

Università Politecnica delle Marche

Corso di Dottorato in Ingegneria Industriale
Curriculum: Energetica

TOWARDS ENERGY EFFICIENT, COMFORTABLE AND CLIMATE RESILIENT BUILT ENVIRONMENT:

Development and application of smart, optimized and mitigation-oriented solutions

Curriculum supervisor:

Prof. Costanzo di Perna

Ph.D. Dissertation of:

Giulia Ulpiani

Ph.D. Course coordinator:

Prof. Ferruccio Mandorli

XVI edition (2014 – 2017) – new series

"As the saying goes, the Stone Age did not end because we ran out of stones; we transitioned to better solutions. The same opportunity lies before us with energy efficiency and clean energy."

Steven Chu

Table of contents

LIST OF FIGURES p. I.8

LIST OF TABLES p. I.16

NOMENCLATURE p. I.20

1. INTRODUCTION

Thematic contents, key concepts and roadmap of the experimental activity

1.1 – ABSTRACT p. 1.2

1.2 – OPTIMIZATION FOR ENERGY EFFICIENCY & COMFORT p. 1.4

1.2.1 Regulatory framework p. 1.5

1.3 – SMART SYSTEMS FOR ENERGY EFFICIENCY AND COMFORT p. 1.9

1.3.1 Smart control of buildings: an overview p. 1.11

1.3.2 Optimal, predictive, adaptive control systems p. 1.12

1.3.3 Computational Intelligence p. 1.13

1.3.4 Multi-agent control systems p. 1.16

1.3.5 Ambient Intelligence p. 1.17

1.4 – MITIGATION TECHNOLOGIES FOR CLIMATE RESILIENCE p. 1.18

1.4.1 Magnitude and characteristics of climate change p. 1.22

1.4.2 International framework of commitment p. 1.26

1.4.3 Building scale p. 1.27

1.4.4 Urban scale p. 1.28

APPENDIX 1 p. 1.32

REFERENCES p. 1.34

2. SMART CONTROL OF ELETRIC RADIATORS

Comparing the performance of on/off, PID and fuzzy controllers applied to the heating system of an energy-efficient building

2.1 – ABSTRACT p. 2.2

2.2 – INTRODUCTION p. 2.2

2.3 – MATERIALS AND METHODS p. 2.3

2.4 – CASE STUDY p. 2.4

2.5 – SENSOR NETWORK p. 2.8

2.6 – CONTROLLERS CONFIGURATION p. 2.13

2.6.1 On/off controller **p. 2.14**
2.6.1.1 Setup **p. 2.14**
2.6.2 PID controller **p. 2.16**
2.6.2.1 Structure **p. 2.17**
2.6.2.2 Control actions **p. 2.18**
2.6.2.3 Tuning **p. 2.19**
2.6.2.4 Setup **p. 2.23**
2.6.3 Fuzzy controller **p. 2.25**
2.6.3.1 Structure **p. 2.25**
2.6.3.2 Setup **p. 2.27**
2.7 – EVALUATION CRITERIA **p. 2.34**
2.7.1 Criterion for energy consumption **p. 2.34**
2.7.2 Criterion for comfort **p. 2.35**
2.8 – RESULTS AND DISCUSSION **p. 2.35**
2.8.1 Energy consumption **p. 2.36**
2.8.1.1 Normalized comsumption **p. 2.36**
2.8.1.2 Energy signatures **p. 2.38**
2.8.2 Indoor thermal comfort **p. 2.42**
2.9 – CONCLUSIONS **p. 2.46**
REFERENCES **p. 2.48**

3. SMART CONTROL OF WINDOW OPENINGS

Maximizing indoor air quality and thermal comfort through a customized adaptive comfort algorithm, tailored for classrooms requirements

3.1 – ABSTRACT **p. 3.2**
3.2 – INTRODUCTION **p. 3.3**
3.3 – METHODOLOGY **p. 3.8**
3.4 – CASE STUDY **p. 3.9**
3.5 – EXPERIMENTAL METHOD **p. 3.12**
3.6 – SMART SYSTEM SPECIFICATIONS **p. 3.17**
3.7 – HUMPHREYS' ALGORITHM - TUNING **p. 3.18**
3.8 – RESULTS **p. 3.19**
3.8.1 Comparison of comfort models **p. 3.20**
3.8.2 Adaptive Comfort Algorithm **p. 3.24**

3.8.3 Test and comparative analysis **p. 3.25**
3.8.4 Questionnaires **p. 3.28**
3.8.5 The effect of wind **p. 3.30**
3.9 – DISCUSSION AND CONCLUSION **p. 3.32**
REFERENCES **p. 3.35**

4. OPTIMIZED DESIGN AND SMART CONTROL OF A SUNSPACE

Experimental monitoring of a sunspace applied to a NZEB mock-up: assessing and comparing the energy benefits of different configurations

4.1 – ABSTRACT **p. 4.2**
4.2 – INTRODUCTION **p. 4.3**
4.3 – MATERIALS AND METHODS **p. 4.9**
4.3.1 Phases **p. 4.10**
4.3.2 Mock-up **p. 4.11**
4.3.3 Sunspace **p. 4.14**
4.3.3.1 Preliminary simulations **p. 4.14**
4.3.3.2 Inputs and outputs **p. 4.15**
4.3.3.3 Results and discussion **p. 4.17**
4.3.3.4 Construction **p. 4.23**
4.3.4 Sensor network **p. 4.25**
4.4 – MONITORING ACTIVITY AND COMPARATIVE ANALYSIS **p. 4.28**
4.4.1 Environmental parameters **p. 4.29**
4.4.2 Energy consumption **p. 4.33**
4.4.3 Simulation models' validation and sunspace efficiency **p. 4.38**
4.5 – CONCLUSIONS **p. 4.39**
REFERENCES **p. 4.42**

5. SMART CONTROL OF FAN COIL UNITS TO COUNTERACT INDOOR OVERHEATING

Overheating phenomena induced by fully-glazed facades: investigation of a sick building in Italy and assessment of the benefits achieved via fuzzy and model predictive control of the AC system

5.1 – ABSTRACT **p. 5.2**
5.2 – INTRODUCTION **p. 5.3**

5.3 – MATERIALS AND METHODS **p. 5.6**
5.3.1 Case study **p. 5.6**
5.3.2 Sensor network **p. 5.12**
5.4 – CONTROL MANAGEMENT **p. 5.17**
5.4.1 On-off controller **p. 5.19**
5.4.2 Fuzzy controllers **p. 5.20**
5.4.3 Model predictive controller **p. 5.21**
5.4.3.1 Setup **p. 5.22**
5.5 – ASSESSMENT CRITERIA **p. 5.24**
5.5.1 Indoor comfort **p. 5.25**
5.5.2 Energy consumption **p. 5.26**
5.6 – RESULTS AND DISCUSSION **p. 5.27**
5.6.1 Operative temperature and PMV **p. 5.28**
5.6.1.1 Summertime results **p. 5.28**
5.6.1.2 Wintertime results **p. 5.34**
5.6.2 Draughts and vertical gradient **p. 5.42**
5.6.2.1 Summertime results **p. 5.42**
5.6.2.2 Wintertime results **p. 5.48**
5.6.3 Energy consumption **p. 5.51**
5.6.3.1 Summertime results **p. 5.51**
5.6.3.2 Wintertime results **p. 5.52**
5.7 – CONCLUSIONS **p. 5.56**
APPENDIX A **p. 5.61**
APPENDIX B **p. 5.63**
APPENDIX C **p. 5.67**
REFERENCES **p. 5.69**

6. CLIMATE CHANGE RESILIENCE

Identify, assess and compare potential countermeasures to cope with climate change for a low-tech building in Austria

6.1 – ABSTRACT **p. 6.2**
6.2 – INTRODUCTION **p. 6.3**
6.3 – CASE STUDY **p. 6.9**
6.3.1 General features **p. 6.11**

6.3.2 Location **p. 6.13**
6.3.3 Sunlight **p. 6.14**
6.3.4 Walls composition **p. 6.15**
6.3.5 Comfort management **p. 6.18**
6.4 – METHODOLOGY **p. 6.19**
6.4.1 Building Information Modelling **p. 6.20**
6.4.2 Energy modelling **p. 6.22**
6.5 – CURRENT STATE RESULTS **p. 6.25**
6.5.1 SWOT analysis **p. 6.25**
6.5.2 Energy consumption **p. 6.26**
6.5.3 Indoor comfort **p. 6.30**
6.6 – CLIMATE CHANGE RESILIENT REDESIGN **p. 6.31**
6.6.1 Problem solving **p. 6.32**
6.6.2 Comfort oriented redesign **p. 6.33**
6.6.3 Redesign options **p. 6.36**
6.6.3.1 Comfort-based comparison **p. 6.41**
6.6.3.2 Energy-based comparison **p. 6.44**
6.7 – FINAL REDESIGN STRATEGY **p. 6.47**
6.8 – CONCLUSIONS **p. 6.52**
REFERENCES **p. 6.53**

7. URBAN HEAT ISLAND MITIGATION

Investigating and comparing the UHI mitigation potential of various technologies via on-site monitoring and urban-scale simulation: a case study in Australia

7.1 – ABSTRACT **p. 7.2**
7.2 – INTRODUCTION **p. 7.3**
7.3 – DARWIN'S MICROCLIMATE **p. 7.4**
7.4 – CURRENT STATE SIMULATION **p. 7.7**
7.5 – MONITORING CAMPAIGN **p. 7.12**
7.5.1 Monitoring plan **p. 7.14**
7.5.2 Aerial survey **p. 7.15**
7.5.2.1 Instruments and methods **p. 7.15**
7.5.2.2 Outputs **p. 7.19**
7.5.2.3 Conclusions **p. 7.24**
7.5.3 Terrestrial survey **p. 7.26**

7.5.3.1 Instruments and methods **p. 7.26**

7.5.3.2 Outputs **p. 7.35**

7.5.3.3 Conclusions **p. 7.48**

7.6 – MITIGATION SCENARIOS **p. 7.49**

7.7 – RESULTS AND DISCUSSION **p. 7.51**

7.8 – CONCLUSIONS **p. 7.55**

REFERENCES **p. 7.58**

8. CONCLUSIONS

Contribution, novelty and perspectives

8.1 – FOREWORKD **p. 8.2**

8.2 – ADVANCES IN THE FIELD OF SMART CONTROL **p. 8.3**

8.3 – ADVANCES TOWARDS CLIMATE CHANGE RESILIENCE **p. 8.6**

8.3.1 Low-tech buildings and future scenarios **p. 8.7**

8.3.2 Urban Heat Island mitigation in tropical climates **p. 8.8**

REFERENCES **p. 8.10**

ACKNOWLEDGMENTS

Through the voice of Indira Gandhi – Speech at the plenary session of United Nations Conference on Human Environment (Stockholm, 1972)

List of figures

1. INTRODUCTION

1.1 – Research topics of the thesis in object and visual interpretation of their interrelations p. 1.3

1.2 – EPBD regulatory framework p. 1.7

1.3 – EU27 heating and cooling demands in residential and services sector per scenario. p. 1.9

1.4 – Adaptive controller basic scheme p. 1.13

1.5 – Fuzzy logic integration into a neural network structure p. 1.15

1.6 – Single and multi-agent control structures for distributed systems p. 1.16

1.7 – Radiative forcing of anthropogenic and natural factors (IPCC 2007: WG1-AR4) p. 1.19

1.8 – Human activities planetary boundaries in terms of safety: activities still within safe margins (green areas), activities that may or may not have exceeded safe margins (yellow areas), activities that have exceeded safe margins (red areas) and activities for which safe margins have not yet been determined (grey areas) p. 1.20

1.9 – Front and back loop of construction sector strategy to cope with climate change p. 1.21

1.10 – IPCC Fourth Assessment Report - FAQ 3.1, Figure 1, Figure 4.2, Figure 5.13 – surface temperatures, sea level and snow cover trends. Observed changes in (a) global average surface temperature, (b) global average sea level from tide gauge (blue) and satellite (red) data and (c) Northern Hemisphere snow cover for March-April. All changes are relative to corresponding averages for the period 1961–1990. Smoothed curves represent decadal average values while circles show yearly values. The shaded areas are the uncertainty intervals estimated from a comprehensive analysis of known uncertainties (a and b) and from the time series (c) p. 1.22

1.11 – IPCC Fourth Assessment Report - FAQ 9.2, Figure 1– global and continental temperature change. Comparison of observed continental- and global-scale changes in surface temperature with results simulated by climate models using natural and anthropogenic forcings. Decadal averages of observations are shown for the period 1906 to 2005 (black line) plotted against the centre of the decade and relative to the corresponding average for 1901–1950. Lines are dashed where spatial coverage is less than 50%. Blue shaded bands show the 5–95% range for 19 simulations from five climate models using only the natural forcings due to solar activity and volcanoes. Red shaded bands show the 5–95% range for 58 simulations from 14 climate models using both natural and anthropogenic forcings p. 1.23

1.12 –IPCC Fourth Assessment Report - Figures 10.4 and 10.29– global and continental temperature change. Solid lines are multi-model global averages of surface warming (relative to 1980–1999) for the scenarios A2, A1B and B1, shown as continuations of the 20th century simulations. Shading denotes the ±1 standard deviation range of individual model annual averages. The orange line is for the experiment where concentrations were held constant at year 2000 values. The grey bars at right indicate the best estimate (solid line within each bar) and the likely range assessed for the six SRES marker scenarios. The assessment of the best estimate and likely ranges in the grey bars includes the AOGCMs in the left part of the figure, as well as results from a hierarchy of independent models and observational constraints p. 1.24

1.13 – IPCC Fourth Assessment Report - Figures 10.8 and 10.28– global and continental temperature change. Projected surface temperature changes for the early and late 21st century relative to the period 1980–1999. The central and right panels show the AOGCM multi-model average projections for the B1 (top), A1B (middle) and A2 (bottom) SRES scenarios averaged over the decades 2020–2029 (centre) and 2090–2099 (right). The left panels show corresponding uncertainties as the relative probabilities of estimated global average warming from several different AOGCM and Earth System Model of Intermediate Complexity studies for the same periods. Some studies present results only for a subset of the SRES scenarios, or for various model versions. Therefore, the difference in the number of curves shown in the left-hand panels is due only to differences in the availability of results p. 1.25

1.14– IPCC Fourth Assessment Report - Figures 10.9– global and continental temperature change. Relative changes in precipitation (in percent) for the period 2090–2099, relative to 1980–1999. Values are multi-model averages based on the SRES A1B scenario for December to February (left) and June to August (right). White areas are where less than 66% of the models agree in the sign of the change and stippled areas are where more than 90% of the models agree in the sign of the change. p. 1.26

1.15 – Per cent electricity demand increase per degree of temperature rise: comparison among different countries. The potential increase ranges between 0.5% and 8.5%. p. 1.29

1.16 - UHI energy penalty indices: comparing data from various cities p. 1.30

1.17 - Per cent peak electricity demand increase per degree of temperature rise: comparison among different cities. The potential increase ranges between from 0.45% to 4.6%, which corresponds to a penalty of about 21 (±10.4) W per degree of temperature rise per person p. 1.30

2. SMART CONTROL OF ELETRIC RADIATORS

2.1 – Experimental mock-up in Agugliano (Ancona, Italy) p. 2.4

2.2 – CAD detail of materials composing mock-up's walls: shots taken during the construction on the right p. 2.8

2.3 – Distribution scheme of the probes inside and outside the mock-up: A) Plan view of the indoor network; B) A-A' cross section of the outdoor network; C) A-A' cross section of the indoor network; D) B-B' cross section of the interface network; E) outdoor network on south-exposed wall p. 2.11

2.4 – Characteristic curve of the on/off controller when the hysteresis is set to 1°C: power command against dry-bulb indoor air temperature p. 2.15

2.5 – Characteristic curve of the on/off controller when the hysteresis is set to 0,5°C: power command against dry-bulb indoor air temperature p. 2.15

2.6 – Turning a manual control into an equivalent automatic control in a typical industrial process: SP=Set Point; PV=Process Variable; CO=Control Output p. 2.17

2.7 – Functional macro-blocks of a PID controller p. 2.18

2.8 – Tuning of the proportional band p. 2.20

2.9 – P, I, D structure of the controller p. 2.23

2.10 - Agugliano's PI controller characteristic curve: the bottom detail is used to gather technical information p. 2.24

2.11 – Fuzzy controller basic scheme p. 2.25

2.12 – Normalized energy consumption ortogram p. 2.38

2.13 – Energy signature regression lines relating power consumption to outdoor air temperature p. 2.40

2.14 – Energy signature regression lines relating power consumption to global solar radiation p. 2.41

2.15 – Predicted mean vote and predicted percentage of dissatisfied people charts over the entire monitoring period p. 2.45

3. SMART CONTROL OF WINDOW OPENINGS

3.1 – Plan view and vertical section of the MT and FR classrooms: red dots and dashes indicate the location of the probes composing the indoor and outdoor sensor network; the dial at the top right displays North orientation p. 3.11

3.2 – FR classroom layout. Red circle to highlight the indoor microclimate station p. 3.12

3.3 – Preliminary analyses on the MT classroom (before the installation of the automatic system): (a) indoor thermal gradient, (b) comfort maps, (c) mean PMV value for each relevant sub-zone of the classroom p. 3.13

3.4 – MT classroom questionnaire template: users' thermal perception, preferences and disturbances investigation p. 3.16

3.5 – Schematization of the sensitive-planning-acting chain behind the automatic system conceptualization p. 3.17

3.6 – Environmental trigger parameters trends over time: comfort and IAQ boundaries displayed for the sake of comparison p. 3.21

3.7 – FR classroom monitoring campaign – linear regression analysis to identify ACA's trigger parameters p. 3.24

3.8 – Thermal (a), IAQ (b) and occupants related information (c) recorded over six representative days for both MT and FR classrooms p. 3.26

3.9 – Comparison of MT and FR classrooms microclimates during two days of different wind conditions p. 3.32

4. OPTIMIZED DESIGN AND SMART CONTROL OF A SUNSPACE

4.1 – Solar gains and heat transfer displayed according to the three operative modes of a sunspace p. 4.5

4.2 – Flow diagram of the operational steps to investigate the potential energy saving achievable when a sunspace works coupled with an energy-efficient building p. 4.11

4.3 – Graphical analysis of the energy saving trends related to the number of glazed panes and the presence of the opening on the partition wall p. 4.21

4.4 – Sunspace construction details p. 4.24

4.5 – Comparison between the mock-up plus sunspace configurations in terms of air temperatures p. 4.30

4.6 – Comparison between the mock-up plus sunspace configurations in terms of surface temperatures p. 4.31

4.7 – Comparison between the mock-up plus sunspace configurations in terms of Solar radiation p. 4.32

4.8 – Energy signatures of the mock-up plus sunspace configurations. Outdoor parameter: daily average difference between indoor and outdoor air temperatures p. 4.34

4.9 – Energy benefit achieved with Conf_3 compared to Conf_2 in absolute terms p. 4.35

4.10 – Energy benefit achieved with Conf_3 compared to Conf_2 in per cent terms p. 4.35

4.11 – Energy signatures of the mock-up plus sunspace configurations. Outdoor parameter: daily Solar radiation hitting the south-facing external wall of the sunspace p. 4.36

5. SMART CONTROL OF FAN COIL UNITS TO COUNTERACT INDOOR OVERHEATING

5.1 – Climatic characterization of Ancona (Italy): monthly averaged values of temperature, relative humidity, global horizontal radiation and rainfall over the year 2016 p. 5.7

5.2 – Case study: a) satellite localization, b) view of the south fully-glazed façade, c) view of the interiors p. 5.8

5.3 – Plan localization and visualization of the sensor network p. 5.14

5.4 – Screenshot of the front panel of the Virtual Instrument developed in LabVIEW to manage the dataflow p. 5.19

5.5 – Global comfort assessment: time trends of operative temperature against setpoint threshold, solar radiation, outdoor temperature and concomitant fan speed p. 5.29

5.6 – Global comfort assessment: histograms of occurrences - operative temperature offset from the setpoint p. 5.30

5.7 – Global comfort assessment: histograms of occurrences - PMV value p. 5.30

5.8 – Thermal distribution of the maximum surface temperatures on the glazed façade p. 5.34

5.9 – Global comfort assessment: time trends of operative temperature against setpoint threshold, solar radiation and concomitant fan speed p. 5.39

5.10 – Global comfort assessment: histograms of occurrences - operative temperature offset from the setpoint p. 5.39

5.11 – Global comfort assessment: histograms of occurrences - PMV value p. 5.40

5.12 – Local comfort assessment: thermal distribution of the maximum surface temperatures on the glazed façade p. 5.42

5.13 – Local comfort assessment: time trends of the draught rates at 0.1m and 1.1m against the comfort limit and the concomitant fan speed p. 5.45

5.14 – Local comfort assessment: histograms of occurrences – DR values at 0.1, 0.6 and 1.1 meters from ground level p. 5.46

5.15 – Local comfort assessment: time trends of the air temperature at 0.1m and 1.1m against the concomitant fan speed p. 5.47

5.16 – Local comfort assessment: histograms of occurrences – vertical thermal gradients p. 5.48

5.17 – Local comfort assessment: time trends of the draught rate at 0.1m and of the vertical gradient against the respective comfort limits and the concomitant fan speed p. 5.50

5.18 – Local comfort assessment: histograms of occurrences – vertical thermal gradients p. 5.51

5.19 – Energy assessment (fuzzy controllers): histograms of occurrences – fan speeds p. 5.52

5.20 – Energy assessment (MPC and FM controllers): histograms of occurrences – fan speeds p. 5.54

5.21 – Energy assessment: time trends of the energy consumptions against solar radiation and the simultaneous offset from the setpoint p. 5.55

C.1 –2C2R circuit of the grey-box model. p. 5.67

6. CLIMATE CHANGE RESILIENCE

6.1 – Deviation from global mean surface temperature (reference given by climatic conditions in the first decade of the 20th century) according to different future evolutions p. 6.4

6.2 – Climate change scenario: weather data for case study location in Austria - 2015 on top, 2050 on bottom p. 6.5

6.3 – Climate change scenario: air temperature and Solar radiation time trends - 2015 on top, 2050 on bottom (adaptive comfort zone compliant to ASHRAE 55) p. 6.6

6.4 – Climate change scenario: wind speed ranges per month - 2015 on top, 2050 on bottom p. 6.7

6.5 – Climate change scenario: air temperature and relative humidity per month - 2015 on top, 2050 on bottom p. 6.8

6.6 – Building 2226 in Lustenau and WISBA 2015 team (students and mentors) p. 6.9

6.7 – Building 2226 natural ventilation systems: windows equipped with ventilating doors (a) and internal stairway (b) p. 6.10

6.8 – Plans, elevations and sections of Building 2226 p. 6.12

6.9 – Architect Eberle showing the monitoring touchscreen during the visit to Building 2226 p. 6.12

6.10 – Lustenau's annual climate p. 6.14

6.11 – Building 2226 structural details: brick layers (a), windows (b), floor structure (c), connection between opaque and glazed components (d) p. 6.17

6.12 – BIM on Building 2226 through Autodesk Revit: (a) materials insertion and quantification: (b) element composition definition p. 6.21

6.13 – BIM-based workflow: links between assessment perspectives and feedback loop of the iterative design process p. 6.22

6.14 – BEM geometry, layout and division in thermal zones p. 6.23

6.15 – Occupancy schedules tailored per each thermal zone: office case p. 6.24

6.16 – Building 2226 current state simulation: daily temperatures and energy loads throughout the year p. 6.28

6.17 – Building 2226 current state simulation: indoor temperatures, carbon dioxide levels and heat balance during a summer day in the westhern zone p. 6.29

6.18 – Building 2226 current state simulation: indoor temperatures, carbon dioxide levels and heat balance during a winter day in the northern zone p. 6.29

6.19 – Building 2226 current state comfort assessment: indoor and outdoor temperatures time trends, overlapped to comfort limits in order to visualize the frequency of satisfactory environmental conditions p. 6.30

6.20 – Dynamic parameters descriptive of building thermal behaviour p. 6.34

6.21 – Re-design flowchart p. 6.36

6.22 – Redesign details for window blinds, interior and exterior walls composition p. 6.39

6.23 – Comparison between different redesign options applied to building 2226 in 2015 in terms of accumulated discomfort [h] p. 6.42

6.24 – Comparison between different redesign options applied to building 2226 in 2050 in terms of accumulated discomfort [h] p. 6.43

6.25 – Orientation and solar gains [Sapa Building System] p. 6.44

6.26 – Base cases in 2015 and 2050: comparing energy consumptions p. 6.44

6.27 – Comparing energy consumptions in 2015 and 2050 when redesigning (a) outer walls, (b) blinds, (c) inner walls, (d) roof, (e) inner floors, (f) ventilation, (g) lighting p. 6.46

6.28 – Final redesign strategy for climate change scenario p. 6.48

6.29 – Comfort assessment for the final redesign: discomfort hours in 2015 and 2050 p. 6.50

6.30 – Overheating and related discomfort for each chosen redesign strategy: comparing 2015 and 2050 scenarios p. 6.50

6.31 – Energy consumptions for base and final redesigned case in 2015 and 2050 p. 6.51

7. URBAN HEAT ISLAND MITIGATION

7.1 – Annual temperature 90th percentile distribution over Australian territory – BoM maps of minimum (a), average (b) and maximum (c) values p. 7.4

7.2 – Ambient temperature distribution for Darwin reference model in summer, 2pm, with winds blowing from: (a)NW at 5m/s, (b) NW at 1m/s, (c) SE at 5m/s and (d) SE at 1m/s p. 7.9

7.3 – Surface temperature distribution for Darwin reference model in summer, 2pm, with winds blowing from: (a)NW at 5m/s, (b) NW at 1m/s, (c) SE at 5m/s and (d) SE at 1m/s p. 7.10

7.4 – Darwin CBD monitoring campaign asset: (a) aerial survey by pilot Aaron Emmett (NT National Drones); (b) terrestrial survey by PhD candidates Giulia Ulpiani and Jonathan Fox p. 7.13

7.5 – Darwin aerial monitoring campaign – thermal shots strategic roadmap p. 7.19

7.6 – Darwin aerial monitoring campaign – thermal shots: (a) area 1.3, 23rd of March, 12pm; (b) area 2.3, 24th of March, 11:30am p. 7.20

7.7 – Darwin aerial monitoring campaign – thermal shots strategic roadmap p. 7.21

7.8 – Mitchell Street – Daly Street crossing & petroleum station carpark (area 1.2) thermal video frames p. 7.22

7.9 –LabVIEW front panel: (a) setting screen - communication with the datataker, dt85 and geographic data retrieval; (b) graphical visualization of net radiometer output time trends; (c) graphical visualization of meteo station output time trends p. 7.31

7.10 – Darwin terrestrial monitoring campaign – points of measurement p. 7.33

7.11 – Darwin terrestrial monitoring campaign –meteo charts p. 7.38

7.12 – Darwin terrestrial monitoring campaign –thermohygrometric differences along Cavenagh Street (a), Woods Street (b) and Daly Street (c) p. 7.40

7.13 – Darwin CBD air temperature differences distribution – maximum, minimum and average values displayed per each monitored location p. 7.43

7.14 – Darwin CBD wind speed differences distribution – maximum, minimum and average values displayed per each monitored location p. 7.45

7.15 – Darwin CBD relative humidity differences distribution – maximum, minimum and average values displayed per each monitored location p. 7.47

7.16 – Distribution of the ambient temperature drop in Darwin CBD, according to the different simulated scenarios p. 7.54

List of tables

1. INTRODUCTION

1.1 – Building categorization p. 1.8

1.2 – Comparison amongst building controllers in terms of functions p. 1.18

2. SMART CONTROL OF ELETRIC RADIATORS

2.1 – Experimental building general data. p. 2.5

2.2 – Walls composition: materials, thicknesses, thermal transmittances p. 2.6

2.3 – Probes specs and location p. 2.9

2.4 – Acquisition systems specs p. 2.11

2.5 – Heating system specs p. 2.11

2.6 – Tuning scheme of a PID (and sub-species) controller p. 2.22

2.7 – Fuzzy controller membership functions p. 2.27

2.8 – Fuzzy controller rules p. 2.30

2.9 – Observation periods and corresponding weather conditions per each controller under test p. 2.36

2.10 – Energy performance evaluation: normalized energy consumption per each controller under test p. 2.37

2.11 – Outdoor temperature related energy signature line equations p. 2.39

2.12 – Solar radiation related energy signature line equations p. 2.40

2.13 – UNI EN ISO 7730:2006 - Categories of thermal environment p. 2.44

2.14 – Time-averaged PPD and PMV and PPD.h values for each control system p. 2.44

3. SMART CONTROL OF WINDOW OPENINGS

3.1 – Comparing PMV/PPD and adaptive comfort models p. 3.4

3.2 – Steps in the implementation of the (a) Humphreys' algorithm from the literature and (b) modified/integrated inputs in the proposed version p. 3.5

3.3 – Case study geographic features p. 3.9

3.4 – Monitored classrooms features p. 3.11

3.5 – Per cent discomfort values and per cent time outside IAQ boundaries (FR classroom) p. 3.22

3.6 – Questionnaires to rate users' thermal sensation in FR classroom - analysis p. 3.23

3.7 – Comparison of thermo-olfactive comfort behaviour between the free-running and motorized classrooms p. 3.28

3.8 – PPD weighted index results: main differences between FR and MT classrooms p. 3.28

3.9 – Comparison of thermal sensation questionnaires for FR and MT classrooms p. 3.29

4. OPTIMIZED DESIGN AND SMART CONTROL OF A SUNSPACE

4.1 – Mock-up walls composition: materials, thicknesses, thermal transmittances. in compliance with the international Standard ISO 13786 p. 4.11

4.2 – Preliminary simulations general settings p. 4.14

4.3 – Sunspace glass properties p. 4.15

4.4 – Preliminary simulation general settings p. 4.16

4.5 – Reference buildings details p. 4.17

4.6 – Preliminary simulations energy results p. 4.17

4.7 – Sunspace walls composition: materials, thicknesses, thermal transmittances p. 4.22

4.8 – Sunspace monitoring stations details p. 4.27

4.9 – Monitoring activity: covered periods and general settings p. 4.28

5. SMART CONTROL OF FAN COIL UNITS TO COUNTERACT INDOOR OVERHEATING

5.1 – Office room walls composition: materials, thicknesses, thermal transmittances and surface mass p. 5.9

5.2 – FCU technical data p. 5.11

5.3 – Sensor network general data p. 5.15

5.4 – Characterization of the monitoring periods p. 5.24

A.1 – FS controller: general settings. p. 5.61

A.2 – FS controller: input membership functions p. 5.61

A.3 – FS controller: output membership functions p. 5.62

A.4 – FS controller: rules p. 5.62

B.1 – FM controller: general settings. p. 5.63

B.2 – FM controller: input membership functions p. 5.63

B.3 – FM controller: output membership functions p. 5.64

B.4 – FM controller: rules p. 5.64

6. CLIMATE CHANGE RESILIENCE

6.1 – Geometric and structural details of building 2226 p. 6.16

6.2 – Building 2226 current state: SWOT analysis p. 6.25

6.3 – Building 2226 current state: pros and cons from SWOT analysis p. 6.26

6.4 – Some guidelines to counteract the deficit in energy performance expected in 2050 scenario p. 6.32

6.5 – Redesign options for building 2226 to face 2050 climate change p. 6.36

6.6 – Trade-offs of the proposed final redesign measures between current and future scenario p. 6.49

7. URBAN HEAT ISLAND MITIGATION

7.1 – Darwin climate specs categorized via clustering technique p. 7.7

7.2 – Statistics on temperatures for the reference scenario p. 7.11

7.3 – Darwin CBD monitoring campaign plan p. 7.14

7.4 – DJI Inspire 1 technical details p. 7.16

7.5 – Zenmuse XT thermal camera technical details p. 7.17

7.6 – Hukseflux NR01 technical details p. 7.28

7.7 – Gill Instrument MetPak Pro technical details p. 7.29

7.8 – Darwin terrestrial monitoring campaign – example of meteorological data collection: time and space details, terrestrial sensor network outputs and mathematical processing (as in sub-paragraph 7.7.1). Refer to the following legend: Wdir = Wind direction; Ws = Wind speed;Ta = Air temperature; P = Barometric pressure; Tdew = Dew-point; RH = Relative humidity p. 7.33

7.9 – Darwin terrestrial monitoring campaign – list and indexing of monitored points p. 7.42

7.10 – List of the terrestrial survey monitoring points in order of decreasing average UHI magnitude – maximum and minimum values additionally showed p. 7.43

7.11 – List of the terrestrial survey monitoring points in order of decreasing average wind speed difference – maximum and minimum values additionally showed p. 7.45

7.12 – List of the terrestrial survey monitoring points in order of decreasing average relative humidity difference – maximum and minimum values additionally showed p. 7.47

7.13 – List of the proposed countermeasures for Darwin urban heat mitigation p. 7.50

7.14 – Simulation results for the combined scenario developed for the dry season p. 7.55

Nomenclature

In alphabetical order

AC	Air Conditioning/Air Conditioned
ACA	Adaptive Comfort Algorithm
AHU	Air Handling Unit
AI	Artificial Intelligence
ANFIS	Adaptive Neuro-Fuzzy Inference Systems
ASHRAE	American Society of Heating, Refrigerating, and Air-Conditioning Engineers
BACS	Building Automation and Control Systems
BEM	Building Energy Modelling
BIEMS	Building Intelligent Energy Management Systems
BIM	Building Information Modelling
BoM	Bureau of Meteorology
CASA	Civil Aviation Safety Authority
CAST	Civil Aviation Safety Team
CBD	Central Business District
CEN	European Committee for Standardization
CFD	Computational Fluid Dynamics
CFMPC	Cooperative Fuzzy Model Predictive Control
CIBSE	Chartered Institution of Building Services Engineers
CO	Control Output
Cops	Conferences of the parties
CSIRO	Commonwealth Scientific and Industrial Research Organisation
DAQ	Data Acquisition
DHW	Domestic Hot Water
DR	Draught Rate [%]
DT	Delta of Temperature [°C]
EED	Energy Efficiency Directive
EPBD	Energy Performance of Buildings Directive
EU	European Union
FCU	Fan Coil Unit
FM	Fuzzy Meteorological control
FR	Free-Running (classroom)
GHG	Greenhouse Gases
HPA	High Performance Architecture cluster
HVAC	Heating Ventilation and Air Conditioning
IAQ	Indoor Air Quality
IEQ	Indoor Environmental Quality
IPCC	Intergovernmental Panel on Climate Change
LCA	Life Cycle Assessment
LCC	Life Cycle Cost
MACS	Multi-Agent Control System
MISO	Multiple-Input Single-Output
MPC	Model Predictive Control
MT	Motorized (classroom)
NDC	Nationally Determined Contribution
NIR	Near Infrared
NNC	Neural Network Controller
NT	Northern Territory
NW	North-West
NZEB	Nearly Zero Energy Building
OECD	Organisation for Economic Co-operation and Development

PCM	Phase Change Material
PID	Proportional-Integral-Derivative control
PMV	Predicted Mean Vote
PPD	Predicted Percentage of Dissatisfied people [%]
PPD.h	Excess-weighted PPD [h]
PPDwC	PPD-weighted Criterion
PV	Process Variable
R&D	Research & Development
RC	Resistor-Capacitor circuit
RePL	Remote Pilot License
RF	Radiative Forcing
RH	Relative Humidity
RHC	Receding Horizon Control
RTD	Resistance Temperature Detector
SBS	Sick Building Syndrome
SE	South-East
SHGC	Solar Heat Gain Coefficient
SP	Set Point
SRES	Special Report on Emission Scenarios
SWOT	Strengths, Weaknesses, Opportunities and Threats
TAR	Third Assessment Report
TCP/IP	Transmission Control Protocol/Internet Protocol
UAV	Unmanned Aerial Vehicle
UHI	Urban Heat Island
UNEP	United Nations Environmental Programme
UNFCCC	United Nations Framework Convention on Climate Change
UNSW	University of New South Wales
VI	Virtual Instrument
VMC	Controlled Mechanical Ventilation
WISBA	Wienerberger Sustainable Building Academy
WMO	World Meteorological Organization
XPS	Extruded Polystyrene
ΔRH	Delta of Relative Humidity [%]
ΔTa	Delta of ambient Temperature [°C]

1

Introduction

Thematic contents, key concepts and roadmap of the experimental activity.

1.1 – ABSTRACT

Several research activities have been carried out during the three years of the Doctorate path spanning the different spatial and temporal aspects of energy efficiency, comfort and resilience throughout diverse scales of the building stock.
Each of these macro-topics has been addressed from an applicative point of view by exploring the frontiers of optimized, smart and mitigation technologies.
The longest monitoring activities took place in Italian case studies and tackled with the design of optimized solutions achieved by means of increased regulation efficiency of specific building components, notably:

- smart control of electric radiators: comparing the performance of on/off, PID and fuzzy controllers applied to the heating system of an energy-efficient building (**chapter 2**);
- smart control of window openings: maximizing indoor air quality and thermal comfort through a customized adaptive comfort algorithm, tailored for classrooms requirements (**chapter 3**);
- optimized design and smart control of a sunspace attached to a NZEB mock-up: experimental monitoring and comparative assessment of the energy benefits for different configurations (**chapter 4**);
- smart control of fan coil units to counteract the overheating induced by fully glazed, sun-exposed façades: exploring the environmental benefits achievable via fuzzy and model predictive control (**chapter 5**).

Chapter 6 collects the outcomes of the four-month experience in Europe, as a member of the 2015 WISBA edition (Wienerberger Sustainable Building Academy), as regards the contents directly developed by the team I belonged to: modelling and assessing the energy and ergonomic performance of Building 2226 from Baumschlager Eberle architects in the frame of the actual climatic conditions and in view of the expected climate change to come in 2050.
Finally, the results of one of the main projects run in the one-year experience in the University of New South Wales (Sydney, Australia) - as a member of the HPA (High Performance Architecture) cluster led by professor Mat Santamouris - are reported (**chapter 7**). In this framework, the focus shifted from indoors to outdoors, yet retaining the core target of optimizing energy consumptions and comfort conditions: magnitude and characteristics of the urban heat island affecting the major Australian cities were monitored, analysed, modelled and tackled by developing customized counterbalance measures.
All things considered, the first macro-block of the present thesis (**chapters 2-5**) deals with smart, optimized controllers to be coupled with various building systems so as to depict and delimit their effectiveness in achieving Nearly Zero Energy Buildings

(NZEBs); while the second macro-block (**chapters 6,7**) investigates the need for mitigation solutions to enhance climate change resilience both on building and urban scale. The overarching aim is to conceive appropriate strategies to be implemented in view of the mutual-empowering effect of global warming and local heat islands, exacerbated by increasingly frequent and massive heat waves.
The roadmap of the main contents is illustrated in **figure 1.1.**



Figure 1.1
Research topics of the thesis in object and visual interpretation of their interrelations.

It should be stressed here that:

- given the broad range of topics and theoretical backgrounds involved, each chapter has been provided with its own introductory paragraph, necessary to contextualize problem, methodology and solutions;
- not all the experimental activities actually run during the Doctorate path are here presented: a selection has been made among those with higher international impact or already published in peer-reviewed journals.

1.2 – OPTIMIZATION FOR ENERGY EFFICIENCY & COMFORT

In the Eurozone, about 40% of energy consumption is related to buildings requirements and, beneath that percentage, space heating is responsible for over 75% **[1.1].** When the energy required for construction and demolition is also considered, the percentage rises up to 50% of the total energy use **[1.2].**
In particular, European residential buildings average consumption for heating is 140 kWh/m^2 per year, while DHW and summer cooling demand is about 25 and 20 kWh/m^2 per year respectively**.** Percentages do not vary significantly for different latitudes in Europe **[1.3].**
Besides, as a general trend (since 1990), total energy consumption undergoes an annual increment of 1% with a peak of 2.5% related to electrical demand **[1.3].**
In terms of delivered energy, the absolute consumption was close to 23.7 PWh in 2010, yet, sticking to the scenario depicted by the International Energy Agency, such figure is expected to overtake 38.4 PWh in 2040 as a result of the huge rate of growth of non OECD countries **[1.4].**
Although the non-negligible benefits in terms of economy and standard of life, building construction presents a high potential to create negative impacts **[1.5].**
As a matter of fact, its aftermaths on the environment are multiple and variously interrelated, thus leading to self-empowering chains and ripple effects**.**
Consider, for instance, the role played by building demand in the distribution of the worldwide resources of raw materials: the manufacture of building components, products and derived materials absorbs between the 40 and the 50% of the global annual raw material use **[1.6].** The percentage drops down to 12% in terms of global potable water (representing a huge quote anyway), and rises up to even 70% when it comes to timber products**.**
The environmental impact of the building sector can be recapped by the following figures: 20–25% of the air pollutants, 25–33% of black carbon emissions, about 70% of halocarbon, 40% of the pollution of drinking water, 50% of the land- fill waste **[1.7]**, 38% of greenhouse gases emissions **[1.8]**
Besides, the urban sprawl in densely packed layouts and the sharp penetration of air conditioners, are strongly contributing to global and local climate change, with a brave counter-trend given by the renovation of existing building stock**.** Such macro and micro climatic phenomena, in turn, have a serious impact on:

- energy consumption by considerably increasing the peak and the total electricity demand **[1.9,1.10]**;
- the concentration of tropospheric ozone and other air pollutants **[1.11]**;
- thermal comfort conditions and liveability of outdoor spaces **[1.12,1.13]**;

- health degradation and indoor environmental sickness (Sick Building Syndrome) **[1.14,1.15]**;
- the global ecological footprint of the cities **[1.16]**;

Data provided by the European Commission underline that, by improving the energy efficiency of buildings, the total energy consumptions in EU could be reduced by 5% up to 6% and CO_2 emissions by nearly 5% **[1.17].**

1.2.1 Regulatory framework

In order to face this emergency, EU introduced, in the 2000s, a series of directives, standards and guidelines promoting energy saving strategies in the building sector, encouraging a rational use of energy and a wide spread of renewable solutions.
The Europe 2020 strategy was the response given by the European Commission in 2010. It sets targets and deadlines for three major energy issues to be accomplished by 2020:

- greenhouse emissions: the goal is -20% (given 1990 level as reference);
- energy efficiency: a 20% increase is required;
- penetration of renewable energy technologies: 20% quote of the final energy consumption.

Beyond 2020's targets, a roadmap until 2050 has been simultaneously conceived to guide the reduction of the carbon emissions. The milestones are: - 40% by 2030; -60% by 2040 and -80% by 2050 (always compared to 1990 figures).
A series of Standards and regulations have been released in order to turn into executive the afore mentioned objectives, targeting the different sectors which play a significant role in the world energy balance.
The reference for the buildings and construction area are 2002/91/CE Energy Performance of Buildings Directive (EPBD) **[1.18]**, its 2010 Recast **[1.19]** and 2012 Energy Efficiency Directive EED **[1.20].** They define tools and methods to reduce the energy demand of buildings and mitigate their carbon footprint in the Eurozone, through:

- maximum exploitation of advantageous effects related to building inertia and response to outdoor climate conditions;
- optimal management of indoor microclimate;
- cost-effective measures for energy saving.

As a consequence, all EU countries are asked to:

- move towards new and retrofitted nearly zero energy buildings (NZEB), through specific national plans. The deadline is 2019 for new public buildings and 2021 for all new buildings;
- apply cost-optimal methodology for setting minimum requirements for both the envelope and the technical systems of new buildings as well as existing ones when replaced/retrofitted;
- define a common methodology to calculate the energy performance of buildings and certificate it in order to allow meaningful comparison between different constructive and/or HVAC solutions and promote users' awareness;
- schedule regular inspections of the heating and AC systems to guarantee optimal performances.
- refurbish 3% of the governmental buildings per year;
- energy savings equal to 1.5% per year.

The third point of the 2020 Strategy was reinforced by the Renewable Energy Directive **[1.21]**, which drives the penetration of green energy throughout the building stock: on the one hand, new buildings or those subject to major renovation must include renewable energy sources in the heating and cooling services; on the other hand new and existing public buildings (subject to major renovation) must stand as prime examples of excellent integration of renewables in the energy mix.

A further legal instrument comes from the Ecodesign Directive [**1.22**] which addresses the world of energy-related products serving the building sector (boilers, pumps, fans, …) by setting rules and minimum performances.

As a consequence, another Directive (the Energy Labelling one) **[1.23]** has been drawn up to categorize and differentiate the products from an energy-efficient perspective.

EU's legislation relates the energy performance of a building to all energetic services: heating, cooling, ventilation, air conditioning, hot water production, lighting and vertical transport. As a consequence, EPBD refers to many other standards covering all building process and providing a complete NZEB design frame (**figure 1.2**).

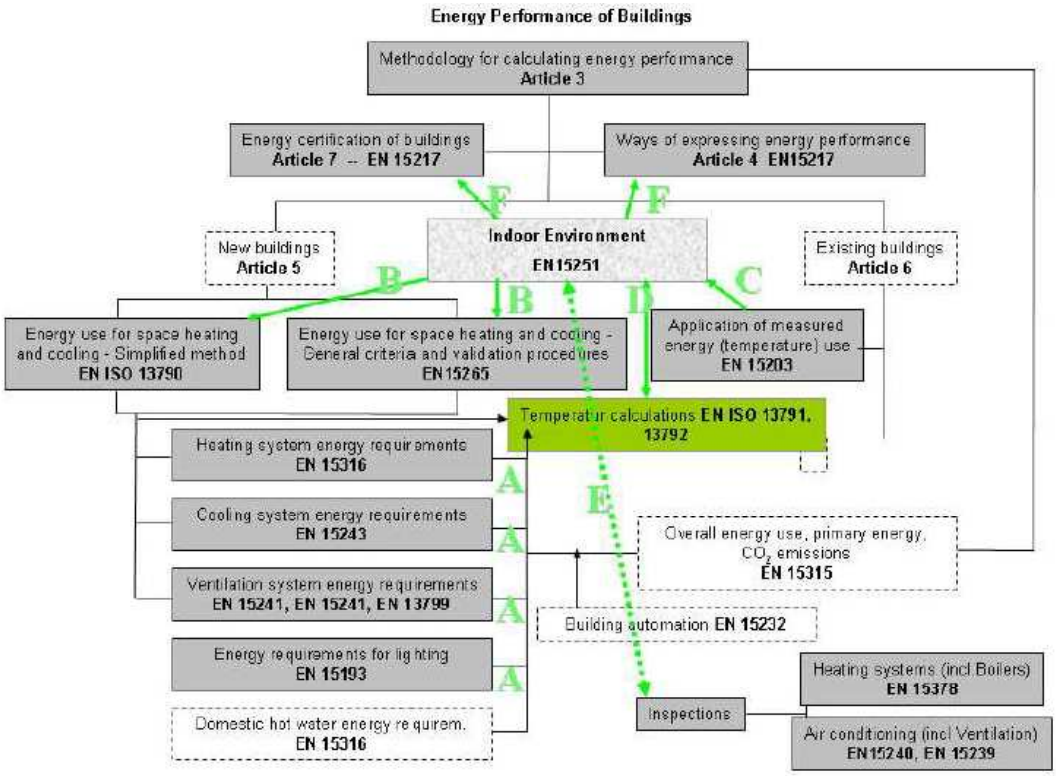


Figure 1.2
EPBD regulatory framework.

In **figure 1.2** some connections are highlighted:

A: indoor environmental criteria for the design of building and HVAC systems:

I. design indoor temperature in winter and summer are used as input for heating (EN 12831) and cooling load (EN 15243) calculations and sizing of the equipment;
II. ventilation rates are used for sizing ventilation systems;
III. lighting levels are incorporated in the design of lighting system (including the use of daylighting).

Output values are used to:

- provide suitable comfort indices;
- size building services;
- fulfil the requirements in the article 4 of EPBD (referring to possible negative effect of indoor environment);
- recommendations on how to improve the energy efficiency of existing buildings (article 6) by limiting the heating (article 8) and cooling (article 9) needs.

B: input values (temperature, ventilation, lighting) to be used:

I. in the calculation of building energy demand, when the space is occupied, (EN ISO 13790, EN 15255, EN 15265);
II. for energy calculations as specified in article 3 of EPBD.

C e D: output values from environmental parameters measurement, to be used in the evaluation of the annual performance in existing buildings (EN 15203, temperature, indoor air quality, ventilation rates, EN ISO 13791, EN ISO 13792 room temperatures). It is necessary in order to display the climatic factors (indoor environment) in the energy performance certificate (article 6 and 7 of EPBD).

E: methods for measurement of the indoor environment and for treating measured data related to the inspection of HVAC systems (EN 15240, EN 15239, EN 15378).

F: method for categorization of indoor environment characteristics (EN 15217) to aggregate the relevant information and easily rank the energy performance in the form of appropriate certificates (article 7 of EPBD). Recommended input values are given for each of the different categories. A short description of the categories is shown in **table 1.1** below: categories are related to the closeness with which indoor conditions should be controlled in order to meet occupants' different expectations.

BUILDING CATEGORIZATION			
Category	**Explanation**	**Thermal state of the body as a whole**	
		PPD %[1]	**PMV[2]**
I	High level of expectation and is recommended for spaces occupied by very sensitive and fragile persons with special requirements like handicapped, sick, very young children and elderly persons.	<6	-0.2÷+0.2
II	Normal level of expectation and should be used for new buildings and renovations.	<10	-0.5÷+0.5
III	An acceptable, moderate level of expectation and may be used for existing buildings.	<15	-0.7÷+0.7
IV	Values outside the criteria for the above categories. This category should only be accepted for a limited part of the year.	>15	<-0.7 OR >+0.2

1 Percentage of Dissatisfied People (comfort index)
2 Predicted Mean Vote (comfort index)
Note: In other standards like EN13779 and EN ISO 7730 categories are also used; but may be named different (A, B, C or 1, 2, 3 etc.)

Table 1.1
Building categorization.

In spite of this nested and strict legislative framework, and the deep increase of the energy efficiency (1.4% per year), data between 1990 and 2012 outline:

- +14% energy consumption for European residential buildings;
- +60% electricity use because of the widespread of electronic appliances and devices.

And as we look towards the future, cooling demands appear to be the greater threat. In 2014, Ciscar et al. **[1.24]**, investigated, by means of simulation, the evolution of buildings expected heating and cooling energy demand in Europe over the period 2010–2050, applying four different climatic scenarios (plus two scenarios without climate change named noC-A1B and noC-E1 in **figure 1.3**).
Their findings outline an average decrement of heating energy needs between 9% and 17%, outweighed by an average increase of cooling energy needs between 40% and 70% depending on the considered scenario.

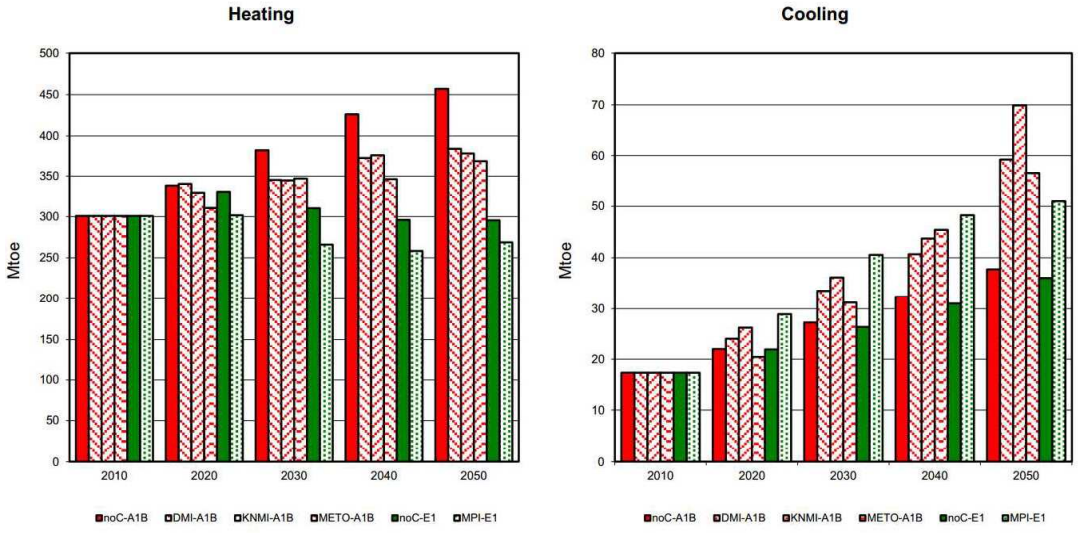


Figure 1.3
EU27 heating and cooling demands in residential and services sector per scenario.

1.3 – SMART SYSTEMS FOR ENERGY EFFICIENCY AND COMFORT

The frontier of NZEB is not just a matter of renewables and advanced design. It can be fully achieved only by mastering the complexity of building thermo-physics and its interlacements with bordering scientific fields.

The goal is to strike a stable balance in building energy flows, tipping between capacity and necessity and appealing to all players: building fabric, user behaviour and lifestyle, technical systems, outdoor climate, local environmental and human resources, Internet of things, …
Apparently, the number of parameters at stake is increasing more and more, thus boosting the need for more precise calculation methods, simulation tools and validation techniques.
Recently, the world of building and electronic engineering has deeply explored the technical issues related to IEQ (Indoor Environment Quality) by developing algorithms, control logics, measurement devices and smart systems **[1.25-1.29].**
Starting from the conventional comfort model, pioneered by Fanger in 1970 **[1.30]** diverse practical solutions and theoretical methodologies have been released over the same substrate to accomplish the hard task of translating comfort into a scientific shape without losing the shades of subjectivity.
Furthermore, several buildings typologies have been studied to point out specific requirements and vulnerabilities due to envelope characteristics, geographic features, climatic conditions, occupancy patterns and user's lifestyle.
Interrelations between pivotal parameters have been outlined in order to infer equations and indices useful to regulate losses and gains and to categorize building performances.
Control logics are gaining comprehensiveness and efficacy thanks to the establishment of new approaches and to the renovation of already known schemes like PID, fuzzy, neural networks, learning, predictive, genetic algorithms and powerful combinations like adaptive neuro-fuzzy inferential systems.
Nowadays home automation paradigms and, in a broader horizon, the challenges of the Internet of Things aim at striking synergies between user and living environment (indoor and outdoor) based on mutual communication and interoperability.
The ultimate ambition is to impart to the buildings kind of chameleon-like skills, so that it could turn into a self-adaptive system that fully masters its resources.
The main uncertainties still linger in the crossover between objective and subjective spheres, since:

- universal comfort solutions do not exist: consequently, IEQ systems design entails customized services and techniques, to be identified and contextualized from time to time. Standards, guidelines and best practices have been framed in the latest decades, yet providing just a track for applicable models **[1.31].** Moreover, such models have to be conceived in a flexible and dynamic way so that continuous adjustments to cater to users' needs can be performed. However, sensing, learning, acting/interacting, communicating represent the basic functions under any circumstances.

- no weighting system to ponder the contributions of each sensory sphere in the overall comfort feeling has been standardized **[1.31]**: such a prioritization would be rewarding to set the order of intervention when competing process have to be optimized. In literature **[1.25,1.32-1.38]**, various efforts have been sunk to hierarchize the key parameters and quantify their role through proper multiplying factors in comfort equations (thermo-hygrometric, acoustic, visive, IAQ, electromagnetic, …) but the approach was basically intuitive and non-rigorous. It should be stressed here that the introduction of a priority scale is a necessary compromise to solve race conditions, but it actually penalizes the optimization of the overall level of satisfaction, since comfort is a Boolean target by its very nature, thus it can either subsist or not. The weighting question assumes a different significance when comfort issues have to be harmonized with other concerns (energy, safety, security ...): multi-purpose, optimized allocation of resources might help in the transversal management of the entire building system. The most promising solutions, in this sense, come from learning algorithms and direct involvement of the users in the initiation phase.
- No detailed specs about measurement techniques, instruments, space-time configurations are actually validated: even though such information is fully supplied by Standards **[1.39]** the application for comfort assessment and building categorization was frequently found to be misleading **[1.40]**. Some of the main issues behind the incorrect handling of environmental conditions are rooted right in the uncertainties and equivocations related to the setup of the sensor network (distribution, accuracy, acquisition rate, …) **[1.31]**. The risk is sourcing the wrong datasets to the control/assessing systems, thus leading to the elaboration of counterproductive measures. Here, a possible solution might come from redundant sensing assemblies.

All the afore mentioned critical points and open issues have been addressed in the experimental activities presented in the following chapters of this thesis.
In the next sub-paragraph an overview of the world of smart systems and commercial solutions, serving the building sector is provided, in order to contextualize some of the choices and the strategies here applied.

1.3.1 Smart control of buildings: an overview

Cutting edge solutions to manipulate building thermo-physics and guarantee liveability, wellness and health are currently based on passive techniques and

technologies, thus relying on eco-design and bio-materials to achieve the maximum reduction of energy consumption and carbon footprint **[1.41, 1.42, 1.43].**
For instance, in the field of bio-climatic architecture, buildings are located and shaped to get the most from local resources to be utilized for heating, cooling and natural ventilation.
Yet, because of high construction costs and other cons, such configurations are usually coupled with active control systems much easier to be handled by the occupants: bang-bang chrono-thermostats, optimal and predictive PID controllers, …
The afore mentioned solutions provide a separated management of environmental parameters, acting on specific aspects of comfort: temperature, relative humidity, ventilation rate…
More complex and sophisticated systems tackle industrial environments (where the risks of a deficient control are crucial), followed by commercial and tertiary buildings (where the risks of a grossly control may threaten the quality of the service) and finally residential ones (where the risks of a poor environmental control affect the standard of living of the inhabitants).
The market of smart systems, serving buildings controls and air-conditioning, is currently dominated by some widespread typologies, which are described below.

1.3.2 Optimal, predictive, adaptive control systems

In the last century, consistent boost was given to the field of optimal **[1.44,1.45]** and predictive control **[1.46]** even though no immediate effect on industrial market was actually recorded **[1.47].**
Such controllers rely on building modelling. Predictive features are imparted through embedded forecasting modules for states, activities and system perturbations.
An example is given by the predictive controller elaborated by Freire et al. **[1.48]**: it collects information from temperature and humidity probes, located indoors and outdoors, to pilot the actuators in charge of preserving thermal-hygrometric comfort inside dwellings.
Adaptive controllers **(figure 1.4)** boast properties of auto-adjustment and adaptation to cope with boundary conditions changes, regardless of the type of building: the most common frameworks are fuzzy logics and parametric estimation techniques (i.e. recursive-least-square).
However, some inconveniences undermine the market uptake for such control systems: the principal ones are the non-linearity, the absence of a user-friendly configuration and the need for building model plus real time parametric estimation.

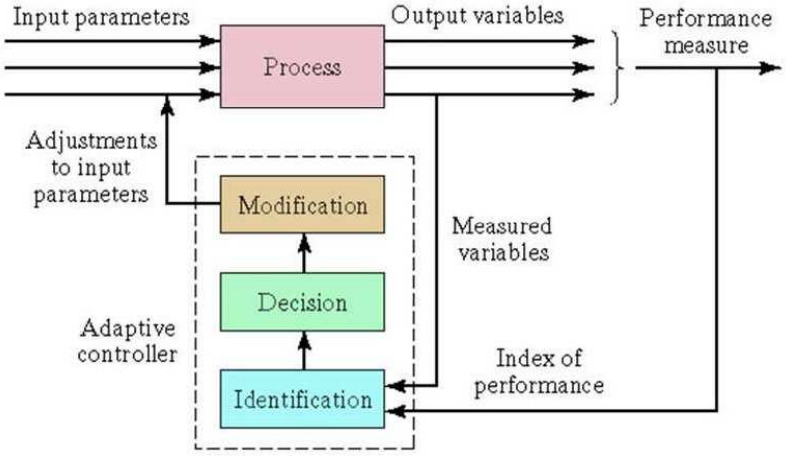


Figure 1.4
Adaptive controller basic scheme.

1.3.3 Computational Intelligence

Computational intelligence applications in the building sector root their earliest appearance in the 90s **[1.47]** in the shape of artificial intelligence techniques, neural networks, fuzzy frameworks and evolutionary algorithms.
The use of BIEMS (Building Intelligent Energy Management Systems) based on fuzzy logics (better if empowered by genetic algorithms **[1.49]**) as well as the application of neural networks to pilot the HVAC (Heating Ventilation and Air Conditioning) systems were found to outperform classic control logics in the optimization of energy efficiency and ergonomics.
Most of the limits exhibited by optimal, predictive and adaptive controllers were overtaken by avoiding the need for modelling and by privileging the role of the user in the definition of the comfort zone.
Further improvement was achieved when fuzzy and neural networks were coupled, since they combine the fuzzy inference process (which is close to human thinking and easier to deal with chaotic or complex non-linear systems) with a back-propagation algorithm based on collection of input/output data **[1.50].** Indeed, when a fuzzy controller becomes part of the hidden layer of a neural network (**figure 1.5**), both the methods get empowered: fuzzy logics are able to demystify extremely articulated phenomena, but rely on experience-based, intuitive configuration; neural network drive the optimal setup of the fuzzy controller, loop by loop, on the basis of past experiences, boundary conditions changes and learning abilities. This is the reason why Adaptive Neuro-Fuzzy Inference Systems (ANFIS) can be used as alternative, cost-

effective and computationally-cheap methods for modelling and predicting the performance of complex energy systems **[1.51]**, like:

- ground-coupled heat pump systems **[1.52,1.53]**,
- thermal energy storage **[1.54]**,
- refrigeration systems **[1.55,1.56],**
- photovoltaic systems **[1.57,1.58],**
- controls in HVAC systems and power generation **[1.59-1.61],**
- fault detection and diagnosis **[1.62,1.63],**
- building energy needs estimation **[1.64],**
- heat exchangers performance modelling **[1.65,1.66].**

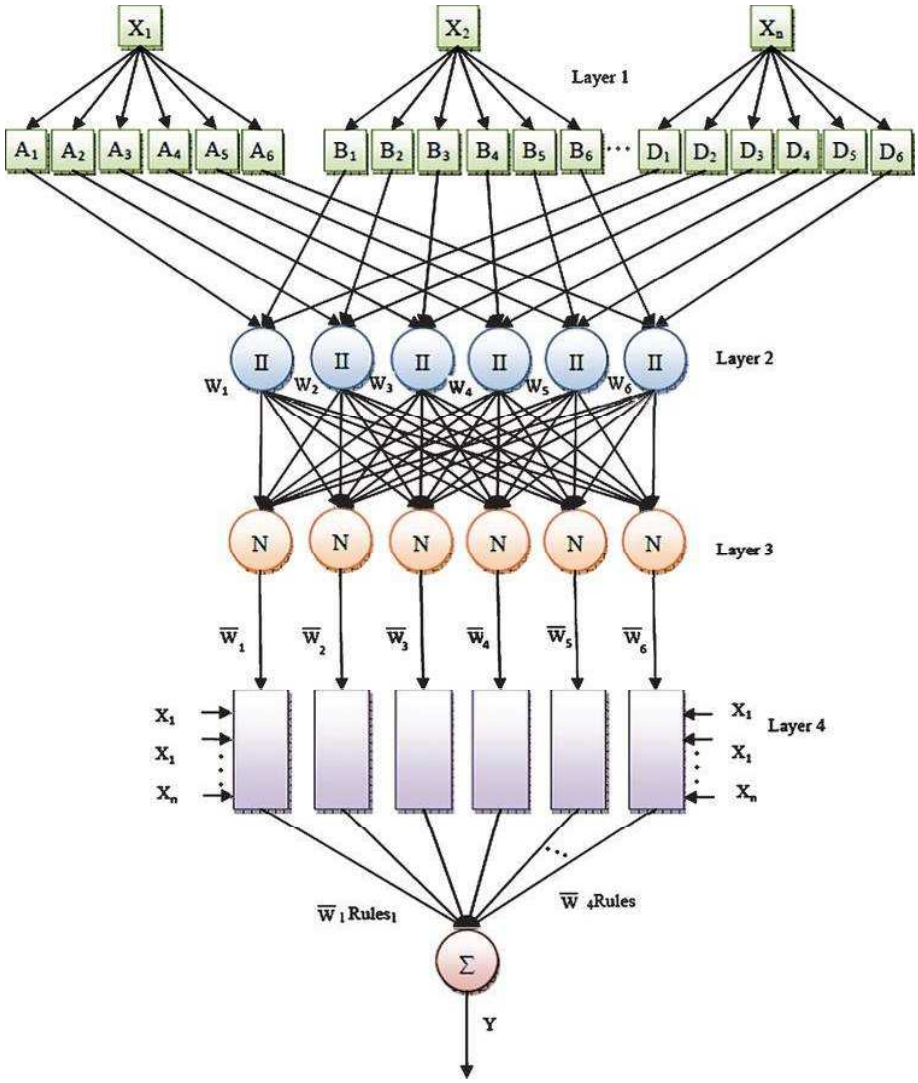


Figure 1.5
Fuzzy logic integration into a neural network structure.

Other promising combinations are fuzzy P closed-loop **[1.67,1.68]**, fuzzy PID, illuminance and adaptive, fuzzy PID controllers **[1.69].**
In the field of thermal control and hydronic heating systems, the NNCs (Neural Network Controllers) are gaining ground **[1.70,1.71]** since they attribute the synaptic weights of the neural network by chasing after the optimization of a cost function**.**

1.3.4 Multi-agent control systems

Multi-Agent Control Systems (MACS) **[1.47,1.72-1.75]** are networks of controllers which cooperate and act simultaneously to pursue a defined strategy (**figure 1.6**).
Each controller is in charge of accomplishing one or more specific task, which involves:

- the resolution of a sub-problem;
- the interaction with a sub-portion of the environment;
- the intercommunication with the other control nodes;
- the coordination of shared information to guarantee the achievement of the ultimate target.

Behaviour-based systems **[1.76,1.77]** (combined with artificial intelligence techniques), are examples of MACs, renowned for their ability to replace theoretical models with real models.

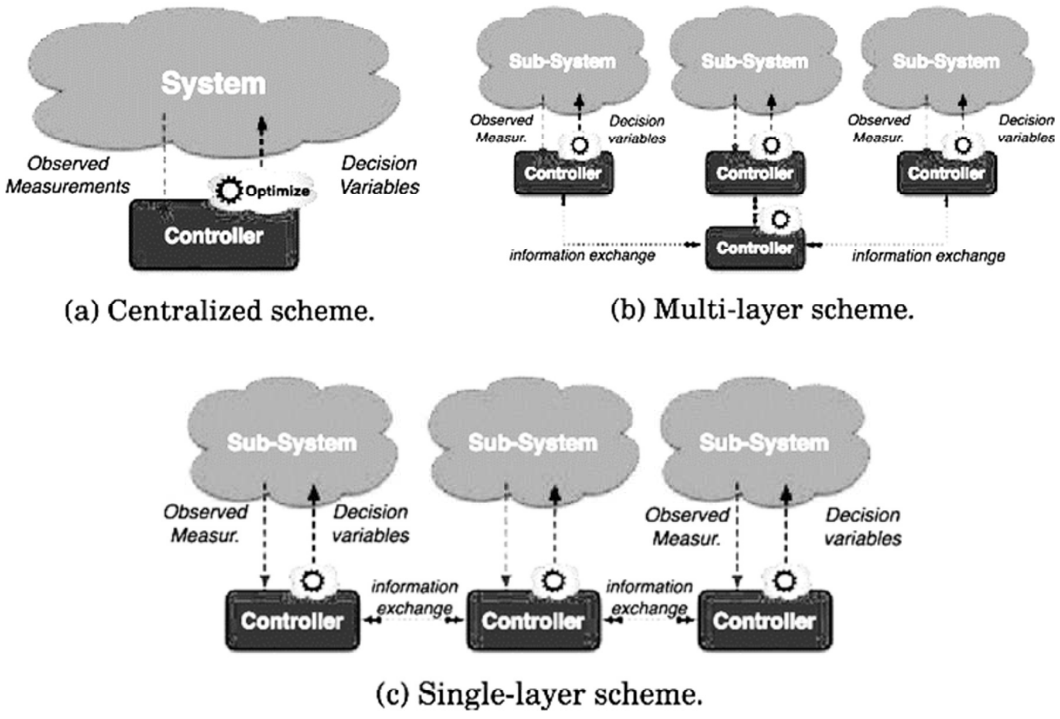


Figure 1.6
Single and multi-agent control structures for distributed systems.

1.3.5 Ambient Intelligence

R&D trends, in the field of ambient intelligence, and particularly of smart homes **[1.78-1.80]**, aim at designing and developing user-centred approaches to the domestic environment management, in order to turn the building fabric into a system serving its occupants, predicting/adapting to their necessities and automatically reacting through diverse, interoperable techniques and technologies.

Following the footprint of the adaptive comfort theories, such systems rely on the detection and the forecast of users' presence and activity. By mapping their lifestyle, a tailored decision making process is developed to manipulate the environment in a fully autonomous way (see, for instance MavHome projects **[1.81-1.83]** and Neural Network House **[1.84]**).

Table 1.2 [1.47] summarizes the various building control techniques, by linking each one to the problems they solved, the targets they achieved and the common applications (either experimental and commercial ones).

ENVIRONMENTAL CONTROL SYSTEMS						
Control System	**Thermal Comfort Control (PMV)**	**IAQ Control (CO_2)**	**Visual Comfort Control (lux)**	**Temperature Control**	**DCV Ventilation Control**	**Global Control Strategy**
On/Off	X	X	X	√	X	X
PID	X	X	X	√	√	X
Fuzzy P	√	√	√	X	√	√
Fuzzy PID	√	√	√	X	√	√
Adaptive fuzzy PD	√	√	√	X	√	√
Fuzzy PI	√	√	√	X	√	√
Adaptive fuzzy PI	√	√	√	X	√	√
Neural network	√	X	X	X	√	X
Agent-based	√	√	√	X	√	√
Predictive	√	X	X	X	√	√
Supervisory	√	√	√	X	√	√
Reinforcement learning	√	√	√	X	√	√
Ambient intelligent	√	√	√	X	√	√
Self adaptive	√	√	√	X	√	√
Optimal	X	X	X	√	√	X

Optimal and robust	X	√	X	X	√	X

Control System	Energy Consumption	Priority to Passive Techniques	User Preferences Learning	Learning	Tuning: fuzzy/GA/neural	Adaptation
On/Off	X	X	X	X	X	X
PID	√	X	X	X	X	X
Fuzzy P	√	√	X	X	X	X
Fuzzy PID	√	√	X	X	X	X
Adaptive fuzzy PD	√	√	X	X	X	√
Fuzzy PI	√	√	√	X	√	X
Adaptive fuzzy PI	√	X	X	X	√	X
Neural network	√	X	X	√	X	X
Agent-based	√	√	X	√	√	√
Predictive	√	√	√	√	√	X
Supervisory	√	√	√	√	√	X
Reinforcement learning	X	√	√	√	X	X
Ambient intelligent	√	X	√	√	X	X
Self adaptive	√	√	√	X	√	X
Optimal	√	√	X	X	X	√
Optimal and robust	√	X	√	X	X	X

Table1.2
Comparison amongst building controllers in terms of functions.

1.4 – MITIGATION TECHNOLOGIES FOR CLIMATE RESILIENCE

Climate change is the "inconvenient truth" of our century and is largely provoked by human activities. According to the Intergovernmental Panel on Climate Change (IPCC) **[1.85]**, global warming is the result of a series of anthropogenic pollutant agents **[1.86]**:

- carbon dioxide (CO_2), mainly coming from fossil fuels combustion processes (for heating and electricity production purposes);
- methane (CH_4), released in considerable amount by agriculture, livestock farming sectors and fossil fuels combustion;
- nitrogen monoxide (N_20), whose main source is the widespread of fertilisers in intensive agriculture.

In **figure 1.7 [1.87]** anthropogenic pollutants and other relevant agents and mechanisms are assessed in spatial scale (geographical extent) and in terms of average, net and range of radiative forcing (RF). RF is a measure of the altering power of a phenomenon on the balance of incoming and outgoing energy in the Earth atmosphere.

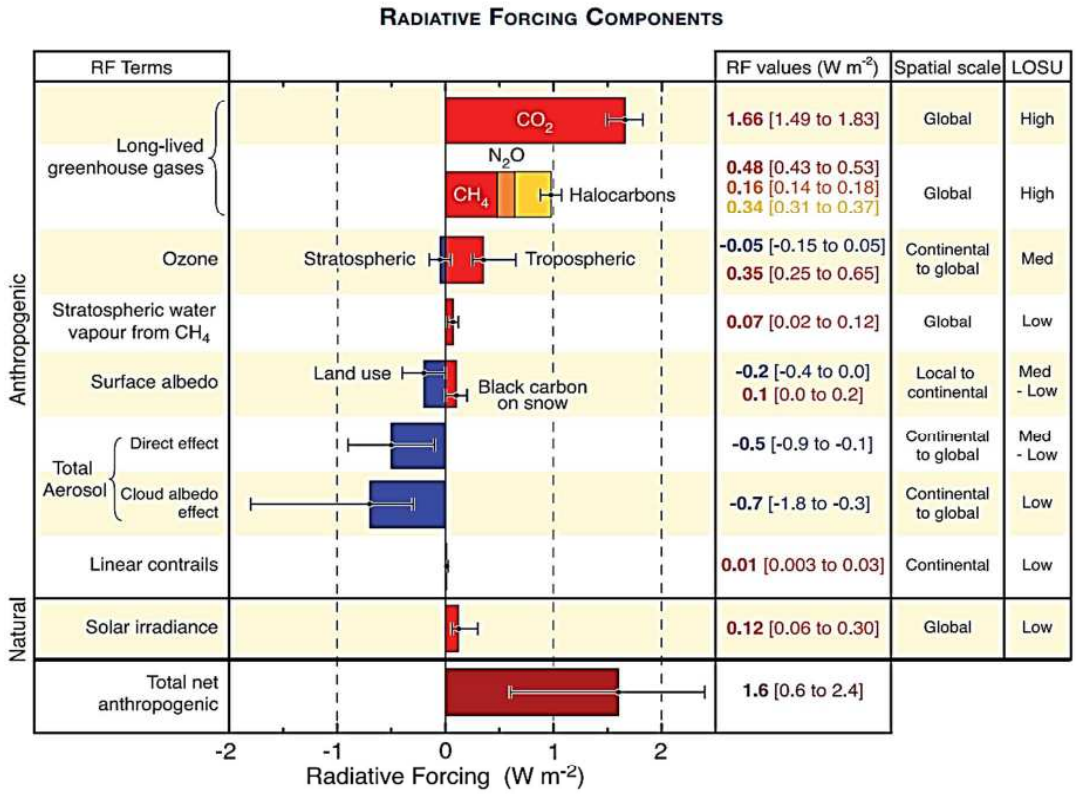


Figure 1.7
Radiative forcing of anthropogenic and natural factors (IPCC 2007: WG1-AR4).

Local climate change has a serious impact on the built environment, especially in terms of energy consumptions and liveability. Higher ambient temperatures and more frequent heat waves increase the energy demand and the peak electricity load for cooling purposes (extra calls and reduced HVAC systems efficiency), affect indoor and outdoor thermal comfort, raise tropospheric ozone and other harmful pollutants concentration, deteriorate human health (triggering morbidity and mortality **[1.88]**), increase the vulnerability of local populations and the ecological footprint of populated areas.

This situation is further aggravated in densely inhabited conurbations (and urban centres in general) where the 74% of the European population lives **[1.89],** experiencing extreme synoptic weather conditions**.** As a consequence, Urban Heat Island (UHI) has become one of the most documented phenomena of local climate change **[1.90].**

Yet, that is a vicious loop since buildings themselves strongly emphasize global and local climate change: the sole construction sector is responsible of about the 38% of the GHG (Greenhouse Gases) **[1.91].**

All things considered, climate change is one of the most daunting global challenges (**figure 1.8**) **[1.92,1.93]**, whose consequences on human wellness are likely to be tremendous and whose risks cannot be underestimated, yet rather counteracted and counter-balanced: indeed, the potential social, environmental, economic benefit of mitigation and adaptation policies is a paramount goal for every country all over the world**.**

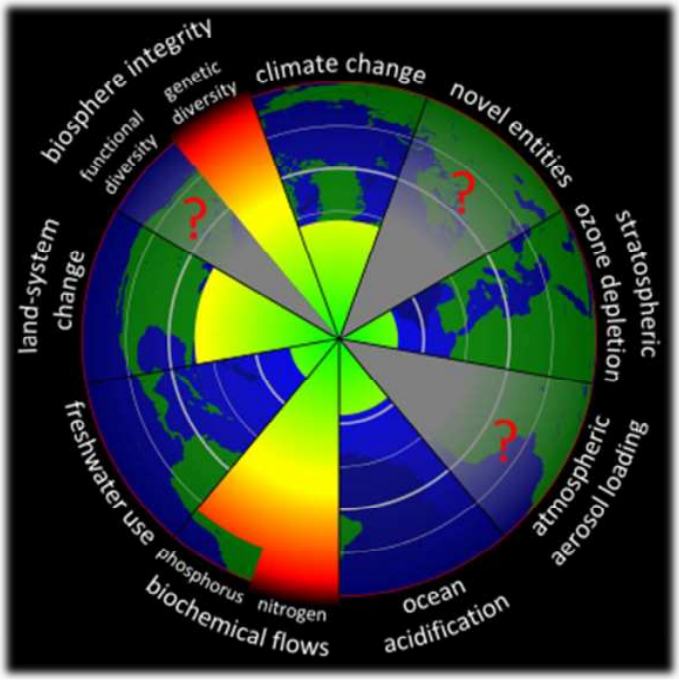


Figure 1.8
*Human activities planetary boundaries in terms of safety: activities still within safe margins (green areas), activities that may or may not have exceeded safe margins (yellow areas), activities that have exceeded safe margins (red areas) and activities for which safe margins have not yet been determined (*grey areas) ***[1.92,1.93]***.

Preventive alarms (warning people about incoming adverse weather conditions), health risks awareness raise, dedicated programs for vulnerable social sub-classes, wider spread of conditioning in public spaces and inside the buildings are some of the adaptive reactions European countries undertook after the 2003 heat wave.
Yet, adaptation is a necessary, but not sufficient condition to eradicate the inherent problem: for instance, the unconditional penetration of air conditioning systems inside the dwellings is a short term positive investment but is severely detrimental in the long term horizon since it increases energy consumptions, CO_2 emissions, local temperature rise, social non-uniformities **[1.94]** …
The ultimate solution would be mitigation, rather than adaptation: various techniques, technologies and strategies are currently available.
However, the urgency for bold decisions to reduce anthropic contribution still lingers: the key-words (**figure 1.9**), in this sense, are energy efficiency, renewables and resilience (timeless design, able to absorb changes and persist) **[1.96].**

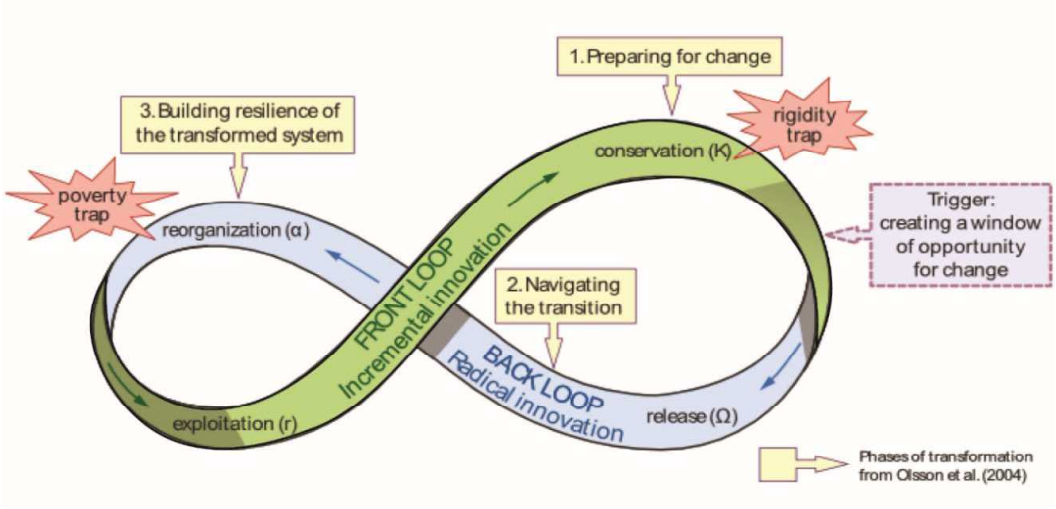


Figure 1.9
*Front and back loop of construction sector strategy to cope with climate change **[1.95]**.*

1.4.1 Magnitude and characteristics of climate change

Climate change involves a huge number of parameters which might change at different rates and spatial distributions.
IPCC Fourth Assessment Report: Climate Change 2007 (AR4) **[1.87]** released a series of assessments and sensible scenarios, which are recapped by the following figures and correspondent captions.
The detailed description of the scenarios is provided in **Appendix 1**: it is taken from the TAR **[1.97]** and has been subject to prior line-by-line approval by the Panel.

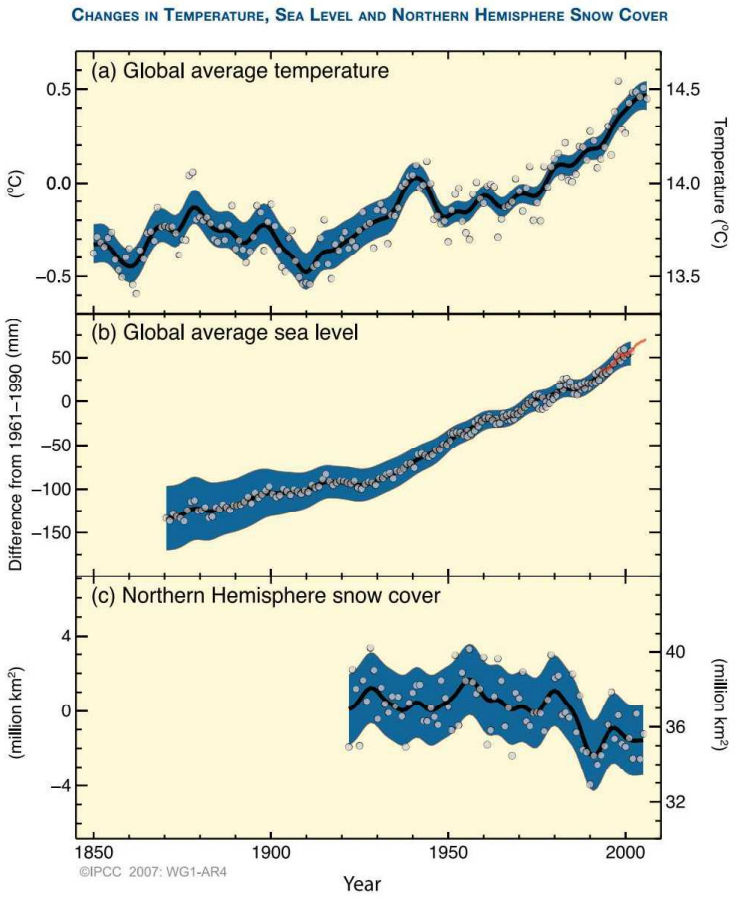


Figure 1.10
IPCC Fourth Assessment Report - FAQ 3.1, Figure 1, Figure 4.2, Figure 5.13 – surface temperatures, sea level and snow cover trends. Observed changes in (a) global average surface temperature, (b) global average sea level from tide gauge (blue) and satellite (red) data and (c) Northern Hemisphere snow cover for March-April. All changes are relative to corresponding averages for the period 1961–1990. Smoothed curves represent

decadal average values while circles show yearly values. The shaded areas are the uncertainty intervals estimated from a comprehensive analysis of known uncertainties (a and b) and from the time series (c).

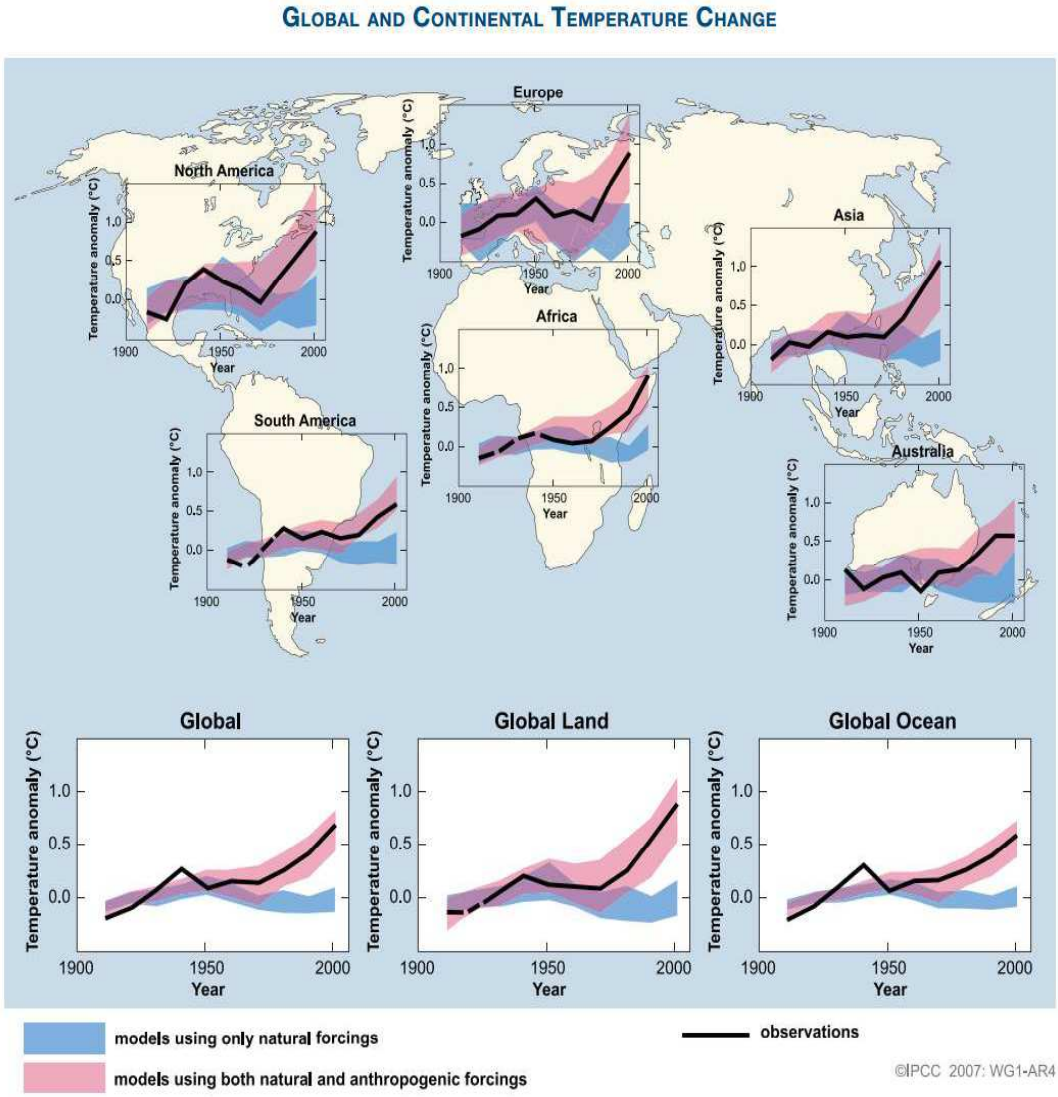


Figure 1.11

IPCC Fourth Assessment Report - FAQ 9.2, Figure 1– global and continental temperature change. Comparison of observed continental- and global-scale changes in surface temperature with results simulated by climate models using natural and anthropogenic forcings. Decadal averages of observations are shown for the period 1906 to 2005 (black line) plotted against the centre of the decade and relative to the corresponding average for 1901–1950. Lines are dashed where spatial coverage is less than 50%. Blue shaded bands show the 5–95% range for 19 simulations from five climate models using only the

natural forcings due to solar activity and volcanoes. Red shaded bands show the 5–95% range for 58 simulations from 14 climate models using both natural and anthropogenic forcings.

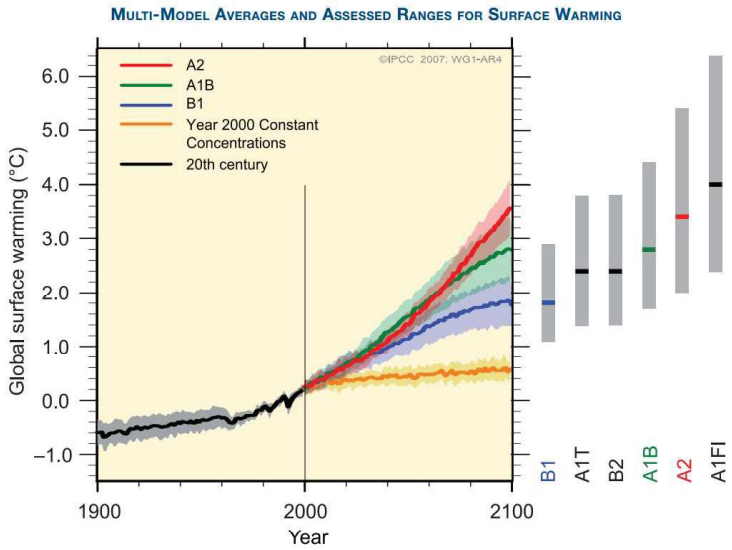


Figure 1.12

IPCC Fourth Assessment Report - Figures 10.4 and 10.29– global and continental temperature change. Solid lines are multi-model global averages of surface warming (relative to 1980–1999) for the scenarios A2, A1B and B1, shown as continuations of the 20th century simulations. Shading denotes the ±1 standard deviation range of individual model annual averages. The orange line is for the experiment where concentrations were held constant at year 2000 values. The grey bars at right indicate the best estimate (solid line within each bar) and the likely range assessed for the six SRES marker scenarios. The assessment of the best estimate and likely ranges in the grey bars includes the AOGCMs in the left part of the figure, as well as results from a hierarchy of independent models and observational constraints.

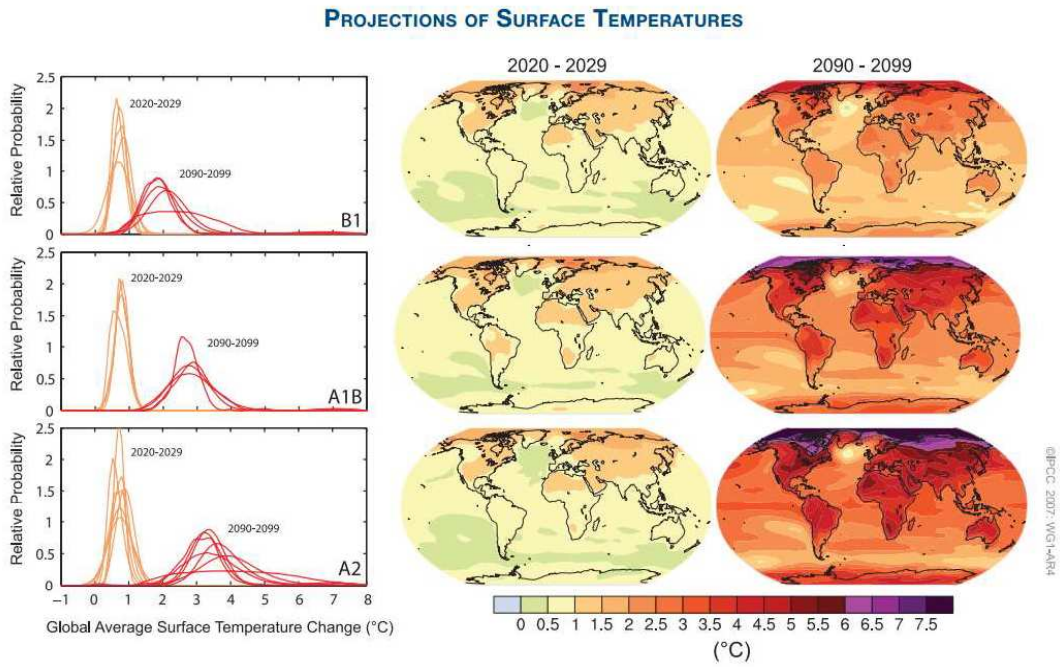


Figure 1.13

IPCC Fourth Assessment Report - Figures 10.8 and 10.28– global and continental temperature change. Projected surface temperature changes for the early and late 21st century relative to the period 1980–1999. The central and right panels show the AOGCM multi-model average projections for the B1 (top), A1B (middle) and A2 (bottom) SRES scenarios averaged over the decades 2020–2029 (centre) and 2090–2099 (right). The left panels show corresponding uncertainties as the relative probabilities of estimated global average warming from several different AOGCM and Earth System Model of Intermediate Complexity studies for the same periods. Some studies present results only for a subset of the SRES scenarios, or for various model versions. Therefore, the difference in the number of curves shown in the left-hand panels is due only to differences in the availability of results.

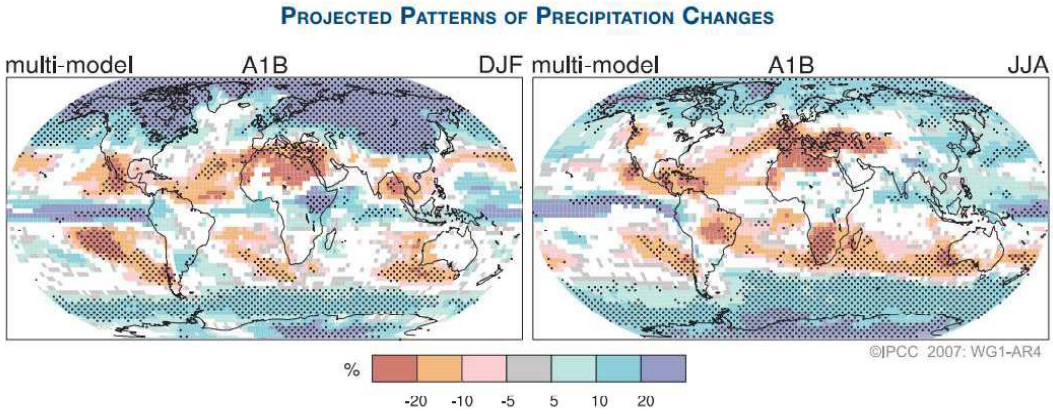


Figure 1.14
IPCC Fourth Assessment Report - Figures 10.9– global and continental temperature change. Relative changes in precipitation (in percent) for the period 2090–2099, relative to 1980–1999. Values are multi-model averages based on the SRES A1B scenario for December to February (left) and June to August (right). White areas are where less than 66% of the models agree in the sign of the change and stippled areas are where more than 90% of the models agree in the sign of the change.

1.4.2 International framework of commitment

The need to preserve planetary balance and face climate change was globally addressed the first time in 1972, during the plenary session of United Nations Conference on Human Environment (Stockholm, 1972).
This philosophy led to the creation of the UNEP (United Nations Environmental Programme), whose aim was to coordinate and enhance eco-initiatives all over United Nations.
In 1988 UNEP and World Meteorological Organization (WMO) combined their efforts by creating the IPCC (Intergovernmental Panel on Climate Change), an inter-governmental institution, gathering the major experts about climatic changes.
Its first report (1990) dealt with the hypothetic aftermaths of GHG emissions from human activities on the modification of world's climate.
The subsequent milestone is represented by 1992's United Nations Framework Convention on Climate Change (UNFCCC), which took place in Rio de Janeiro with the presence of the major heads of State. It kick-started a series of Cops (Conferences of the parties) about environmental issues in each of the acceding Countries.
Five years later, during Cop3, the globally renowned Kyoto Protocol was signed off by more than 160 Countries, to join forces and counteract global warming. It turned into executive shape on the 16th of February 2005: the target was set to -8% of GHG

emissions (1990 levels as benchmark) per each Member State to be accomplished within the period 2008-2012.
Then, during Cop13 (2007) in Bali (Indonesia), an action plan was ratified in order to enhance Kyoto's obligations and include emerging economies (China, India, Brazil), to set some boundaries to their industrial development and impose some constraints to their emissions. It should have become executive during Cop15 (Copenhagen, 2009).
The meeting didn't end up as forecasted: a mere political agreement was established without any practical constraint or tangible target. The only achievement was enclosed in the following statement: "the increase in global temperature should be below 2 degrees Celsius, on the basis of equity and in the context of sustainable development".
2011-2012 Cops extended the global agreement on CO2 reduction to 2020, thus delaying the achievement of the final goal.
A real step forward came with the creation of the Green Climate Fund, which granted contributions to stimulate and sustain measures of adaption and mitigation of climate change in developing countries. EU is the major founder: 14,5 billion euros were already provided in 2014 out of a total of 91 billion euros to be released by 2020.
From the 30th of November to the 11th of December 2015, Cop21 took place in Paris: an historic agreement was stricken by 196 Countries (actually almost all the International community) to kick-start bold and massive strategies to stem the tide of global mean temperature increase far below the 2°C threshold, previously defined.
The Paris Agreement entered officially into force on the 4th of November 2016.
Progress of work was checked during the Cop22 in Marrakech: a broad involvement of local firms, multinational corporations third sector, city councils was established.
The 2017 UN Climate Change Conference will take place from the 6th to the 17th of November 2017 at the World Conference Centre in Bonn, Germany. The focus will be on NDCs (Nationally Determined Contributions), long-term strategies, adaptation, inspiration for action, undertakings in adaptation planning, capacity-building, climate finance, mitigation… **[1.98]**.

1.4.3 Building scale

Nowadays, it is universally acknowledged in the world of building construction that the nature of climatic events is unlikely to remain the same during the lifetime of a building.
Therefore, one of the main challenges engineers and architects are facing today is to integrate in the design process, the need for resilient solutions which could cope with changes and avoid premature obsolescence.

Adaptation of buildings for climate change deals with the prediction and management of increased extreme or average temperatures and air pollution.
The crucial point is what level of adaptation is needed and which kind of preventive strategies should be applied as general recommendations and specific solutions.
From the comfort and energy perspective the main concern is about the rise of the average outdoor temperature which is expected to occur as a direct consequence of global warming. The goal is to provide solutions to prevent the risk of overheating and therefore deal with the simultaneously increasing demand of cooling (necessary to maintain the operative temperature within the comfort range).
Achieving this target is very complex and time consuming as significant uncertainties affect both input and output data. The first challenge is to properly depict future scenarios and take into account local peculiarities.
The second challenge is to safely predict the vulnerability of buildings and cities to climate change and to react properly in terms of new design concepts. Passive strategies are the most recommended **[1.41, 1.42, 1.43]**:

- Thermal mass to mitigate internal temperature variations.
- Insulation and/or low emissivity roofing paints and/or high performance glazing to reduce the rate of heat transfer through building structures.
- External shading of building surfaces exposed to direct sunlight (and strategic siting of deciduous vegetation).
- Cross ventilation and mixed-mode design to cool internal spaces.

1.4.4 Urban scale

When it comes to densely inhabited conurbations, Urban Heat Island (UHI) exacerbates the effects of local climate change. It refers to the thermal gap between ambient temperature within the urban fabric and the surrounding rural and suburban spaces.
The magnitude and peculiar characteristics of such positive urban thermal balance depends upon a suite of factors (both natural and anthropogenic) **[1.99]:**

- the morphological, structural and physical characteristics of cities;
- the type of materials used in the urban fabric
- the synoptic climatic conditions;
- the released anthropogenic heat in the city…

UHI is a well-documented phenomenon: data from hundreds of cities are currently available and the number is increasing **[1.90]**, yet, non-negligible inconsistencies and disaggregation about experimental protocols, theoretical analyses and assessment methodologies undermine the comparison among collected pieces of knowledge.

Despite data scattering, the impact of UHI on energy and comfort issues has been widely addressed. The main findings outline that:

- UHI exacerbates the effects of global warming, thus intensifying the need for cooling and the related energy consumption (**figure 1.15**). Various indices to quantify the penalty have been proposed and calculated for different cities (**figure 1.16**). However, the major drawback is recorded in terms of increased peak electricity demand, since it is usually covered by energy-consuming power plants and might drive to the installation of new facilities, thus stressing both consumers and energy networks (**figure 1.17**). It should be underlined that in case of heating-dominated climates, the situation might get reversed since the temperature rise is likely to be beneficial in terms of energy balance;
- UHI deteriorates outdoor thermal comfort: a glaring example was assessed by Papanastasiou et al. **[1.102]** during a heat wave episode in Athens: discomfort was recorded over the entire period with 50% of people under sever thermal stress and 13% under emergency medical conditions;
- UHI affects global environmental quality of cities: the ecological footprint may rise up to 1,5-2 times just to compensate the environmental impact **[1.103].** Strong increase of the concentration of tropospheric ozone and of other harmful pollutants is also documented, as a consequence of reduced convection phenomena within urban canyons.

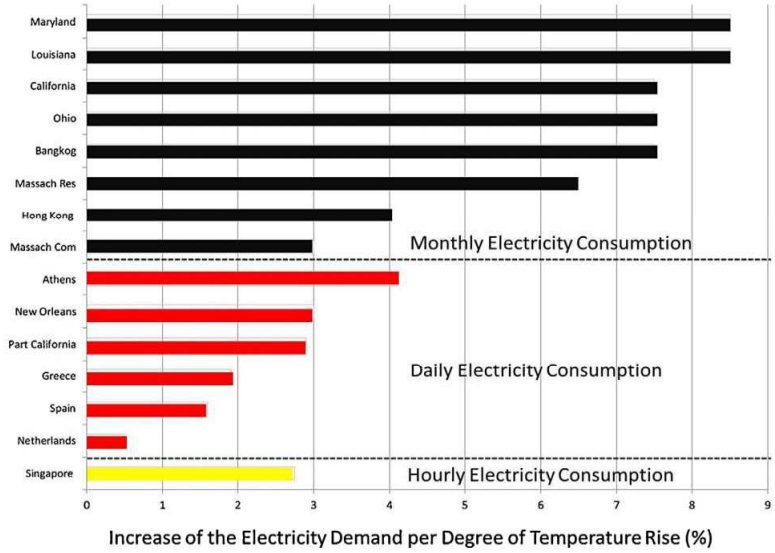


Figure 1.15
*Per cent electricity demand increase per degree of temperature rise: comparison among different countries. The potential increase ranges between 0.5% and 8.5% **[1.100]**.*

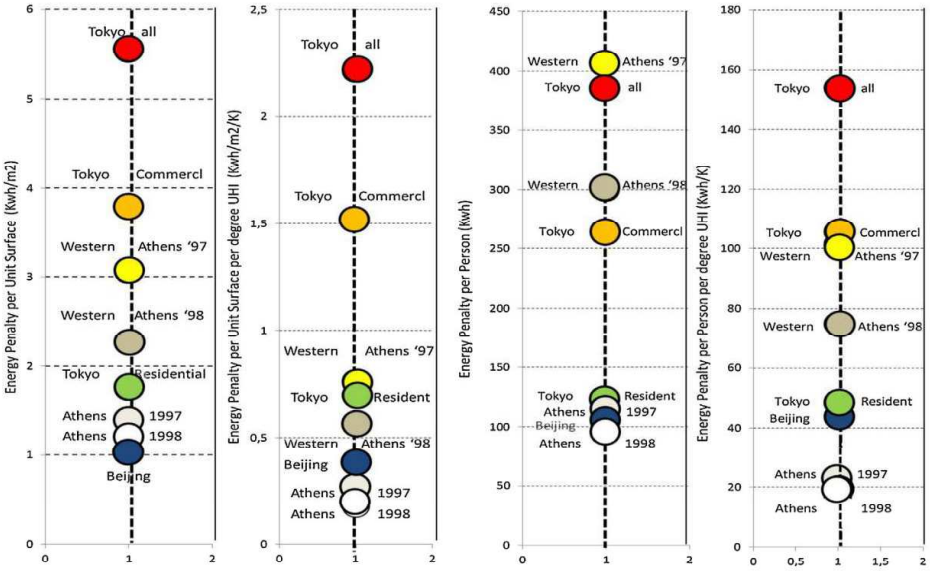


Figure 1.16
UHI energy penalty indices: comparing data from various cities ***[1.101]****.*

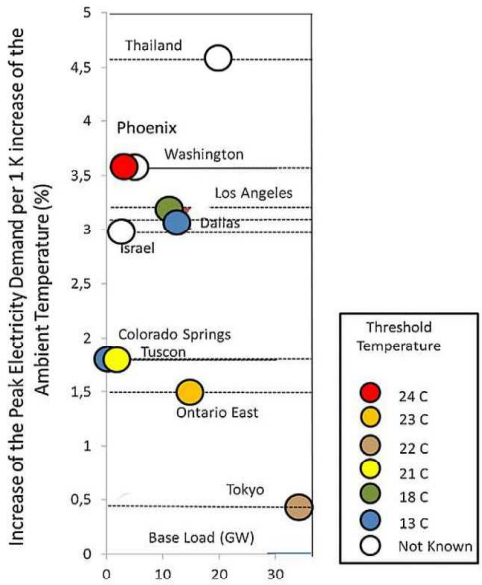


Figure 1.17
Per cent peak electricity demand increase per degree of temperature rise: comparison among different cities. The potential increase ranges between from 0.45% to 4.6%, which corresponds to a penalty of about 21 (±10.4) W per degree of temperature rise per person. ***[1.100]****.*

In order to reduce the impact of UHI, NZEB-oriented building-scale transition is a necessary **[1.104]** but not sufficient solution. Advanced urban adaptation and mitigation techniques and technologies (tailored to the specific features and sources of UHI) should be integrated to furtherly reduce urban temperatures **[1.105,1.106].**
Some of the most successful and widespread technologies are listed below:

- cool roofs and pavements: their high solar reflectance increase the albedo of urban fabric and reduce solar radiation absorption. As a result, urban surfaces stay cooler and release less heat into the ambient air;
- trees, greenery and green roofs: evapotranspiration absorbs the heat in the air, reduces local temperatures and substantially improve thermal comfort;
- street shading: they prevent solar beams from reaching the street level and heating up the surface (thereby reducing the radiant emission in the air);
- fountains, ponds and sprinklers: water bodies act as heat sinks and through evaporation process cool the surrounding ambient air.

UHI magnitude may be reduced up to 2.5°C when proper design and installation of the mitigation solution is applied **[1.106].**

APPENDIX 1 - Emission scenarios of the IPCC special report on emission scenarios (SRES) [1.97]

- A1. The A1 storyline and scenario family describes a future world of very rapid economic growth, global population that peaks in mid-century and declines thereafter, and the rapid introduction of new and more efficient technologies. Major underlying themes are convergence among regions, capacity building and increased cultural and social interactions, with a substantial reduction in regional differences in per capita income. The A1 scenario family develops into three groups that describe alternative directions of technological change in the energy system. The three A1 groups are distinguished by their technological emphasis: fossil-intensive (A1FI), non-fossil energy sources (A1T) or a balance across all sources (A1B) (where balanced is defined as not relying too heavily on one particular energy source, on the assumption that similar improvement rates apply to all energy supply and end use technologies). A2. The A2 storyline and scenario family describes a very heterogeneous world. The underlying theme is self-reliance and preservation of local identities. Fertility patterns across regions converge very slowly, which results in continuously increasing population. Economic development is primarily regionally oriented and per capita economic growth and technological change more fragmented and slower than other storylines.
- B1. The B1 storyline and scenario family describes a convergent world with the same global population, that peaks in mid-century and declines thereafter, as in the A1 storyline, but with rapid change in economic structures toward a service and information economy, with reductions in material intensity and the introduction of clean and resource-efficient technologies. The emphasis is on global solutions to economic, social and environmental sustainability, including improved equity, but without additional climate initiatives.
- B2. The B2 storyline and scenario family describes a world in which the emphasis is on local solutions to economic, social and environmental sustainability. It is a world with continuously increasing global population, at a rate lower than A2, intermediate levels of economic development, and less rapid and more diverse technological change than in the B1 and A1 storylines. While the scenario is also oriented towards environmental protection and social equity, it focuses on local and regional levels.
- An illustrative scenario was chosen for each of the six scenario groups A1B, A1FI, A1T, A2, B1 and B2. All should be considered equally sound.

The SRES scenarios do not include additional climate initiatives, which means that no scenarios are included that explicitly assume implementation of the United Nations Framework Convention on Climate Change or the emissions targets of the Kyoto Protocol.

REFERENCES

[1.1] Position of the European Parliament of 23 April 2009 (not yet published in the Official Journal), position of the Council at first reading of 14 April 2010 (not yet published in the Official Journal), position of the European Parliament of18 May 2010 (not yet published in the Official Journal).
[1.2] WBCSD, 2009
[1.3] European project iNSPiRe report, EURAC (European Academy of Bozen/Bolzano), 2015.
[1.4] IEA, 2013
[1.5] M. Santamouris, Innovating to zero the building sector in Europe: Minimising the energy consumption, eradication of the energy poverty and mitigating the local climate change, Solar Energy 128 (2016) 61–94
[1.6] Hultgren, 2011
[1.7] UNEP, 2012; BIMHow, 2015; IIASA, 2015
[1.8] UNEP, 2012
[1.9] S. Hassid, M. Santamouris, N. Papanikolaou, A. Linardi, N. Klitsikas, C. Georgakis,D.N. Assimakopoulos, Effect of the Athens heat island on air conditioning load, Energy and Buildings 32 (2) (2000) 131–141.
[1.10] M. Santamouris, N. Papanikolaou, I. Livada, I. Koronakis, C. Georgakis, A.Argiriou, D.N. Assimakopoulos, On the impact of urban climate on the energy consumption of building, Solar Energy 70 (3) (2001) 201–216.
[1.11] E. Stathopoulou, G. Mihalakakou, M. Santamouris, H.S. Bagiorgas, On the impact of temperature on tropospheric ozone concentration levels in urban environments, Journal of Earth System Science 117 (3) (2008) 227–236.
[1.12] K. Pantavou, G. Theoharatos, M. Santamouris, D. Asimakopoulos, Outdoor thermal sensation of pedestrians in a Mediterranean climate and a comparison with UTCI, Building and Environment 66 (2013) 82–95.
[1.13] K. Pantavou, G. Theoharatos, A. Mavrakis, M. Santamouris, Evaluating thermal comfort conditions and health responses during an extremely hot summer in Athens, Building and Environment 46 (2) (2011) 339–344.
[1.14] A. Sakka, M. Santamouris, I. Livada, F. Nicol, M. Wilson, On the thermal performance of low income housing during heat waves, Energy and Buildings 49(2012) 69–77.
[1.15] M. Santamouris, J.A. Paravantis, D. Founda, D. Kolokotsa, P. Michalakakou, A.M. Papadopoulos, N. Kontoulis, A. Tzavali, E.K. Stigka, Z. Ioannidis, A. Mehilli, A.Matthiessen, E. Servou, Financial crisis and energy consumption: a household survey in Greece, Energy and Buildings 65 (Oct. (0)) (2013) 477–487.

[1.16] M. Santamouris, K. Paraponiaris, G. Mihalakakou, Estimating the ecological footprint of the heat island effect over Athens, Greece, Climatic Change 4 (2007)265–276.
[1.17] European Commission Report, Directorate-General for Energy, 2015.
[1.18] Directive 2002/91/EC of the European Parliament and of the Council of 16 December 2002 on the energy performance of buildings (EPBD).
[1.19] Directive 2010/31/EU of the European Parliament and of the Council of 19 May 2010 on the energy performance of buildings (EPBD Recast).
[1.20] Directive 2012/27/EU of the European parliament and of the Council of 25October 2012 on energy efficiency (EED), amending Directives 2009/125/E Cand 2010/30/EU and repealing Directives 2004/8/EC and 2006/32/EC.
[1.21] Renewable Energy Directive, European Parliament and Council, L.140, 5 June 2009, pp. 16-62
[1.22] Directive 2009/125/EC of the European Parliament and of the Council of 21 October 2009 establishing a framework for the setting of ecodesign requirements for energy-related products
[1.23] Directive 2010/30/EU of the European Parliament and of the Council of 19 May 2010 on the indication by labelling and standard product information of the consumption of energy and other resources by energy-related products
[1.24] J. Ciscar, P. Dowling, Integrated assessment of climate impacts and adaptation in the energy sector, Energy Economics 46 (2014) 531–538.
[1.25] D,Heinzerling, S. Schiavon, T. Webster, E. Arens, Indoor environmental quality assessment models: A literature review and a proposed weighting and classification scheme, Building and Environment 70 (2013) 210e222
[1.26] Fisk WJ. Health and productivity gains from better indoor environments and their relationship with building energy efficiency. Annual Review of Energy and the Environment 2000; 25:537e66.
[1.27] Wargocki P, Seppänen O. Indoor climate and productivity in offices. REHVA Guidebook 2006.
[1.28] REHVA. Indoor climate quality assessment. Brussels: Federation of European Heating, Ventilation and Air-conditioning Associations; 2011.
[1.29] Lai CK, Mui KW, Wong LT, Law LY. An evaluation model for indoor environmental quality (IEQ) acceptance in residential buildings. Energy and Buildings 2009; 41:930e6.
[1.30] P.O. Fanger, Thermal Comfort, Danish Technical Press, Copenhagen, DK, 1970.
[1.31] F. R. d'Ambrosio Alfano, B.W. Olesen, B.I. Palella, G. Riccio, Thermal comfort: Design and assessment for energy saving, Energy and Buildings 81 (2014) 326–336.
[1.32] Frontczak M, Wargocki P. Literature survey on how different factors influence human comfort in indoor environments. Building and Environment 2011;46: 922e37.

[1.33] Marino C, Nucara A, Pietrafesa M. Proposal of comfort classification indexes suitable for both single environments and whole buildings. Building and Environment 2012; 57:58e67.
[1.34] Ncube M, Riffat S. Developing an indoor environment quality tool for assessment of mechanically ventilated office buildings in the UK e a preliminary study. Building and Environment 2012; 53:26e33.
[1.35] Cao B, Ouyang Q, Zhu Y, Huang L, Hu H, Deng G. Development of a multivariate regression model for overall satisfaction in public buildings based on field studies in Beijing and Shanghai. Building and Environment 2012; 47:394e9.
[1.36] Chiang CM, Lai CM. A study on the comprehensive indicator of indoor environment assessment for occupants' health in Taiwan. Building and Environment 2002; 37:387e92.
[1.37] Chiang CM, Chou PC, Lai CM, Li YY. A methodology to assess the indoor environment in care centres for senior citizens. Building and Environment 2001; 36:561e8.
[1.38] Wong LT, Mui KW, Hui PS. A multivariate-logistic model for acceptance of indoor environmental quality (IEQ) in offices. Building and Environment 2008; 43:1e6.
[1.39] ISO 7726, Ergonomics of the thermal environment – Instruments formeasuring physical quantities, 1998.
[1.40] F. R. d'Ambrosio Alfano, B.W. Olesen, B.I. Palella, G. Riccio, Thermal comfort: Design and assessment for energy saving, Energy and Buildings 81 (2014) 326–336.
[1.41] K. Huang, R. HwangFuture trends of residential building cooling energy and passive adaptation measures to counteract climate change: The case of Taiwan, Applied Energy, Volume 184, 15 December 2016, Pages 1230–1240
[1.42] A. Tripathi, A. K. Mishra knowledge and passive adaptation to climate change: An example from Indian farmers, Climate Risk Management, Available online 24 November 2016
[1.43] A. Tejero-González,, M. Andrés-Chicote, P. García-Ibáñez, E. Velasco-Gómez, F. J. Rey-Martínez, Assessing the applicability of passive cooling and heating techniques through climate factors: An overview, Renewable and Sustainable Energy Reviews, Volume 65, November 2016, Pages 727–742
[1.44] C. Bernard, B. Guerrier, M. Rasset-Louerant. Optimal building energy management. Part II: Control. ASME Journal of Solar Energy Engineering, 1982, p. 114:13.
[1.45] J. House, T. Smith. A system approach to optimal control for HVAC and building systems. HVAC&R Research, 14(1), 2008.
[1.46] P. Curtis, G. Shavit, J. Kreider. Neural Networks Applied to Buildings-A Tutorial and Case Studies in Prediction and Adaptive Control. ASHRAE Transactions part 2, 100(1), 1996.

[1.47] A. Dounis, C. Caraiscos. Advanced control systems engineering for energy and comfort management in a building environment. A review, Renewable and Sustainable Energy Reviews, 13, 2009, p. 1247-1261.
[1.48] R. Freire, G. Oliveira, N. Mendes. Predictive controllers for thermal comfort optimization and energy savings. Energy and Buildings, 40, 2008, p. 1353–1365.
[1.49] C. Altrock, H. Arend, B. Krause, C. Steffens, E. Behrens-Rommler. Adaptive fuzzy control applied to home heating system. Fuzzy Sets and Systems, 61(1), 1994, p. 29-35.
[1.50] W. Yaïci, E. Entchev, Adaptive Neuro-Fuzzy Inference System modelling for performance prediction of solar thermal energy system, Renewable Energy 86 (2016) 302e315
[1.51] B. Kosko, Neural Networks and Fuzzy Systems, A Dynamical Systems Approach, Prentice Hall, New Jersey, 1991.
[1.52] H. Esen, M. Inalli, A. Sengur, M. Esen, Modelling a ground-coupled heat pump system using adaptive neuro-fuzzy inference system, Int. J. Refrig. 31 (2007) 65e74.
[1.53] H. Esen, M. Inalli, ANN and ANFIS models for performance evaluation of a vertical ground source heat pump system, Expert Syst. Appl. 37 (2010) 8134e8147.
[1.54] K. Ermis, A. Erek, I. Dincer, Heat transfer analysis of phase change process in a finned-tube thermal energy storage system using artificial neural network, Int. J. Heat Mass Transf. 50 (2007) 3163e3175.
[1.55] H.M. Ertunca, M. Hosoz, Comparative analysis of an evaporative condenser using artificial neural network and adaptive neuro-fuzzy inference system, Int. J. Refrig. 31 (2008) 1426e1436.
[1.56] A.S. Sahin, Performance analysis of single-stage refrigeration system with internal heat exchanger using neural network and neuro-fuzzy, Renew. Energy 31 (2011) 2747e2752.
[1.57] A. Mellit, S.A. Kalogirou, ANFIS-based modeling for photovoltaic power supply system: a case study, Renew. Energy 36 (2011) 250e258.
[1.58] R.K. Kharb, S.L. Shimi, S. Chatterji, M.F. Ansari, Modelling of solar PV module and maximum point tracking using ANFIS, Renew. Sustain. Energy Rev. 33 (2014) 602e612.
[1.59] S. Soyguder, H. Alli, Predicting of fan speed for energy saving in HVAC system based on adaptive network based fuzzy inference system, Expert Syst. Appl. 36 (2009) 8631e8638.
[1.60] S. Soyguder, H. Alli, An expert system for the humidity and temperature control in HVAC systems using ANFIS and optimization with fuzzy modelling approach, Energy Build. 41 (2009) 814e822.
[1.61] S.R. Khuntia, S. Panda, Simulation study for automatic generation control of a multi-area power system by ANFIS approach, Appl. Soft Comput. 12 (2012) 333e341.

[1.62] K. Salahshoor, M. Kordestani, M.S. Khoshro, Fault detection and diagnosis of an industrial steam turbine using fusion of SVM (support vector machine) and ANFIS (adaptive neuro-fuzzy inference system) classifiers, Energy 35 (2010) 5472e5482.
[1.63] R.A. Saeed, A.N. Galybin, V. Popov, 3D fluid-structure modelling and vibration analysis for fault diagnosis of Francine turbine using ANN and ANFIS, Mech. Signal Process. 34 (2013) 259e276.
[1.64] B. Ekici, U.T. Aksoy, Prediction of building energy needs in early stage of design by using ANFIS, Expert Syst. Appl. 38 (2011) 5352e5358.
[1.65] T.H. Lee, J.Y. Yun, J.S. Lee, J.J. Park, K.S. Lee, Determination of airside heat transfer coefficient on wire-on tube type heat exchanger, Int. J. Heat Mass Transf. 44 (2001) 1767e1776.
[1.66] T.A. Tahseen, M. Ishak, M.M. Rahman, Performance predictions of laminar heat transfer and pressure drop in an in-line flat tube bundle using an adaptive neuro-fuzzy inference system (ANFIS) model, Int. Commun. Heat Mass Transf. 50 (2014) 85e97.
[1.67] A. Dounis, D. Manolakis. Design of a fuzzy system for living space thermal comfort regulation. Applied Energy, 69, 2001, p. 119–144.
[1.68] A. Dounis, M. Santamouris, C. Lefas, A. Argiriou. Design of a fuzzy set environment comfort system. Energy and Buildings, 22, 1994, p. 81–87.
[1.69] D. Kolokotsa. Design and implementation of an integrated intelligent building indoor environment management system using fuzzy logic, advanced decision support techniques, local operating network capabilities and smart card technology. PhD., Technical University of Crete, 2001.
[1.70] A. Kanarachos, K. Geramanis. Multivariable control of single zone hydronic heating systems with neural networks. Energy Conversion Management, 13(13), 1998, p. 1317–1336.
[1.71] J. Liang, R. Du. Thermal comfort control based on neural network for HVAC application. Proceedings of the control applications conference, 2005, p. 819–824.
[1.72] D. Cook. Multi-agent smart environments. Journal of Ambient Intelligence and Smart Environments, 1, 2009, p. 47-51.
[1.73] V. Lesser, M. Atighetchi, B. Benyo, B. Horling, A. Raja, R. Vincent, T. Wagner, P. Xuan, S. Zhang. A Multi-Agent System for Intelligent Environment Control. Umass Computer Science Technical Report 1998-40.
[1.74] B. Huberman, S. Clearwater. A Multi-Agent System for Controlling Building Environments. Proceedings from the First International Conference on MultiAgent Systems, 1995, p. 171-176.
[1.75] G. Evans, Solving Home Automation Problems using Artificial Intelligence Techniques. IEEE Transactions on Consumer Electronics, 37(3), 1991, p. 395-400.
[1.76] A. Breemen, T. Vries. Design and implementation of a room thermostat using an agent-based approach. Control Engineering Practice, 9(3), p. 233-248.

[1.77] H. Hagras, V. Callaghan, M. Colley, G. Clarke. A Hierarchical Fuzzy-Genetic Multi-Agent Architecture for Intelligent Buildings Online Learning, Architecture and Control. Information Sciences, 150, 2003, p. 33–57.
[1.78] D. Cook, J. Augusto, V. Jakkula. Ambient intelligence: Technologies, applications, and opportunities. Pervasive and Mobile Computing, 5, 2009, p. 277-298.
[1.79] J. Vidal. Fundamentals of multiagent systems with NetLogo examples. 2010. http://jmvidal.cse.sc.edu/papers/mas.pdf.
[1.80] D. Cook, S. Das. How smart are our environments? An updated look at the state of the art. Pervasive and Mobile Computing, 3, 2007, p. 53–73.
[1.81] D. Cook, M. Youngblood, E. Heierman, K. Gopalratnam, S. Rao, A. Litvin, F. Khawaja. MavHome: An Agent-Based Smart Home. Proceedings of the First IEEE International Conference on Pervasive Computing and Communications (PerCom), 2003, p. 521-524.
[1.82] D. Cook, M. Huber, K. Gopalratnam, M. Youngblood. Learning to Control a Smart Home Environment. Innovative Applications of Artificial Intelligence, 2003
[1.83] S. Das, D. Cook, A. Bhattacharya, E. Heierman, T. Lin. The Role of Prediction Algorithms in the MavHome Smart Home Architecture. IEEE Wireless Communications, 9(6), 2002, p. 77-84.
[1.84] M. Mozer. The Neural Network House: An Environment that Adapts to its Inhabitants. Proceedings of the American Association for Artificial Intelligence Spring Symposium on Intelligent Environments, 1998, p. 110-114.
[1.85] IPCC Climate Change 2007. http://www.ipcc.ch
[1.86] P. Michelozzi, M. De Sario, Climate changes: health effects and mitigation interventions Epidemiol Prev 2009; 33 (6): 195-198
[1.87] IPCC Fourth Assessment Report: Climate Change 2007 (AR4)
[1.88] WHO, The world health report 2007 - A safer future: global public health security in the 21st century
[1.89] The World Bank Annual Report 2015
[1.90] M. Santamouris, Innovating to zero the building sector in Europe: Minimising the energy consumption, eradication of the energy poverty and mitigating the local climate change, Solar Energy, Volume 128, April 2016, Pages 61–94
[1.91] UNEP 2012 Annual Report
[1.92] Rockström et al., 2009. Nature, 461, 472-475
[1.93] Steffen, W.; Richardson, K.; Rockström, J.; Cornell, S. E.; Fetzer, I.; Bennett, E. M.; Biggs, R.; Carpenter, S. R.; de Vries, W.; de Wit, C. A.; Folke, C.; Gerten, D.; Heinke, J.; Mace, G. M.; Persson, L. M.; Ramanathan, V.; Reyers, B.; Sorlin, S. (2015). "Planetary boundaries: Guiding human development on a changing planet". Science. 347 (6223): 1259855

[1.94] Ayres JG, Forsberg B, Annesi-Maesano I et al, on behalf of the Environment and health committee of the European Respiratory Society. Climate change and respiratory disease: European Respiratory Society position statement. Eur Respir J 2009; 34: 295-302.
[1.95] L. Olsson, A. Jerneck, H. Thoren, J. Persson, D. O'Byrne Why resilience is unappealing to social science: Theoretical and empirical investigations of the scientific use of resilience, *Science Advances* 22 May 2015:Vol. 1, no. 4, e1400217 DOI: 10.1126/sciadv.1400217
[1.96] Biggs et al., 2010. Navigating the back loop: fostering social innovation and transformation in ecosystem management. Ecology and Society, 15, 9
[1.97] IPCC Third Assessment Report, 2001
[1.98] United Nations Framework Convention on Climate Change COP 23/CMP 13/CMA 1.2: Information for Participants
[1.99] K. Gobakis, D. Kolokotsa, A. Synnefa, M. Saliari, K. Giannopoulou, M. Santamouris, Development of a model for urban heat island prediction using neural network techniques, Sustainable Cities and Society 1 (2011) 104–115
[1.100] M. Santamouris, C. Cartalis, A. Synnefa, D. Kolokotsa, On the impact of urban heat island and global warming on the power demand and electricity consumption of buildings - A review, Energy and Buildings 98 (2015) 119–124
[1.101] M. Santamouris, On the energy impact of urban heat island and global warming on buildings, Energy and Buildings 82 (2014) 100–113
[1.102] D.K. Papanastasiou, D. Melas, H.D. Kambezidis, Heat waves characteristics and their relation to air quality in Athens, Global Nest Journal 16(5):919-928 · December 2014
[1.103] M. Santamouris, K. Paraponiaris, G. Mihalakakou, Estimating the ecological footprint of the heat island effect over Athens, Greece. Climate Change. 2007, Vol. 80, pp. 265-276.
[1.104] M. Hekkenberg, R.M.J. Benders, H.C. Moll, A.J.M. Schoot Uiterkamp, Indications for a changing electricity demand pattern: the temperature dependence of electricity demand in the Netherlands, Energy Policy 37 (2009) 1542–1551.
[1.105] M. Santamouris, Cooling the cities—a review of reflective and green roof mitigation technologies to fight heat island and improve comfort in urban environments, Solar Energy 103 (2014) 682–703.
[1.106] M. Santamouris, A. Synnefa, T. Karlessi, Using advanced cool materials in the urban built environment to mitigate heat islands and improve thermal comfort conditions, Solar Energy 85 (12) (2011) 3085–3102.
[1.107] M. Santamouris,D. Kolokotsa, Urban Climate Mitigation Techniques, Routledge, 2016.

2

Smart control of electric radiators

Comparing the performance of on/off, PID and fuzzy controllers applied to the heating system of an energy-efficient building[1]

[1] Published in Energy and Buildings, Volume 116, 15 March 2016, Pages 1-17

2.1 – ABSTRACT

This research activity aimed at investigating and comparing the energetic and ergonomic performance of three different control logics (on–off, PID, fuzzy), used to regulate the emission of the heating system of an energy-efficient building.
Tests were carried out on an experimental building, equipped with three electric radiators and a sensor network mapping internal, external and surface thermal conditions.
The building–technical system ensemble was evaluated in real time for a monitoring period of five/six days of non-occupancy, winter/midseason weather and Mediterranean climate.
All controllers were assessed with regard to thermal comfort and energy consumption in order to return an exhaustive scenario of possible strengths and weaknesses.
The comparison showed that fuzzy logic, properly configured, outperformed both PID and on/off controllers reducing energy consumption of 30–70% and maintaining thermal dissatisfaction between comfort limits for all the monitoring period.

2.2 – INTRODUCTION

EU's legislation relates the energy performance of a building to all energetic services: heating, cooling, ventilating, air conditioning, hot water production, lighting and load handling.
As a consequence, EPBD refers to many other standards covering all building process and providing a complete NZEB design frame.
Since the present research focuses on the role of regulation systems in heating energy demand, the Standard to refer to is EN 15316– 2008 **[2.1]**. It standardizes inputs and outputs that are necessary to apply a common methodology to calculate energy demand and energy performance related to heating and DHW systems.
In particular, EN 15316-2.1 **[2.2]** concerns energetic approach to heat emission terminals.
The emission system supplies (by convection and/or radiation) the thermal power necessary to maintain the ambient temperature at a specified set-point.
Most common emission systems are radiators, radiant panels and aeraulic diffusers.
In the calculation of the energy demand of an emission system, the above-mentioned Standard takes into account the effects of a non-ideal control: physical properties of the heating systems and of the controller itself, imprecise positioning of the sensors…
The main consequences are temperature non-uniformities and drifts around set-point, leading to additional losses through the building envelope.

Nowadays, building thermal control is generally performed by room thermostats or thermostatic valves on radiators **[2.3–2.5]** driven by on–off, and in the best cases, PID logics to ensure desired indoor temperature and, at the same time, minimize overheating phenomena.
In spite of their diffusion, these controllers are not conceived for optimal performance in heating applications either in terms of energy saving or in terms of internal comfort. Besides, no detailed information is given about the way they react to weather conditions, occupancy patterns and building inertia **[2.6].**
The aim of this research activity was to provide on-site validated data, collected during field experimental tests on three different control logics, in order to identify the real energy potential of their use, the response to different combination of indoor-outdoor climate conditions and the effects on perceived internal comfort.

2.3 – MATERIALS AND METHODS

Optimizing heating controller can be translated into taking maximum advantage of the weather and the building thermal inertia so as to ensure comfort conditions with minimal energy expenditure.
In order to investigate the dynamics of these correlations, different operational steps were required:

1. preliminary definition of control logics to be tested: on/off, PID and fuzzy ones;
2. programming a software for input acquisition and output actuation in order to enable automatic management of the control algorithms;
3. setting PID parameters through trial-and-error tuning procedure of proportional gain, integral time and derivative time in order to customize the control system to the specific application and heating terminal;
4. setting up the sensor network in an experimental building in order to analyse outside and inside climate conditions during heating period as well as envelope and/or technical systems performance;
5. detailed on-site monitoring (10-day measurements for each control system), in order to collect local, real-time data;
6. analytical and graphical assessment of regulation performance in terms of energy savings and comfort levels for each controller typology;
7. definition of assessment criteria and calculation of normalized parameters allowing significant comparison between the control logics.

In this study, no occupancy pattern was tested (included typical residential intermittent one) since no one inhabited the experimental building during the monitoring period. As a consequence, the set point temperature was fixed at a constant value of 20°C, as suggested by Italian legislation in winter season **[2.7].**

In order to investigate how the regulation system interacted with the heating emission, the building characteristics and the climate conditions, it was necessary to develop a sensing, controlling and acting frame.
The determination of an evaluating method comparing meaningful indices was therefore required.

2.4 – CASE STUDY

The experimental building is a hyper-insulated mock-up in Italy, exposed to a typical Mediterranean climate (**figure 2.1**).
It consists of a single room, rectangular in plan and perfectly oriented according to cardinal points. General information is resumed in **table 2.1**.



Figure 2.1
Experimental mock-up in Agugliano (Ancona, Italy)

AGUGLIANO MOCK-UP: GENERALITIES	
	Location
Address	Borgo Ruffini Agugliano (AN) ITALY
Latitude	43.54°
Longitude	13.37°
Elevation [a.s.l.]	137
Climatic Zone	D
	Geometrical characteristics
Gross area [mxm]	3.23x5.23
Net area [m^2]	12.20
Indoor volume [m^3]	36.18
Casing surface [m^2]	67.60
	Physical characteristics
Surface/Volume Ratio [m^2/m^3]	0.33
Thermal transmittance [W/m^2*K]	0.974
Surface mass [kg/m^2]	60

Table 2.1
Experimental building general data.

Design is compliant with national **[2.8]** and town-council legislation **[2.9]**; walls composition (**table 2.2** and **figure 2.2**) follows the International Standard ISO 13786 **[2.10]**.

1. As a mock-up, it respects the typical features of test-rooms:
    - minimal load-bearing structure;
    - external plugging to reduce thermal bridges;
    - dry construction technique facilitating structural assembling and modifying (enabling rapid test changing);
    - no internal partitions to avoid local non-uniform thermal conditions;
    - above-ground planking level in order to inhibit heat exchanges with the soil and capillary rise phenomena;
    - minimal and south-exposed fenestration to limit ventilation per cent weight on global heat loss.
2. As a reduced-scale NZEB, it integrates high thermal insulation performance with high HVAC efficiency. The first requirement is achieved through adequate walls composition and thermal bridges treatment, while the second requirement is assigned to the heating regulation system.

In particular, the load-bearing structure is hyper-isolated x-lam (thickness 12 cm).
The only opening, interrupting the continuity of walls, is the entry door, on the north side of the building.

In order to minimize air permeability, the door is double-shuttered, obtained coupling an internal and an external door and filling the gap with a high density insulating material.
The double-pitched roof is in larch, while the floor decking is all-fir. All the wooden surfaces are treated with water-repellent paint.
Interstitial gaps are filled with PU foam and insulating tape, applied both on the outside and on the inside. All the x-lam structure is externally coated with a high-density insulating layer (thickness 1 cm).
Building external finishing is traditional plasterboard. Internal finishing is in plasterboard panels (thickness 1.25 cm), except for half the surface of the south-exposed wall which is covered with a clay microencapsulated PCM (phase change material) panel (thickness 1.6 cm).
The recommended number of air changes (obtained by blower door test and application of UNI EN 13829 **[2.11]**) is 7.9 per hour.

MOCK-UP WALLS COMPOSITION

FLOORING

Material	**Specific heat Cp [J/kgK]**	**Density ρ [kg/m³]**	**Weight [kg/m²]**	**Thermal conductivity λ [W/mK]**	**Thickness [mm]**	**Thermal resistance R [m²K/W]**	**Thermal transmittance U (W/m²K)**
mineralized fir wood wool bound with grey Portland cement	1810	400	16	0.07	40	0.6	
Insulating over CLS	1000	150	-	0.01	10	0.76	
EPS (polystyrene)	1500	20	-	0.04	120	3.33	
Vapour barrier	1500	425	0.07	0.17	0.18	0.00	
Wood	1660	550	-	0.12	34	0.28	
Air space	-	-	-	0.20	40	0.205	
Tot.					244.18	5.18	0.193

ROOFING FLOOR

Material	**Specific heat Cp [J/kgK]**	**Density ρ [kg/m³]**	**Weight [kg/m²]**	**Thermal conductivity λ [W/mK]**	**Thickness [mm]**	**Thermal resistance R [m²K/W]**	**Thermal transmittance U (W/m²K)**
EPS (polystyrene)	1500	20	-	0.04	120	3.33	
Vapour barrier	1800	940	188	0.4	0.2	0.00	
Sheath slated	1470	1200	4	0.17	7	0.04	

coupled with 40 mm XPS	1200	30	3.5	0.33	40	1.2	
Wood	1000	580	-	0.17	25	0.15	
Tot.					192.20	4.72	0.212

WALLS

Material	**Specific heat Cp [J/kgK]**	**Density ρ [kg/m³]**	**Weight [kg/m²]**	**Thermal conductivity λ [W/mK]**	**Thickness [mm]**	**Thermal resistance R [m²K/W]**	**Thermal transmittance U (W/m²K)**
Vapour barrier	1500	425	0.07	0.17	0.18	0.00	
Internal plasterboard	837	760	15	0.2	125	0.63	
PCM panel	Ca. 1300	1000	13.5	0.47	16	0.03	
x-lam	2700	500	-	0.14	120	0.86	
Rock wall (external coating)	1030	90	-	0.036	100	2.75	
Rock wall (internal coating)	1030	70	-	0.035	50	1.4	
XPS (60 cm from foundation mat)	1200	30	-	0.038	100	2.85	
adhesive/levelling grey powder for insulating panels	1000	1150	-	0.48	10	0.02	
Cement mortar	-	-	-	-	10	-	
Tot.					531.18	5.69	0.176

Table 2.2

Walls composition: materials, thicknesses, thermal transmittances.

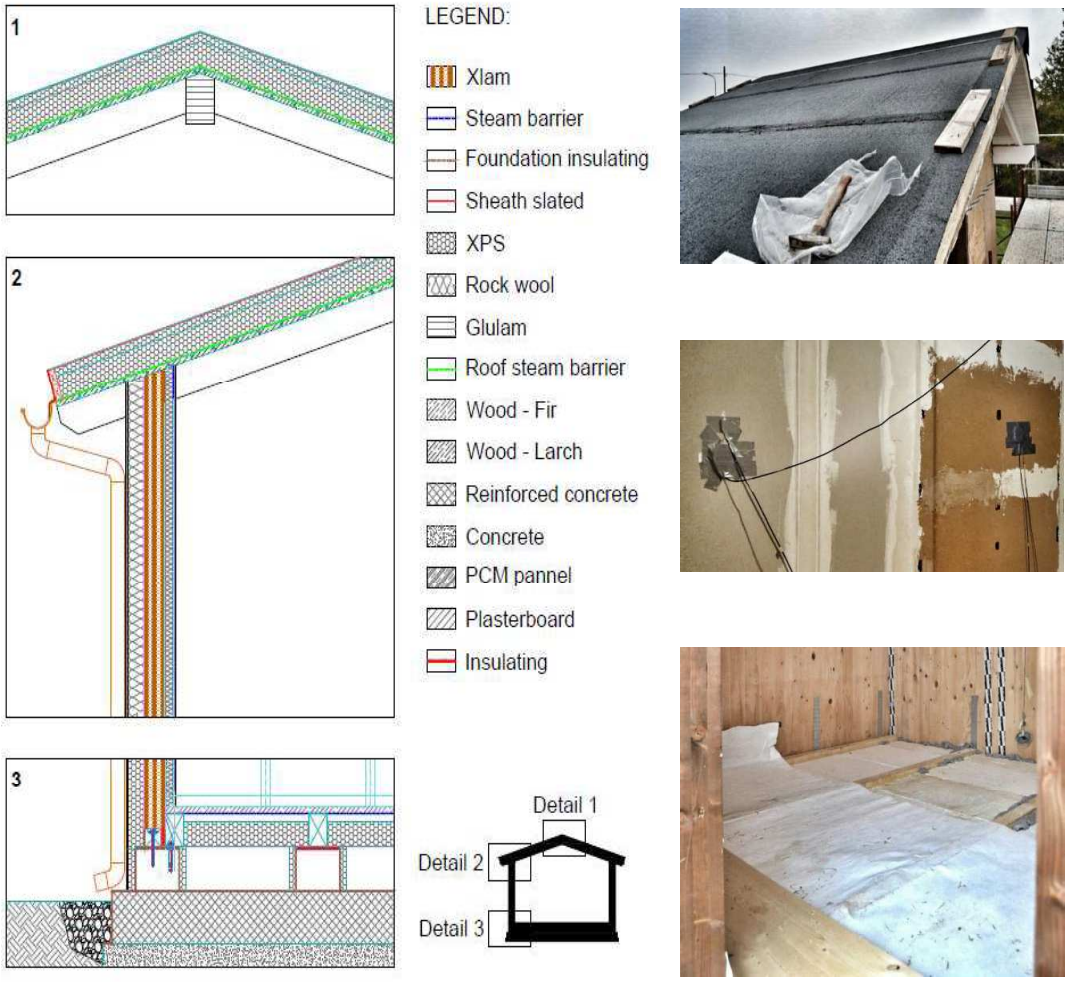


Figure 2.2
CAD detail of materials composing mock-up's walls: shots taken during the construction on the right.

2.5 – SENSOR NETWORK

Experimental setup was conceptualized in order to:

- provide exhaustive description of indoor/outdoor climate conditions;
- record the building response to different boundary conditions;
- collect all data necessary to:
  1. quantify the performance of tested regulatory systems;
  2. identify possible connections between energy consumption profiles and building thermal behaviour.

As a consequence, the settlement of different monitoring stations was necessary:

1. outdoor monitoring station, including air temperature, relative humidity, global solar radiation and wind speed sensors. Data collection allowed the reconstruction of boundary conditions;
2. indoor monitoring station, composed by dry-bulb air temperature, relative humidity, air velocity and mean radiant temperature probes. Data collection allowed the description of internal global comfort. In addition to environmental measurement, consumption rate was determined too, inserting a power metre in the feeding line to the electric radiators;
3. interface monitoring station, consisting of surface temperature and thermal flux probes installed on different walls or on different sides of the same wall. Data collection allowed the characterization of the building envelope in terms of thermal transmittance, permeability, capacity and lag.

Sensors composing the network were compliant to UNI EN ISO 7726:1998 **[2.12]** and its last review **[2.13]** requirements and were suitable for accurately measuring thermal comfort parameters according to ISO 7730:2006 **[2.14].** The output signal is analogic for all the listed probes.
Measuring instruments and multi-acquisition systems technical data are summarized respectively in **table 2.3** and **table 2.4**, while **table 2.5** provides radiators data sheet (technical specs are the same for all the three terminals installed).
Figure 2.3 shows the probes distribution in plant and vertical views.

SENSOR NETWORK							
INDOOR MONITORING STATION							
Measure	**Sensor type**	**Production house**	**Acquisition system**	**Rating**	**Position**	**Range**	**Accuracy**
Air Temp.**	Platinum resistor	Tersid	Datataker	5 min.	H 0.10 mt	-40°C ÷ +80°C	0.05 °C
Air Temp.	Platinum resistor	Tersid	Datataker	5 min.	H 1.10 mt	-40°C ÷ +80°C	0.05 °C
Air Temp.	Platinum resistor	Tersid	Datataker	5 min.	H 2.00 mt	-40°C ÷ +80°C	0.05 °C
Air Temp.	Platinum resistor	Tersid	NI 9219	20 sec.	H 1.30 mt	-40°C ÷ +80°C	0.05 °C
Average radiant temp.	Globe thermometer	LSI LASTEM	Babuc 1530	5 min.	Babuc Station	-40°C ÷ +80°C	0.15 °C
Relative Humidity	Thermo hygro meter	LSI LASTEM	Babuc 1530	5 min.	Babuc Station	0 ÷ 100%	±1.5%
INTERFACE MONITORING STATION							

Measure	Sensor type	Production house	Acquisition system	Rating	Position	Range	Accuracy
Thermal flow	Thermo-flow meter	Hukseflux	Datataker	5 min.	South wall - indoor	-2000 to +2000 W/m^2	+5/ -5 %
Surface temp.	Thermistor	Tersid	Datataker	5 min.	PCM -south-wall - indoor	-40°C ÷ +80°C	0.05 °C
Surface temp.	Thermistor	Tersid	Datataker	5 min.	floor - indoor	-40°C ÷ +80°C	0.05 °C
Surface temp.	Thermistor	Tersid	Datataker	5 min.	Plasterboard - south wall - indoor	-40°C ÷ +80°C	0.05 °C
Surface temp.	Thermistor	Tersid	Babuc 1530	5 min.	PCM - south wall – inner surface	-40°C ÷ +80°C	0.05 °C
Surface temp.	Thermistor	Tersid	Babuc 1530	5 min.	Ceiling - indoor	-40°C ÷ +80°C	0.05 °C
Surface temp.	Thermistor	Tersid	Babuc 1750	5 min.	Plasterboard - south wall - outdoor	-40°C ÷ +80°C	0.05 °C
Surface temp.	Thermistor	Tersid	Babuc 1750	5 min.	North wall - outdoor	-40°C ÷ +80°C	0.05 °C
Surface temp.	Thermistor	Tersid	Babuc 1750	5 min.	PCM - south wall – outdoor	-40°C ÷ +80°C	0.05 °C
Surface temp.	Thermistor	Tersid	Babuc 1750	5 min.	North wall - indoor	-40°C ÷ +80°C	0.05 °C
Thermal flow	Thermo-flow meter	Hukseflux	Babuc 1750	5 min.	North wall - indoor	-2000 to +2000 W/m2	+5/ -5 %
Surface temp.	Thermistor	Tersid	Babuc 1750	5 min.	North wall – inner surface	-40°C ÷ +80°C	0.05 °C

OUTDOOR MONITORING STATION

Measure	Sensor type	Production house	Acquisition system	Rating	Position	Range	Accuracy
Air Temp.	thermo hygrometer	LSI LASTEM	Datataker	5 min.	weather station	-30 ÷ 70 °C	0.20°C
Relative Humidity	thermo hygrometer	LSI LASTEM	Datataker	5 min.	weather station	0 ÷ 100 %	±1.5%

Wind direction	Anemometer	Eurelettronica icas	Datataker	5 min.	weather station	0 – 270 °	± 2° (± 4° if wind speed ≥ 5 m/s)
Wind velocity	Anemometer	Eurelettronica icas	Datataker	5 min.	weather station	0 – 75 m/s	0.1 m/s (± 2%)
Solar radiation	Radiometer	LSI LASTEM	Datataker	5 min.	weather station	0 - 2000	< 5%

Note 1 *Ch=channel number. Note 2 ** temp=temperature.

Table 2.3
Probes specs and location.

DATALOGGERS					
Model	**Production house**	**Analogic Channels**	**Digital Channels**	**Acquisition rating**	**PC Connection**
Babuc A (1530)	LSI Lastem	11		5 minutes	RS232 - Usb
Babuc A (1750)	LSI Lastem	11		5 minutes	RS232 - Usb
DT85M Series 3	DataTaker	16	8	5 minutes	Usb
NI Usb 6008	National Instruments	4		1 minute	Usb
NI 9219	National Instruments	12		1 minute	Usb

Table 2.4
Acquisition systems specs.

ELECTRIC RADIATORS				
Model	**Production house**	**Type**	**Heat exchange type**	**Power [W]**
PR 15044	Thermal Technology	Electric wall radiator	Radiation	330
Supply [V]	Weight [kg]	Dimensions [cm]	Electronic control unit and safety systems	Heated surface $[\frac{mq\ (surface)}{mc\ (air)}]$
230	8.5	150 x 44	NI USB 6008 – Static Relay	$\frac{11}{30}$

Table 2.5
Heating system specs.

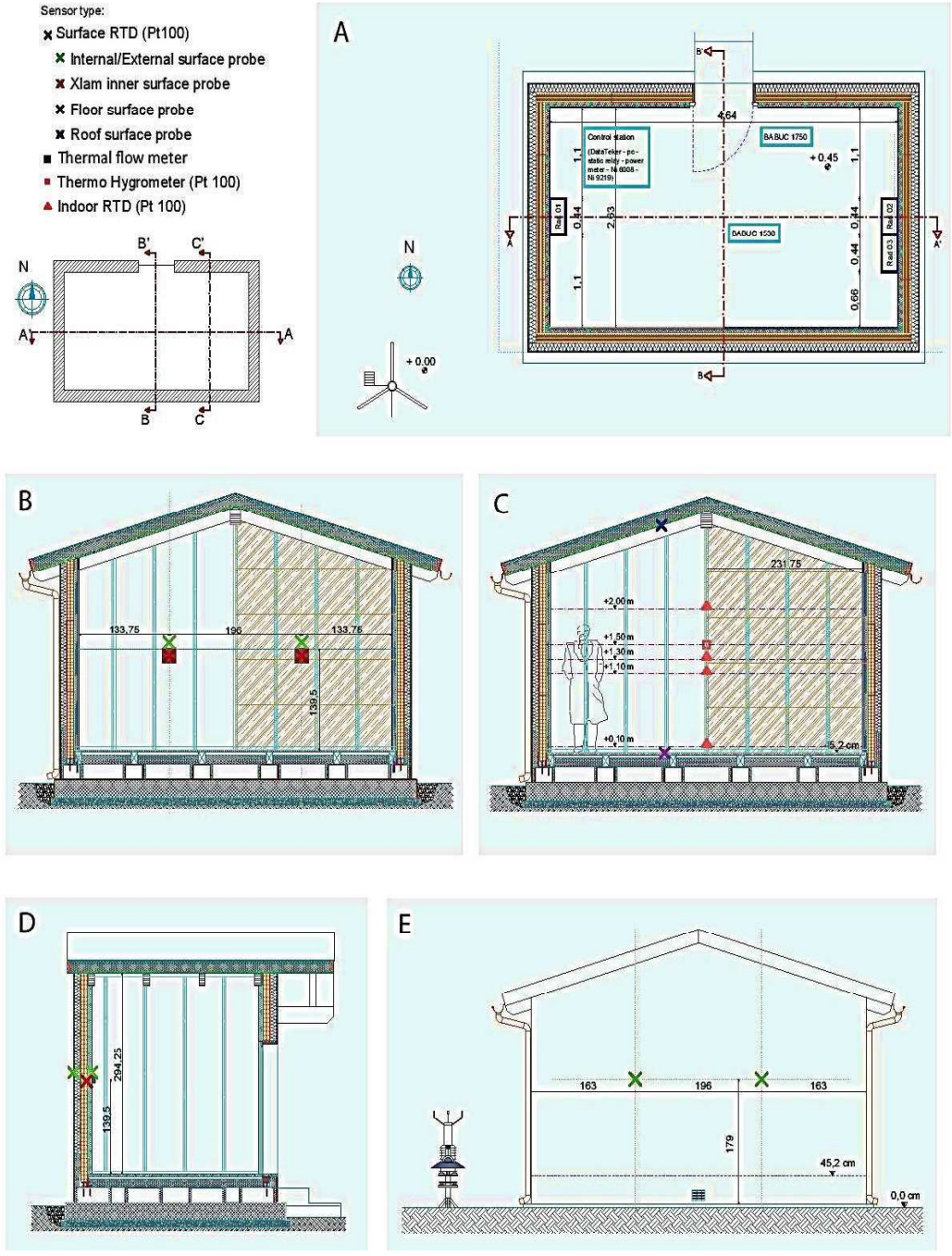


Figure 2.3

Distribution scheme of the probes inside and outside the mock-up: A) Plan view of the indoor network; B) A-A' cross section of the outdoor network; C) A-A' cross section of the indoor network; D) B-B' cross section of the interface network; E) outdoor network on south-exposed wall.

2.6 – CONTROLLERS CONFIGURATION

The thermal emission of electric radiators is a function of the voltage established at the ends of the internal resistors. Indeed, Ohm's first law (**equation 2.1**) states that, when the voltage ΔV at the ends of a resistive element (resistance R) in an electrical circuit is increased, a proportional increase of the current I is experienced as well, as the driving force which induces the motion of the electrons is amplified. Then, Joule effect (**equation 2.2**) transforms the linear increment of the amperage into a quadratic increase of the thermal power P emitted by the resistor.

$$\Delta V = RI \quad (2.1)$$

$$P = RI^2 \quad (2.2)$$

Against this theoretical backdrop, the output of the control system was identified in the voltage to be imposed to the feeding line of the three electric radiators.

In these tests the software used to sense and react according to the selected logic was LabVIEW, the system design software provided by National Instrument S.r.l.

It managed the dataflow using the G-Language (Graphic Language) to build up a Virtual Instrument (VI) which simulated the interaction between physical devices.

It looped (unless stopped by the user) repeating the following actions:

- real time sampling: DAQ data capture cards acquired and digitized connected sensors outputs (ambient RTD and power metre). The user set the acquisition delay [ms];
- control logic selection and activation: each case acted as a black box containing setting parameters and control algorithm processing the inputs (actual temperature, its derivative, outdoor temperature) into a voltage output between 0 and 5 V.
- power supply to the static relays driving the electric resistances of the radiators;
- computation of accumulated energy consumption [kJ] as:

  $$E_{heating}[kJ] = \sum_{i=o}^{n} P_i \cdot dt_i \quad (2.3)$$

  where "n" is the number of cycles completed in the period of observation, "dt_i" is the time taken for a cycle to be completed, "P_i" is the power metre ith output;
- data storing in a database application.

LabVIEW visualized the time trends of the following parameters: power [W], accumulated energy [kJ], outdoor, set point and actual ambient temperatures [°C]. Outdoor temperature data were imported in the VI by configuring the Datataker TCP/IP connection.

2.6.1 On/off controller

The on/off controllers (going by the name of hysteresis or bang-bang controllers too) belong to the category of feedback loop control systems with the peculiar feature of exerting their regulatory action through sharp switches between the active status (generally corresponding to the maximum power release) and the inactive status (generally corresponding to no power release).
The application in the field of thermal conditioning is quite a must since such controllers can be coupled to the majority of heating and cooling systems. Yet the choice is often more dependent on the ease in implementation/management rather than on a wise optimization of the control.
Actually, the manipulation of an environmental parameter via on/off loops is rewarding when the time to reach the set-point value is a major issue compared to the need to maintain it (in this case the adoption of a continuous-output control system – like a PID – is recommended) **[2.15].**
In fact, the output signal of an on/off controller is typically discontinuous and this affects the control variable time trend which becomes fluctuating around the set-point with a sawtooth shape (while the ideal is a flat one, every time environmental wellness is among the end targets).
Therefore, even though such configuration is not representative of comfort requirements, the great majority of thermostats applied in residential buildings is piloted via on/off logic **[2.15].**
Hence, the hysteresis controller had been included among the ones tested during this experimental activity in order to provide a baseline for the comparative performance assessment.

2.6.1.1 Setup

Setting up an on/off controller for HVAC purposes is fundamentally a matter of proper hysteresis selection so that timing and efficacy of the activation/deactivation loop is optimized for the specific application and thermophysical phenomenon:

- an excessively wide gap between on and off thresholds leads to systematic and substantial overshoots of the limit values imposed to the control variable which causes a strong penalization in both ergonomic (considerable deviations from comfort temperature) and energetic aspects (highly detrimental drawback in terms of consumptions in the rising phase after the activation and in compensating the overshoot after the deactivation);
- an excessively strict gap leads to a highly-pulsed on/off cycling of the emission terminal since little distance from the set-point value is tolerate before sending a corrective command. The main risk is the reduction on

technical systems life span, particularly in presence of metallic components which might suffer of thermal-cycling fatigue.

Hence, two different settings were implemented and tested. The choice was made among the hysteresis values suggested by the Standard UNI TS 11300 part 2 **[2.16]**:

- hysteresis = 1°C;
- hysteresis = 0.5°C.

The corresponding characteristic curves are plotted in **figure 2.4** and **figure 2.5.**

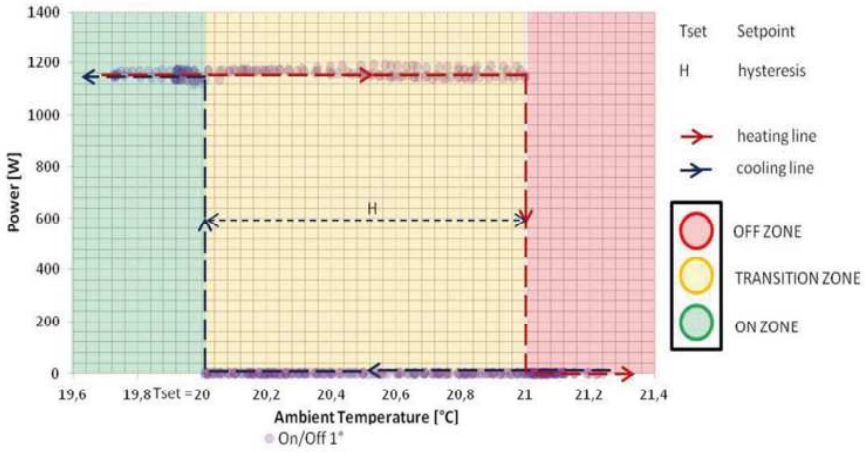


Figure 2.4

Characteristic curve of the on/off controller when the hysteresis is set to 1°C: power command against dry-bulb indoor air temperature.

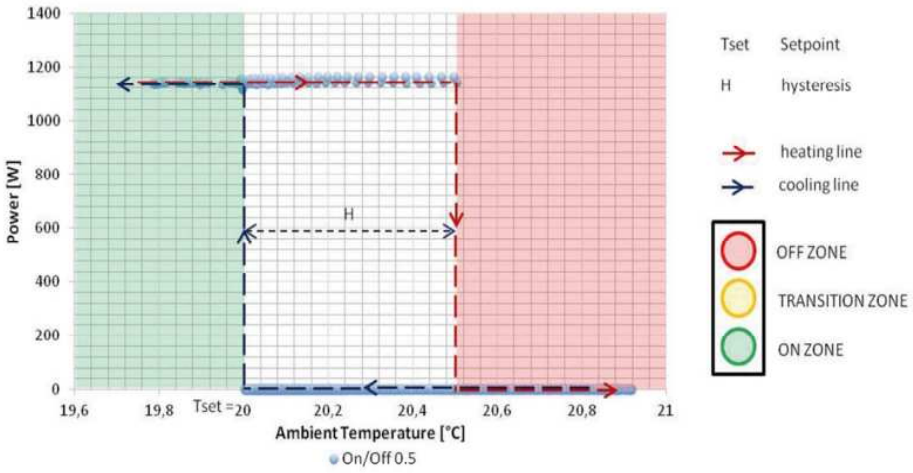


Figure 2.5

Characteristic curve of the on/off controller when the hysteresis is set to 0.5°C: power command against dry-bulb indoor air temperature.

2.6.2 PID controller

Although not yet well established on the real estate market (in particular residential sector), PID controllers represent a must in several industrial applications, as demonstrated by the percentage of implementation in plants control systems: 95% (including PID sub-species, especially PI) **[2.17].**

The main reason is that the inner methodology a PID controller applies perfectly caters to the regulation needs of industrial environments thanks to a set of peculiar features, which could be recapped as follows:

- ability to manage whatever control variable in function of set-point and output range by looping a retroactive logic: such is the key characteristics which makes PID controllers the proper low-level element in countless control strategies, no matter their global complexity and degree of hierarchy. In a time and cost-effective way, even articulated processes might be broken down in simpler sub-routines, each one conceived and tuned in order to optimize a single target parameter;
- no complex phenomenological models behind the corrective actions since PID controllers act on the error signal e(t) – defined as the difference between current and target values of the control variable – rather than on the interactions between control variables and the other parameters involved in the same sub-universe of interest. Such feature turns PID intro an all-purpose, one-fits-all, rapidly applicable solution: no detailed preliminary study is required);
- micro-processor-based technology: this means resilience as it entails a series of plus points in all applications where fast, precise, recurrent decision making is required and user's intervention is preferably driven to zero (to speed up the process, to increase the level of automation, to avoid specialized and expensive workforce, …): automatic tuning, continuous adjustment of setting parameters…

Therefore, it is actually because of PID introduction that industrial plants evolved from manual control to smart control (**figure 2.6**), without losing the benefit of a continuous adaption (in time and output range) of the target parameter to track its ideal trend.

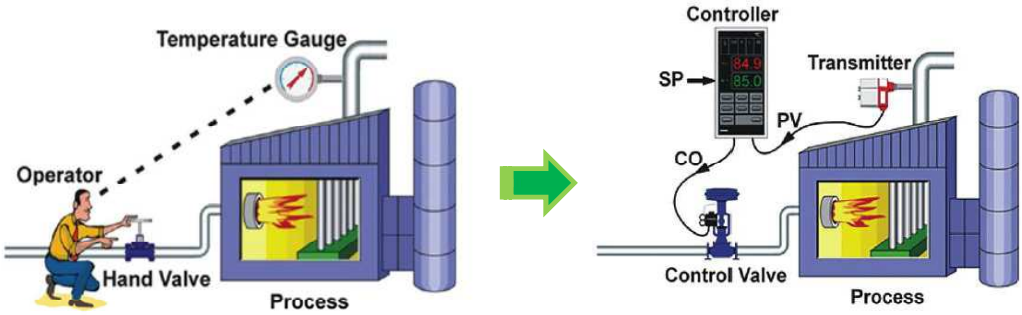


Figure 2.6
Turning a manual control into an equivalent automatic control in a typical industrial process: SP=Set Point; PV=Process Variable; CO=Control Output.

2.6.2.1 Structure

The PID control loop is composed by three functional macro-blocks (**figure 2.7**):

1. PROCESS: inside this box is the physical system on which the controller operates to adjust one of its pivotal parameters (by the name of process variable) around the strictest possible neighbourhood of a defined target value (representing its optimum). What happens inside this macro-block is subject not only to internal phenomenological dynamics but also to the forcing induced by the command elaborated by the controller in the previous loop and to the noise that might enter its boundaries.
2. SENSOR: this block indicates whatever measurement system used to sense and detect the process variable instantaneous value y(t). The output from the sensorial block is the input used to weight the corrective action in the subsequent block.
3. CONTROLLER: this is the PID core block: here a sequence of reading-computing-writing operations is performed loop by loop. While reading, the controller requires in input the contingent value of the process variable and the corresponding set-point. Then, a subtracter node calculates the difference between the two values to quantify the error signal and apply the corrective action (detailed description in the following paragraph) on it. The writing step consists in the elaboration of the output o(t) and its feeding to the process macro-block. Hence the loop is closed.

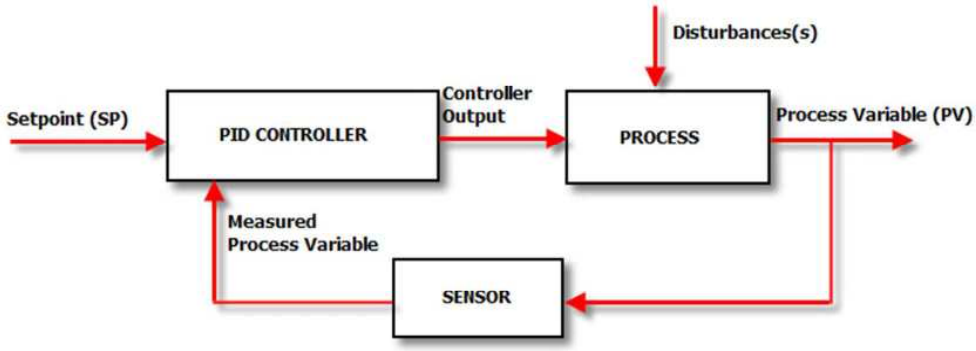


Figure 2.7
Functional macro-blocks of a PID controller.

2.6.2.2 Control actions

As previously mentioned, PID controllers act not directly on the process variable PV but on the gap between PV and the set-point value SP, named error signal e(t). The final aim is to drive e(t) to zero. It might be stressed here that SP is not necessarily a constant value but could be a variable itself (and even, in the most complex cases, the output of another sequential/nested PID)

The ultimate output signal Co(t) is the sum of the single proportional P, integral I and derivative D corrective actions, as mathematically expressed by the following control law:

$$Co(t) = K_c e(t) + K_i \int_{t_0}^{t} e(\tau) d\tau + K_d \frac{d}{dt} e(t) \qquad (2.4)$$

Such equation describes a dynamic, SISO (single input, single output), steady-state, linear, in continuous time and improper control system.

It is immediately noticeable that as the error comes to zero (which means that PV equals SP), each addendum is nil and the controller macro-block actually acts as a short circuit.

In every other case, each regulatory mode (P, I and D) return a component of the overall action, obtained by multiplying the error signal, its integral and its derivative with the corresponding constant K_x. This triplet of coefficients goes by the name of PID gains or PID degrees of freedom.

As a consequence, not just the present discrepancy between actual and ideal condition is taken into account, but also the gap accumulated in the past (which memory is stored in the result of the integration) and the future trend (which indication is expressed by the result of the differentiation).

Nevertheless, such potential must be carefully handled since it can result counterproductive when indiscriminately used: indeed, the implementation of all the three modes might not necessarily be the most rewarding configuration.

It actually depends on the shape of the error signal, which, in turn, is influenced partly by the physical process and partly by the quality of the sensor network: i.e. when e(t) follows a highly oscillatory trend (due to internal dynamics and/or considerable noise and/or probes' not filtered spikes) the D term introduces an extreme sensitivity to the trend reversals even though they might not be associated to the natural error signal evolution. This leads to inappropriate and generally pronounced corrective actions which emphasize the distance between PV and SP.
As a matter of fact, the most common PID and sub-PID configurations on the market, in order of decreasing spread, are: PI controller (major quote); PID and P controllers; PD controllers (very rare).
As a rule of thumb, the proportional action is always necessary as it brings the process variable much closer to the target value compared to the other two modes; the integral term addition tends to have a beneficial effect since it generally refines the result of the control; the derivative term, instead, is often disregarded since the balance between pros and cons turns positive in a limited number of scenarios.
Apparently, tuning is a crucial process which must be carefully handled in full awareness of the consequences every time PID gains are tweaked, since they define the amplitude of each corrective action and must be harmonized to get the optimal setting of the controller.

2.6.2.3 Tuning

Nowadays most of PID controllers are sourced with auto-tuning functions already embedded. Nevertheless, in many cases, manual tuning procedures lead to better results, tailored to the contingent application and process: the trial-and-error method and the tuning algorithm by Ziegler and Nichols are the most diffused **[2.18]**.
The former, in particular, is the one discussed and applied in the research activity in object. It consists in a progressive "guess and check" adjustment of the degrees of freedom.
According to the discussion in **sub-paragraph 2.6.2.2**, the first gain to be tuned is the proportional one, namely the K_c constant.
It determines the ratio of the output of a purely proportional controller to the error signal given in input: for instance, if e(t) amplitude is 10, the implementation of a P controller with a K_c equal to 5, generates an output signal Co(t) of 50.
While setting a P controller it is necessary to keep in mind that an increase in K_c value entails:

- faster response and higher readiness of the controller: this happens because K_c is actually a measure of the pitch by which the process variable approaches its set-point. On the one hand, this speeds up the reactions of the controller, yet, on the other hand, it emphasizes fluctuations and triggers overshoot.

- reduced steady state offset (stable gap between PV and SP). This can be measured just after the initial transient phase in which PV trend is remarkably oscillatory and, in particular, when the control variable falls steadily within a certain tolerance band around SP. Hence steady state conditions are achieved and it can be noticed that current PV value stabilizes on a time line parallel and below the one representing the set-point. The vertical gap between the two lines is called steady state offset. An increment in the proportional action magnitude contracts such discrepancy.

When it comes to purely proportional controllers, the proper tuning procedure consists in increasing K_c until the best compromise between offset and oscillation amplitude is accomplished. Conversely, when at least a second corrective mode is to be added, the proportional gain is set to the maximum value before observing a waving trend for the PV.

K_c can be either positive and negative. It depends on the physical characteristics of the process: for instance, when the controller is coupled with a cooling device the sign is typically positive, while when it regulates the emission of a heating system K_c is a negative value.

Another way to configure the proportional action is to quantify the proportional band B which represents the error range on which the regulation operates. B and K_c are strictly interrelated as expressed by the following equation:

$$B = e_{max} - e_{min} = \frac{PV_{max} - SP}{K_c} - \frac{PV_{min} - SP}{K_c} = \frac{PV_{max} - PV_{min}}{K_c} \quad (2.5)$$

This means that all consequences of increasing K_c are equally recorded by reducing B [**figure 2.8**].

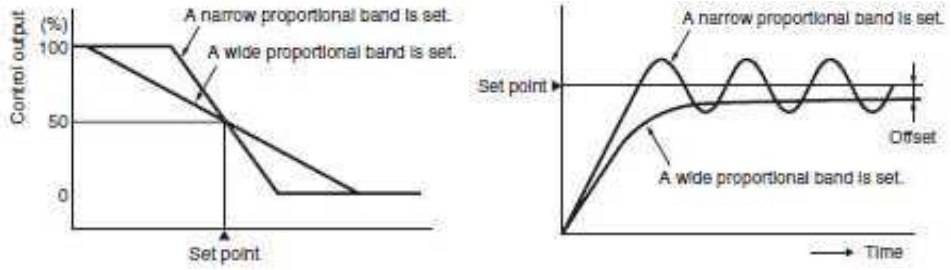


Figure 2.8
Tuning of the proportional band.

By adding the integral term, it is possible to weight the control action according to what happened in the past, in particular, to the error accumulated in the previous loops. As displayed in **equation 2.4**, the "I" component sums up the error signal over

time so that its magnitude intensifies until the steady state offset is filled and the error signal is driven to zero.
The main consequence is a finer control, especially during transient phases. This is the reason why PI and PID controllers are preferred whenever the process evolves in a dynamic rather than static equilibrium.
On the other hand, the exacerbation of the integral action might produce frequent and considerable overshoot (since the correction is weighted on a massive accumulation of the error).
In practical terms, the K_i (integral gain) tuning comes through a progressive reduction of its reciprocal, the so-called integral time constant T_i, which represents the integration interval.
In the case of a PI controller, the optimal value is the one which guarantees the best trade-off between offset reduction and signal fluctuation; whereas, in case of a complete PID regulation, T_i is lowered until the steady state error is equal to zero, although a certain degree of oscillation in reasonably accepted.
Indeed, the derivative term determines the error rate by means of differentiation between the last two values. This is why the D component might be completely misleading when it comes to noisy probes' signal and/or low loop rate so that the corresponding corrective action might easily emphasises the gap between PV and ST.
Consequently, the choice of adopting the derivative mode as well as its quantification are particularly delicate matters.
However, when properly tuned, the D term plays a strategic role in the overall control algorithm: it reacts to perturbing events (i.e. change in the distribution/number of loads, set-point adjustment, significant variation in the boundary conditions, …) by dumping the reaction of the controller and smoothing its output signal: the dumping effect intensifies with the slope of the rising/decreasing error signal, or, in other words, with the speed at which the PV is converging/diverging from the SP value.
So, if the P term is the gear stick of the controller, the I term its accelerator pedal, the D term is the brake pedal. Its maximum potential is released in case of clean signals and highly perturbed processes.
The K_d gain is most commonly referred to as T_d, derivative time constant. When T_d increases:

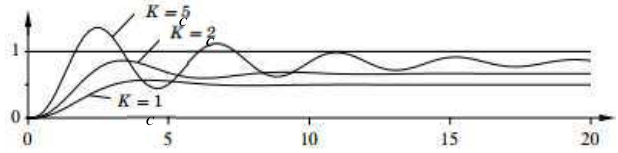
- the counteraction against error signal variation is amplified;
- the response of the controller gets faster;
- the overshoot frequency drops.

All things considered (and recapped in **table 2.6**), the macro-blocks scheme in **figure 2.7** can be now turned into the structure in **figure 2.9**, with all components unpacked.

PID CONTROLLER AND (SUB-TYPOLOGIES) TUNING

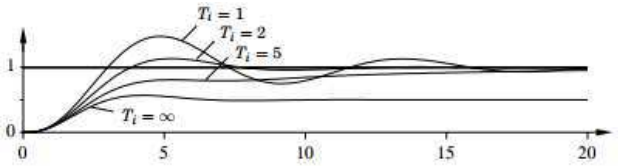
P CONTROLLER

Control law	Gains tuning	PROs	CONs
$Co(t) = K_c e(t)$	**K_c ↑** **T_i=∞** **T_d=0**	* response readiness increases * steady-state error decreases	*oscillation tendency and amplitude increases *control stability decreases



PI CONTROLLER

Control law	Gains tuning	PROs	CONs
$Co(t) = K_c e(t) + K_i \int_{t_0}^{t} e(\tau) d\tau$	**K_c≠0** **T_i ↓** **T_d=0**	* offset is driven to zero more rapidly	*control instability is enhanced



PID CONTROLLER

Control law	Gains tuning	PROs	CONs
$Co(t) = K_c e(t) + K_i \int_{t_0}^{t} e(\tau) d\tau + K_d \frac{d}{dt} e(t)$	**K_c≠0** **T_i≠0** **T_d ↑**	* overshooting frequency declines; * response dynamism and control stability increase	*high sensitivity to noisy environments

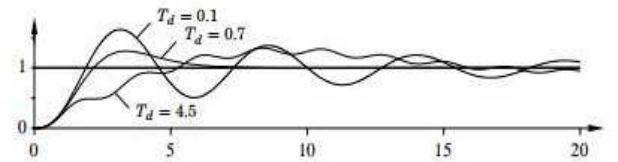


Table 2.6
Tuning scheme of a PID (and sub-species) controller.

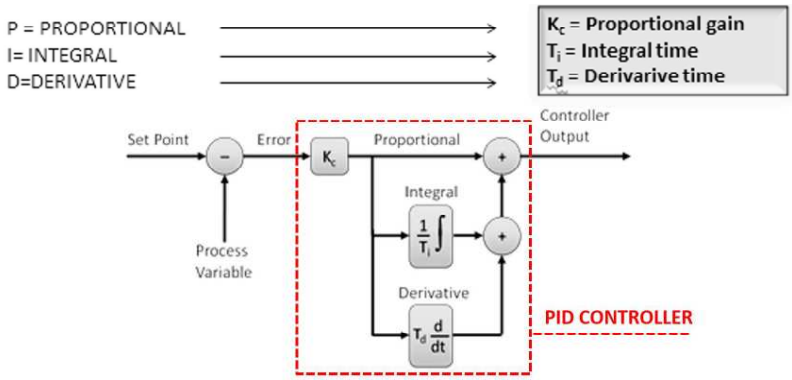


Figure 2.9
P, I, D structure of the controller.

2.6.2.4 Setup

The control law describing the tuning procedure adopted for the heating emission regulation in the mock-up is expressed as follows:

$$Co(t) = \frac{PV_{max} - PV_{min}}{B} e(t) + \frac{1}{T_i}\int_{t_0}^{t} e(\tau)d\tau + T_d \frac{d}{dt} e(t) \qquad (2.6)$$

Proportional band, integral time constant and derivative time constant were tweaked according to the trial-and-error procedure until an optimal coupling with the specific process was achieved.

The final characteristic parameters are listed below:

- B = 2°C.
  The corresponding time trend of the indoor temperature (PV) was slightly fluctuating but very close to the set-point value of 20°C (limited offset).
- T_i = 10 min.
  The corresponding average steady state error was driven to zero.
- T_d = 0 min.

Since RTDs are vulnerable sensors in terms of electrical interferences and white noise, the introduction of the D term was found to be detrimental for the sake of control stability as it extolled such undesired oscillations.

In similar cases the best practise is to avoid differentiation and optimize the PI version of the controller **[2.19].**

With this triplet of gains, the characteristic curve of the PI controller installed in the mock-up was shaped like in **figure 2.10.** Several pieces of information could be drawn:

- Rise time (time passed before SP line was crossed for the first time) = 1h, 8 mins, 4 secs;

- Peak time (time to reach the maximum overshoot) = 1h, 9 mins, 22 secs;
- Settling time (time to get to steady state conditions) = 1h, 9 mins, 32 secs (δ = acceptability range around SP = 0.5°C);
- Overshoot (maximum SP overpassing) = 0.57 °C;
- Steady state error (maximum gap between PV and SP in steady state conditions) = 0.4°C.

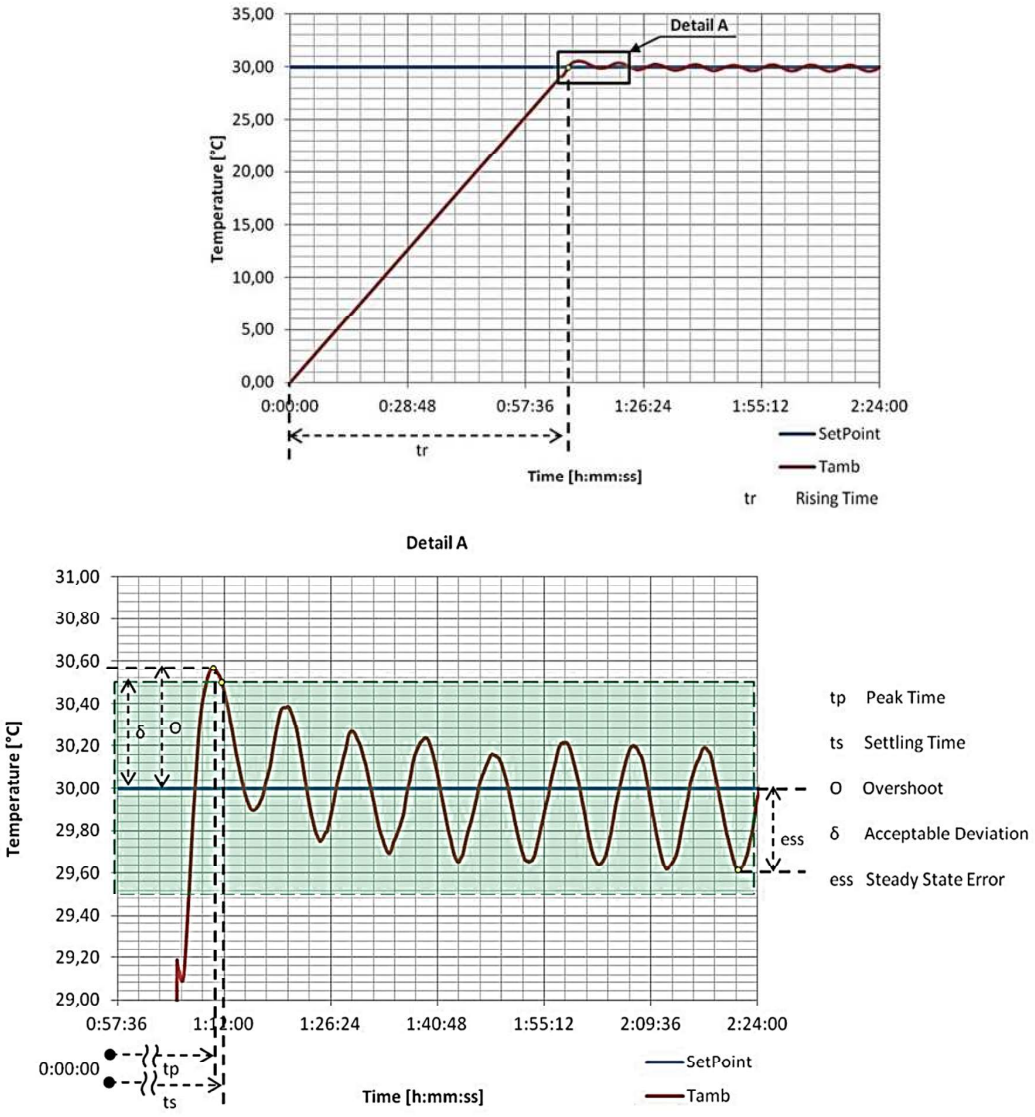


Figure 2.10
Agugliano's PI controller characteristic curve: the bottom detail is used to gather technical information.

2.6.3 Fuzzy controller

When it comes to comfort issues, both objective and subjective considerations are to be drawn in order to maximize users' environmental satisfaction. Approximate reasoning (in the shape of fuzzy logic) is thus widely renown to be a more successful control strategy than a classically designed scheme **[2.20].**

Fuzzy control logic mainstay and efficacy lies in its intuitive nature, which results in a series of strengths:

- flexibility: no need to deploy complex calculation algorithms in order to set precise thresholds and rigorous interrelations: this mathematical-model-free approach avoids a series of cost and time consuming preliminary studies (frequently discarded/ignored in the industrial world) whilst offering better management of chaotic/nonlinear time-variant working conditions compared to conventional PID controllers;
- multiple-input system: the decision-making process can embrace a virtually limitless number of parameters, weighting their role according to specific membership functions. Generally, the optimal set of inputs is the result of a previous sensitivity study, otherwise even a mere experience-based screening might suffice;
- heuristics and past experience can be integrated into the control system, mimicking human reasoning **[2.21].**

2.6.3.1 Structure

Fuzzy controllers are made up of four main components which transform and inverse transform crisp input data to return crisp output data **[2.22]**: fuzzifier, rules, inference engine, and defuzzifier (**figure 2.11**).

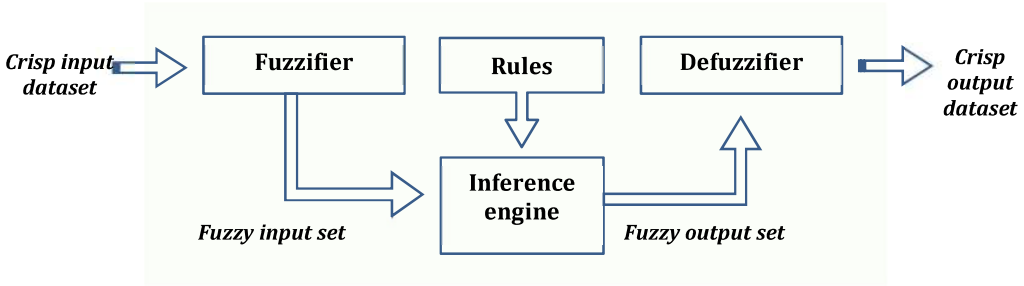


Figure 2.11
Fuzzy controller basic scheme.

The process of fuzzification takes place in the first component, which gathers and manipulates the input variables to turn them into a fuzzy shape through a metric of linguistic variables, linguistic terms and membership functions.
The decision-making process relies on statistical inference and a preliminarily defined set of rules: fuzzy output set is eventually released as the consequence of a series of antecedents and logic connectors. The crisp mapping process is played by the defuzzifier, which applies the output membership functions to reconvert the fuzzified output set into a "legible" command.
Fuzzy controller configuration is a sequence of three steps (called initialization), to define, in order:

1. linguistic variables and terms: numerical values are translated in natural language and replaced by words or sentences. Once maximum and minimum thresholds are defined per each input/output variable, the whole range is split into significant sub-sets: a linguistic variable is assigned to represent the overall parameter while set of linguistic terms is used to label the portions of sub clusters.
2. membership functions: they represent the graphical code to execute the conversion between crisp and fuzzy values by quantifying each linguistic term. It should be stressed here that a numerical value can belong to diverse sets at the same time with different degree of memberships.
3. rule base: it is a series of IF-THEN clauses involving all input and output linguistic variables to set a connection between each combination of input linguistic terms and the output counterpart.

Each rule returns a result which has to be assessed and then combined with the others to get the final outcome. This is performed through fuzzy set operations: in the present work the AND (intersection) MIN (minimum value among competing membership functions) is selected.
There are different algorithms for defuzzification too. The most common (here adopted too) is the Centre of Gravity, defined by the following formula:

$$O_{CoG} = \frac{\int_{min}^{max} o\ \mu(o)\ do}{\int_{min}^{max} \mu(o)\ do} \tag{2.7}$$

Where "O_{CoG}" is the result of defuzzification, "μ" is the "accumulated" membership function, "max" and "min" are the upper and lower limits for defuzzification.

2.6.3.2 Setup

Fuzzy controller configuration was completely developed via an ad-hoc toolkit available for LabVIEW **[2.23].**

It was conceived as a MISO system (multiple input – single output) so that three input variables could be involved in the decision-making process:

- dry-bulb indoor air temperature (instantaneous value, taken in the middle of the room to be representative of the average thermal conditions): it represents the driving information for all the controllers;
- dry-bulb indoor air temperature time derivative (trend): since the fuzzy controller is able to quantify (in a continuum of values within the 0-1 range) the effect of each input variable subset on the output one/ones, it is definitely the perfect solution to include the temperature derivative in a moderate decision-making process and avert the risk of an excessively sharp and impulsive reaction (quite likely to happen with a Not-Null-D-mode PID controller). Additionally, by contemplating the derivative in the identification of the proper corrective action, the controller gains predictive characteristics, as it acts and reacts anticipating the evolution on the process in the subsequent loop.
- Outdoor temperature (acquisition in parallel with indoor one): this choice caters to the need of considering the mutual influence between indoor and outdoor thermodynamical systems. Such control strategy empowers the predictive aspect and the climatic resilience of the controller.
  It should be stressed here that the simultaneous acquisition of outdoor and indoor temperatures doesn't actually represent a plus point in this context: in fact, further improvement to the control algorithm would be achieved by integrating the time lag and the dumping of the thermal heat wave crossing the walls because of the thermal inertia of the envelope. The new input variable would be the outdoor temperature recorded a certain number of loops before the current one (given by the rounded integer part of the ratio of the time lag to the loop rate) and reduced by the decrement factor.

The general settings of the fuzzy controller are summarized in the following tables (**tables 2.6-2.8**).

FUZZY CONTROLLER VARIABLES AND METHODS

INPUT VARIABLES

Variable	Name	Range	Number of membership functions
Actual ambient air temperature	T_ATT	0 -> 40	5
Ambient air temperature	dT/dt	-0.1 -> 0.1	3

derivative			
Outdoor temperature	T_out	-10 -> 45	4
	OUTPUT VARIABLES		
Variable	**Name**	**Range**	**Number of membership functions**
Feeding voltage	VOLT	0 -> 5	8
DEFUZZIFICATION METHOD:	Center of Area*	**ANTECEDENT CONNECTIVE**:	AND (Minimum)**
IMPLICATION:	Minimum	**DEGREE OF SUPPORT**:	1.00

Note 1 *it calculates the geometric center of the area under the scaled membership functions and within the range of the output variables.

Note 2 **it specifies to use the smallest degree of membership of the antecedents as aggregated value.

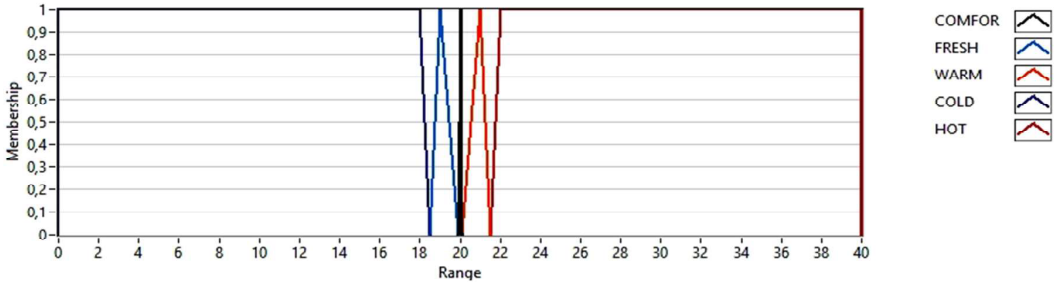
Table 2.6

Fuzzy controller general settings.

INPUT MEMBERSHIP FUNCTIONS

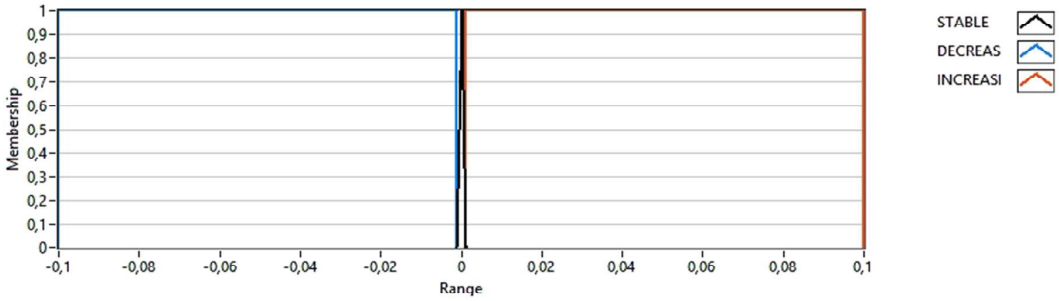
T_ATT

Membership function	**Shape**	**Points**
COMFORT	Triangle	19,9 ; 20 ; 20,1
FRESH	Triangle	18,5 ; 19 ; 19,9
WARM	Triangle	20,1 ; 21 ; 21,5
COLD	Trapezoid	0 ; 0 ; 18 ; 18,5
HOT	Trapezoid	21,5 ; 22 ; 40 ; 40



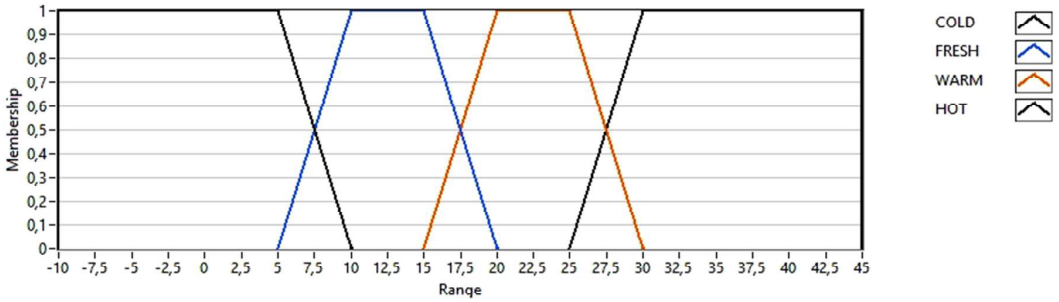
dT/dt

Membership function	**Shape**	**Points**
STABLE	Triangle	-0,001 ; 0 ; 0,001
DECREASING	Trapezoid	-0,1 ; -0,1 ; -0,001 ; -0,001
INCREASING	Trapezoid	0,001 ; 0,001 ; 0,1 ; 0,1



T_out

Membership function	Shape	Points
COLD	Trapezoid	-10 ; -10 ; 5 ; 10
FRESH	Trapezoid	5 ; 10 ; 15 ; 20
WARM	Trapezoid	15 ; 20 ; 25 ; 30
HOT	Trapezoid	25 ; 30 ; 45 ; 45



OUTPUT MEMBERSHIP FUNCTIONS

VOLT

Membership function	Shape	Points
VERY LOW	Triangle	0 ; 0 ; 0,5
OFF	Singleton	0
FULL	Singleton	5
LOW	Trapezoid	0 ; 0,5 ; 1 ; 1,5
MEDIUM-LOW	Trapezoid	1 ; 1,5 ; 2,5 ; 3
MEDIUM-HIGH	Trapezoid	2 ; 2,5 ; 3,5 ; 4
HIGH	Trapezoid	3,5 ; 4 ; 4,5 ; 5
VERY HIGH	Triangle	4,5 ; 5 ; 5

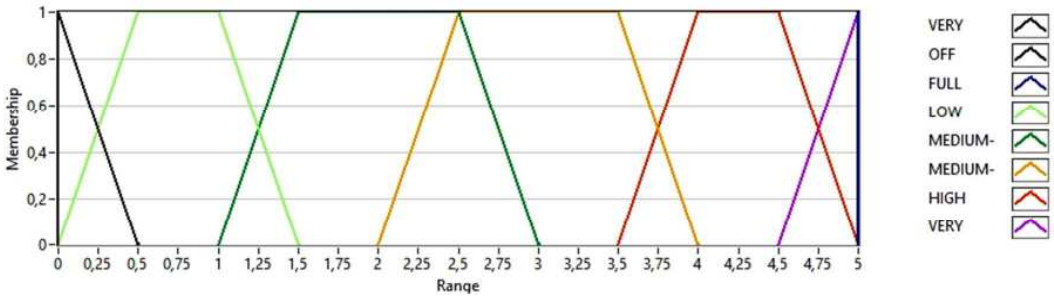


Table 2.7
Fuzzy controller membership functions.

FUZZY RULES SET

1. IF 'T_ATT' IS 'COMFORT' AND 'dT/dt' IS 'STABLE' AND 'T_out' IS 'COLD' THEN 'VOLT' IS 'MEDIUM-LOW'
connective: AND (Minimum) ; implication: Minimum ; degree of support: 1,00

2. IF 'T_ATT' IS 'COMFORT' AND 'dT/dt' IS 'STABLE' AND 'T_out' IS 'FRESH' THEN 'VOLT' IS 'LOW'
connective: AND (Minimum) ; implication: Minimum ; degree of support: 1,00

3. IF 'T_ATT' IS 'COMFORT' AND 'dT/dt' IS 'STABLE' AND 'T_out' IS 'WARM' THEN 'VOLT' IS 'VERY LOW'
connective: AND (Minimum) ; implication: Minimum ; degree of support: 1,00

4. IF 'T_ATT' IS 'COMFORT' AND 'dT/dt' IS 'STABLE' AND 'T_out' IS 'HOT' THEN 'VOLT' IS 'OFF'
connective: AND (Minimum) ; implication: Minimum ; degree of support: 1,00

5. IF 'T_ATT' IS 'COMFORT' AND 'dT/dt' IS 'DECREASING' AND 'T_out' IS 'COLD' THEN 'VOLT' IS 'MEDIUM-HIGH'
connective: AND (Minimum) ; implication: Minimum ; degree of support: 1,00

6. IF 'T_ATT' IS 'COMFORT' AND 'dT/dt' IS 'DECREASING' AND 'T_out' IS 'FRESH' THEN 'VOLT' IS 'MEDIUM-LOW'
connective: AND (Minimum) ; implication: Minimum ; degree of support: 1,00

7. IF 'T_ATT' IS 'COMFORT' AND 'dT/dt' IS 'DECREASING' AND 'T_out' IS 'WARM' THEN 'VOLT' IS 'LOW'
connective: AND (Minimum) ; implication: Minimum ; degree of support: 1,00

8. IF 'T_ATT' IS 'COMFORT' AND 'dT/dt' IS 'DECREASING' AND 'T_out' IS 'HOT' THEN 'VOLT' IS 'VERY LOW'
connective: AND (Minimum) ; implication: Minimum ; degree of support: 1,00

9. IF 'T_ATT' IS 'COMFORT' AND 'dT/dt' IS 'INCREASING' AND 'T_out' IS 'COLD' THEN 'VOLT' IS 'LOW'
connective: AND (Minimum) ; implication: Minimum ; degree of support: 1,00

10. IF 'T_ATT' IS 'COMFORT' AND 'dT/dt' IS 'INCREASING' AND 'T_out' IS 'FRESH' THEN 'VOLT' IS 'VERY LOW'

connective: AND (Minimum) ; implication: Minimum ; degree of support: 1,00

11. IF 'T_ATT' IS 'COMFORT' AND 'dT/dt' IS 'INCREASING' AND 'T_out' IS 'WARM' THEN 'VOLT' IS 'VERY LOW'
connective: AND (Minimum) ; implication: Minimum ; degree of support: 1,00

12. IF 'T_ATT' IS 'COMFORT' AND 'dT/dt' IS 'INCREASING' AND 'T_out' IS 'HOT' THEN 'VOLT' IS 'OFF'
connective: AND (Minimum) ; implication: Minimum ; degree of support: 1,00

13. IF 'T_ATT' IS 'FRESH' AND 'dT/dt' IS 'STABLE' AND 'T_out' IS 'COLD' THEN 'VOLT' IS 'VERY HIGH'
connective: AND (Minimum) ; implication: Minimum ; degree of support: 1,00

14. IF 'T_ATT' IS 'FRESH' AND 'dT/dt' IS 'STABLE' AND 'T_out' IS 'FRESH' THEN 'VOLT' IS 'VERY HIGH'
connective: AND (Minimum) ; implication: Minimum ; degree of support: 1,00

15. IF 'T_ATT' IS 'FRESH' AND 'dT/dt' IS 'STABLE' AND 'T_out' IS 'WARM' THEN 'VOLT' IS 'HIGH'
connective: AND (Minimum) ; implication: Minimum ; degree of support: 1,00

16. IF 'T_ATT' IS 'FRESH' AND 'dT/dt' IS 'STABLE' AND 'T_out' IS 'HOT' THEN 'VOLT' IS 'MEDIUM-HIGH'
connective: AND (Minimum) ; implication: Minimum ; degree of support: 1,00

17. IF 'T_ATT' IS 'FRESH' AND 'dT/dt' IS 'DECREASING' AND 'T_out' IS 'COLD' THEN 'VOLT' IS 'FULL'
connective: AND (Minimum) ; implication: Minimum ; degree of support: 1,00

18. IF 'T_ATT' IS 'FRESH' AND 'dT/dt' IS 'DECREASING' AND 'T_out' IS 'FRESH' THEN 'VOLT' IS 'FULL'
connective: AND (Minimum) ; implication: Minimum ; degree of support: 1,00

19. IF 'T_ATT' IS 'FRESH' AND 'dT/dt' IS 'DECREASING' AND 'T_out' IS 'WARM' THEN 'VOLT' IS 'FULL'
connective: AND (Minimum) ; implication: Minimum ; degree of support: 1,00

20. IF 'T_ATT' IS 'FRESH' AND 'dT/dt' IS 'DECREASING' AND 'T_out' IS 'HOT' THEN 'VOLT' IS 'FULL'
connective: AND (Minimum) ; implication: Minimum ; degree of support: 1,00

21. IF 'T_ATT' IS 'FRESH' AND 'dT/dt' IS 'INCREASING' AND 'T_out' IS 'COLD' THEN 'VOLT' IS 'FULL'
connective: AND (Minimum) ; implication: Minimum ; degree of support: 1,00

22. IF 'T_ATT' IS 'FRESH' AND 'dT/dt' IS 'INCREASING' AND 'T_out' IS 'FRESH' THEN 'VOLT' IS 'VERY HIGH'
connective: AND (Minimum) ; implication: Minimum ; degree of support: 1,00

23. IF 'T_ATT' IS 'FRESH' AND 'dT/dt' IS 'INCREASING' AND 'T_out' IS 'WARM' THEN 'VOLT' IS 'VERY HIGH'
connective: AND (Minimum) ; implication: Minimum ; degree of support: 1,00

24. IF 'T_ATT' IS 'FRESH' AND 'dT/dt' IS 'INCREASING' AND 'T_out' IS 'HOT' THEN 'VOLT' IS 'HIGH'
connective: AND (Minimum) ; implication: Minimum ; degree of support: 1,00

25. IF 'T_ATT' IS 'WARM' AND 'dT/dt' IS 'STABLE' AND 'T_out' IS 'COLD' THEN 'VOLT' IS 'OFF'
connective: AND (Minimum) ; implication: Minimum ; degree of support: 1,00

26. IF 'T_ATT' IS 'WARM' AND 'dT/dt' IS 'STABLE' AND 'T_out' IS 'FRESH' THEN 'VOLT' IS 'OFF'
connective: AND (Minimum) ; implication: Minimum ; degree of support: 1,00

27. IF 'T_ATT' IS 'WARM' AND 'dT/dt' IS 'STABLE' AND 'T_out' IS 'WARM' THEN 'VOLT' IS 'OFF'

connective: AND (Minimum) ; implication: Minimum ; degree of support: 1,00

28. IF 'T_ATT' IS 'WARM' AND 'dT/dt' IS 'STABLE' AND 'T_out' IS 'HOT' THEN 'VOLT' IS 'OFF'
connective: AND (Minimum) ; implication: Minimum ; degree of support: 1,00

29. IF 'T_ATT' IS 'WARM' AND 'dT/dt' IS 'DECREASING' AND 'T_out' IS 'COLD' THEN 'VOLT' IS 'VERY LOW'
connective: AND (Minimum) ; implication: Minimum ; degree of support: 1,00

30. IF 'T_ATT' IS 'WARM' AND 'dT/dt' IS 'DECREASING' AND 'T_out' IS 'FRESH' THEN 'VOLT' IS 'VERY LOW'
connective: AND (Minimum) ; implication: Minimum ; degree of support: 1,00

31. IF 'T_ATT' IS 'WARM' AND 'dT/dt' IS 'DECREASING' AND 'T_out' IS 'WARM' THEN 'VOLT' IS 'OFF'
connective: AND (Minimum) ; implication: Minimum ; degree of support: 1,00

32. IF 'T_ATT' IS 'WARM' AND 'dT/dt' IS 'DECREASING' AND 'T_out' IS 'HOT' THEN 'VOLT' IS 'OFF'
connective: AND (Minimum) ; implication: Minimum ; degree of support: 1,00

33. IF 'T_ATT' IS 'WARM' AND 'dT/dt' IS 'INCREASING' AND 'T_out' IS 'COLD' THEN 'VOLT' IS 'OFF'
connective: AND (Minimum) ; implication: Minimum ; degree of support: 1,00

34. IF 'T_ATT' IS 'WARM' AND 'dT/dt' IS 'INCREASING' AND 'T_out' IS 'FRESH' THEN 'VOLT' IS 'OFF'
connective: AND (Minimum) ; implication: Minimum ; degree of support: 1,00

35. IF 'T_ATT' IS 'WARM' AND 'dT/dt' IS 'INCREASING' AND 'T_out' IS 'WARM' THEN 'VOLT' IS 'OFF'
connective: AND (Minimum) ; implication: Minimum ; degree of support: 1,00

36. IF 'T_ATT' IS 'WARM' AND 'dT/dt' IS 'INCREASING' AND 'T_out' IS 'HOT' THEN 'VOLT' IS 'OFF'
connective: AND (Minimum) ; implication: Minimum ; degree of support: 1,00

37. IF 'T_ATT' IS 'COLD' AND 'dT/dt' IS 'STABLE' AND 'T_out' IS 'COLD' THEN 'VOLT' IS 'FULL'
connective: AND (Minimum) ; implication: Minimum ; degree of support: 1,00

38. IF 'T_ATT' IS 'COLD' AND 'dT/dt' IS 'STABLE' AND 'T_out' IS 'FRESH' THEN 'VOLT' IS 'FULL'
connective: AND (Minimum) ; implication: Minimum ; degree of support: 1,00

39. IF 'T_ATT' IS 'COLD' AND 'dT/dt' IS 'STABLE' AND 'T_out' IS 'WARM' THEN 'VOLT' IS 'FULL'
connective: AND (Minimum) ; implication: Minimum ; degree of support: 1,00

40. IF 'T_ATT' IS 'COLD' AND 'dT/dt' IS 'STABLE' AND 'T_out' IS 'HOT' THEN 'VOLT' IS 'FULL'
connective: AND (Minimum) ; implication: Minimum ; degree of support: 1,00

41. IF 'T_ATT' IS 'COLD' AND 'dT/dt' IS 'DECREASING' AND 'T_out' IS 'COLD' THEN 'VOLT' IS 'FULL'
connective: AND (Minimum) ; implication: Minimum ; degree of support: 1,00

42. IF 'T_ATT' IS 'COLD' AND 'dT/dt' IS 'DECREASING' AND 'T_out' IS 'FRESH' THEN 'VOLT' IS 'FULL'
connective: AND (Minimum) ; implication: Minimum ; degree of support: 1,00

43. IF 'T_ATT' IS 'COLD' AND 'dT/dt' IS 'DECREASING' AND 'T_out' IS 'WARM' THEN 'VOLT' IS 'FULL'
connective: AND (Minimum) ; implication: Minimum ; degree of support: 1,00

44. IF 'T_ATT' IS 'COLD' AND 'dT/dt' IS 'DECREASING' AND 'T_out' IS 'HOT' THEN 'VOLT' IS 'FULL'
connective: AND (Minimum) ; implication: Minimum ; degree of support: 1,00

45. IF 'T_ATT' IS 'COLD' AND 'dT/dt' IS 'INCREASING' AND 'T_out' IS 'COLD' THEN 'VOLT' IS 'FULL' connective: AND (Minimum) ; implication: Minimum ; degree of support: 1,00

46. IF 'T_ATT' IS 'COLD' AND 'dT/dt' IS 'INCREASING' AND 'T_out' IS 'FRESH' THEN 'VOLT' IS 'FULL' connective: AND (Minimum) ; implication: Minimum ; degree of support: 1,00

47. IF 'T_ATT' IS 'COLD' AND 'dT/dt' IS 'INCREASING' AND 'T_out' IS 'WARM' THEN 'VOLT' IS 'FULL' connective: AND (Minimum) ; implication: Minimum ; degree of support: 1,00

48. IF 'T_ATT' IS 'COLD' AND 'dT/dt' IS 'INCREASING' AND 'T_out' IS 'HOT' THEN 'VOLT' IS 'FULL' connective: AND (Minimum) ; implication: Minimum ; degree of support: 1,00

49. IF 'T_ATT' IS 'HOT' AND 'dT/dt' IS 'STABLE' AND 'T_out' IS 'COLD' THEN 'VOLT' IS 'OFF' connective: AND (Minimum) ; implication: Minimum ; degree of support: 1,00

50. IF 'T_ATT' IS 'HOT' AND 'dT/dt' IS 'STABLE' AND 'T_out' IS 'FRESH' THEN 'VOLT' IS 'OFF' connective: AND (Minimum) ; implication: Minimum ; degree of support: 1,00

51. IF 'T_ATT' IS 'HOT' AND 'dT/dt' IS 'STABLE' AND 'T_out' IS 'WARM' THEN 'VOLT' IS 'OFF' connective: AND (Minimum) ; implication: Minimum ; degree of support: 1,00

52. IF 'T_ATT' IS 'HOT' AND 'dT/dt' IS 'STABLE' AND 'T_out' IS 'HOT' THEN 'VOLT' IS 'OFF' connective: AND (Minimum) ; implication: Minimum ; degree of support: 1,00

53. IF 'T_ATT' IS 'HOT' AND 'dT/dt' IS 'DECREASING' AND 'T_out' IS 'COLD' THEN 'VOLT' IS 'OFF' connective: AND (Minimum) ; implication: Minimum ; degree of support: 1,00

54. IF 'T_ATT' IS 'HOT' AND 'dT/dt' IS 'DECREASING' AND 'T_out' IS 'FRESH' THEN 'VOLT' IS 'OFF' connective: AND (Minimum) ; implication: Minimum ; degree of support: 1,00

55. IF 'T_ATT' IS 'HOT' AND 'dT/dt' IS 'DECREASING' AND 'T_out' IS 'WARM' THEN 'VOLT' IS 'OFF' connective: AND (Minimum) ; implication: Minimum ; degree of support: 1,00

56. IF 'T_ATT' IS 'HOT' AND 'dT/dt' IS 'DECREASING' AND 'T_out' IS 'HOT' THEN 'VOLT' IS 'OFF' connective: AND (Minimum) ; implication: Minimum ; degree of support: 1,00

57. IF 'T_ATT' IS 'HOT' AND 'dT/dt' IS 'INCREASING' AND 'T_out' IS 'COLD' THEN 'VOLT' IS 'OFF' connective: AND (Minimum) ; implication: Minimum ; degree of support: 1,00

58. IF 'T_ATT' IS 'HOT' AND 'dT/dt' IS 'INCREASING' AND 'T_out' IS 'FRESH' THEN 'VOLT' IS 'OFF' connective: AND (Minimum) ; implication: Minimum ; degree of support: 1,00

59. IF 'T_ATT' IS 'HOT' AND 'dT/dt' IS 'INCREASING' AND 'T_out' IS 'WARM' THEN 'VOLT' IS 'OFF' connective: AND (Minimum) ; implication: Minimum ; degree of support: 1,00

60. IF 'T_ATT' IS 'HOT' AND 'dT/dt' IS 'INCREASING' AND 'T_out' IS 'HOT' THEN 'VOLT' IS 'OFF' connective: AND (Minimum) ; implication: Minimum ; degree of support: 1,00

Table 2.8

Fuzzy controller rules.

2.7 – EVALUATION CRITERIA

The overarching aim of the present work was to assess the comfort and energetic performance of different control logics, specific criteria were defined to evaluate both these aspects.

At the end of every running test, a representative period of 5/6 days in which the sensor network showed no breakdowns, was selected and the following performance criteria were applied.

2.7.1 Criterion for energy consumption

As the only elements absorbing energy, in the heating terminals, were the electrical resistances inside the radiators, the total power necessary to keep ambient temperature at the imposed set point was directly obtained from the output signal of the power metre.

Then, total energy consumption was calculated programmatically, as exposed in the **paragraph 2.3.**

In order to allow significant comparison between data collected in different observation periods, making them independent from contingent thermal conditions (both inside and outside the building), the total energy consumption was normalized over the average difference between indoor (T_{amb}) and outdoor (T_{out}) temperature:

$$E_{norm} = \frac{E_{heating}}{\frac{1}{n}\sum_{i=1}^{n}(T_{amb} - T_{out})_i} \quad (2.8)$$

In **equation 2.7** "n" is the number of temperature records, stored in the observation period T.

In addition, graphical analysis was carried out to diagnose the real energy consumption related to the building-HVAC coupled system. Hourly averaged power consumption was chartered in function of:

- outdoor air temperature;
- global solar radiation.

These charts, called energy signatures, returned meaningful information about building energy performance and thermal behaviour (thermal transmittance), efficiency gains and losses recorded with the different control logics and allowed rapid individuation of extraordinary working conditions: particularly windy/sunny days, starts-up after long inactive periods, system breakdowns **[2.24–2.28].**

2.7.2 Criterion for comfort

Conventional comfort theory lies on Fanger's equations and indices **[2.29]**, in particular Predicted Mean Vote (PMV) and Predicted Percentage of Dissatisfied people (PPD).
They quantify user's expected level of global satisfaction towards the surrounding microclimate, according to the actual environmental conditions. As a consequence, they only provide information about instantaneous comfort/discomfort status.
In order to enlarge the temporal horizon of the assessment, several long-term indices have been developed **[2.30]**, summarizing building comfort behaviour over the entire period of observation.
Among them, excess-weighted PPD (PPD.h) has been adopted in European Standard EN 15251 **[2.31]** and applied in previous similar studies returning meaningful information **[2.18,2.32,2.33].** It summarizes time intervals over which PPD exceeds the PPD_{min} value of 10% (lower limit of comfort zone for category 2 in EN 15251, the suggested category for new buildings), weighted according to the following function wf_i:

$$wf_i = \begin{cases} \dfrac{PPD}{PPD_{min}}, per \;\; PPD > 10 \\ 0, per \; PPD \;\; \leq 10 \end{cases} \tag{2.9}$$

PPD.h analytical expression is:

$$PPD.h = \sum_{i=1}^{n} wf_i \cdot t_{wfi} \tag{2.10}$$

where "n" represents the number of different values calculated for the weighting function and "t_{wfi}" is the total period of time over which wf_i assumes the ith value.
PPD.h is a comfort model based, category-dependent and cumulative index. It is not upper-limited; hence its absolute value cannot be used for a meaningful evaluation. It was calculated for all the monitoring periods: the difference between the results allowed comparison between the relative controllers in terms of comfort stability each one guaranteed.

2.8 – RESULTS AND DISCUSSION

Each controller was tested for a monitoring period of about 10days.
Building inertia, sensors' settling time and working anomalies reduced the sampling to 5/6 days of validated data, summarized in **table 2.9**.
The post-elaboration results on data collected by the three monitoring stations are reported in the following sub-paragraphs.

TIME SCHEDULING AND BOUNDARY CONDITIONS			
Controller	**Monitoring Period**		**Valid days***
PID	10\12\2014 – 21\01\2015		6
	Average weather conditions		
Air Temperature [°C]	**Relative umidity [%]**	**Solar radiation [W]**	**Wind Speed [m/s]**
9.47	71.97	60.05	/**
Controller	**Monitoring Period**		**Valid days***
On/Off-1°C	22\01\2015 – 12\02\2015		6
	Average weather conditions		
Air Temperature [°C]	**Relative umidity [%]**	**Solar radiation [W]**	**Wind Speed [m/s]**
5.61	66.55	173.95	/**
Controller	**Monitoring Period**		**Valid days***
On/Off-0.5°C	13\02\2015 –01\03\2015		5
	Average weather conditions		
Air Temperature [°C]	**Relative umidity [%]**	**Solar radiation [W]**	**Wind Speed [m/s]**
8.23	83.32	69.88	2.27
Controller	**Monitoring Period**		**Valid days***
Fuzzy	27\03\2015 – 07\04\2015		6
	Average weather conditions		
Air Temperature [°C]	**Relative umidity [%]**	Solar radiation [W]	**Wind Speed [m/s]**
11.71	57.46	191.63	3.23

Note 2 *no breakdowns recorded by the instruments composing the sensor network
Note 2 **unavailability of tacogonioanemometer

Table 2.9
Observation periods and corresponding weather conditions per each controller under test.

2.8.1 Energy consumption

On/off, PID and fuzzy controllers tracked the set point temperature with a power supply characteristic curve very different one to another. Besides the heating load necessary to cover the building winter requirement varied significantly with the weather conditions and, in particular, the thermal gradient between indoor and outdoor environments and the solar radiation.
For these reasons, comparison was made on normalized consumption data and energy signatures.

2.8.1.1 Normalized consumption

Indoor environment thermal condition was the main driving force for power consumption.
However, the energy supplies necessary to keep ambient temperature at the desired set-point were also influenced by outdoor temperature, wind speed and direction, solar radiation contribution.

A correct approach to compare the energy performance of the controllers was to use these external parameters as terms of normalization for power consumption.
In this study, the selected reference parameter was the average difference between indoor and outdoor air temperature in the monitoring period:

$$C_{norm,i} = \frac{Q_i}{\left|T_{amb,i} - T_{out,i}\right|}\Delta t_i \qquad (2.11)$$

where "$C_{norm,i}$" is the normalized energy consumption related to the ith monitoring period [Wh/°C], "Δt_i" is the total number of hours corresponding to the ith monitoring period, $T_{amb,i}$ and $T_{out,i}$ are the ith time-averaged ambient air and outdoor temperatures [°C].
Results are summarized in **table 2.10** and **figure 2.12.**
The conclusion was that the best energy performance, evaluated through normalized energy consumption, was achieved by the fuzzy controller: the saving was about 67.8% compared to the on/off-1°C controller, 43.8% compared to the PID controller and 31.4% compared to the on/off-0.5°C controller.
That was an expected result since the fuzzy controller was the only one directly including outdoor temperature in its regulation algorithm.

ENERGY PERFORMANCE ASSESSMENT (1)

CONTROLLER	NORMALIZED ENERGY CONSUMPTION		
	DATE	IN A DAY	OVER THE PERIOD
PID	15/01/2015	276.42	2286.73
	16/01/2015	484.12	
	17/01/2015	456.38	
	18/01/2015	309.86	
	19/01/2015	326.59	
	20/01/2015	485.20	
On/Off 1°	27/01/2015	408.94	2668.40
	28/01/2015	674.97	
	29/01/2015	366.55	
	30/01/2015	460.44	
	31/01/2015	377.95	
	01/02/2015	373.54	
On/Off 0.5°	25/02/2015	718.38	2089.62
	26/02/2015	343.07	
	27/02/2015	372.89	
	28/02/2015	411.20	
	01/03/2015	277.18	
	/	/	

Fuzzy	30/03//2015	281.92	1589.85
	31/03/2015	258.12	
	01/04/2015	463.04	
	02/04/2015	210.72	
	03/04/2015	194.21	
	04/04/2015	289.99	

Table 2.10
Energy performance evaluation: normalized energy consumption per each controller under test.

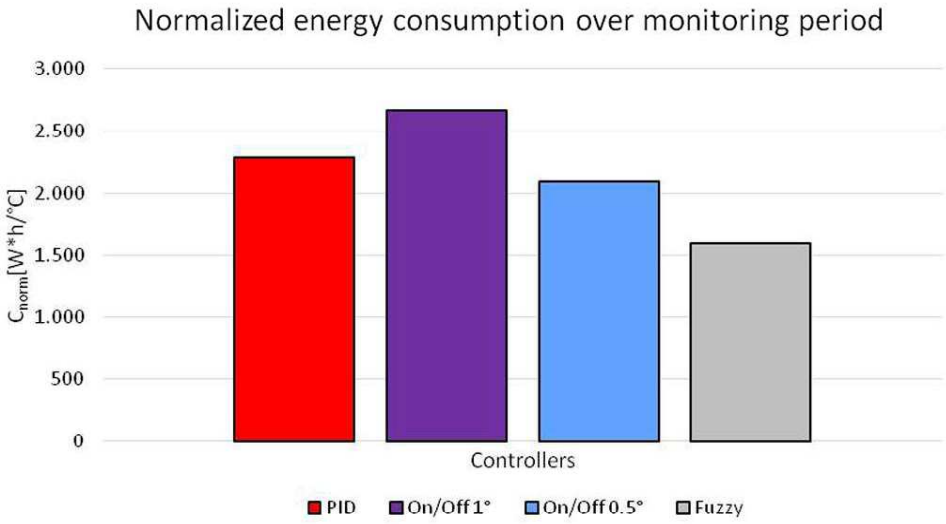


Figure 2.12
Normalized energy consumption ortogram.

2.8.1.2 Energy signatures

Energy signatures were obtained plotting hourly averaged power consumption in function of an external parameter. The line interpolating the cloud of points represented building-technical system combined energy performance.

In the present research, the selected external parameters were outdoor air temperature and global solar radiation, because of their direct influence in the heating process.

The linear regression curve adopted is described by the following equations:

$$y = A + Bx \tag{2.12}$$

$$A = \frac{[(\sum x_i^2) * (\sum y_i) - (\sum x_i) * (\sum y_i^2)]}{\Delta} \tag{2.13}$$

$$B = \frac{[N(\sum x_i * y_i) - (\sum x_i) * (\sum y_i)]}{\Delta} \quad (2.14)$$

$$\Delta = N\left(\sum x_i^2\right) - \left(\sum x_i\right)^2 \quad (2.15)$$

where y represents the consumed power [W], x the corresponding outdoor temperature [°C] or solar radiation [W/m²], A and B are the intercept and slope constants, respectively, describing the regression lines. A and B are the comparison parameters.

The results for the four tested settings of the controllers were presented in the form of:

- tables (**table 2.11, table 2.12**) relating controlling periods average x values to regression lines equations;
- charts (**figure 2.13, figure 2.14**) overlapping the regression lines and enabling direct assessment of the main differences.

ENERGY PERFORMANCE ASSESSMENT (2)				
Controller	**Period**	**Outdoor Temperature (daily average) [°C]**	**Set-point [°C]**	**Energy signature [line equation]**
PID	15/01/2015 16/01/2015 17/01/2015 18/01/2015 19/01/2015 20/01/2015	10.94 11.01 13.44 9.79 5.72 5.94	20	y = -9.7923x + 241.71
On/Off 1°	27/01/2015 28/01/2015 29/01/2015 30/01/2015 31/01/2015 01/02/2015	4.12 4.90 5.91 7.53 7.33 3.84	20	y = -4.4065x + 279.41
On/Off 0.5°	25/02/2015 26/02/2015 27/02/2015 28/02/2015 01/03/2015 /	7.08 9.72 8.99 8.94 7.52 7.13	20	y = -8.9049x + 247.56
Fuzzy	30/03//2015 31/03/2015 01/04/2015 02/04/2015 03/04/2015 04/04/2015	17.67 17.83 14.68 13.99 11.30 9.19	20	y = -7.4133x + 170.09

Table 2.11
Outdoor temperature related energy signature line equations.

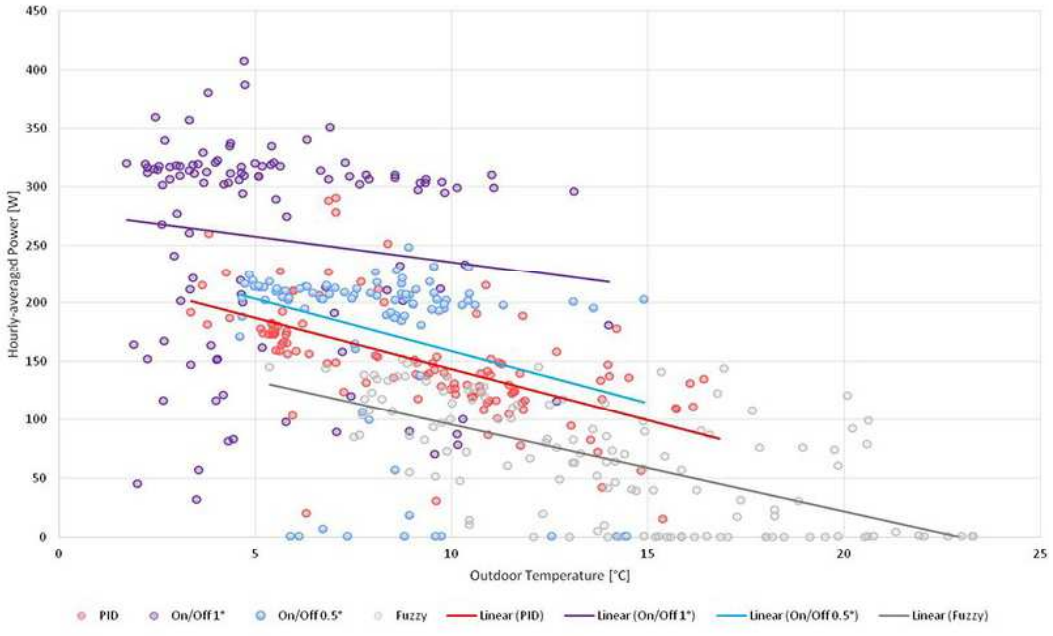


Figure 2.13
Energy signature regression lines relating power consumption to outdoor air temperature.

ENERGY PERFORMANCE ASSESSMENT (3)				
Controller	**Period**	**Solar radiation (daily average) [W/m²]**	**Set-point [°C]**	**Energy signature [line equation]**
PID	15/01/2015 16/01/2015 17/01/2015 18/01/2015 19/01/2015 20/01/2015	228.77 207.52 165.37 107.25 235.28 31.73	20	y = 0.0119x + 152.4
On/Off-1°C	27/01/2015 28/01/2015 29/01/2015 30/01/2015 31/01/2015 01/02/2015	200.86 184.30 151.10 117.40 271.38 113.84	20	y = -0.0237x + 273.07
On/Off-0.5°C	25/02/2015 26/02/2015 27/02/2015 28/02/2015 01/03/2015 /	163.50 83.46 83.11 195.36 359.55 /	20	y = -0.0028x + 168.04

Fuzzy	30/03//2015	359.97	20	y = -0.0118x + 69.139
	31/03/2015	293.44		
	01/04/2015	262.13		
	02/04/2015	243.05		
	03/04/2015	236.70		
	04/04/2015	98.58		

Table 2.12
Solar radiation related energy signature line equations.

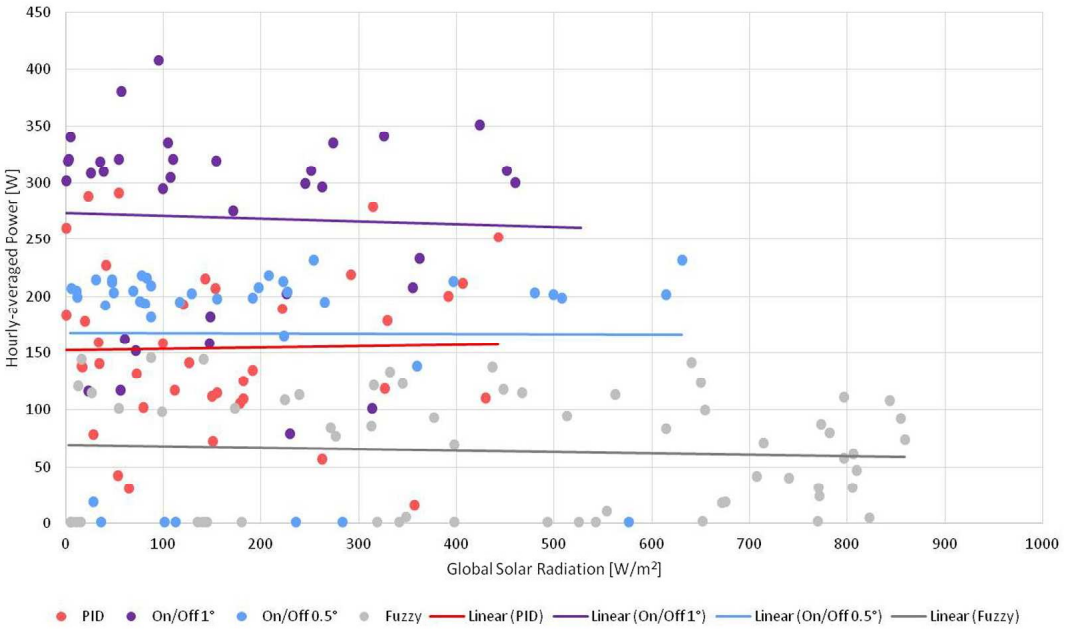


Figure 2.14
Energy signature regression lines relating power consumption to global solar radiation.

Both the energy signature typologies showed the same trend:

- the best energy saving performance was achieved by the fuzzy controller, which regression line lied below all the others. When outdoor temperature was 0°C, power consumption was about 64% lower than using on/off-1°C and over 40% lower than using the other controllers. Even if the slope constant was not the highest absolute value (20–30% less sensitive than PID and on/off-0.5°C) it significantly reduced the power consumption with increasing outdoor temperature. In the solar radiation energy signature, the gap was even greater because all regression lines were quite horizontal (denoting a

substantial insensitiveness to solar incomes for all the regulation systems) while the intercept was, in every case, less than half the others.

- The highest power consumption was recorded with the on/off-1°C controller in terms of response both to outdoor average temperature and solar radiation. It was an expected result since this regulation system was the less refined one and delivered full power until the ambient temperature filled the 1°Cgap between turn-on and turn-off temperatures. Consequent inertial phenomena typically produced significant overshoots penalizing the comfort performance too (**see next paragraph**).
- PID and on/off-0.5°C controllers showed an intermediate energy performance. Their behaviour during cold and cloudy days was very similar: intercepts differed of almost 6 watts in the outdoor temperature energy signature and of almost 16 watts in the solar radiation one (greater values were always recorded with the on/off controller). But the sensitiveness to outdoor temperature increase was much higher in the PID case since the slope constant was 10% greater than that recorded in the on/off-0.5°C regression line (and the highest one between all tested controllers).

The conclusion was that the most energy efficient controller to be coupled with the electrical radiators installed in the hyper-isolated mock-up was the fuzzy one. The second choice was a PID controller to be tuned with a trial and error method in presence of real working boundary conditions. However, a simpler on/off controller, with a hysteresis of 0.5°C performed in a similar way, in particular when outdoor temperatures and direct solar radiation were almost zero. The most energy consuming controller was the on/off-1°C since its power consumption was about three times the fuzzy one in the solar radiation energy signature and over +60% in the outdoor temperature energy signature.

2.8.2 Indoor thermal comfort

Comfort assessment was conducted from two perspectives:

- global evaluation through the calculation of PMV and PPD, chartered and averaged over the entire monitoring period of each controller: charts allowed a qualitative assessment of the oscillating trend of the comfort indices (useful for building categorization according to the UNI EN ISO 7730 **[2.14]** classification (**table 2.13**), while averaged values returned a quantitative assessment of the overall perceived thermal satisfaction;
- long-term performance evaluation, through the calculation of the excess weighted PPD, according to the prescriptions of EN 15251 Standard **[2.31]**. It takes into account not just the magnitude of global comfort/discomfort

perceived, but the duration of each predicted sensation too. In this way it was possible to discriminate control systems which reached greater discomfort values, but just for very restricted periods of time, from those control systems which provoked slight discomfort perception but for extended periods of time.

By analysing PMV and PPD time trends (**figure 2.15**) (without taking into account the spikes related to anomalous working conditions), it was concluded that:

- the on/off-1°C controller was the one producing more discomfort situations among all tested logics: PMV chart oscillated from 0.2 and 0.8 entering and exiting category I, II and III. PPD chart oscillated of about 5% from an average value of 10%. This means that just half the time it guaranteed the respect of the boundaries for a medium-level of expectation building (category II);
- the on/off-0.5°C controller, instead, maintained for all the monitoring period a general comfort condition: PMV chart, even if highly oscillating (typical trend of on/off systems), lied within the 0.2–0.5 range, guaranteeing constant thermal neutrality for category II buildings. PPD chart oscillated around 6%, overcoming the 10% limit for relatively short periods of time;
- the PID controller achieved a good comfort performance: PMV respected category II limits for all the monitoring period, with minimal variations around the average value of 0.1. The PPD chart obviously reflected the same PMV trend, lying below 10% for almost all the time and stabilizing on an average value of about 5%;
- the fuzzy controller guaranteed the best comfort performance: PMV was, by far, within the category II boundaries with an average value of 0.26 and a variability range of 0.04–0.44. PPD chart lied on an average value of 6.4%, never overcoming the10% limit.

By analysing **table 2.14** results obtained for average PMV, average PPD and PPD.h (over the entire monitoring period), some conclusions could be drawn:

- according to an average PMV-PPD evaluation, the PID controller was the best system in terms of comfort performance. It ensured almost a perfect thermal neutrality and the lowest percentage of dissatisfied people;
- according to a long-term evaluation, the fuzzy controller achieved the highest stability and an ideal comfort performance totalizing a PPD.h of 0. However, PID controller's performance was, by far, the closest one, with a PPD.h of 0.63. The on/off controller, set with a hysteresis of 1°C, was responsible of the worst comfort management: it recorded the highest percentage of people dissatisfied by the surrounding microclimate and, at the same time, the longest cumulative period exceeding category II comfort limits (52.33 h), almost one third of the total monitoring period. The on/off-0.5°C controller improvement was substantial: in terms of average PMV-PPD it achieved a comfort performance

even more virtuous than the fuzzy controller, while in terms of PPD.h, the value of 2.60 made it competitive with all the other non-on/off systems.

COMFORT-BASED BUILDING CATEGORIES						
Category	**Thermal state of the body as a whole**		**Local discomfort**			
	PPD [%]	**PMV**	**DR [%]**	**PD [%] caused by**		
				vertical air temperature difference	**warm or cool floor**	**radiant asymmetry**
A	< 6	-0.2 < PMV < +0.2	< 10	< 3	< 10	< 5
B	< 10	-0.5 < PMV < +0.5	< 20	< 5	< 10	< 5
C	< 15	-0.7 < PMV < +0.7	< 30	< 10	< 15	< 10

Table 2.13
UNI EN ISO 7730:2006 - Categories of thermal environment.

COMFORT ASSESSMENT			
Controller	**Comfort indices**		
	PPD %	**PMV**	**PPD.h**
PID	5.20	0.10	0.63
On/Off-1°	8.83	0.43	52.33
On/Off-0.5°	5.57	0.17	2.60
Fuzzy	6.36	0.26	0.00

Table 2.14
Time-averaged PPD and PMV and PPD.h values for each control system.

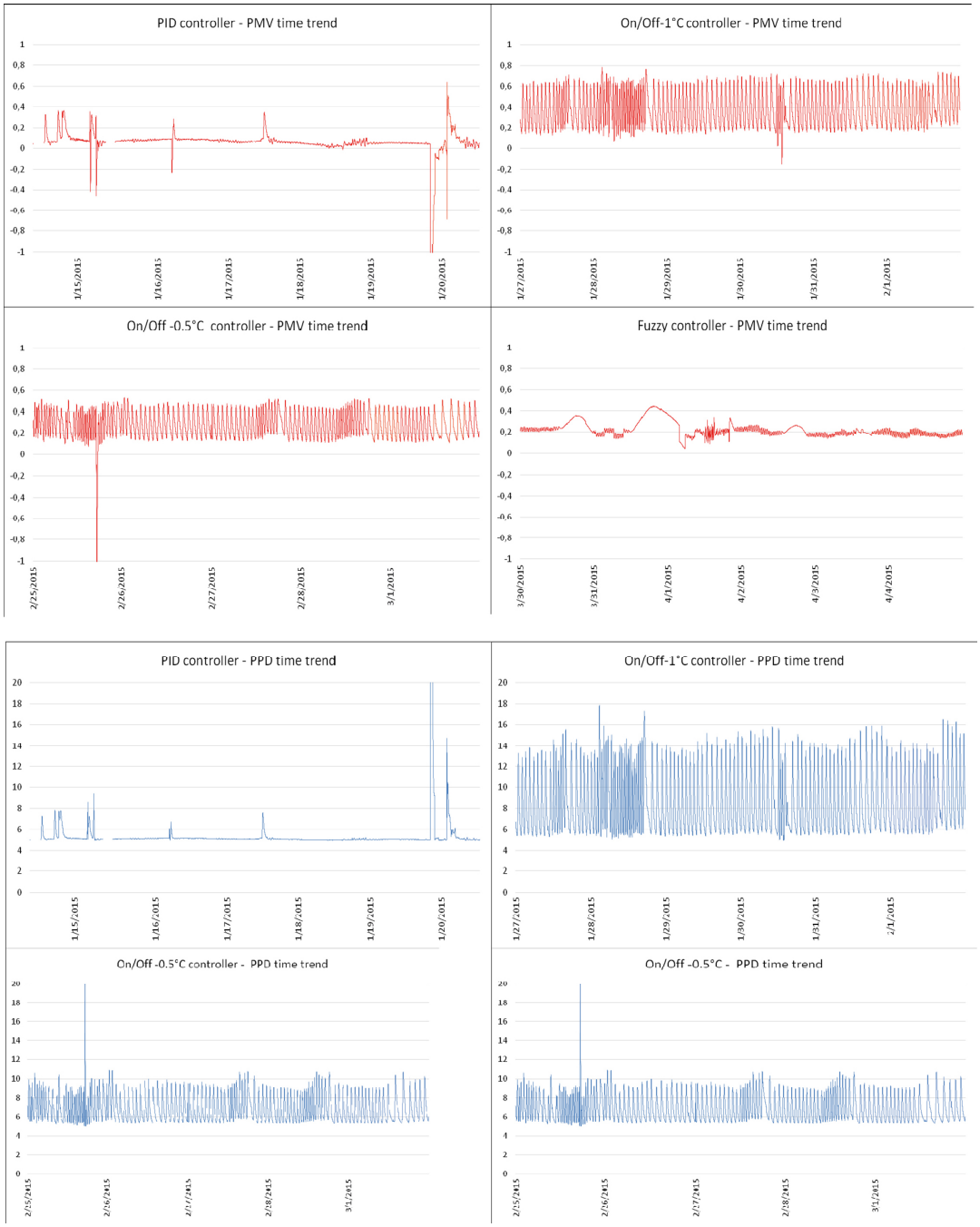


Figure 2.15
Predicted mean vote and predicted percentage of dissatisfied people charts over the entire monitoring period.

2.9 – CONCLUSIONS

An experimental and numerical study **[2.34]** was carried out in order to compare different regulation solutions applied to the heating system of an energy efficient small-scale building, composed by three electric radiators. The control logics under test were:

- on/off controller, set with a hysteresis value of 1°C;
- on/off controller, set with a hysteresis value of 0.5°C;
- PID controller, set with a proportional band of 2°C, an integral time of 10 minutes and no derivative action;
- fuzzy controller, acting as a MISO (multiple input, single output) system in function of actual ambient temperature, its derivative and outdoor air temperature.

Each regulatory configuration was tested for 10 days in a single room, hyper-isolated mock-up (used as case study), equipped with three different monitoring stations, in order to get a full database about indoor and outdoor climate conditions, heating emission status and building thermal behaviour.

Post-processing and assessment procedures were conducted over 5/6 days of validated data. Evaluation was made from both the perspectives of energy consumption and comfort performance. Energy analyses were carried out applying:

- an analytical approach, by normalizing energy consumption over the absolute value of the difference between time-averaged ambient and outdoor temperatures;
- a graphical approach, by plotting building energy signatures in function of outdoor air temperature and global solar radiation.

Comfort analyses were carried out applying:

- a qualitative approach, by observing PMV and PPD time trends over each monitoring period;
- a quantitative approach, by calculating PMV and PPD averaged values and excess weighted PPD (PPD.h) as long-term comfort index.

The results highlighted that the fuzzy controller achieved the best energetic-ergonomic combined performance, offering, at the same time, the lowest energy consumption and the highest comfort level.

In particular, data analyses outlined:

- 67.8%, 43, 8% and 31.4% benefit in terms of normalized energy consumption, compared respectively to the on/off-1°C con-troller, the PID controller and the on/off-0.5°C controller;
- 64% and over 40% energy saving observing the outdoor temperature energy signature, compared respectively to on/off-1°C and the other controllers. The benefit increased between 50% and 300% in the case of the solar radiation energy signature;

- even if the most comfortable averaged values of PMV and PPD were those recorded with the PID controller, the fuzzy logic was the only one never provoking discomfort conditions, totalizing a PPD.h equal to zero. As a consequence, it achieved the best comfort performance in terms of stability.

Among the other controllers, PID guaranteed an optimal combined performance, close to the semi-ideal one achieved by using the fuzzy logic. The on/off-1°C controller resulted (as expected) the worst in terms both of energy consumption, comfort level and comfort stability.

However, halving the hysteresis value, the over-all performance improved significantly, becoming comparable to fuzzy and PID alternatives. Nevertheless, on/off-0.5°C controller maintained the highly oscillating trend typical of all on/off systems.

Anyway, it has to be underlined that the above-exposed result scan be considered effective just in presence of boundary conditions similar to those experienced in this specific case (Mediterranean climate, hyper-isolated building, no occupancy) and may lose their validity as one or more of these parameters changes. Further research will be carried out in the future to extend their applicability and integrate the effects of different occupancy patterns, different climate zones, different building specifics.

REFERENCES

[2.1] EN 15316, Heating systems in buildings, 2008.

[2.2] EN 15316-2.1, Heating systems in buildings – Method for calculation of system energy requirements and system efficiencies – Part 1: General,2008.

[2.3] A.I. Dounis, C. Caraiscos, Advanced control systems engineering for energy and comfort management in a building environment — a review, Renew. Sustain. Energy Rev. 13 (2009) 1246–1261.

[2.4] Z. Liao, M. Swainson, A.L. Dexter, On the control of heating systems in the UK,Build. Environ. 40 (2005) 343–351.

[2.5] L. Peeters, J. Van der Veken, H. Hens, L. Helsen, W. D'Haeseleer, Control of heating systems in residential buildings: current practice, Energy Build. 40(2008) 1446–1455.

[2.6] I. Hazyuk, C. Ghiaus, D. Penhouet, Model Predictive Control of thermal comfort as a benchmark for controller performance, Autom. Construct. 43(2014) 98–109.

[2.7] Legge ordinaria del Parlamento n°373/76, Norme per il contenimento del consumo energetico per usi termici negli edifici, 1976.

[2.8] NTC2008 – Norme tecniche per le costruzioni, D.M., 14 Gennaio 2008.

[2.9] P.R.G.C. Agugliano (AN), Italy, 2011.

[2.10] ISO 13786, Thermal performance of building components – Dynamic thermal characteristics - Calculation methods, 2007.

[2.11] UNI EN 13829, Thermal Performance of Buildings – Determination of Air Permeability of Buildings – Fan Pressurization Method, 2002.

[2.12] ISO 7726, Ergonomics of the thermal environment – Instruments for measuring physical quantities, 1998.

[2.13] ISO 7726, Influence of Measurement Uncertainties on the Thermal Environmental Assessment, International Organization for Standardization,2012.

[2.14] ISO 7730, Ergonomics of the thermal environment – analytical determination and interpretation of thermal comfort using calculation of the PMV and PPD indices and local thermal comfort criteria, International Organization for Standardization, 3rd edition, 2006.

[2.15] M. Sen, A review of principles and applications of thermal control, Journal of the Mexican Society of Mechanical Engineering 1.4 (2004): 115-131.

[2.16] UNI TS 11300-2, Energy performance of buildings – Part 2: Evaluation of primary energy need and of system efficiencies for space heating, domestic hot water production, ventilation and lighting for non-residential buildings,2014.

[2.17] D. Meneghel, M.E. Valcher, PID: design techniques and implementation issues, 2009/2010.

[2.18] W. Tan, J. Liu, T. Chen, H.J. Marquez, Comparison of some well-known PID tuning formulas, Comp. Chem. Eng. 30 (2006) 1416–1423.

[2.19] Q.-G. Wang, Handbook of PI and PID Controller Tuning Rules, Aidan O'Dwyer, Imperial College Press, London, 2003, 375pp, ISBN 1-86094-342-X.
[2.20] A.I. Dounis, M.J. Santamouris, C.C. Lefas, Building visual comfort control with fuzzy reasoning, Energy Conversion and Management, Volume 34, Issue 1, January 1993, Pages 17-28
[2.21] Babuska R, Verbruggen HB. An overview of fuzzy modeling for control. Control Eng Pract 1996;4(11):593–606.
[2.22] J. Mendel. Fuzzy logic systems for engineering: a tutorial. Proceedings of the IEEE, 83(3):345–377, Mar 1995.
[2.23] National Instruments, LabVIEW™ PID and Fuzzy Logic Toolkit User Manual, June 2009.
[2.24] 95/05548 Performance lines and energy signatures – analysis with reference to the CIBSE building energy code, Fuel Energy Abst. 36 (September (5) (1995) 384.
[2.25] F. Flouquet, Local weather correlations and bias in building parameter estimates from energy-signature models, Energy Build. 19 (2) (1992)113–123.
[2.26] F.W. Yu, K.T. Chan, Energy signatures for assessing the energy performance of chillers, Energy Build. 37 (7) (2005) 739–746, 06/01019.
[2.27] A. Rabl, A. Rialhe, Energy signature models for commercial buildings: test with measured data and interpretation, Energy Build. 19 (2) (1992) 143–154.
[2.28] L. Belussi, L. Danza, Method for the prediction of malfunctions of buildings through real energy consumption analysis: holistic and multi-disciplinary approach of Energy Signature, Energy Build. 55 (December) (2012) 715–720.
[2.29] P.O. Fanger, Thermal Comfort Analysis and Application in Environmental Design, McGraw-Hill, New York, NY, 1972.
[2.30] S. Carlucci, L. Pagliano, A review of indices for the long-term evaluation of the general thermal comfort conditions in buildings, Energy Build. 53 (2012)194–205.
[2.31] CEN Standard EN 15251, Indoor environmental input parameters for design and assessment of energy performance of buildings addressing indoor air quality, thermal environment, lighting and acoustics, CEN, Brussels, 2007.
[2.32] B.W. Olesen, M. de Carli, Long term evaluation of the general thermal comfort conditions, in: Proceedings: Indoor Air, 2002.
[2.33] B.W. Olesen, M. de Carli, Field measurements of thermal comfort conditions in buildings with radiant surface cooling systems, in: Clima 2000/Napoli 2001World Congress, Napoli (I), 15–18 September, 2001.
[2.34] G. Ulpiani, M. Borgognoni, A. Romagnoli, C. Di Perna, Comparing the performance of on/off, PID and fuzzy controllers applied to the heating system of an energy-efficient building, Energy and Buildings, Volume 116, 15 March 2016, Pages 1-17.

3

Smart control of window openings

Maximizing indoor air quality and thermal comfort through a customized adaptive comfort algorithm, tailored for classrooms requirements.[1]

[1] Published in Energy and Buildings, Volume 139, 15 March 2017, Pages 732-746

3.1 – ABSTRACT

Thermal comfort and indoor air quality assume a deeper meaning when it comes to school environments as they represent essential requirements for the correct accomplishment of the core functions on which teaching and learning processes rely on.

Staying on target, keeping attention and concentration are delicate matters, remarkably sensitive to diverse sources of distraction, included poor environmental quality.

Against this general backdrop, an experimental activity was conceived to investigate how an automatic system for window openings (based on thermal comfort and indoor air quality correlations) could enhance students' and teachers' productivity, reduce the number and magnitude of adaptive actions to restore users' comfort zone and prevent health symptoms/absenteeism.

The research involved two parallel monitoring campaigns run in that many similar and adjacent classrooms. As a starting point, a series of assessments were carried out to dig into:

- existing environmental conditions in the classrooms;
- contingent validity of objective and subjective comfort models proposed in literature for similar purposes;
- trigger parameters discriminating the occurrence of window opening events.

Once these pieces of information had been gathered, a basic scheme of the inputs and outputs of the control system was drafted. An ACA (Adaptive Comfort Algorithm) was finally applied and tuned according to the specs of the case study (climatic conditions and occupancy patterns fundamentally).

The final goal of the implemented automatic system was an optimized management of the hopper windows opening/closing loops in terms of both IAQ (Indoor Air Quality) and thermal satisfaction. The main challenge was to properly cope with the CO_2 content in the air, since it is a major source of loss of mental acuity/somnolence and it is far less detectable by the users until it reaches alarming levels.

Just one of the classrooms was geared with the motor actuators while the "twin" adjacent classroom served as reference for the sake of comparison.

The research findings underpinned the relevance of IAQ control in school environments and confirmed, on the other hand, the key role of temperature in maintaining environmental satisfaction. Indeed, it was concluded that "the stronger driving force for undertaking adaptive actions is thermal comfort, while the need to improve the air quality is a secondary constraint", but easily underestimated and likely to jeopardize the liveability of school places.

Moreover, the efficacy of the proposed automatic system was demonstrated via objective and subjective analyses.

3.2 – INTRODUCTION

School classrooms represent a challenging environment on which applying and testing comfort theories as the need to preserve a pleasant and healthy microclimate, suitable for teaching purposes, is a major issue, considering that students can spend most of their time **[3.1-3.3]** inside such living spaces.

Air temperature and air quality are discriminatory. The natural consequence is that the paramount means of manipulating the comfort parameters is governing the air ventilation. This can be done resorting to all the building physics phenomena enhancing air circulation from cross ventilation to VMC (Controlled Mechanical Ventilation). Indeed, inadequate ventilation rates have been identified to be common source of user's declining performances and growing absenteeism **[3.4,3.5]**. In particular, carbon dioxide levels tend to rise in an almost unnoticed way, thus overtaking healthy thresholds very frequently before any kind of corrective action is performed **[3.6,3.7].**

Furthermore, classrooms are typical built environments were adaptive comfort theories apply. "Adaptive" means that "if a change occurs such as to produce discomfort, people react in ways which tend to restore their comfort" **[3.13].**

Therefore, whenever occupants have non negligible access to environmental controls, (engaged in sedentary activities with metabolic rates of 1-1.3 met and prevailing mean temperature falls within 10°÷33.5°C) the new-born adaptive theories should be preferred to the traditional PMV-PPD based method (**see chapter 2**).

Classrooms are typically approached in an adaptive way since users (either students and teachers) might actively interact with the thermal surrounding, applying means of acclimatization and control in order to keep and restore their environmental satisfaction: a wider thermal tolerance has to be considered likely to occur.

Moreover, classrooms are highly responsive to thermo-hygrometric inputs, because:

- their "small" dimensions (compared to commercial blocks, gyms, theatres…) allow greater and more frequent variability;
- fluctuating internal gains can rapidly affect indoor temperature;
- variation in occupancy pattern can modify the required ventilation rate;
- nearly all forms of behavioural adaptation are applicable within small time slots (operating windows and fans, adjusting blinds/shades, changing clothes, consuming food and drinks…).

Finally, many scientific papers demonstrate that the adaptive model is the most proper and realistic one when natural ventilation is applied to enhance air circulation (instead of mechanic or mixed modes). For instance, following a sort of reductio ad absurdum approach, Humphreys and Nicol checked out the validity of Fanger's steady-state comfort theory **[3.14,3.15]** and drew the conclusion that it remarkably fails in reflecting human real tolerance to both frequency and extent of temperature

deviations from the comfort zone. Therefore, most of the discomfort phenomena detected in compliance with UNI EN ISO 7730 methodology **[3.16]** weren't actually experienced by the users **[3.17,3.18].**

Later on, their findings were scientifically substantiated by de Dear and Brager **[3.19]** as well as various other researchers **[3.20,3.21].**

Shifting from the traditional method (rooted in Fanger's studies) to the adaptive methods (rising from the experimental researches by M.A. Humphreys, J.F. Nicol, R. de Dear, G. Brager…) entails a series of aftermaths, summarized in **table 3.1**:

PMV/PPD METHOD	ADAPTIVE METHOD
Based upon principles of heat balance and experimental data collected in a controlled climate chamber under steady state conditions	Based upon data collected from field studies without forcing control parameters under dynamically changing conditions.
Passive users, wearing standardized uniforms and executing sedentary activities	Active users in everyday life
Suitable to indoor air conditioned buildings	Suitable to buildings with no (running) mechanical conditioning system.
Acceptable comfort temperature ranges very narrow	Wider acceptable comfort temperature ranges
Constant optimal comfort temperatures (according to the six independent parameters)	Variable optimal comfort temperature (according to a wider set of involved parameters)
No consideration for outdoor conditions	Strict relation between outdoor conditions and indoor thermal expectancy
Typically energy-consuming approach	Typically comfort/sustanaibility bivalent approach

Table 3.1
Comparing PMV/PPD and adaptive comfort models.

Accordingly, the equations and algorithms to be applied in order to identify the comfort temperatures and IAQ settings have to take into account the two pillars of adaptive theory:

1) users' activeness and the wider range of environmental conditions they are able to tolerate without sacrificing their comfort zone;
2) outdoor climate influence on indoor comfort (plus past thermal history as it affects building occupants' thermal expectations and preferences).

In recent years, many different ACAs have been proposed **[3.9–3.12]** to translate into practice this user-centred approach with the final aim of foreseeing time and type of adaptive actions descriptive of the average-user behavioural patterns.

Humphreys and Nicol formulated two equations to calculate the comfort temperature in free-running buildings **[3.22].** The results of their application were tested and trimmed for various climatic areas **[3.8].** Finally, the equations got transposed into various Standards (ASHRAE, ATL CEN, CIBSE).

On the other side, particular emphasis was given to find suitable ACAs to drive the operation of windows. The reason behind is that such adaptive pattern is the most recurrent one whatever the intended use of the building is **[3.23].**

However, the great majority of windows-related ACAs were tailored for residential **[3.24–3.26]** and commercial sectors **[3.9,3.10,3.27,3.28]**, while little space was reserved to the academic environment **[3.6].**

Against this lack of specific information, Humphreys adaptive algorithm **[3.11]** was identified as the proper basic logical structure to kick-start the tuning process on the peculiar requirements of the case study, since:

- it is based on an officially recognized adaptive comfort theory (as above mentioned);
- it requires few environmental parameters to be detected thus sustaining its potential applicability in various real conditions;
- it is easily adjustable to various environmental conditions since no a priori assumptions on metabolic rates, clothing insulation and IAQ requirements are embedded and driven to a fixed value.

Therefore, even if the original algorithm was shaped on office buildings requirements, its structure (summed up in **table 3.2**) is highly scalable to meet other end-use environments specs.

A) HUMPHREYS' ALGORITHM

No.	Window algorithm parameter	Symbol	Sample	Derivation or source
1	Outdoor air temperature	T_{out}	1 per hour	Interpolated from climate file (hourly data in file)
2	Daily mean outdoor air temperature	T_{odm}	1 per day	Calculated from 24 hourly data points per day
3	Running mean outdoor temperature (CEN)	T_{rm}	1 per day	$T_{rm}(init) = (1-a)(T_{odm-1} + a\,T_{odm-2} + a^2\,T_{odm-3}\ldots)$ initial value calculated from previous 20 days daily mean, then $T_{rm} = (1-a)T_{odm-1} + aT_{rm-1}$
4	Running mean response to Tout	a	Const	Default a=0.8 (0.01–0.99 allowed range)
5	Comfort temperature	T_{comf}	1 per day	If $T_{rm} > 10$, $T_{comf} = 0.33\,T_{rm} + 18.8$ (CEN Standard (1)) If $T_{rm} \leq 10$, $T_{comf} = 0.09\,T_{rm} + 22.6$ (CIBSE Guide A(2))

6	Indoor air temperature	T_{ai}	1 per hour	Available at each timestep
7	Indoor operative temperature	T_{op}	1 per hour	Available at each timestep (50% mrt, 50% Tai)
8	Comfort	Comf	1 per hour	Comf = "yes" if abs (T_{op}- T_{comf}) ≤2 K Comf = "hot" if (T_{op}- T_{comf}) >2 K Comf =" cold" if (T_{op}- T_{comf}) <−2 K
9	Logit function	Func	1 per hour	Func = logit(P_W) = 0.171 T_{op} + 0.166 T_{out}- 6.43
10	Probability function for window open	P_W	1 per hour	P_W = exp(Func)/(1 + exp(Func))
11	Random number between 0 and 1	R_n	1 per hour	Generate from Fortran RNG
12	Windows status (0 = closed, 1 = open)	iwin	1 per hour	If Comf = "hot" and window closed (w = 0) then if P_W> R_n then window open (w = 1) If Comf = "cold" and window open (w = 1) then if R_n > P_W then window closed (w = 0)

(B) MODIFIED/INTEGRATED INPUTS OF HUMPHREYS ALGORITHM				
8		Comf	1 per minute	Comf = "yes" if abs(T_{op}- T_{comf}) ≤1 K Comf = "hot" if (T_{op} – T_{comf}) >1 K Comf = "cold" if (T_{op} – T_{comf}) <−1 K
8 bis		CO_2	1 per minute	Available at each timestep (variable)
8 ter		CO_2 limit	Const	CO_2 limit = 1250 ppm
12	Windows status (0 = closed, 1 = open)	iwin	1 per minute	If CO2 >1250PPM and window closed (w=0) then window open (w = 1) If Comf = "hot" and window closed (w = 0) then if Pw> Rn, then window open (w = 1) If Comf = "cold" and window open (w = 1) then if Rn > Pw then window closed (w = 0)

Table 3.2
Steps in the implementation of the (a) Humphreys' algorithm from the literature and (b) modified/integrated inputs in the proposed version.

Given that either offices and classrooms present a quite narrow variability in terms of met and clo, no amendments to the original scheme were applied to account for a wider range of activity rates or outfits **[3.29].** Hence the metabolic rate is the sedentary one in both case (met: 1.1 according to ISO 7730 Table B.1) and the

thermal insulation provided by the garments is substantially constant along each season **[3.30].**

Besides, another similarity between the two indoor microclimates consists in the prevailing occupancy pattern, which is not a remarkably intermittent one (applicable for residential buildings) but an almost continuous profile. As a matter of fact, it is well acknowledged that students' lifestyle allows for spending the vast majority of time indoors, inside the classrooms in particular **[3.1-3.3].**

The main consequence is that a strong adaptation from outdoor climate conditions to indoor climate conditions occurs just in the early morning, thus a total disregard for transient thermal perceptions leads to negligible inaccuracies.

Conversely, CO_2 is a pivotal variable for classrooms environmental quality since high carbon dioxide limits are likely to be overtaken and represent a major issue every time small, reasonably tight, air volumes are coupled with high-density occupancy **[3.31],** regardless of the specific climatic zone **[3.32].** Hence its inclusion in the algorithm among the other decision-making parameters wad deemed compulsory, being IEQ (Indoor Environmental Quality) the final goal.

As an evidence supporting this claim, several studies all around the world **[3.33,3.34]**, including Italy **[3.35,3.36]** and involving European projects as well **[3.41,3.42]**, addressed the issue of IAQ inside school environments and the vast majority remarks poor indoor ventilation rates and high CO2 concentration **[3.37–3.40].** Few solutions which do not take advantage of mechanical ventilation are yet proposed [**3.43].**

In order to cope with this contextual lack, this research activity was conceived to build up an automatic system driving windows operation in order to adjust natural ventilation rates to the target temperature defined by an ad-hoc developed adaptive comfort algorithm.

The proposed control logic can be represented as a black box, receiving in input temperature and CO_2 concentration real time recordings and returning in output a Boolean value which defines the status of the mechanical actuators moving the hopper windows.

Moreover, the study could rely on the availability of a solid and wide set of experimental data, collected during a previous monitoring campaign run in the same school building, which served as benchmark for the planning and the design of the entire survey.

3.3 – METHODOLOGY

The experimental study was structured according to the following roadmap:

1) Characterization of the "undisturbed" baseline through on-site data collection in order to depict the "as is" condition and detect the potential of an automatic management of the natural ventilation over user's thermal comfort and IAQ concerns.
2) Post processing of the recordings to identify trigger parameters and comfort models suitable to properly intervene on windows operation.
3) Design and physical installation of the automatic system in charge of driving opening/closing looping of the hopper windows.
4) Monitoring campaign run simultaneously in two thermo-dynamically equal classrooms, one in free-running mode to serve as benchmark and the other equipped with the ACA-driven mechanism.
5) Data analysis and multi-perspective comparisons to highlight pros and cons of the proposed intervention and define means and methods to achieve further improvement.

In order to satisfy the first point, indoor and outdoor environmental parameters were recorded, while occupancy patterns and users' actions on windows were noted as well.

The second step led to the identification, by comparing a certain number of ACAs proposed in literature, of the one better matching user's behavioural patterns and trigger parameters emerging from on-site data analyses.

The following point in the strategic roadmap required to assemble and program the various hardware and software elements composing the automatic system. An ad hoc structure was realized in order to break loose from the dependency on proprietaries command languages and market products thus allowing for in-itinere modification of the control logic to explore the aftermaths of tuning actions.

The fourth step was accomplished by acquiring environmental and windows status information for both the classrooms in parallel. Therefore, both ACA-driven and user-driven management of indoor thermal comfort and air quality were tested.

Finally, the comfort benefit and the energy saving achieved in the motorized classroom was highlighted by:

- comparing the per cent dissatisfaction expressed towards the surrounding microclimate in both classrooms, assessed by diverse means of objective and subjective investigation;
- comparing the maximum deviation from the comfort zone and stableness of control of the indoor operative temperature;

- outlining the efficacy of the wash effect adduced by the wind coming from outdoors according to different boundary conditions and typology of windows operation.

3.4 – CASE STUDY

Automated HVAC systems and environmental controls are going to be more and more widely used throughout the building sector, in particular the residential quote (domotics) and the public one.
Smart components will be directly embedded in the new-built environment since regulation efficiency is gaining ground among the means of matching EPDB requirements.
In this context, a recently built secondary school (2010) was selected as case study for this experimental activity. The institute is representative of the Italian typical school buildings in terms of:

- occupancy patterns, occupancy density and timetable;
- floor area and air volume;
- HVAC equipment (manually-operated windows, radiators-based heating system, no cooling system)

Besides the same building was investigated in previous researches, focused on thermal comfort as well, thus coming with an extensive ready-to-use set of monitored dataset **[3.44].**
Basic geographical and climatological information are provided in **table 3.3**:

SECONDARY SCHOOL "PODESTI – CALZECCHI ONESTI"	
Location	Ancona (Central Italy)
Latitude	43°58'49''30 N
Longitude	13°52'57''01 E
Altitude amsl	67 m
Climate	hot-summer Mediterranean climate (Köppenclimatic classification)
heating degree days	1688
Surroundings	residential zone, no traffic-noise

Table 3.3
Case study geographic features.

From a constructive point of view, the external envelope is composed by insulated cavity walls for what concerns opaque elements, while transparent surfaces are made

of two-per-classroom, double-glazed windows in aluminium frame, each one structured into a casement plus top hopper window unit.
As the final aim of the project was to install and test ah highly efficient, comfort-oriented, automatic controller of the air ventilation, no instrumentation was applied to the casement window: just the hopper one was geared to open and close according to the ad-hoc tuned ACA. In this way no local discomfort phenomena due to air draughts could be associated to the change made on the fenestration. Furthermore, a well-conceived, fine regulation system needs to handle small "packages" of air incomes in order to avoid excessive wear and tear of the mechanical components and avoid excessive oscillation of the indoor air temperature. By mechanizing the opening loop of the casement windows both these conditions couldn't be respected. Additionally, the operation of such windows was forbidden to the users throughout the monitoring period to isolate and assess the effects of the sole automatic controller.
That was the "motorized" configuration imposed to one of the ground floor classrooms (named "MT" from now on). A second adjacent classroom, similar to the former in terms of exposition (north-west), volumetry, occupancy (16/17 students aged between 14 and 15 years) and timetable (lessons scheduled from 8:00am to 2:00pm from Monday to Friday) was simultaneously conducted in "free-running" to provide the baseline for comparisons on equivalent boundary conditions (named "FR"). The location and global clearances are visualized in **figure 3.1**, while **table 3.4** adds details to the tested spaces. FR classroom layout is further characterized in **figure 3.2**.

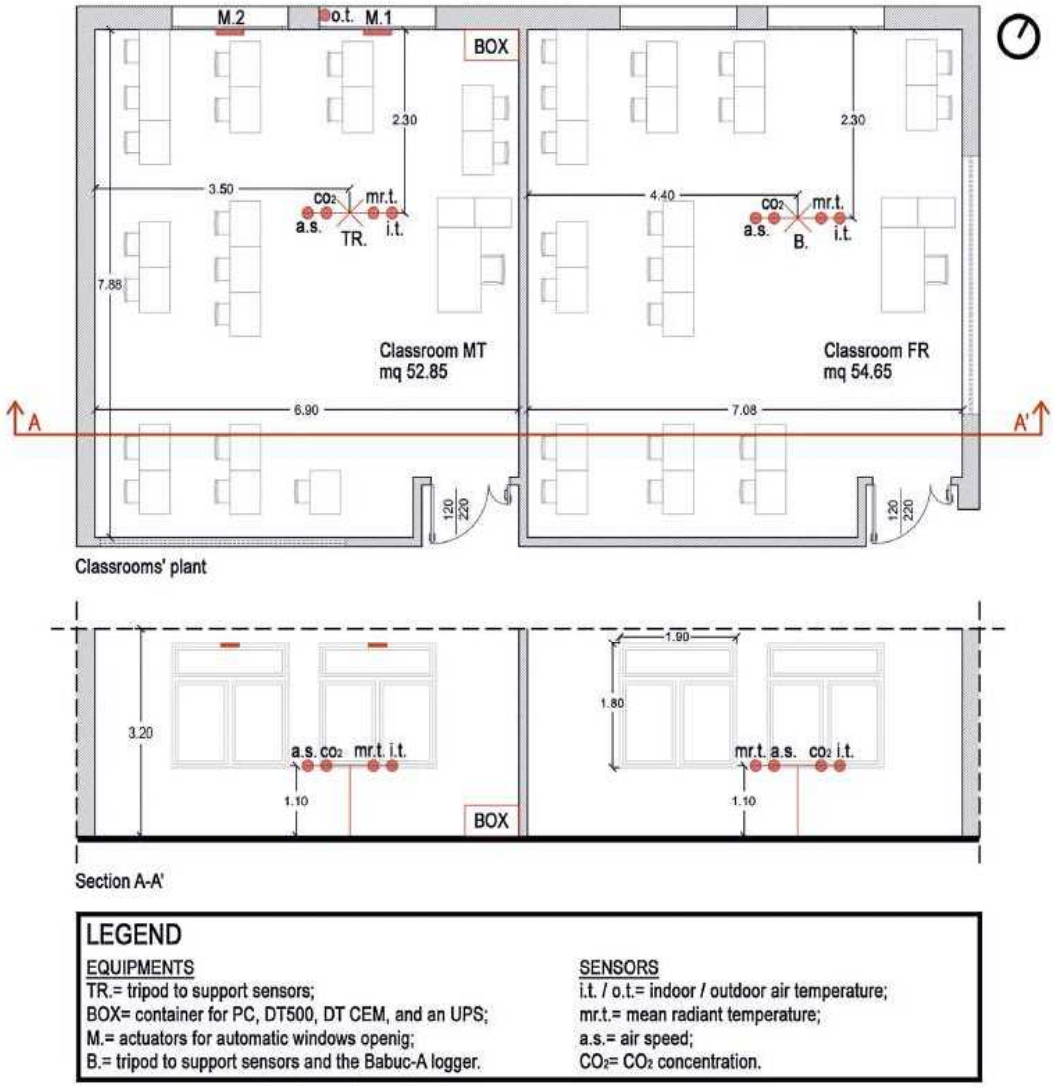


Figure 3.1
Plan view and vertical section of the MT and FR classrooms: red dots and dashes indicate the location of the probes composing the indoor and outdoor sensor network; the dial at the top right displays North orientation.

MT & FR CLASSROOMS GENERAL SPECS		
Features	**Class MT**	**Class FR**
Size (m)	6.9 × 7.88	7.08 × 7.88
Net floor area (m²)	52.85	54.65

Internal height (m)	3.20	3.20
Heated volume (m^3)	169.12	174.88
Ratio S/V	0.313	0.313
Surface mass external side (kg/m^2)	547	547
Surface mass floor on the ground (kg/m^2)	595	595
Thermal transmittance external wall (W/m^2K)	0.324	0.324
Thermal transmittance ground floor slab (W/m^2K)	0.269	0.269
Thermal transmittance window (W/m^2K)	2.23	2.23

Table 3.4
Monitored classrooms features.



Figure 3.2
FR classroom layout. Red circle to highlight the indoor microclimate station.

3.5 – EXPERIMENTAL METHOD

The monitoring campaign was scheduled so as to cover the entire heating period, resulting in a total number of 57 days. The reason behind this choice was the need to assess both the benefits in indoor comfort level and the aftermaths in terms of energy consumption linked to the "smartization" of the windows.
Hence the network and the automatic mechanism were kept in place from the 15th to the 28th of January 2013 (wintertime with the heating system on) and from the 19th of March to the 15th of April 2015 (midseason with the heating system still on).

Some preliminary assessments from the previous monitoring campaign were carried out (**figure 3.3**) in order to identify the proper arrangement for the comfort probes to be representative of the indoor microclimate: temperature gradient maps (**figure 3.3.a**), subjective questionnaires and comfort maps (**figure 3.3.b**) plus PMV values calculated for four thermo-irradiative sub-areas of the classroom (**figure 3.3.c**) were produced and perused to define global environmental conditions and locate the sensor network accordingly.

Since the thermal characteristics inside the classroom were found to be reasonably uniform, the indoor microclimate station was set in the middle of the room. Plan and vertical views of the sensor network are provided in **figure 3.1.**

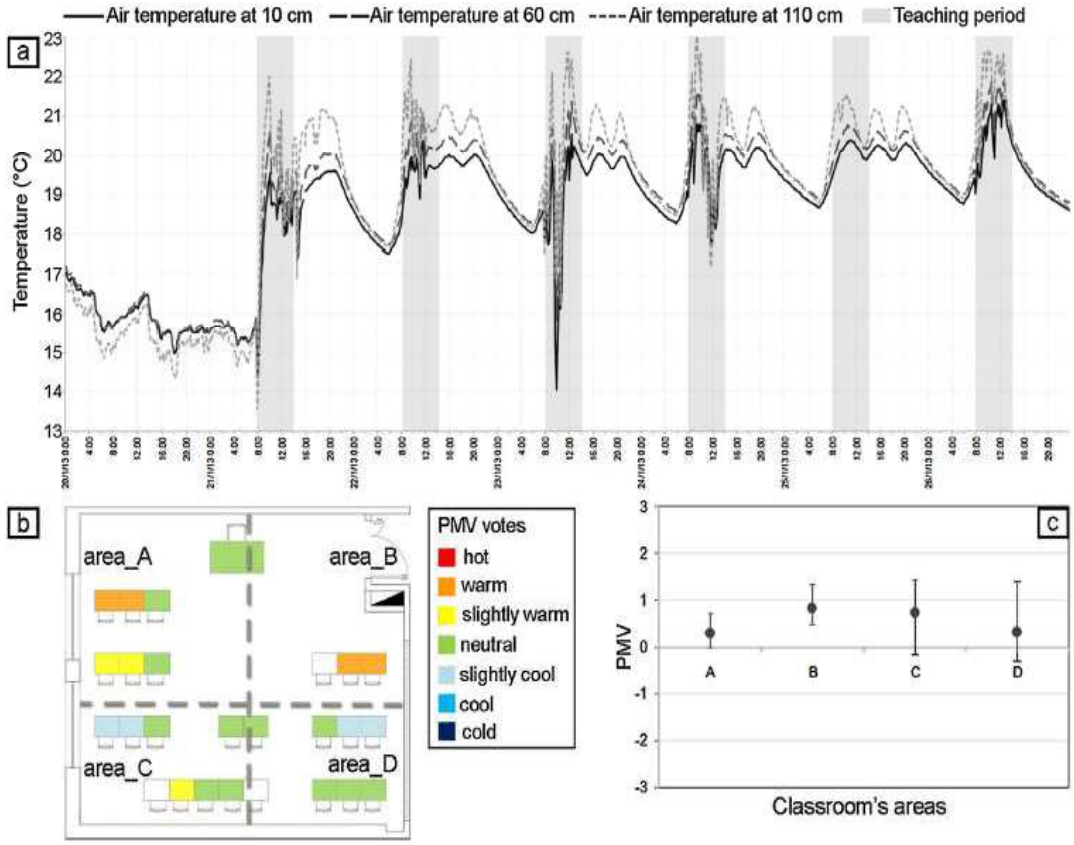


Figure 3.3

Preliminary analyses on the MT classroom (before the installation of the automatic system): (a) indoor thermal gradient, (b) comfort maps, (c) mean PMV value for each relevant sub-zone of the classroom.

Measurements were performed in compliance with Standard ISO 7726:2001 **[3.45]** and conceived to match outdoor thermal dynamics with indoor ones and the role played by windows openings as well.

Outdoor environmental conditions were recorded by Marche Civil Defence meteorological station, located 1 km far from the school and operative since 2009. Air temperature, solar radiation, wind speed and direction datasets are the ones used in the research in object.

Indoor climate conditions were detected by two equivalent microclimate stations, composed by:

- a resistance thermometer (PT 100) with an accuracy of 0.15°C to measure indoor and local outdoor dry-bulb air temperature;
- a globe thermometer to measure mean radiant temperature;
- a hot sphere anemometer with an accuracy of ±0.01 m/s to measure air velocity;
- a CO_2 probe with an accuracy range of 20÷70 ppm to measure carbon dioxide level indoors.

From the vertical perspective, the height of the probes was defined according to the Standard ISO 7726:2001 **[3.45]:** indoor comfort measurements for a typically seated user take place at 1.1m above the floor.

Data collection and retrieval passed through two dataloggers: a Datataker DT500 acquired the probes' signals in the MT classroom while a Babuc/A was set up in the FR classroom.

Alongside probes' measurements, daily adjournment of user behavioural logbook was pursued by two specifically appointed supervisors (one per classroom) via:

- real occupancy annotation (number of teachers in the classroom and of students attending the lessons). That was regularly done for both the classrooms.
- adaptive actions notification: each thermo-hygrometric adjustment (performed by opening/closing the entry door or operating the casement windows…) was recorded and detailed with the consequent environmental modifications.

This logging activity was particularly profitable in the first phase of the monitoring campaign, run just in the FR classroom, to establish users' "undisturbed" behaviour. In that procedural phase the dominant means of adaptation was the interaction with the windows: actually, the entry door remained always closed, apart from the twenty-minute break scheduled from 10:50 to 11:10 and few minutes between each lesson.

Perturbing actions and events analysis led to the definition of the trigger parameters to be included in the ACA design.

Humphreys' basic algorithm, trigger parameters and their weights on occupants' reactions to restore their comfort were combined to shape the final controller to be installed in the

MT classroom: the hopper windows were instrumented to respond to the controller commands, while casements windows operation was interdicted over the entire observation period.

Once the parallel monitoring in the FR and MT classrooms was established, both objective and subjective tools to assess indoor comfort level were implemented so as to get quantitative data and users' perception as well. PMV-based and adaptive comfort models served the former purpose, while tailored questionnaires were used to get personal thermal feeling and give a voice to the non-strictly-rational side of comfort evaluation.

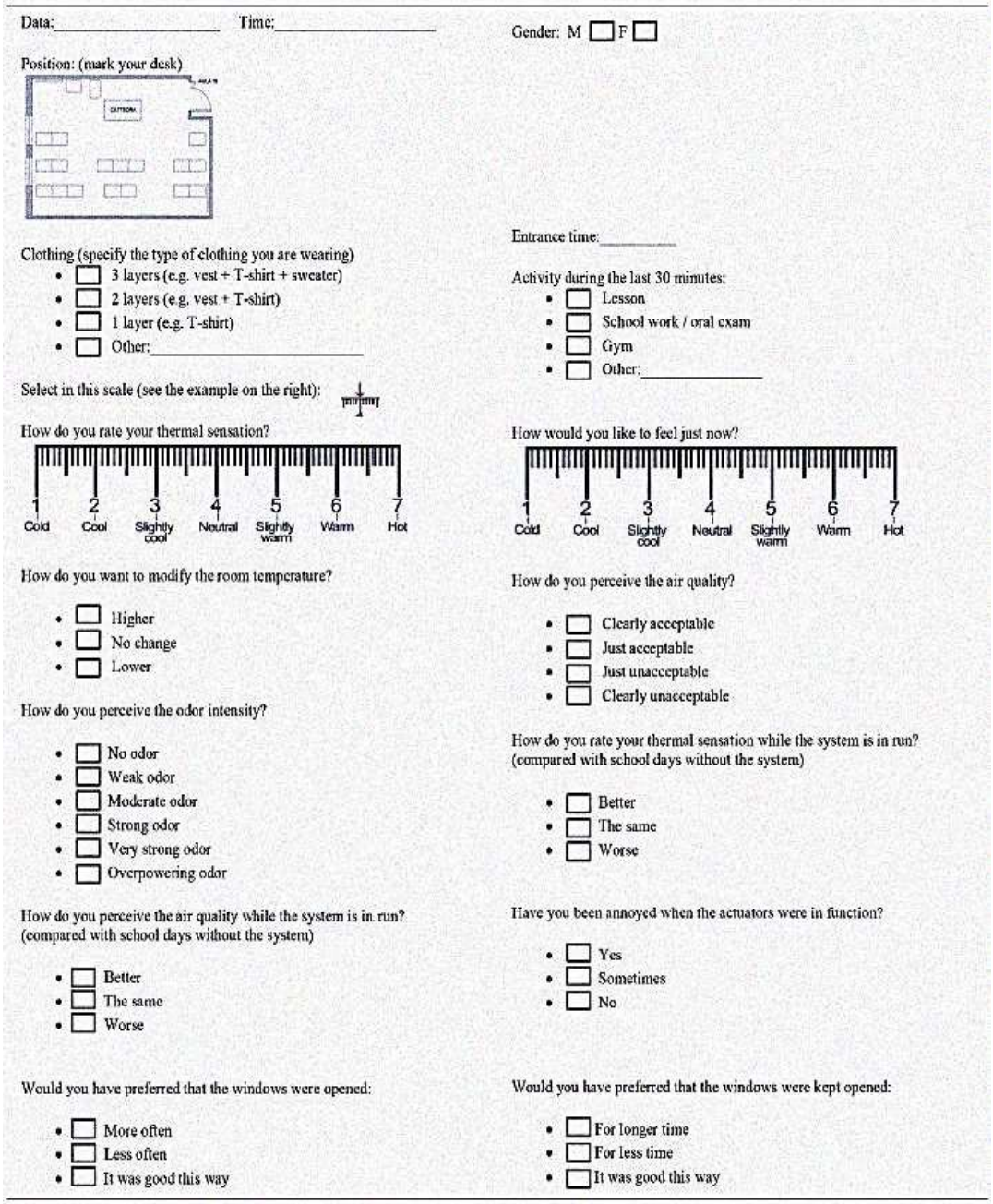
Accordance between the two assessment strategies was used to reinforce the validity of the proposed ACA, while discrepancies (when reasonably validated) were used to define the scope for improvement.

Besides, as already pursued in the previous experimental activity described in **chapter 2**, PPD-weighted (PPDwC) criterion was applied to retrieve information in the long run too.

Hence hourly accumulation of users' dissatisfaction was calculated accordingly.

Students and teachers, in both the classrooms, were asked to fill in the questionnaires every working day before the morning break (around 10:50 am) in order to get environmental preferences and disturbances right at the most critical time in terms of indoor comfort. Indeed, after the break, the reduction in occupancy and the air circulation between the classroom and the corridor through the entry door dramatically mitigated the microclimatic conditions inside.

The basic format for the questionnaires was drawn from the Standard UNI 15251 **[3.47]** and then adjusted to include the specific thermo-hygrometric and acoustic comfort issues related to the stepped motorization of the hopper windows (**figure 3.4**).



Data:_____ Time:_____

Gender: M ☐ F ☐

Position: (mark your desk)

Entrance time:_____

Clothing (specify the type of clothing you are wearing)
- ☐ 3 layers (e.g. vest + T-shirt + sweater)
- ☐ 2 layers (e.g. vest + T-shirt)
- ☐ 1 layer (e.g. T-shirt)
- ☐ Other:_____

Activity during the last 30 minutes:
- ☐ Lesson
- ☐ School work / oral exam
- ☐ Gym
- ☐ Other:_____

Select in this scale (see the example on the right):

How do you rate your thermal sensation?

1 Cold 2 Cool 3 Slightly cool 4 Neutral 5 Slightly warm 6 Warm 7 Hot

How would you like to feel just now?

1 Cold 2 Cool 3 Slightly cool 4 Neutral 5 Slightly warm 6 Warm 7 Hot

How do you want to modify the room temperature?
- ☐ Higher
- ☐ No change
- ☐ Lower

How do you perceive the air quality?
- ☐ Clearly acceptable
- ☐ Just acceptable
- ☐ Just unacceptable
- ☐ Clearly unacceptable

How do you perceive the odor intensity?
- ☐ No odor
- ☐ Weak odor
- ☐ Moderate odor
- ☐ Strong odor
- ☐ Very strong odor
- ☐ Overpowering odor

How do you rate your thermal sensation while the system is in run? (compared with school days without the system)
- ☐ Better
- ☐ The same
- ☐ Worse

How do you perceive the air quality while the system is in run? (compared with school days without the system)
- ☐ Better
- ☐ The same
- ☐ Worse

Have you been annoyed when the actuators were in function?
- ☐ Yes
- ☐ Sometimes
- ☐ No

Would you have preferred that the windows were opened:
- ☐ More often
- ☐ Less often
- ☐ It was good this way

Would you have preferred that the windows were kept opened:
- ☐ For longer time
- ☐ For less time
- ☐ It was good this way

Figure 3.4
MT classroom questionnaire template: users' thermal perception, preferences and disturbances investigation.

A total number of 614 questionnaires from 68 people were handed in by the end of the monitoring campaign.

The post-processing of the subjective answers was approached following the procedure drawn by Humphreys and Hancock in 2007 **[3.48]**. Therefore, a seven-point assessment scale was used to slot personal thermal sensation: it ranges from 1 which represents a very cold perception to 7 which represents the very hot counterpart. Comparison between the results allowed to check whether there was accordance between ACA's actions timing and users' feeling in the MT. Additionally a measure of the different level of environmental satisfaction between the two management modes was derived.

3.6 SMART SYSTEM SPECIFICATIONS

In order to properly mimic the behavioural adjustments an active user can perform to restore his comfort, an equally adaptive framework had to be conceived for the "smart" automatic system.

This is the reason why a hierarchical/deliberative paradigm, coming from the world of robotics, was set as basic structure. Three primitive actions were enclosed in a continuous decision-making loop: the system "sensed" the environment and gathered the information to recreate a global world model, then interpreted and decided ("planned") the next move, and finally "acted" according to its inner reasoning.

This very generic baseline was then declined and detailed according to the specs of the case (**figure 3.5**)

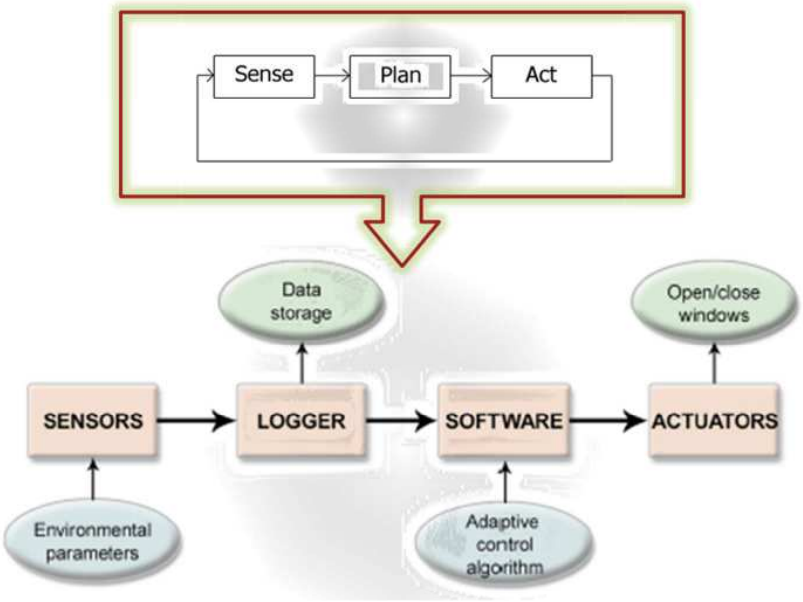


Figure 3.5
Schematization of the sensitive-planning-acting chain behind the automatic system conceptualization.

The sensorial action was split into two components: the probes recorded in continuous, but time stepped mode all the pivotal parameters. Their signals were then received by the datalogger which acted like a storage and access point gathering all the information to recreate a fictitious single-point based model of the surroundings.
The planning action was charged to the software which processed the ACA calculations. In this case, as in the experimental study described in **chapter 2**, the programming language used is graphical, in particular a virtual instrument developed in LabVIEW 2014.
The ACA compared the measurements with the corresponding target or limit values (imposed after the analysis of trigger parameters) in order to get a measure of the "error" between real and ideal conditions. Every time a discomfort phenomenon was detected, the status of the windows was modified accordingly: an electrical input was sent to the actuators moving the stepping motors (acting action) so that the hopper windows could be opened/closed.
It should be stressed that a priority among IAQ and thermal comfort had to be established since it was reasonably expected that in some cases they could act as competing objectives.
Hence a nested case structure was developed inside the ACA to solve race conditions and privilege the need to reduce the CO_2 content in the air anytime it overtook a certain critical point.
The loop time was set to 1 minute.

3.7 HUMPHREYS' ALGORITHM - TUNING

As previously mentioned, the technical scaffolding of the control logic was Humphreys' adaptive algorithm **[3.28]**.
The environmental parameters that played a major role in the output of such ACA were operative and comfort temperature (indicated as Top and Tcomf respectively) as they actually conveyed all the main information about both indoor and outdoor microclimatic conditions:

- the operative temperature combines dry-bulb air temperature and mean radiant temperature into a sole numerical quantity thus providing a comprehensive estimation of human body's response to both convective and irradiative energy exchange with the surroundings.
- the comfort temperature is defined, in the adaptive comfort theory, as a linear function of the outdoor temperature.

As a consequence, matching Top and Tcomf actually means matching all the thermal phenomena behind microclimatic perception, whether they depend on outdoor weather conditions or indoor thermodynamics.

During each loop, the algorithm checked if the instantaneous values of Top fell within a certain acceptability range (dead band) around Tcomf:

- as long as this condition was respected no corrective action was fed to the actuators;
- if Top exceeded the upper limit (given by Tcomf + ΔT, with ΔT set to 2°C in Humphreys' original version) the windows were forced to open.
- If Top fell below the lower limit, a closing command was sent to the motors.

This is, in a nutshell, the general procedure developed in **[3.28]**.

In order to customize the decision-making process to the peculiarities of the case study, two main adjustments were proposed and tested (**table 3.2b**):

1. the introduction of CO_2 level as a driving force for enhancing air ventilation. A threshold of 1250 ppm was found to return the best results from a bivalent perspective (IAQ and thermal comfort): it was identified by averaging Building Bulletin and ASHRAE Standard suggested limits (1500 and 1000 ppm respectively), each of which previously tested. The 1000 ppm boundary was usually trespassed just after 30 minutes of lessons and then frequently crossed: this led to a frenetic on/off cycling thus increasing the noise and the wear and tear of the mechanism. The 1500 ppm value, applied to the volumetry of the classroom, provoked excessive overshoot in most of the cases thus undermining the efficiency of such belated interventions.
2. the contraction of the "dead band" around comfort temperature from ±2°C to ±1°C. This change was found to be rewarding in terms of indoor air temperature stability since it averted the threat of excessive air stratification in transient conditions.

3.8 RESULTS

The main findings of this experimental study can be categorized into three main blocks, each one detailed in the following sub-paragraphs:

1. indoor comfort models for school buildings: application and comparison of comfort models and indices to highlight the best practice;
2. sensitivity analysis to pinpoint the trigger parameters: linear regression analyses on environmental parameters to define the proper way to include them in the ACA design;
3. thermal comfort and IAQ achievements due to the "smartization" of the air ventilation: identification and discussion of the discrepancies between MT and

FR classroom to assess the performance of the ACA-driven, automatic controller.

3.8.1 Comparison of comfort models

The monitoring campaign, run all over winter 2013 and spring 2015, allowed to gather sufficient information to detect the main inner workings beyond comfort and IAQ dynamics inside the FR classroom. Once the pivotal thermo-physical variables were defined and interrelated, it was possible to identify both the most proper comfort theory framework and the most pertaining question marks for the subjective survey.

Indeed, the observation period was representative of all the annual patterns going on inside an Italian school building since the academic year starts in mid-September and ends around the first week of June.

An extensive analysis of time trends and fluctuations was primarily accomplished (**figure 3.6**): five days per each time of the heating period (winter, intermediate season and kick-off of the warm season) were selected to plot and assess the trigger parameters trends (operative temperature for thermal comfort and CO_2 content for IAQ), in particular:

- operative temperature time trend was chartered together with comfort temperature (**figure 3.6a**): this is a comprehensive way of linking indoor and outdoor environments and check if the thermal adaptive tolerance of the occupants is satisfied by the instantaneous combo of the two thermodynamic systems. The comfort range was set according to CIBSE Guide A **[3.49].** It is immediately noticeable that the likelihood of occurrence of acceptable conditions was rather low: operative temperature seldom fell within the limits and almost never reached optimal values.
- CO_2 concentration time trend was overlapped to the International Standards suggested limits (**figure 3.6b**). The 1000 ppm limit was always exceeded during occupied hours. The 1500 ppm limit was crossed at least once a day (but for limited time slots) in the first period, about half this frequency was recorded during the second period, while during the last one the number of occurrences was dramatically reduced. This is because outdoor temperature increase is generally followed by a stronger appeal to natural air ventilation.

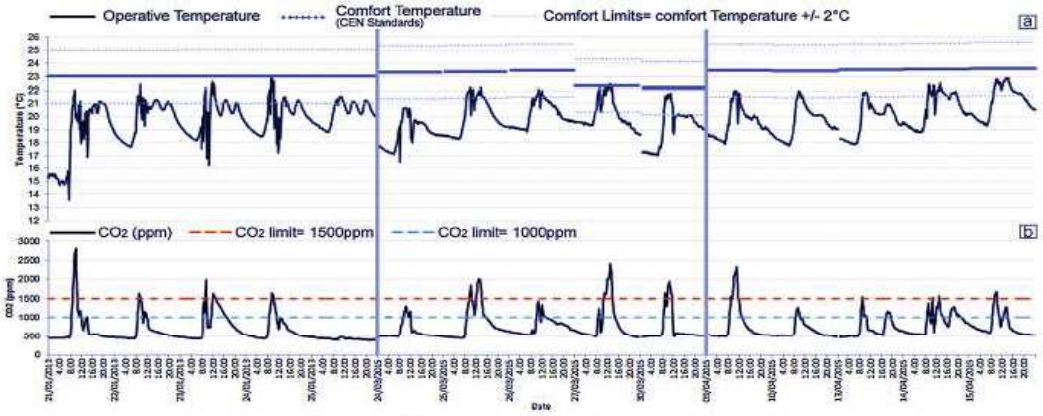


Fig. 5. Extensive analysis of environmental variables trends.

Figure 3.6
Environmental trigger parameters trends over time: comfort and IAQ boundaries displayed for the sake of comparison.

An assessment of "undesired" environmental conditions recurrence was thus required for both thermal comfort and IAQ issues: **table 3.5** shows the results of the accumulated percentages out of the boundaries imposed to:

- operative temperature according to both adaptive and PMV-based comfort models (second and third column respectively). The acceptability range for PMV was set to [-0.5, 0.5], in line with ISO 7730 **[3.16]** and EN 15251 **[3.47]** prescriptions for existing buildings with no peculiar comfort requirements. A metabolic rate of 1.1 mets was adopted as representative of sedentary activities, while the thermal insulation adduced by the garments was adjusted to the season and the questionnaires answers time after time.
- carbon dioxide according to Building Bulletin and ASHRAE thresholds (fourth and fifth column respectively).

These values were calculated for each period (first column) and in the hours of actual occupation. The total percentage over the entire observation time is given in the last row.

At that point, some conclusions could be drawn:

- "adaptive" discomfort phenomena tended to decrease while approaching the warm season: this finding reinforces the suitability of such model in free-running mode **[3.19,3.50]**. As a double-check, the highest PPD values were recorded during milder seasons;
- the maximum gap between the two comfort models is related to wintertime (adaptive discomfort is slightly less than three times the PMV-based one). The minimum gap is 1.79% and is returned between March and April;

- the lowest time percentages in which out-of-the-boundary CO_2 levels were detected pertain to the wintry observation period: 19.8% above 1500ppm limit and 59.6% above 1000ppm limit);
- the time percentage, in which ASHRAE limit was overpassed, increased substantially from winter time to mid-season and slightly from mid-season to warm period, while Building Bulletin's limit excess reached its peak per cent value during the mid-season and decreased again with the beginning of the warm period.

In any case, looking at the last raw of **table 3.5**, it is apparent that the ASHRAE limit of 1000ppm, exceeded for the 73,1% of the time, was too much restrictive for a feasible and actually comfortable control of the air quality inside the classroom. On the other hand, the limit value of 1500ppm left considerable scope for excessive inertial increase of the carbon dioxide content in the air. However, the total percentage of excess was dramatically lower that the 1000ppm-related one (28,6%) suggesting that a moderately lower value could be used as a proper set-point for an automatic control system.

FR CLASSROOM – UNDESIRED ENVIRONMENTAL CONDITIONS ASSESSMENT				
Time interval	**% of discomfort "Adaptive model"**	**% of discomfort "PMV model"**	**% of time with CO_2 > 1500 ppm**	**% of time with CO_2 > 1000 ppm**
15/01/'13–28/01/'13	64.5	24.2	19.8	59.5
19/03/'15–1/04/'15	35.1	33.3	31.6	71.0
8/04/'15–15/04/'15*	20.4	32.3	26.9	76.4
All	39.3	29.2	28.6	73.1

* from the 2nd to the 7th of April 2015: Easter holidays.

Table 3.5
Per cent discomfort values and per cent time outside IAQ boundaries (FR classroom)

Parallel subjective investigation via daily distributed questionnaires led to a different rating of thermal comfort and indoor air quality compared to the one coming out the two objective comfort models, even though the adaptive one followed much closer users' reported thermal perception.
More in detail, the analyses pursued on the answers given by the occupants (**table 3.6**), remarked that:

- environmental satisfaction votes were similarly distributed regardless of the observation period: the vast majority (60%) outlined a thermally neutral

perception; an almost equal percentage of students (ranging from 15.4% to 16.9%) found themselves in a slightly warm or cold condition; extreme assessments were rarely reported.

- discomfort phenomena were much more likely to occur over wintertime: their frequency and magnitude considerably decreased while approaching milder seasons to the point that, in the last period, no vote exceeded the range -1, 1;
- questionnaires and adaptive model showed very strong agreement. The only remarkable discrepancy is in the source of discomfort: the distribution of votes was apparently skew, exhibiting a certain bend to the positive side of the 7-point scale, thus remarking a predominance of hot conditions as main cause of discomfort. More in detail, an overall percentage of 24,7% was obtained by summing up the individual +1, +2 and +3 sub-sets, while -1, -2 and -3 votes covered a total of 18.3% of students. Conversely adaptive model predicted dissatisfaction was mainly due to cool conditions, with T_{op} below T_{comf}.

FR CLASSROOM – THERMAL SENSATION QUESTIONNAIRES							
Time interval	**Percentage of votes (%)**						
	Cold (−3)	**Cool (−2)**	**Slightly cool (−1)**	**Neutral (0)**	**Slightly warm (+1)**	**Warm (−2)**	**Hot (−3)**
15/01/'13–28/01/'13	0.0	3.6	13.6	41.8	13.6	20.0	7.3
19/03/'15–1/04/'15	0.0	0.7	19.2	62.3	16.4	1.4	0.0
8/04/'15–15/04/'15*	0.0	0.0	17.1	67.1	15.9	0.0	0.0
All	0.0	1.5	16.9	60.0	15.4	7.0	2.3
* from the 2nd to the 7th of April 2015: Easter holidays.							

Table 3.6

Questionnaires to rate users' thermal sensation in FR classroom - analysis

Notwithstanding the specific environmental combinations leading to diverse thermal sensations, both PMV-based and adaptive comfort models showed a definite tendency to overestimate temperature expectations and preferences, particularly in the heating period (even if the latter was much more accurate in depicting user's sensations). This finding underpins previous researches, although conducted in different climates **[3.51,3.52]**).

3.8.2 Adaptive Comfort Algorithm

As a first step in the definition of the ACA, trigger parameters were identified by means of linear regression analysis applied to the datasets coming from FR classroom's monitoring campaign. The results are plotted in **figure 3.7**: black solid lines represent the outcome of the regression, while diamond red dots represent raw data from on-site collection. R^2 values are displayed as well.

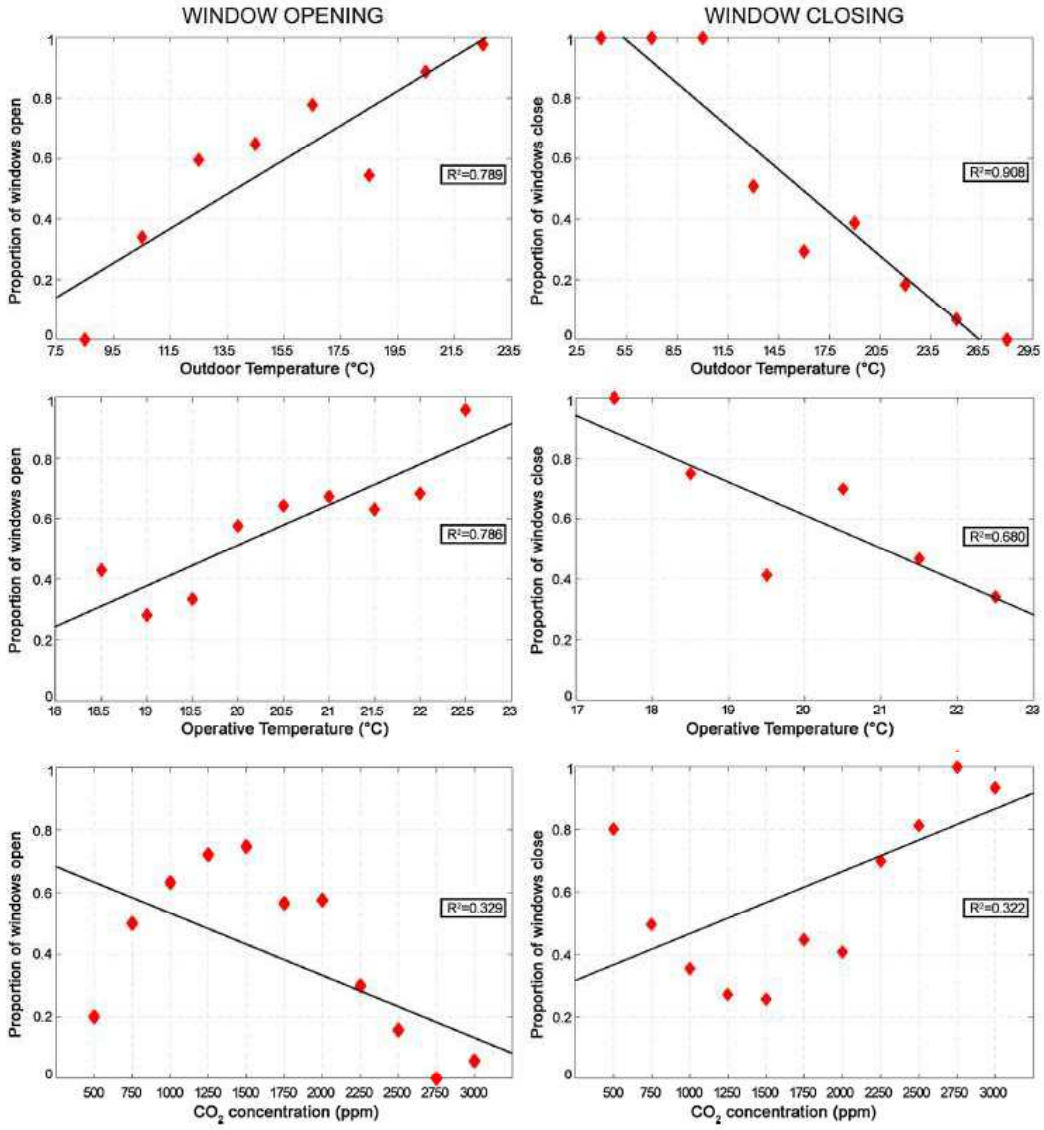


Figure 3.7
FR classroom monitoring campaign – linear regression analysis to identify ACA's trigger parameters.

The main findings might be recapped as follows:

- operative and outdoor temperatures were highly correlated to both windows opening events, as witnessed by the correspondent R^2 values (0.786 and 0.789, respectively) and windows closing events (R^2= 0.680 and R^2= 0.908, respectively);
- carbon dioxide content in the air was found to play a minor role (opening-related-R^2=0.329, closing-related-R^2= 0.322) thus not appearing as a driving force behind air ventilation boost.

Several previous researches **[3.6,3.11,3.27,3.53]** came to the same conclusion, namely that temperature (indoor as well as outdoor) is the pivotal parameter piloting users' adaptive behaviour, while IAQ issues take second place.

It should be stressed here that the reason behind such an underestimation of the CO_2 effect is not its effective negligibility, but actually its tendency to go unnoticed: occupants are much less sensitive to poor indoor air quality rather than thermal stimuli **[3.6,3.38]** so that their responsiveness is far more triggered by even small temperature variations compared to considerable carbon dioxide increase.

Against this backdrop, both temperature and CO_2 variables were included in the ACA framework.

3.8.3 Test and comparative analysis

The installation of the automatic system required both the physical coupling of the hopper windows with the stepper motor and the implementation of the ACA on a software platform (LabVIEW).

The monitoring campaign was carried out over ten days, during the non-heating season and regular scholastic activities. Two main management modes were programmed and tested:

- from the 22nd to the 27th of April 2015 the automatic system operated as discussed in paragraph 3.2.
- from the 28th of April to the 1st of May 2015 the ACA was refined by adding a sub-routine driving preventive ventilation in the early morning, in order to maximize IAQ levels before students' arrival (7:30am – 8:00am).

Six representative days were selected to run the post-processing assessment. The main findings are summarized in **figure 3.8**, which displays, in order:

1. the environmental variables trends, retrieved from the recordings simultaneously taken in MT and FR classroom (**figure 3.8a**), in particular: operative temperature, outdoor temperature, comfort temperature are plotted against comfort limits. Hatched green rectangles are used to highlight whenever MT classroom indoor conditions matched comfort criteria.

2. The CO_2 levels on the same time axis (**figure 3.8b**): the dotted red line stands for the fixed-threshold of 1250ppm, while hatched red areas emphasize poor IAQ time slots in the MT classroom.
3. The occupancy and proportion of opened windows in MT classroom (blue zones) and FR classroom (grey zones) occurring over the same observation period (**figure 3.8c**).

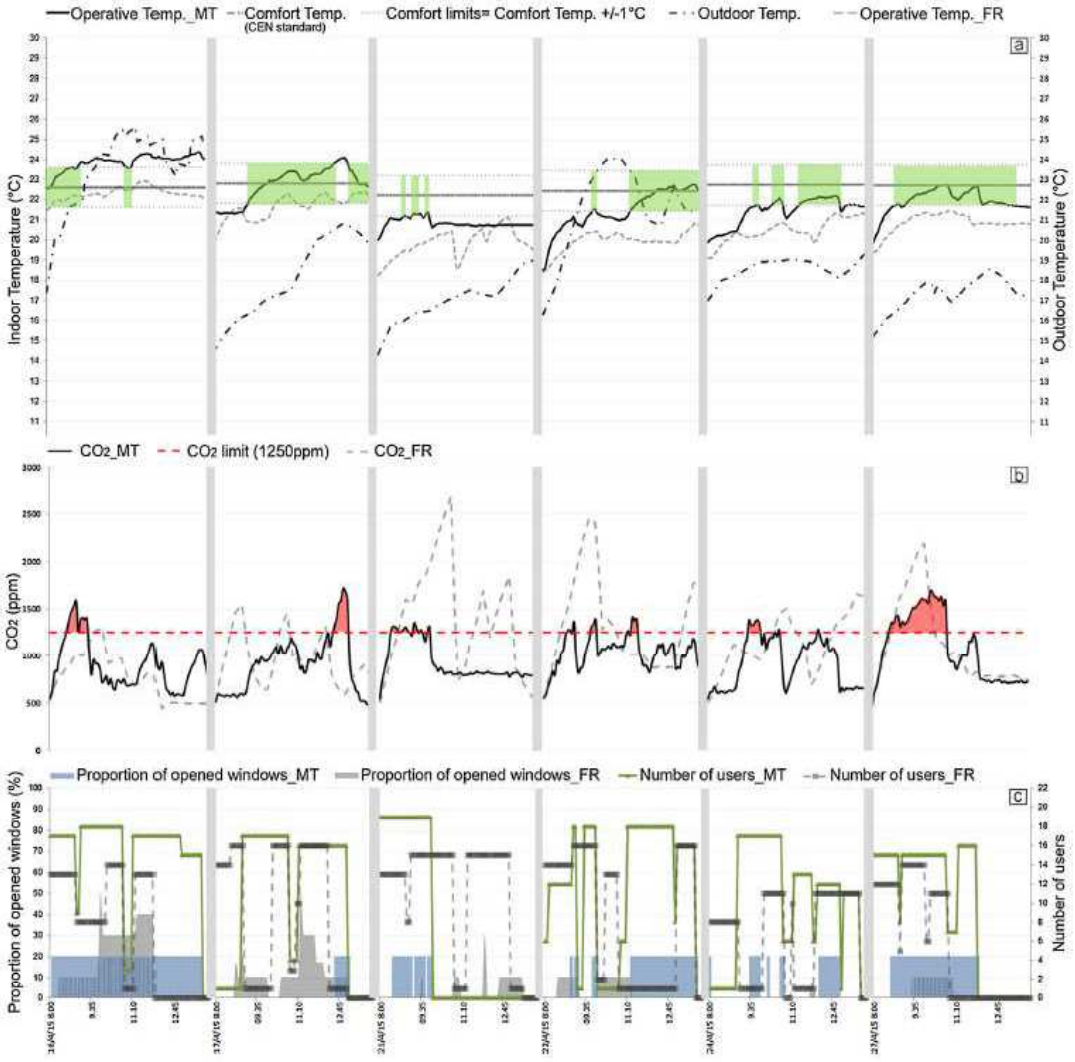


Figure 3.8
Thermal (a), IAQ (b) and occupants related information (c) recorded over six representative days for both MT and FR classrooms.

The following conclusions could be drawn:

- MT classroom abided by comfort condition the most of the time (operative temperature inside the ±1°C comfort temperature neighbourhood).
- The automatic operation of the hopper windows didn't cause any appreciable temperature drop, thus it didn't affect comfort conditions (nor global since the change rate was perfectly manageable, nor local since vertical and horizontal gradient remained negligible). Whenever significant reductions occurred it was because of people moving in and out the classroom, which meant, on the one side, less internal gains and, on the other side, cross ventilation through the entry door with fresh air flows coming from not-AC environments.
- FR classroom exhibited low temperatures the most of the time; MT classroom showed cool conditions just in the early morning when "preventive ventilation" was active. The temperature jumped as soon as full occupancy was achieved and the door was closed for the beginning of the lesson. By the first hour the operative temperature fell within the comfort range.
- In the MT classroom the CO_2 was prevented from reaching the 1250 threshold in many cases. Building Bulletin limit was never trespassed. Preventive ventilation had no aftermaths on carbon dioxide content in the air, which stayed around 500ppm until students' arrival.
- The opening of the windows was IAQ-driven, while the closing events were thermally-triggered. That happened because, in the morning, the pitch by which CO_2 content approached its limit value was much higher than the rate by which air temperature approached comfort upper limit. Consequently, the operative temperature exceeded the upper limit far later since its increase had already been interrupted several times to preserve indoor air quality. On the other side, automatic closings occurred because of Top falling below the lower comfort limit.

Table 3.7 extends the results displayed in **figure 3.8** over the whole occupied period and summarizes the main differences between the two operative modes: the percentage of dissatisfied people in the FR classroom was found to be about five times MT one set with a ±2°C dead band (46.9% vs 8.6%). By reducing the dead band to ±1°C, such percentages soared in both the classrooms: 53.7% in MT and 83.6% in FR.

Remarkable differences could be outlined in terms of CO_2 content as well: the 1500ppm limit was overtaken for only the 8,7% of the time in the MT classroom, whilst this figure almost quadruplicated in the free running one (30,7%). The benefit is strong even in comparison with other naturally ventilated buildings documented performance **[3.1,3.38–3.40].**

The 1250 ppm threshold led to completely different percentages in both the tested environments (33.9% in MT classroom and 51.4% in the FR one).

DISCOMFORT AND POOR IAQ PHENOMENA FOR MT AND FR CLASSROOMS				
Classroom (16/04/'15–29/04/'15)	**% of discomfort "Adaptive model" _T = ±2°C**	**% of discomfort "Adaptive model" _T = ±1°C**	**% of time with CO2 > 1500 ppm**	**% of time with CO2 > 1250 ppm**
MT	8.6	53.7	8.7	33.9
FR	46.9	83.6	30.7	51.4

Table 3.7
Comparison of thermo-olfactive comfort behaviour between the free-running and motorized classrooms.

PPD-weighted criterion analysis was furtherly accomplished: the results are summarized in **table 3.8.** Even though absolute values are not significant (since PPDwC is a cumulative index without upper threshold) the percentage difference between the values obtained from each classroom was calculated. FR classroom figure was more than two times higher than the MT counterpart.

PPD ASSESSMENT				
	Class FR	**Class MT**	**FR- MT**	**Difference (%)***
Occupancy (hours)	42	42	0	0
PPD> PPDlimit (hours)	34	15	19	55.9
PPDwC (hours)	2766	1290	1476	53.4

*the percentage difference between the results obtained from the MT classroom and those from the FR one.

Table 3.8
PPD weighted index results: main differences between FR and MT classrooms.

3.8.4 Questionnaires

Experimental studies in the field of comfort, whether indoor or outdoor, and in case users' thermal tolerance might be enhanced by means of adaptation, require both comfort-model based and subjective assessment in order to be fully comprehensive.
Accordingly, students' actual feeling towards the surrounding microclimate, were collected via daily questionnaires and then perused to identify statistical occurrences,

preferences and check the agreement between objective global comfort evaluation and individual local response.
Thermal sensation personal information is retrieved by calculating the percentage of each vote given on the corresponding 7-point-scale. **Table 3.9** collects the results:

THERMAL SENSATION QUESTIONNAIRES – COMPARISON BETWEEN FR AND MT CLASSROOMS							
Classroom (16/04/'15 – 29/04/'15)	**Percentage of votes (%)**						
	Cold (–3)	**Cool (–2)**	**Slightly cool (–1)**	**Neutral (0)**	**Slightly warm (+1)**	**Warm (–2)**	**Hot (–3)**
MT	0.00	1.41	10.56	77.46	9.15	1.41	0.00
FR	0.00	0.91	12.72	66.36	19.09	0.91	0.00

Table 3.9
Comparison of thermal sensation questionnaires for FR and MT classrooms.

The distribution of votes, even in this second monitoring run, was quite similar to the one pertaining the FR classroom and recapped in **table 3.6.** In fact:

- for both tested rooms, the highest percentages report a feeling of thermal neutrality: 77.5% of occupants felt satisfied in the MT classroom microclimate, thus reinforcing the results given by the objective assessments. A smaller, but still very high percentage (66,4%) was recorded in the FR reference room;
- for both tested rooms, a modest per cent quote is attributed to slightly warm and cool thermal sensations: more in detail, FR classroom figures are 19.1% and 12.7%, respectively, while MT classrooms ones are 9.15% and 10.56%. These values highlight the main difference in the running modes applied to the ventilation rate: motorized management was more likely to provoke low temperature discomfort phenomena, while free management tended to overheating issues since windows operation usually occurred with a certain amount of delay and fewer times compared to MT activations. However, the difference for cooler sensations is much less significant: the reason is that in FR classroom, the casement windows were operable and much more effective in refreshing the indoor air compared to the cooling potential of the sole hopper windows air flow;
- for both tested rooms, negligible percentages of votes witnessed cool and warm sensations experienced by the occupants;
- subjective votes analysis reinforced the fundamental finding coming from adaptive and PPDwC objective criteria that discomfort events were much

more likely to affect FR classroom environment rather than the motorized room. Besides, the operation of the stepper motor showed no relevant drawbacks in terms of noise (acoustic comfort) or of draughts (local comfort). Conversely the operation of the casement windows, in a time-and-duration-uncontrolled mode, was found to be far less efficient in terms of comfort (and reasonably of energy saving too) since air ventilation and its enthalpy content management was imprecise and overabundant for the most of the time, plus causing the occupants to interrupt their activities to undertake corrective actions and easily get distracted during the lesson.

3.8.5 The effect of wind

Outdoor climatic conditions deeply influence the efficacy and the thermodynamic convenience of indoor air ventilation in a complex scenario of competing and/or self-empowering interrelations. In particular, outdoor air properties (enthalpy, speed, direction and quality) play a major role.

In this framework, the synergies of wind speed and direction on the performance of the smart system were assessed in relation to CO_2 reduction and indoor temperature control.

The graph in **figure 3.9** outlines the effect of the wind by comparing a day of "positive" potential (high module, right-to-window-incoming velocity vector) - 21st of April 2015 - with a day of "negative" potential (mild intensity, right-to-window-outgoing velocity vector) – 27th of April 2015.

For the sake of comparison and to isolate the sole contribution of the wind, the two selected days showed similar outdoor temperatures, ranging from 14°C to 19°C.

The north-west, abundant air flow blowing on the 21st exhibited a strong dilution capacity thus succeeding in restoring CO_2 level below the fixed threshold in few loops by granting consensus to window openings (**figure 3.9c**, solid line).

Conversely, the eastern wind, dominant on the 27th, hardly kept the indoor air quality at the desired level. The overshoot and the extra time required to force the trend reversal highly reduced the percentage of time over which the 1250ppm limit was respected (**figure 3.9d**, solid line).

In terms of indoor temperature, no critic role was played by the wind, since in both cases, the automatic openings were never triggered by the overtaking of thermal comfort upper limit (**figure 3.9c** and **d**, dashed lines). Actually, some differences could be highlighted since the variability range of indoor temperature was significantly narrower on the 21st: that might seem controversial since the inlet of a high-cooling-potential wind from the hopper windows could be expected to cause much more thermal gradient, yet it should be considered that the opening time slots

in this case were much shorter thus not significantly impacting on the temperature of the indoor air volume.

Whatever wind condition occurred, MT classroom air ventilation management outperformed by far the FR free conduction. This is immediately noticeable by comparing the vertical aligned charts **c-e** and **d-f** of the same **figure** and by taking into consideration the adaptive actions undertaken by the users inside the two environments: in the FR classroom students intervened by opening the casement windows (thus activating a massive outdoor air income) just when the operative temperature and/or CO_2 content had already reached critical levels thus coercing to much longer restoring times to recreate sufficiently good thermal and air quality conditions. Consequently, indoor temperatures dropped and local discomfort phenomena were usually recorded.

The inner minor readiness of FR management was due to both occupants' low sensitivity to IAQ and the much more cumbersome procedure to apply the adjustments: students had to interrupt their activities, stand up, move and operate the windows, once to open them and once to close. So adaptive actions mainly took place during breaks, losing simultaneity with the environmental changes boosting the discomfort (as outlined in other papers as well **[3.1,3.60]**).

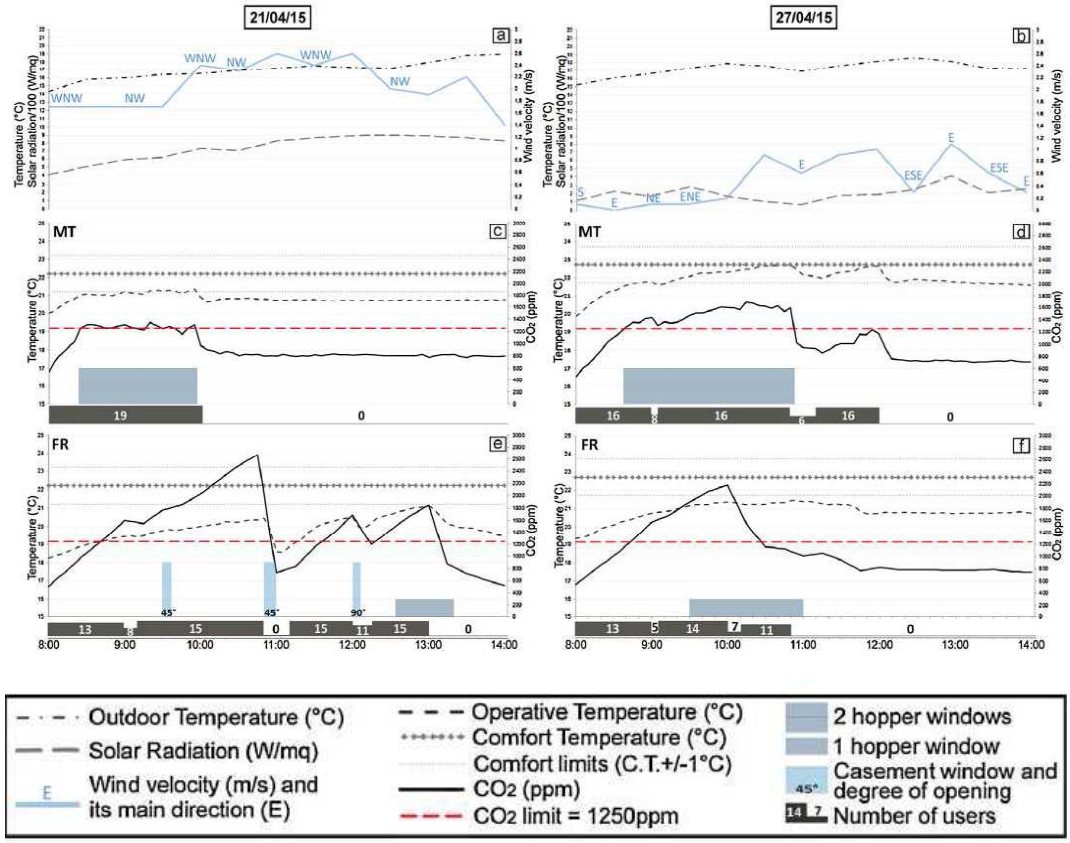


Figure 3.9
Comparison of MT and FR classrooms microclimates during two days of different wind conditions.

3.9 DISCUSSION AND CONCLUSION

Thermal comfort and indoor air quality are two major concerns inside school buildings, since clear-headedness, concentration and health are crucial points when it comes to education and training.

Classrooms represent strategic living environments, as well as residential buildings, since youngsters spend a considerable quote of their time inside them **[3.54]**, yet they tend to be vulnerable to poor indoor air quality, high uncontrolled contents of carbon dioxide and overheating **[3.55-3.59].**

Previous research activities and European projects - first in line the SIMPHONIE project **[3.42] –** attempted to produce proper guidelines to demystify the concern of poor IEQ inside school buildings, but such recommendations were recently found to fail: 20 primary schools were configured according to SINPHONIE's prescriptions

[3.43] and then assessed in terms of pollutants contents in the air. Ventilation rates were inadequate, thus underpinning the general highlight, coming from literature, that naturally ventilated schools still represent an open issue in terms of substantial improvements in the management of IAQ.
The research activity in object [3.61] actually demonstrated that CO_2 levels can be tweaked in an efficient, comfort-respective way without threatening students' attention (by making noise or triggering local draughts) and without getting them feel deprived of their direct control over the surroundings.
The availability of upper located, hopper windows is expected to be an essential factor for the achievement of the same results in similar applications. However further investigation might be carried out in the future to supply design indications as well.
Trigger parameters were identified by means of linear regression analysis: priority was eventually given to thermal driving forces, thus operative temperature (and its distance from adaptive comfort temperature) was set as pivotal variable. A nested decision-making loop was implemented so that CO_2 level took second place in the algorithm giving consensus to windows operation.
This priority scale was in line with previous works findings **[3.62, 3.63].**
Humphreys' adaptive comfort algorithm was found to be a powerful base to correlate outdoor, indoor and comfort temperatures inside school buildings (and not just office buildings like originally outlined in SCATs project **[3.64]**) because of two main strengths: user-centred approach and flexible structure.
The latter property allowed to integrate CO_2 content as control variable, setting the threshold to 1250ppm, which represented the trade-off between ASHRAE and Building Bulletin suggested limits.
A second modification to the basic structure was the reduction of the acceptability range around comfort temperature from ±2 to ±1°C.
During the monitoring campaign the window-opening patterns in the two adjacent classrooms under test were soundly different: MT relied on a slightly frequent, but energetically weighted operation of the sole hopper windows, while FR's ventilation rate was directly managed by the occupants through quite sparse but generally overabundant air flows coming from the casement windows.
In FR classroom the driving force for undertaking behavioural adaptation was the increase of the operative temperature. In MT classroom, windows opening was generally triggered by the high levels of carbon dioxide, while the following temperature drop led to the closing action.
It should be stressed here that such a IAQ-driven behaviour is related to the mild climatic conditions of the seasons over which the monitoring activity took place: in the coldest days of winter, as well as the hottest days in summer a major role is expected to be played by thermal issues in both operation commands.

Both objective and subjective means of evaluation were applied to return a full screening of the main improvements an automatic system to pilot windows open/close loops was able to ensure, compared to a free running management of air ventilation. The vast majority of users witnessed a sensation of thermal neutrality in both the classrooms, but the figure was much higher in MT rather than FR. Such result was furtherly reinforced by adaptive model assessments.

The only discrepancy amongst the two judging approaches was found in the skewness of votes distribution: questionnaires outlined a tendency to suffer warm microclimates, while comfort-model-based methods highlighted a stronger vulnerability to cool conditions.

From the IAQ perspective, the proposed methodology guaranteed a huge reduction of per cent time above the limit: in MT classroom 1500pm was overpassed three times less than FR (8,7% vs 30,7%).

From an energy perspective, even if no detailed calculation was performed to quantify the gap between the two management modes, it was crystal clear that much lower consumptions were achieved through the implementation of the smart system: the "spy" parameter, in this context, is the indoor operative temperature, or, more precisely, its deviation from the defined range of comfort values. In the MT classroom the comfort zone was seldom not respected and the oscillatory trend of the temperature was much less pronounced. Indoor temperature was quite constant thus avoiding all the extra calls to the heating terminals to catch up the gap provoked by strong temperature drops (like the ones simultaneously occurring after casements windows operations in FR classroom).

From a functional perspective, the automatic operation of the hopper windows allowed students and teachers to never interrupt their activities just to restore their comfort, preserving attention, concentration and responsiveness without any distraction and by enhancing learning capabilities by keeping the right air quality conditions.

All things considered, a huge benefit went alongside the proposed smartization of the classrooms. Obviously further investigation is needed to confirm such performance even in other geographical, seasonal and design conditions.

Furthermore, a greater number of classrooms, should serve as sample base in order to take into account even the microclimatic differences of the diverse zones of a building (exposure, volumetry, adjacent AC, not-AC environments, …).

Finally, the modified version of Humphreys ACA we proposed could be furtherly refined to tune its equations on the specific synoptic weather conditions of each case study.

REFERENCES

[3.1] V. De Giuli, O. Da Pos, M. De Carli, Indoor environmental quality and pupil perception in Italian primary schools, Build. Environ. 56 (2012) 335–345, http://dx.doi.org/10.1016/j.buildenv.2012.03.024

[3.2] S. Brasche, W. Bischof, Daily time spent indoors in German homes-baseline data for the assessment of indoor exposure of German occupants, Int. J. Hyg. Environ. Health 208 (2005) 247–253, http://dx.doi.org/10.1016/j.ijheh.2005.03.003.

[3.3] T. Hussein, P. Paasonen, M. Kulmala, Activity pattern of a selected group of school occupants and their family members in Helsinki – Finland, Sci. Total Environ. 425 (2012) 289–292, http://dx.doi.org/10.1016/j.scitotenv.2012.03.002.

[3.4] Z. Bakó-Biró, D.J. Clements-Croome, N. Kochhar, H.B. Awbi, M.J. Williams, Ventilation rates in schools and pupils' performance, Build. Environ. 48 (2012)215–223, http://dx.doi.org/10.1016/j.buildenv.2011.08.018.

[3.5] D.A. Coley, R. Greeves, The effect of low ventilation rates on the cognitive function of a primary school class, Int. J. Vent. 6 (2) (2004).

[3.6] M. Santamouris, A. Synnefa, M. Asssimakopoulos, I. Livada, K. Pavlou, M.Papaglastra, et al., Experimental investigation of the air flow and indoor carbon dioxide concentration in classrooms with intermittent natural ventilation, Energy Build. 40 (2008) 1833–1843, http://dx.doi.org/10.1016/j.enbuild.2008.04.002.

[3.7] V. Richalet, B. Beheregaray, G. Guarracino, C. Dornier, L. Janvier, Ventilation by the windows in classrooms: a case study, in: Role Vent. 15th AIVC Conf. Buxton, Gt. Britain, 1994.

[3.8] K.J. McCartney, J. Fergus Nicol, Developing an adaptive control algorithm for Europe, Energy Build. 34 (2002) 623–635, http://dx.doi.org/10.1016/S0378-7788(02)00013-0.

[3.9] R. Fritsch, a. Kohler, M. Nygård-Ferguson, J.-L. Scartezzini, A stochastic model of user behaviour regarding ventilation, Build. Environ. 25 (1990) 173–181, http://dx.doi.org/10.1016/0360-1323(90)90030-U.

[3.10] G.Y. Yun, P. Tuohy, K. Steemers, Thermal performance of a naturally ventilated building using a combined algorithm of probabilistic occupant behaviour and deterministic heat and mass balance models, Energy Build. 41(2009) 489–499, http://dx.doi.org/10.1016/j.enbuild.2008.11.013.

[3.11] H.B. Rijal, P.G. Tuohy, M. Humphreys, J.F. Nicol, A.A. Samuel, J. Clarke, Using results from field surveys to predict the effect of open windows on thermal comfort and energy use in buildings, Energy Build. 39 (2007) 823–836, http://dx.doi.org/10.1016/j.enbuild.2007.02.003.

[3.12] C.F. Reinhart, Lightswitch-2002: A model for manual and automated control of electric lighting and blinds, Sol. Energy 77 (2004) 15–28, http://dx.doi.org/10.1016/j.solener.2004.04.003.

[3.13] J.F. Nicol, M. a. Humphreys, Adaptive thermal comfort and sustainable thermal standards for buildings, Energy Build. 34 (2002) 563–572, http://dx.doi.org/10.1016/S0378-7788(02)00006-3.

[3.14] M.A. Humphreys, J. Fergus Nicol, The validity of ISO-PMV for predicting comfort votes in every-day thermal environments, Energy Build. 34 (2002)667–684, http://dx.doi.org/10.1016/S0378-7788(02)00018-X.

[3.15] M.A. Humphreys, J.F. Nicol, Understanding the adaptive approach to thermal comfort, ASHRAE The ch. Data Bull. 14 (1988) 1–14 http://search.proquest.com/docview/192527084/fulltextPDF?accountid=12152.

[3.16] I. 7730, Ergonomia degli ambienti termici Determinazione analitica e interpretazione del benessere termico mediante il calcolo degli indici PMV ePPD e dei criteri di benessere termico locale UNI EN ISO 7730, 2006.

[3.17] M.A. Humphreys, Field studies of thermal comfort compared and applied, J.Inst. Heat. Vent. Eng. 44 (1976) 5–27.

[3.18] M. a. Humphreys, Outdoors temperatures and comfort indoors, Build. Res. Pract. 6 (2) (1978) 92–105.

[3.19] R.J. de Dear, G.S. Brager, Thermal comfort in naturally ventilated buildings: revisions to ASHRAE Standard 55, Energy Build. 34 (2002) 549–561, http://dx.doi.org/10.1016/S0378-7788(02)00005-1.

[3.20] I. Fato, F. Martellotta, C. Chiancarella, Thermal Comfort in the Climatic Conditions of Southern Italy., ASHRAE Trans. 110 PART I (2004) 578–593.

[3.21] S. Heidari, S. Sharples, A comparative analysis of short-term and long-term thermal comfort surveys in Iran, Energy Build. 34 (2002) 607–614, http://dx.doi.org/10.1016/S0378-7788(02)00011-7.

[3.22] M.A. Humphreys, J.F. Nicol, An adaptive guideline for UK office temperatures, in: Stand. Therm. Comf. Indoor Air Temp. Stand. 21 St Century, E FN Spon, London, UK, 1995.

[3.23] S. Barlow, D. Fiala, Occupant comfort in UK offices - How adaptive comfort theories might influence future low energy office refurbishment strategies, Energy Build. 39 (2007) 837–846, http://dx.doi.org/10.1016/j.enbuild.2007.02.002.

[3.24] T. Johnson, T. Long, Determining the frequency of open windows in residences: a pilot study in Durham, North Carolina during varying temperature conditions, J. Expo. Anal. Environ. Epidemiol. 15 (2005) 329–349, http://dx.doi.org/10.1038/sj.jea.7500409.

[3.25] V. Fabi, R. Andersen, S. Corgnati, B. Olesen, A methodology for modelling energy-related human behaviour: application to window opening behaviour in residential buildings, Build. Simul. (2013), http://dx.doi.org/10.1007/s12273-013-0119-6 (Accessed July 8 2015) http://link. springer. com/article/.

[3.26] R. Andersen, V. Fabi, J. Toftum, S.P. Corgnati, B.W. Olesen, Window opening behaviour modelled from measurements in Danish dwellings, Build. Environ.69 (2013) 101–113, http://dx.doi.org/10.1016/j.buildenv.2013.07.005.

[3.27] F. Haldi, D. Robinson, Interactions with window openings by office occupants, Build. Environ. 44 (2009) 2378–2395, http://dx.doi.org/10.1016/j.buildenv.2009.03.025.

[3.28] M.a. Humphreys, H.B. Rijal, J.F. Nicol, Updating the adaptive relation between climate and comfort indoors; new insights and an extended database, Build.Environ. 63 (2013) 40–55, http://dx.doi.org/10.1016/j.buildenv.2013.01.024.

[3.29] D. Daum, F. Haldi, N. Morel, A personalized measure of thermal comfort for building controls, Build. Environ. 46 (2011) 3–11, http://dx.doi.org/10.1016/j.buildenv.2010.06.011.

[3.30] R.-L. Hwang, T.-P. Lin, C.-P. Chen, N.-J. Kuo, Investigating the adaptive model of thermal comfort for naturally ventilated school buildings in Taiwan, Int. J.Biometeorol. 53 (2009) 189–200, http://dx.doi.org/10.1007/s00484-008-0203-2.

[3.31] D.J. Clements-Croome, H.B. Awbi, Z. Bakó-Biró, N. Kochhar, M. Williams, Ventilation rates in schools, Build. Environ. 43 (2008) 362–367, http://dx.doi.org/10.1016/j.buildenv.2011.08.018.

[3.32] T. Salthammer, E. Uhde, T. Schripp, A. Schieweck, L. Morawska, M. Mazaheri,et al., Children's well-being at schools: impact of climatic conditions and air pollution, Environ. Int. 94 (2016) 196–210, http://dx.doi.org/10.1016/j.envint.2016.05.009.

[3.33] J.M. Daisey, W.J. Angell, M.G. Apte, Indoor air quality, ventilation and health symptoms in schools: an analysis of existing information, Indoor Air 13(2003) 53–64, http://dx.doi.org/10.1034/j.160-0668.2003.00153.x.

[3.34] O. Seppänen, W. Fisk, M. Mendell, Association of ventilation rates and CO_2 concentrations with health and other responses in commercial and institutional buildings, Indoor Air 9 (1999) 226–252 (Accessed July 8 2015) http://energy.lbl.gov/ie/viaq/pubs/LBNL-43334.pdf.

[3.35] Gard-I, La qualità dell'aria nelle scuole e rischi per malattie respiratorie e allergiche (in Italian), 2010.

[3.36] Legambiente, Ecosistema scuola XVI Rapporto Legambiente sulla qualitàdell'edilizia scolastica, delle strutture e dei servizi (in Italian), 2014.

[3.37] M. Griffiths, M. Eftekhari, Control of CO2 in a naturally ventilated classroom, Energy Build. 40 (2008) 556–560, http://dx.doi.org/10.1016/j.enbuild.2007.04.013.

[3.38] L. Dias Pereira, D. Raimondo, S.P. Corgnati, M. Gameiro da Silva, Assessment of indoor air quality and thermal comfort in Portuguese secondary classrooms: methodology and results, Build. Environ. 81 (2014) 69–80, http://dx.doi.org/10.1016/j.buildenv.2014.06.008.

[3.39] P.V. Dorizas, M.-N. Assimakopoulos, C. Helmis, M. Santamouris, An integrated evaluation study of the ventilation rate, the exposure and the indoor air quality in

naturally ventilated classrooms in the Mediterranean region during spring, Sci. Total Environ. 502 (2015) 557–570, http://dx.doi.org/10.1016/j.scitotenv.2014.09.060.

[3.40] V. Turanjanin, B. Vuˇci´cevi´c, M. Jovanovi´c, N. Mirkov, I. Lazovi´c, Indoor CO2 measurements in Serbian schools and ventilation rate calculation, Energy 77(2014) 290–296, http://dx.doi.org/10.1016/j.energy.2014.10.028.

[3.41] SEARCH II Project, Making Schools Healthy: Meeting Environment and Health Challenges. Final publication of the SEARCH II project, 2013. http://search.rec.org/outcomes/uploads/documents/SearchMakingSchoolsHealthy WebDec2013.pdf.

[3.42] Sinphonie, Guidelines for Within Healthy Environments Within European Schools, 2014, http://dx.doi.org/10.2788/89936.

[3.43] J.C. Rufo, J. Madureira, I. Paciência, L. Aguiar, J.P. Teixeira, A. Moreira, et al., Indoor air quality and atopic sensitization in primary schools: a follow-upstudy, Porto Biomed. J. (2016) 3–7, http://dx.doi.org/10.1016/j.pbj.2016.07.003.

[3.44] F. Stazi, A. Vegliò, C. Di Perna, Experimental assessment of a zinc-titanium ventilated facade in a Mediterranean climate, Energy Build. 69 (2014)525–534, http://dx.doi.org/10.1016/j.enbuild.2013.11.043.

[3.45] ISO, EN ISO 7726:2001 Ergonomics of the Thermal Environment –Instruments for Measuring Physical Quantities, Comité Européen deNormalisation, Bruxelles, 2001.

[3.46] S. Carlucci, L. Pagliano, A review of indices for the long-term evaluation of the general thermal comfort conditions in buildings, Energy Build. 53 (2012)194–205, http://dx.doi.org/10.1016/j.enbuild.2012.06.015.

[3.47] CEN Standard EN 15251, Indoor environmental input parameters for design and assessment of energy performance of buildings- addressing indoor air quality, thermal environment, lighting and acoustics Contents, 2006.

[3.48] M.a. Humphreys, M. Hancock, Do people like to feel neutral? Energy Build. 39(2007) 867–874, http://dx.doi.org/10.1016/j.enbuild.2007.02.014.

[3.49] CIBSE Guide A, Environment Design, 8th ed., 2007, http://dx.doi.org/10.1016/B978-0-240-81224-3.00016-9.

[3.50] G. Brager, R. de Dear, Thermal adaptation in the built environment: a literature review, Energy Build. 17 (1998) (accessed April 22 2015) http://www. sciencedirect. com/science/article/pii/S0378778897000534.

[3.51] D. Teli, M.F. Jentsch, P. a, B. James, Naturally ventilated classrooms: an assessment of existing comfort models for predicting the thermal sensation and preference of primary school children, Energy Build. 53 (2012) 166–182, http://dx.doi.org/10.1016/j.enbuild.2012.06.022.

[3.52] R. De Dear, J. Kim, C. Candido, M. Deuble, Summertime thermal comfort in australian school classrooms, 8th Wind Conf. (2014) (p21).

[3.53] S. D'Oca, T. Hong, A data-mining approach to discover patterns of window opening and closing behavior in offices, Build. Environ. 82 (2014) 726–739, http://dx.doi.org/10.1016/j.buildenv.2014.10.021.

[3.54] M. Turunen, O. Toyinbo, T. Putus, A. Nevalainen, R. Shaughnessy, U.Haverinen-Shaughnessy, Indoor environmental quality in school buildings and the health and wellbeing of students, Int. J. Hyg. Environ. Health 217(2014) 733–739, http://dx.doi.org/10.1016/j.ijheh.2014.03.002.

[3.55] M. Mendell, G. Heath, Do indoor pollutants and thermal conditions in schools influence student performance? A critical review of the literature, Indoor Air (2005) (Accessed July 3 2015) http://onlinelibrary.wiley.com/doi/10.1111/j.1600-0668.2004.00320.x/pdf.

[3.56] N. Michelot, M. Carrega, Monitoring indoor air quality in French schools and day-care centres. Results from the first phase of a pilot survey, Heal. Build.2012, 10th Int. Conf. Brisbane (2012) 1–6.

[3.57] S. Lee, M. Chang, Indoor and outdoor air quality investigation at schools in Hong Kong, Chemosphere 41 (2000) 109–113, http://dx.doi.org/10.1016/S0045-6535(99)00396-3.

[3.58] D.G. Shendell, R. Prill, W.J. Fisk, M.G. Apte, D. Blake, D. Faulkner, Associations between classroom CO2 concentrations and student attendance in Washington and Idaho, Indoor Air 14 (2004) 333–341, http://dx.doi.org/10.1111/j.1600-0668.2004.00251.x.

[3.59] R. de Dear, J. Kim, C. Candido, M. Deuble, Adaptive thermal comfort in Australian school classrooms, Build. Res. Inf. 43 (2015) 383–398.

[3.60] K.K. Kalimeri, D.E. Saraga, V.D. Lazaridis, N.A. Legkas, D.A. Missia, E.I. Tolis,et al., Indoor air quality investigation of the school environment and estimated health risks: two-season measurements in primary schools in Kozani, Greece, Atmos. Pollut. Res. 1 15 (2016), http://dx.doi.org/10.1016/j.apr.2016.07.002.

[3.61] F. Stazi, F. Naspi, G. Ulpiani, C. Di Perna, Indoor air quality and thermal comfort optimization in classrooms developing an automatic system for windows opening and closing, Energy and Buildings, Volume 139, 15 March 2017, Pages 732-746.

[3.62] K. Schakib-Ekbatan, F.Z. C¸ akıcı, M. Schweiker, A. Wagner, Does the occupant behavior match the energy concept of the building? –Analysis of a German naturally ventilated office building, Build. Environ. 84 (2015) 142–150, http://dx.doi.org/10.1016/j.buildenv.2014.10.018.

[3.63] M. Schweiker, F. Haldi, M. Shukuya, D. Robinson, Verification of stochastic models of window opening behaviour for residential buildings, J. Build. Perform. Simul. 5 (2012) 55–74, http://dx.doi.org/10.1080/19401493.2011.567422.

[3.64] Nicol F., Sykes O., Smart controls for thermal comfort, the SCATS project, International conference on indoor air quality ventilation and energy conservation in buildings; 3; 844-849;1998.

4

Optimized design and smart control of a sunspace

Experimental monitoring of a sunspace applied to a NZEB mock-up: assessing and comparing the energy benefits of different configurations.[1]

[1] Published in Energy and Buildings, Volume 152, October 2017, pages 194-215

4.1 – ABSTRACT

This chapter collects the outcomes of an experimental study focused on the energy benefits achieved by coupling an energy efficient building with a sunspace in winter season and Mediterranean climate.

Acting as passive solar heating elements, sunspaces are intended to be a valuable tool among sustainable and energy-efficient constructive and/or retrofitting strategies.

In order to assess the energy saving potential of the above-mentioned coupling and relate it to the main design parameters, two operative steps were carried out: the numerical step allowed different simulated configurations to be evaluated in order to identify the optimal one from an energy perspective and physically realize it; the monitoring phase served the double purpose of calibrating the simulation model and provide on-site validated data for subsequent assessments and comparisons.

Three main sunspace configurations were tested: irradiative single-glazed, irradiative double-glazed and convective double-glazed.

The convective double glazed configuration was found to outperform the others since the daily energy consumption reduction exceeded the 27% (compared to the irradiative, double glazed counterpart) for all weather conditions. Besides, the activation of a mechanical ventilation system was slightly counterproductive in terms of discomfort phenomena since a less stable indoor air temperature was guaranteed.

Comparing the two irradiative configurations, it was found that the addition of an extra glass layer was responsible of a quite constant reduction of 1 kWh/day, thus increasing the percent heating energy demand saving achieved through the insertion of the sunspace from approximately 3,3% to 8,7%, while minimizing indoor air temperature fluctuations too.

4.2 – INTRODUCTION

According to the energy efficiency regulatory framework **[4.1-4.5]**, the design of energy-efficient buildings represents one of the most accredited ways of reducing buildings environmental impact as it requires both high-performance components and technical systems able to exploit the local/remote availability of renewable energy sources.

Among renewable sources, Solar energy is one of the most attractive (in particular in countries typically characterized by a high sunlight potential, like Mediterranean ones) as it can be turned both into electric and thermal energy and can rely on various technologies already well-established on the market **[4.6]**.

Those solutions can behave actively or passively: in the first case, Solar energy is accumulated and converted through specific technical systems (Solar thermal collectors, photovoltaic panels, ...); in the second case, Solar energy is stored as heat in ad-hoc indoor/outdoor spaces and then transferred across the building walls in order to replace the role of traditional heating systems (bioclimatic sunspaces).

This research activity investigated the latter solution.

Sunspaces do not represent an innovation since their use is rooted in Roman times **[4.7]**, but the application as a buffer zone allowing the entrance of a large quantity of Solar radiation between the house and the external environment **[4.8]** has been only recently found to be an effective means to mitigate the environmental impact of buildings **[4.9]**.

A sunspace recreates in small-scale the macroscopic phenomenon of the greenhouse effect occurring between Earth and the atmosphere. The essential role is played by the glazed surfaces, properly oriented in order to receive the highest and longest lasting Solar radiation. In this way, it is possible to turn the internal air volume into an efficient heat collector that reduces the thermal gap between indoor and outdoor environments thus lowering the energy demand required to the heating systems for balancing the heat losses.

This is why, as long as adequately designed, the bioclimatic sunspace exploits Solar gains to minimize or even invert the heat flows from the conditioned environment to the outdoors.

Sunspaces are conceived for the heating season as they capture the maximum sunlight coming in through the glazed surface (which is transparent to the visible wavelengths and opaque to the NIR's) causing the internal air and wall surfaces to increase their temperatures. In this way, both the indoor dry-bulb air temperature and the mean radiant temperature rise concurring to a higher operative temperature.

In this way, sunspaces serve the double purpose of buffer zone against the heat losses towards the outdoors and of heat collector which charges during the hottest hours (when Solar radiation peaks) and then gradually releases the stored heating power

during the hours of darkness thus providing a free energy income when needed more (in the evening and the night). The internal surface of the partition acts as a irradiative element becoming a passive heating component to be coupled with the active HVAC system commonly installed in buildings.

Yet, the energy benefit linked up with the application of a passive Solar system depends on the capability of the system for overtaking its inner inefficiencies.

In fact, the passive thermo-physical principle underlying a sunspace operation conveys two main consequences: on the one hand it guarantees the least energy expenditure as it behaves receptively, but on the other hand it limits the optimal management of the obtained free heat gain as there is no concurrence between maximum yield time intervals (typically occurring in summer) and peak demand ones (typically occurring in winter).

Besides, another problem to be taken into account (according to the construction requirements for NZEB buildings) is the eventual overheating a sunspace can provoke - even temporarily - in case of building wall blocks with very low thermal transmittances **[4.10].**

Sunspaces can behave in three different ways according to the role played by the partition wall and to the thermal coupling between the indoor air volumes:

- direct gain (**figure 4.1a**): the partition is completely removable. This means that indoor environment and sunspace create a sole air volume where the heating power collected by the sunspace is directly released to the internal living space. In the Italian region where the experimental activity in object took place, this typology is currently forbidden as it is in contrast with the regional law dated 20th April 2015;
- irradiative heat transfer (**figure 4.1b**): the partition consists of a wall whose indoors-overlooking surface rises in temperature because of the heat power collected inside the sunspace and gradually releases it via radiation.
- convective heat transfer (**figure 4.1c**): the partition is provided with adjustable openings on the top and the bottom or with controlled mechanical ventilation (VMC) ducts in order to enable the mixing between the two air volumes or even with the outdoor air and/or non-adjacent thermal zones. The open/close cycling can respond to specific control algorithms.

According to the Italian legislation, the present research analyzed the energy saving potential of both the last two operative modes, once closing whatever kind of direct air flowing between indoor environment and sunspace once enabling mechanical ventilation.

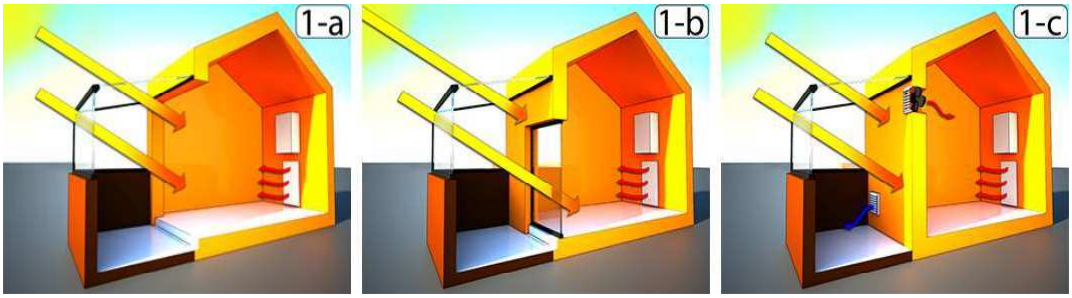


Figure 4.1

Solar gains and heat transfer displayed according to the three operative modes of a sunspace.

As a matter of fact, regardless of the specific thermal mechanism, the energy performance of a sunspace as a passive, climate-responsive design component is an often-troubled issue, mainly because it relies on countless variables (geometry, materials, users lifestyle, occupancy patterns, equipment, tree shading, orientation, local weather phenomena, …).

Besides there is still no broad consensus about the most proper calculation procedure to be adopted when it comes to describing sunspace thermal behaviour.

The effect of Solar greenhouses in the energy balance of a building during the heating period can be evaluated with different approaches: among the steady state (or semi steady state) procedures, the "Method 5000" **[4.11]** and the calculation process described in the Standard EN ISO 13790 **[4.12];** among the dynamic codes EnergyPlus **[4.13]** or TRNSYS software **[4.14].** Against this backdrop, Asdrubali et al. **[4.15]** performed the energy analysis of a sunspace located in Perugia (mid Italy) via the four above-mentioned methodologies and then compared the results with the real energy consumptions of the same building attached sunspace. Their findings showed that the average reduction of the winter energy demand due to the sunspace was about 20%, and that all methodologies were in good agreement: Method 5000 slightly overestimated the contribution of the sunspace, while the dynamic tool Energy Plus produced the closest results to the real ones (as it takes into account the role of unsteady meteorological data).

As the aim of the study in object was to truthfully depict the inner workings of the energy phenomena participating and/or competing in the operation of the sunspace, the "conventional" semi-steady approach provided by EN ISO 13790 was disregarded in favour of a dynamic approach (EnergyPlus).

Apart from the calculation procedure issues, particular emphasis has to be placed on correctly designing the sunspace in order to saturate its energy-saving potential. Widely accepted beliefs around solar heating design **[4.16,4.17]** state that, as a rule of thumb, Solar spaces should face no more than 30° from the south, roof glazing should

be minimized and vertical south-facing glazing should be maximized: this is because too shallowly sloped surface are unlikely to intercept sufficient Solar radiation in winter (when the Sun path is lower), while, conversely, they represent a trigger for overheating phenomena occurring in summer when their Solar receptivity is enhanced **[4.18-4.28].**

Unconventional, evidence-based alternatives are yet running in parallel, underpinning the suitability of such systems even in wider design configuration and even in geographic areas where overcast skies are predominant **[4.29-4.31].** For instance, Rempel et al. **[4.32]** found that conventional wisdom about sunspace application tend to underestimate the beneficial effect of diffuse Solar radiation, thus supporting wide deviations from southerly orientation to be taken into account. Besides tree shading, over-massing and insufficient insulation of thermal storage were found to be the main threats leading to under-heating, in agreement with previous similar works too **[4.33].**

The key parameters piloting the thermal behaviour of building attached sunspaces are addressed by many other theoretical and/or experimental studies: Mottard et al. **[4.34]**, for instance, focused on long infrared radiation exchanges as well as on the distribution of Solar radiation in the sunspace; Roux **[4.35]** ran a sensitivity analysis to point out the pivotal parameters driving the thermal exchanges through the sunspace walls.

Furthermore, the thermal performance of building attached sunspaces is strongly related to the ratio of glazed surface area to opaque surface area, walls and floor absorption coefficients and number of glass layers. Betaineh and Fayez **[4.36]**, for example, tested six configurations. Their findings show that heating load requirements are reduced by increasing the ratio of glazed surface area to opaque surface area and by utilizing a double layer of glass. Oliveti et al. **[4.37]** reached the same conclusions by demonstrating that the collecting capacity of Solar energy of a volume depends mostly on the configuration and optical properties of the surfaces.

In addition, the optimization of sunspace design must be conceived with due attention to outdoor boundary conditions, like weather and geographic features, which are major players in its expected and real energy performance. Case studies all around the world served the double purpose of finding general good practices and get a sense of the adjustments to be performed in an ad-hoc-developed design strategy.

Bakos and Tsagas **[4.38]** tested the thermal behaviour and the economic consequences of building attached sunspace located in northern Greece. Mihalakakou picked several locations throughout Europe to investigate the energy potential of a sunspace (both in wintertime and in summertime) as a function of diverse climatic conditions **[4.39].** His findings underpin the beneficial impact of sunspaces all over Europe during the heating season. Alfredo Fernandez-Gonzalez compared the wintertime thermal performance of five different passive solar test-cells (Direct Gain, Trombe-wall, Water wall, Sunspace, and Roof pond) and a control test-cell in America (Muncie, Indiana) **[4.40].**

Bataineh et al. **[4.36]** assessed the energy-saving effectiveness of six sunspace configurations (different ratio of glazed surface area to opaque surfaces) according to the climatic conditions in Jordan in order to extrapolate the optimal customized solution. Oliveti et al. **[4.41]** varied several key parameters (the exposure, the optical properties and the thermal capacity of the opaque surfaces, the amount of ventilation and the shading device) to define the correlation with the solar gains of the sunspace and the adjacent spaces for some Italian localities.

As a general result, many national and regional legislations have favoured the use of sunspaces in temperate climates, allowing incentives or extra building volumes, all while energy efficient buildings (NZEB) were gaining ground.

Against the above described backdrop, the actual challenge is developing and validating more accurate simulation and design tools for these systems with extensive field measurements to disclose characteristic patterns of heat gain, storage and loss and finally establish valuable design criteria which might be applicable throughout the year, adjustable for diverse climatic conditions and energy/cost effective even in case of hyper-insulated buildings **[4.39]**. Accordingly, Chiesa et al. **[4.42]** investigated the potential applicability of attached sunspaces in Southern and Central Europe, during wintertime, comparing different technological choices both in terms of insulation level (walls thermal transmittance ranging from 1,589 W/m^{2}K to 0,287 W/m^{2}K) and window system (single, double, triple glazing, low-e infilled with argon). Potential maps are finally reported to help designers optimise the use of sunspaces: as expected, the highest is the level of insulation of the building the highest must be the quality of the glazing in order to get significant advantage from the intervention measure. The results were obtained via EnergyPlus simulations, yet not validated with on-site collected real data.

The need for monitoring activities to support simulation models is highly underlined in various scientific papers: a recent one **[4.43]**, for example, demonstrated that the results of dynamic simulations can deviate by more than 30% by just changing the source of the typical meteorological year in input.

Being this the general context, the aim of this study was to take a step forward in the investigation of the energy benefits achievable when a sunspace is coupled with an energy efficient building (U-value below 0,2 W/m^{2}K in the specific case) by performing both a numerical and an experimental analysis.

The goals in particular were:

1. understand the weight of the main design parameters on the energy performance of a sunspace applied to a NZEB building: according to this target, 132 preliminary simulations were carried out (relying on the software DesignBuilder **[4.44]** and EnergyPlus) before building the physical experimental setting thus releasing a sort of database to support designers who approach this specific issue;

2. assess the effective energy saving achievable by coupling a sunspace and a NZEB mock-up by collecting on-site monitored data and processing the information to point out pros and cons of the different configurations under test (chosen among the above-mentioned proposed ones). Meaningful performance parameters were selected to allow a multi-perspective comparison;
3. validate the output of DesignBuilder and EnergyPlus by comparing the real case data set with the preliminary simulations. In this way, it was given proof of the scientific base underlying the information gathered in the previous step and it was possible to refine the building model by inserting an ad-hoc built weather file.

Therefore, the research in object is focused on the wintertime performance of an ad-hoc realized sunspace. Nevertheless, optimized solutions are to be looked for throughout the year.

Since the sunspace operates as a warm zone interposed between the conditioned indoor environment and the outdoors it is actually an architectural element very sensitive to summertime overheating phenomena.

Indeed, some considerations affecting the sunspaces sited on the Mediterranean coast climates, are to be referred for the necessary disposition of active/passive strategies.

The effect of attached sunspaces on the building thermal behaviour during the cooling season in warm/hot summer climates has been addressed in diverse papers, mainly focusing on passive design strategies and measures useful to mitigate or prevent the overheating blowbacks.

For instance, Oliveti et al. **[4.41]** compared through simulation, the overheating adduced by attached-sunspaces at three different latitudes - Cosenza (39◦N), Rome (41◦N) and Milan (45◦N). They verified that if a properly conceived Solar shading and ventilation strategy is applied, the sunspace can reach a temperature close to the exterior one, so that the buffer zone effect is actually by-passed.

Mihalakakou et al. **[4.45]** ran an extensive sensitivity investigation to analyse the impact of various parameters affecting the sunspace energy potential for a range of cases covering existing design practice. Apart from night ventilation and Solar protection, the passive technique of buried pipes was proposed **[4.46-4.49].** As a conclusion all the measures reduced overheating, although the best results were obtained with a combination of the three passive techniques.

Torra et al. **[4.50]** tracked and analysed three attached sunspaces in Barcelona, with the final aim of proposing design guidelines suitable to counteract the summertime sensitivities and disadvantages too: thermal regulation, full exploitation of the stack effect via natural and cross ventilation, plus the use of Solar filters were found to be efficient means of tackling undesired high indoor temperatures.

Similar end point for Bataineh et al. **[4.36]**, who simulated the thermal performance of a sunspace attached to a living room located in Amman-Jordan. They found that

adequate ventilation, Solar protection and an active/adaptive use of the sunspace (versus a static one), throughout the day, could lead to a global heating and cooling loads reduction of 42%.
Additionally, Aelenei et al. **[4.51]** studied four sunspace configurations in Portugal (two attached, one integrated and one partially integrated) in six different climatic zones. They found that the best energy performance was achieved by coupling natural ventilation of fully integrated sunspaces and inner shading devices with high reflectance.
Overall, all these studies show that sunspaces can be an appropriate and effective system all year round and even in extremely hot summer conditions **[4.52]** if properly designed to take full advantage of local climate and if overheating is addressed by combining the following counterbalancing measures:

- thermal regulation, since it controls nocturnal losses during winter, adjusts the gains during intermediate seasons and prevents excessive gains during summer: movable insulation like inside dark rollers, exterior or interior dark ventilation blinds (during summer the exterior one is better, whereas the interior one is preferred for the intermediate seasons), outside movable horizontal louvers, etc.
- Eolic orientation, natural and cross ventilation (through accurately distributed openings, superior chimneys or shunts), given that the stack effect is a high efficient regulating mechanism as well as of easy adaptation to most of the designs.
- use of canvas or solar filters together with damp zones inside/outside the sunspace.

On the basis of all these findings further experimental activities will be performed in the future to complete the contents of the present research.

4.3 – MATERIALS AND METHODS

Assessing the energy behavior of a sunspace applied to a NZEB building requires both an experimental and a numerical activity in order to build up an on-site validated model and then decline it to test the effects of alternative configurations.
As a consequence, the overall study has been planned in order to get all necessary information for an optimal design of the sunspace itself, its physical realization and its monitoring with the final purpose of quantifying how much it passively exploited the renewable energy coming from the Sun to reduce buildings heating requirements.
In the next paragraphs, the operational steps driving the conduction of the experimental study are described in detail as well as the specifics of the case study (composed by mock-up and sunspace).

4.3.1 – Phases

The research in question is multi-disciplinary activity aiming at providing useful information about potential energy saving achievable when a sunspace works coupled with an energy-efficient building.

The general strategy (**figure 4.2**) has been structured involving several sequential phases:

1. building up of the model of the mock-up without sunspace (used as baseline for next-coming analyses) by means of the dynamic simulation software DesignBuilder and EnergyPlus **[4.53,4.54]**;
2. simulation of different sunspace configurations starting from the most common solutions compliant to the minimum requirements imposed by the national legislation and then varying both technical specs and boundary conditions **[4.55,4.56]**;
3. selection of the most proper sunspace typology to serve as basic structure;
4. design and realization of the sunspace forecasting adaptable means for testing different configurations (further glass layers, holes and fans to enable mechanical ventilation between the sunspace and the mock-up, ...);
5. setting up of the sensor network in order to record both outdoor and indoor microclimate conditions during the heating period and to define envelope's and technical systems' energy performance;
6. detailed on-site monitoring;
7. comparison of the energy benefit achieved by each configuration according to specific performance parameters;
8. validation of the building (mock-up plus sunspace) model via DesignBuilder and EnergyPlus by comparing simulated and on-site-collected data.

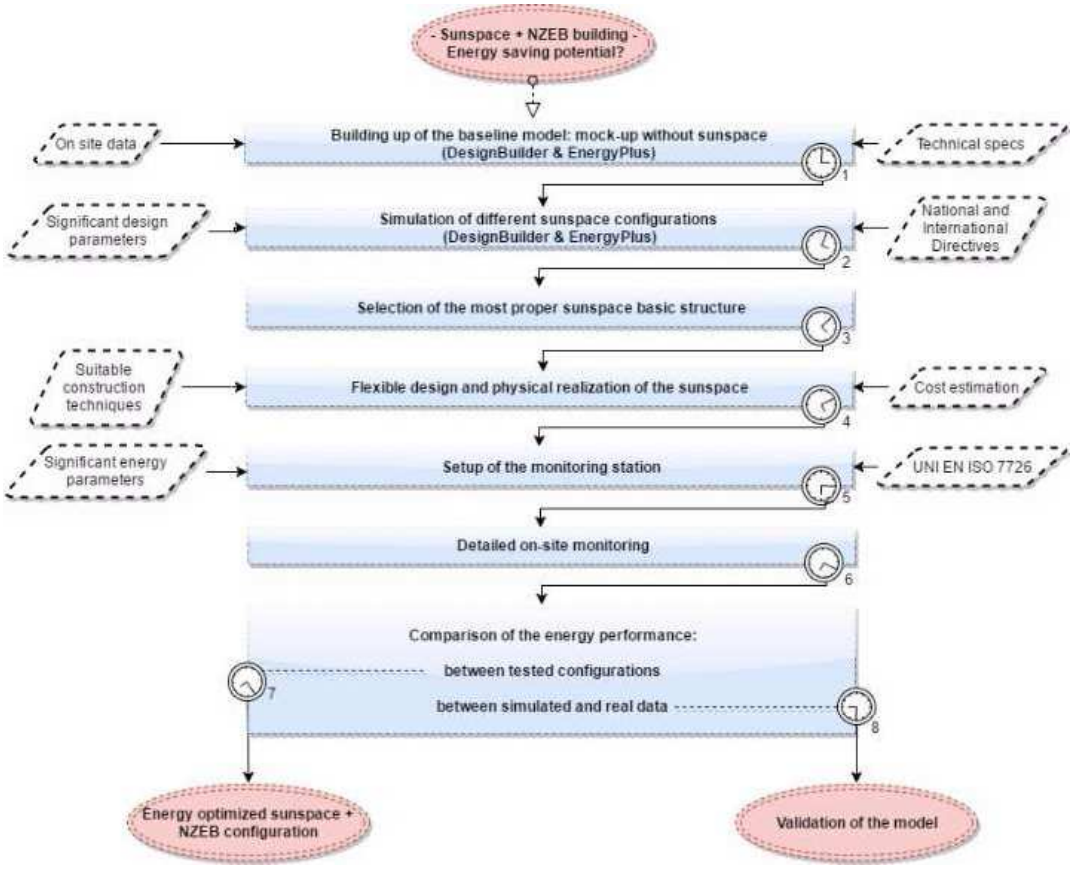


Figure 4.2

Flow diagram of the operational steps to investigate the potential energy saving achievable when a sunspace works coupled with an energy-efficient building.

4.3.2 – Mock-up

The experimental building is the hyper-insulated mock-up described in **chapter 2**, with slight variations.

The main geometrical and thermal properties are summarized in **table 4.1.**

MOCK-UP WALLS COMPOSITION				
Material	**Specific heat, C_p** [J/kg K]	**Thermal conductivity, λ** [W/m K]	**Thickness, t** [mm]	**Thermal resistance, R** [m²K/W]
Flooring				
Surface reisistance (external)	-	-	-	0.10
Air space	1000	0.3	182	0.18

Mineralized fir wood wool bound with grey Portland cement	1000	2.5	250	0.10
EPS (polystyrene)	1500	0.036	120	3.33
Air space	1000	0.3	40	0.21
Vapour barrier	1500	0.17	1	0.01
Wood	1660	0.12	34	0.28
Surface reisistance (internal)	-	-	-	0.17
Tot.			627	4.38
Thermal transmittance U (W/m^{2}K)				0.228
Roofing floor				
Surface reisistance (internal)	-	-	-	0.1
Wood	1000	0.17	25	0.15
Vapour barrier	1800	0.4	1	0.00
EPS (polystyrene)	1500	0.036	120	3.33
Sheath slated coupled with 40 mm XPS	1470	0.17	7	0.04
	1200	0.033	40	1.21
Surface reisistance (External)	-	-	-	0.17
Tot.			193	5.01
Thermal transmittance U (W/m^{2}K)				0.200
Walls				
Surface reisistance (internal)	-	-	-	0.13
Internal plasterboard	837	0.2	12.5	0.06
Vapour barrier	1500	0.17	1	0.01
Rock wool (internal coating)	1030	0.035	50	1.43
X-lam	2700	0.14	120	0.86
XPS (60 cm from foundation mat)	1200	0.038	100	2.63
Rock wool (external coating)	1030	0,036	100	2.78
Cement mortar	1000	0.48	10	0.02
Surface reisistance (External)	-	-	-	0.04
Tot.			293.5	5.32
Thermal transmittance U (W/m^{2}K)				0.188

Table 4.1
Mock-up walls composition: materials, thicknesses, thermal transmittances. in compliance with the international Standard ISO 13786 ***[4.57]***

Just to recap, the basic structure is in X-Lam, coated with a high-density insulating layer. The recommended number of air changes per hour is 7.9 according to UNI EN 13829 **[4.58]**.

As for the technical systems, the mock-up is provided with three radiant electric radiators hung on the west and east oriented walls and there fixed with dowels into the plasterboard supporting upright. The overall nominal power is close to 1200 W. Their activation is submitted to both an on/off controller programmed in graphical

language (LabVIEW by National Instruments) and a safety overheat thermostat connected in series to properly react to potential system breakdowns.
Radiators' technical specifics are summarized in **table 2.5.**
During all the monitoring activity the indoor setpoint temperature was kept fixed at a constant value of 20°C in compliance with the Italian law on building heating requirements **[4.59].**
On the partition wall, which separates the mock-up from the sunspace, two 100mm diameter holes (bored at a height of 2.50m and 0.20m respectively) house a couple of fans whose operation allows to activate mechanical ventilation.

4.3.3 – Sunspace

The overall process of design and construction of the sunspace was internal to the resources made available by the Università Politecnica delle Marche. It required four main steps:

1. preliminary design, based on several dynamic simulations run on a calibrated model;
2. definitive and executive design collecting all quantitative data to proceed with the physical implementation of the new component;
3. construction phase (10th-23th December 2015);
4. monitoring plan to define the typology, the number and the location of the sensors required to get all needed information.

In the following sub-paragraph, preliminary simulations made to optimize the sunspace conception are described in order to justify the final adopted configuration.

4.3.3.1 – Preliminary simulations

As long as an engineering solution is well established on the market and consolidated design guidelines are readily available to the various stakeholders there is no need to verify every time what is the configuration that most closely matches one or more target functions. In the specific case of a sunspace lying on the hyper insulated walls of a NZEB building, preliminary analyses were necessary to exclude the less effective solutions and keep just the most promising ones for further investigation.
Dynamic simulation tools (DesignBuilder 4.5.0.148 graphics and EnergyPlus 8.3.0 calculation modules) were adopted in this phase to assess the potential energy benefits occurring when the mock-up plus sunspace configuration was somehow modified in order to tune the pivotal design parameters.
General settings are reported in **table 4.2**.

PRELIMINARY SIMULATIONS - SETTINGS	
General Features	
Loads Convergence Tolerance Value	0.04
Temperature Convergence Tolerance Value [delta]	0.4
Solar Distribution	Full Interior and Exterior
Maximum Number of Warmup Days	25
Minimum Number of Warmup Days	6
Number of Timesteps per Hour	30
Heat Balance Algorithm	
Algorithm	Conduction Transfer Function
Surface temperature upper limit [°C]	2000
Surface Convection Algorithm: Outside	DOE-2: correlation from measurements by Klems and Yazdanian for rough surfaces
Surface Convection Algorithm: Inside	TARP: Thermal Analysis Research Program, by blending correlations from ASHRAE and flat plate experiments by Sparrow et. al.
Shadow Calculation	
Calculation method	Average over days in frequency
Calculation frequency	20
Maximum figures in shadow overlap calculations	15000
Polygon clipping algorithm	Sutherland Hodgman
Sky diffuse modeling algorithm	Simple Sky Diffuse Modeling

Table 4.2
Preliminary simulations general settings.

The main target of this preliminary comparative step is to get out as much verifiable information as possible to lead the subsequent design and construction phases with the double intent of setting a proper experimental building and pre-configuring it in a flexible way so that different tests could be carried out on the same basic structure.

4.3.3.2 – Inputs and outputs

To achieve the afore-mentioned goal a total number of 132 simulations were run varying on a case-by-case basis the dimensions of the sunspace (both in terms of depth and of glazed surface) and/or the number of the glass panes and/or the partition settings intervening, in particular, on:

1. the percentage of the glazed surface of the sunspace:
   - 0% (completely opaque walls);
   - 30% of the overall sunspace perimeter surface (4.80m^2 glass over 15.80 m^2);
   - 50% of the overall sunspace perimeter surface (7.08m^2 glass over 15.80 m^2);

2. the typology of glazed surface:
   - single layer;
   - double layer;
3. the depth of the sunspace (in plan):
   - 1.50m;
   - 2.00m;
   - 2.20m;
   - 2.50m.
4. the glazed opening on the partition wall, which could be:
   - absent;
   - present (dimensions=2.10x0.80m, thermal transmittance=2.67 W/m²·K).

The outputs of the simulations were primarily used to investigate the interrelations between the geometry of the sunspace components, the Solar gains and the heat losses occurring in the overall observation period (**table 4.5**) as directly linked to the building surface area, the percentage of glazed surface and the number of layers composing the glazed panel.

The weather file used in input was the one referred to the town of Falconara, 11,6 km distant from Agugliano (**table 4.4**). The thermal transmittances adopted to model the NZEB mock-up were: 0.19 W/m²K for the walls, 0.20 W/m²K for the ceiling and 0.23 W/m²K for the above ground floor. The typology of glass set in the simulations was the same used to build the sunspace and tested during the monitoring activity. Technical specs are summarized in **table 4.3.**

In order to better understand the energy aftermaths related to the varied design parameters, a benchmark value for each energy parameter was identified to provide a common baseline for the comparative analysis by running the simulations on reference buildings composed by the same mock-up (with or without the opening on the partition wall), but without the sunspace (**table 4.5**).

SUNSPACE FENETRATION FEATURES				
Optical properties				
Light transmission -T_v	88		75	
Light Reflection - ρ_v (%)	8		17	
Internal light reflection - ρ_{vi} (%)	8		16	
Colour Rendering - RD65 - R_a (%)	98		98	
Thermal properties (EN 673)				
U_g-Value	5.6		1.6	
Energy properties (EN 410 - ISO 9050)	**EN 410**	**ISO 9050**	**EN 410**	**ISO 9050**
Solar factor - g (%)	78	77	70	68

Energy Reflection - ρ_e (%)	7	7	14	14
Direct Energy Transmission - τ_e(%)	73	71	61	58
Solar abs. Glass 1 - α_e (%)			15	17
Solar abs. Glass 2 - α_e (%)			10	11
Total Energy absorption - α_e (%)	20	22	25	28
Shading coefficient - SC	0.9	0.89	0.8	0.78
UV Transmission - UV (%)	0		0	
Selectivity	1.13	1.14	1.07	1.1
Thickness and weight				
Nominal thickness (mm)	8.38		22.38	
Weight (kg/m^2)	21		26	

Table 4.3
Sunspace glass properties.

PRELIMINARY SIMULATIONS – CLIMATIC DATA		
Observation period: 01/11/2015 - 15/04/2016		
Assessment days	[dd]	166
Assessment hours	[hh]	3984
Outdoor mean temperature	[°C]	7.54
Outdoor max temperature	[°C]	22
Outdoor min temperature	[°C]	-4
Mean Solar radiation	[W/m^2]	69.88
Max Solar radiation	[W/m^2]	802
Min Solar radiation	[W/m^2]	0
Mean relative humidity	[%]	82.42
Max relative humidity	[%]	100
Min relative humidity	[%]	31
Mean wind velocity	[m/s]	1.97
Max wind velocity	[m/s]	26
Min wind velocity	[m/s]	0
Degree days	[DD]	49981.8
Sunspace surface	[m^2]	12.18

Table 4.4
Preliminary simulation general settings.

REFERENCE BUILDINGS			
Sunspace		NO	NO
Door		NO	YES
Estimated energy requirements	[kWh]	741.76	723.95
Energy requirements per square meter	[kWh/m^{2}year]	60.90	59.44
Energy requirements per degree days	[Wh/DD]	1.48406	1.44843
Average estimated daily energy requirements	[kWh/d]	4.47	4.36

Table 4.5
Reference buildings details.

4.3.3.3 – Results and discussion

Table 4.6 summarizes the results coming out of the entire simulation activity: the differences between single-glazed, double-glazed and 0%, 30% or 50% glazed area percentages are displayed according to four macro-categories which refer to the depth of the sunspace.

PREMILINARY SIMULATIONS - RESULTS										
SUNSPACE SIZE: 150cm										
Typology of glass panels	No glass	No glass	Single	Double	Single	Double	Single	Double	Single	Double
Percentage of glazed surface[%]	-	-	30%	30%	30%	30%	50%	50%	50%	50%
Door?	No	Yes	No	No	Yes	Yes	No	No	Yes	Yes
Estimated energy demand [kWh]	743.4	841.2	713.3	697.6	737.2	705.3	708.7	683.3	717.0	663.2
Annual specific energy demand (per unit area) [kWh/m^{2}year]	61.03	69.06	58.57	57.27	60.53	57.91	58.19	56.10	58.87	54.45
Specific energy demand (per degree day) [Wh/DD]	1.487	1.683	1.4272	1.3956	1.4749	1.4112	1.418	1.367	1.4345	1.327
Estimated average daily energy demand [kWh/d]	4.48	5.07	4.30	4.20	4.44	4.25	4.27	4.12	4.32	4.00
Difference in energy demand (absolute terms) [kWh]	1.6	99.4	-28.4	-44.2	-4.6	-36.4	-33.1	-58.5	-24.8	-78.6
Difference in energy demand	0.22%	16.2%	-3.83%	-5.96%	1.83%	-2.57%	-4.46%	-7.88%	-0.96%	-8.40%

(per cent terms) [%]										
SUNSPACE SIZE: 200cm										
Typology of glass panels	No glass	No glass	Single	Double	Single	Double	Single	Double	Single	Double
Percentage of glazed surface [%]	-	-	30%	30%	30%	30%	50%	50%	50%	50%
Door?	No	Yes	No	No	Yes	Yes	No	No	Yes	Yes
Estimated energy demand [kWh]	745.4	848.61	717.49	705.88	753.21	727.91	712.39	692.56	734.16	689.08
Annual specific energy demand (per unit area) [kWh/m²year]	61.19	69.67	58.91	57.95	61.84	59.76	58.49	56.86	60.28	56.57
Specific energy demand (per degree day) [Wh/DD]	1.4912	1.6978	1.4355	1.4123	1.5070	1.4564	1.4253	1.3856	1.4689	1.3787
Estimated average daily energy demand [kWh/d]	4.49	5.11	4.32	4.25	4.54	4.39	4.29	4.17	4.42	4.15
Difference in energy demand (absolute terms) [kWh]	3.6	124.7	-24.3	-35.9	29.3	4.0	-29.4	-49.2	10.2	-34.9
Difference in energy demand (per cent terms) [%]	0.48%	17.22%	-3.27%	-4.84%	4.04%	0.55%	-3.96%	-6.63%	1.41%	-4.82%
SUNSPACE SIZE: 220cm										
Typology of glass panels	No glass	No glass	Single	Double	Single	Double	Single	Double	Single	Double
Percentage of glazed surface [%]	-	-	30%	30%	30%	30%	50%	50%	50%	50%
Door?	No	Yes	No	No	Yes	Yes	No	No	Yes	Yes
Estimated energy demand [kWh]	745.98	851.05	718.9	705.88	759.79	736.72	713.68	695.55	740.86	698.95
Annual specific energy demand (per unit area) [kWh/m²year]	61.25	69.87	59.02	57.95	62.38	60.49	58.59	57.11	60.83	57.39
Specific energy demand (per degree day) [Wh/DD]	1.4925	1.7027	1.4383	1.4123	1.5201	1.4740	1.4279	1.3916	1.4823	1.3984
Estimated average daily energy demand [kWh/d]	4.49	5.13	4.33	4.25	4.58	4.44	4.30	4.19	4.46	4.21
Difference in energy demand (absolute terms) [kWh]	4.2	127.1	-22.9	-35.9	35.8	12.8	-28.1	-46.2	16.9	-25.0

Difference in energy demand (per cent terms) [%]	0.57%	17.56%	-3.08%	-4.84%	4.95%	1.76%	-3.79%	-6.23%	2.34%	-3.45%
SUNSPACE SIZE: 250cm										
Typology of glass panels	No glass	No glass	Single	Double	Single	Double	Single	Double	Single	Double
Percentage of glazed surface [%]	-	-	30%	30%	30%	30%	50%	50%	50%	50%
Door?	No	Yes	No	No	Yes	Yes	No	No	Yes	Yes
Estimated energy demand [kWh]	746.77	854.52	720.8	711.83	769.32	748.77	715.41	699.45	750.89	711.9
Annual specific energy demand (per unit area) [kWh/m²year]	61.31	70.16	59.18	58.44	63.16	61.48	58.74	57.43	61.65	58.45
Specific energy demand (per degree day) [Wh/DD]	1.4941	1.7097	1.4421	1.4242	1.5392	1.4981	1.4313	1.3994	1.5023	1.4243
Estimated average daily energy demand [kWh/d]	4.50	5.15	4.34	4.29	4.63	4.51	4.31	4.21	4.52	4.29
Difference in energy demand (absolute terms) [kWh]	5.0	130.6	-21.0	-29.9	45.4	24.8	-26.4	-42.3	26.9	-12.1
Difference in energy demand (per cent terms) [%]	0.68%	18.04%	-2.83%	-4.03%	6.27%	3.43%	-3.55%	-5.70%	3.72%	-1.66%

Table 4.6
Preliminary simulations energy results.

The first immediately noticeable outcome was that the 150cm deep sunspace guaranteed the best energy performance, regardless of the constructive typology and the other pivotal parameter values. The maximum energy saving was 8% reached with a 50% glazed surface. The presence of an opening on the partition wall (realistically conceivable since sunspaces are mainly obtained by closing existing balconies and terraces) was totally counterproductive when increasing the sunspace depth: the energy benefit plummeted hitting a negative low and the ratio between the recovered heat and the global Solar energy incident on the external surfaces of the sunspace barely exceeded the unit. This means that a deep sunspace attached to a NZEB wall provided with an opening is expected to raise the energy demand of the system rather than to improve the energy performance.

A second analysis, carried out fixing the sunspace depth at 150cm, focused on the role played by the number of panes composing the glazed surface and the glass percentage

over the overall perimeter surface. It highlighted that, regardless of the specific wall composition, the best energy performance was guaranteed by keeping the aforementioned percentage within the range 40% to 80%. Borderline case of 100% (walls plus flat roof) glazed surface configuration was included to better define the trend lines.

Indeed, the other finding was that the relocation of the glazed surfaces on the side walls (east and/or west exposed) was detrimental in terms of energy saving as it penalized the overall benefit. The underlying reason is supposed to be that by increasing the thermal transmittance of the walls which are not as heated up by the Sun as the south-exposed ones it is likely that greater heat losses might be recorded compared to the configuration with opaque side walls.

Finally, by analyzing both the charts in **figure 4.3** (which display the percent energy saving occurring when the glazed opening on the partition wall is respectively absent and present), it is evident that the achievable energy saving tends to be directly related to the increase of vertical glazed surface. In any case, extending the glazed panels to the roofing floor reveals itself to be substantially counterproductive. The explanation is that a side effect of replacing the existent roof with a higher-thermal-transmittance composition is the rise up in terms of heat losses towards both the outside and the canopy that, in the case of a horizontal surface, is not compensated by the amount of Solar radiation captured during winter season when the angle of elevation of the Sun is particularly low at such latitudes.

The difference between the two models (the one with the opening and the one without it) lies on the energy saving optimal percentage of glazed area: in the first case it is around 50%, while in the second one it is 70% which means that all vertical walls are glazed surfaces. This is because the opening on the partition allows to better exploit the direct Solar radiation income so that the increase in the heat losses (compared to a highly insulated opaque wall) is far outweighed by the increase in Solar gains. However, this result can be guaranteed just in case the materials composing the glass panels are characterized by low thermal transmittance and, contemporarily, high Solar factor.

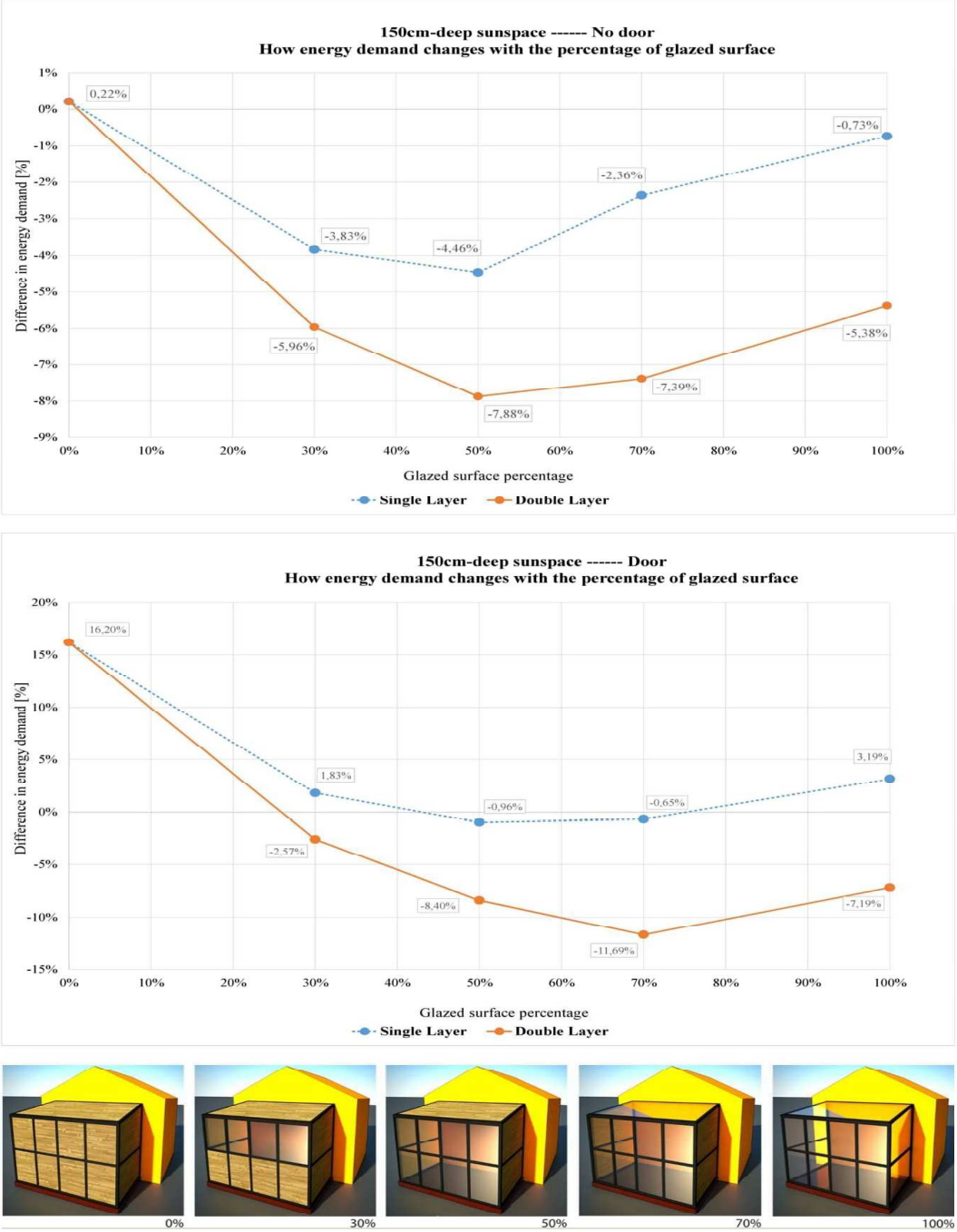


Figure 4.3

Graphical analysis of the energy saving trends related to the number of glazed panes and the presence of the opening on the partition wall.

4.3.3.4 – Construction

Taking into account the results emerged from the preliminary simulations campaign, it was decided to apply some specific design techniques in order to set a sort of flexible basic structure of the sunspace: the initial configuration (which is the one monitored in this experimental study) was characterized by a depth of 150 cm and a glazed percentage of 30%. Both the parameters could be easily and rapidly varied intervening on the flexible structure.

The sunspace (**figure 4.4**) was built on the south wall of the mock-up by applying an earlier wood construction technique, called balloon framing, widely spread in the recent years as it fastens and reduces the costs of house building compared to timber or platform framing **[4.60].** The reticular structure made with very long pieces of lumber ran from the foundation to the top. Wall cavities were retrofitted by inserting rigid insulating panels within mullions and transoms (providing a fire blocking action too).

The only modification to this general structure regarded the decking floor where the insulating panels were covered with a protective plywood sheet to make it viable.

Foundations were realized posing fir beams on a load-bearing structure composed by seven zinc-coated metal tip bars mechanically anchored to the ground and a beam directly fixed to the mock-up X-lam structure. Another analogue beam was used to support the roof whose fir planks were stroked with bituminous sealing paints and overprotected with riveted bituminous slated tiles.

The walls were made of beaded fir beams just screwed to the structure in order to ease the change to other planned configurations, while the glass facade was mechanically mounted on a wooden batten support frame fixed with both screws and polyurethane glue.

The sunspace was provided with three openings: a lateral entry door and two small windows located at the top of the west and east oriented walls enabling natural ventilation during the cooling period.

All wooden surfaces were waterproofed, treated against insects and fungi with specific wood stains and internally insulated with XPS panels fixed with acrylic glue.

Geometrical and thermal properties are summarized in **table 4.7.**

SUNSPACE WALLS COMPOSITION				
Material	**Specific heat, Cp [J/kg K]**	**Thermal conductivity, λ [W/m K]**	**Thickness, d [mm]**	**Thermal resistance, R [m2K/W]**
Flooring				
Surface reisistance (External)	-	-	-	0.10

Wood	1660	0.12	35	0.29
EPS (polystyrene)	1200	0.034	40	1.18
Surface reisistance (internal)	-	-	-	0.17
Tot.			75	1.74
Thermal transmittance U (W/m²K)				0.575
Roofing floor				
Surface reisistance (internal)	-	-	-	0.10
XPS	1450	0.036	40	1.11
Wood	1660	0.12	25	0.21
Sheath slated	1470	0.17	7	0.04
Surface reisistance (External)	-	-	-	0.17
Tot.			72	1.63
Thermal transmittance U (W/m²K)				0.613
Walls				
Surface reisistance (internal)	-	-	-	0.13
XPS	1450	0.036	40	1.11
Wood	1660	0.12	25	0.21
Surface reisistance (External)	-	-	-	0.04
Tot.			65	1.49
Thermal transmittance U (W/m²K)				0.671

Table 4.7

Sunspace walls composition: materials, thicknesses, thermal transmittances.



Figure 4.4
Sunspace construction details.

4.3.4 – Sensor network

The setup of the monitoring station (working from December 2015 to April 2016) was conceived to collect all useful information to:

- properly fill the input parameters required by DesignBuilder and EnergyPlus in order to recreate the boundary conditions and simulate the building dynamic energy behavior, both before and after the construction of the sunspace;
- assess how the presence of the sunspace affects the energy performance of the NZEB mock-up both in absolute and per cent terms;
- record the building response to different outdoor conditions providing means for a proper normalization of energy consumption data and for an adequate assessment of the efficiency of the sunspace as a passive Solar energy collector;
- compare the energy performance of the four tested configurations.

Being these the main targets, a rich list of components (sensors, data loggers, acquisition modules, storage devices, controllers, actuators) were installed both on the inside and on the outside of mock-up and sunspace.

In particular, the settlement of different monitoring stations was necessary:

I. meteorological station: it included air temperature, relative humidity, global Solar radiation and wind speed sensors. Data collection allowed the recreation of boundary conditions, necessary to the double purpose of turning the results into a non-climate-dependent format and of assessing the energy efficiency of the sunspace in collecting Solar radiation;

II. mock-up indoor microclimate station: it was composed of a PT100 sensor to record the dry-bulb temperature and a hygrometer to measure the moisture content inside the conditioned space. Both the probes were installed in a central point to be representative of the average values. In addition, three other sensors were located inside the mock-up: two thermocouples to acquire the temperature of the air passing through the VMC canals and a power meter to measure the energy consumption of the technical systems.

Data collection allowed the ventilation and the heating systems to properly work according to the specific thermal operative conditions inside the building, providing the inputs for the automated control which drove the on/off cycling.

III. mock-up interface monitoring station: it was distributed on the envelope of the mock up and consisted of four flat platinum resistors coupled with an equal number of flux-meters.

Data collection allowed the heat wave path and attenuation across the partition wall to be investigated in order to check in real time the effect of the NZEB thermal inertia. Meaningful information was then provided to understand the differences between heating phenomena inside the sunspace (when working in irradiative mode) and inside the mock-up.

IV. sunspace indoor monitoring station: it involved three RTDs located at different heights in the center of the sunspace.
Data collection allowed the thermal stratification inside the sunspace to be investigated in response to different climate conditions. Besides the records were used to determine the delta T piloting the activation of the fans.

V. sunspace interface monitoring station: it included six flat RTDs, two flux-meters and two radiometers located both on the surface of the partition wall and on the south-exposed external wall surface.
Data collection allowed a full comprehension of thermal phenomena occurring across the partition wall and at the same time the collection of more accurate information about Solar radiation actually hitting the sunspace.

Sensors composing the network were calibrated and set up in compliance with UNI EN ISO 7726:1998 **[4.61]** and its last review **[4.62]** requirements. Particular attention was paid during the monitoring design to avoid the installation of the probes near the electric radiators and, in this way, minimize eventual interferences and get good signal-to-noise ratios.
Sensors signals coming from the mock-up indoor microclimate station and the meteorological station were collected by an LSI Lastem dataTaker 8xx series; sunspace indoor and outdoor monitoring stations were connected to other two LSI Lastem data loggers (a Babuc-A and an E-Log).
Finally, the technical systems (heating and ventilating devices) were piloted via National Instruments digital output module (NI USB 6008). In the feeding line from the NI module (processing the command signal) and the electric radiators, three additional elements were inserted:

- a static relay whose double aim was to adjust the power variations and to provide electric insulation between the control circuit and the electrical system by acting as a circuit breaker;
- mechanical relays to pilot the on/off of the fans and the opening/closing of the ventilation duct grids;
- a power meter, used to determine the consumption rate.

Data loggers were connected to a central PC working both as a storage device and a data processor thanks to an ad-hoc developed LabVIEW software. The building was provided with network connection so that remote control was enabled during all monitoring activity ensuring just-in-time data observation and operational readiness (TeamViewer10 software).
Measuring instruments and sensor network specifics are summarized in **table 4.8**.

SUNSPACE SENSOR NETWORK							
Measure	**Sensor**	**Model**	**Logger**	**Rate**	**Position**	**Range**	**Accuracy**
Indoor monitoring station Mock-up							
Air temp.	Platinum resistor	PT100	Datataker	1 min	Centre of the room - 1.10 m	-40°C÷+80°C	0.05°C
Relative humidity	Thermo hygrometer	DME775	Datataker	1 min	Centre of the room - 1.10 m	-30°C÷+70°C	0.2°C
Air temp.	Thermocouple	TC Tipo T	Datataker	1 min	South wall - Fan channel - 2.50 m	-100°C÷+400°C	±1°C
Air temp.	Thermocouple	TC Tipo T	Datataker	1 min	South wall - Fan channel – 0.20 m	-100°C÷+400°C	±1°C
Power meter	Wattmeter	S500	Datataker	1 min	Centre of the room – 0.10 m	230-415 V	±0.5%
Indoor monitoring station - sunspace							
Air temp.	Platinum resistor	PT100	Elog	5 min	Centre of the Sunspace – 1.90 m	-40°C÷+80°C	0.05°C
Air temp.	Platinum resistor	PT100	Elog	5 min	Centre of the Sunspace – 1.20 m	-40°C÷+80°C	0.05°C
Air temp.	Platinum resistor	PT100	Elog	5 min	Centre of the Sunspace – 0.60 m	-40°C÷+80°C	0.05°C
Interface monitoring station Mock-up							
Surface temp.	Platinum resistor	PT100	Datataker	1 min	Earthen-walled south wall - inner surface – 1.10 m	-40°C÷+80°C	0.05°C
Surface temp.	Platinum resistor	PT100	Datataker	1 min	Plasterboard south wall - inner surface - 1.10 m	-40°C÷+80°C	0.05°C
Surface temp.	Platinum resistor	PT100	Datataker	1 min	Earthen-walled south wall - internal side – 1.10 m	-40°C÷+80°C	0.05°C
Surface temp.	Platinum resistor	PT100	Babuc A	5 min	XLAM south wall - internal side – 1.10 m	-40°C÷+80°C	0.05°C
Thermal flow	Platinum resistor	HFP01	Datataker	1 min	Plasterboard north wall - inner surface – 1.10 m	-2000to +2000W/m²	+5/-5%
Thermal flow	Platinum resistor	HFP01	Datataker	1 min	Earthen-walled south wall - inner surface – 1.10 m	-2000to +2000W/m²	+5/-5%
Thermal flow	Platinum resistor	HFP01	Datataker	1 min	Earthen-walled south wall - internal side – 1.10 m	-2000to +2000W/m²	+5/-5%
Thermal flow	Platinum resistor	HFP01	Datataker	1 min	Plasterboard south wall - inner surface – 1.10 m	-2000to +2000W/m²	+5/-5%
Interface monitoring station – sunspace side							
Surface temp.	Platinum resistor	PT100	Babuc A	5 min	Cement mortar partition wall - inner surface – 1.10 m	-40°C÷+80°C	0.05°C
Surface temp.	Platinum resistor	PT100	Babuc A	5 min	Cement mortar partition wall - inner surface – 1.10 m	-40°C÷+80°C	0.05°C
Surface temp.	Platinum resistor	PT100	Babuc A	5 min	XPS west wall - inner surface – 0.50 m	-40°C÷+80°C	0.05°C
Surface temp.	Platinum resistor	PT100	Elog	5 min	XPS est wall - inner surface - 0.80 m	-40°C÷+80°C	0.05°C
Thermal flow	Platinum resistor	HFP01	Datataker	1 min	Cement mortar partition wall - inner surface – 1.10 m	-2000to +2000W/m²	+5/-5%
Thermal flow	Platinum resistor	HFP01	Datataker	1 min	XPS South wall - inner surface – 0.80 m	-2000to +2000W/m²	+5/-5%
Solar radiation	Radiometer	DPA 806	Babuc A	5 min	Cement mortar partition wall - inner surface - 1.10 m	0 - 1500 W/m²	±10%
Surface temp.	Platinum resistor	PT100	Elog	5 min	Cement mortar partition wall - inner surface – 0.80 m	-40°C÷+80°C	0.05°C
Surface temp.	Platinum resistor	PT100	Elog	5 min	Glass - external surface – 1.20 m	-40°C÷+80°C	0.05°C
Solar radiation	Radiometer	DPA 806	Babuc A	5 min	XPS South wall - external surface – 0.70 m	0 - 1500 W/m²	±10%
Outdoor monitoring station							
Air temp.	Thermo hygrometer	DMA875	Datataker	1 min	Weather station	-30°C÷+70°C	0.2°C
Relative humidity	Thermo hygrometer	DMA875	Datataker	1 min	Weather station	0 ÷ 100%	±0.25
Atmospheric pressure	Piezoelectric	DQA801	Datataker	1 min	Weather station	800÷1100 hPA	0.5 hPa
Atmospheric pressure	Piezoelectric	DQA801	Datataker	1 min	Weather station	800÷1100 hPA	0.5 hPa
Wind velocity	Anemometer	WMT700	Datataker	1 min	Weather station	0 ÷ 75m/s	/
Wind direction	Anemometer	WMT700	Datataker	1 min	Weather station	0 ÷ 270°	/
Solar radiation	Radiometer	DPA 153	Datataker	1 min	Weather station	0 - 2000 W/m²	< 5%

Table 4.8

Sunspace monitoring stations details.

4.4 – MONITORING ACTIVITY AND COMPARATIVE ANALYSIS

In this paragraph, the data collected during the monitoring of the experimental building are displayed and discussed. The baseline for the comparison in terms of energy performance is represented by the reference building without openings on the partition wall, as it recreates the mock-up as it was before attaching the sunspace. Besides, in order to take into account the different climate conditions occurring during the three monitoring time periods (**table 4.9**), a normalized version of the energy parameters is proposed.

The on-site data also demonstrated the validity of the preliminary simulation model developed in DesignBuilder and EnergyPlus as the outcomes were consistent to each other. Some refinements were introduced to make the results almost equal.

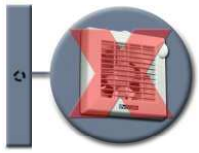
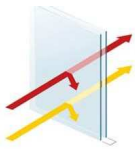
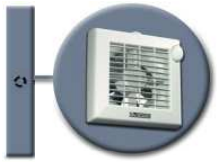
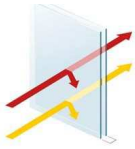
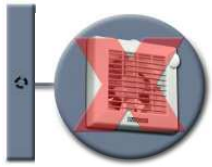
MONITORING SCHEDULE			
Monitoring time period		**29\12\2015 - 28\01\2016**	
Glazed panels characteristics	Number of panes	1	 
	Thermal transmittance	5.6 W/m²K	
	Solar factor	78%	
	Light transmission	88%	
VMC system	OFF		
Monitoring time period		**17\03\2016 - 21\03\2016**	
Glazed panels characteristics	Number of panes	2	 
	Thermal transmittance	1.6 W/m²K	
	Solar factor	70%	
	Light transmission	75%	
VMC system	ON		
Monitoring time period		**01\04\2016 - 15\04\2016**	
Glazed panels characteristics	Number of panes	2	 
	Thermal transmittance	1.6 W/m²K	
	Solar factor	70%	
	Light transmission	75%	
VMC system	OFF		

Table 4.9
Monitoring activity: covered periods and general settings.

4.4.1 – Environmental parameters

The comparison between the tested configurations is first of all conducted on the basis of the thermal conditions subsisting during the monitoring, in particular:

- the air temperatures (outdoor, indoor mock-up and sunspace dry-bulb temperatures **figure 4.5**);
- the surface temperatures (partition wall mock-up side and sunspace external side **figure 4.6**);
- the Solar radiation (external and internal side of the sunspace **figure 4.7**).

In these figures, those parameters are plotted by selecting 3 significant days, representative of the entire monitoring period in terms of average climate conditions. Each figure includes 3 graphs to compare the different configurations under test, which are:

1. Irradiative sunspace with a single-glazed facade (from here on out named Conf_1): in this case the absence of a mechanical ventilation system (directly connecting the two air volumes) and the higher thermal transmittance given by the single pane glass panel emphasize the thermal sensitivity of the building to changing boundary conditions. In fact, the most nervous trends for the sunspace temperatures (**figure 4.5** and **figure 4.6**) are those recorded for Conf_1. Besides internal Solar radiation trend follows more closely the external one in **figure 4.7** compared to the correspondent lines recorded for the other configurations.
2. Irradiative sunspace with a double-glazed facade (from here on out named Conf_2): here the presence of a higher-performance glass panel mitigates the transmission losses thus providing stronger robustness to outdoor climate changes. Moreover, since no convective transfer is habilitated between mock-up and sunspace, Conf_2 represents the configuration where mock-up and sunspace air volumes are less sensitive to the reciprocal changes. In accordance with all these remarks, both the sunspace and the mock-up temperatures displayed in **figure 4.5** and **figure 4.6** show the smoothest trends. Finally, as expected for both the tested double-glazed configurations, the gap between the external and the internal Solar radiation lines is considerably greater than the one occurring for Conf_1.
3. Convective sunspace with a double-glazed facade (from here on out named Conf_3): in this case the air communication between mock-up and sunspace given by fans operation (enabled every time the difference between sunspace and mock-up air temperatures exceeds +2°C) increases the sensitivity of the mock-up internal and surface temperatures to the rise and fall of the correspondent sunspace lines thus showing a reduced tendency to plateau (**figures 4.5, 4.6**). Conf_3 in the only one directly exploiting the higher temperatures reached inside the sunspace to lower the number and duration of

the calls for heating to the radiators via VMC. This means higher energy efficiency, paid by accepting a less stable indoor temperature and therefore a higher probability of discomfort phenomena.

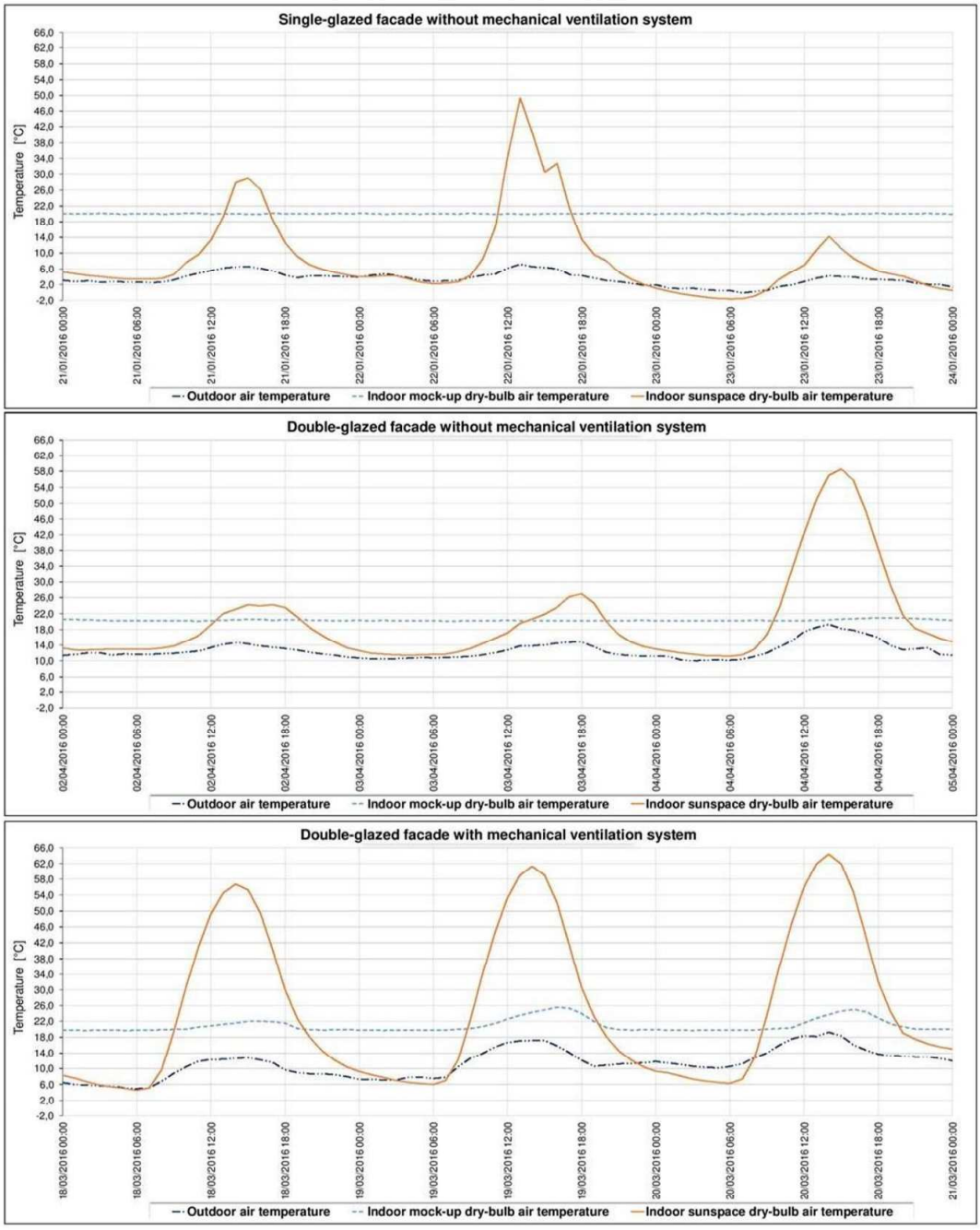


Figure 4.5

Comparison between the mock-up plus sunspace configurations in terms of air temperatures.

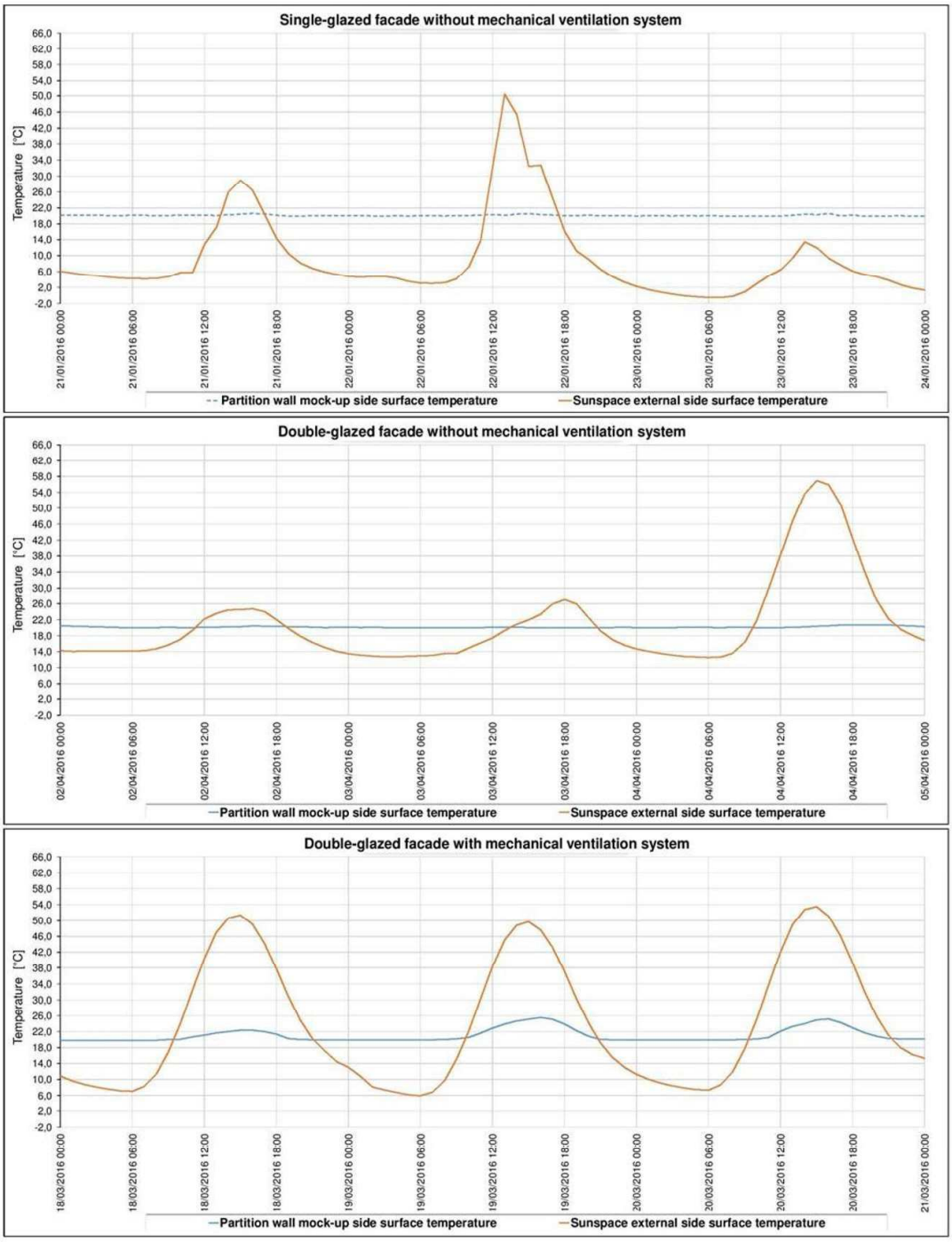


Figure 4.6

Comparison between the mock-up plus sunspace configurations in terms of surface temperatures.

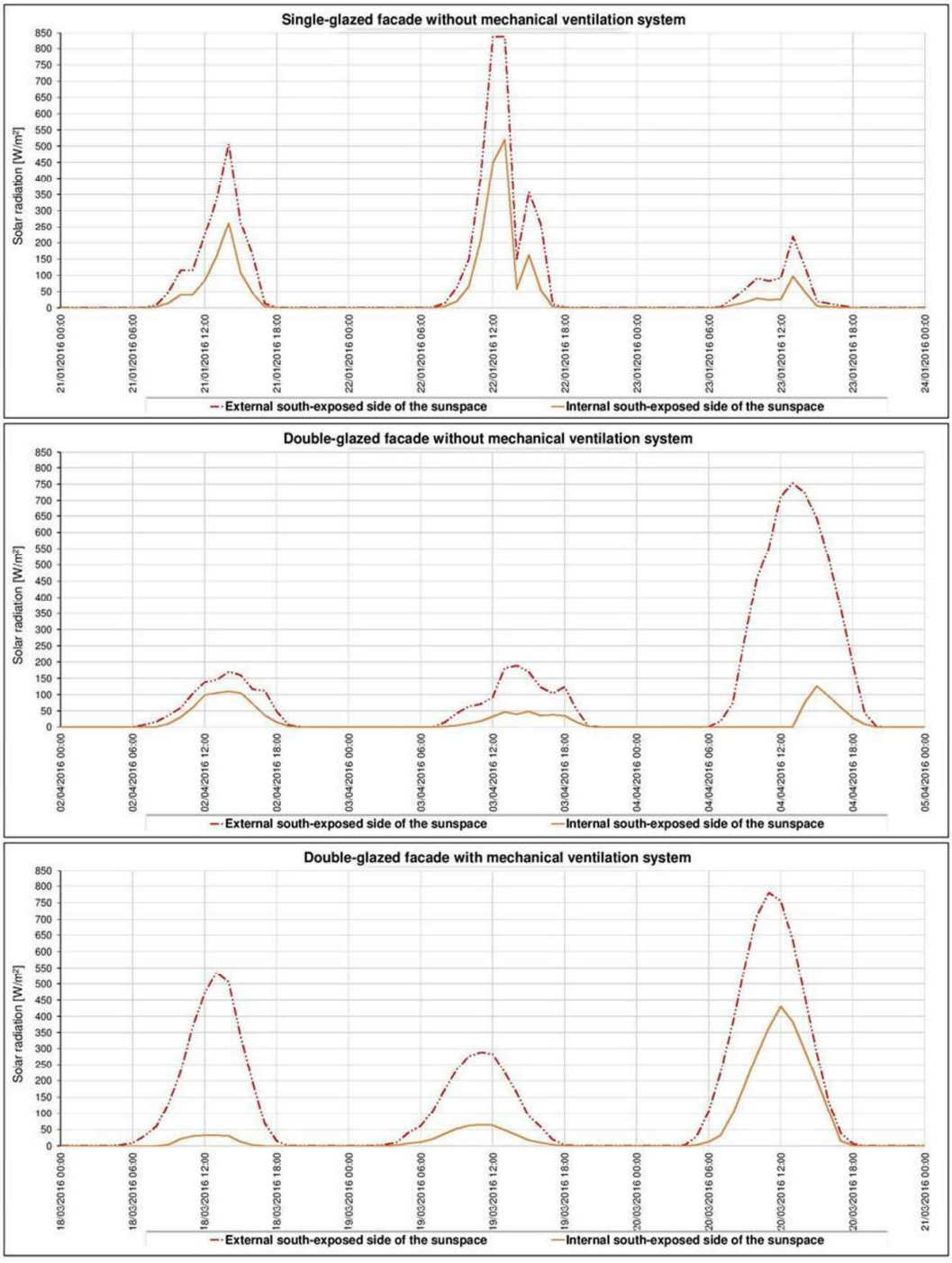


Figure 4.7

Comparison between the mock-up plus sunspace configurations in terms of Solar radiation.

4.4.2 – Energy consumption

Being the main goal of this experimental study the quantification of the energy saving potential of a sunspace leant against the south-exposed wall of a NZEB building, the monitoring activity was mainly focused on getting all data necessary to depict the energy consumption profiles of each configuration.

The monitoring of the three configurations took place in different time periods thus experiencing unequal climate conditions and practical concerns (mainly linked to physical damages due to unusual storms and bad weather) which invalidated most of the data collected during the testing of Conf_2 and the entire data set related to the forth configuration planned to be monitored (irradiative, single-glazed sunspace).

In order to get meaningful information despite of the disturbances given by such leakage of boundary conditions, two normalized versions of the daily energy consumption are presented and discussed. The first proposed term of normalization is the difference between indoor and outdoor air temperatures on hourly basis, named "DT".

The following chart (**figure 4.8**) shows the DT-related energy signatures of the building: on the x-basis is the daily average value of DT, while on the y-axis is the daily average energy consumption; the line interpolating the cloud of points represents the building plus technical system combined energy performance. The analysis of the trends underpins what was expected:

- in the case of irradiative configurations, a quite constant reduction of almost 1 kWh/day is recorded by adding an extra glass layer (passing from Conf_1 to Conf_2). This means that the energy benefit gained by reducing the thermal transmittance of the glazed panels is independent of the specific outdoor temperatures.
- in the case of convective configuration, the energy signature, compared to Conf_2 line, reveals a quite constantly increasing reduction of the daily energy consumption with growing DT. This means that the energy benefit connected to the activation of the VMC system depends on the outdoor conditions: a minimum DT value of about 4°C is required to justify its operation.

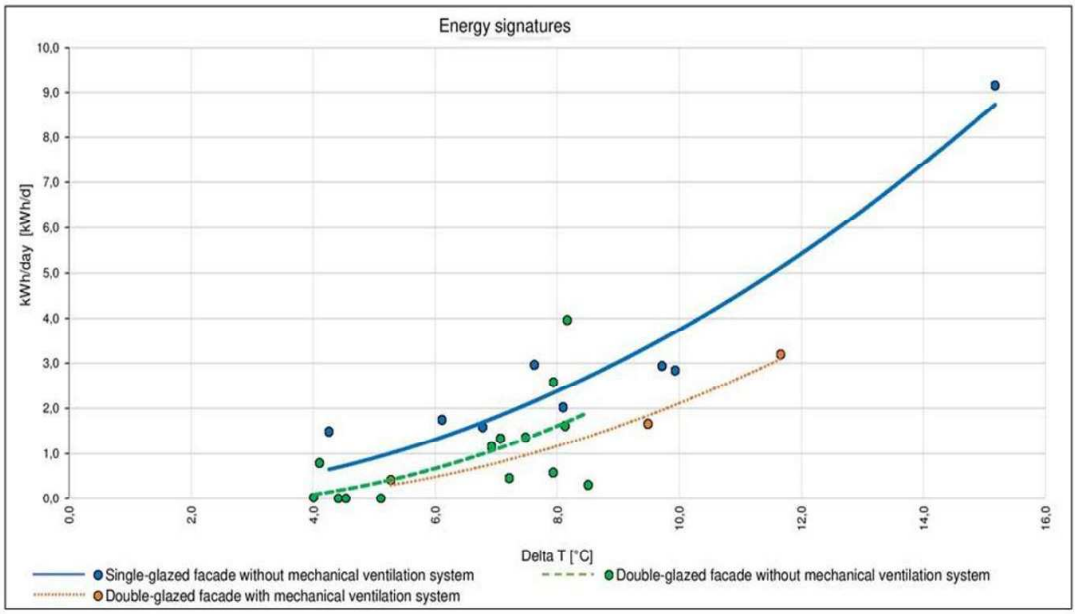


Figure 4.8

Energy signatures of the mock-up plus sunspace configurations. Outdoor parameter: daily average difference between indoor and outdoor air temperatures.

More detailed information about the energy benefit achievable with a convective, double-glazed sunspace is displayed in absolute terms in **figure 4.9** and in relative terms in **Figure 4.10** (taking Conf_2 energy performance as the basis of differentiation and comparison respectively). It is noticeable that from a DT value of 4°C on out, the saving always exceeds the 25%.

Obviously, since the sunspace acts as a Solar collector, the other key parameter to be involved to get meaningful information while comparing the energy efficiency of the different tested configurations is the Solar radiation. This is the reason why the second proposed term of normalization is represented by the Solar radiation hitting the south-facing external wall of the sunspace, named "Is".

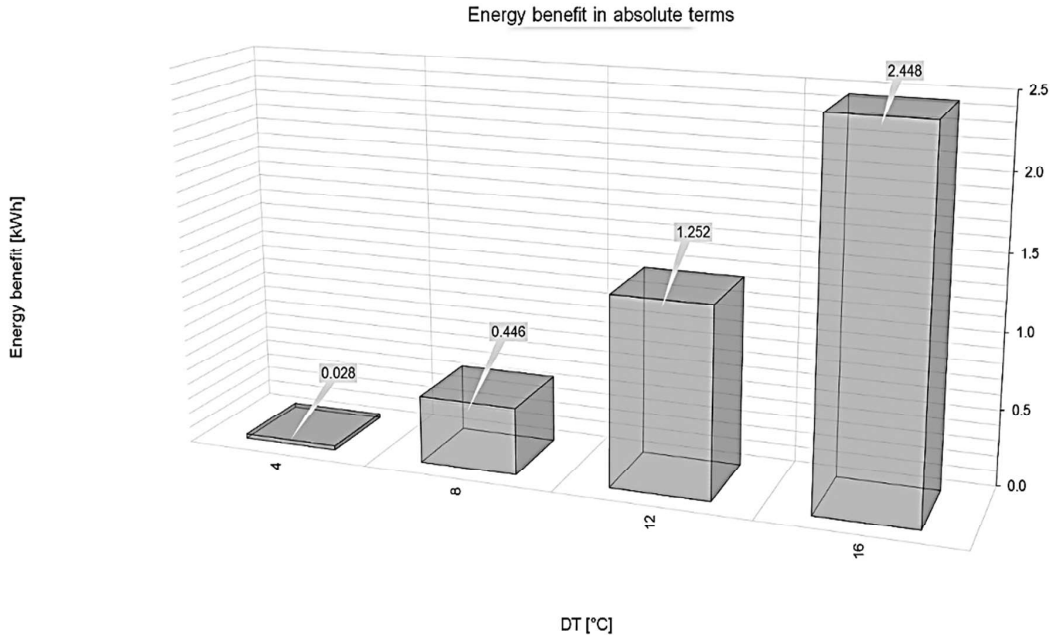


Figure 4.9

Energy benefit achieved with Conf_3 compared to Conf_2 in absolute terms.

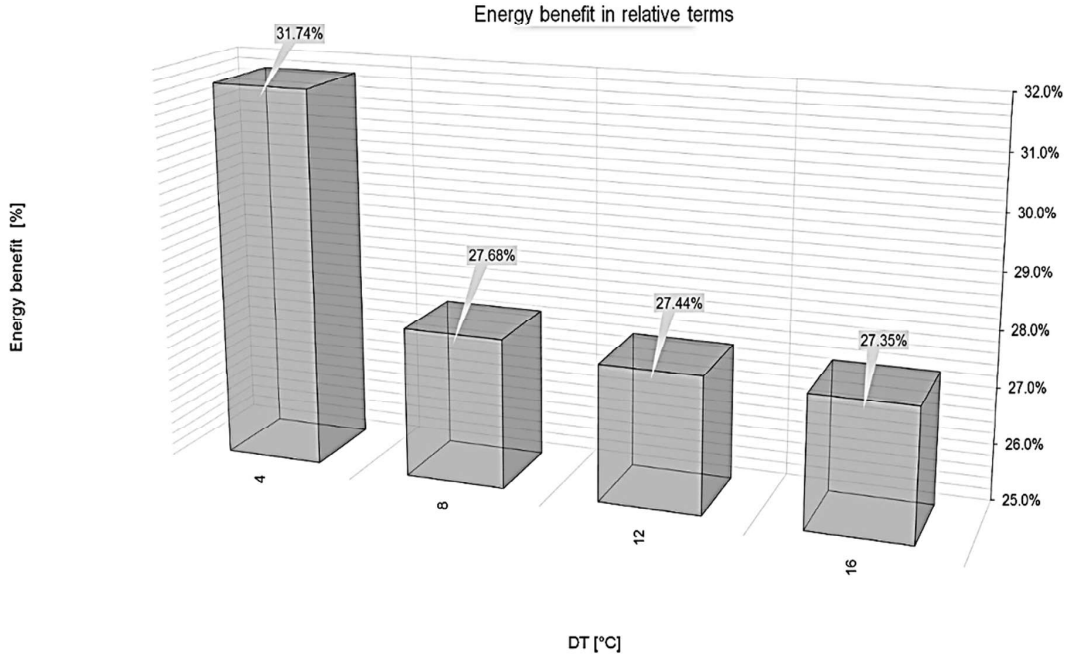


Figure 4.10

Energy benefit achieved with Conf_3 compared to Conf_2 in per cent terms.

Figure 4.11 shows the Is-related energy signatures of the building: the daily average energy consumption is plotted against daily average value of Is.

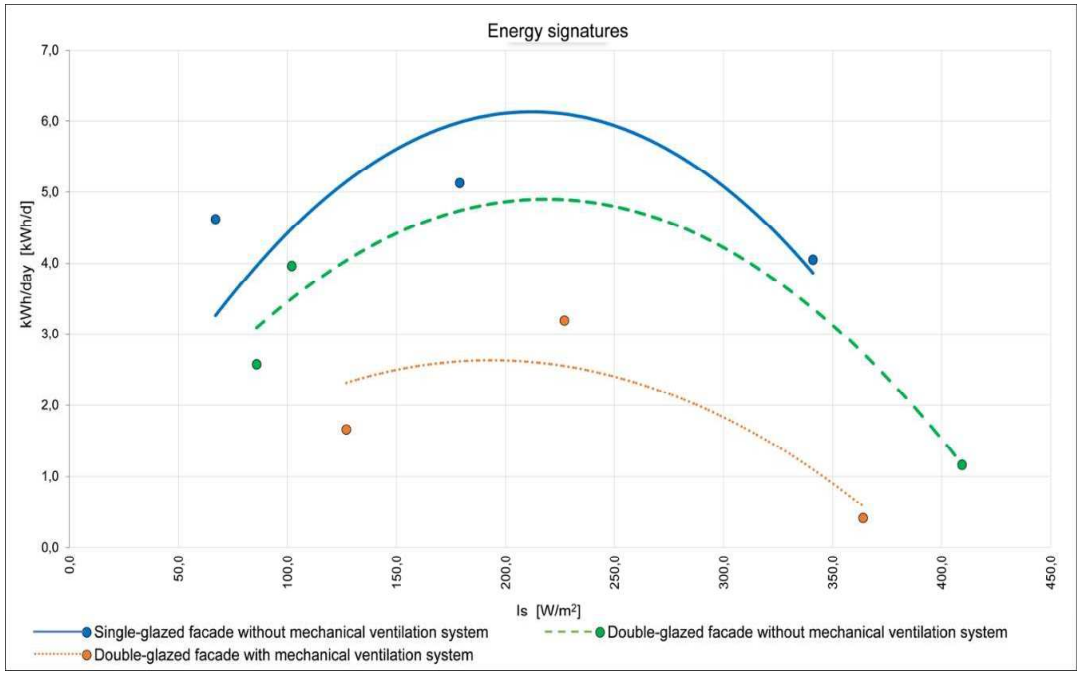


Figure 4.11

Energy signatures of the mock-up plus sunspace configurations. Outdoor parameter: daily Solar radiation hitting the south-facing external wall of the sunspace.

The analyses of the trends we obtained are performed from to two main perspectives: the amount of Solar radiation and the sunspace configuration.

According to the first criterion, it is noticeable that regardless of the specific configuration, the concave shape of each curve indicate three different "operational areas":

- the first one covers the x-axis in the range between 0-150W/m^2 and represents the diffuse-radiation-dominated section. The ascending trend of the curves reveals that when the sky is overcast during the day, all day long, the climate tends to be milder because of the blanketing effect exerted by the clouds and this mitigates the transmission transfers through the walls. In this case the increase in Solar radiation is counterproductive as the raise in Solar gains is overridden by the one in heat losses.

  However, the average energy consumption in this operational area is far less from the maximum one. This finding seems to underpin previous studies **[4.29-**

4.32] demonstrating that diffuse Solar radiation plays a major role in the heat collected by building attached sunspaces, therefore, even in geographic areas where the Sun is typically elusive and frequently cloaked by clouds, sunspaces might act as efficient passive energy collectors.

- The second operational area refers to Solar radiation between 150W/m^2 and 250W/m^2 approximately. Here the daily energy consumption lines reach the peak value before inverting the trend. This can be considered the worst case for a building attached sunspace to operate.
- The third one represents the energy performance during direct-radiation dominated days (x-values above 250W/m^2). Here the trend lines assume the expected shape of a sloped, monotonically decreasing function so that, i.e. when Solar radiation rises from 300 W/m^2 to 350 W/m^2 a minimum reduction of 1kWh/d is recorded for each sunspace configuration.

According to the second criterion, both the heat transfer mechanism and the insulation level of the specific sunspace configuration play a significant role in the way energy consumption is related to Solar radiation. In particular:

- in the case of irradiative configurations, the slope of the curves is much more pronounced then in Conf_3, as expected since the inner mechanism is directly dependent of Solar radiation. The difference between Conf_1 and Conf_2 energy consumptions increases near the peak values, reaching a maximum of 1kWh/d, and decreases when approaching the limit values on the x-axis. This means that the reduction in thermal transmittance achieved by doubling the number of glass panes exerts its maximum relative role when the sunspace energy performance is affected more by the difference between indoor and outdoor temperatures than by Solar radiation.

  Besides, the effect of increased thermal insulation is apparent in the diffuse-radiation-dominated operational area: the slope for Conf_2 is significantly reduced compared to Conf_1 one since the sensitivity to outdoor climate conditions is limited.
- in the case of convective configuration, the energy signature shows a much more substantial energy-saving profile and a much flatter trend, compared to Conf_1 and Conf_2. A remarkable dependency between heating consumption and Solar radiation still lingers in the direct-radiation-dominated operational area: here the energy benefit is linked to the thermal logic behind the activation of the VMC system: the highest the temperatures reached inside the sunspace the highest the frequency of convective flows between the sunspace and the heated environment.

4.4.3 – Simulation models' validation and sunspace efficiency

After the first monitoring campaign we were allowed to use the on-site collected weather data to refine the boundary conditions required by EnergyPlus and double check the consistency of the preliminary analysis outputs. Some adjustments on the input settings (internal convective heat transfer coefficient, infiltration rate, diffuse and direct solar radiation contributes) were required to train the model in order to minimize the deviation between simulated and real case energy performance.

As we got a fully calibrated model we ran further simulations at the end of every monitoring campaign in order to confirm the validity of the model for each modified configuration and to get the reference values (those referred to the mock-up without sunspace) needed to calculate the sunspace efficiency case-by-case.

In fact, thanks to the calculation schedules provided by EnergyPlus, it was possible to split the W/m^2 of global incident Solar radiation into the contribution hitting the opaque components of the sunspace, and the one hitting the glazed surface, while quantifying (for fixed time intervals and specific incident angles) the correspondent amount of surface directionally irradiated.

Therefore, the incident Solar power (P_{inc}) was obtained by multiplying the incident Solar radiation (I_{inc}) with the relative irradiated surface (S_{irr}). Then we could get the incident Solar energy E_{inc} by counting the time intervals t_i over which I_{inc} hitted S_{irr}:

$$E_{inc} = P_{inc} \cdot \sum t_i = I_{inc} \cdot S_{irr} \cdot \sum t_i \qquad (4.1)$$

Finally we were allowed to calculate the sunspace efficiency η_s (in order to use it as a comparative parameter) by dividing the heating energy demand saving E_s achieved by inserting the sunspace with the global Solar energy E_g (which is the sum of the one involving the opaque surface $E_{inc,op}$ and the one involving the glazed surface $E_{inc,gl}$, each one calculated according to equation 4.1):

$$\eta_s = \frac{E_s}{E_g} = \frac{E_s}{E_{inc,op} + E_{inc,gl}} \qquad (4.2)$$

However, it must be pointed out that no ad-hoc routines to simulate the specific VMC system serving the experimental building is provided among EnergyPlus ready-to-use schedules. That is why, even though that customized schedules can be developed, in this first stage of the research activity, the aforementioned energy parameters focusing on the energy benefits achieved by adding the sunspace were not calculated for Conf_3.

For Conf_1 and Conf_2 configurations, the sunspace yields (calculated as the ratio of E_s to the heating energy demand recorded without the sunspace) reached approximately 3,3% and 8,7% respectively. These values are in line with the ones returned by the preliminary simulations (3,8% and 5,96%) as the discrepancies are easily attributable to the different weather file in input (on-site collected outdoor temperature and Solar radiation values were meanly 2°C and 50 W/m^2 higher respectively).

4.5 – CONCLUSIONS

An experimental and numerical study was carried out in order to compare the energy performance of a NZEB mock-up plus sunspace coupled system according to different setup configurations (physically realized or just simulated) **[4.63]**.
This specific combination has not been widely investigated yet, hence the main purpose of the research activity in question was to define its optimal design criteria in the perspective of energy efficiency, relying on the on-site collected data obtained by monitoring a small scale prototype.
The first step was the construction of the sunspace, taking into account both the geometrical and constructive details of an existent NZEB mock-up in Agugliano (AN, Italy). Various solutions were explored in terms of glazed surface typologies, dimensions and disposition. The south orientation responded to the main design criterion for a sunspace which is to receive the maximum possible Solar radiation, while the vertical dimensions (width and height) were adjusted to the ones of the existent building. Different depths in plan (150cm, 200cm, 220cm, 250cm), different window panes (single-glazed, low-e double-glazed), different glazed surface percentages (0%, 30%, 50% of the overall perimeter surface) and different partition operative modes (radiative and convective) were used as key parameters to tune the sunspace design towards an optimal configuration (or at least reduce the number of setups to be physically tested).
After having created the virtual model of the combined system in DesignBuilder, 132 simulations were run exploiting EnergyPlus calculation tools to check the energy performance parameters over an observation period of 166 days (from the 1st of September to the 15th of April) in order to cover the entire heating season in Italy.
All the findings emerging from the simulations served as technical base for the subsequent step, which was the physical realization of the sunspace to be attached to the existing mock-up in Agugliano. The final configuration was the following:

- the depth of the sunspace was 150cm as unequivocally rewarding from an energy perspective;
- the continuity of the partition wall was interrupted by two holes, bored at different heights, in order to arrange a mechanical ventilation system composed by an electric supply fan (top hole), an electric exhaust fan (bottom one), a differential thermostat and a remote controller enabling to actively recover the free heat gain collected by the sunspace whenever the thermal gap between the two environments justified the mixing of the air volumes.
- The south-exposed wall structure was predisposed to potentially replace the wood panels with the window panes in two lines: if just the upper line was replaced, the glazed area was about 30% of the entire perimeter area, if both

the lines were provided with glazed panels the percentage rose up to 50%. During the monitoring activity the 30% configuration was the only one tested.

- The sensor network was installed both inside and outside the building thus providing all necessary data to link the thermal parameters characterizing the three involved environments: sunspace, mock-up and outdoors. Flux meters and surface RTDs were added to the monitoring equipment in order to record the energy behavior of the envelope and the partition wall as well. All the output signals were collected by three data loggers and sent to a central PC where a virtual instrument developed in G-language charted the trends, handled the savings, processed the calculations and elaborated the command outputs to the electric radiators and the fans via specific digital output modules. An indoor setpoint temperature of 20°C represented the target value piloting the on/off algorithm of the technical system.

The monitoring activity took place from December 29, 2015 to April 15, 2016 according to the following timetable:

- December 29, 2015 - January 21, 2016: single-glazed sunspace, VMC off (Conf_1);
- March 17, 2016 - March 21, 2016: double-glazed sunspace, VMC on (Conf_3);
- April 1, 2016 - April 15, 2016: double-glazed sunspace, VMC off (Conf_2).

All things considered, the best energy performance was the one achieved by Conf_3 since the relative energy benefit compared to the irradiative counterpart (Conf_2) reached a low of 27,35% and peaked at 31,74% when the average daily difference between indoor and outdoor air temperatures was about 4°C.

This was the expected result since the activation of the VMC system according to a thermo-driven automatic logic enabled direct exploitation of the heat gain conveyed by the air volume inside the sunspace to lower the call for heating required to the radiators every time it resulted profitable.

As regards the energy aftermaths related to the doubling of the glazed panes (keeping the same sunspace operative mode, in particular the irradiative one), it was found that the saving was about 1 kWh/day, regardless of the contingent outdoor temperature. This result is underpinned by the calculation of the sunspace efficiency too as it reached approximately 3,3% and 8,7% for Conf_1 and Conf_2 respectively.

Apart from the need for on-site monitoring of the 50% glazed surface sunspace, the need for developing an ad-hoc EnergyPlus schedule for modelling sunspace convective mode and the need for investigating the aspects linked to the walls thermal inertia, another opened issue needs to be addressed in order to enhance further deepening.

In the perspective of following European directives specifications **[4.5]**, the efficiency of buildings must be achieved throughout the year and should be approached in a long-term, resilient way in order to cope with expected climate change **[4.64].**

Against this backdrop, future research activities are planned to involve the same mock-up plus sunspace building in order to check that no overheating is caused by the sunspace in summer. The calculation procedure given by Standard UNI EN ISO 13790 can be used to quantify the Solar gains for the cooling (summer) mode, taking into account any extra (seasonal) Solar protection and ventilation provisions, if present.
Passive techniques of night ventilation and/or modification of the current configuration (i.e. installing blinds or shutters on the outside of the glazed part of the sunspace) might be necessary to provide solutions to improve the overall performance as it was found in previous works **[4.36,4.41,4.45-4.52]**.

REFERENCES

[4.1] Cereto FB, Santalucia F. Prestazione energetica degli edifici comunali ed agevolazioni e/o incentivi comunali per interventi di edilizia sostenibile. s.l. : APAT, 2004.

[4.2] EU Renewable Energy Directive 2009/28/EC. s.l. : European Parliament and Council, 5 June 2009. L 140, pp. 16–62.

[4.3] Directive on the energy performance of buildings 2002/91/EC (EPBD). s.l. : European Parliament and Council, 16 December 2002.

[4.4] Directive 2010/31/EU on the energy performance of buildings (EPBD recast). s.l. : European Parliament and of the Council, 19 May 2010 .

[4.5] Directive 2012/27/EU on energy efficiency. s.l. : European Parliament and of the Council, 25 October 2012.

[4.6] Task 7, Photovoltaic Power Systems Programme Annual Report. s.l. : International Energy Agency, December 2001.

[4.7] Del Corno B, Mottura G. Serre e verande. s.l. : Maggioli Editore, 2014.

[4.8] Hestnes AG. Building integration of solar energy systems. s.l. : Sol. Energy, 67, 181–187. , 2000.

[4.9] Zappone C. La serra solare - criteri di progettazione e risparmio energetico, architettura, funzionamento, materiali, aspetti normativi. s.l. : Architettura Sostenibile, Esselibri S.p.A., 2009.

[4.10] Pizzo S. Architetture nZEB: Come Si Vive in una Casa a Zero Consumi? Houzz Italia. 11 luglio 2016.

[4.11] Achard P, Gicquel R. European Passive Solar Handbook: Basic Principles and Concepts for Passive Solar Architecture. s.l. : Commission of the European Communities: Brussels, Belgium, 1986.

[4.12] UNI EN ISO 13790: Energy performance of buildings - Calculation of energy use for space heating and cooling. 2012.

[4.13] ENERGY PLUS 6.0, User's Guide. s.l. : Lawrence Berkley Laboratory: Berkeley, CA, USA, 2011.

[4.14] User's Guide for TRNSYS 17.0. s.l. : Thermal Energy System Specialists: Madison, WI, USA, 2011.

[4.15] Asdrubali F, Cotana F, Messineo A. On the Evaluation of Solar Greenhouse Efficiency in Building. s.l. : Energies, 2012. Vol. 5.

[4.16] Wilson A. Passive solar heating. s.l. : Environ Build News 2012;21:1e15.

[4.17] Reynolds JS. Design tools. In: Balcomb JD, editor Passive solar buildings.Cambridge MA: MIT Press; 1992. p. 485e514.

[4.18] Mazria E. The passive solar energy book. Emmaus PA: Rodale Press; 1979.

[4.19] Niles PWB, Haggard K. Passive solar handbook. Sacramento CA: California Energy Commission; 1980.

[4.20] Crosbie M, editor. The passive solar design and construction handbook. New York: Stephen Winter Associates: John Wiley & Sons; 1998.

[4.21] Brown GZ, DeKay M. Strategy 60: direct-gain rooms, and Strategy 61: sunspaces. In: Sun, wind, & light: Architectural design strategies. New York: John Wiley & Sons; 2001. p. 169e73.

[4.22] Grondzik WT, Kwok AG, Stein B, Reynolds JS. Mechanical and electrical equipment for buildings. 11th ed. New York: John Wiley & Sons; 2009.

[4.23] Isolated gain (sunspaces) [Internet]. Washington DC: US Department of Energy, Office of Energy Efficiency and Renewable Energy. Available from: http://www.energysavers.gov/your_home/designing_remodeling/index.cfm?mytopic¼10310 [accessed 15.07.12]. .

[4.24] Chiras DD. The solar house: passive heating and cooling. White River Junction VT: Chelsea Green Publishing Co; 2002. .

[4.25] Kachadorian J. The passive solar house. White River Junction VT: Chelsea Green Publishing Co; 1997. .

[4.26] Anderson B, Wells M. Passive solar energy: the homeowner's guide to natural heating and cooling. 2nd ed. Amherst NH: Brick House Publishing Company; 1994. .

[4.27] Sunspace basics. Report No.: DOE/CH10093-350 FS124. Golden (CO): National Renewable Energy Laboratory Technical Information Program; 1994. p. 6. .

[4.28] Shapiro AM. Add-on solar greenhouses and sunspaces. Emmaus PA: Rodale Press; 1985.

[4.29] Reynolds JS. Solar energy for Pacific Northwest buildings. Eugene OR: Center for Environmental Research, School of Architecture and Allied Arts, University of Oregon; 1974. .

[4.30] Mithun OL. Solar design for Puget Sound. In: Proceedings of solar 79 Northwest. Seattle WA: Pacific Northwest Solar Energy Association; Aug 10e12 1979. p. 59e60. .

[4.31] Cole RJ. Solar research and design e closing the gap. In: Proceedings of solar 79 Northwest. Seattle WA: Pacific Northwest Solar Energy Association; Aug 10e12 1979. p. 61e4.

[4.32] Rempel AR, Rempel AW, Cashman KV,Gates KN, Page CJ, Shaw B. Interpretation of passive solar field data with EnergyPlus models: Un-conventional wisdom from four sunspaces in Eugene, Oregon,Building and Environment 60 (2013) 158e172 .

[4.33] Baker MS, Lorenzen R. Oregon monitored solar building study. Eugene OR: Solar Energy Center, University of Oregon; 1979.

[4.34] Mottard J, Fissore A. Thermal simulation of an attached sunspace and its experimental validation. Sol. Energy 2007, 81, 305–315. .

[4.35] Roux JJ et al. Validation of a glazed space simulation model using full-scale experimental data. Energy Build. 2004, 36, 557–565. .

[4.36] Bataineh KM, Fayez N. Analysis of thermal performance of building attached sunspace. Energy Build. 2011, 43, 1863–1868. .

[4.37] Oliveti G, De Simone M, Ruffolo S. Evaluation of the absorption coefficient for solar radiation in sunspaces and windowed rooms. Sol. Energy 2008, 82, 212–219.
[4.38] Bakos GC, Tsagas NF. Technology, thermal analysis and economic evaluation of a sunspace located in northern Greece. Energy Build. 2000, 31, 261–266. .
[4.39] Mihalakakou G. On the use of sunspace for space heating/cooling in Europe. Renew. Energy 2002, 26, 415–429. Energies 2012, 5 1880.
[4.40] Fernandez-Gonzalez A. Analysis of the thermal performance and comfort conditions produced by five different passive solar heating strategies in the United States Midwest. Sol. Energy 2007, 81, 581–593.
[4.41] Oliveti G et al. Solar heat gains and operative temperature in attached sunspaces. Renew. Energy 2012, 39, 241–249.
[4.42] Chiesa G, Simonetti M, Ballada G. Potential of attached sunspaces in winter season comparing different technological choices in Central and Southern Europe, Energy and Buildings 138 (2017) 377-395.
[4.43] Chiesa G, Grosso M. The influence of different hourly typical meteorological years on dynamic simulation of buildings, Energy Procedia 78 (2015) 2560-2565.
[4.44] DesignBuilder 2.1 User's Manual October 2009.
[4.45] Mihalakakou G. et al. Energy conservation and potential of a sunspace: sensitivity analysis, Energy Conversion and Management, Volume 41, Issue 12, August 2000, Pages 1247–1264.
[4.46] Santamouris M, Mihalakakou G, Balaras CA, Argiriou A, Asimakopoulos D, Vallindras M. Use of buried pipes for energy conservation in cooling of agricultural greenhouses. Solar Energy 1995; 55:111±24.
[4.47] Tombazis A, Argiriou A, Santamouris M. Performance evaluation of passive and hybrid cooling components for a hotel complex. Int J of Solar Energy 1990; 9:1±12.
[4.48] Agas G, Matsagos T, Santamouris M, Argiriou A. On the use of the atmospheric heat sinks for heat dissipation. Energy and Buildings 1991; 17:321±9.
[4.49] Mihalakakou G, Santamouris M, Asimakopoulos D. Use of the ground for heat dissipation. Energy 1994; 19:17±25.
[4.50] Torra C et al. Some experiences on design and calculation of sunspaces in Mediterranean climates, Solar & Wind Technology, Volume 5, Issue 4, 1988, Pages 365-378.
[4.51] Aelenei D et al. The use of attached-sunspaces in retrofitting design: the case of residential buildings in Portugal, Energy Procedia, Volume 48, 2014, Pages 1436-1441.
[4.52] Monge-Barrio A et al. Energy efficiency and thermal behaviour of attached sunspaces, in the residential architecture in Spain. Summer Conditions, Energy and Buildings, Volume 108, 1 December 2015, Pages 244–256.
[4.53] Calzolari M. Prestazione energetica delle architetture storiche: sfide e soluzioni. s.l. : Franco Angeli, 2016. Volume 101 "Ricerche di tecnologia dell'architettura".

[4.54] Greco A, Quagliarini E. L'involucro edilizio: una progettazione complessa . s.l. : Alinea Editrice, 2007.

[4.55] LEGGE REGIONALE 20 aprile 2015, n. 17. B.U. 30 aprile 2015, n. 37.

[4.56] Delibera di Giunta regionale n. 2215. 21 dicembre 2015.

[4.57] ISO 13786 Thermal performance of building components - Dynamic thermal characteristics - Calculation methods. 2007.

[4.58] EN 13829 Thermal Performance of Buildings - Determination of Air Permeability of Buildings - Fan Pressurization Method. January 15, 2001.

[4.59] UNI/TS 11300-1: Energy performance of buildings – Part 1: Evaluation of energy need for space heating and cooling. 2014 .

[4.60] Tronconi O. Costruzioni lignee: il "balloon frame" e il "platform". 2009.

[4.61] UNI EN ISO 7726: Ergonomics of the thermal environment -- Instruments for measuring physical quantities. 22 October1998.

[4.62] UNI EN ISO 7726-2002 Ergonomics of the thermal environment - Instruments for measuring physical quantities. 1 January 2002.

[4.63] G. Ulpiani, D. Giuliani, A. Romagnoli, C. Di Perna, Experimental monitoring of a sunspace applied to a NZEB mock-up: assessing and comparing the energy benefits of different configurations, Energy and Buildings, Volume 152, October 2017, pages 194-215.

[4.64] O'Neill BC, Nakicenovic N, Moss RH. Towards New Scenarios for Analysis of Emissions, Climate Change, Impacts, and Response Strategies. . IPCC, Geneva. : s.n., 2008. ISBN 978-92-9169-125-8.

5

Smart control of fan coil units to counteract indoor overheating

Overheating phenomena induced by fully-glazed facades: investigation of a sick building in Italy and assessment of the benefits achieved via fuzzy and model predictive control of the AC system.[1]

[1] Published in Solar Energy, Volume 158, December 2017, Pages 572-594
and in Solar Energy, Volume 157, 15 November 2017, Pages 830-852

5.1 – ABSTRACT

This chapter addresses the potential benefit achievable via fuzzy and model-based, predictive control of the AC system in overheated buildings with large glazed façades.
A sick building in Italy (and more specifically a protractedly and intensely sunlit office on the south-exposed, fully-glazed façade) was selected as case study.
It was monitored both over summertime and wintertime. The sensor network mapped the indoor climatic conditions, the surface temperature distribution on the glazed façade and the thermodynamic parameters of the air inlet from the 3-speed fan coil unit serving the room (originally in manual mode).
Both the typologies of controller were conceived to involve the outdoor conditions in the decision making process to better tackle the specific target.
The ultimate configuration of the fuzzy controller was a MISO (multiple input, single output) system contemplating both solar radiation and external temperature, measured in real time. It was tested over one week in September 2016.
The MPC relied on a grey-box model of the room's thermal dynamics, built on a short-term monitoring dataset (4-day-lasting collection in November) and tuned during the first day of testing. Its ergonomic and energetic performance was assessed on the two days of maximum and minimum solar radiation over the testing week in December 2016.
Considerably high operative temperature persisted all over the period of observation. However, while in free running the room reached peak values of almost 28°C, during the operation of the fuzzy the offset from the setpoint of 26°C was considerably narrowed down, guaranteeing PMV<1 for the 97.2% of the time.
In wintertime, with the MPC controller on, the setpoint value of 24°C was never exceeded by more than 2°C. Indeed, the offset stayed within ±0.5°C for the 95.8% of the time on the sunnier day and for the 60.8% on the cloudier day, while the PMV remained within the ±0.5 range for the 85% and the 80% respectively.
No local discomfort from vertical gradients or drafts occurred with the ultimate configurations of both the controllers.
Furthermore, the energy consumptions were remarkably contained since the fan operated at minimum speed for nearly the 67% and the 80% of time respectively.

5.2 – INTRODUCTION

Architecture and construction engineering have been dealing with glazed solutions' ins and outs since long ago. Year round efficient operation of windows is found to be the outcome of a series of wise choices **[5.1]**: orientation, dimensions, materials and design of all the components (windows glass, sash, frame but also trickle vents, clearstory openings) have to be properly selected to achieve a good working balance **[5.2].**

Indeed, in order to fully benefit of view, natural daylight and ventilation without paying the energy penalty, a delicate equilibrium needs to be stricken among thermal transmittance, solar transmittance and air tightness **[5.3].**

Recently, the widespread of highly-glazed façades and curtain walls has exacerbated the need to counteract the vulnerability to overheating and excessive heat losses, notably in cooling-dominated climates.

In 2000, a Zurich journal published an article entitled "*Wer im Glashaus sitzt, der schwitzt*", which means "those who live in glass houses sweat". Such statement addressed the experience of working in the Zurich Department of Dentistry, built in 1998: the all-glass façade forced the users to work under unbearably hot indoor climate in summer and drafts in the winter. The same concerns arise from the findings of many research activities.

For instance, Hwang et al. **[5.4]** simulated occurrences and severity of the overheating in presence of highly-glazed façade with different combinations of glazing types, areas and depths of overhang. They concluded that unless a proper shading device is installed, large window surfaces represent a major source of discomfort whichever material is used.

Kalmár **[5.5]** investigated the risk for uncomfortably hot conditions in ante-1970 buildings with high window-to-wall ratios: he concluded that "in case of existing buildings with large transparent surfaces on the façades, extreme hot indoor environments may occur even in May or September. In such environments, the occupants cannot perform the daily activities".

An akin situation was witnessed in Germany **[5.6]**, where indoor spaces liveability was seriously jeopardised inside buildings with very high proportions of windowed components if no full mechanical cooling was provided.

The alarming conclusion was that glass structures are likely to be the wrong answer in the perspective of energy efficient office buildings: in such climates, cooling needs are the predominant voice among the energy consumptions and affect an extended summer period starting from spring time de facto. Air conditioning and cooling techniques must work at high power ratings to counteract the overheating and preserve productivity, breaching all the paradigms of sustainability.

In England, Altan et al. **[5.7]** investigated the rise in ambient temperature inside each floor of an office building with a fully glazed façade on the heliothermic axis over late

spring and summer months. They found that solar shadings and efficient ventilation systems were paramount to mitigate the overheating risk, since thermal discomfort persisted even when natural ventilation was widely deployed.

In Lithuania, a field study tackled the same issue **[5.8]**: two office buildings with large glazed façades were monitored during the heating season. Despite the mild summery weather conditions at such latitudes, some offices exhibited average temperatures out of recommended comfort limits. Subjective questionnaires were distributed to check on users' environmental sensations and preferences: many complains arose in terms of excessively high temperatures and other SBS symptoms (irritation in eyes, cough and dry skin of the hands) because of overabundant solar gains.

Moving on to arid climates, a recent on-topic publication **[5.9]** concluded that in countries like South Arabia the maximum recommendable window-to-wall ratio should be 10%.

All things considered, excessive solar gains in indoor environments is a global-scale issue affecting the ergonomics (and the sustainability) of living spaces.

Nonetheless, the definition of a correct design approach is overcomplicated by the multiple interrelations between indoor microclimate and dimensions/properties of glazed façades: a truthful modelling of all the mechanisms by which solar energy enters the building (conduction, direct and diffuse radiation, absorption and thermal emission from lit surfaces) is paramount.

Several papers propose simulation-based and/or experimental-based procedures to depict the indoor thermal aftermaths due to solar heat gain through glazed surfaces by calculating, for instance: the solar heat gain through glazed surfaces in AC buildings **[5.10]**, the thermal radiant field induced by solar radiation over individuals **[5.11,5.12]**, the impact of different shades and glazing solutions for office buildings with a high window area **[5.13],** the dynamic distribution of solar radiation onto a person not directly struck by the direct beam **[5.14]**.

Equally extensive literature approaches such issue from the comfort perspective, by suggesting methodologies to assess how solar radiation from windows perturbates occupants' thermal and visual sensation both on global and local scale: practical tools **[5.15]**, adjusted comfort indices (out of parametric **[5.16,5.17]** or test chamber studies **[5.18]**), spatial distributions **[5.19]** (some of which considering both direct and diffuse radiation components **[5.20,5.21]**) are proposed.

Lyons et al. **[5.16]**, in particular, addressed long-wave, solar radiation and draft effects on the net PPD by means of computational fluid dynamics (CFD). It was demonstrated that "in summer, solar load dominates the perception of comfort. Discomfort increases with both clothing insulation and glazing solar heat gain coefficient (SHGC)."

Indeed, high window-to-wall ratios are not just a trigger for overheating since they might cause also draughts and radiant asymmetries (which might turn into thermal gradients in case of prolonged persistency) when geometry and exposition of the

transparent components is not conceived taking care of skew distributions. And the drawbacks are furtherly emphasized when the users are expected to statically stay in close proximity to the glazed façade (i.e. offices, classrooms, auditoriums, …) as discomfort might turn into heat stress and affect the immunological system, stimulating the symptoms of the so called Sick Building Syndrome (SBS) **[5.22]**.
Existing examples of low energy buildings generally adopt double/triple glazing (low-e and heat absorptive and/or reflective) provided with external solar shading systems, smartly controlled in the most virtuous cases **[5.23,5.24]**.
Yet, such combinations might be costly and seldom supported. The rather convenient, alternative opportunity to mitigate the overheating risk (yet without tackling the problem at source) might come from the sole optimisation of the HVAC action through an efficient control logic.
Nonetheless, the synergy among glazed components, AC and lighting systems needs to be handled with care so as to ensure a sustainable built environment.
Against this backdrop, the present research investigates the overheating rate in a "sick" office building in Italy designed with externally unshaded, south-exposed, fully-glazed façade and equipped with different controllers piloting the heating/cooling emission of the local AC unit **[5.25]**.
In summertime, ad-hoc conceived fuzzy controllers were implemented and assessed to quantify the eventual improvement in terms of ergonomics and energy consumptions. Although the severity and frequency of extremely uncomfortable conditions was dampened by the final configuration of the controller, the operative temperature overtook the comfort limits almost all over the summer period.
Therefore, another monitoring campaign was arranged in the same indoor space during wintertime with the double purpose of checking on the temporal extent of the overheating phenomena (annual/seasonal) and of testing if a different control logic compared to the heuristic approach could be more successful.
A mathematical-model based, predictive controller (MPC) was developed and evaluated accordingly.
Extensive information is nowadays available on traditional and advanced PID and fuzzy logics used to calibrate the HVAC equipment for energy conservation and/or pleasantness of indoor environments **[5.26–5.31]**.
Less is known, instead, on the benefits on comfort levels and energy efficiency achievable by predictive controllers based on customized and on-site calibrated grey-box models of the building thermal dynamics, especially when the heat transfer is massively influenced by direct and diffuse solar radiation.
This research activity aimed at disclosing information on such potential advantage from various viewpoints, outlines pros and cons in absolute and comparative terms and pinpoints the scope for further refinement on the basis of the measured response of the tested environment.

5.3 – MATERIALS AND METHODS

The choice, design and customization of the controllers followed a robust planning phase, based on a massive screening of the on-topic literature and of the body of knowledge gained by interpreting the measurements performed during the previous environmental monitoring campaigns of the same building.
Accordingly, the roadmap was conceived as follows:

1. analysis of the thermal behaviour of the case study from on-site collected datasets;
2. definition of the control logic in view of the thermo-physical phenomena involved and the proved suitability in akin applications by comparing strengths, weaknesses, opportunities and threats of the most promising solutions;
3. identification of the pivotal parameters to be fed in input to the controller so as to install the proper sensor network and arrange the hardware components;
4. setup of the monitoring stations and of the logging components;
5. development of the software platform to manage the dataflow, integrate the control algorithm, give consent to the actuators and retrieve the data packs;
6. on-site monitoring and remote management to potentially intervene on the basis of the observed trends;
7. numerical and graphical assessment of the controller's performance in terms of global comfort, local discomfort and energy consumptions.

The access to the office was forbidden to all non-authorized personnel; maintenance/corrective actions were remotely managed whenever possible. By excluding the contribute of people on the energy balance of the tested room it was possible to directly link the diurnal thermal evolution of the indoor parameters to the corresponding solar gains.
In any case, the controllers were provided with an occupancy schedule, taking into account the typical use of an office building.

5.3.1 – Case study

The monitoring campaigns took place in one of the buildings (Polo Eustachio) composing the ensemble of the university polyclinic in Ancona (Italy).
According to the Köppen-Geiger classification, the area (lat. 43,60°, long. 13,46°) is characterized by a humid, subtropical climate with mild, warm and rather rainy weather conditions throughout the year. **Figure 5.1** displays the monthly histograms of temperature, solar radiation, rainfall and relative humidity over the year 2016, so as to frame the general meteorological context.

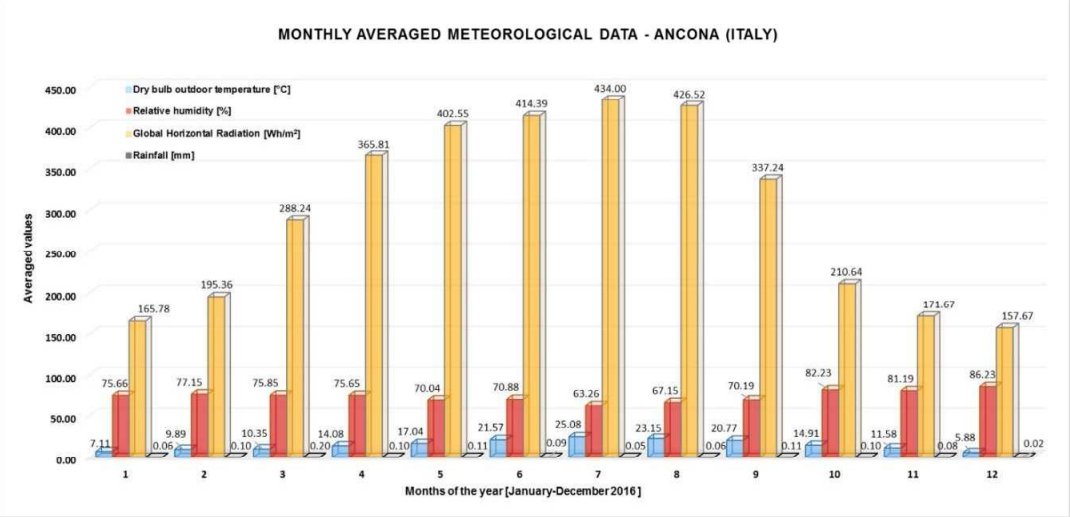


Figure 5.1

Climatic characterization of Ancona (Italy): monthly averaged values of temperature, relative humidity, global horizontal radiation and rainfall over the year 2016.

Polo Eustachio was built in the '90s to accommodate the medical school's offices, classrooms and library. It is a multi-storey complex (6 floors) developed on two longitudinal blocks with a rectangular ground plan (**Figure 5.2a**).
On the heliothermic axis are the fully-glazed façades (**Figure 5.2b** and **Figure 5.2c**), responsible of the overheating.



Figure 5.2

Case study: a) satellite localization, b) view of the south fully-glazed façade, c) view of the interiors.

The experimental activity took place in a 3.70m x 5.64m x 3.00m, south-exposed office on the third floor: the small indoor air volume (57.51m^3) and the considerable surface area to volume ratio (0.33m^{-1}, used as an indicator of the amount of thermal exchange taking place between the indoor and the outdoor air volumes) guaranteed high responsiveness to solar gains, considerable radiant asymmetry and full inclusion of the workstation into the influence area of the glazed façade; the altitude ensured a high sky-view factor, therefore massive, long-lasting irradiation.

Such characteristics exacerbated the risk of overheating thus providing the exemplary casuistry to perform the tests.

The double-glazed window is split in three modules by aluminium uprights for a total area of 3.50m x 1.67m. Its g value (percentage of the total incident radiation that enters through the glass) is equal to 0.504.

A 1-metre high, shielded and insulated panel runs from floor level, juxtaposed to the internal side of the glass, to mitigate the energy loss through the façade: it consists of a 6-mm thick prepainted steel sheet and 55mm of hot-injected polyurethane foam at the interface with the window.
In this way, the local thermal transmittance drops from 2.8 W/m²K to less than 0.5 W/m²K (thus reducing the magnitude of the overall heat transfer through the façade) and the penetration of solar beams is dampened. Yet, no remarkable relief to the overheating is provided since just a small portion of the indoor surface stays cooler throughout the day: the twilight zone reaches significative dimensions right approaching the sunset, thus not affecting the hours of maximum radiation.
More details of the glazed façade and the walls' composition are given in **Table 5.1.**

WALLS COMPOSITION

Material	**Density ρ** [kg/m³]	**Thermal conductivity λ** [W/m K]	**Thickness t** [mm]	**Thermal resistance R** [m²K/W]
Flooring/ Roofing floor (3th/4th floor)				
Surface resistance (internal)	-	-	-	0.130
Stoneware tiles	2300	1.300	10	0.008
Alveolar Concrete screed	450	0.580	100	0.172
Reinforced concrete and hollow tiles mixed floor	2200	-	300	0.300
Plastering	1200	0.700	15	0.021
Surface resistance (external)	-	-	-	0.130
Tot.			425	0.761
Thermal transmittance U (W/m²K)				1.314
Corridor ceiling				
Surface resistance (internal)	-	-	-	0.130
Internal plasterboard	900	0.250	25	0.100
Air space	-	-	400	0.426
Reinforced concrete and hollow tiles mixed floor	2200	-	300	0.300
Alveolar Concrete screed	450	0.580	100	0.172
Stoneware tiles	2300	1.300	10	0.008
Surface resistance (external)	-	-	-	0.130
Tot.			835	1.266
Thermal transmittance U (W/m²K)				0.790
East/West Walls				
Surface resistance (internal)	-	-	-	0.130
Internal plasterboard	700	0.210	25	0.119
Fiberglass	16	0.046	50	1.087

External plasterboard	700	0.210	25	0.119
Surface resistance (external)	-	-	-	0.130
Tot.			100	1.585
Thermal transmittance U (W/m²K)				0.631
Surface mass (kg/m²)				35.8
North Wall				
Surface resistance (internal)	-	-	-	0.130
Plastering	1400	0.700	10	0.014
Hollow bricks	800	0.400	80	0.200
Plastering	1400	0.700	10	0.014
Surface resistance (external)	-	-	-	0.130
Tot.			100	0.488
Thermal transmittance U (W/m²K)				2.049
Surface mass (kg/m²)				64
South Horizontal Shielded Band				
Surface resistance (internal)	-	-	-	0.130
Steel sheet	7800	52	6	0.000
Polyurethane foam	70	0.050	55	1.100
Hardened reflective glass	2500	1.000	6	0.006
Surface resistance (external)	-	-	-	0.040
Tot.			67	1.276
Thermal transmittance U (W/m²K)				0.784
Surface mass (kg/m²)				65.65
South Glazing				
Surface resistance (internal)	-	-	-	0.130
Stratified inner glass	2500	1.000	7	0.007
Air space	-	-	12	0.173
Hardened reflective glass	2500	1.000	6	0.006
Surface resistance (external)	-	-	-	0.040
Tot.			25	0.356
Thermal transmittance U_g (W/m²K)				2.809
Surface mass glass (kg/m²)				32.5
Surface mass frame (kg/m²)				270

Table 5.1
Office room walls composition: materials, thicknesses, thermal transmittances and surface mass.

The office is served by a false-ceiling, ducted fan coil unit (FCU), connected to one of the three rooftop Air Handling Units (AHUs) supplying mechanical air to the top three floors: the primary stream (fresh air treated by the AHU) mixes with the secondary stream (return air, recirculated and conditioned by the room coil) in a dedicated plenum box attached directly to the supply outlet of the FCU, where the velocity

pressure drops and equalize, the combined airflow gets uniformly dispersed and the momentum stabilizes. Thanks to such plant configuration the fresh and return air mixing is facilitated and both sensible and latent loads are controlled.
The technical specs of the FCU are summarized in **Table 5.2.** The original operation of the 3-speed centrifugal fan was manual, exerted via a local thermostat.

FAN COIL UNIT SPECIFICATIONS				
Model	**Production house**	**Motor**	**Fan Power [W]**	**Number of fans**
STRO 1.2 mod. 2	Galletti Air Conditioning	3-speed, electric	Centrifugal, airfoil shaped blades 330	1
SPEED	**Global cooling power[1] [kW]**	**Sensible cooling power[1] [kW]**	**Water flow[1] [l/h]**	**Pressure drop[1] [kPa]**
Min speed	1.04	0.79	179	7
Med speed	1.24	0.97	213	9
Max speed	1.54	1.20	264	13
SPEED	**Heating power[2] [kW]**	**Pressure drop[2] [kPa]**	**Heating power[3] [kW]**	**Water flow[3] [l/h]**
Min speed	1.4	6	2.5	216
Med speed	1.7	8	3.0	263
Max speed	2.1	11	3.7	325
SPEED	**Pressure drop[3] [kPa]**	**Air flow [m³/h]**	**Power consumption [W]**	
Min speed	7	178	21	
Med speed	10	233	28	
Max speed	15	319	37	

[1] Water temperature 7/12°C, air temperature 27°C dry-bulb, 19°C wet-bulb (47% RH).
[2] Water temperature 50°C, same water flow as in cooling, air inlet temperature 20°C.
[3] Water temperature 70/60°C, air temperature 20°C.

Table 5.2
FCU technical data

When the indoor microclimate is mechanically regulated, adaptive comfort theory does not apply **[5.32]**: consequently the comfort zone of the occupants cannot be enlarged in view of a potential higher thermal tolerance. That put even more emphasis on the need to automatically preserve good environmental quality.
The office was monitored in mid-season (February-June 2016), when the technical systems were switched off, so as to get the magnitude of the overheating occurring in free running mode. Operative temperatures rose dramatically during solar peak hours (monthly maximum always close to 30°C) and were remarkably high even on overcast days. A warning signal came from the analysis of the surface temperature of the

window frame, which exceeded 45°C during days of high direct radiation, thus remarkably affecting the mean radiant temperature.

5.3.2 – Sensor network

An articulated sensor network was designed to get a global understanding of the thermal dynamics involved, with particular emphasis on the roles played by the glazed façade and the HVAC system.
Since ergonomics was the overarching focus of the monitoring activity, the technical specs and the distribution of the probes were mostly defined in compliance with UNI EN ISO 7726 **[5.33]**, thus abiding by the conditions to address indoor thermal comfort parameters according to ISO 7730 **[5.34].**
The sensor network consisted of a web of more than 20 probes, split into four main interconnected sub-systems (**Figure 5.3**):

I. outdoor monitoring station, composed by air temperature, relative humidity, global solar radiation, wind speed and direction sensors. The mast was placed, and conveniently secured, on the rooftop of one of the arms of the transversal connection between the two longitudinal blocks. Such location was selected since:
   - it provided good exposition to Sun and wind, with no shading from trees, surrounding buildings or other physical barriers;
   - it extended over a horizontal flat surface;
   - it was forbidden to non-authorized people.

   The power and signal cables ran through the door to the datalogger (LSI Lastem E-log) and a dedicated laptop, placed inside an existing technical cavity wall and connected to the local area network. The acquisition rate was set to 5 minutes. Obviously, the readings of such station were actually used just by the fuzzy controllers, while the MPC retrieved forecasted data.

II. Indoor microclimatic station, composed by the comfort-conceived ensemble by Dantec Dynamics, named ComfortSense. It includes three draught probes to perform local discomfort analysis, a capacitive hygrometer to measure the moisture content in the air and an ellipsoidal-thermometer, which was inclined of 30° from vertical to get the mean radiant temperature in consideration of both the radiosity of the walls and the effective radiation area of a seated person. All the probes were connected to the main frame which logged and packed the dataflow through a National Instrument acquisition platform. A dedicated palette is embedded in LabVIEW to easily communicate with the station and perform the calculation of indoor comfort parameters, such as operative temperature, turbulence intensity, draught rate, PMV and PPD.

The calculation of operative temperature and PMV might be misleading when performed in the middle of a room whose thermal conditions are expected to be non-uniform because of the presence of local heat sources and sinks, like a large window **[5.5]**. Indeed, in order to test the comfort perceived by the occupants, the station was installed very close to the workbench, slightly decentralized on the South-North axis towards the glazed façade and right in front of the central glazed module on the East-West axis.

The draught probes were placed at 0.1m, 0.6m and 1.1m according to the standardized procedure **[5.35]** when the user is expected to stay seated for the vast majority of time.

III. Glazed façade thermo-station: the internal side of the south-exposed wall was littered with flat Resistance Temperature Detectors (Pt100) to map the surface temperature distribution and detect when and where the main alterations occurred, in function of:
   - position (readings from the different glass modules and pieces of frame);
   - materials and composition of the layers (readings from the frame, from the glass and from the horizontal shielded band).

IV. Air ventilation station, whose composition was changed between the summertime and the wintertime monitoring runs to properly feed the different controllers. In summertime, it consisted of four cylindrical RTDs detecting the air temperature of the inlet and outlet, both in the recirculation ducting and the fresh air ducting, right before the mixing in the plenum. While, in wintertime, the FCU sensor network consisted of two thermo-hygrometers to characterize the airflow processed through the FCU and through the AHU, plus a KIMO anemometer (Ø 100 mm vane probe), used for a spot measurement of the air velocity from the technical system, for each speed of the fan. Such measuring system was setup to feed the controller with the necessary information about the power supply.

In addition to the above-described stations, a Hobo ZW Series Wireless Network, composed by four thermo-hygrometers, was installed in the experimental area. Three sensors were hanging from the ceiling of the adjacent offices and of the corridor to get the air temperature of the surrounding environments, while another one was placed next to the comfort station. They were utilized to build up the mathematical model of the building embedded in the MPC.

The output signals were logged every 5 minutes by a suite of acquisition cards by National Instruments (for what concerns the indoor stations), while the wireless sensors data were acquired every minute by means of a receiver connected to the PC inside the room.

An additional module (NI 9401) transformed the output of the control algorithm into the digital command to the 220V electric motor of the FCU to set the defined speed.
For the sake of safety, three static relays were interposed so that low voltage and high voltage circuits could be separated and potential competing requests to the fan averted.
A detailed description of the specs and spatial distribution of the devices composing the sensor network is given in **Tables 5.3 and 5.4.**

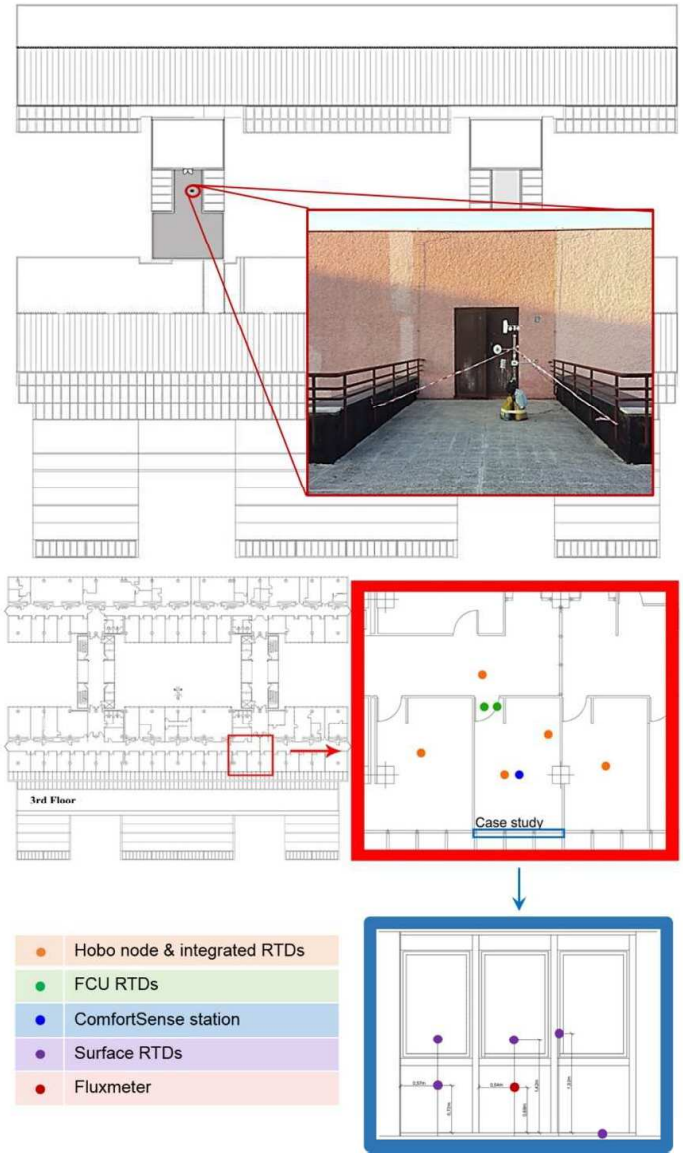


Figure 5.3
Plan localization and visualization of the sensor network.

SENSOR NETWORK CONFIGURATION

Wintertime run | Summertime run | All monitoring period

Measure	Sensor	Rate	Position	Range	Accuracy
INDOOR COMFORT MONITORING STATION					
Air temp. and velocity	Draught probe	5 min	Centre of the room. 2.5m from the window - H 0.10m Centre of the room. 2.5m from the window - H 0.60m Centre of the room. 2.5m from the window - H 1.1m	0.05-5 m/s. indicates up to 10 m/s	0-1 m/s: ± 2% OR* ± 0.02 m/s 1-5 m/s: ± 5% OR* 5-10 m/s: ±10% OR*
Relative Humidity	Capacitive Hygrometer	5 min	Centre of the room. 2.5m from the window - H 1.9m	0-100% RH	+2% RH (0-10°C); +1.5% RH (10-30°C); +2% RH (30-45°C)
Operative temperature	Ellipsoidal-thermometer	5 min	Centre of the room. 2.5m from the window - H 0.6m	0-45°C	±0.5 K (0-10°C); ±0.2 K (10-40°C); ±0.5 K (40-45°C)
Air temp.	Thermo hygrometer	1 min	Centre of the room. 2.5m from the window - H 1.1m	-20°C÷+70°C	±0.21 °C (0-50°C)
Air temp.	Thermo hygrometer	1 min	Corridor - H 2.5 m	-20°C÷+70°C	±0.21 °C (0-50°C)
Air temp.	Thermo hygrometer	1 min	Eastern adjacent office - H 2.5 m	-20°C÷+70°C	±0.21 °C (0-50°C)
Air temp.	Thermo hygrometer	1 min	Western adjacent office - H 2.5 m	-20°C÷+70°C	±0.21 °C (0-50°C)
FANCOIL MONITORING STATION					
Air temp.	Platinum resistor	5 min	Recirculation fancoil inlet - H 2.8m	-40°C÷+80°C	0,05°C
Air temp.	Platinum resistor	5 min	Recirculation fancoil outlet - H 2.8m	-40°C÷+80°C	0,05°C
Air temp.	Platinum resistor	5 min	Fresh air fancoil inlet - H 2.8m	-40°C÷+80°C	0,05°C
Air temp.	Platinum resistor	5 min	Fresh air fancoil outlet - H 2.8m	-40°C÷+80°C	0,05°C
External air temp.	Thermo hygrometer	1 min	Fancoil outlet - H 2.8 m	-20°C÷+70°C	±0.21 °C (0-50°C)
External air temp.	Thermo hygrometer	1 min	AHU outlet - H 2.8 m	-20°C÷+70°C	±0.21 °C (0-50°C)
Air velocity	Thermo-anemometer	1 min	Fancoil outlet/AHU outlet - H 2.8 m	0.25÷35 m/s	±3% of reading ±0,1m/s (0,25÷3 m/s), ±1% of reading ±0,3m/s (3,1÷35 m/s)
GLAZED FAÇADE MONITORING STATION					
Surface temp.	Platinum resistor	5 min	Center of the leftmost glazed module - H 1.40 m	-40°C÷+80°C	0,05°C

Surface temp.	Platinum resistor	5 min	Center of the central glazed module - H 1.40 m	-40°C÷+80°C	0,05°C
Surface temp.	Platinum resistor	5 min	Inter-modules frame - H 1.5 m	-40°C÷+80°C	0,05°C
Surface temp.	Platinum resistor	5 min	Floor frame - H 0.03 m	-40°C÷+80°C	0,05°C
Surface temp.	Platinum resistor	5 min	Center of the leftmost horizontal shielded band - H 0.7 m	-40°C÷+80°C	0,05°C
Thermal flow	Platinum resistor	5 min	Center of the central horizontal shielded band - H 0.7 m	-2000to +2000W/m^2	+5/-5%
OUTDOOR MONITORING STATION					
Air temp.	Thermo hygrometer	5 min	Weather station – H 1.0m	-30°C÷+70°C	0,2°C
Relative humidity	Thermo hygrometer	5 min	Weather station – H 1.0m	0 ÷ 100%	±0,25
Wind velocity	Tacogonioan emometer	5 min	Weather station – H 1.6m	0 ÷ 75m/s	/
Wind direction	Tacogonioan emometer	5 min	Weather station – H 1.6m	0 ÷ 270°	/
Solar radiation	Radiometer	5 min	Weather station – H 1.3m	0 - 2000 W/m^2	< 5%

Table 5.3
Sensor network general data

DATALOGGING					
Model	**Production house**	**Analogic Channels**	**Digital Channels**	**Acquisition rating**	**PC Connection**
E-Log (ELO305)	LSI Lastem	8 differential, 16 single-ended	4	5 minutes	RS232
ComfortSense main frame	LSI Lastem	Up to 16 input channels and 2 output channels with build in A/D converter		5 minutes	Usb
NI 9217	National Instruments	16		5 minutes	Usb
NI 9219	National Instruments	12		5 minutes	Usb
NI 9401	National Instruments		8	5 minutes	Usb
Hobo ZW-RCVR	Onset Computer Corporation			1 minute	Usb

Table 5.4
Acquisition systems specs

5.4 – CONTROL MANAGEMENT

As introduced in **sub-paragraph 1.3.1**, in the framework of an increasingly pressing need for energy-efficient (preferably nZEB) and sustainable buildings, new paradigms and R&D perspectives are emerging to introduce the built environment in the era of artificial intelligence (AI) and impel the integration within smart infrastructures. Indeed, a massive potential in the optimization of both energy savings and comfort levels is represented by the Building Automation and Control Systems (BACS).

Control theory arises from a cross-disciplinary compendium of mathematical, physical and engineering knowledge, particularly when the controller is not conceived to merely maintain a process in a defined operational state, yet also to govern the transient phases according to a wide variety of combinations and constraints.

All controllers deal with both manipulated inputs and disturbances (which might be either measurable or not) so as to manage and optimize the performance of the systems they are coupled with.

Given the complexity of the interaction among the factors that determine the thermal behaviour of a building (particularly in presence of strong non-uniformities), several strategies can be pursued.

Advanced control systems are the major opportunity for coping successfully in complex scenarios. This is because, apart from sensors and actuators, they deploy a supervisory control layer **[5.36–5.38]** which basically adjusts the settings (setpoints, weather/occupancy/operating schedules, tariffs, coefficients, functions…) of the basic control layer to adapt to variable conditions **[5.39–5.41].**

The supervisory layer can be either rule-based or model-based **[5.42].**

Fuzzy controllers belong to the former category, thereby a certain suite of rules (shaped on the formalism "if initial conditions, then action") is pre-set to guide the elaboration of the input data into the proper output to track the setpoint **[5.43,5.44].** Their approximate reasoning proved to be more successful than a classically designed scheme (on/off, PID, …) when it comes to comfort issues, since the subjective preferences of the users tend to be better contemplated **[5.45–5.50].**

This is why, in the framework of the present research, two different nonlinear, heuristic-based fuzzy controllers were tested to check whether they could counteract the excessive rise in operative temperature and to identify which could represent the best practice in such a weather-affected typology of buildings.

Nonetheless, such controllers critically depend on the correct configuration of linguistic terms, membership functions and rules which results in strong limitations to their scope for adaptation, particularly in transient phases which might not be included in the casuistry covered by the conditional clauses **[5.44].**

A model-based approach overtakes this limitation: indeed, process modelling can capture complex dynamic interrelations so that the controller can adjust its framework loop by loop though a dynamic optimization logic **[5.40,5.51].**
Furthermore, when supplemented with predictive capabilities, such controllers can generate and analyse multiple possible scenarios and calculate the optimal settings accordingly **[5.52–5.54].** The acronym RHC (Receding Horizon Control) is used to identify the class of control methods that forecasts future conditions and disturbances, to interpolate the best trajectory of actions in the light of optimizing an objective function **[5.37,5.55–5.58].**
Among them, Model Predictive Control (MPC) is gaining ground in building applications **[5.37,5.40,5.43,5.44,5.55–5.64]** and was thereby selected as piloting system for the technical systems of the overheated office in object (more detailed explanation in the next paragraph).
Both the fuzzy controllers and the MPC were conceived as MISOs (multiple-input, single-output systems) so as to include both indoor and outdoor parameters.
Indeed, as the overheating proved to affect the building throughout the day and throughout the year, all the countermeasures were conceived to properly intervene on indoor parameters given outdoor weather changes, thus striking a link between the two air volumes standing on the opposite sides of the glazed wall. The only exception was the on/off controller which merely served as reference case.
The feedback loop of all the controllers was developed in graphical language (LabVIEW 2015 by National Instrument S.r.l.) and repeated the following steps all over the time window of expected occupancy inside the office (7am to 7pm during weekdays, 7am to 2pm on Saturdays, full-day off on Sundays):

- input acquisition: the data from the monitoring stations were invoked and used to feed the controller, to perform comfort assessments, to check on the response of the glazed façade in terms of surface temperatures and display the weather data so as to visually strike correlations with the thermal evolution inside and outside the building;
- control logic selection: a drop-down menu allowed the activation of each controller, thus enabling the corresponding data flow. A separate case was developed per each typology of controller containing settings and input values. The output from the case structure was an integer between 0 and 3, standing for the fan speed identified by the control algorithm;
- power supply to the electric motor of the fan via the digital output module and the buffer board hosting the static relays;
- data storing in a database application.

The front panel (**Fig. 5.4**) was remotely managed for ongoing debugging, maintenance and data analysis (via TeamViewer 10).

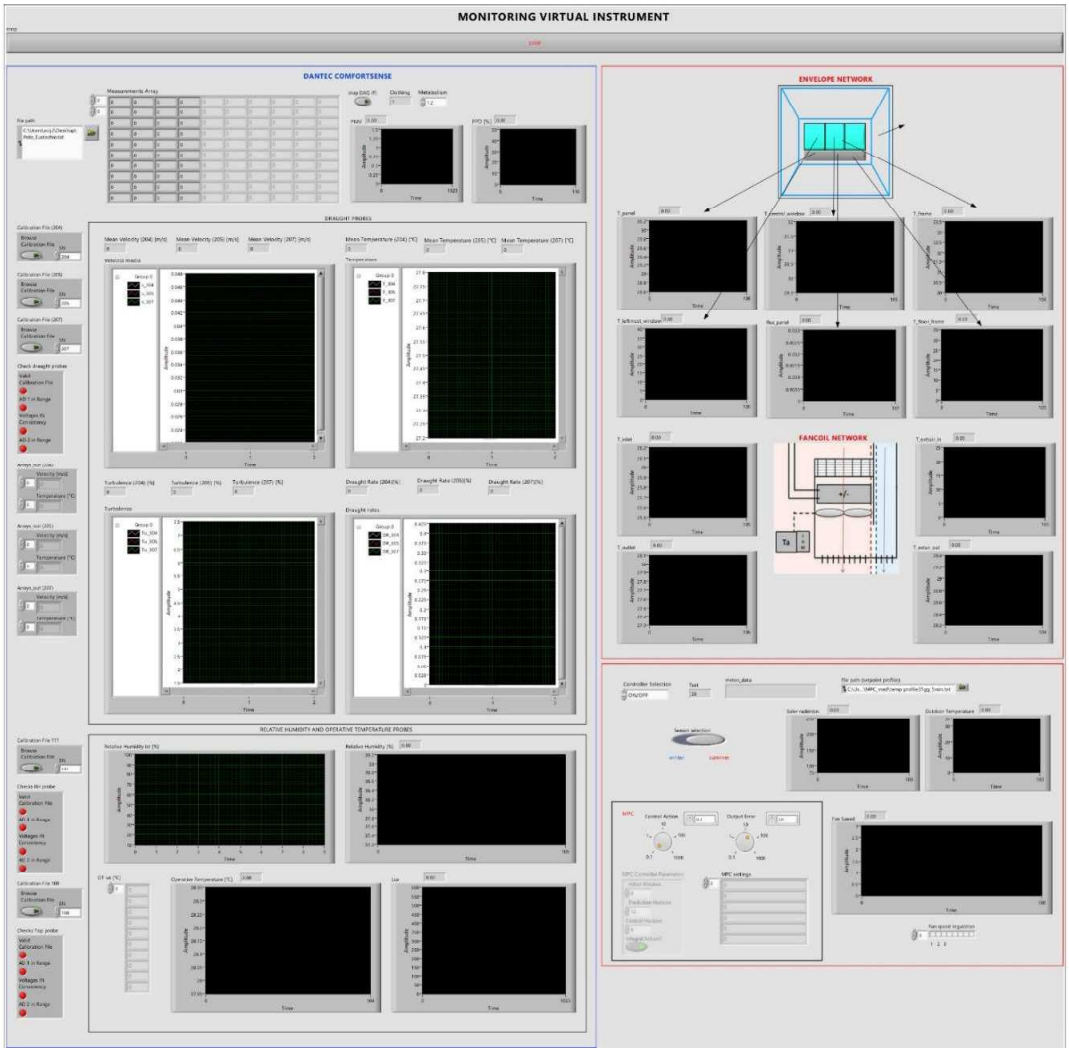


Figure 5.4
Screenshot of the front panel of the Virtual Instrument developed in LabVIEW to manage the dataflow.

5.4.1 – On-off controller

As described in **paragraph 2.6.1 and sub-paragraphs**, the setup of an on-off system consists in properly defining the hysteresis between switch-on and switch-off values of the process variable, necessary to avoid a hectic operation of the terminal**.**

In the specific case of a 3-speed FCU, each operative mode has to be defined in its turn-on and turn-off thresholds**.** Consequently, the following basic algorithm was implemented, since it was found to be the one that more truly depicted the existing manual management:

- if x≤0°C then y=0;
- if x>0°C and x≤0.5°C then y=1;
- if x>0.5°C and x≤1°C then y=2;
- if x>1°C then y=3;

where "x" represents the difference between the air temperature and the set point and "y" is the fan speed.

5.4.2 – Fuzzy controllers

The fuzzy controllers were configured, in LabVIEW, by defining:

1. the linguistic variables to represent each input/output parameter and a set of linguistic terms to label properly-identified subsets of their numerical ranges;
2. the membership functions, which shape the conversion between crisp and fuzzy values by assigning to each numerical value its degree of membership to the pertaining linguistic terms.
3. The rule base, made of a suite of IF-THEN clauses to strike the proper causal links between fuzzy input and output.

Each rule returns a result which has to be assessed and then combined with the others to get the final outcome. This is performed through logical operations: in the study here presented the AND (intersection) MIN (minimum value among competing membership functions) was selected. The adopted defuzzification algorithm was the Centre of Gravity.

In view of the specific "sickness" of the room, the fuzzy basic structure was conceived as a MISO system (multiple input – single output) so as to include both indoor and outdoor parameters.

The selection of the input variables was the outcome of a preliminary sensitivity analysis, used to rank the meteorological data in order of decreasing weight on internal thermal dynamics: solar radiation and outdoor temperature were found to be the main drivers for indoor air temperature rises and falls.

Accordingly, two fuzzy controllers were developed, one assuming solar radiation as dominant perturbing action (from now on named FS), the other involving both radiation and temperature collected by the meteorological station (from now on named FM).

The difference between indoor ambient temperature and the corresponding setpoint was the pivotal input for both the controllers, in order to size the correct cooling call in all operative conditions (minimum power or off mode around thermal neutrality and full capacity at start-off). However, the amplitude of the ranges referred to each linguistic term was reduced in FM compared to FS, in response to the results collected during the testing of the FS controller.

The selection of the set point was guided by standardized values afferent to the Italian legislation **[5.87].** As a result, summertime target value was set to 26°C, in line with the acceptable operative temperatures given also by the ASHRAE Standard 55 **–** 2010 **[5.35].**
The detailed settings of the controllers are presented in **Appendix A** (FS controller) and **Appendix B** (FM controller)**.**

5.4.3 – Model predictive controller

MPC logic is based on the minimization of a cost function to produce the optimal control action**.**
Compared to the success and widespread use in the industrial world **[5.71]**, MPC applications in the construction sector, although widely addressed at research level, still linger in a very early stage**.** Nonetheless the potential in many applications has been already outlined**.**
In 1985, a first study took place to check whether a controller of a solar energy system based on weather predictions and dynamic programming could be beneficial in terms of energy consumptions **[5.72].** Such publication boosted many other research activities (mostly based on simulation rather than on experimentation) in the field of thermal storage **[5.63,5.73,5.74]**, radiant heating systems **[5.52,5.56,5.75]** and cooling systems **[5.76,5.77].**
MPC controllers were found to outperform conventional ones in the most cases, partly thank to the inclusion of the variability of energy price in the optimization process **[5.78,5.79].**
The potential in terms of thermal comfort was outlined by Freire et al**. [5.58]**: they tested two sets of MPCs, one targeting energy efficiency, the other users' environmental satisfaction, and concluded that all controllers succeeded in reducing energy consumption while maintaining the comfort zone over the 100% of the time thanks to their ability to handle personal parameters**.** Similar conclusions were drawn by Carrascal et al**. [5.80].**
Nevertheless, full-scale applications are very limited: the main deterrent is the need to develop a reliable, explicit, reduced-order building model **[5.63,5.81].** Common practice in research is to resort to simulation tools (i**.**e**.** EnergyPlus, TRNSYS, …) **[5.82,5.83]**, which not always fit well with high-performance controllers **[5.84]** and introduce considerable computational complexity**.**
An alternative approach (here adopted) for existing buildings is to create grey-box models **[5.85,5.86]**, which match on-site collected data (from short-term campaigns) with parameter estimation and statistical analysis**.** Such algorithm relies on the analogy between building physics and electric RC circuits (where capacitive elements mimic

thermal mass, resistive elements represent thermal resistance and current generators are iconic of heat fluxes under the potential difference given by the difference between indoor and outdoor temperatures).

The MPC developed in the framework of the research in object collects the environmental data in short-term monitoring loops, gathers weather forecasts and occupancy estimations (reflected via dedicated sub-routines) and creates the dynamic thermal model accordingly. All information is fed to the controller to solve the optimization problem and keep the process variable within the desired range.

5.4.3.1 – Setup

MPC is a mathematical-model-based, constrained, feedback control. Its design requires the setting of multiple inputs and calculation procedures **[5.87].**

The basic functioning of such controllers relies on the optimization of an objective cost function which encapsulates the wished process evolution, on the basis of a reliable dynamic model of the phenomenology to be steered and a suite of limitations to obey to physical laws, namely ranges and thresholds.

The optimal control problem loops in feedback and in such receding horizon it propagates states, disturbances (i.e. internal gains), time-dependencies of input variables (weather forecasts, occupancy schedules, …) and constraints (comfort parameters, energy price, …) to properly conceive the corrective action fort the new state **[5.37].**

Basically, the configuration of the basic control scheme of an MPC consists in designing its three main components:

1. Cost function J(k), formulized in **equation (5.1)**:

$$J(k) = \sum_{l=N_0}^{N_p} [\hat{y}(k+l|k) - r(k+l|k)]^T \cdot Q \cdot [\hat{y}(k+l|k) - r(k+l|k)] + \sum_{l=0}^{N_c-1} [\Delta u^T(k+l|k) \cdot R \cdot \Delta u(k+l|k)] \quad (5.1)$$

where "N_p"and "N_c" are the prediction horizon and the control horizon respectively, "N_0" is the lower bound of the prediction horizon, equal or greater than one so as to exclude the current state (N_0=0) from the predictive term, "k" is the discrete time step for the completion of a single loop, "$\hat{y}(k+l|k)$", "$r(k+l|k)$" and "$\Delta u(k+l|k)$" are, in order, the predicted output, the output set-point profile and the predicted rate of change of the control action at time $k+l$ given all previous measurements, "Q" and "R" are weight matrices, the former referred to the output error (difference between $\hat{y}$ and r), the latter to the rate of change in control action (Δ u) used to set priorities. At first instance, Q and R were set to 1 and 10 respectively so as to give to energy consumption

and comfort level the same priority. Such values derived from the tuning procedure, run on the first day of monitoring: the differences between absolute maximum and minimum values of both ambient temperature and FCU power were used to set the respective operative ranges and so the terms of normalization (2.1 kW for the control action and 6.6 °C for the output error). Then, since $\hat{y} - r$ and Δ u are squared quantities in the cost function, Q and R were initially set on a one-to-ten ratio so as to harmonize the weights.

The prediction horizon was fixed at 1 hour in consideration of the time lag between weather changes and indoor reactions, caused by the thermal mass of the glazed façade. According to the calculation methodology described in the standard UNI EN ISO 13786:2008 **[5.88]**, such delay amounts to 0.43 hours, based on the dynamic thermal characteristics of the layers composing the glass. A certain margin of safety was introduced to take into account potential slowdowns of the control system.

The control horizon "N_c" (a value between 0 and "N_p") was tuned to 30 minutes, as trade-off between two competing objectives: on the one hand, the need to preserve the predictive nature of the MPC controller in place of a traditional feedback controller and, on the other hand, the wish to avoid abrupt changes in the control action, and so, the wear and tear of the system **[5.89]**.

2. Constraints: given the technical specifications of the FCU, a linear constraint (**equation 5.2**) was applied to the control action to fix its lower and upper limits:

$$0 \leq u_k \leq 2.1 \text{ [kW]} \quad (5.2)$$

3. Dynamics/building model: as previously mentioned, the grey-box approach was here adopted to fill the lack of information based on a limited set of experimental data and thus estimate the necessary parameters without excessive computational load (which might had penalized the controller responsiveness). The model relied on building thermal physics laws (principles of energy balance and heat transfer) **[5.90],** used to translate the building components into the corresponding elements of the analogous electric circuit (**Appendix C**). Its formalization is given by the following first-order stochastic differential **equations (5.3 and 5.4)**:

$$dX(t) = A(\theta)X(t)dt + B(\theta)U(t)dt + \sigma(\theta)d\omega \quad (5.3)$$

$$Y(t) = C(\theta)X(t) + D(\theta)U(t) + \varepsilon \quad (5.4)$$

Where "θ" is the vector of unknown parameters (namely the undefined elements composing the circuit), "X(t)" is the vector of states (temperatures of the office room), "U(t)" is the vector of measured inputs (global horizontal radiation, outdoor temperature, power consumption of the FCU and the AHU, air temperature of the corridor – adjacent offices were neglected since they didn't trigger any significant thermal process through the walls), "ω" is a

random function of time (standard Wiener process with independent increments), "σ" is the standard deviation of the Wiener process, "Y(t)" is the vector of measured outputs, formulated in function of the current state and inputs, "A", "B", "C" and "D" are non-linear functions of θ, while "ε" represents the white noise introduced by the measurement error **[5.86]**.
Maximum likelihood estimation is applied to derive the "θ" vector **[5.91]**.

5.5 – ASSESSMENT CRITERIA

The experimental activity was designed and developed to address two main issues:

- provide a full assessment of the overheating affecting the sick building under investigation – exemplary case of a particularly vulnerable construction typology (fully glazed façades) – throughout the year, in order to quantify the extent in time and space of the ergonomic and energetic drawbacks of excessive solar gains.
- check if a smart controller, able to ponder its action on multiple inputs (simultaneously detected or forecasted), could represent a valuable solution to manipulate the environmental parameters in such a thermo-physically complex context.

Against this context, the post-processing phase was primarily focused on comfort parameters.
In the summertime monitoring run, the performance of each fuzzy controller was evaluated by selecting a representative day in terms of solar radiation among an overall monitoring period of seven days in September.
In the wintertime monitoring run, two representative days were selected: the most overcast (15th of December 2016) and the sunniest (16th of December 2016) over the entire observation period around the winter solstice (13rd-22nd of December).
Such choice served the double purpose of investigating lower and upper limits for the overheating occurring inside the office and evaluating the performance of the controllers under different borderline circumstances.
Detailed information on the boundary conditions is provided in **Table 5.5.**

SUMMERTIME MONITORING CAMPAIGN		
Controller	**Period of observation**	**Representative day**
On/off	23/06/2016 - 30/06/2016	28/06/2016
Average weather conditions during business hours on the representative day		
Air Temperature [°C]	**Relative umidity [%]**	**Global Solar radiation [W/m^2]**
28.40	46.41	324.11
Controller	**Period of observation**	**Representative day**

FS	18/09/2016-21/09/2016	20/09/2016
Average weather conditions during business hours on the representative day		
Air Temperature [°C]	**Relative umidity [%]**	**Global Solar radiation [W/m²]**
24.24	57.29	446.59
Controller	**Period of observation**	**Representative day**
FM	22/09/2016-25/09/2016	22/09/2016
Average weather conditions during business hours on the representative day		
Air Temperature [°C]	**Relative umidity [%]**	**Global Solar radiation [W/m²]**
22.42	46.66	462.57
WINTERTIME MONITORING CAMPAIGN		
Controller	**Period of observation**	**Representative day**
MPC	13/12/2016 – 22/12/2016	15/12/2016
Average weather conditions during business hours on the representative day		
Air Temperature [°C]	**Relative umidity [%]**	**Global Solar radiation [W/m²]**
5.40	33	40.75
Controller	**Period of observation**	**Representative day**
MPC	13/12/2016 – 22/12/2016	16/12/2016
Average weather conditions during business hours on the representative day		
Air Temperature [°C]	**Relative umidity [%]**	**Global Solar radiation [W/m²]**
6.25	32	66.22

Table 5.5
Characterization of the monitoring periods.

An indication of the energy benefit was included too, based on the frequency of activation of the three speeds of the FCU.
Each assessment was performed over the hours of expected occupancy.
It should be stressed here that, on the 15th of December some issues occurred with the technical system of the office, indeed no control action could be exerted before 8:00 in the morning (one-hour delay in respect of scheduled operation). Therefore, such anomaly has been contemplated in the assessment phase and served the purpose of checking on how the office would have thermally performed in free running (without any intervention of the controller): in fact, before the implementation of the smart system, the FCU was manually controlled and thus activated just at the arrival of the workers (8:00am).

5.5.1 – Indoor comfort

When it comes to comfort-oriented controllers in mechanically ventilated buildings, the aspects to be taken into account are multiple since multiple are the ways the air jet affects the local and the global air volume in terms of temperature, stratification and turbulence.

Indeed, each speed of the fan guaranteed a certain penetration of the air inlet both along the longitudinal axis (distance spanned) and along the transversal axis (effective area) resulting in different throws, spreads and drops.
Consequently, each action and each switch of the controller caused a perturbation of the thermal field inside the room by mixing the air layers with different intensities and by triggering more or less pleasant draughts.
Therefore, the comfort aftermaths were quantified by calculating the draught rate (DR) and the vertical gradient per each loop. Then the time trends were derived and chartered, together with the corresponding fan speed, so as to define whether the global thermal benefit - which might have been achieved at full-power activations - was counterbalanced by local discomfort phenomena.
Finally, in order to address the magnitude of radiant asymmetry and check on the main reasons behind the increase of mean radiant temperature, the output of the RTD network installed on the glazed façade was analysed to:

- identify the maximum values per each of the materials and the positions involved in the measurements;
- investigate the time lag between maximum solar radiation and maximum surface temperatures.

Global comfort evaluations focused on both the environmental and the users' point of view: accordingly, the operative temperature trends and the PMV values were computed and analyzed. Besides, in order to strike potential causal correlations, the simultaneous levels of solar radiation and outdoor temperature were retrieved and comparatively assessed.
For each performance parameter, along with or in place of the graphical representation of the time trends, a suite of charts (histograms of occurrences) was produced to get the dimension of the dispersion around setpoint values and/or comfort limits, generally by splitting the datasets into progressively wider gaps from the ideal target. The occurrences refer to the 5-minute-averaged recordings.
Even though the boundary conditions over the summertime and then the wintertime monitoring runs were completely different (the weather time trends are displayed for the sake of comprehensiveness) some peculiarities in the different underlying approaches were identified and discussed.

5.5.2 – Energy consumption

The energy consequences of the entrance of over-abundant solar gains through the glazed façade were addressed by investigating the need for higher or lower speeds of the fan as they stand for both electric and thermal consumptions.

The histograms for the MPC controller are accompanied by those referred to the FM controller to verify if any abnormal pattern occurred in view of the predictive features. Furthermore, during the testing of the MPC, the thermal power supplied by the FCU was calculated based on the on-site, instantaneous measurements of the thermal difference between supply and indoor air and the velocity of the air jet (KIMO anemometer).

Such information was analysed in absolute and relative terms:

- by plotting the time trends of the energy consumption, together with the parallel solar radiation and difference between setpoint and operative temperature so as to strike correlations between the energy use and the main triggers for its demand;
- by comparing the frequency of activation of the 3 speeds so as to identify the proportion of corrective action in response to more or less solar gains.

5.6 – RESULTS AND DISCUSSION

The presentation of the main findings is conceived to outline both the overall concern for overheating and the potential benefit driven by the smart control of the AC system, according to the above criteria.

Accordingly, the post-elaboration of the datasets collected by the monitoring stations is hereby introduced by addressing global and local comfort first and subsequently energy consumptions and by respecting the time frame of the experimental activities (namely summertime monitoring with fuzzy controllers first and then wintertime monitoring with the MPC).

In order to comprehensively describe the way the fully glazed façade affected the indoor environmental conditions, both the global and local contribution of convective and irradiative heat flows were addressed to characterize the competing/mutual-empowering interactions between the entrance of solar radiation and the emission of cool air jets from the aeraulic system.

Local phenomena, in particular, were assessed in view of the extensive asymmetries triggered by both the envelope and the HVAC design: indeed, the presence of the large glazed area on one side and of the FCU on the other side (given that the outlet grids were not shaped to take maximum advantage of the Coanda effect) represented a major source for non-uniform distribution of the isotherms.

5.6.1 – Operative temperature and PMV

The operative temperature (Top) was adopted in the context of this experimental activity since it is a particularly meaningful parameter when irradiative heat transfer plays a major role in the thermal balance between occupants and surrounding environment: it is calculated as the average of the mean radiant and ambient air temperatures, weighted by the respective heat transfer coefficients.

The suitability of such approach is underpinned both by on-topic Standards **[5.32,5.33,5.35,5.86]** and akin scientific papers addressing the same issue **[5.5]**.

5.6.1.1 – Summertime results

Figure 5.5 displays the time trends from 7am to 7pm, along with the concomitant weather conditions and FCU speed: operative, setpoint and outdoor temperatures are on the primary y-axis, while global solar radiation is reported on the secondary y-axis. The fan speed representation is overlapped (together with its graduated scale) in order to link all the three major players in the thermal balance (AC system, indoor and outdoor environments).

Furthermore, the histograms in **Figure 5.6** indicate the dispersion of the operative temperature readings around the setpoint value (per each of the tested configurations), representative of the stability of the control strategy.

The PMV index was calculated, assuming a metabolic rate of 1.2 met (equal to 70 watts per unit of body area and representative of sedentary activities like desk jobs) and a clothes thermal insulation of 0.5 clo (equal to 0.0775 m^2K/W and typical of summertime garments) (ISO, 2006). The results were summarized in another set of occurrences distributions (**Figure 5.7**) splitting the datasets into the ranges pertaining to the thresholds of each comfort category identified in Standard ISO 7730 (ISO, 2006) so as to verify the time during which different levels of environmental satisfaction were guaranteed in each tested configuration.

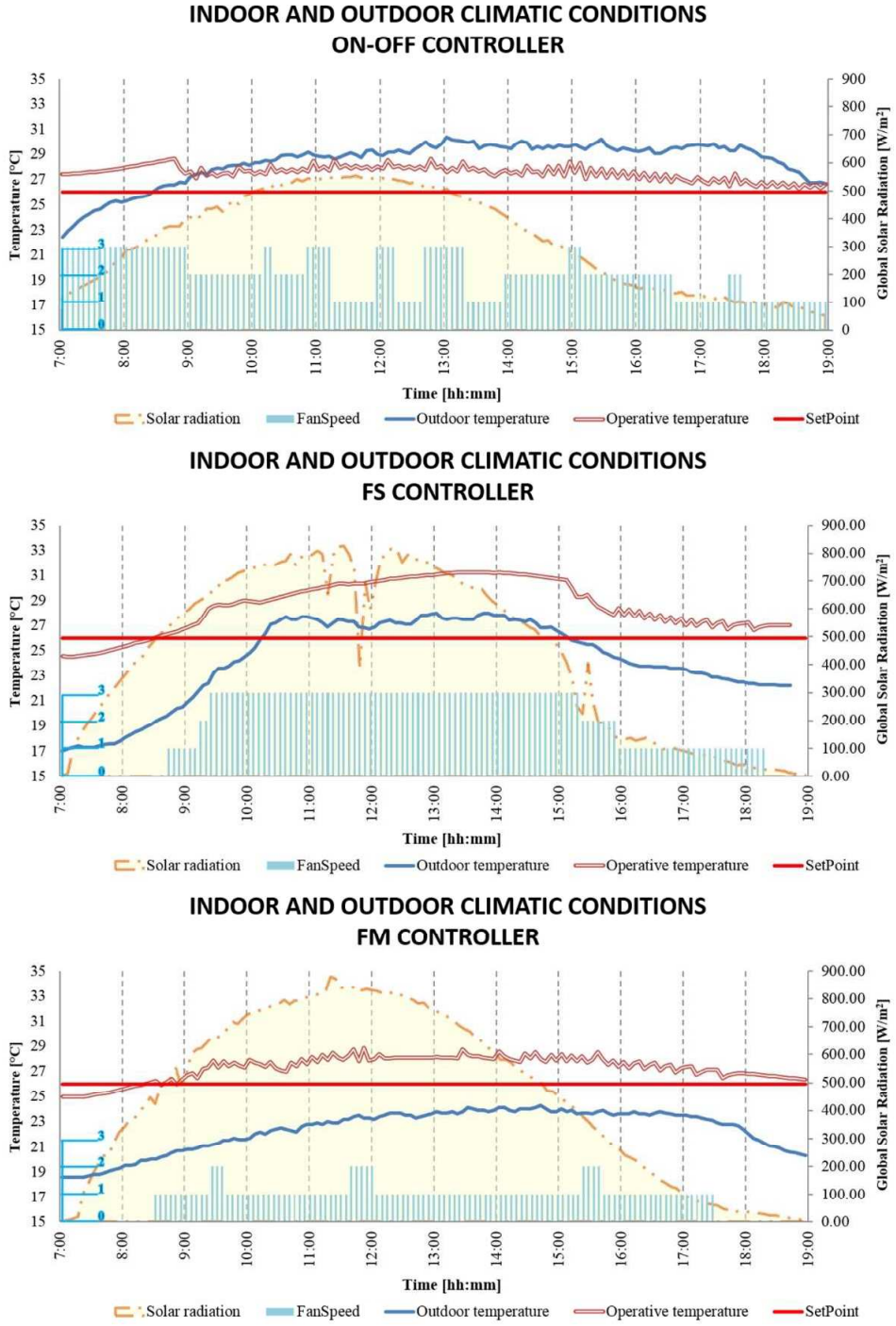


Figure 5.5

Global comfort assessment: time trends of operative temperature against setpoint threshold, solar radiation, outdoor temperature and concomitant fan speed.

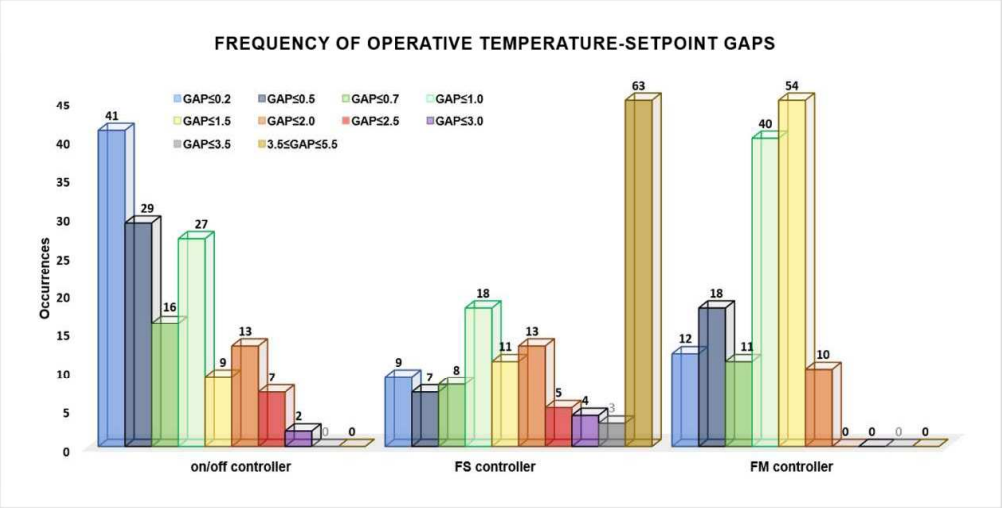


Figure 5.6

Global comfort assessment: histograms of occurrences - operative temperature offset from the setpoint.

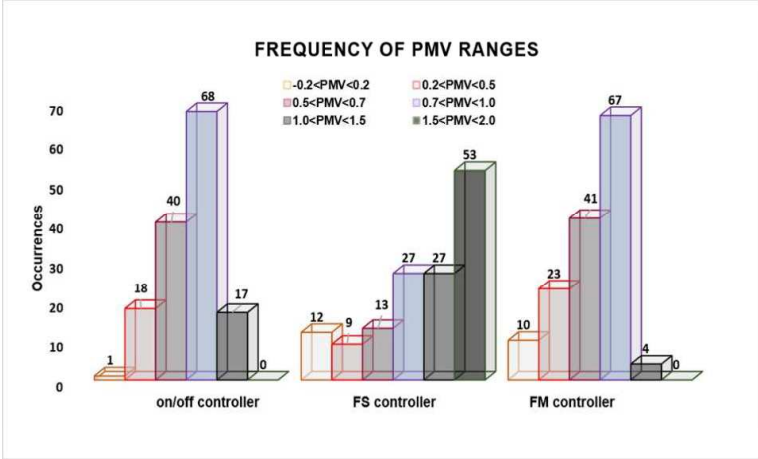


Figure 5.7

Global comfort assessment: histograms of occurrences - PMV value.

By combining the information conveyed by **Figure 5.5, Figure 5.6** and **Figure 5.7** some observations could be drawn:

- during the operation of the on/off controller, the operative temperature never crossed the setpoint line, staying above 26°C all over the occupied period, despite the full-power activation of the FCU for the most time. Just approaching the sunset, a certain temperature reduction was experienced, even though outdoor temperature remained high. Such findings underpinned the need to include solar radiation and, secondly, outdoor temperature in the control logic.

As regards thermal stability, during the period of the on/off control the operative temperature stayed within a quite close neighbourhood of the setpoint value. The 5-minute-averaged measurements fell within the ±0.2°C range around the setpoint for almost the 30% of the time and in the ±0.2 to ±0.5°C range for another 20%. The recorded maximum was 28.7°C, the minimum 26.3°C and the average 27.6°C.

The situation dramatically worsened in September, when the fuzzy controllers were under test, since considerably higher Solar radiation was experienced, thus the energy gains were much more abundant and hard to manage. Outdoor temperatures were, instead, higher in June (on/off controller monitoring period): this indicates again that Solar contribution is preponderant.

The PMV assessment revealed that category A conditions were guaranteed for less than 1% of the time, category B for almost the 15% and category C for the 41%. For the highest time percentage (47%) the PMV fell within the 0.7÷1 range.

- During the operation of the FS controller (which introduced the solar radiation among the driving parameters), the operative temperature fell below the setpoint line for less than 13% of the time, during the early morning when both solar radiation and outdoor temperature hit their low. For the remaining 87%, the trend was almost steadily increasing forcing the fan to operate at full power until sunset.

  As regards thermal stability, the FS controller failed in avoiding drifting. The 5-minute measurements fell within the ±0.2°C and the ±0.2°C to ±0.5°C ranges just for the 6% and the 5% of the time, respectively. Mostly the operative temperature was more than 4°C higher than the setpoint. The recorded maximum was 31.2°C, the minimum 24.5°C and the average 28.6°C.

  All things considered, the combination of September weather conditions and FS controller were found to be the worst case.

  The PMV assessment revealed that category A conditions were guaranteed for the 8.5% of the time, category B for almost the 15% and category C for the 24%. For the highest time percentage (38%) the PMV fell within the 1.5÷2 range.
- During the operation of the FM controller (which pondered its action over smaller deviations from the setpoint compared to the FS one and included the outdoor temperature among the input variables), the operative temperature exceeded 26°C for the 88% of time.

  However, the frequency of extreme deviations was much lower compared to the FS controller, without over-stressing the AC system (which operated just resorting to speed 1 and 2): the 5-minute-averaged measurements fell within the ±0.2°C and the ±0.2°C to ±0.5°C ranges for the 8.3% and the 12.5% of the time, respectively. The greater percentages were distributed between ±0.7°C to

±1°C and ±1°C to ±1.5°C ranges (27.8% and 37.5% respectively). The setpoint values was never exceeded by more than 2.5°C. The recorded maximum was 28.87°C, the minimum 25.0°C and the average 27.3°C.

The PMV assessment revealed that category A conditions were guaranteed for the 7% of the time, category B for almost the 23% and category C for the 51%. For the highest time percentage (46%) the PMV fell within the 0.7÷1 range.

Indeed, the FM controller exhibited a quite stable and valuable performance, especially given the combination of very high solar radiation and outdoor temperature.

Nonetheless, the overheating affecting the building was never rectified, notably because of the massive amount of radiant heat released by the glazed façade. In order to check on this point and verify if the smart control of the FCU was somehow beneficial, the thermal mapping of the glazed façade components (performed by the dedicated sensor station) was analyzed and interpreted.

During all the three observation periods, the solar radiation peaked at around 11:30am, while the maximum surface temperatures were always reached with a certain delay (between 1pm and 2pm with the on/off controller, between 12:30pm and 13:30 pm with the FS controller and at 12:50pm with the FM controller).

Figure 5.8 maps the maximum values: the data can be addressed from different perspectives:

- comparison among controllers' operative conditions.

  The on/off controller tackled with much lower surface temperatures since, albeit considerably higher outdoor temperatures in June, the average solar radiation was below the levels experienced by the other controllers and so was the radiosity of the indoor walls. Notably, the windows and the frame (at window level) were 6-6.5°C cooler compared to FS' conditions (which stand for the hottest case), the horizontal shielded band and the frame (at ground level) were 4°C and almost 2°C cooler respectively.

  The FS controller operated under the worst conditions in terms of mean radiant temperature: compared to the FM period, all the surfaces in close proximity to the perimeter (leftmost windowed module, horizontal shielded band and ground level frame) stayed 2.5-3°C warmer, while the probes on the central windowed module and on the frame at window level revealed milder increases (below 2°C): that could be explained in view of the higher outdoor temperature witnessed during the FS period which kept warmer the external surfaces of the construction elements bordering the window thus empowering the radiant emissions hitting the closer portions of the glazed façade.
- Comparison between measurements performed at different heights (role of position).

  As expected the most central elements (which received the longest-lasting and most-undisturbed contribute from the Sun) showed higher surface

temperatures compared to akin recordings in more outlying positions. In particular, the central windowed module was 0.66°C, 0.25°C and 0.89°C warmer than the leftmost module during the operation of the on/off, FS and FM controller respectively. Much more significant were the frame's surface temperature differences between window level (1.5m above the floor approximately) and ground level: +7,77°C, +12.18°C and +13.11°C. Such considerably diverse behaviour is directly related to the opto-thermal properties of the materials composing the windowpane and the window frame, furtherly evidenced in the following point.

- Comparison between measurements performed on different materials.
  Number and typology of the layers composing the south-exposed façade impinged on prominent differences in the amount of thermal energy absorbed and thus converted in rise of surface temperature. The major discrepancy was recorded by the RTDs placed on the leftmost glazed module and the shielded horizontal band directly below: the gap between the maximum values ranged between +6.1°C and +6.4°C during the operation of the fuzzy controllers, in respect of the +3.6°C witnessed in June. As a matter of fact, the lower level of solar radiation, experienced during the on/off control of the FCU, was responsible for the halving.
  Further significant heterogeneity arose between the surface temperatures detected by the two central probes on the windowpane and the window frame: the frame was up to 1°C warmer than the glazed counterpart during the on/off and the FS control periods. The gap more than doubled during the FM operation: since the strongest variation in weather conditions was by far experienced passing from the on/off controller to the FS one, such increase might be explained by looking at the major difference between the FM management of the cold air jet and the other two modes: speed 3 was never activated, consequently the throw might not have reached the glazed surface and cooled the frame at window level.

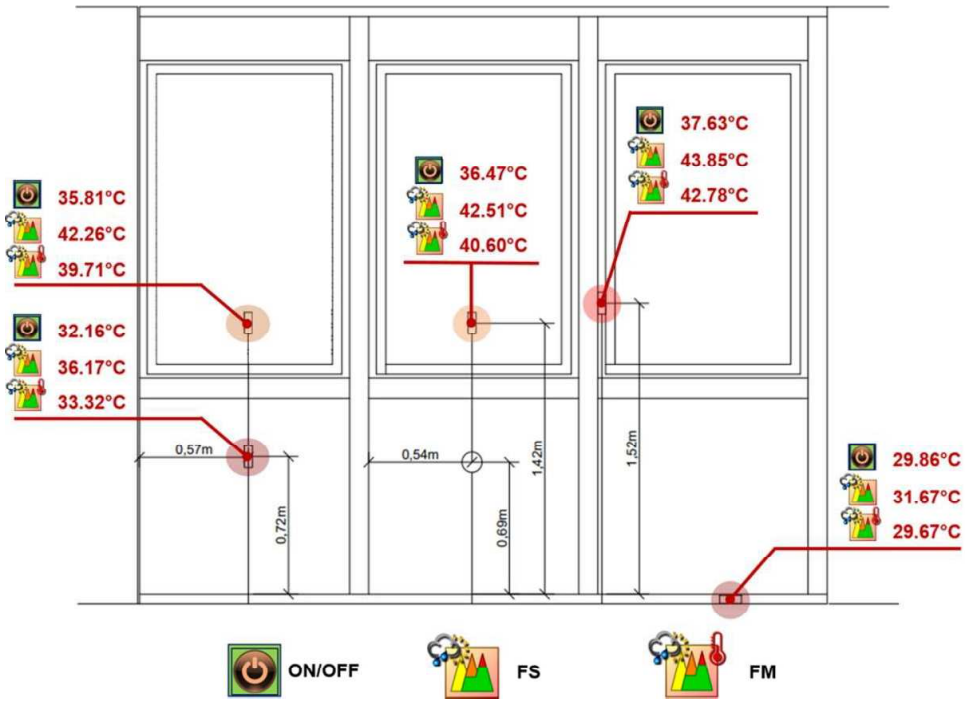


Figure 5.8
Thermal distribution of the maximum surface temperatures on the glazed façade.

All things considered, very high surface temperature persisted on almost all the internal side of the south-exposed façade throughout the time slot of occupancy with remarkable variations depending on weather conditions, mutual influences among construction elements, materials' properties and geometry, and radiant field perturbations indirectly triggered by the mechanical ventilation.

5.6.1.2 – Wintertime results

In order to potentially intervene on the settings of the MPC at any given time on the basis of the achieved comfort performance, the calculation of the operative temperature was programmed in LabVIEW, within the same Virtual Instrument governing the control process. The time trend was chartered in the front panel together with the parallel speed of the fan so that a gross, prompt indication of the interrelation could be retrieved.
Thanks to such precaution, a strong overheating was notified since the first day of the monitoring activity which forced to correct the settings of the controller.
In fact, the MPC was originally tuned to track a setpoint of 20°C, in compliance with the standardized values afferent to the Italian legislation **[5.87]**.

De facto, on the 13th of December, the operative temperature never dropped below 20°C, thus forcing to raise the setpoint value to 24°C (still within the acceptable range of wintry operative temperatures and air speeds for the comfort zone according to the ASHRAE Standard 55 - 2010 **[5.35]**) in order to check on the performance of the controller.

Nonetheless, that was the major proof of the ongoing occurrence of uncomfortable conditions.

Therefore, it was unequivocally demonstrated that the vulnerability to overheating for such building typology is a major issue which might undermine the productivity of the occupants and trigger other-SBS related inconveniences/illnesses throughout the year. Since no means of effective counteraction was identified neither in summer (the cooling load supplied by the FCU, even smartly controlled, was insufficient) nor in winter (the AHU did not operate in cooling mode during the heating season) a substantial retrofitting is apparently necessary (replacement of the current glazed solution with high-performance glasses or electronically switchable glasses, installation of external shadings, …).

In analogy with **Figure 5.5**, the graphs in **Figure 5.9** plot the time trend of operative and outdoor temperatures along with global solar radiation (on the secondary y-axis) for both the days under investigation. The horizontal, thickest red line stands for the setpoint value, while the light-blue graduated scale on the left side defines the legend for the piled column chart representing the fan speeds.

Other two sets of charts are provided to comprehensively depict the global comfort condition, as it was done for the fuzzy controllers:

- the histograms in **Figure 5.10** (analogous to **Figure 5.6**) are illustrative of the stability of the control action according to different perturbing inputs from the outdoors.
- the histograms in **Fig. 5.11** (analogous to **Figure 5.7**), which show how many times the environmental conditions established inside the office fell within the different categories of comfort defined in the on-topic standards **[5.32,5.33,5.88]**.

Again, the results are based on the 5-minute spaced calculation of the PMV index. It was assumed a metabolic rate of 1.2 met (equal to 70 watts per unit of body area), recommended for sedentary activities and a thermal resistance of the clothes equal to 1.0 clo (0.0775 m^2K/W), typical of wintry garments **[5.33]**.

It should be stressed here that The Predicted Mean Vote is representative of the expected feedback on thermal sensation of a homogeneous sample of people living the thermodynamics of indoor environments **[5.89]**, thus it stands for the overall pleasantness of the microclimate. This means that it includes the negative effect of the unavoidable baseline of overheating that led to the adjustment of the setpoint value during the configuration of the controller. Consequently, closest sensations to thermal

neutrality are concomitant with morning hours when lower temperatures persisted inside the office. Therefore, such analysis should not be considered representative of the quality of the MPC management (which tended to emphasize the occurrence of sightly warm conditions by tracking the 24°C setpoint), yet it truly depicts the drawbacks of over-abundant solar gains on the proper comfort-driven running of the FCU.

By analysing the trends in **Figure 5.9** it is possible to investigate the way the controller handled the information about current indoor and forecast outdoor parameters to keep the operative temperature in the closest possible neighbour of the setpoint.

Both on the 15th and the 16th of December, the controller started to manipulate the emission of heat when Top was approximately 22.5°C (in the first case around 8am, in the second at 7am) and initiated a progressive escalation of the fan speeds. Then, two different operative patterns were established on the representative days, due to the different start time and amount of solar gains affecting the room:

- on the 15th, speed 1 was initially activated and maintained (in view of the increase of solar radiation predicted for the following hours) until Top exhibited a trend reversal and stabilized at a certain offset under the setpoint. Consequently, the controller corrected its action by boosting the fan from speed 1 to speed 2. Speed 3 was eventually reached because of the combination of Top below the target value and the forecast of decreasing solar radiation. The full power mode persisted (regardless of the increase of the outdoor temperature, expected for the next hour) until the setpoint was twice overtaken in a time slot of less than 10 minutes. The MPC logic intervened by drastically switching off the fan for a while. As soon as Top showed a mild, but steady decrease, the fan was activated again at minimum power. The maximum overshoot occurred because of the subsequent escalation to speed 2 and 3 around 3pm, in response to a quite stable Top and the prediction of sunset. This suggests that the controller slightly outweighed the effect of solar radiation when its predicted value approached zero and overreacted by releasing more heat than necessary. Indeed, once the overshoot was detected, the algorithm corrected the emission by stepping back directly to speed 1. From 4pm on, neither solar radiation nor outdoor temperature changes perturbed the thermal balance of the office; therefore speed 1 was enough to compensate the heat losses and keep a very stable operative temperature.
- On the 16th of December, the MPC rapidly proceeded through the three power levels to emphasize the natural rise of Top and quickly drive it to the target value. Until no significant increase of the solar radiation was forecast, speed 3 persisted without causing any relevant overshoot, even with Top very close to or slightly exceeding the setpoint. Such behaviour demonstrates the suitability of the developed grey-box model in depicting the sensitivity of the test room to

solar gains so that the control action could be pondered on the right driving forces. At 9am the MPC detected a significant increase of solar radiation expected for the next hour and corrected the action by directly switching to speed 1. Such setting persisted until 2.15pm since a minimum heat influx was necessary to compensate the heat losses (thanks to more favourable weather conditions than those recorded the previous day). Given the dramatical drop of solar radiation predicted to occur at 3pm, a 20-minute-lasting action at maximum power was preventively adopted until a certain overshoot of the setpoint was detected. Another activation, even briefer, of speed 3 occurred in view of the sunset, thus remarking the potential room for improvement in the settings of the controller to better manage the forecast zeroing of the solar contribute.

Despite such occasional boosts of the fan, the controller succeeded in preserving a steady operative temperature close to the target value by resorting to the minimum power throughout the operative time frame.

As regards the overheating affecting the building, from 7am to 8am on the 15th of December, when the system breakdown prevented any control action, the operative temperature rose from around 20°C to 22.5°C as a result of the sole effect of solar gains entering through the glazed façade.

Moreover, on the 13th of the month, when the test started and the MPC settings were defined, the operative temperature ranged between a minimum of 21.6°C and a maximum of 27.7°C in the time slot of expected occupancy, given an average solar radiation of 170 W/m^2 (higher than that experienced during the other days of monitoring of the MPC): this means that, around winter solstice solar gains are still so abundant to drive the operative temperature not just over the heating setpoint, but even over the cooling setpoint (26°C) without any active intervention.

Moving on to the statistical figures, the histograms in **Figure 5.10** display how the operative temperature recordings distributed around the setpoint during the operation of the MPC, thus comparing the stability of the control action in response to the two different boundary conditions.

An additional set of histograms is provided to check on the differences with the performance of the fuzzy controller which piloted the FCU during the previous test, run in summertime. Even though the weather conditions that accompanied the two experimental rounds were completely different, such frequency distributions are representative of the level of indoor comfort achieved inside the office as a result of the smart management of cooling/heating loads. Therefore, some comparative conclusions can be drawn between the predictive, model-based logic and the heuristic approach.

The MPC proved to better master the building thermal dynamics on sunnier days. Indeed, on the 16th of December, its action was never belated and promptly

compensated the predicted necessary corrections right before the steepest rises and falls of the solar radiation curve (at 10am and 3pm approximately). That caused minimum overshooting (even less than during more overcast days) and minimum offsets from the setpoint. In detail:

- on the 16th of December, the 5-minute-spaced Top measurements fell within the ±0.2°C range around the setpoint for more than the 77% of the time. The almost total remainder fitted the range ±0.2 to ±0.5°C.
- on the 15th of December, most of the readings were distributed between the two above ranges (35.4% of the time in the former and 25.4% in the latter) thus validating the quality of the control action in the event of diverse boundary conditions. The residual 40% was quite equally distributed among the other subsets in **Figure 5.10**.

The limit of ±2°C was never exceeded.

This happened with the fuzzy controller too, in summertime, yet the setpoint tracking was much grosser: for the 65% of the time, the overshoot was between 0.7°C and 1.5°C thus substantially jeopardising the establishment of stable comfort conditions inside the room.

Anyhow, it should be stressed here that the fuzzy controller relied on a very intuitive and evidence-based configuration with no need for a wide sensor network and a dynamic model of the building **[5.25]**. Besides, while solar gains were partly positive in the maintaining of indoor thermal comfort in wintertime, their drawbacks in terms of over-saturation of the cooling needs were exacerbated in September.

Nonetheless, the differences in terms of perceived comfort are indivertibly evident from the frequency distribution of the Predicted Mean Vote index (**Figure 5.11**).

As regards the fuzzy management of the FCU, more than half the time, during the selected day of high solar radiation (22nd of September 2016), the level of comfort was outside acceptable criteria (Category IV). In Standard EN 15251 **[5.32]** it is specifically stated that such conditions "should only be accepted for a limited part of the year". In the light of the monitoring results, the fuzzy operation in summertime might represent a borderline solution. Potential improvement could be achieved by implementing the MPC, since its management in wintertime led to more encouraging results.

Indeed, Category IV conditions were always averted by the model-based, predictive logic. Category II (the recommended one for existing buildings) was ensured for the 85% and the 80% of the time on the 16th and the 15th of December respectively.

The coldest temperatures on the overcast day allowed to establish even Category I conditions over a considerable time window (from 8am to 10am, standing for the 18% of the occurrences approximately), while the higher solar gains on the 16th were responsible for non-negligible persistence (13.1% of the time) of Category III comfort levels (still moderately acceptable for existing buildings).

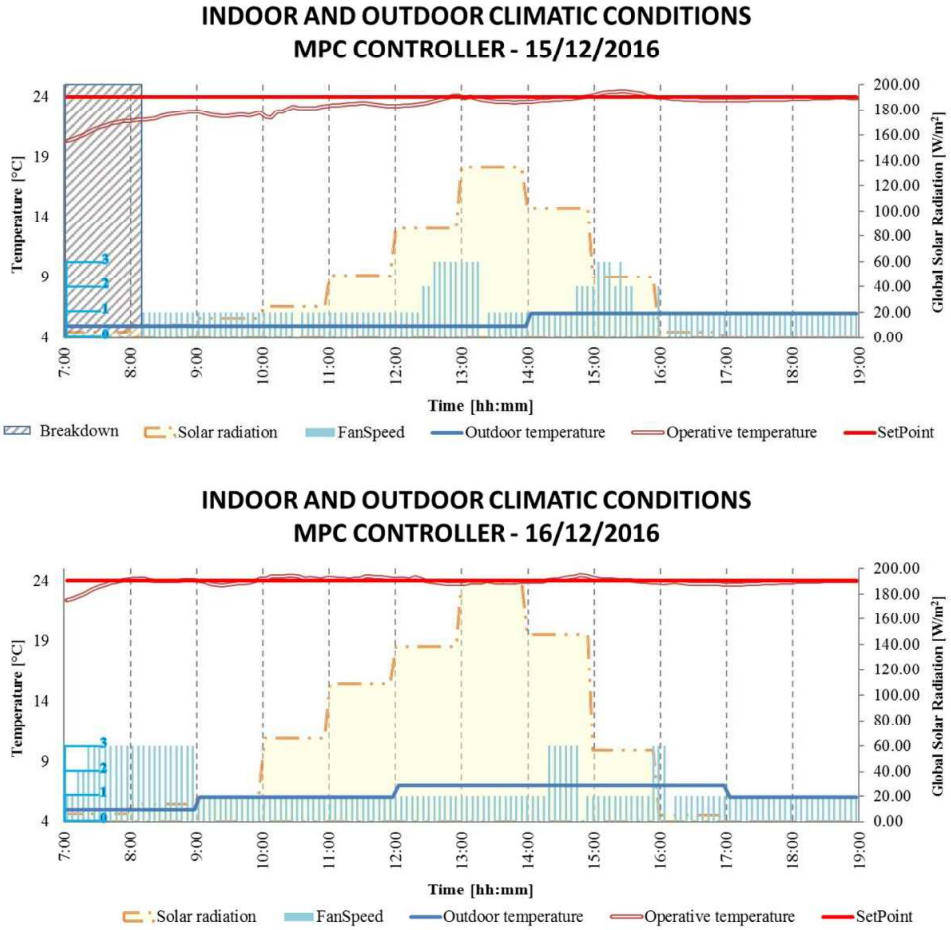


Figure 5.9

Global comfort assessment: time trends of operative temperature against setpoint threshold, solar radiation and concomitant fan speed.

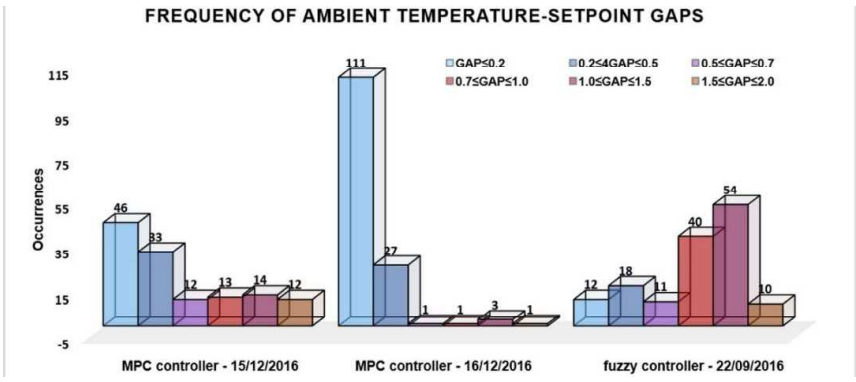


Figure 5.10

Global comfort assessment: histograms of occurrences - operative temperature offset from the setpoint.

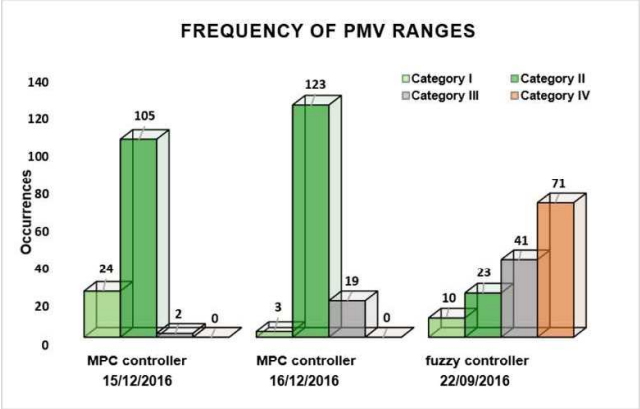


Figure 5.11
Global comfort assessment: histograms of occurrences - PMV value.

On the other side, some relevant information was derived by commenting on the temperature distribution on the internal side of the south-exposed façade.
On both the representative days of December, solar radiation peaked between 1pm and 2pm, while the maximum surface temperatures were recorded two hours later on the 15th and one hour later on the 16th.
Figure 5.12 maps the distribution of the maximum values. Multiple comparisons can be drawn.
Firstly, by comparing the pairs of values displayed per each probe, it is possible to point out the differences between days dominated by direct or diffuse solar radiation.
Regardless of materials and position, on the 16th all surfaces reached higher temperatures and kept them longer. The only negligible increase is the one on the frame at floor level: this might be explained considering the shadowing effect of the shielded horizontal band in the first 1 meter of the façade which, de facto, annulled the local contribution of direct solar radiation.
As expected the maximum differences were recorded by the Pt100s installed on the glazed panes, in particular, +1.46°C on the central module and +1.37°C on the leftmost module. The different location, in fact, impinged on the amount of solar radiation received in the early morning, when the sunbeams on the lateral window were temporarily obstructed by the bordering construction elements.
The shielded panel and the inter-window frame exhibited milder increments, yet close to 1°C (0.92°C and 0.86°C respectively), in view of their lower thermal transmittances.
Another consequence of the different resistances to the heat flow exerted by the variously composed portions of the south façade, is that the glazed components (and the opaque elements in close proximity) stayed cooler over the entire monitoring

period, as the thermal gradient between outdoors and indoors impelled stronger heat transfers.

In fact, a second comparison between different materials (same height of the probes) revealed that the leftmost glazed module stayed 1°C and 0.55°C cooler than the shielded horizontal band directly below on the 15th and the 16th, while the recordings from the RTDs on the central windowpane and window frame differed by -1.12°C and -0.53°C respectively.

The gaps were halved on the sunnier day because the glazed components could absorb much more radiation.

A third comparison aimed at investigating the role of position by juxtaposing the pairs of values recorded on the same day and on equal materials, yet different heights of the probes.

Since the maximum levels of solar radiation were recorded in the afternoon, the leftmost elements were more intensely irradiated and heated up: accordingly, the probe on the lateral module detected a surface temperature greater than that recorded by the aligned probe on the central module by 0.22°C and 0.13°C on the 15th and 16th of December respectively. The difference was less noticeable on the sunnier day since the maximum surface values were reached one hour earlier (between 2:15pm and 3pm) than on the 15th when the sun was still high upon the horizon.

A substantial discrepancy (+1°C) arises by comparing the recordings of the probes on the frame, between floor level and window level in overcast conditions: that might depend on the higher thermal losses by conduction experienced by the aluminum uprights towards the adjacent cooler glazed surfaces when the direct sunlight was not sufficient to properly counterbalance. Conversely, the floor frame and the shielded horizontal band surface temperatures were always very close thus not impelling any significant conductive transfer (thereby keeping the frame warmer). On the 16th of December, such gap was dramatically reduced: the inter-window frame stayed just 0.15°C cooler than the floor frame. The reason is that the thermal gradient between frame and window was halved with respect to the correspondent recordings on the 15th, as previously discussed.

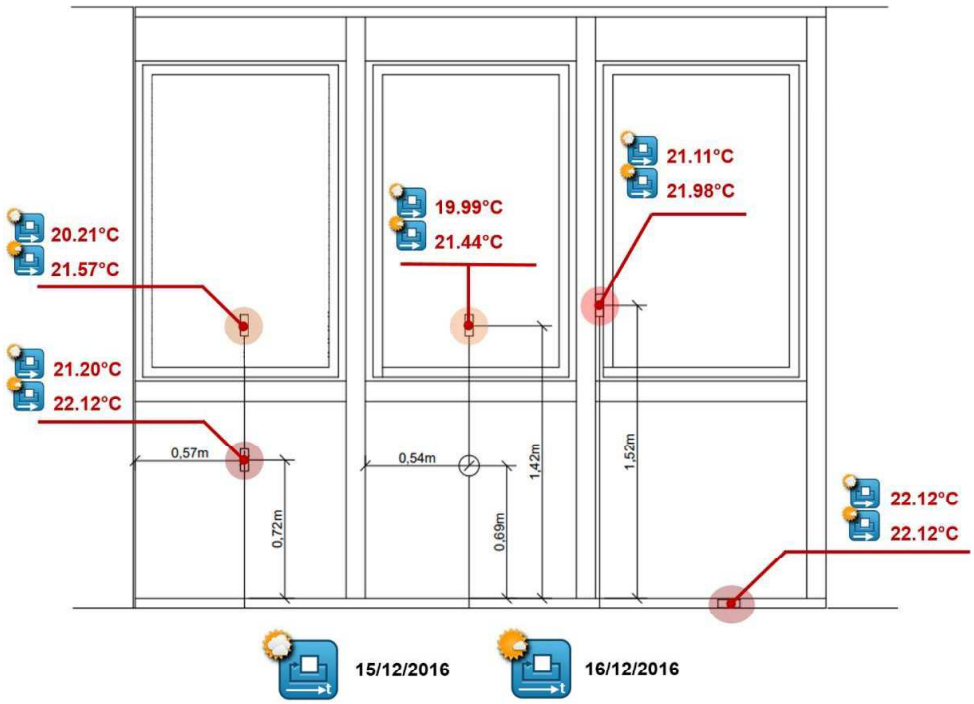


Figure 5.12
Local comfort assessment: thermal distribution of the maximum surface temperatures on the glazed façade.

5.6.2 – Draughts and vertical gradient

Although comfort criteria might be successfully fulfilled on a spatially-averaged scale, situations might differ on a local-scale.
In presence of a single FCU serving a small indoor volume, the likelihood of discomfort phenomena, namely drafts and vertical gradients, tends to be non-negligible. Besides, the presence of a single, very large glazed façade is a major trigger for asymmetries.
Accordingly, a series of evaluations based on measured data was carried out to check on confined areas of high potential for thermal dissatisfaction.

5.6.2.1 – Summertime results

In order to define the extent of the discomfort inside the office in object, the occurrence of draughts was investigated. The likelihood of excessive or excessively variable air velocity in the casuistry in object was mainly linked to:

- the protracted exposition to solar radiation, that heated up the internal surfaces, which, in turn, gradually released the stored energy to the neighboring air volumes thus creating a vertical thermal gradient and impelling convective updrafts;
- the air jet from the FCU, which was responsible for considerable air movement, beneficial in terms of mixing and homogenizing, yet detrimental in terms of local air acceleration and turbulence (sparsely tolerated in wintertime **[5.33]**).

The second trigger for local environmental non-uniformities, addressed in this study in view of the specs of the case study, is the vertical thermal gradient.

The vertical gradient of the air temperature depends on the distribution of the heat sources, especially along the height (AC systems. lighting, occupants…). Given the denial to access the room all over the monitoring campaign, the potential uneven stratification of the air could be directly related to the air jet from the fan coil and to the penetration of solar beams (no other internal gains).

Against this backdrop, the outputs of the draught probes were post-processed to calculate the draught rate (DR) and the vertical gradient at 1.1 m and 0.1m, according to the formulation in ISO 7730 and other Standards **[5.33,5.35,5.86]**:

$$DR = (34 - t_a)(v - 0{,}05)^{0{,}62}(0{,}37 \cdot v \cdot Tu + 3{,}14) \quad (5.5)$$

where "ta" is the indoor air temperature (°C), "v" is the air velocity and "Tu" the turbulence intensity, defined as the air speed standard deviation divided by its average. Equation (5) applies to people at light sedentary activity, with an overall thermal sensation close to neutral. The recommended upper limit to guarantee local comfort conditions in existing buildings (category B) is 20%.

Against this backdrop, the occurrence of drafts in the reference case (on-off controller) and with the high-performance controllers was analysed.

Figure 5.13 plots the time trends (over the hours of occupancy) of the draught rates measured at head level (1.1m) and ankle level (0.1) per each controller, with respect to the comfort limit (highlighted by the horizontal red line). On the secondary axis is the fan speed, overlapped to the other lines so as to strike correlations between the occurrence of draughts and the momentum of the air outlet from the FCU.

Drafts mostly developed at ground level, in particular:

- the maximum DR values at 0.1m are 60% (on/off controller), 55% (FS controller) and 29.2% (FM controller), which, compared to the correspondent maximum values recorded at 1.1m, are respectively 7 times, 3.5 times and 4 times greater;
- the average DR values at 0.1m are 10.8% (on/off controller), 11.4% (FS controller) and 4.9% (FM controller), while the correspondent values at 1.1m are 1.54%, 2% and 0.9% respectively.

A reasonable explanation for such behaviour is that, at ground level, the fluid jet from the FCU interacts with the local convective updraft triggered by the sunlit floor surface

which transfers part of its exergy to the air volumes blowing past it, thus impelling higher turbulence.
The fan speed management tremendously affected the overall situation: every time the speed abruptly increased (as when the on/off controller directly switched from 1 to 3) the DR peaked, sharply overtaking the comfort limit. Speed 1 was the only operative mode that didn't generate discomfort. A brief activation of speed 2 led to limited concerns, while prolonged commands were substantially detrimental. Speed 3 caused immediate and consistent discomfort regardless of the duration of the action.

The frequency of DR-driven discomfort phenomena is displayed in **Figure 5.14** that plots the occurrences of DR values over the 20% upper limit.
Among the different controllers, the best DR performance was by far achieved by the FM controller, which totalized just three discomfort events at 0.1m, one at 0.6m and none at 1.1m. The FS configuration wasn't beneficial to the base case since the discomfort occurred with almost the same distribution.

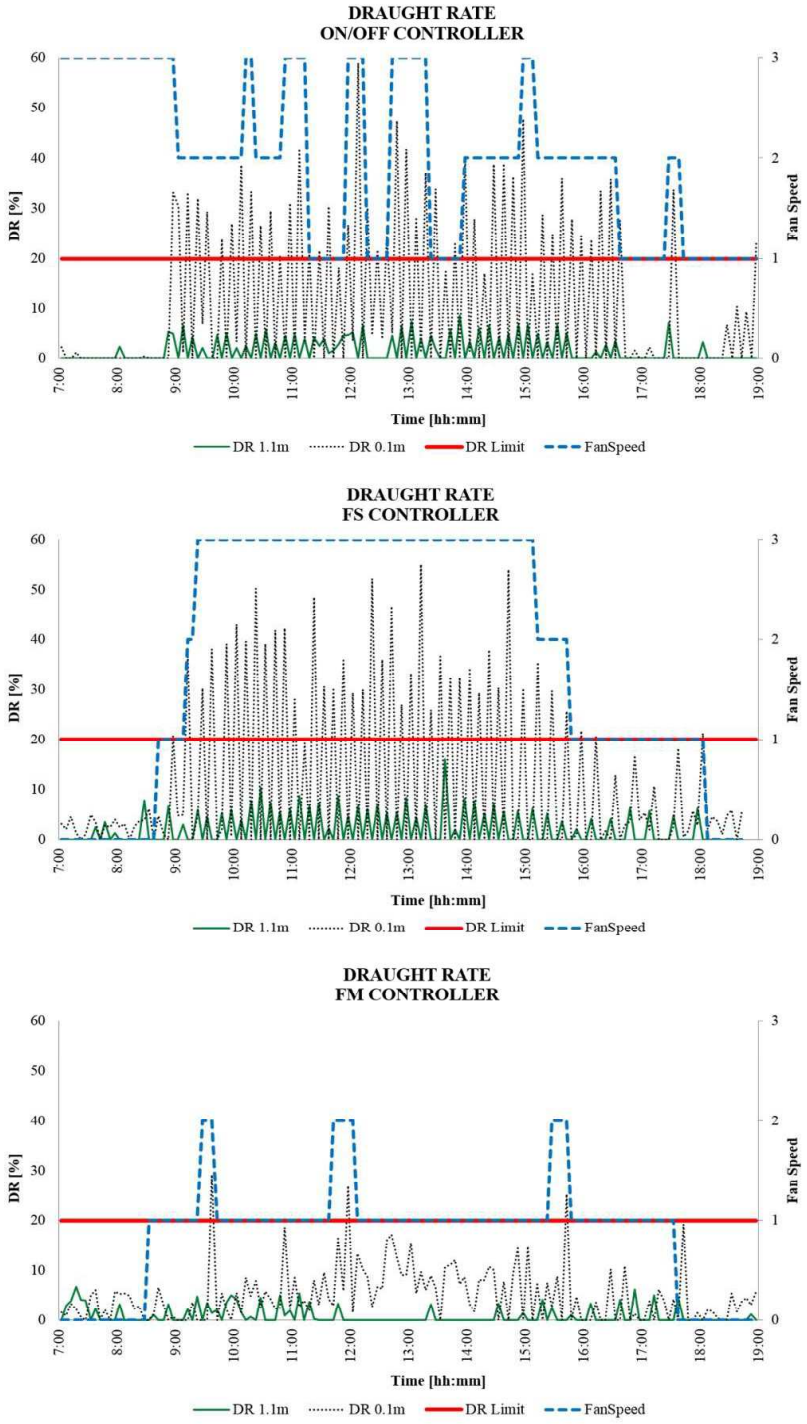


Figure 5.13

Local comfort assessment: time trends of the draught rates at 0.1m and 1.1m against the comfort limit and the concomitant fan speed.

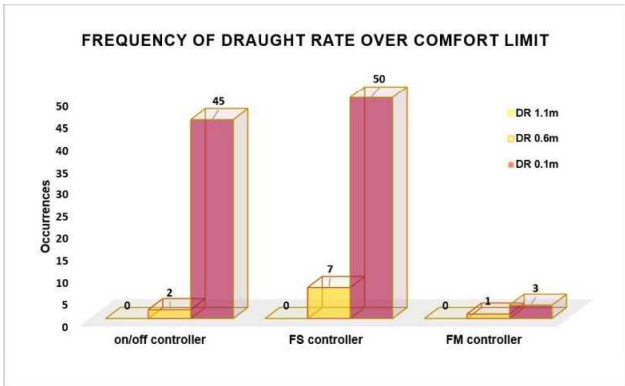


Figure 5.14

Local comfort assessment: histograms of occurrences – DR values at 0.1, 0.6 and 1.1 meters from ground level.

As regards air stratification, the case study basically didn't show any concern due to vertical thermal gradient, since the afore mentioned comfort condition was respected all over the hours of occupancy, regardless of the controller in run (as apparent in **Figure 5.15**).

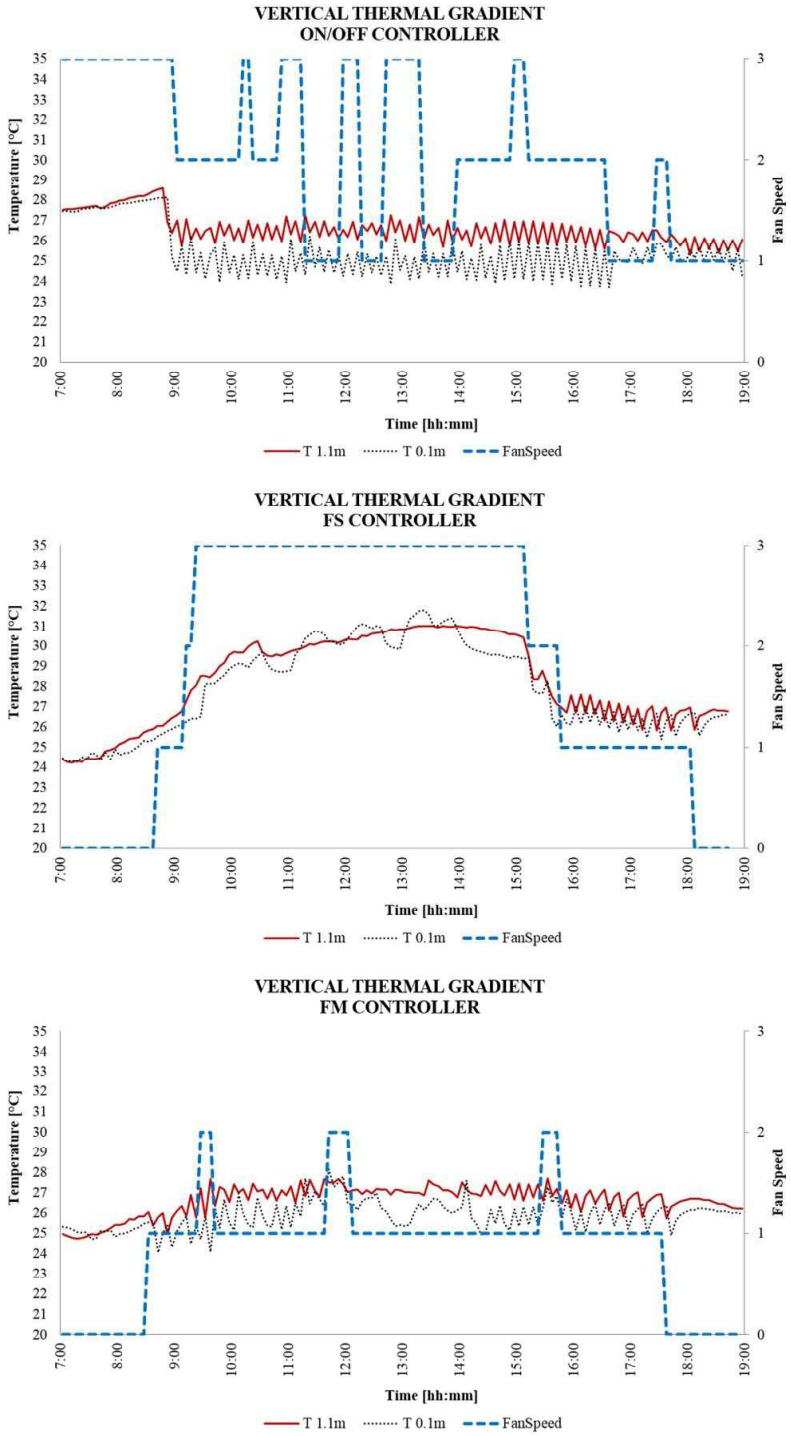


Figure 5.15

Local comfort assessment: time trends of the air temperature at 0.1m and 1.1m against the concomitant fan speed.

However, the frequency plot of progressively wider vertical gradients (**Figure 5.16**) outlines that both the fuzzy controllers were beneficial in terms of air stratification: the on/off controller followed a quite symmetrical distribution, thus exhibiting vertical gradients close to 3°C for almost the 20% of the time. Such percentage was dramatically reduced by the FM controller (1.4%) and even annulled by the FS controller.

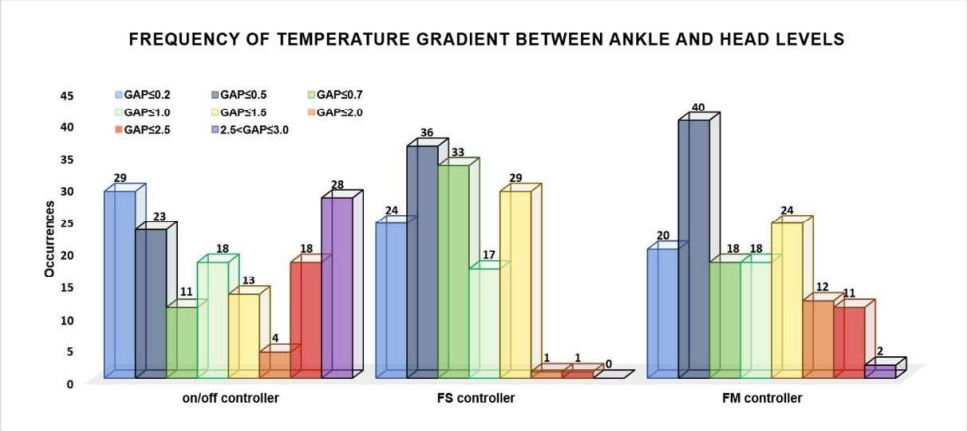


Figure 5.16
Local comfort assessment: histograms of occurrences – vertical thermal gradients.

5.6.2.2 – Wintertime results

Almost the same analyses were performed for both the representative days of the MPC control, by producing:

- plots of the time trends (**Figure 5.17)**, compared to the recommended upper limits in compliance with Category II requirements set out in EN ISO 7730 (20% for DR and 3°C for vertical gradients). On the secondary axis is reported the action of the FCU in terms of activated speed so as to strike causal links between the intensity of the local discomfort and the momentum of the air jet. It should be stressed that only the 0.1-metre value for the DR is displayed since the measurements at higher heights were negligible.
- histograms (**Figure 5.18**), which display how many times the 5-minute calculations of the vertical gradient fell within progressively wider ranges approaching the comfort limit. When mixing devices are deployed, instead of displacement ventilations, the thermal uniformity tends to be jeopardised when high airflow rates are activated **[5.90].** Therefore, the least the need for full-power air conditioning, the least the impact on local discomfort.

The main reason behind imparting predictive features to an AC controller was to prevent strong, delayed corrective actions and to distribute the energy loads on

smoother, longer-lasting low-power calls. Consequently, the risk for strong vertical gradients was expected to get mitigated. In order to check on this point, a third group of histograms is added in **Figure 5.18**, based on the fuzzy controller's performance in summertime, which provides the reference for comparison with non-predictive logics. The main observations can be recapped as follows:

- the comfort limits were never exceeded. Consequently, no local discomfort was generated by the control action pursued by the MPC;
- on the 15th of December, the maximum and average DR values at 0.1m (excluding the spikes due to the initial breakdown) were 7.4% and 2.0%, when speed 1 was activated, whereas the respective percentages under full-power air jets were 10.4% and 4.6% (speed 2 ran too briefly to be reasonably evaluated). The correspondent figures recorded on the 16th were 6.9% and 3.1% for speed 1, whilst 2.26% and 1.13% were detected for speed 3. This might be explained by contemplating the effect of solar radiation at ground level: on the 16th of December, the floor surface was more intensively heated up by the Sun, thus reaching a higher temperature and transferring more thermal energy to the air volumes blowing past it. Consequently, higher thermal uniformity was achieved throughout the room and lower turbulence was impelled since the warm fluid jet from the FCU better mixed with the local convective updrafts;
- on the 15th of December, the maximum, minimum and average vertical gradients were 1.46°C, 0.47°C and 0.88°C, when speed 1 was activated, whilst the respective values at speed 3 were 1.68°C, 0.71°C and 1.06°C. The correspondent figures recorded on the 16th were 1.38°, 0.45°C and 0.85°C for speed 1, whereas 1.73°C, 0.74°C and 1.38°C were detected for speed 3. Therefore, on sunnier days, higher-power injects triggered more substantial thermal gradients, as expected. Instead, very cloudy conditions (predominance of diffuse radiation) led to a complete reversal of the usual thermal behaviour pattern: this suggests that more vigorous air mixing is beneficial when floor temperature is lower since it helps to amalgamate the stratified air layers.

Overall, the thermal gradients were more pronounced on the 16th, because of the protracted use of speed 3 in the early morning, when the indoor surfaces where still cold: in such conditions, the thermal gap between ankle and head level was remarkably higher since the momentum of the air jet could span a major area and cover a greater distance.

Finally, by plotting the different frequencies of progressively wider vertical gradients (**Figure 5.18**), it was possible to underline whether the predictive nature of the MPC was beneficial in terms of air stratification compared to the rule-based, heuristic approach, regardless of the specific boundary conditions.

As expected, the vertical gradient never exceeded 2.0°C under the regulation of the predictive logic, while such level of non-uniformity occurred with the fuzzy controller for almost the 10% of the time (even though the comfort threshold of 3°C was never

crossed in any case). The greater time percentages corresponded to the 0.7°C÷1.0°C and the 1.0°C÷1.5°C ranges all over the MPC control: 62.6% and 20.6% on the 15th of December versus 58.6% and 24.8% on the 16th.
Much lower were the correspondent percentages experienced on the 22nd of September: 12.4% and 16.6%.
On the other hand, the fuzzy controller succeeded in establishing minimum temperature differences among 0.1m and 1.1m, totalizing 13.8% and 27.6% of the time within the 0.0°C÷0.2°C and the 0.2°C÷0.5°C ranges respectively. The correspondent proportion with the MPC was totally negligible. Nevertheless, that might have been the result of a substantial inefficacy of the cooling action of the FCU on the massive overheating affecting the office in summertime.

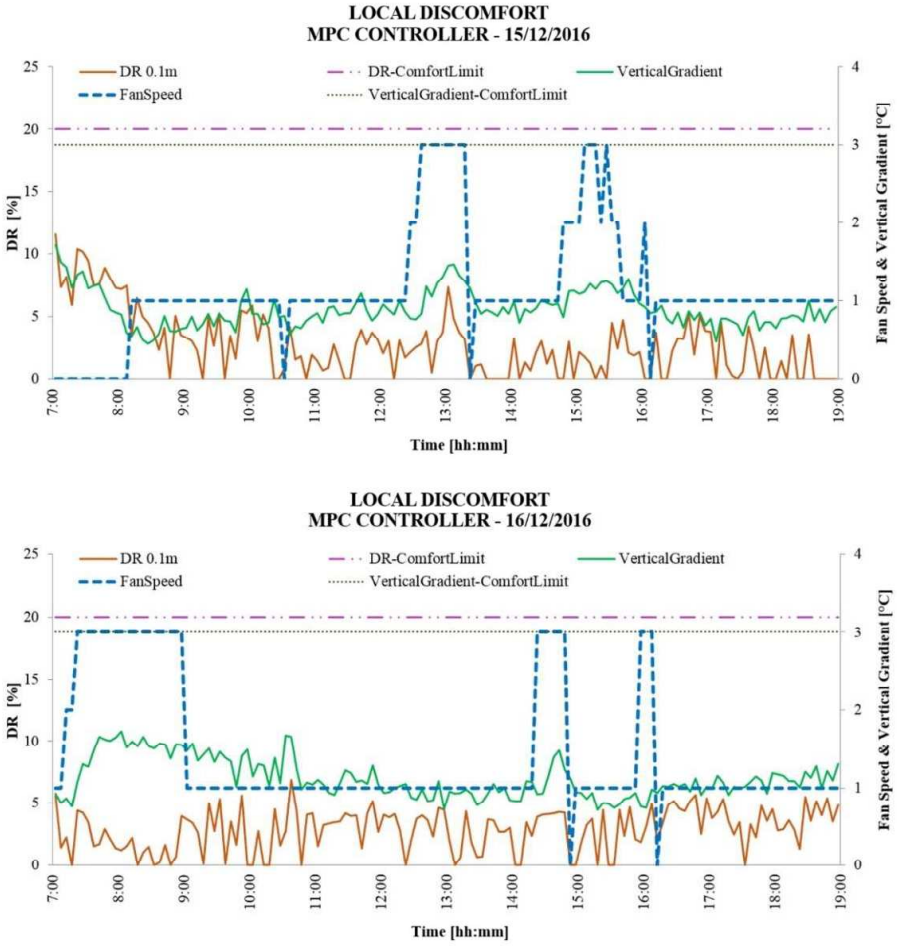


Figure 5.17
Local comfort assessment: time trends of the draught rate at 0.1m and of the vertical gradient against the respective comfort limits and the concomitant fan speed.

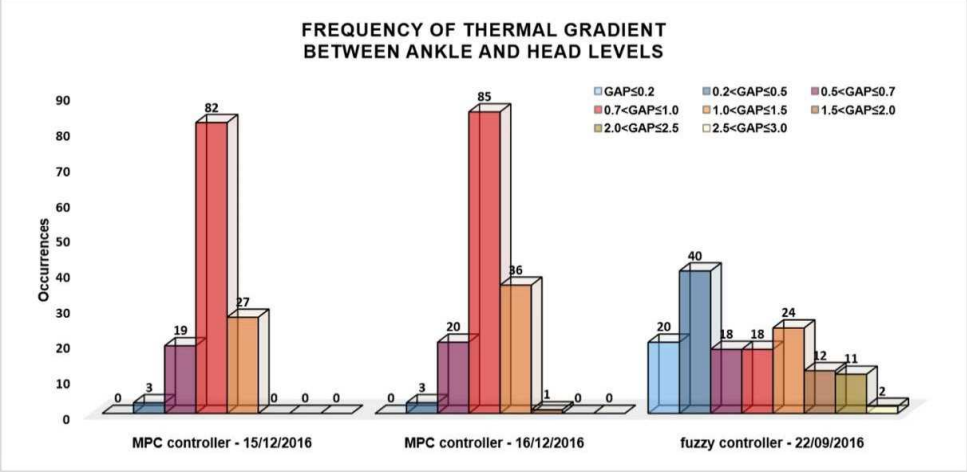


Figure 5.18

Local comfort assessment: histograms of occurrences – vertical thermal gradients.

5.6.3 – Energy consumption

Comfort and energy savings are commonly antagonist targets in building design.

Nevertheless, in case the source of discomfort leads to the exacerbation of the cooling/heating loads the two purposes might align.

Therefore, some of the conclusions drawn for the comfort assessment are de facto illustrative of the energy aspects too.

The main indicator for energy consumptions is the fan speed, since each operative mode of the motor corresponds to different thermal/electric power levels (**Table 5.2**).

5.6.3.1 – Summertime results

The histograms in **Figure 5.19** were produced to compare the energy behavior of the three operation modes and verify if the deployment of the different powers obeyed to any sort of scheme or if imbalances occurred as result of an improper configuration of the controllers.

In terms of control action equalization, the on/off controller divided up quite equally among the three speeds (32% of the time at speed 1, 36% at speed 2 and 32% at speed 3) even though it never switched off.

The FS controller exhibited an evident misuse of speed 2 which was seldom activated (6% of the time) thus frequently leading to sharp switches between speed 1 and 3 (impelling drafts and exacerbating the consumptions): indeed, both speed 3 and off-mode were overused compared to the other controllers (almost 50% and 20% of the

time respectively): this is the result of an excessively loyal tracking of global solar power distribution. Such an overcompensation of solar gains, was a strong indicator of the unbalances in the setup of the FS controller which led to its improved version (FM controller): the ranges corresponding to the different linguistic terms of the leading input variable (difference between ambient temperature and setpoint) were reallocated and the outdoor temperature was introduced (refer to **Appendix A** and **B**), to help getting better performances right approaching the sunset where a certain AC action was still needed despite the consistent reduction of direct solar penetration.
The FM controller showed quite an optimal distribution of the fan speeds (in terms of tradeoffs between global and local comfort concerns) giving great emphasis (67% of the time) to speed 1 (which is the only one leading to no local discomfort phenomena), making a pondered use of speed 2 (8%) and never resorting to speed 3. However, since the global overheating was not compensated, some occasional, short-lasting activations of full-power mode might have been beneficial in all respects. Besides, a certain overabundance of off-periods late in the day was experienced in this case too.
Nonetheless, the FM configuration of the controller led to a significantly improved management of comfort and energy loads.

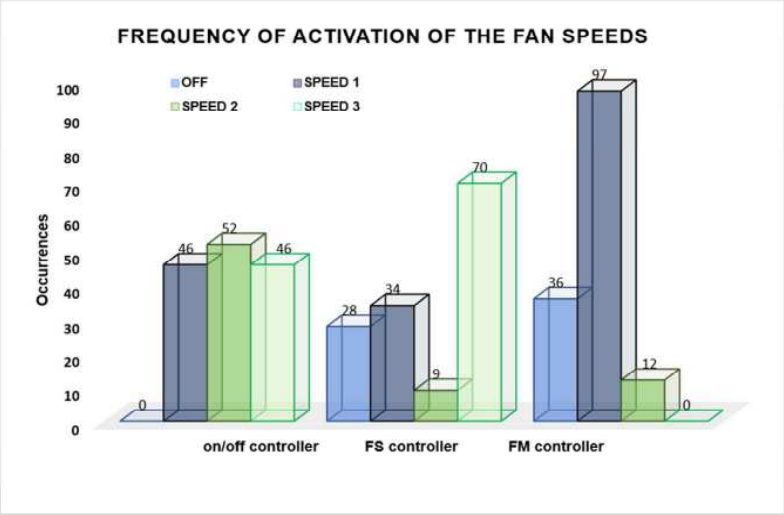


Figure 5.19
Energy assessment (fuzzy controllers): histograms of occurrences – fan speeds.

5.6.3.2 – Wintertime results

The wintertime analysis of energy consumption followed the same procedure as in summertime. Yet, in order to strike causal relationships between the performance of

the controller and the concomitant weather conditions, a further assessment was carried out.

In fact, thanks to the installation of the anemometer and the thermo-hygrometers upstream and downstream the heating terminal, it was possible to measure the power supply to the indoor environment and calculate the energy consumption. **Figure 5.20** displays its time trend, overlapped to the curves of solar radiation and of the distance between operative temperature and setpoint: these parameters were selected as major driving forces for the heating calls (since the perturbing action of outdoor temperature was found to be less extensive).

In terms of balanced operation, the MPC showed a systematic low utilization of the medium power, regardless of the specific boundary conditions: it seldom activated speed 2 for protracted time slots (7.6% and 1.4% on the sunnier and cloudier days), privileging quite abrupt switches from speed 1 to speed 3 and vice versa. Indeed, minimum power levels were deployed for the 80.2% on the 15th and the 77.2% on the 16th, while full-power runs occurred for the 10% and the 20% of the time respectively. Such result outlines that a certain scope for improvement, in terms of energy savings, might come from a different setting of the speed activation conditions so as to enlarge the intermediate power zone and compress the time slots of maximum consumption.

The FCU switched off over a very limited time window (2.3% on the 15th and 1.4% on the 16th in percentage terms) as it seldom occurred that the operative temperature was above the setpoint line in concomitance with high or predicted high solar radiation.

The time trends in **Figure 5.21** reveal that minimum energy consumptions occurred in three instances:

- peak hours of solar radiation, since little energy release was necessary to counterbalance the heat losses and contain the potential overheating, given that the predictive controller had already boosted its action in the hour before;
- operative temperature slightly below the setpoint and concomitant/forecast high radiation, since solar gains were predicted to suffice in maintaining comfort conditions;
- after sunset, since no significant perturbing action existed and the heat losses were mostly compensated by the heat re-emitted by the surfaces into the enclosed space.

On the other hand, maximum energy consumptions possibly occurred in three main occasions too:

- operative temperature considerably below the target value and concomitant/predicted low solar radiation;
- consistent predicted increments/decrements in the level of solar gains (especially right before sunset);

- operative temperature above the setpoint accompanied by concomitant/predicted high solar radiation.

The strongest control actions always occurred when the indoor temperature drifted: it is evident that the MPC better handled direct than diffuse radiation (given its mathematical-model-based nature) as both the major crests and the major troughs of the temperature offset took place on the 15th of December.

The total energy consumption was 11.96kWh/day and 7.82kWh/day over the period of expected occupancy on the two consecutive representative days. It should be stressed here that the prominent call for heating concentrated in the first hour of operation (7am to 8am) when the operative temperature was far below the setpoint, thus the consumptions on the 15th of December were slightly underestimated because of the initial breakdown.

According to the outcomes of the previous, summery monitoring round, also the fuzzy controller showed an unbalanced operation since it never resorted to speed 3, even though the operative temperature was frequently above the setpoint even at medium power activation.

Unfortunately, in that case speed 3 was found to impel dramatic local discomfort conditions: therefore, a more distributed operative speed pattern might not have been beneficial in the cooling season.

Moreover, during the regulation of the fuzzy controller, a more sustained utilization of speed 2 allowed to extend the proportion of off-periods, which covered almost the 25% of the time **[5.25]**: such observation underpins the energy saving potential of better balancing medium power levels within the control logic.

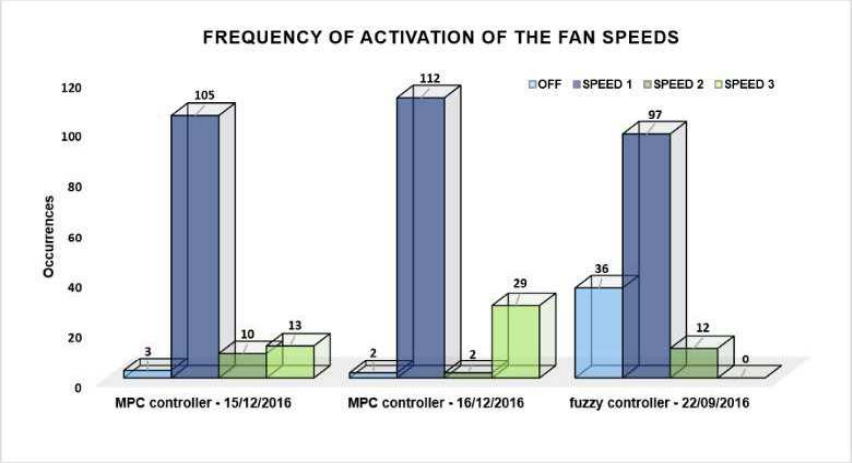


Figure 5.20

Energy assessment (MPC and FM controllers): histograms of occurrences – fan speeds.

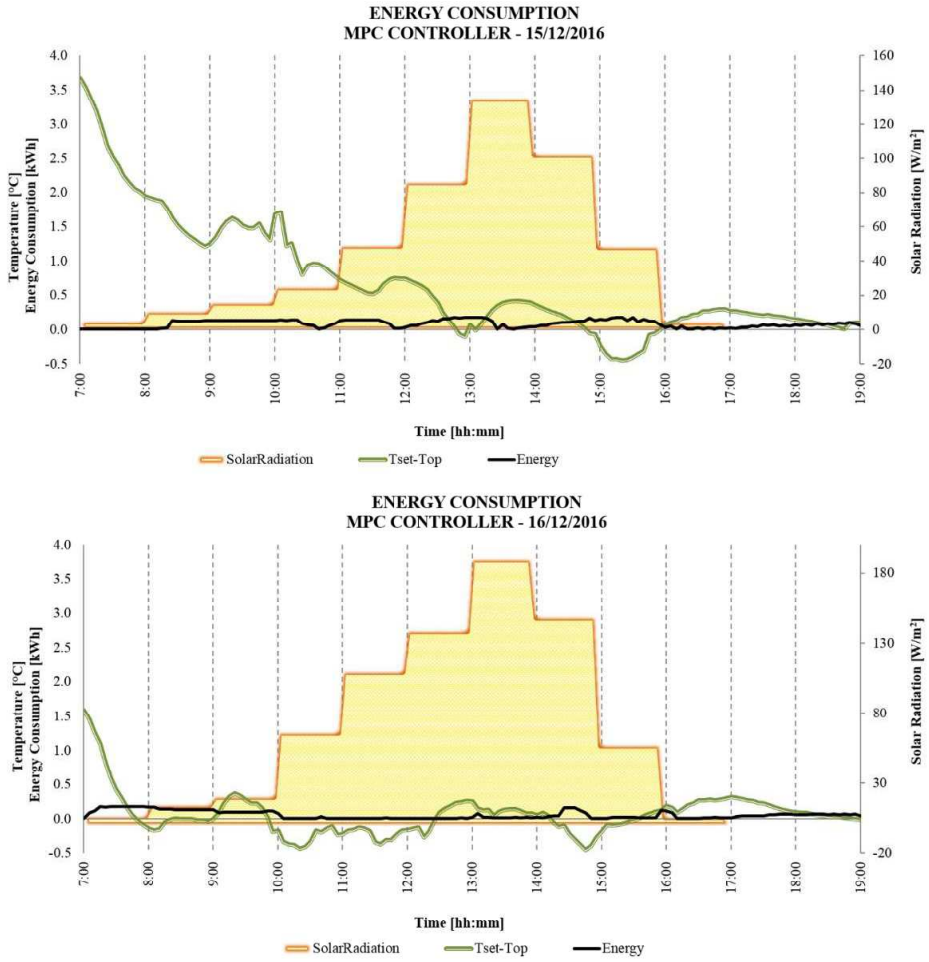


Figure 5.21

Energy assessment: time trends of the energy consumptions against solar radiation and the simultaneous offset from the setpoint.

5.7 CONCLUSIONS

Buildings with large glazed façades are tremendously vulnerable to overheating of indoor spaces (and other discomfort issues) whenever a proper control strategy is missing.

The risk for overabundant solar gains might extend throughout the year even in temperate climates **[5.92,5.93]**: in summer time, it is exacerbated by the massive income of direct beams, while in winter time it might get empowered by the heating emission of the technical systems.

In order to restore and maintain satisfactory comfort conditions in buildings with reasonably low energy utilization, several potential solutions might be adopted: a suitable, rather convenient approach, in presence of terminal units, is to optimize the emission of conditioned air according to befitting control logics.

Different control logics were applied to pilot the output of the technical system in summertime:

- on/off controller, whose triplet of hysteresis values on the detected ambient temperature was selected in order to mimic the manual operation of the system so as to provide the baseline for further analyses;
- FS fuzzy controller, incorporating ambient temperature, setpoint temperature and solar radiation among its input variables in order to address the specific source of discomfort with a pondered conditioning action;
- FM fuzzy controller, which resulted from a suite of improvements on the FS structure, in terms of input variables, namely boosting the responsiveness to slight deviations of the ambient temperature from the setpoint and including the outdoor temperature in the decision-making process.

Each configuration was monitored via an ad-hoc conceived sensor network, basically composed by an indoor comfort station, a meteorological pole, a net of temperature probes on the glazed façade and a set of air temperature probes dedicated to the heating/cooling terminal. Such configuration allowed to get a full database of indoor and outdoor climate conditions, FCU emission and building thermal behaviour. No one accessed the office over the entire observation period, yet the occupancy pattern was included in the settings of each controller.

Post-processing and assessment procedures were conducted over representative days in terms of overheating: the sunniest days among each monitoring period were selected in agreement with the results of a previous monitoring campaign, which outlined a substantial predominance of solar radiation among the driving forces for discomfort phenomena.

Evaluation was made from both the perspectives of global and local comfort, even though a marginal assessment of energy consumptions was addressed as well.

The results highlighted that the operative temperature exceeded the setpoint values (26°C) over almost all the observation period: for less than the 15% of the time the overheating was averted with both the fuzzy controllers and just early in the morning as result of favorable combinations of solar radiation and outdoor temperature. A strong indication on the radiant contribution to such uncomfortable conditions came from the analysis of the surface temperatures on the glazed façade: values over 40°C were frequently recorded.

Despite the inherent comfort deficiency, the FM controller outperformed by far the FS version and achieved a non-negligible improvement from all perspectives, in primis by keeping the operative temperature close to the set point. Indeed, the readings:

- fell within ±0.5°C from the set point for the 21% of the time, almost doubling the result achieved with the FS controller;
- never exceeded the setpoint value by more than ±2.5°C (while during the FS control the gap was greater than 4°C for the 44% of the time);
- hit a maximum of 28.87°C (-8.1% compared to FS's peak value);
- maintained an average of 27.3°C (-4.8% compared to FS's mean value).

Calculations of the PMV index never exceeded the warm threshold (+2).

The best performance was achieved by the FM controller since it succeeded in maintaining category B conditions for the 23% of the time (versus 14.9% attained by the FS). Besides, while the FS control led to prolonged time windows beyond category C (38% of time with PMV values between 1.5 and 2), the FM counterpart usually provided conditions close to slightly warm sensation (28% of the time with PMV between 0.5 and 0.7; 46.2% of the time with PMV between 0.7 and 1).

In terms of local discomfort, vertical thermal gradients didn't affect the comfort level in any case: air stratified quite homogeneously whichever speed of the FCU was activated. Indeed, such finding might be the result of the inherent inefficacy of the technical system in triggering significant temperature drops inside the room.

In terms of drafts, they massively occurred at ground level (0.1m), while they tended to extinguish at head level (1.1m) because of the interaction with the floor surface, whose higher temperature triggered small-scale convective updrafts which interacted with the air jet from the FCU in competing/mutual-empowering ways thus resulting in higher local turbulence.

Even from this perspective, the FM controller achieved a considerable improved performance:

- the maximum and average draught rates (DRs) were 29.2% and 4.9%, almost halving the respective values reached by the FS controller;
- the comfort limit (20%) was quite never overtaken, against the 5-minute-averaged 50 events recorded with the FS controller.

Such discrepancy was mainly due to the tendency of the FS controller to abruptly switch from speed 1 to speed 3, which provoked instantaneous spikes of the DR value and prolonged the persistency of discomfort conditions.

Finally, from the energy point of view, some differences in the way the power consumption was managed by the controllers could be highlighted.

The FM controller privileged long-lasting activations of speed 1 (67% of the time versus the 23.6% allocated by the FS controller), made a limited use of speed 2 and never resorted to speed 3 thus drastically reducing both the energy consumptions and the incidence of local discomfort phenomena. The FS controller, instead, worked at full power for almost the 50% of the time.

It should be stressed here that on the 20th of September (FS controller) the average outdoor temperature was 1.8 degrees higher than on the 22nd (FM controller). This mirrored in higher surface temperatures on the glazed façade which exacerbated the radiant emission towards the indoors and led to major corrective actions. Anyway, most of the penalty recorded with the FS controller resulted from an overcompensation of solar gains which led to a general misuse of both speed 3 and off-mode and which dictated the main amendments to the settings incorporated by the FM version.

All things considered, the overheating of the room was never averted, suggesting that a major renovation is required to properly rectify the thermal behaviour of the building. The data collected all over the monitoring campaign made it crystal clear that an oversaturation of the FCU energy demand was unavoidable to counteract the rise of indoor air temperature in response to solar radiation, thus underpinning the need for more sustainable solutions.

In terms of smart control, a certain room for improvement was identified in either:

- deriving the heuristic information to setup the fuzzy controller from extensive mathematical modelling or neural networking (Ghadi et al., 2016; Killian et al., 2016, 2014; Moon et al., 2011; Pombeiro et al., 2017) in order to impart learning skills and optimise the decision-making process;
- designing a model-based predictive control.

Accordingly, in the subsequent monitoring run (December 2016) an MPC system was set, implemented and field-tested

The sensor network was enriched of a suite of probes to characterize the emission of the FCU and the temperatures of the adjacent rooms so as to properly feed the controller.

The same software platform was employed to design the control logic.

The monitoring campaign took place over a week around winter solstice to check on the magnitude of overheating occurring even in the coldest period of the year. No one accessed the office so that the retrieved measurements were directly attributable to the sole effect of solar gains (no other internal gains competed).

The two days of maximum and minimum solar radiation were selected for assessment. The severity of global discomfort was evident from the very beginning of the field-test: the MPC couldn't be tuned to track a setpoint value of 20°C (according to the Italian legislation **[5.87]**) since the operative temperature naturally rose above such threshold all over the time window of expected occupancy (7am-7pm), thus forcing to raise the target value to 24°C.
Besides, during the first day of measurements (to tune the MPC), when the room was in free-running, the operative temperature ranged between a minimum of 21.6°C and a maximum of 27.7°C given an average solar radiation of 170 W/m^2.
The control action of the MPC strongly mitigated the risk of discomfort: it succeeded in preserving a steady operative temperature close to the target value by properly anticipating the perturbing action of weather changes and by pondering the power released by the FCU accordingly. Indeed:

- the operative temperature mostly fell within the ±0.5°C range around the setpoint (95.8% of the time on the sunnier day and 60.8% on the cloudier day). The limit of ±2°C was never exceeded. Given the almost optimal performance in conditions of high solar gains (and so higher surface temperatures of the glazed façade components), it was proved that the MPC mastered the thermal dynamics of the building by successfully preventing both the overshoot of the setpoint and considerable temperature drops;
- the PMV never exceeded Category III limits, while Category II conditions were satisfied for the 85% and the 80% of the time respectively;
- vertical temperature gradients and draught rates stayed always below the respective discomfort thresholds (maximum 1.7°C on the sunnier day and maximum 10.4% on the cloudier day);
- the fan operated at minimum speed for the greater time percentage on both the sunny and the cloudy day (77.2% and 80.2% respectively). Full-power activations occurred just for the 20% and the 10%of the time.

Overall, even though the overheating proved to be a major risk for the liveability of the indoors (of all the south exposed rooms of the building with all probability) even in winter time, the smart control of the technical system via MPC logic resulted in non-negligible improvements from all considered perspectives.
Moreover, by comparing the quality of the control action, it was found that the model-based, predictive approach outperformed the heuristic, fuzzy controller, tested in the previous monitoring run on the same case study **[5.25]**.
Nonetheless, by perusing the datasets of the field test, a certain scope for refinement was pinpointed: the MPC seldom activated medium power emissions thus emphasizing the use of speed 3 and compressing the time slot of shut-off. Consequently, the energy saving potential might be maximized by better balancing the control action.

Besides, the major calls for full power occurred right before sunset, when the MPC predicted the annulment of the contribution of solar gains. A milder corrective action might be beneficial in minimizing the consumptions and the overshoot events.
All things considered, potential further research might include the design of a cooperative fuzzy model predictive control (CFMPC) to combine the advantages of both the algorithms. Encouraging results emerge from the studies by Killian et al. **[5.94]**. They demonstrated that the integration of the rule-based approach into the grey-box-model-based control action overcomes most of the limits of the state-of-the-art MPCs since it extends their suitability to all seasons and all buildings and technical systems typologies, by achieving high control performance at less energy expenditure.
However, their findings are supported only by simulation results. For this reason, on-site validation could represent the next step.

APPENDIX A. FS fuzzy controller configuration

In the following tables (tables A1-A4), the main settings of the FS fuzzy controller are presented.

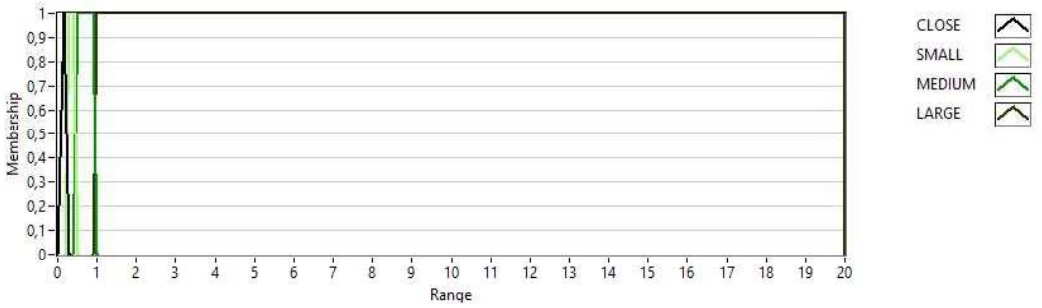
Table A.1
FS controller: general settings.

INPUT VARIABLES			
Variable	**Name**	**Range**	**Number of membership functions**
Instantaneous gap between ambient air temperature and setpoint value	deltaTset	0 -> 20	4
Global solar radiation	solar radiation	0 -> 1200	3
OUTPUT VARIABLES			
Variable	**Name**	**Range**	**Number of membership functions**
Speed of the electric motor of the fancoil	fan speed	0 -> 3	4
DEFUZZIFICATION METHOD:	Center of Area*	**ANTECEDENT CONNECTIVE:**	AND (Minimum)**
IMPLICATION:	Minimum	**DEGREE OF SUPPORT:**	1,00

*it calculates the geometric center of the area under the scaled membership functions and within the range of the output variables.
**it specifies to use the smallest degree of membership of the antecedents as aggregated value.

Table A.2
FS controller: input membership functions.

deltaTset		
Membership function	**Shape**	**Points**
CLOSE	Trapezoid	0 ; 0 ; 0,8; 1
SMALL	Trapezoid	0,8 ; 1 ; 1,8 ; 2
MEDIUM	Trapezoid	1,8 ; 2 ; 2,8 ; 3
LARGE	Trapezoid	2,8 ; 3 ; 20 ; 20



Solar radiation		
Membership function	**Shape**	**Points**
CLOUDY	Trapezoid	0 ; 0 ; 150 ; 200
PARTLY CLOUDY	Trapezoid	150 ; 200 ; 350 ; 400
SUNNY	Trapezoid	350 ; 400 ; 1200 ; 1200

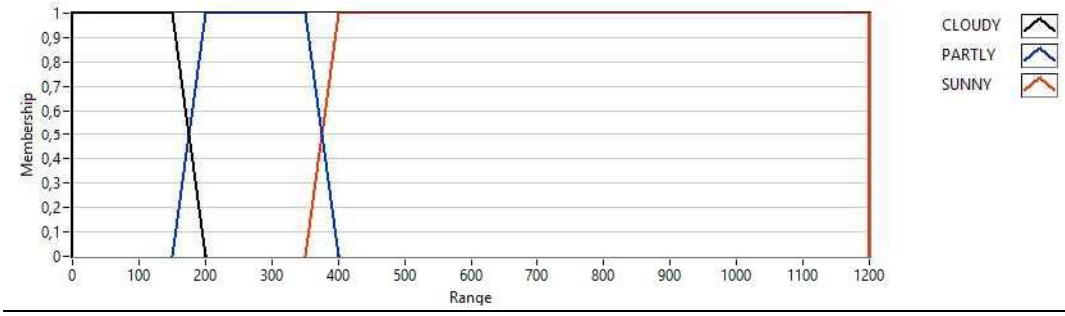


Table A.3
FS controller: output membership functions.

	Fan speed	
Membership function	**Shape**	**Points**
0	Singleton	0
1	Singleton	1
2	Singleton	2
3	Singleton	3

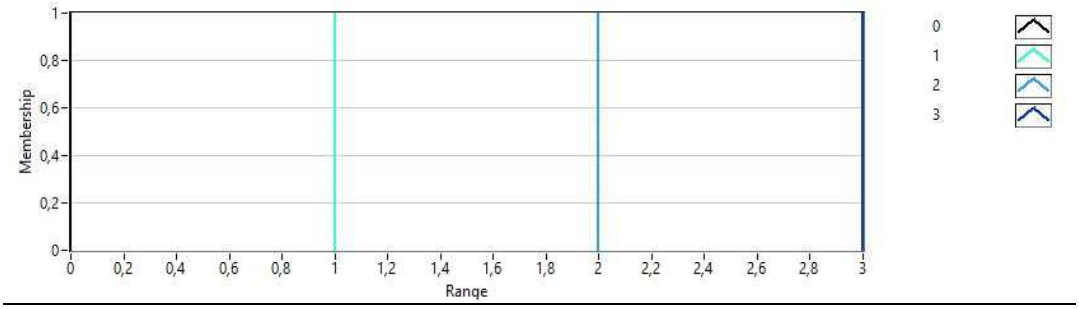


Table A.4
FS controller: rules.

1. IF 'deltaTset' IS 'CLOSE' AND 'solar radiation' IS 'CLOUDY' THEN 'fan speed' IS '0'
connective: AND (Minimum) ; implication: Minimum ; degree of support: 1,00

2. IF 'deltaTset' IS 'CLOSE' AND 'solar radiation' IS 'PARTLY CLOUDY' THEN 'fan speed' IS '0'
connective: AND (Minimum) ; implication: Minimum ; degree of support: 1,00

3. IF 'deltaTset' IS 'CLOSE' AND 'solar radiation' IS 'SUNNY' THEN 'fan speed' IS '1'
connective: AND (Minimum) ; implication: Minimum ; degree of support: 1,00

4. IF 'deltaTset' IS 'SMALL' AND 'solar radiation' IS 'CLOUDY' THEN 'fan speed' IS '1'
connective: AND (Minimum) ; implication: Minimum ; degree of support: 1,00

5. IF 'deltaTset' IS 'SMALL' AND 'solar radiation' IS 'PARTLY CLOUDY' THEN 'fan speed' IS '1'
connective: AND (Minimum) ; implication: Minimum ; degree of support: 1,00

6. IF 'deltaTset' IS 'SMALL' AND 'solar radiation' IS 'SUNNY' THEN 'fan speed' IS '2'
connective: AND (Minimum) ; implication: Minimum ; degree of support: 1,00

7. IF 'deltaTset' IS 'MEDIUM' AND 'solar radiation' IS 'CLOUDY' THEN 'fan speed' IS '2'
connective: AND (Minimum) ; implication: Minimum ; degree of support: 1,00

8. IF 'deltaTset' IS 'MEDIUM' AND 'solar radiation' IS 'PARTLY CLOUDY' THEN 'fan speed' IS '2'
connective: AND (Minimum) ; implication: Minimum ; degree of support: 1,00

9. IF 'deltaTset' IS 'MEDIUM' AND 'solar radiation' IS 'SUNNY' THEN 'fan speed' IS '3'
connective: AND (Minimum) ; implication: Minimum ; degree of support: 1,00

10. IF 'deltaTset' IS 'LARGE' AND 'solar radiation' IS 'CLOUDY' THEN 'fan speed' IS '3'
connective: AND (Minimum) ; implication: Minimum ; degree of support: 1,00

11. IF 'deltaTset' IS 'LARGE' AND 'solar radiation' IS 'PARTLY CLOUDY' THEN 'fan speed' IS '3'

connective: AND (Minimum) ; implication: Minimum ; degree of support: 1,00

12. IF 'deltaTset' IS 'LARGE' AND 'solar radiation' IS 'SUNNY' THEN 'fan speed' IS '3'
connective: AND (Minimum) ; implication: Minimum ; degree of support: 1,00

APPENDIX B. FM fuzzy controller configuration

In the following tables (tables B1-B4), the main settings of the FS fuzzy controller are presented.

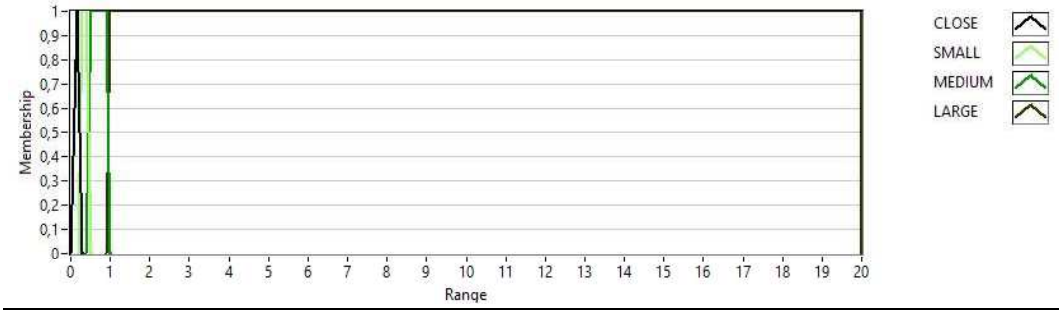
Table B.1
FM controller: general settings.

INPUT VARIABLES			
Variable	**Name**	**Range**	**Number of membership functions**
Instantaneous gap between ambient air temperature and setpoint value	deltaTset	0 -> 20	4
Global solar radiation	solar radiation	0 -> 1200	3
Instantaneous gap between setpoint value and outdoor air temperature	deltaTsetTout	0 -> 30	4
OUTPUT VARIABLES			
Variable	**Name**	**Range**	**Number of membership functions**
Speed of the electric motor of the fancoil	fan speed	0 -> 3	4
DEFUZZIFICATION METHOD:	Center of Area*	**ANTECEDENT CONNECTIVE:**	AND (Minimum)**
IMPLICATION:	Minimum	**DEGREE OF SUPPORT:**	1,00

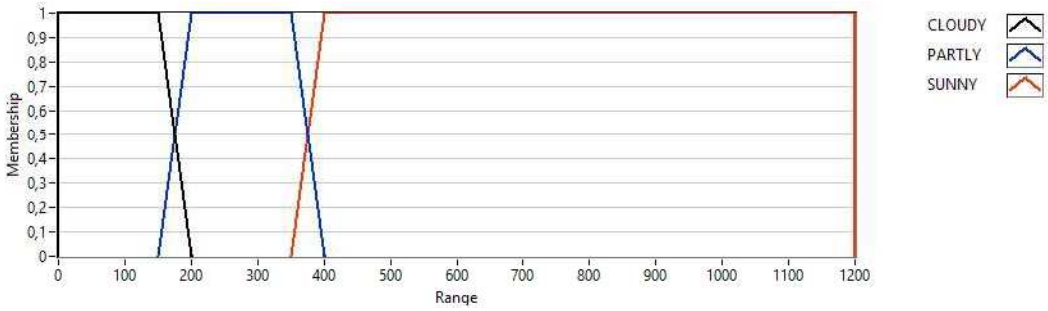
*it calculates the geometric center of the area under the scaled membership functions and within the range of the output variables.
**it specifies to use the smallest degree of membership of the antecedents as aggregated value.

Table B.2
FM controller: input membership functions.

deltaTset		
Membership function	**Shape**	**Points**
CLOSE	Triangle	0 ; 0,15 ; 0,3
SMALL	Trapezoid	0,2 ; 0,3 ; 0,4 ; 0,5
MEDIUM	Trapezoid	0,4 ; 0,5 ; 0,9 ; 1
LARGE	Trapezoid	0,9 ; 1 ; 20 ; 20
CLOSE	Triangle	0 ; 0,15 ; 0,3



Solar radiation		
Membership function	**Shape**	**Points**
CLOUDY	Trapezoid	0 ; 0 ; 150 ; 200
PARTLY CLOUDY	Trapezoid	150 ; 200 ; 350 ; 400
SUNNY	Trapezoid	350 ; 400 ; 1200 ; 1200



DeltaTsetTout		
Membership function	**Shape**	**Points**
CLOSE	Trapezoid	0 ; 0 ; 1 ; 2
SMALL	Trapezoid	1 ; 2 ; 3 ; 4
MEDIUM	Trapezoid	3 ; 4 ; 5 ; 6
LARGE	Trapezoid	5 ; 6 ; 30 ; 30

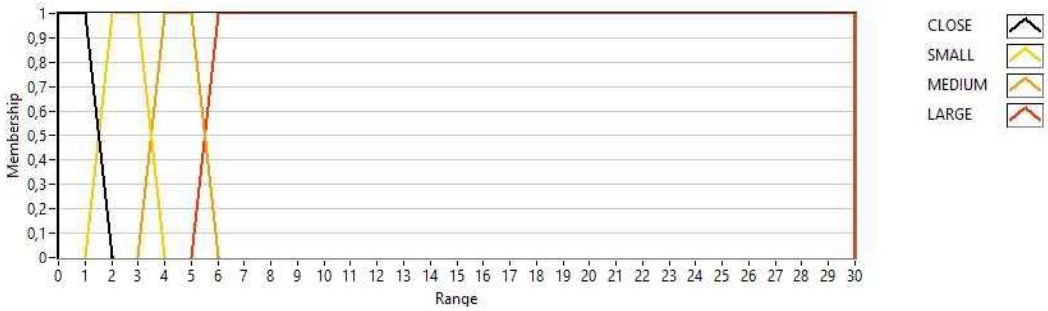


Table B.3
FM controller: output membership functions.

Fan speed		
Membership function	**Shape**	**Points**
0	Singleton	0
1	Singleton	1
2	Singleton	2
3	Singleton	3

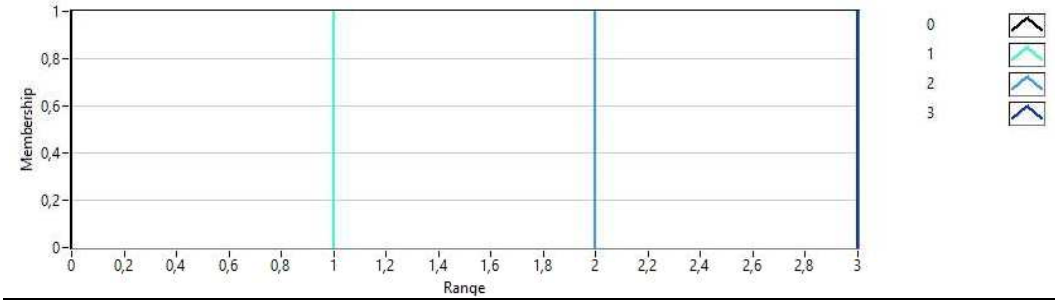


Table B.4
FM controller: rules.

1. IF 'deltaTset' IS 'CLOSE' AND 'solar radiation' IS 'CLOUDY' AND 'deltaTsetTout' IS 'CLOSE' THEN 'fan speed' IS '0'
connective: AND (Minimum) ; implication: Minimum ; degree of support: 1,00

2. IF 'deltaTset' IS 'CLOSE' AND 'solar radiation' IS 'CLOUDY' AND 'deltaTsetTout' IS 'SMALL' THEN 'fan speed' IS '0'
connective: AND (Minimum) ; implication: Minimum ; degree of support: 1,00

3. IF 'deltaTset' IS 'CLOSE' AND 'solar radiation' IS 'CLOUDY' AND 'deltaTsetTout' IS 'MEDIUM' THEN 'fan speed' IS '0'

connective: AND (Minimum) ; implication: Minimum ; degree of support: 1,00

4. IF 'deltaTset' IS 'CLOSE' AND 'solar radiation' IS 'CLOUDY' AND 'deltaTsetTout' IS 'LARGE' THEN 'fan speed' IS '0'
connective: AND (Minimum) ; implication: Minimum ; degree of support: 1,00

5. IF 'deltaTset' IS 'CLOSE' AND 'solar radiation' IS 'PARTLY CLOUDY' AND 'deltaTsetTout' IS 'CLOSE' THEN 'fan speed' IS '0'
connective: AND (Minimum) ; implication: Minimum ; degree of support: 1,00

6. IF 'deltaTset' IS 'CLOSE' AND 'solar radiation' IS 'PARTLY CLOUDY' AND 'deltaTsetTout' IS 'SMALL' THEN 'fan speed' IS '0'
connective: AND (Minimum) ; implication: Minimum ; degree of support: 1,00

7. IF 'deltaTset' IS 'CLOSE' AND 'solar radiation' IS 'PARTLY CLOUDY' AND 'deltaTsetTout' IS 'MEDIUM' THEN 'fan speed' IS '0'
connective: AND (Minimum) ; implication: Minimum ; degree of support: 1,00

8. IF 'deltaTset' IS 'CLOSE' AND 'solar radiation' IS 'PARTLY CLOUDY' AND 'deltaTsetTout' IS 'LARGE' THEN 'fan speed' IS '0'
connective: AND (Minimum) ; implication: Minimum ; degree of support: 1,00

9. IF 'deltaTset' IS 'CLOSE' AND 'solar radiation' IS 'SUNNY' AND 'deltaTsetTout' IS 'CLOSE' THEN 'fan speed' IS '0'
connective: AND (Minimum) ; implication: Minimum ; degree of support: 1,00

10. IF 'deltaTset' IS 'CLOSE' AND 'solar radiation' IS 'SUNNY' AND 'deltaTsetTout' IS 'SMALL' THEN 'fan speed' IS '0'
connective: AND (Minimum) ; implication: Minimum ; degree of support: 1,00

11. IF 'deltaTset' IS 'CLOSE' AND 'solar radiation' IS 'SUNNY' AND 'deltaTsetTout' IS 'MEDIUM' THEN 'fan speed' IS '0'
connective: AND (Minimum) ; implication: Minimum ; degree of support: 1,00

12. IF 'deltaTset' IS 'CLOSE' AND 'solar radiation' IS 'SUNNY' AND 'deltaTsetTout' IS 'LARGE' THEN 'fan speed' IS '1'
connective: AND (Minimum) ; implication: Minimum ; degree of support: 1,00

13. IF 'deltaTset' IS 'SMALL' AND 'solar radiation' IS 'CLOUDY' AND 'deltaTsetTout' IS 'CLOSE' THEN 'fan speed' IS '0'
connective: AND (Minimum) ; implication: Minimum ; degree of support: 1,00

14. IF 'deltaTset' IS 'SMALL' AND 'solar radiation' IS 'CLOUDY' AND 'deltaTsetTout' IS 'SMALL' THEN 'fan speed' IS '1'
connective: AND (Minimum) ; implication: Minimum ; degree of support: 1,00

15. IF 'deltaTset' IS 'SMALL' AND 'solar radiation' IS 'CLOUDY' AND 'deltaTsetTout' IS 'MEDIUM' THEN 'fan speed' IS '1'
connective: AND (Minimum) ; implication: Minimum ; degree of support: 1,00

16. IF 'deltaTset' IS 'SMALL' AND 'solar radiation' IS 'CLOUDY' AND 'deltaTsetTout' IS 'LARGE' THEN 'fan speed' IS '1'
connective: AND (Minimum) ; implication: Minimum ; degree of support: 1,00

17. IF 'deltaTset' IS 'SMALL' AND 'solar radiation' IS 'PARTLY CLOUDY' AND 'deltaTsetTout' IS 'CLOSE' THEN 'fan speed' IS '1'
connective: AND (Minimum) ; implication: Minimum ; degree of support: 1,00

18. IF 'deltaTset' IS 'SMALL' AND 'solar radiation' IS 'PARTLY CLOUDY' AND 'deltaTsetTout' IS 'SMALL' THEN 'fan speed' IS '1'
connective: AND (Minimum) ; implication: Minimum ; degree of support: 1,00

19. IF 'deltaTset' IS 'SMALL' AND 'solar radiation' IS 'PARTLY CLOUDY' AND 'deltaTsetTout' IS 'MEDIUM' THEN 'fan speed' IS '1'
connective: AND (Minimum) ; implication: Minimum ; degree of support: 1,00

20. IF 'deltaTset' IS 'SMALL' AND 'solar radiation' IS 'PARTLY CLOUDY' AND 'deltaTsetTout' IS 'LARGE' THEN 'fan speed' IS '1'
connective: AND (Minimum) ; implication: Minimum ; degree of support: 1,00

21. IF 'deltaTset' IS 'SMALL' AND 'solar radiation' IS 'SUNNY' AND 'deltaTsetTout' IS 'CLOSE' THEN 'fan speed' IS '1'
connective: AND (Minimum) ; implication: Minimum ; degree of support: 1,00

22. IF 'deltaTset' IS 'SMALL' AND 'solar radiation' IS 'SUNNY' AND 'deltaTsetTout' IS 'SMALL' THEN 'fan speed' IS '1'
connective: AND (Minimum) ; implication: Minimum ; degree of support: 1,00

23. IF 'deltaTset' IS 'SMALL' AND 'solar radiation' IS 'SUNNY' AND 'deltaTsetTout' IS 'MEDIUM' THEN 'fan speed' IS '1'
connective: AND (Minimum) ; implication: Minimum ; degree of support: 1,00

24. IF 'deltaTset' IS 'SMALL' AND 'solar radiation' IS 'SUNNY' AND 'deltaTsetTout' IS 'LARGE' THEN 'fan speed' IS '2'
connective: AND (Minimum) ; implication: Minimum ; degree of support: 1,00

25. IF 'deltaTset' IS 'MEDIUM' AND 'solar radiation' IS 'CLOUDY' AND 'deltaTsetTout' IS 'CLOSE' THEN 'fan speed' IS '1'
connective: AND (Minimum) ; implication: Minimum ; degree of support: 1,00

26. IF 'deltaTset' IS 'MEDIUM' AND 'solar radiation' IS 'CLOUDY' AND 'deltaTsetTout' IS 'SMALL' THEN 'fan speed' IS '2'
connective: AND (Minimum) ; implication: Minimum ; degree of support: 1,00

27. IF 'deltaTset' IS 'MEDIUM' AND 'solar radiation' IS 'CLOUDY' AND 'deltaTsetTout' IS 'MEDIUM' THEN 'fan speed' IS '2'
connective: AND (Minimum) ; implication: Minimum ; degree of support: 1,00

28. IF 'deltaTset' IS 'MEDIUM' AND 'solar radiation' IS 'CLOUDY' AND 'deltaTsetTout' IS 'LARGE' THEN 'fan speed' IS '2'
connective: AND (Minimum) ; implication: Minimum ; degree of support: 1,00

29. IF 'deltaTset' IS 'MEDIUM' AND 'solar radiation' IS 'PARTLY CLOUDY' AND 'deltaTsetTout' IS 'CLOSE' THEN 'fan speed' IS '2'

connective: AND (Minimum) ; implication: Minimum ; degree of support: 1,00

30. IF 'deltaTset' IS 'MEDIUM' AND 'solar radiation' IS 'PARTLY CLOUDY' AND 'deltaTsetTout' IS 'SMALL' THEN 'fan speed' IS '2'
connective: AND (Minimum) ; implication: Minimum ; degree of support: 1,00

31. IF 'deltaTset' IS 'MEDIUM' AND 'solar radiation' IS 'PARTLY CLOUDY' AND 'deltaTsetTout' IS 'MEDIUM' THEN 'fan speed' IS '2'
connective: AND (Minimum) ; implication: Minimum ; degree of support: 1,00

32. IF 'deltaTset' IS 'MEDIUM' AND 'solar radiation' IS 'PARTLY CLOUDY' AND 'deltaTsetTout' IS 'LARGE' THEN 'fan speed' IS '2'
connective: AND (Minimum) ; implication: Minimum ; degree of support: 1,00

33. IF 'deltaTset' IS 'MEDIUM' AND 'solar radiation' IS 'SUNNY' AND 'deltaTsetTout' IS 'CLOSE' THEN 'fan speed' IS '2'
connective: AND (Minimum) ; implication: Minimum ; degree of support: 1,00

34. IF 'deltaTset' IS 'MEDIUM' AND 'solar radiation' IS 'SUNNY' AND 'deltaTsetTout' IS 'SMALL' THEN 'fan speed' IS '2'
connective: AND (Minimum) ; implication: Minimum ; degree of support: 1,00

35. IF 'deltaTset' IS 'MEDIUM' AND 'solar radiation' IS 'SUNNY' AND 'deltaTsetTout' IS 'MEDIUM' THEN 'fan speed' IS '2'
connective: AND (Minimum) ; implication: Minimum ; degree of support: 1,00

36. IF 'deltaTset' IS 'MEDIUM' AND 'solar radiation' IS 'SUNNY' AND 'deltaTsetTout' IS 'LARGE' THEN 'fan speed' IS '3'
connective: AND (Minimum) ; implication: Minimum ; degree of support: 1,00

37. IF 'deltaTset' IS 'LARGE' AND 'solar radiation' IS 'CLOUDY' AND 'deltaTsetTout' IS 'CLOSE' THEN 'fan speed' IS '2'
connective: AND (Minimum) ; implication: Minimum ; degree of support: 1,00

38. IF 'deltaTset' IS 'LARGE' AND 'solar radiation' IS 'CLOUDY' AND 'deltaTsetTout' IS 'SMALL' THEN 'fan speed' IS '3'
connective: AND (Minimum) ; implication: Minimum ; degree of support: 1,00

39. IF 'deltaTset' IS 'LARGE' AND 'solar radiation' IS 'CLOUDY' AND 'deltaTsetTout' IS 'MEDIUM' THEN 'fan speed' IS '3'
connective: AND (Minimum) ; implication: Minimum ; degree of support: 1,00

40. IF 'deltaTset' IS 'LARGE' AND 'solar radiation' IS 'CLOUDY' AND 'deltaTsetTout' IS 'LARGE' THEN 'fan speed' IS '3'
connective: AND (Minimum) ; implication: Minimum ; degree of support: 1,00

41. IF 'deltaTset' IS 'LARGE' AND 'solar radiation' IS 'PARTLY CLOUDY' AND 'deltaTsetTout' IS 'CLOSE' THEN 'fan speed' IS '3'
connective: AND (Minimum) ; implication: Minimum ; degree of support: 1,00

42. IF 'deltaTset' IS 'LARGE' AND 'solar radiation' IS 'PARTLY CLOUDY' AND 'deltaTsetTout' IS 'SMALL' THEN 'fan speed' IS '3'
connective: AND (Minimum) ; implication: Minimum ; degree of support: 1,00

43. IF 'deltaTset' IS 'LARGE' AND 'solar radiation' IS 'PARTLY CLOUDY' AND 'deltaTsetTout' IS 'MEDIUM' THEN 'fan speed' IS '3'
connective: AND (Minimum) ; implication: Minimum ; degree of support: 1,00

44. IF 'deltaTset' IS 'LARGE' AND 'solar radiation' IS 'PARTLY CLOUDY' AND 'deltaTsetTout' IS 'LARGE' THEN 'fan speed' IS '3'
connective: AND (Minimum) ; implication: Minimum ; degree of support: 1,00

45. IF 'deltaTset' IS 'LARGE' AND 'solar radiation' IS 'SUNNY' AND 'deltaTsetTout' IS 'CLOSE' THEN 'fan speed' IS '3'
connective: AND (Minimum) ; implication: Minimum ; degree of support: 1,00

46. IF 'deltaTset' IS 'LARGE' AND 'solar radiation' IS 'SUNNY' AND 'deltaTsetTout' IS 'SMALL' THEN 'fan speed' IS '3'
connective: AND (Minimum) ; implication: Minimum ; degree of support: 1,00

47. IF 'deltaTset' IS 'LARGE' AND 'solar radiation' IS 'SUNNY' AND 'deltaTsetTout' IS 'MEDIUM' THEN 'fan speed' IS '3'
connective: AND (Minimum) ; implication: Minimum ; degree of support: 1,00

48. IF 'deltaTset' IS 'LARGE' AND 'solar radiation' IS 'SUNNY' AND 'deltaTsetTout' IS 'LARGE' THEN 'fan speed' IS '3'
connective: AND (Minimum) ; implication: Minimum ; degree of support: 1,00

APPENDIX C. Electric analogy for the grey-box model

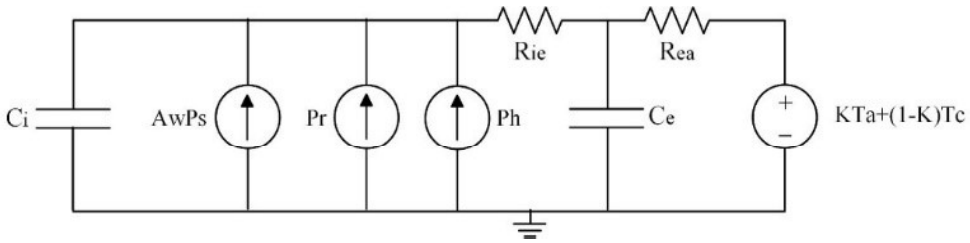


Fig. C1 2C2R circuit of the grey-box model.

In this study, a grey-box approach was selected to characterize the thermal model used by the MPC controller for the optimization process.

The grey-box model structure derives from the formal analogy between thermal and electrical elements, depicted in **Fig. A1**: C_i and C_e [kWh/°C] represent the thermal capacities of the room and stand for the heat stored by the interiors and the envelope respectively; R_{ie} and R_{ea} [°C/kW] represent the building envelope resistance to the heat transfer from the interior and the exterior.

The heat dynamics are described by the following system equations (C1-C2), which correspond to the general formulation in (5.3), as easily verifiable in (C3):

$$dT_i = \frac{1}{R_{ie}C_i}(T_e - T_i)dt + \frac{A_w}{C_i}P_s dt + \frac{1}{C_i}P_h dt + \frac{1}{C_i}P_r dt + \sigma_i d\omega_i \quad (C1)$$

$$dT_e = \frac{1}{R_{ie}C_e}(T_i - T_e)dt + \frac{1}{R_{ea}C_e}\left((KT_a + (1-K)T_c) - T_e\right)dt + \sigma_e d\omega_e \quad (C2)$$

$$dT = ATdt + BUdt + \sigma d\omega \quad (C3)$$

The output is the observation equation (A4), in which, for each time k, the measured operative temperature, Y_k [°C], equals the state T_{ik} [°C] plus a measurement error e_k [°C].

$$Y_k = T_{ik} + e_k \quad (C4)$$

The stochastic differential equations (C1, C2) are one per each state variable depending on the model order (here T_i, indoor temperature and T_e, temperature of the envelope). P_h [kW], P_r [kW] and P_s [kW/m²] constitute the inputs, respectively related to the power supply of the fan coil, the AHU and the sun (which depends on the effective window area A_w [m²]). The outdoor temperature T_a [°C] and the air temperature measured in the corridor T_c [°C] represent the boundary conditions. The symbols in (C3) correspond to those in (5.3), namely: A and B are non-linear functions of the unknown parameters, T represents the state of the room in terms of temperature and U stands for the measured inputs.

The maximum likelihood method is adopted to estimate the unknown parameters of the system by means of CSTM-R software **[5.80].**

The resistance/capacitance parameters are estimated as well as the stochastic terms ($\sigma d\omega$) and the initial values of the temperatures (T_{i0} and T_{e0}). K is another estimated parameter, which is used to linearly combine the boundary temperatures. The time is expressed in hours.

REFERENCES

[5.1] D.D. Chiras, The solar house, Chelsea Green Publishing, 2002.

[5.2] I.C. Ward, Energy and environmental issues for the practising architect, Thomas Telford, 2004.

[5.3] A. Gasparella, G. Pernigotto, F. Cappelletti, P. Romagnoni, P. Baggio, Analysis and modelling of window and glazing systems energy performance for a well insulated residential building, Energy Build. 43 (2011) 1030–1037.

[5.4] R.-L. Hwang, S.-Y. Shu, Building envelope regulations on thermal comfort in glass facade buildings and energy-saving potential for PMV-based comfort control, Build. Environ. 46 (2011) 824–834.

[5.5] F. Kalmár, Summer operative temperatures in free running existing buildings with high glazed ratio of the facades, J. Build. Eng. 6 (2016) 236–242.

[5.6] D.-I.W. Eicke-Hennig, H. Energiespar-Aktion, Glasarchitektur-Lehren aus einem Großversuch, Hess. Energiespar-Aktion. Inst. Für Wohn. Und Umwelt (IWU), Darmstadt. (2004).

[5.7] H. Altan, I. Ward, J. Moheln'\iková, F. Vajkay, Daylight, Solar Gains and Overheating Studies in a Glazed Office Building, Int. J. Energy Environ. 2 (2008) 129–138.

[5.8] L. Šeduikyte, V. Paukštys, Evaluation of indoor environment conditions in offices located in buildings with large glazed areas, J. Civ. Eng. Manag. 14 (2008) 39–44.

[5.9] M. Alwetaishi, Impact of glazing to wall ratio in various climatic regions: A case study, J. King Saud Univ. –Engineering Sci. (2017).

[5.10] G. Oliveti, N. Arcuri, R. Bruno, M. Simone, An accurate calculation model of solar heat gain through glazed surfaces, Energy Build. 43 (2011) 269–274.

[5.11] M. La Gennusa, A. Nucara, M. Pietrafesa, G. Rizzo, A model for managing and evaluating solar radiation for indoor thermal comfort, Sol. Energy. 81 (2007) 594–606.

[5.12] M. La Gennusa, A. Nucara, G. Rizzo, G. Scaccianoce, The calculation of the mean radiant temperature of a subject exposed to the solar radiation?, Build. Environ. 40 (2005) 367–375.

[5.13] A. Tzempelikos, M. Bessoudo, A.K. Athienitis, R. Zmeureanu, Indoor thermal environmental conditions near glazed facades with shading devices – Part II, Build. Environ. 45 (2010) 2517–2525.

[5.14] A. Trombe, L. Serres, M. Moisson, Solar radiation modelling in a complex enclosure, Sol. Energy. 67 (1999) 297–307.

[5.15] R. Zmeureanu, S. Iliescu, D. Dauce, Y. Jacob, Radiation from cold or warm windows, Build. Environ. 38 (2003) 427–434.

[5.16] P.R. Lyons, D. Arasteh, C. Huizenga, Window performance for human thermal comfort, Trans. Soc. Heat. Refrig. Air Cond. Eng. 106 (2000) 594–604.

[5.17] R. Sullivan, Thermal comfort issues in the LRI study, internal memorandum/report, window and daylighting group, Lawrence Berkeley Natl. Lab. (1986).

[5.18] T. Ohnaka, S. Hodder, K. Parsons, The effects of simulated solar radiation to the head and trunk on the thermal comfort of seated subjects, Elsevier Ergon. B. Ser. 3 (2005) 305–311.

[5.19] M.Y. Chan, C.W. Mak, Thermal comfort levels in a room with solar radiation, Indoor Built Environ. 17 (2008) 516–524.

[5.20] C. Marino, A. Nucara, M. Pietrafesa, Thermal comfort in indoor environment, Sol. Energy. 144 (2017) 295–309.

[5.21] F. Cappelletti, A. Prada, P. Romagnoni, A. Gasparella, Passive performance of glazed components in heating and cooling of an open-space office under controlled indoor thermal comfort, Build. Environ. 72 (2014) 131–144.

[5.22] L. Mølhave, The sick buildings and other buildings with indoor climate problems, Environ. Int. 15 (1989) 65–74.

[5.23] A.S. Bahaj, P.A.B. James, M.F. Jentsch, Potential of emerging glazing technologies for highly glazed buildings in hot arid climates, Energy Build. 40 (2008) 720–731.

[5.24] E. Dascalaki, M. Santamouris, On the potential of retrofitting scenarios for offices, Build. Environ. 37 (2002) 557–567.

[5.25] G. Ulpiani, Overheating phenomena induced by fully-glazed facades: investigation of a sick building in Italy and assessment of the benefits achieved via fuzzy control of the AC system., Submitt. Publ. (2017).

[5.26] A.P. Wemhoff, Calibration of HVAC equipment PID coefficients for energy conservation, Energy Build. 45 (2012) 60–66.

[5.27] M. Xu, S. Li, W. Cai, L. Lu, Effects of a GPC-PID control strategy with hierarchical structure for a cooling coil unit, Energy Convers. Manag. 47 (2006) 132–145.

[5.28] S.M. Attaran, R. Yusof, H. Selamat, A novel optimization algorithm based on epsilon constraint-RBF neural network for tuning PID controller in decoupled HVAC system, Appl. Therm. Eng. 99 (2016) 613–624.

[5.29] Z. Tianyi, Z. Jili, S. Dexing, Experimental study on a duty ratio fuzzy control method for fan-coil units, Build. Environ. 46 (2011) 527–534.

[5.30] C. Ghiaus, Fuzzy model and control of a fan-coil, Energy Build. 33 (2001) 545–551.

[5.31] H. Moradi, H. Setayesh, A. Alasty, PID-Fuzzy control of air handling units in the presence of uncertainty, Int. J. Therm. Sci. 109 (2016) 123–135.

[5.32] E.C. for Standardization, CEN, EN 15251:2007. Indoor environmental input parameters for design and assessment of energy performance of buildings addressing indoor quality, thermal environment, lighting and acoustics., (n.d.).

[5.33] G.I.O. for Standardization, ISO Standard 7730. Moderate thermal environments -determination of PMV and PPD indices, (1994).

[5.34] I.O. for Standardization, ISO Standard 7726: Ergonomics Of The Thermal Environment - Instruments For Measuring Physical Quantities, (2002).

[5.35] A. Inc, ASHRAE Standard 55 - 2010 Thermal Environmental Conditions for Human Occupancy, (n.d.).

[5.36] M. Castilla, J.D. Álvarez, M. Berenguel, F. Rodríguez, J.L. Guzmán, M. Pérez, A comparison of thermal comfort predictive control strategies, Energy Build. 43 (2011) 2737–2746.

[5.37] J. Široky, F. Oldewurtel, J. Cigler, S. Prívara, Experimental analysis of model predictive control for an energy efficient building heating system, Appl. Energy. 88 (2011) 3079–3087.

[5.38] M. Maasoumy, A. Sangiovanni-Vincentelli, Total and peak energy consumption minimization of building hvac systems using model predictive control, IEEE Des. Test Comput. 29 (2012) 26–35.

[5.39] R.H. Katz, D.E. Culler, S. Sanders, S. Alspaugh, Y. Chen, S. Dawson-Haggerty, P. Dutta, M. He, X. Jiang, L. Keys, A. Krioukov, K. Lutz, J. Ortiz, P. Mohan, E. Reutzel, J. Taneja, J. Hsu, S. Shankar, An information-centric energy infrastructure, Sustain. Comput. Informatics Syst. 1 (2011) 7–22.

[5.40] V.M. Zavala, D. Skow, T. Celinski, P. Dickinson, Techno-economic evaluation of a next-generation building energy management system, Math. Comput. Sci. Div. Tech. Memo. ANL/MCS-TM-313. (2011).

[5.41] V. Marinakis, H. Doukas, C. Karakosta, J. Psarras, An integrated system for buildings' energy-efficient automation, Appl. Energy. 101 (2013) 6–14.

[5.42] N. Aste, M. Manfren, G. Marenzi, Building Automation and Control Systems and performance optimization, Renew. Sustain. Energy Rev. 75 (2017) 313–330.

[5.43] F. Oldewurtel, A. Parisio, C.N. Jones, M. Morari, D. Gyalistras, M. Gwerder, V. Stauch, B. Lehmann, K. Wirth, Energy efficient building climate control using stochastic model predictive control and weather predictions, Am. Control Conf. (ACC), 2010. (2010).

[5.44] F. Oldewurtel, A. Parisio, C.N. Jones, D. Gyalistras, M. Gwerder, V. Stauch, B. Lehmann, M. Morari, Use of model predictive control and weather forecasts for energy efficient building climate control, Energy Build. 45 (2012) 15–27.

[5.45] A.I. Dounis, M.J. Santamouris, C.C. Lefas, Building visual comfort control with fuzzy reasoning, Energy Convers. Manag. 34 (1993) 17–28.

[5.46] G. Ulpiani, M. Borgognoni, A. Romagnoli, C. Di Perna, Comparing the performance of on/off, PID and fuzzy controllers applied to the heating system of an energy-efficient building, Energy Build. 116 (2016) 1–17.

[5.47] M. Košir, Adaptive Building Envelope, in: Autom. Control Trends, InTech, 2016.

[5.48] C. Price, B.P. Rasmussen, Optimal tuning of cascaded control architectures for nonlinear HVAC systems, Sci. Technol. Built Environ. (2017) 1–13.

[5.49] S. Huang, Model based Technologies for Enhancing Building Operation, (2016).

[5.50] S. Merabti, B. Draoui, F. Bounaama, A review of control systems for energy and comfort management in buildings, Model. Identif. Control (ICMIC), 2016 8th Int. Conf. (2016) 478–486.

[5.51] A. Foucquier, A. Brun, G.A. Faggianelli, F. Suard, Effect of wall merging on a simplified building energy model, Proc. Build. Simul. (2013).

[5.52] S.H. Cho, M. Zaheer-Uddin, Predictive control of intermittently operated radiant floor heating systems, Energy Convers. Manag. 44 (2003) 1333–1342.

[5.53] A. Mahdavi, C. Pröglhöf, A model-based approach to natural ventilation, Build. Environ. 43 (2008) 620–627.

[5.54] J.A. Candanedo, V.R. Dehkordi, P. Lopez, A control-oriented simplified building modelling strategy, 13th Conf. Intl. Build. Perf. Simul. Ass. (2013).

[5.55] M. Kummert, P. André, Simulation of a model-based optimal controller for heating systems under realistic hypothesis, (2005).

[5.56] S. Prìvara, J. Široky`, L. Ferkl, J. Cigler, Model predictive control of a building heating system, Energy Build. 43 (2011) 564–572.

[5.57] E. Žáčeková, S. Prívara, Control relevant identification and predictive control of a building, Control Decis. Conf. (CCDC), 2012 24th Chinese. (2012) 246–251.

[5.58] R.Z. Freire, G.H.C. Oliveira, N. Mendes, Predictive controllers for thermal comfort optimization and energy savings, Energy Build. 40 (2008) 1353–1365.

[5.59] M. Morari, J.H. Lee, Model predictive control, Comput. Chem. Eng. 23 (1999) 667–682.

[5.60] I. Hazyuk, C. Ghiaus, D. Penhouet, Optimal temperature control of intermittently heated buildings using Model Predictive Control, Build. Environ. 51 (2012) 379–387.

[5.61] B. Lehmann, D. Gyalistras, M. Gwerder, K. Wirth, S. Carl, Intermediate complexity model for model predictive control of integrated room automation, Energy Build. 58 (2013) 250–262.

[5.62] V.M. Zavala, C. Thomas, M. Zimmerman, A. Ott, others, Next-generation building energy management systems and implications for electricity markets, Argonne National Laboratory (ANL), 2011.

[5.63] S. Privara, J. Cigler, Z. Váňa, F. Oldewurtel, C. Sagerschnig, E. Žáčeková, Building modeling as a crucial part for building predictive control, Energy Build. 56 (2013) 8–22.

[5.64] J.H. Lee, M. Morari, C.E. Garcia, State-space interpretation of model predictive control, Automatica. 30 (1994) 707–717.

[5.65] S.J. Qin, T.A. Badgwell, A survey of industrial model predictive control technology, Control Eng. Pract. 11 (2003) 733–764.

[5.66] W. Grünenfelder, J. Tödtli, The use of weather predictions and dynamic programming in the control of solar domestic hot water systems, 3rd Mediterr. Electrotech. Conf. (Melecon). Madrid, Spain. (1985).

[5.67] M.E. Snyder, T.A. Newell, Cooling cost minimization using building mass for thermal storage, ASHRAE Trans. (American Soc. Heating, Refrig. Air-Conditioning Eng. States). 96 (1990).

[5.68] G.P. Henze, C. Felsmann, G. Knabe, Evaluation of optimal control for active and passive building thermal storage, Int. J. Therm. Sci. 43 (2004) 173–183.

[5.69] T.Y. Chen, Application of adaptive predictive control to a floor heating system with a large thermal lag, Energy Build. 34 (2002) 45–51.

[5.70] Y. Ma, F. Borrelli, B. Hencey, A. Packard, S. Bortoff, Model predictive control of thermal energy storage in building cooling systems, Decis. Control. 2009 Held Jointly with 2009 28th Chinese Control Conf. CDC/CCC 2009. Proc. 48th IEEE Conf. (2009) 392–397.

[5.71] Y. Ma, F. Borrelli, B. Hencey, B. Coffey, S. Bengea, P. Haves, Model predictive control for the operation of building cooling systems, IEEE Trans. Control Syst. Technol. 20 (2012) 796–803.

[5.72] I. Hazyuk, C. Ghiaus, D. Penhouet, Model Predictive Control of thermal comfort as a benchmark for controller performance, Autom. Constr. 43 (2014) 98–109.

[5.73] J.E. Braun, others, Load control using building thermal mass, Trans. Soc. Mech. Eng. J. Sol. ENERGY Eng. 125 (2003) 292–301.

[5.74] E. Carrascal, I. Garrido, A.J. Garrido, J.M. Sala, Optimization of the Heating System Use in Aged Public Buildings via Model Predictive Control, Energies. 9 (2016) 251.

[5.75] M. Killian, M. Kozek, Ten questions concerning model predictive control for energy efficient buildings, Build. Environ. 105 (2016) 403–412.

[5.76] J.A. Orosa, A.C. Oliveira, Software tools for HVAC research, Adv. Eng. Softw. 42 (2011) 846–851.

[5.77] M. Trčka, J.L.M. Hensen, Overview of HVAC system simulation, Autom. Constr. 19 (2010) 93–99.

[5.78] A. Afram, F. Janabi-Sharifi, Gray-box modeling and validation of residential HVAC system for control system design, Appl. Energy. 137 (2015) 134–150.

[5.79] G. Reynders, J. Diriken, D. Saelens, Quality of grey-box models and identified parameters as function of the accuracy of input and observation signals, Energy Build. 82 (2014) 263–274.

[5.80] P. Bacher, H. Madsen, Identifying suitable models for the heat dynamics of buildings, Energy Build. 43 (2011) 1511–1522.

[5.81] M. J., Predictive control with constraints, Prentice Hall. (2001).

[5.82] E.C. for Standardization, UNI EN ISO 13786.Thermal performance of building components - Dynamic thermal characteristics - Calculation methods, (2008).

[5.83] N. Instruments, LabVIEW Control Design Toolkit User Manual, (n.d.).

[5.84] M. Benedettelli, A. Carbonari, B. Naticchia, M. Vaccarini, Reduced-order Models for Supporting Energy Audits of Buildings, ISARC. Proc. Int. Symp. Autom. Robot. Constr. 33 (2016).

[5.85] H. Madsen, J.M. Schultz, Short time determination of the heat dynamics of buildings, in: Therm. Insul. Lab. Rep. No. 243, Technical University of Denmark USA, 1993.

[5.86] E.D. CIBSE, CIBSE Guide a, Chart. Inst. Build. Serv. Eng. London. (1999).

[5.87] n. 74 Decreto del Presidente della Repubblica 16 aprile 2013, Regolamento recante definizione dei criteri generali in materia di esercizio, conduzione, controllo, manutenzione e ispezione degli impianti termici per la climatizzazione invernale ed estiva degli edifici e per la preparazione dell'acqua calda per usi ig, (n.d.).

[5.88] E.C. for Standardization, CEN. 2004. Standard EN 13779. Ventilation for non-residential buildings - performance requirements for ventilation and room-conditioning systems. Brussels., (n.d.).

[5.89] P.O. Fanger, others, Thermal comfort. Analysis and applications in environmental engineering, Therm. Comf. Anal. Appl. Environ. Eng. (1970).

[5.90] Z. Lin, T.T. Chow, K.F. Fong, Q. Wang, Y. Li, Comparison of performances of displacement and mixing ventilations. Part I, Int. J. Refrig. 28 (2005) 276–287.

[5.91] P.O. Fanger, B.M. Ipsen, G. Langkilde, B.W. Olessen, N.K. Christensen, S. Tanabe, Comfort limits for asymmetric thermal radiation, Energy Build. 8 (1985) 225–236.

[5.92] J. Carmody, S. Selkowitz, E. Lee, D. Arasteh, T. Willmert, Window System for High-Performance Buildings, (2004).

[5.93] J. Ramanauskas Bliūdžius, R. and Stankevičius, V., Langu šilumines savybes [Thermal properties of windows], 135Kaunas: Technologija. p. ISBN 9955–09–983–6, (n.d.).

[5.94] M. Killian, B. Mayer, M. Kozek, Cooperative fuzzy model predictive control for heating and cooling of buildings, Energy Build. 112 (2016) 130–140.

6

Climate change resilience

Identify, assess and compare potential countermeasures to cope with climate change for a low-tech building in Austria.

6.1 – ABSTRACT

The research activity, discussed in this chapter, was carried out as part of Wienerberger Sustainable Building Academy (WISBA) 2015 edition **[6.1]**.
As the name suggests, this International education programme focuses on sustainability, framed in its different facets which might go under the macro-headings of life span optimization and resource efficiency.
The final goal is to revitalize the limelight on brick solutions by testing their potential in coping with changes (of building function or of climatic conditions).
24 students from six different countries (Austria, Belgium, Italy, Hungary, Poland and Switzerland) were asked to answer a question: is it possible for a low-tech building (with reference to the renowned building 2226 in Lustenau, Austria) to adapt and escape obsolescence by contemplating the most likely casuistry of changes from now to 2050?
Two major scenarios were identified: change of weather conditions (team A) and change of intended use (team B). In four workshops, taken in various European locations, the "as-is" situation was preliminarily assessed, providing a common benchmark for both the lines of research, then ad-hoc conceived re-design options were selected, modelled, simulated and compared in terms of energy consumptions, indoor comfort, environmental impact (Life Cycle Assessment - LCA) and economic matter (Life Cycle Cost – LCC).
The final outputs were an integrated conceptual design and a fully comprehensive report of the upgraded proposal of the current state, highlighting the implications of all four sustainability dimensions.
As a member of team A, my role was mainly focused on the investigation of energy consumptions and comfort issues related to 2050's expected climatic changes ending with the development of proper resilient measures. The contents here presented and restated are part of the final report of the programme.
Not all the technical data, provided by Baumschlager+Eberle company during the project (about design details and related costs) are mentioned in the present thesis since they represent proprietary information.

6.2 – INTRODUCTION

Sustainability is a leitmotiv gaining more and more ground in the design of new buildings as well as in the retrofitting of the existing fabric.
Indeed, the fast-paced and energy demanding evolution of current built environment, requires a multi-perspective approach in order to contemplate all possible issues and stakeholders involved all over the lifespan of a building so as to give it the means to tackle premature ageing and depreciation.
Working on the resilience of a building means to preserve the original vision, emphasize its resource and environment-sparing features and enhance its design flexibility.
The SWOT (Strengths, Weaknesses, Opportunities and Threats) analysis represent the first step for critical reflections to size the room for improvement.
When all the pieces of information are ready to be implemented in a proper simulation tool (here Autodesk Revit and DesignBuilder), the re-design phase can start: results are extracted to be fed back in an iterative loop until the optimal configuration is achieved (according to one or more target functions).
In a climate change scenario, the focus is on how the performance of a building might divert when an increase of mean global temperature, magnitude and frequency of extreme events and air pollution is expected to occur. The aftermaths span through the dimensions of:

- ecology (environmental impact, depletion of resources and raw materials, increase of energy consumptions);
- economy (costs, incentives, deconstruction and reassembling strategies);
- society (comfort, liveability, property value).

The crucial question is what level of adaptation is needed and which kind of preventive/corrective measures should be applied as general recommendations and specific solutions.
From the comfort and energy perspective, the main concern is the risk of overheating as a direct consequence of global warming. It is reflected in the increase of cooling demand (necessary to maintain the operative temperature within the comfort range).
The inner complexity of dealing with future climatic scenarios is the tremendous uncertainty that affects both input and output data.
Several forecasts have been proposed in recent times, yet the rule of thumb is to select the one which better depicts local peculiarities. Therefore, since the case study in object is located in Lustenau, the choice fell on the Austrian Assessment Report on Climate Change 2014 **[6.2]**.
In **figure 6.1** the increase of global surface temperature is displayed according to different hypothesis on future emission reduction policies.

Yet, considering no bold measure has not yet been implemented to meet the Austrian global -2°C target (see **sub-paragraph 1.4.2**), a precautionary approach was taken and the worst case (A1) was selected.

The following boundary conditions were applied to depict 2050 scenario (**figures 6.2 – 6.5**):

- dry bulb temperature increased by between 3°C and 4°C (maximum of 34°C instead of 31.5 °C. minimum of -7.5°C instead of -10°C);
- wind speed increased by 1 m/s;
- relative humidity and solar radiation moderately invariant.

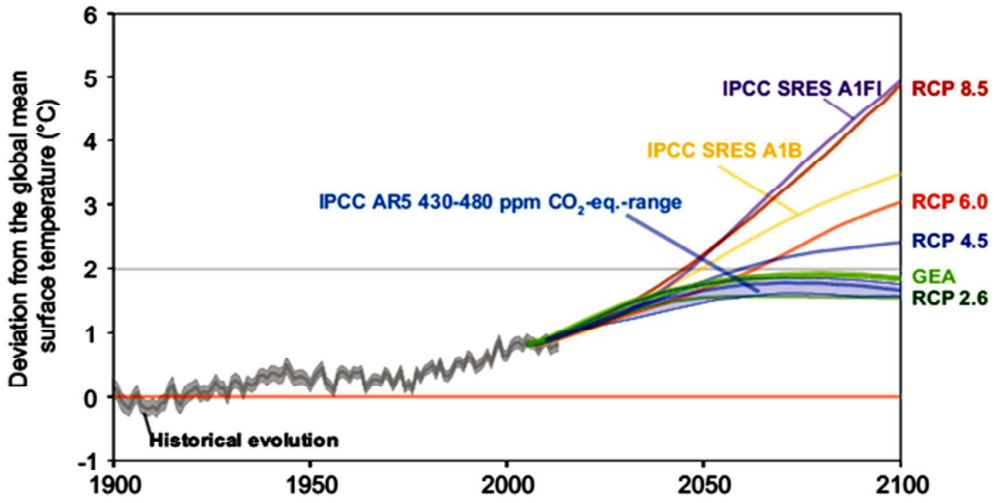


Figure 6.1

Deviation from global mean surface temperature (reference given by climatic conditions in the first decade of the 20th century) according to different future evolutions ***[6.3]****.*

WEATHER DATA SUMMARY

LOCATION: Haus2226_BAumschlager, -, -
Latitude/Longitude: 47.42° North, 9.668° East, **Time Zone from Greenwich** 1
Data Source: MN7 999 WMO Station Number, **Elevation** 403 m

MONTHLY MEANS	JAN	FEB	MAR	APR	MAY	JUN	JUL	AUG	SEP	OCT	NOV	DEC	
Global Horiz Radiation (Avg Hourly)	116	171	238	308	332	352	351	327	269	192	120	93	Wh/sq.m
Direct Normal Radiation (Avg Hourly)	129	215	212	281	257	275	292	256	230	202	105	122	Wh/sq.m
Diffuse Radiation (Avg Hourly)	76	87	133	147	174	180	167	176	147	107	85	60	Wh/sq.m
Global Horiz Radiation (Max Hourly)	376	555	744	883	914	1105	963	913	797	610	511	322	Wh/sq.m
Direct Normal Radiation (Max Hourly)	870	933	986	964	985	984	977	958	972	948	765	830	Wh/sq.m
Diffuse Radiation (Max Hourly)	201	264	362	383	438	464	459	416	357	314	223	162	Wh/sq.m
Global Horiz Radiation (Avg Daily Total)	1013	1705	2817	4140	4961	5524	5360	4581	3331	2049	1093	776	Wh/sq.m
Direct Normal Radiation (Avg Daily Total)	1120	2149	2504	3756	3825	4327	4443	3580	2856	2158	955	1017	Wh/sq.m
Diffuse Radiation (Avg Daily Total)	672	863	1573	1991	2620	2826	2563	2465	1825	1130	776	506	Wh/sq.m
Global Horiz Illumination (Avg Hourly)	12523	18401	25802	33534	36432	38846	38937	36437	29880	21454	13399	10295	lux
Direct Normal Illumination (Avg Hourly)	11018	19619	20019	26376	24300	25135	28116	23300	21080	17694	8854	10172	lux
Dry Bulb Temperature (Avg Monthly)	0	2	6	10	15	18	19	19	14	10	5	1	degrees C
Dew Point Temperature (Avg Monthly)	-2	-1	1	4	9	12	14	14	11	7	2	-1	degrees C
Relative Humidity (Avg Monthly)	82	80	74	71	71	72	72	75	80	82	84	84	percent
Wind Direction (Monthly Mode)	260	260	250	250	290	290	290	270	240	300	310	290	degrees
Wind Speed (Avg Monthly)	1	1	1	1	1	1	1	1	1	0	1	1	m/s
Ground Temperature (Avg Monthly of 1 Depths)	7	6	5	6	7	10	13	14	15	14	13	10	degrees C

WEATHER DATA SUMMARY

LOCATION: Haus2226_BAumschlager, -, -
Latitude/Longitude: 47.42° North, 9.668° East, **Time Zone from Greenwich** 1
Data Source: MN7 999 WMO Station Number, **Elevation** 403 m

MONTHLY MEANS	JAN	FEB	MAR	APR	MAY	JUN	JUL	AUG	SEP	OCT	NOV	DEC	
Global Horiz Radiation (Avg Hourly)	114	163	234	322	338	358	370	343	301	208	126	92	Wh/sq.m
Direct Normal Radiation (Avg Hourly)	142	205	179	274	299	326	326	298	331	269	166	133	Wh/sq.m
Diffuse Radiation (Avg Hourly)	70	86	144	168	149	157	166	168	129	93	72	56	Wh/sq.m
Global Horiz Radiation (Max Hourly)	403	503	736	858	990	999	1025	913	780	673	433	324	Wh/sq.m
Direct Normal Radiation (Max Hourly)	889	907	952	979	1004	963	980	973	987	957	812	833	Wh/sq.m
Diffuse Radiation (Max Hourly)	200	278	359	418	433	465	461	426	375	296	219	155	Wh/sq.m
Global Horiz Radiation (Avg Daily Total)	994	1607	2768	4329	5033	5629	5673	4795	3711	2219	1155	769	Wh/sq.m
Direct Normal Radiation (Avg Daily Total)	1235	2000	2118	3671	4431	5120	5003	4152	4043	2867	1518	1107	Wh/sq.m
Diffuse Radiation (Avg Daily Total)	618	855	1705	2260	2236	2472	2550	2352	1617	995	658	471	Wh/sq.m
Global Horiz Illumination (Avg Hourly)	12335	17657	25405	35071	36915	39694	41171	38268	33417	23141	13981	10243	lux
Direct Normal Illumination (Avg Hourly)	11993	18537	16803	25049	28774	30823	30722	27213	31838	25017	14053	11553	lux
Dry Bulb Temperature (Avg Monthly)	4	6	8	12	16	19	22	22	18	14	7	4	degrees C
Dew Point Temperature (Avg Monthly)	1	3	3	7	11	14	17	17	14	10	5	1	degrees C
Relative Humidity (Avg Monthly)	81	80	74	74	73	75	73	75	80	82	84	82	percent
Wind Direction (Monthly Mode)	260	260	250	250	290	290	290	270	240	270	310	290	degrees
Wind Speed (Avg Monthly)	2	2	2	2	2	2	2	2	1	1	2	2	m/s
Ground Temperature (Avg Monthly of 1 Depths)	10	9	8	9	10	13	15	17	17	17	15	13	degrees C

Figure 6.2
Climate change scenario: weather data for case study location in Austria - 2015 on top, 2050 on bottom.

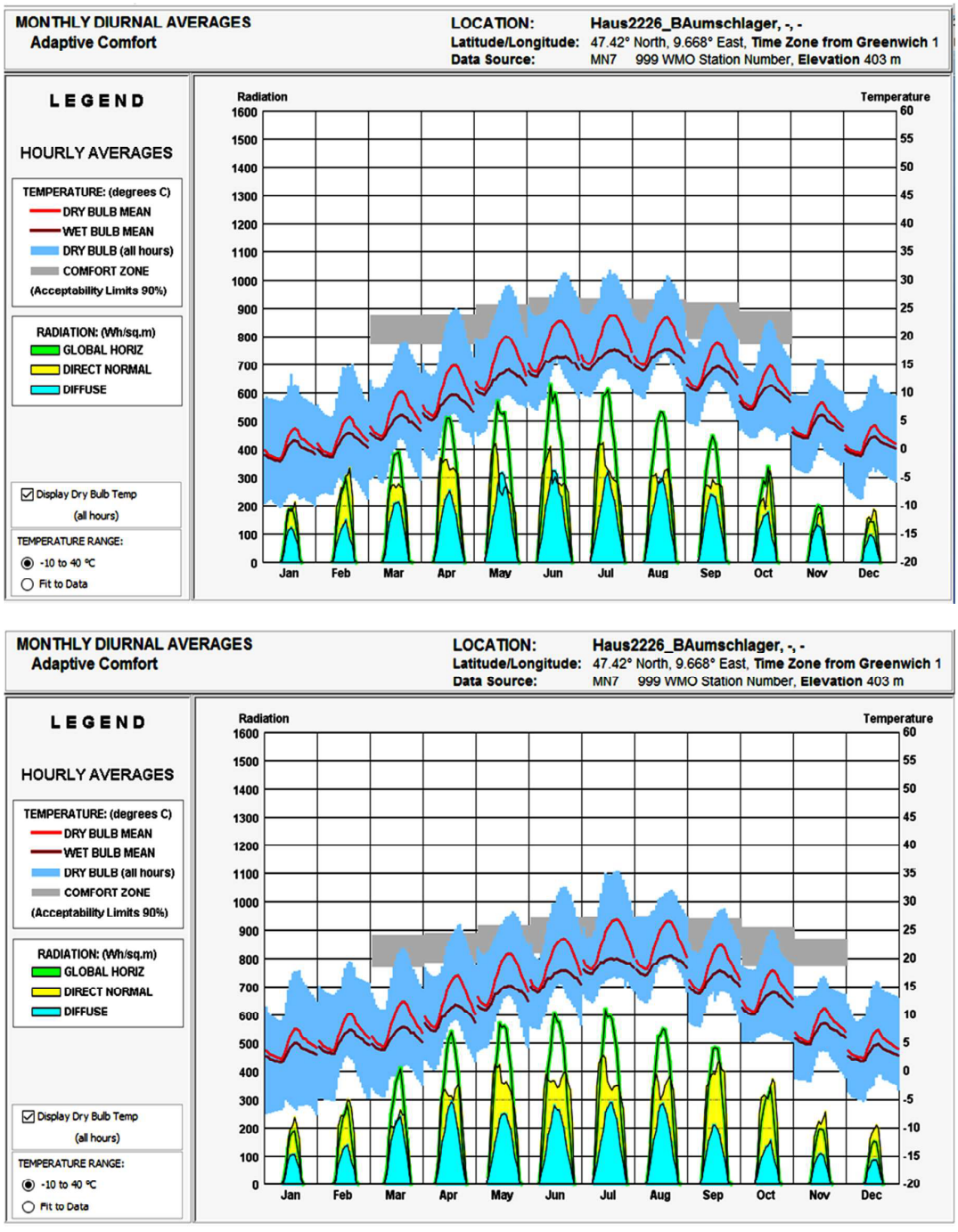


Figure 6.3

Climate change scenario: air temperature and Solar radiation time trends - 2015 on top, 2050 on bottom (adaptive comfort zone compliant to ASHRAE 55).

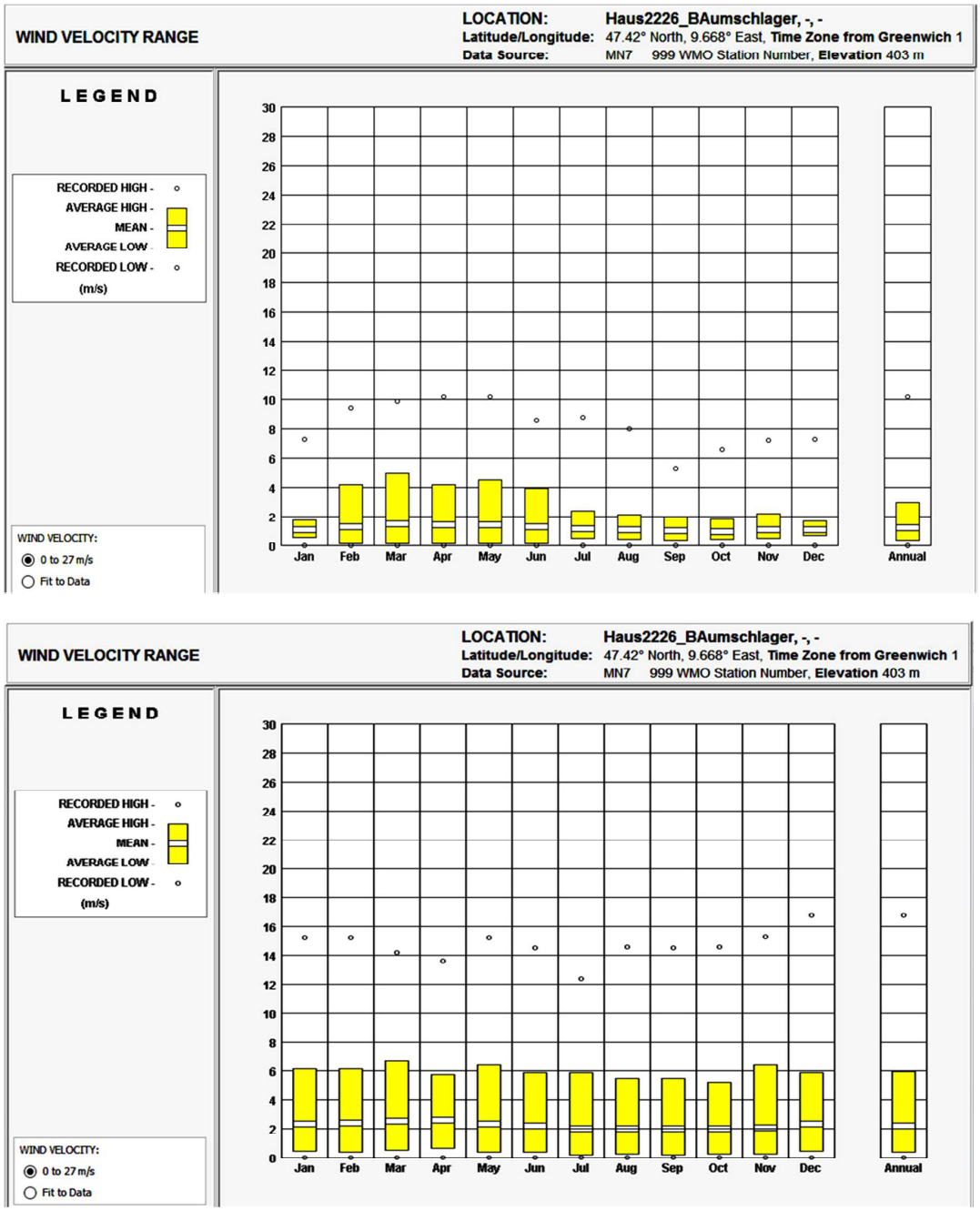


Figure 6.4

Climate change scenario: wind speed ranges per month - 2015 on top, 2050 on bottom.

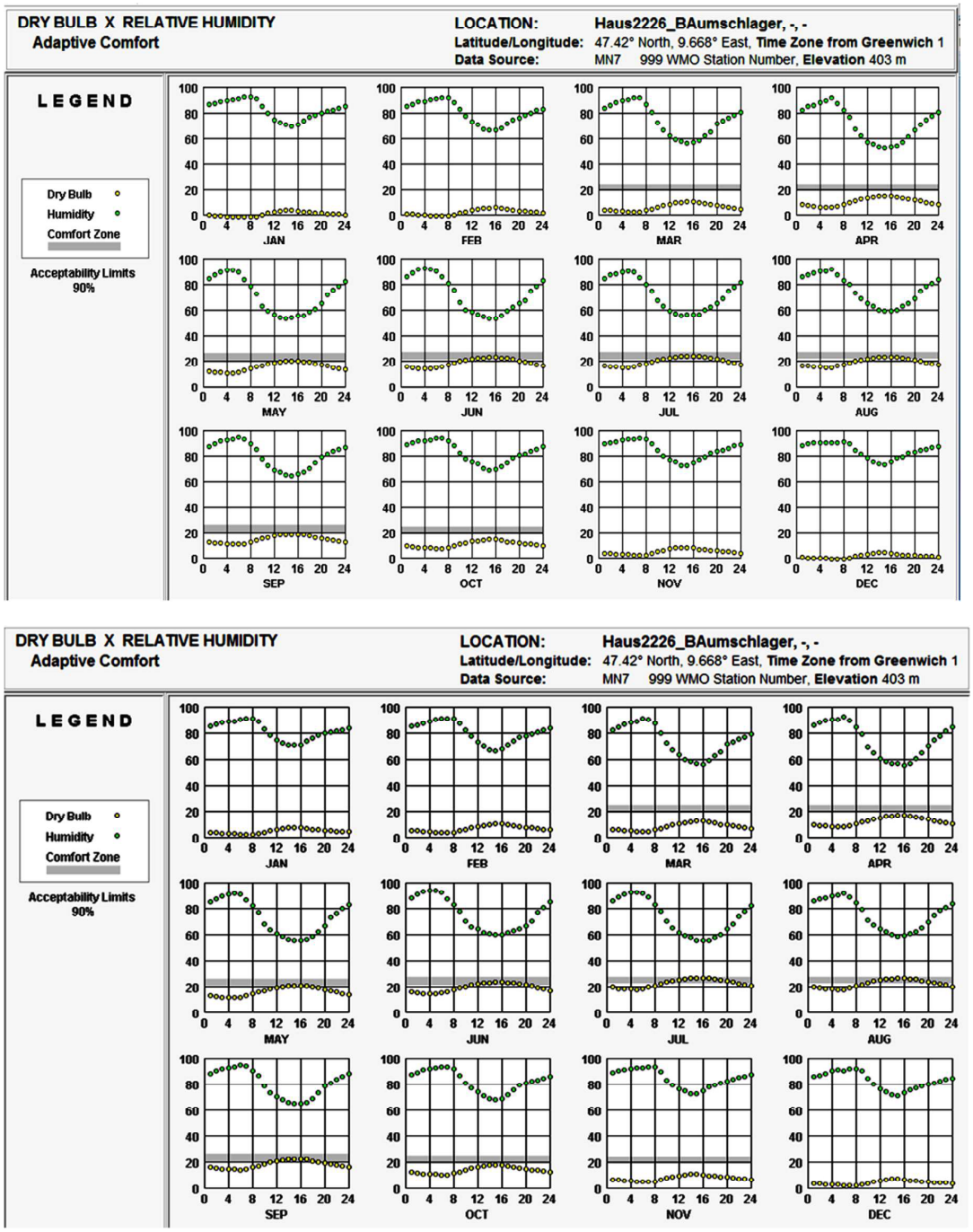


Figure 6.5

Climate change scenario: air temperature and relative humidity per month - 2015 on top, 2050 on bottom.

6.3 – CASE STUDY

In the framework of WISBA 2015, the low-tech building 2226 designed by the architectural office Baumschlager and architect Eberle was selected as testing platform, since it represents a borderline case, given the following features:

- Ultra-low energy building
- No heating, cooling or mechanical ventilation systems
- CO_2 controlled natural ventilation system
- Double layer monolithic brick walls
- No additional insulation (except roof and floor)

Architect Dietmar Eberle developed the concept of building 2226, based on the upstream vision that modern building is a low-tech one, yet smart enough to adapt and give value to the local resources.

The pursuit of resilience paradigm is demonstrated by the adoption of a timeless, simplistic design (**figure 6.6**) and a software-centred, low-impact energy concept.



Figure 6.6
Building 2226 in Lustenau and WISBA 2015 team (students and mentors).

The emphasis is on the user and its pivotal role in the management of the space and microclimate around him: a monitoring system, measuring the inside climate (temperature, humidity, carbon dioxide, …) was introduced to raise occupants' awareness of their surroundings and enhance their control power, even though the building's natural ventilation system automatically reacts whenever the indoor environmental conditions are out of the comfort zone.
Natural ventilation is the key-element to counter-balance, in a precautionary way, the occurrence of discomfort phenomena, without additional cooling and heating system.
It is charged to five (per side and per floor) large windows with ventilating door (**figure 6.7a**). Air circulation is additionally reinforced by means of cross ventilation through the internal stairway (**figure 6.7b**).
Simultaneously, the windows are deep-set into the wall, which allows to mitigate the solar gains during summer when the risk of overheating is stronger.



Figure 6.7
Building 2226 natural ventilation systems: windows equipped with ventilating doors (a) and internal stairway (b).

The user-centred principle of the building is based on researches on optimal temperature comfort range for an adaptive occupant throughout the year: such comfort zone was found to lie within the range 22-26°C, therefore the project has been named likewise – 2226.
One of the pillars over which the general concept was structured is that "the building has replaced hardware by software" (words of architect Eberle). That is the result of a strong scepticism and distrust in the power of simulation tools to properly depict all

building physical or nonphysical phenomena. According to this vision, the idea of a deterministic calculation of all environmental parameters makes no sense if the main variables are connected to users' behaviour and so not rationally (especially in the long-term horizon) predictable.
From an energy perspective, the basic concept is that by reducing the amount of required energy (kWh) more than finding more efficient ways of producing it, it is possible to guarantee high living standards as well, thus reducing anthropic impact on the environment.
Consequently, a crucial role is given to structural materials and their high thermal mass. A "slow-moving" building is reluctant to divert from its behaviour when boundary conditions change: this is the keystone to preserve an optimal indoor environment despite of the changes in internal/solar gains, weather turns and any other perturbation of the energy loads.
Additionally, according to the architect, energy efficiency it is not only about technical innovation but it is deeply rooted in the valorisation of the local peculiarities and strengths: employing local materials and craftsmen's work contributes to the minimisation of transport costs and energy consumptions too.

6.3.1 – General features

Building 2226 is an office block and exposition space, located in Vorarlberg (Austria), thereby occupancy pattern is concentrated on workdays, while over the weekend it is expected to stay inhabited. Since the working timetable usually ends at 8pm, there's plenty of scope in exploiting the refreshing power of night ventilation, when needed.
More in detail, the storeys asset is the following:

- the ground floor hosts a café and an open space used as a gallery;
- on the first and second floors are Baumschlager+Eberle's employees' offices;
- fourth and fifth floors are rented out to other companies.

Each storey has the same layout (**figure 6.8**): a huge open plan divided in four spaces by the load-bearing walls. Currently, the only non-static walls are those dividing the bathroom and the kitchen.
Two staircases and an elevator between them provide the means for inter-communication among the floors and are positioned not to interfere with the penetration of sunlight into the space.

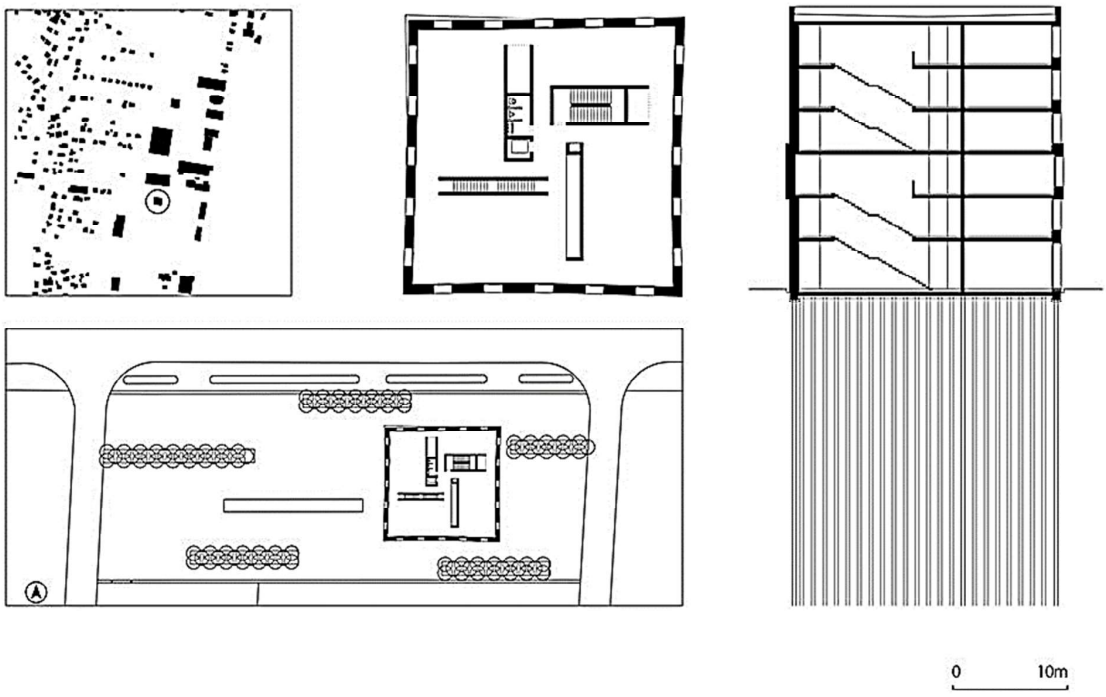


Figure 6.8
Plans, elevations and sections of Building 2226.

Smart technology is essential for building self-regulation: as previously mentioned, a touchscreen (**figure 6.9**) is installed on each floor, approximately in the same position, plotting present time trends of CO_2 level, temperature, illuminance and humidity, recorded by sensors placed in close proximity.



Figure 6.9
Architect Eberle showing the monitoring touchscreen during the visit to Building 2226.

The software detects whenever one of these parameters falls out of the defined range and balances it back. Nevertheless, users are not deprived of their control power as they can still override the software in case they want to impose a new pattern.
However, it should be stressed that:

- user direct action actually lasts for a limited time window before the automatic control is restored;
- sensors' measurements provide a single-point analysis of the microclimate, thus they are not representative of local heterogeneities: therefore, if, for any reason, the density of occupants in a limited area of the room increases, the local temperature rise due to internal gains is not recognized by the system and so not counter-balanced;
- weather anomalies (heat waves mostly) are likely to perturb the correct operation: given that night ventilation is a key factor in preserving the 22-26°C target, the occurrence of tropical night events is a massive threat. For instance, during summer 2014, indoor temperature overtook 27 °C for a whole week. Such episodes are expected to gain importance in the future, since both amplitude and frequency are deemed to increase because of global warming;
- the high thermal mass of structural materials (bricks vertically and concrete horizontally) results counterproductive during long-lasting periods of high outdoor temperatures, since they actually act as thermal batteries, gradually releasing the stored heat to the indoor air volume;
- the windows are not provided with shadings thus increasing the risk of overheating and glare;
- the heating of the building comes from the contributions of both solar gains and internal gains: if insufficient (the temperature falls below 22°C), the lights turn on to help restore the comfort zone. This method tends to be slow and hardly predictable. Back in the day when WISBA 2015 took place, the building was not yet fully occupied, therefore no on-site validation of such strategy was available.
- Open floorplans and high ceilings play a beneficial role in terms of air quality and penetration of daylight, but are detrimental in terms of acoustics, since each floor in divided into big open spaces with no partitions which might act as sound absorbers.

6.3.2 – Location

Building 2226 stands close to the Austria-Switzerland border, in a quite isolated (no other buildings in the close neighbourhood), industrial area.

Therefore, no problems of traffic noise, pollution, urban heat island or poor penetration of daylight is experienced. Greenery and vegetation frame the surrounding space, plus a stretch of water goes from the front of the building to the lawn around: these are natural heat sinks which continuously refresh the air via evapotranspiration and evaporation phenomena.
Obviously, such characteristics are crucial for the correct performance of the 22-26 scheme: nevertheless, in an all-inclusive future scenario, the expansion of the residential area is actually likely to occur, with all its aftermaths in terms of quality of outdoor air and sky view.
Lustenau is Vorarlberg's fourth largest town, lying on the River Rhine.
According to The Köppen-Geiger classification, the climate is warm and temperate (Cfb), experiencing a significant rainfall throughout the year (**figure 6.10**):

- 9.1 °C is the mean annual temperature, which hits the minimum in January (-0.7 °C) and the maximum in July (18.4 °C);
- 1148 mm is the annual rainfall, which hits the minimum in February with 62 mm of rain and the maximum in June with 135mm.

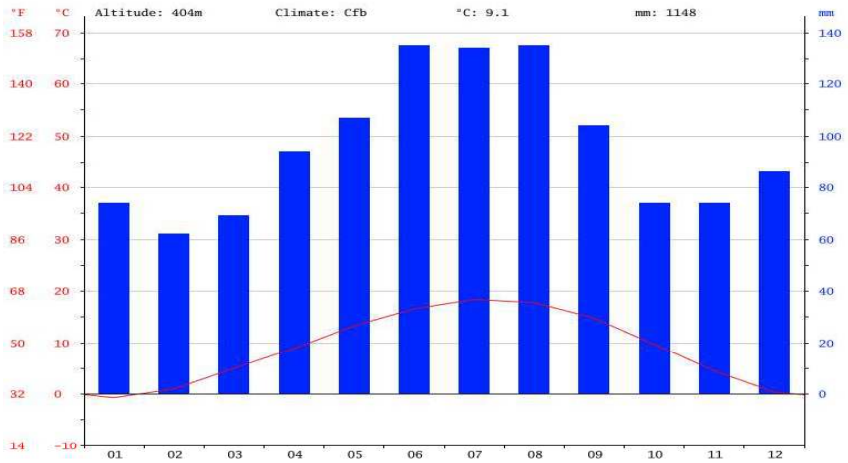


Figure 6.10
*Lustenau's annual climate **[6.4]**.*

6.3.3 – Sunlight

As previously mentioned, the sky is frequently cloaked by clouds in Lustenau.
From a design perspective, such climatological feature entails special care in the developing of a low-tech concept since solar power exploitation is crucial.

The first strategically efficient choice is to orient the façades according to the four principal cardinal points, so that each one can be optimized to the different sun paths and heights in order to build up a balanced distribution of solar incomes throughout the building.
The second escamotage exploits the principle that the less the air volume the higher the responsiveness to energy gains and losses. Consequently:

- smaller spatial units have been north-oriented. In this way, even though the surfaces stay lit for a very limited window of time, the thermal capacity of the inside air is optimized to collect sufficient free heat from the sun and maintain comfort conditions;
- larger spatial units have been distributed all along the rising path of the Sun. In this case, the threat comes from excessive solar penetration both in terms of temperature (overheating) and visual comfort (glare). The height of the rooms (around 3.5m) and the openness of the layout responds to the first issue thus triggering a powerful updraft that disperse potential hot spots at man level by natural convection, without any further, active intervention.

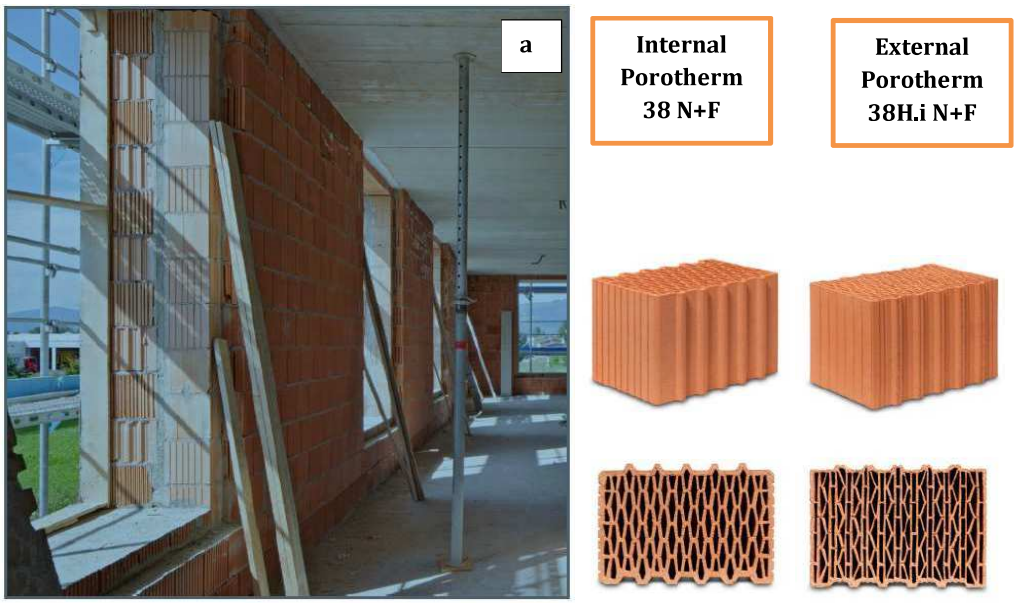
6.3.4 – Walls composition

Vertical elements' composition is quite homogeneous: external and internal walls are actually made of the same materials, the only difference in the number of brick layers (two and one respectively). Horizontal elements are made of concrete, yet differ in the outer layer, which is plastering for inner floors and gravel for the roof.
Besides, inner floors boast a flexible design in order to provide a super-user-friendly management of the technical systems: water and electricity distribution have been conceived as a radial-shaped network, having its origin in the geometrical centre of each floor, where the control panel is easily accessible through removable wooden boards of the suspended floor.
The ceiling does not show the same flexibility because of the presence of the large windows running all the height long.
Table 6.1 and **figure 6.11** provide some information and illustration of structural components.

BUILDING 2226 – GENERAL FEATURES			
Geometry			
Ratio of gross floor area to usable area	1,24	Ratio of enveloping area to usable area	1,08
Ratio of facade surface to window surface	23%	Ratio of facade surface to glass surface	16%
Design			
U-Value - wall	0.13 W/m² K	U-Value - glass	0.5 W/m² K
air tightness	n50 = 0.51 1/h	G-Value - glass	48 %
Wall structure		**Floor structure**	
Lime plaster	8mm	Anhydrite screed	50mm
Lime-cement plaster	12mm	Acoustic mat	10mm
Perforated bricks, U-value	380mm, 0.24 W/m² K	Hardwood	24mm
Mortar joint	18mm	Upholstered wood	56mm
Perforated bricks, U-value	380mm, 0.34 W/m² K	Concrete	180mm
Lime-cement plaster	15mm	Preload precast concrete	110mm
Lime plaster finishing	5mm	Finishing	5mm

Table 6.1

Geometric and structural details of building 2226.



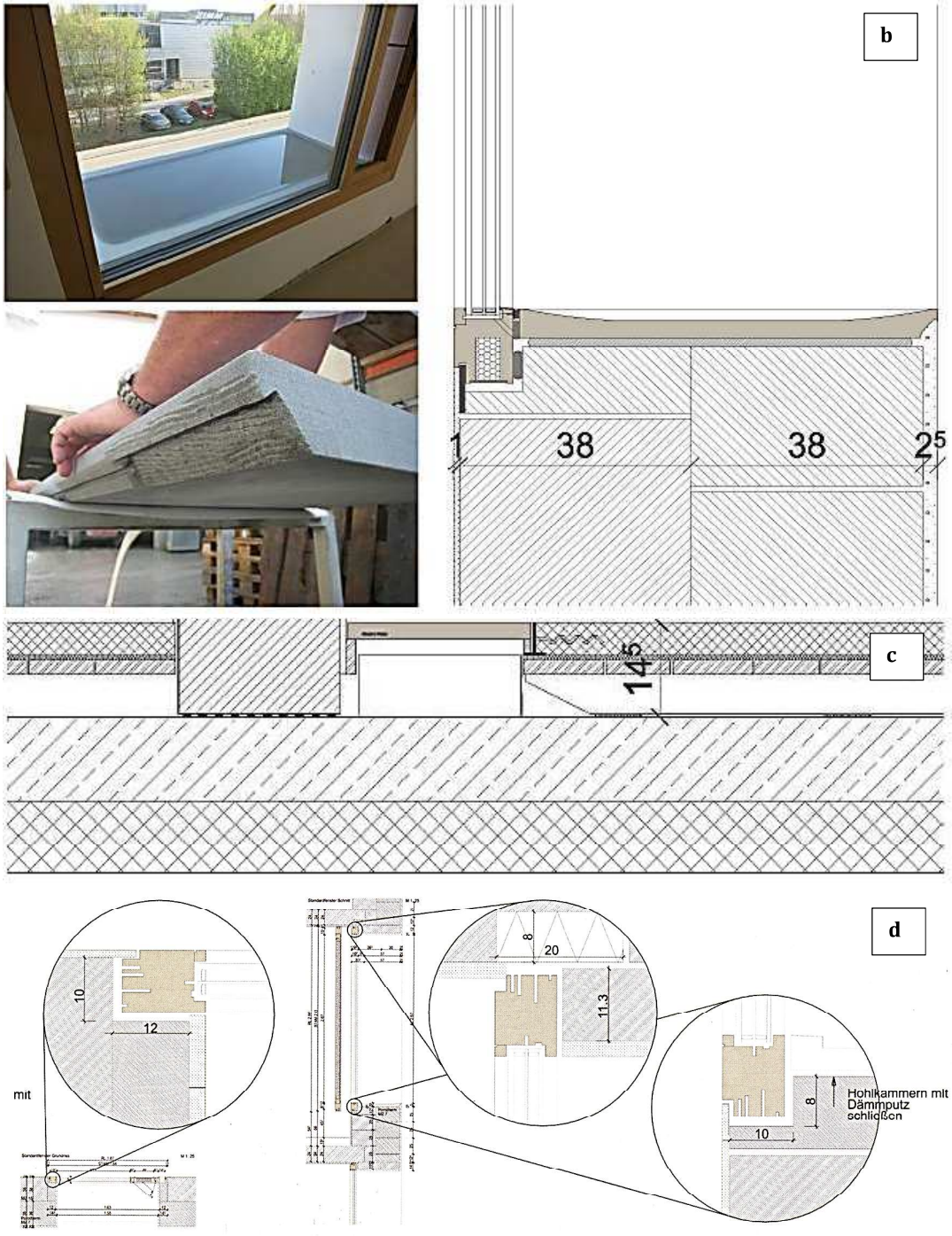


Figure 6.11

Building 2226 structural details: brick layers (a), windows (b), floor structure (c), connection between opaque and glazed components (d)

6.3.5 – Comfort management

When indoor comfort has to be preserved by passive means (without any mechanical system forcing the environment to evolve according to users' settings), the building energy balance is actually the control law, thus all the contributions have to be somehow governed in order to achieve the 22-26°C target:

- outdoor conditions (temperature, relative humidity, wind and solar radiation);
- internal heat gains related to human presence (eating, breathing, moving);
- other thermal sources (computers, lights, electronic devices, …);

Besides, walls "interference" has to be fully quantified in terms of thermal resistance, thermal inertia, decrement factor, …

Thermal inertia and natural ventilation are the key-players in Building 2226: by analogy with electric circuits, massive walls play the role of capacitors, thus storing the heat as internal load, while the ventilating doors play the role of breakers. In this way, heat accumulation (alias electrical charge in the afore mentioned analogy) and gradual release (like through internal resistances) is regulated by activating the natural ventilation when needed.

When free heat income, from the sun mostly, is available, such massive walls initiate their "charge cycle", absorbing the heat during daytime, when outdoor temperature and radiation peak, and slowly releasing it ("discharge cycle") with a certain delay. When walls composition is properly designed it is possible to synch the afore mentioned discharge cycle with the time of maximum need, when outdoor temperature drops, generally after the sunset.

Against this backdrop, summer risk of overheating might be enhanced. This is actually true whenever night ventilation isn't performed or effective: by activating natural and cross ventilation through the building during night time, it is possible to execute a sort of "reset" of indoor conditions, cooling the air, the surfaces and recreating optimal air quality, thus mitigating the risk of discomfort.

Nevertheless, such refreshing action, even if contemplated in the design of the building, is not always rewarding: abnormally hot weather conditions, known as "tropical nights" might annul and even reverse the beneficial effect of air ventilation.

In building 2226, night ventilation is charged to the vertical openable panels integrated in the window case: the consensus is given by wind and temperature probes,

All things considered, slow responsiveness is pivotal in passively maintaining a satisfying indoor climate throughout the year **[6.5-6.13]**: massive walls act as stabilizers of indoor temperature since they are strongly reluctant to change their

thermal status, even when the weather undergoes significant variability or the occupancy suddenly increases/decreases.

Furthermore, the adoption of gypsum plaster on the internal surface allows to control the humidity level in the air through moisture buffering and mould inhibition. On the exterior, the lime plaster mixed with hemp acts as a fungicide. It is a sturdier solution which resists to thermal-cracking.

Moisture control is necessary to counteract the risk of mucous membrane irritation, difficulties in breathing, declining immunity and other sick-building-syndrome symptoms.

The target for Building 2226 was to keep the relative humidity (RH) within the range 40-60% as diverse scientific sources [**6.14-6.16**] deem such values appropriate to reduce the probability of illnesses.

At the time of the research study, when occupancy was much below the capacity of the building, RH values always fell between 40% and 55%

Therefore, thermo-hygrometric comfort is mostly controlled by the building envelope itself.

Yet, as universally acknowledged, users' satisfaction towards the living environment is also affected by IAQ, fundamentally defined by the concentration of CO_2 and the microbiological level. As Lustenau boasts a high quality of outside air, it was decided to charge natural ventilation with the task of preserving the right chemical content of indoor air volumes. The 3.5-meter high walls contributed in two main ways:

- Air stratification: thanks to the huge availability of space, the heat released by internal gains and re-emitted by the surfaces lit by the sun, activates a considerable convective warm updraft that washes the indoor volume from the bottom to the top until it layers right beneath the ceiling. Comfort is preserved since the warm updraft is immediately replaced by a moderately fresher downdraft at users' level.
- Increase of the average air volume per occupant: this has a direct effect on the concentration (in terms of volume fractions) of CO_2 and other micro biologicals, since they can diffuse more efficiently.

6.4 – METHODOLOGY

As afore mentioned, all the dimensions of sustainability were contemplated in Building 2226 assessments, whichever the configuration under analysis. In order to

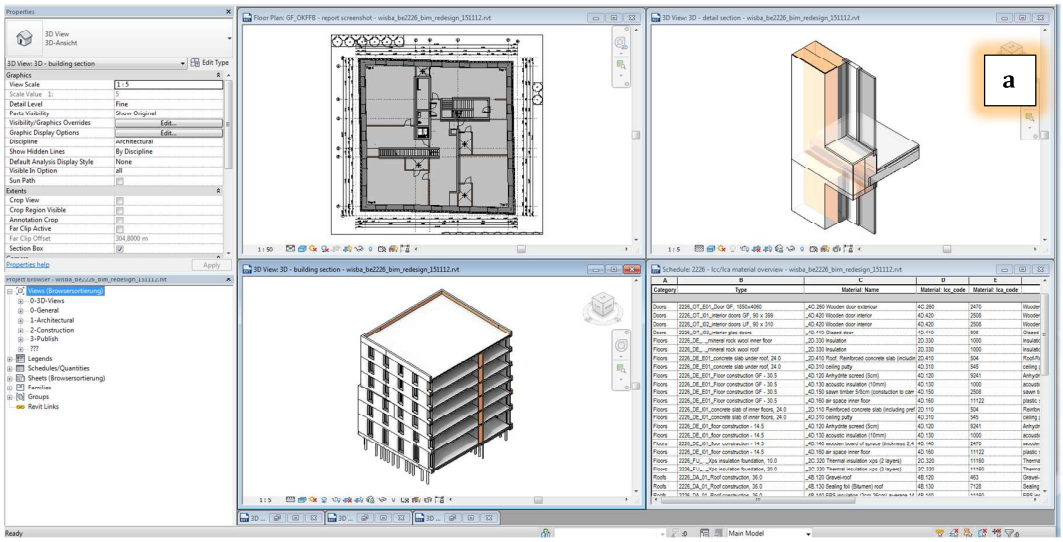
accomplish the task, diverse software and database were interlaced to extract complete and consistent screenings.

6.4.1 – Building Information Modelling

Building Information Modelling (BIM) was selected to collect and compare information in different scenarios in a comprehensive and time-saving way. In fact:

- it returns relevant parametric data about a building throughout its life cycle (design and planning process, building phase, use stage and eventually reuse and disposal stage of buildings);
- its output can be exported to various software to perform function-specific analyses **[6.17].**

Autodesk Revit was adopted. A couple of screenshots of the user interface are visualized in **figure 6.12.**



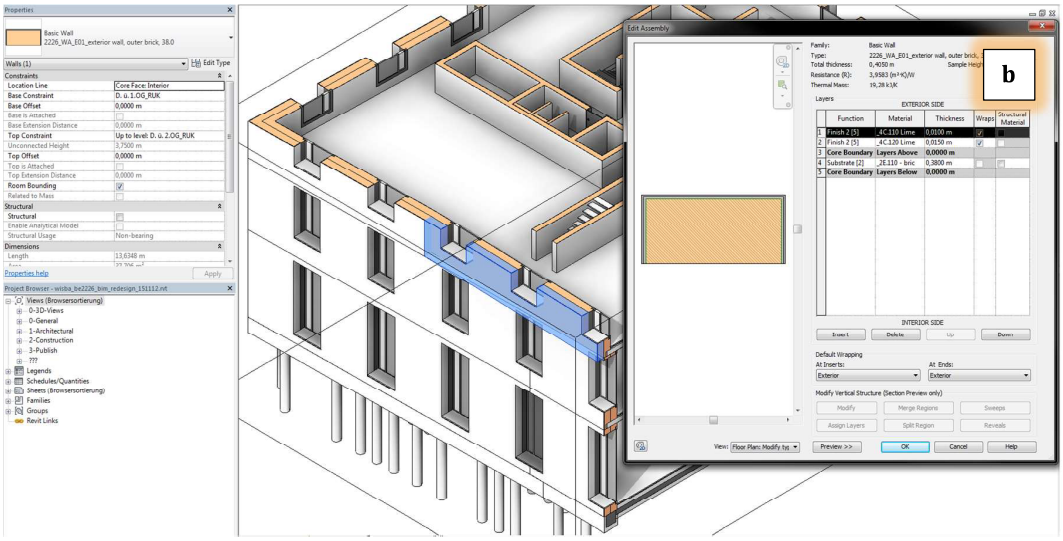


Figure 6.12

BIM on Building 2226 through Autodesk Revit: (a) materials insertion and quantification: (b) element composition definition.

Therefore, a BIM-based workflow (**figure 6.13**) was used to extract elements and materials information and run an iterative assessment of sustainable options, inherent to both the design stage and the optimization process.

Indeed, the output of BIM analysis provided the common baseline for all further investigation around the sphere of LCA (Ecoinvent database), LCC (ASPEN), energy efficiency and comfort (DesignBuilder).

It should be stressed here that, in order to standardise and compare costs and environmental assessments, the current European Standards on BIM **[6.18]** was assumed as the main guideline.

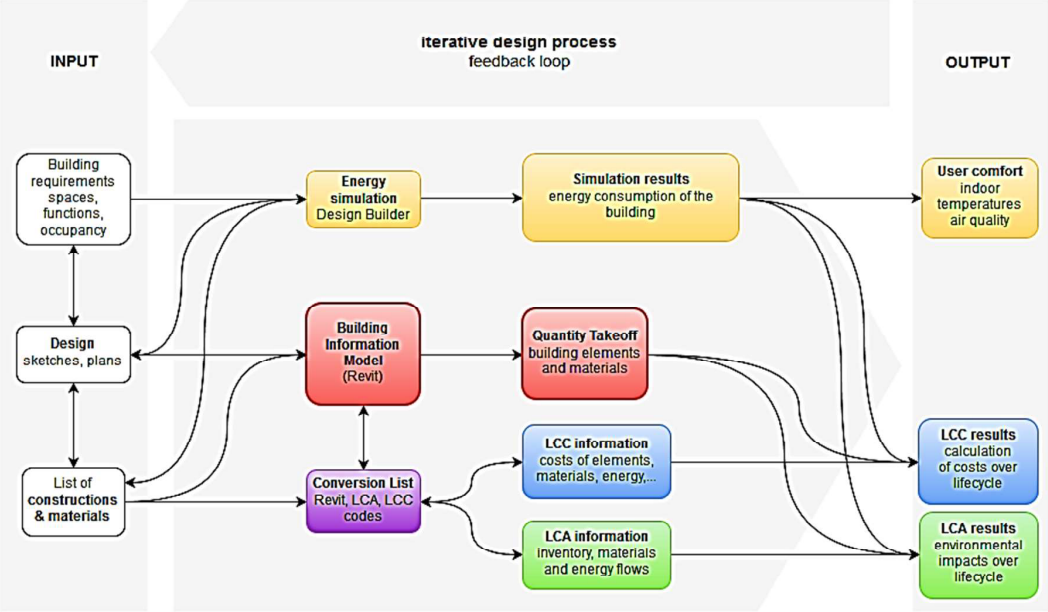


Figure 6.13

BIM-based workflow: links between assessment perspectives and feedback loop of the iterative design process.

Each model was based on:

- project data and technical drawings (floorplans, sections and details) provided by the Baumschlager+Eberle company for the reference building;
- sketches and conceptual plans for the re-design options as conceived by each WISBA sub-group;

Quantitative evaluation of the materials is directly performed within the software on the basis of width, length and height data, thus accounting for all of the multiple layers and parts composing the building.

6.4.2 – Energy Modelling

A whole building energy simulation was accomplished via DesignBuilder (version 4.2.0.054) to quantify the current performance and to catch energy-consuming components as well as the relationship between the different energy services (natural ventilation and lighting mostly, since no heating or cooling equipment is installed).

As outlined before, the energy passive management of building 2226 is achieved by combining low thermal transmittance and high thermal mass walls with high performance window panes. Heating is the result of solar and internal gains.
Indoor temperature and IAQ are actively controlled via smart activation of natural ventilation and lighting.
Against this framework, modelling challenges raised and customized solutions had to be implemented:

- floor plan layout was split into thermal zones in order to differentiate the loads according to the use of the space (offices, cafeteria, toilets, exhibition hall) and the expected occupancy, as shown in **figure 6.14.** 80 people were considered to enter the building daily: such information was given in input to the BEM (as people/m^2) and used to define occupancy and consumption schedules (**figure 6.15**).
  It was assumed a total amount of 4-8 people per zone, each one with a personal workstation including a computer of 50W and two monitors, with an individual mean consumption of 30W **[6.19].** The total electric load per zone was calculated accordingly and entered as a W/m^2 value **[6.20,6.21].** The radiant fraction (accounting for the heat gains released into the environment) was set to 0.2 as default.

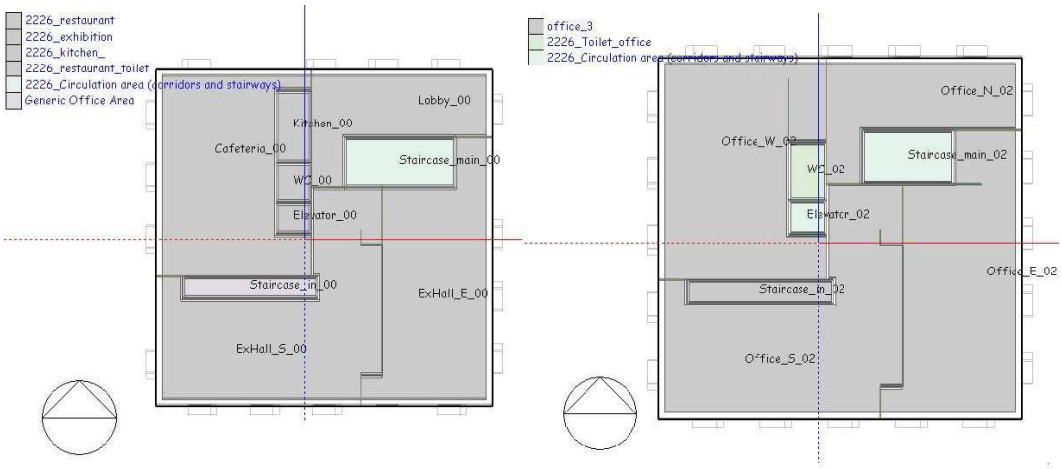


Figure 6.14
BEM geometry, layout and division in thermal zones.



Figure 6.15

Occupancy schedules tailored per each thermal zone: office case.

- the geometrical distortion in the façade was not taken into account, due to its minor impact on the energy performance: a simplified cubic shape was adopted;
- In order to stick to the maximum value of wall thickness allowed in Design Builder (50 cm) without corrupting the actual thermal behaviour and the number/order of layers, exterior walls composition was manipulated as follows: half thickness of the bricks, double density and half conductivity. As a result the total thickness of the external wall was reduced from 81cm to 42cm **[6.22]**.
- Air tightness was set according to the 4-n50 (ac/h at 50 Pa) model infiltration: the rate of air change resulted 0.51, which meant that, when a 50Pa pressure difference was set between indoors and outdoors, the 51% of the total volume of air was leaked through the construction per hour.
- Radiant fractions per each lighting appliance and some of luminaries was defined according to the specs sourced by the official product web page of Zumtobel **[6.23]**.
- As said before, the lighting is also used in guise of smart heating terminals to counteract excessive temperature drops: such mechanism was modelled through an additional EnergyPlus sub-algorithm turning on the lights every time the temperature fell below 20°C.

Smart natural ventilation was recreated via EnergyPlus too, by coding a customized schedule. The activation had to abide by one of the following conditions: indoor temperature overpassing both set point and outdoor temperatures or CO_2 concentration exceeding 1000 ppm.

Both codes are set to each of the perimeter zones separately, which allows independent operation.

6.5 – CURRENT STATE RESULTS

Building 2226 was preliminarily analysed from several perspectives, both qualitative and quantitative, with the overarching aim of collecting as much information as possible to properly address the re-design phase.
Each sub-result is given and discussed in the following paragraphs.

6.5.1 – SWOT analysis

As a preliminary step, a SWOT analysis (**table 6.2**) was performed to size the room for improvement.
A revised version of the outcomes is here proposed in the shape of a pros-and-cons table (**table 6.3**).

BUILDING 2226 CURRENT STATUS – SWOT ANALYSIS		
	Threats	**Opportunities**
Strengths	• Natural ventilation + increase of tropical nights » Inability of the building to reduce inner temperature.	• Low investment cost (building compactness) + small variety of materials used + absence of HVAC » Beneficial low tech design for future climate change scenario + less uncertainties. • Very low U-Value of external building elements + material inertia » Use and strategically improve this property to improve comfort. • Windows ratio + room height » Beneficial for inner lighting (changes made should maintain this aspect).
	• Windows to wall ratio/solar radiation » Source of overheating. • Shadings » Decrease of daylight comfort.	• Maintenance of wooden framed windows (high costs) » Blinds could increase the life span of this building element. • Staircases not part of the

Weaknesses	• Increase of artificial lighting (due to shadings) » Increase in energy consumption. • Building not adaptable to a change of site and function (current state) » Disturbance of comfort in a future climate change scenario.	ventilation » Air circulation improvement (stack/chimney effect) by introducing a roof window.

Table 6.2
Building 2226 current state: SWOT analysis.

BUILDING 2226 – CURRENT STATE ASSESSMENT	
ADVANTAGES	**DISADVANTAGES**
Low density industrial area	Adapted to a specific function / climate
Trees and water plan in the surrounding	Acoustic issues through glass doors
Compact geometry	High environmental impact materials
Open floorplan	Materials with not enough thermal mass
Local materials	Amount of windows
Efficient use of materials	No shading system
No additional insulation layer	Natural ventilation
Low U-values	Energy consumption of lighting devices
Good wall to windows ratio	Maintenance of the windows
High ceilings	Overheating in summer
Removable part of the floor for technical system	Position of the sensors
Natural ventilation	
No heating / cooling system needed	
Low energy consumption	
Low cost of investment	
Focus on user comfort	

Table 6.3
Building 2226 current state: pros and cons from SWOT analysis.

6.5.2 – Energy consumption

As a paramount step, settings and results of DesignBuilder model were calibrated by comparison to the actual, measured values. Once harmonization between the two outcomes was achieved, some analyses could be performed and some observations could be drawn.

Anyway, two main factors undermined the inherent accuracy of the virtual model:

- unknown behaviour of the occupants, in terms of released sensible and latent heat, amount and management of electronic devices and lights, air

contamination… In this research, the building was considered fully occupied, although the last floor was still currently unoccupied;

- no full software support in recreating the automated systems (CO_2 driven ventilation and lighting devices as heating sources).

Consequently, some discrepancies were identified between simulation and measurements thus preventing a good calibration of the model. For instance:

- simulated energy loads (**figure 6.16**) were found to be 15% lower than measured values; that was not unexpected: in fact, given that future scenarios are likely to consider a fully-occupied pattern, the simulated baseline had to be adjusted accordingly, thereby considering additional internal gains in the overall energy balance, thus reducing the overall consumption charged to the lighting.

  Nevertheless, in order to calibrate the model, a comparison between simulated fully and not-fully occupied (last floor still unutilized for instance) building was performed to highlight the per cent discrepancy. Such corrective factor was then applied to the following simulations thus harmonizing the simulated with the experienced.
- abnormal higher indoor temperatures (due to tropical nights and night ventilation inefficacies) were not recorded in the simulations, neither in the hottest case (summer day, west side - **figure 6.17**) or in the coldest case (winter day, north side - **figure 6.18**).

The main consequence of such difference is the driving force activating air ventilation: for instance, according to DesignBuilder output, CO_2 contamination is the most frequent trigger for natural ventilation in summertime; while, during the on-site monitoring activity, mean air temperature was found to be the pivotal parameter.
However, since all re-design measures have been compared to the fully-occupied model, meaningful information could be retrieved.

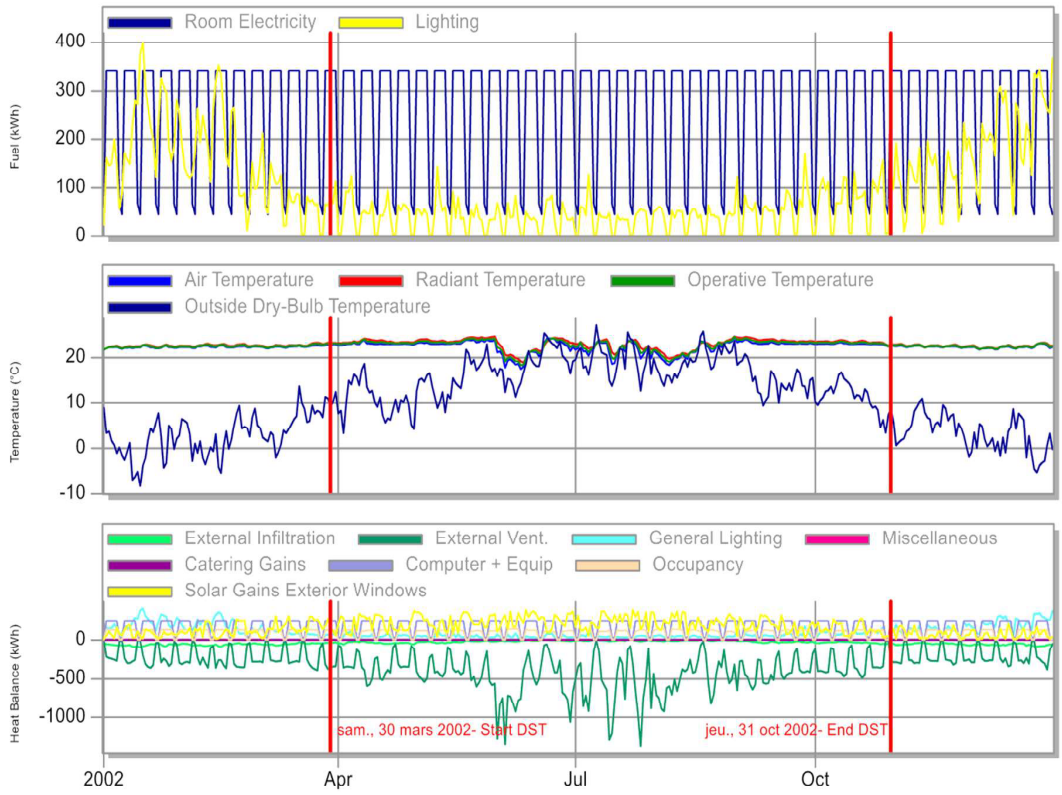


Figure 6.16

Building 2226 current state simulation: daily temperatures and energy loads throughout the year.

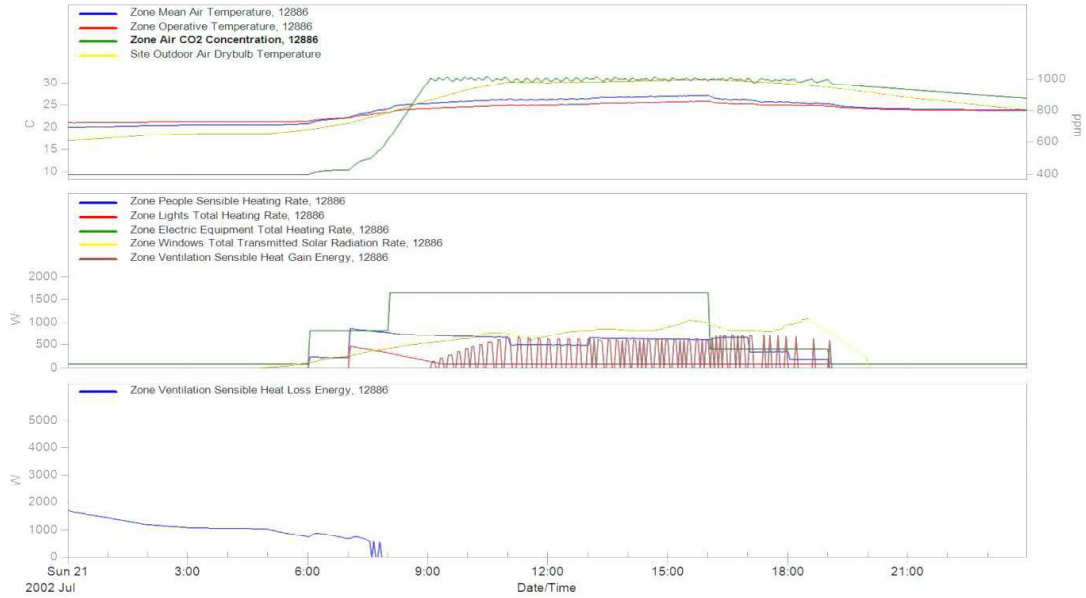


Figure 6.17

Building 2226 current state simulation: indoor temperatures, carbon dioxide levels and heat balance during a summer day in the westhern zone.

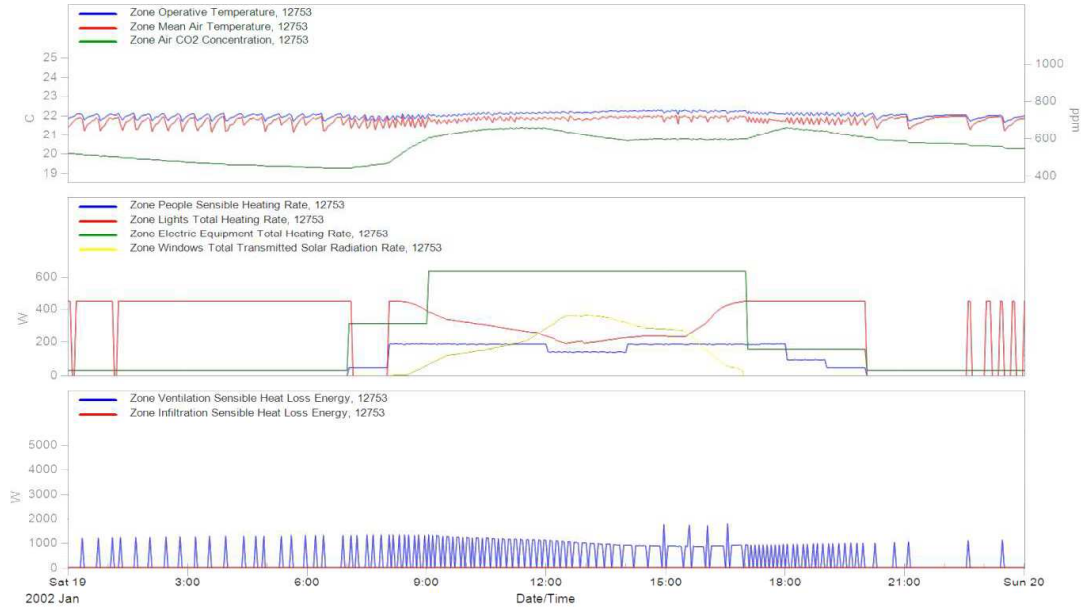


Figure 6.18

Building 2226 current state simulation: indoor temperatures, carbon dioxide levels and heat balance during a winter day in the northern zone.

6.5.3 – Indoor comfort

Comfort is a multi-faceted concept lying on the borderline between objective and subjective spheres. It results from a complex interaction of different variables, coming from the two thermodynamic systems involved, namely the environment and the user.

In the perspective of testing Building 2226 resilience to climate change, only thermal comfort was addressed, and among the tenths of comfort indices proposed in the last five decades, operative temperature was selected as discriminating performance parameter, given its plus point of considering both temperature-driven convective phenomena and solar radiation-driven radiative ones.

Calculation of PMV and PPD was also accomplished (as further output given by Energy Plus simulation engine DOE-2) and discussed.

As for the energy assessment, current comfort level too could be investigated both through on-site measurements of the partly-occupied configuration **[6.24]** and through DesignBuilder simulation of the fully occupied status:

- the former returned the time trend displayed in **figure 6.19**: it is immediately noticeable that the building was able to preserve almost perfectly the indoor temperature within the limits of the comfort zone;
- the latter outlined a very slightly cold sensation, as witnessed by the average value of the PMV (equal to -0,6, corresponding to a PPD of 12%). According to such assessment, building 2226 falls out of the boundaries of category II **[6.25]**.

Anyway, as afore discussed, on-site measurement should be trusted more than simulated results, which cannot account for extraordinary events and cannot provide a truthful reflection of users' lifestyle, adaptive actions and real occupancy. Nevertheless, there is a certain scope for improvement in the recreation of the automatic routines through the simulation software which might be addressed in a subsequent step of the research.

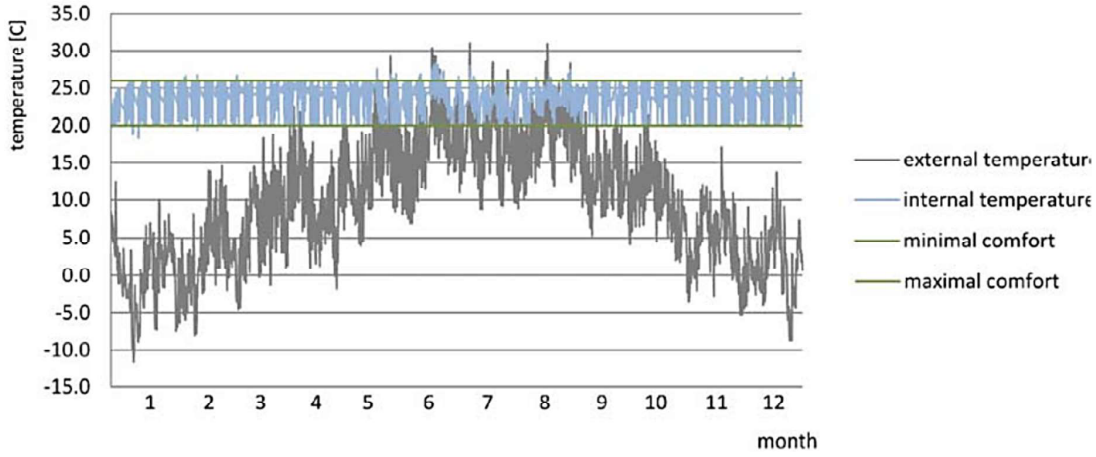


Figure 6.19

Building 2226 current state comfort assessment: indoor and outdoor temperatures time trends, overlapped to comfort limits in order to visualize the frequency of satisfactory environmental conditions.

All things considered, positive conclusions in terms of thermal comfort could be drawn, since the 22-26 target was mostly respected.

6.6 – CLIMATE CHANGE RESILIENT REDESIGN

As abundantly discussed in **chapter 1** and in the **introduction** of the chapter in object, climate change is expected to put to the test most of current building stock, particularly those elements considerably relying on passive techniques to adapt to diverse boundary conditions.

In the specific case of building 2226, the challenge is hidden behind average temperature rise, expected increase of occurrences of heat waves and tropical nights, potential urbanization (and related IAQ, acoustic, sky view consequences). likely increase of occupancy,

Without touching the inherent concept giving life to Eberle's creation, which is the user-centred approach and the limelight on comfort issues, several re-design options were assessed during the last phase of WISBA 2015. Pros and cons of each alternative were highlighted in order to quantify the room for improvement in terms of resilience.

6.6.1 – Problem solving

The overall energy strategy used to provide indoor comfort with no traditional active heating or cooling system, yet giving value to natural ventilation and solar radiation, proved to be a happy choice.
However, sticking to the energy consumption data (**sub-paragraph 6.5.2**), there are some inefficacies about using lighting devices as heating terminals, even when there is no lack of sunlight to compensate.
Fortunately, the low U-values and high thermal mass of the envelope actually preserve a pleasant indoor microclimate in winter, thereby no excessive non-standard use of lights was recorded nor simulated.
Conversely, because of the same reasons, summertime comfort efficacy was frequently imperilled and sometimes corrupted by insufficient release of the stored heat. Besides the absence of any kind of solar shading (except the physical obstruction given by walls' overhangs) gave no chance to control such energy gains.
Obviously, the implementation of shading devices is synonymous to more frequent use of lighting. Such competing effects could paradoxically annul any potential improvement, with the only certain result of increased cost and environmental impacts.
All things considered, it was presumable that building 2226 could maintain a high energy performance in 2050 expected winter time (with mild intervention on heating devices), while summer performance was expected to be strongly endangered by overheating phenomena, empowered in intensity and frequency whichever the chosen future scenario.
In order to reduce indoor temperature fluctuation when outdoor conditions are expected to change in a wider and more hectic way, some rules of thumb might be kept in mind.
A list of the most common strategies to achieve thermal comfort in order of decreasing effectiveness is provided in **table 6.4** [**6.3**].

GOOD PRACTICES TO COPE WITH CLIMATE CHANGE

STRATEGY	REASONS
Windows well shaded and oriented to prevailing breezes in warm weather	Reduction or elimination of air conditioning through good natural ventilation
Exterior wingwalls and planting to divert wind direction up to 45 degrees	Capture of natural ventilation
Door and window openings on opposite side of the building, with larger openings facing up-wind if possible	Facilitated cross ventilation

Ceiling fans or indoor air motion stimulators to be activated on hot days	Decreased apparent temperature by 2.8°C or more, thus less air conditioning needed
Open plan interiors, louvered doors or instead jump ducts if privacy is required	Promotion of natural cross ventilation
Maximized vertical height between air inlet and outlet (open stairwells, two story spaces, …)	Production of stack ventilation even when wind speeds are low
Night ventilation and high mass interior surfaces	Storage of night time freshness (night flushing) to reduce or eliminate air conditioning
Shaded outdoor buffer zones (porch, patio, ...) oriented to the prevailing breezes	Protection from heat entrance through an intermediate environment in summer, extension of living and working areas throughout the year
Plant materials (bushes, trees, ivy-covered walls) especially on the west	Minimization of heat gains (if summer rains support native plant growth)
Window overhangs (designed for the specific latitude) or operable sunshades (awnings that extend in summer)	Reduction or elimination of air conditioning
…	…

Table 6.4
Some guidelines to counteract the deficit in energy performance expected in 2050 scenario.

Accordingly, strategies typically orbited around the key elements of passive design. However, active solutions were not disregarded since a huge potential was connected to the use of renewable energy sources and cutting-edge energy-efficient technologies (green or cool roof, photovoltaics, solar, biomass, and wind-powered cooling technology, co-generation technologies, etc.).
A certain room for improvement was hidden in the material properties too. Therefore, in order to cope with an increase of outdoor temperature, some modifications and alternatives to the original walls composition were tested.

6.6.2 – Comfort oriented redesign

Team A was asked to develop a comfort-oriented and climate change-resilient re-design of Building 2226. Consequently, the key target was identified in equalizing indoor temperature fluctuation.
Such goal could be achieved by playing with two pivotal actors: thermal transmittance and thermal mass of construction components. They define heat resistance, heat storage capacity, decrement and delay of outdoor daily heat wave, which, in turn, determine timing and extent of building's reactions to weather changes.

Indeed, according to EN13786 Standard **[6.26],** thermal mass contribution could be assessed by calculating the following parameters:

- "k1" factor: it measures the ability of the wall to absorb and store the heat carried by indoor air.
- "f" (decrement factor): it reflects the thermal dampening given by the layers of the walls and leading to the reduction in magnitude of the temperature oscillation imposed on one face of the fabric as the heat wave passes through the structure.
- Time lag "s": it defines the time (in hours) the heat wave takes to pass from one side of a structure to the other side.

A graphic representation is given (**figure 6.20**).
While thermal transmittance (U-value) is representative of winter performance (when steady state conditions are reasonably applicable), these three parameters depict summer performance dynamically.

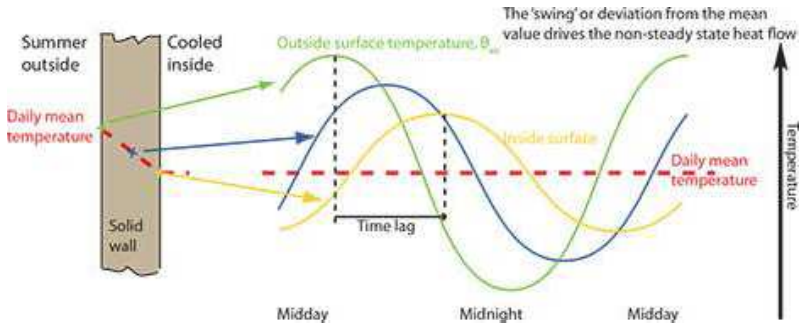


Figure 6.20
Dynamic parameters descriptive of building thermal behaviour.

Keeping in mind that the main threat was overheating, the following list of redesign strategies was conceived:

- reduction of internal heat load: when it comes to energy balance, one of the easiest and most effective ways to cope with excessive indoor temperatures, is to minimize the heat generation inside the building. It could be accomplished by supporting the removal of extra loads and/or reducing the thermal dissipation of the appliances.
  According to the specific issues of building 2226, the suggested interventions were:
  - Vented staircase enhancing chimney effect with the contribution of an external sensing system which improved the internal air circulation:
  - Cool lights because of the heat load reduction connected to their energy efficiency.

Nevertheless, it could be presumed that future technology (particularly in the world of PCs, printers, scanners, etc.) will be oriented to less dissipative devices, thus limiting the contribution of internal sources to indoor thermal dynamics.

- Reduction of solar income: building 2226 suffers of two sun-related issues, which are abundant heat gains and risk of glare. With a window to wall ratio reaching 20%, a properly-designed system of shadings was found to be the only solution to deal with such exacerbation of discomfort phenomena.
  Two redesign options were proposed:
  - mounted blinds, as it was effective both for thermal and visual comfort requirements. Depending on the orientation horizontal and vertical blinds were modelled for the simulation.
  - increased reflectance of the roof, as it filtered the income of solar radiation wavelengths.
- Increase of thermal mass: building materials and their thickness were tuned to find the compositions which could better moderate internal temperatures by averaging outdoor diurnal (day–night) extremes (thus enhancing comfort and mitigating energy costs). The use of even more massive elements was expected to be beneficial throughout the year: in winter, more heat could be stored during the day and released at night, when temperature drops because of nor solar nor internal gains (office building); in summer released heat could be transferred to the cooling breezes introduced inside the building through night ventilation.
  This measure could include both external and internal walls, as well as internal slab, in particular:
  - External walls: two main layer structures were considered for external walls. The first option was to replace the porotherm 38 n+f brick from the inside and exchange it with a denser brick: the porotherm bioplan 40 with which the thermal mass could be increased.
    The second option was a sandwich layer structure, in which the inner brick was the Porotherm 42.5, while the outer layer was built from Ashington Red Multi. In addition, a wooden fibre was put in the structure as heat insulation.
  - Internal walls: the first proposal was to replace the current plaster with clay plaster, as it had a higher density.
    The second option was substituting the bricks with reinforced concrete since it had a 2.5 times higher density than the currently used bricks.
  - Internal slabs: the suggestion was to replace anhydrite with cement based screed in order to increase density and thermal capacity.

6.6.3 – Redesign options

The workflow that led to the proposal and the assessment of the redesign option is represented in **figure 6.21.**
Redesign directions were extrapolated by cross relating SWOT analysis, data coming from ante-WISBA monitoring campaigns and DesignBuilder simulations. Certain strategies were chosen for further investigation: a discriminatory filter was imposed by the dynamic parameters of the components.

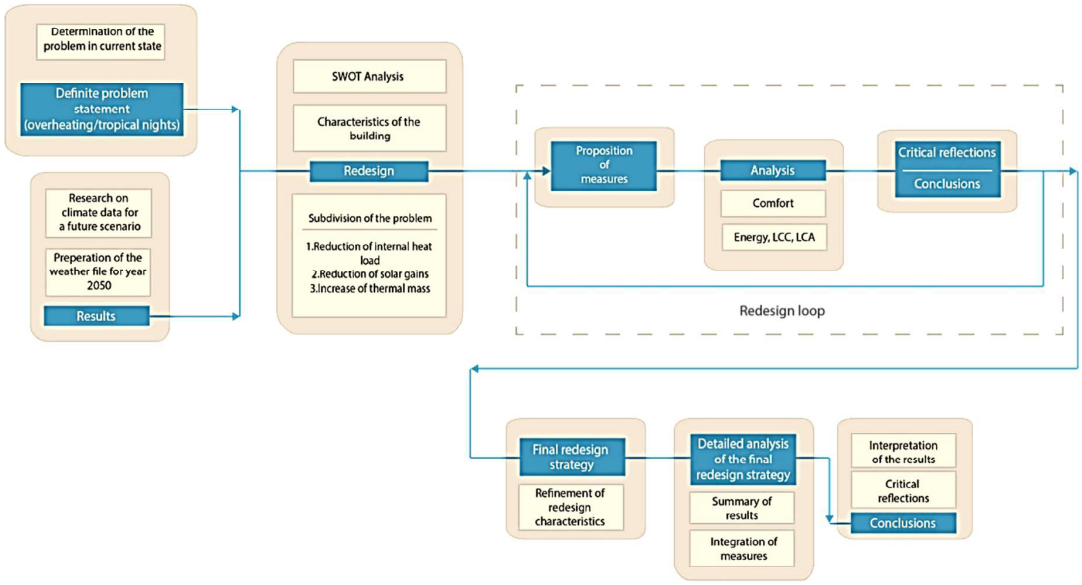


Figure 6.21
Re-design flowchart.

The ultimate redesign measures are summarized in **table 6.5** and represented in **figure 6.22.**

CLIMATE CHANGE SCENARIO – BUILDING 2226 RE-DESIGN			
ELEMENT	**LAYERS**	**THICKNESS**	**THERMAL PROPERTIES**
External wall			
Current state	Lime plastering	10 mm	U-value 0.142 W/m^{2}K Thermal Lag 19.54 hrs Decrement factor 0.0002 k1 dynamic factor 50.9 kJ/m^{2}K
	Porotherm 38 N+F	380mm	
	Cement mortar	18mm	
	Porotherm H.i. 38	380mm	

	Lime plastering	25mm	
Option 1	Lime plastering	10mm	U-value 0.141 W/m^{2}K Thermal Lag 21.87 hrs Decrement factor 0.0001 k1 dynamic factor 53.5 kJ/m^{2}K
	Porotherm Bioplan 40	400mm	
	Cement mortar	18mm	
	Porotherm H.i. 38	380mm	
	Lime plastering	25mm	
Option 2	Lime plastering	10mm	U-value 0.140 W/m^{2}K Thermal Lag 11.56 hrs Decrement factor 0.0014 k1 dynamic factor 58.6 kJ/m^{2}K
	Porotherm 42.5-25/19	425mm	
	Cement mortar	18mm	
	Wooden fiber	180mm	
	Façade brick	88mm	
	White painting		
Inner wall			
Current state	Lime plastering	10mm	U-value 0.717 W/m^{2}K Thermal Lag 10.20 hrs Decrement factor 0.2950 k1 dynamic factor 60.08 kJ/m^{2}K
	Aerated brick	250mm	
	Lime plastering	10mm	
Option 1	Clay plastering	10mm	U-value 0.710 W/m^{2}K Thermal Lag 12.53 hrs Decrement factor 0.2183 k1 dynamic factor 100.17 kJ/m^{2}K
	Aerated brick	250mm	
	Clay plastering	10mm	
Option 2	Lime plaster	10mm	U-value 2.569 W/m^{2}K Thermal Lag 7.49 hrs Decrement factor 0.2480 k1 dynamic factor 240.04 kJ/m^{2}K
	Reinforced concrete	250mm	
	Lime plaster	10mm	
Roof			
Current state	Gravel	60mm	U-value 0.114 W/m^{2}K Thermal Lag 13.98 hrs Decrement factor 0.1042 k1 dynamic factor 277.02 kJ/m^{2}K
	Bitumen sheet	10mm	
	PUR insulation	140mm	
	EPS insulation	140mm	
	Bitumen sheet	10mm	
	Reinforced concrete	240mm	
	Lime plastering	10mm	
Option 1	Reflective membrane	18mm	U-value 0.114 W/m^{2}K Thermal Lag 11.79 hrs Decrement factor 0.1225 k1 dynamic factor 277.07 kJ/m^{2}K
	Bitumen sheet	10mm	
	PUR insulation	140mm	
	EPS insulation	140mm	

	Bitumen sheet	10mm	
	Reinforced concrete	240mm	
	Lime plastering	10mm	
Inner floors			
Current state	Anhydrite screed	50mm	U-value 1.191 W/m^{2}K Thermal Lag 9.37 hrs Decrement factor 0.1510 k1 dynamic factor 41.82 kJ/m^{2}K
	Air layer	10mm	
	Chipboard	24mm	
	Air layer	60mm	
	Reinforced concrete	240mm	
	Lime plastering	10mm	
Option 1	Concrete screed	50mm	U-value 1.72 W/m^{2}K Thermal Lag 10.44 hrs Decrement factor 0.1513 k1 dynamic factor 146.34 kJ/m^{2}K
	Air layer	10mm	
	Chipboard	24mm	
	Air layer	60mm	
	Reinforced concrete	240mm	
	Gypsum plastering	10mm	
Lightning			
Current state	LED lights		
Option 1	Cold lights		
Ventilation			
Current state	Automated ventilation		
Option 1	Improvement of current state with external sensors and chimney effect		
Blinds			
Current state	None		
Option 1	Wooden		
Option	Aluminum		

Table 6.5

Redesign options for building 2226 to face 2050 climate change.


2226 Baumschlager Eberle
SAMPLING DETAILS
Detail 01
Detail 02
Detail 03


Detail 01
WINDOW BLINDS
Mounted Blinds
Depending on the orientation horizontal or vertical
blinds movement mechanism
closed blinds
opened blinds
2226
LUSTENAU
Building Redesign Illustrations



Figure 6.22
Redesign details for window blinds, interior and exterior walls composition.

6.6.3.1 – Comfort-based comparison

The above redesign measures were tested both for current state (2015) and climate change scenario (2050). Assessments focused on Life Cycle Assessment (LCA), Life Cycle Costing (LCC), comfort and energy demand, yet, as preliminarily declared, only the last two perspectives are here presented and discussed, on the basis of DesignBuilder simulations.

The comparison between the different redesign solutions in terms of comfort was not based on Fanger indices as adaptive theory was found to be more representative of Building 2226 inherent concept: PMV/PPD calculations would have imposed restrictive comfort ranges thus underestimating users' thermal tolerance.

An alternative procedure taking into account long term discomfort phenomena was tailored to the specific case. Consequently, comfort performance was estimated by comparing the number of hours (in a year) when the operative temperature exceeded 26°C (the upper limit for Eberle's building). In this way, a meaningful categorization of the different solutions was achieved.

The simulation was made for offices, cafeteria and exhibition area during occupied hours. Discomfort hours were summed up for each zone and then compared:

- 2015: the cumulated discomfort is approximately 1095 hours/year for the whole building. Redesign potential benefits were checked (**figure 6.23**): the replacement of bricks with reinforced concrete in the inner wall structure outperformed the other strategies reducing to a quarter the current cumulated discomfort hours. Second place for the redesign of the inner floor structure, with a total of 515 hours of discomfort (half of the current one). The worst case is given by the vented staircase, hitting the minimum (even if still present) reduction of the discomfort hours (-14%).

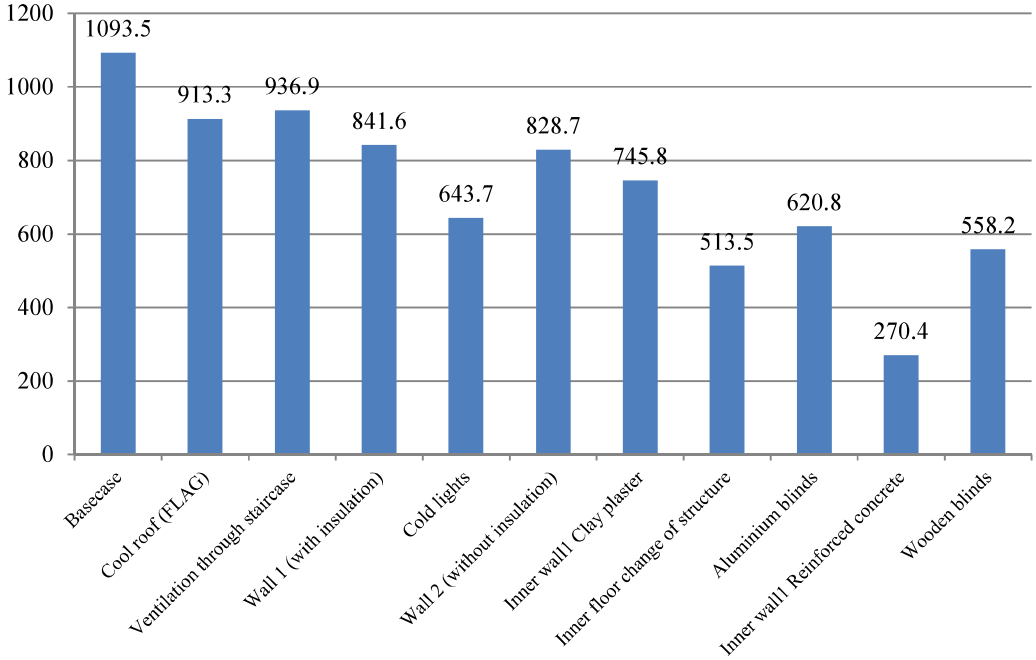


Figure 6.23

Comparison between different redesign options applied to building 2226 in 2015 in terms of accumulated discomfort [h]

- 2050: cumulated discomfort hours soared to approximately 6559 hours/year (six times the amount in 2015). With redesign measured applied (**figure 6.24**), diverse impacts were denoted: the best practise was found to be the use of wooden blinds (-25% hours of discomfort in comparison to the base case), then reinforced concrete in the inner wall structure instead of bricks (- 22% in total), while cool roof, vented staircase, wall with/without insulation and cold lights did not show any appreciable effect (roughly 6100-6200 hours of discomfort, corresponding to an average reduction of 5-6%).

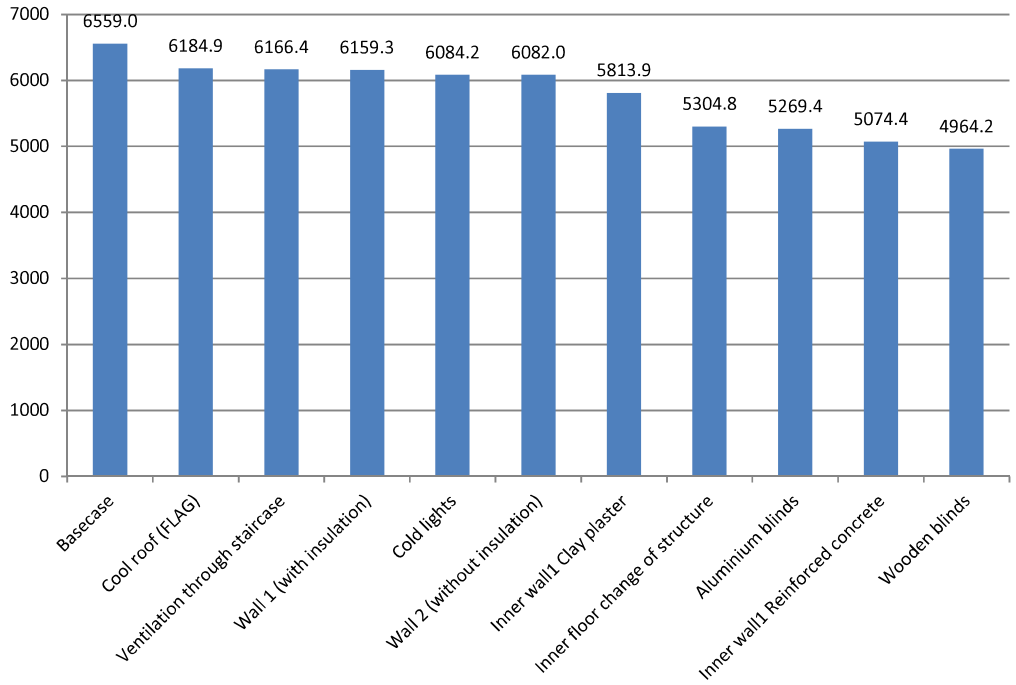


Figure 6.24

Comparison between different redesign options applied to building 2226 in 2050 in terms of accumulated discomfort [h]

A deeper examination revealed that, out of the 24 thermal zones, the south-west oriented one, located on the third floor recorded the worst comfort performance. That could be explained by contemplating two main factors:

- orientation: such area is directly lit by the sun until late afternoon: that is totally detrimental from a comfort perspective since the risk of overheating is emphasized when already heated up building components continue to receive radiation (see **figure 6.25**).
- The story: third floor receives unobstructed sun rays which sum up with higher internal gains (due to occupancy and working appliances).

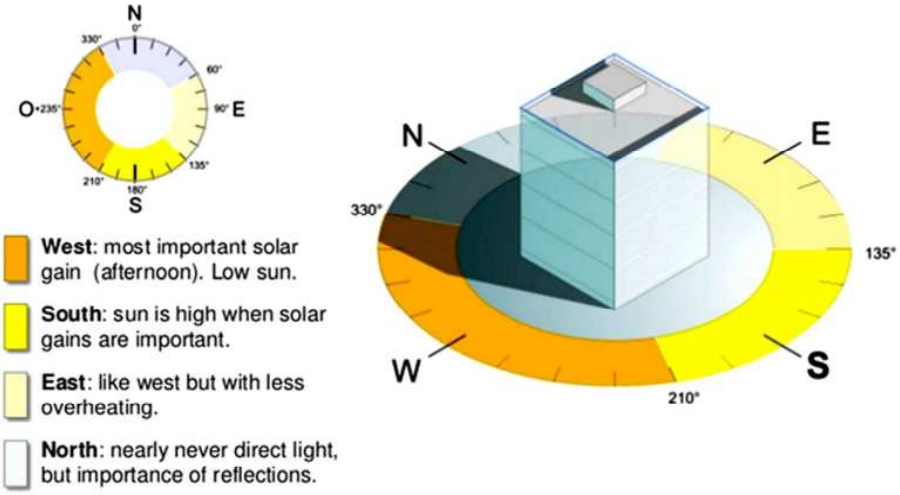


Figure 6.25

Orientation and solar gains [Sapa Building System]

6.6.3.2 – Energy-based comparison

From an energy perspective, the redesign was oriented to better managing the activation of the lighting system.

Accordingly, a 5% energy saving is already shown by comparing the two base cases for 2015 and a warmer (thus less heating-dominated) 2050 (**figure 5.26**).

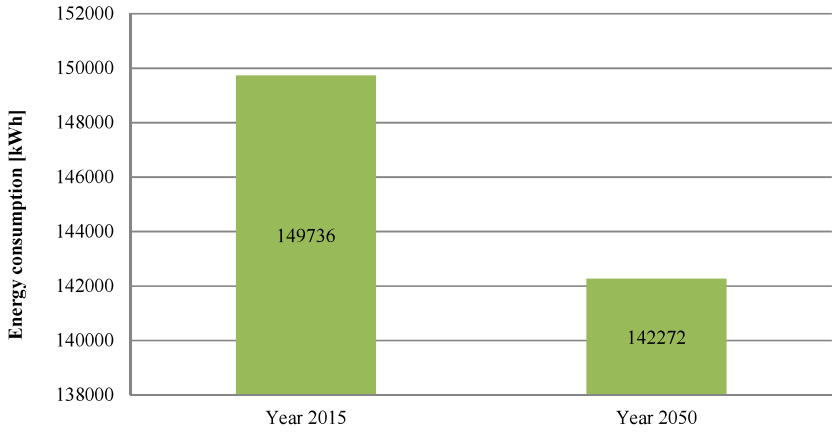


Figure 6.26

Base cases in 2015 and 2050: comparing energy consumptions.

As expected, the redesign options did not contribute significantly to the reduction of the energy consumption as they addressed summer overheating mostly.
More in detail:

- outer walls (**figure 6.26a**): by changing density and thermal capacity of materials composing the layer, the energy benefit was negligible (<2% for wall 1, and <1% for wall 2);
- blinds (**figure 6.26b**): the two typologies (differing in material, thicknesses, conductivity and orientation) were modelled and scheduled to shut as soon as the solar radiation reached a threshold value of 120W/m^2. As expected, the contribution was detrimental in terms of energy consumption (+4% for aluminium blinds, +6% for wooden blinds): by preventing the penetration of the solar radiation, winter performance was imperilled and the use of lights for heating purposes was emphasized;
- inner walls (**figure 6.26c**): in this case the energy benefits were slightly more consistent (3% in 2015 and 2% in 2050);
- roof (**figure 6.26d**): by replacing gravel with a high reflective material, the heat gains from the roof were imperceptibly reduced (less than 1% consumption reduction);
- inner floors (**figure 6.26e**): same negligible energy results as roof by increasing their thermal mass;
- ventilation (**figure 6.26f**): by inserting a new window in the second staircase, the stack effect was activated and a warm updraft rose across the floors. That helped in removing heat from lived zones, yet did not affect energy loads in a significant way (<1% again);
- lighting (**figure 6.26g**): by replacing the existing lights with more efficient solutions (lower heating fraction and higher visible fraction) the energy benefit rose up to 4%. Such percentage is still minimal if considered that this measure directly acted on the source of consumptions.

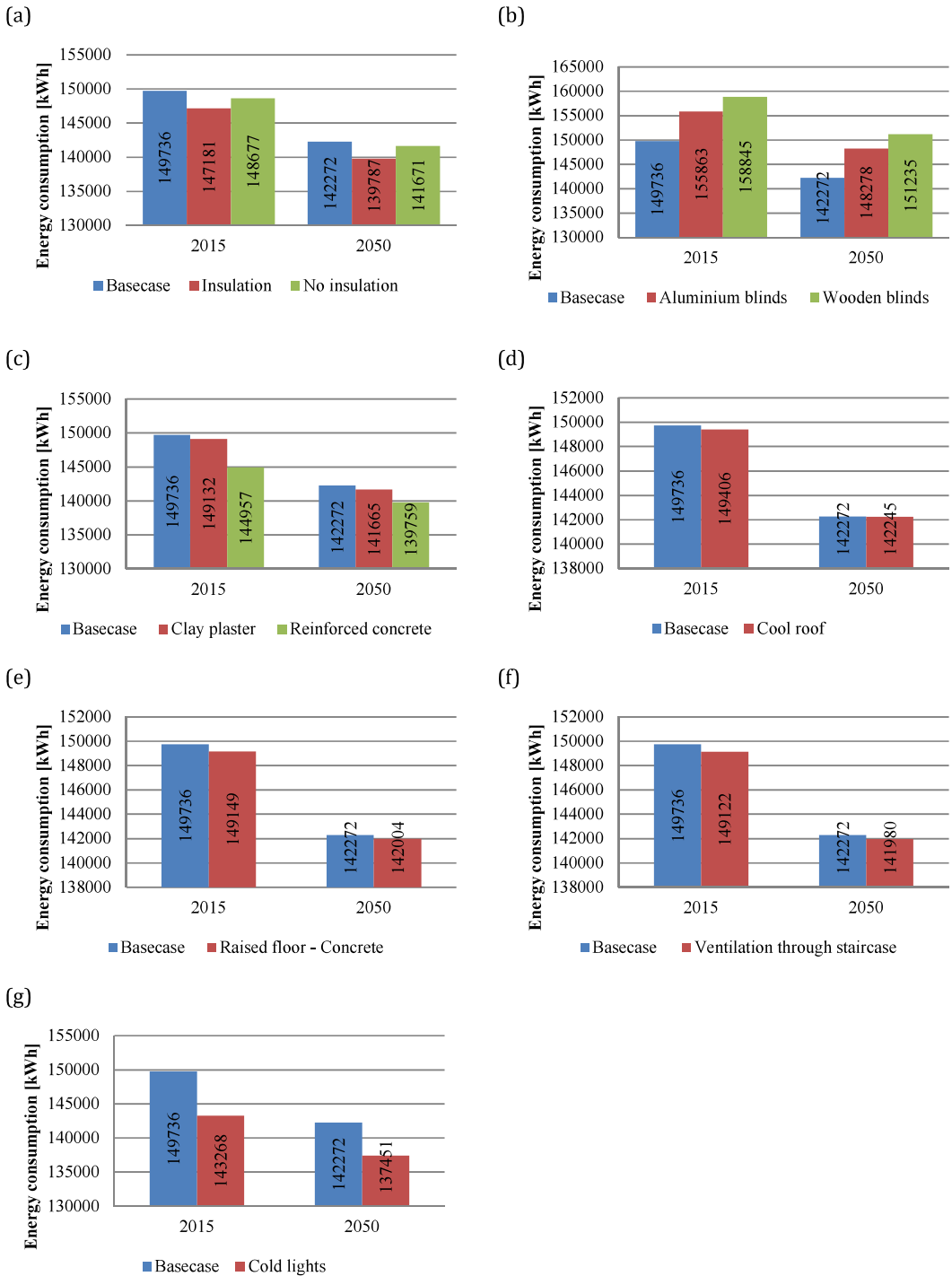


Figure 6.27

Comparing energy consumptions in 2015 and 2050 when redesigning (a) outer walls, (b) blinds, (c) inner walls, (d) roof, (e) inner floors, (f) ventilation, (g) lighting.

All things considered, the redesign options did not lead to noticeable energy impacts, since they come from a comfort-oriented conception. Anyway, the maximum energy saving was achieved by changing lights and replacing the inner wall (3-4% was the simulated room for improvement).
Blinds had the worst drawback (increase of consumptions).

6.7 – FINAL REDESIGN STRATEGY

Comfort issues were pivotal in the design of the ultimate climate resilient solution (**figure 6.28**); energy impact was less sound yet considered as well.
Shading system and air circulation through the staircases led to a significant increase of environmental satisfaction, thereby they were included, even though the other assessment spheres (energy, LCA and LCC) were negatively affected. For instance, wooden blinds were beneficial in terms of comfort and LCA, but detrimental in terms of energy and LCC;
Inner walls replacement with reinforced concrete walls (R.C. Core) led to the same conclusions: comfort was highly improved (that is why such measure was finally implemented), but environmental impacts almost triplicate (LCC and energy consumption were substantially invariant).
External walls were the only ones whose selection was based on LCA and LCC analysis, since all options slightly enhanced discomfort (less than 0,1% impact) and improved all other aspects.
The inner floors and roof renovation were hundred per cent rewarding since comfort was reinforced and the other issues remained almost unaffected.
Table 6.6 recaps the trade-offs/conflicting benefits of the proposed redesign measures in comparison with the current state for the climate change scenario.

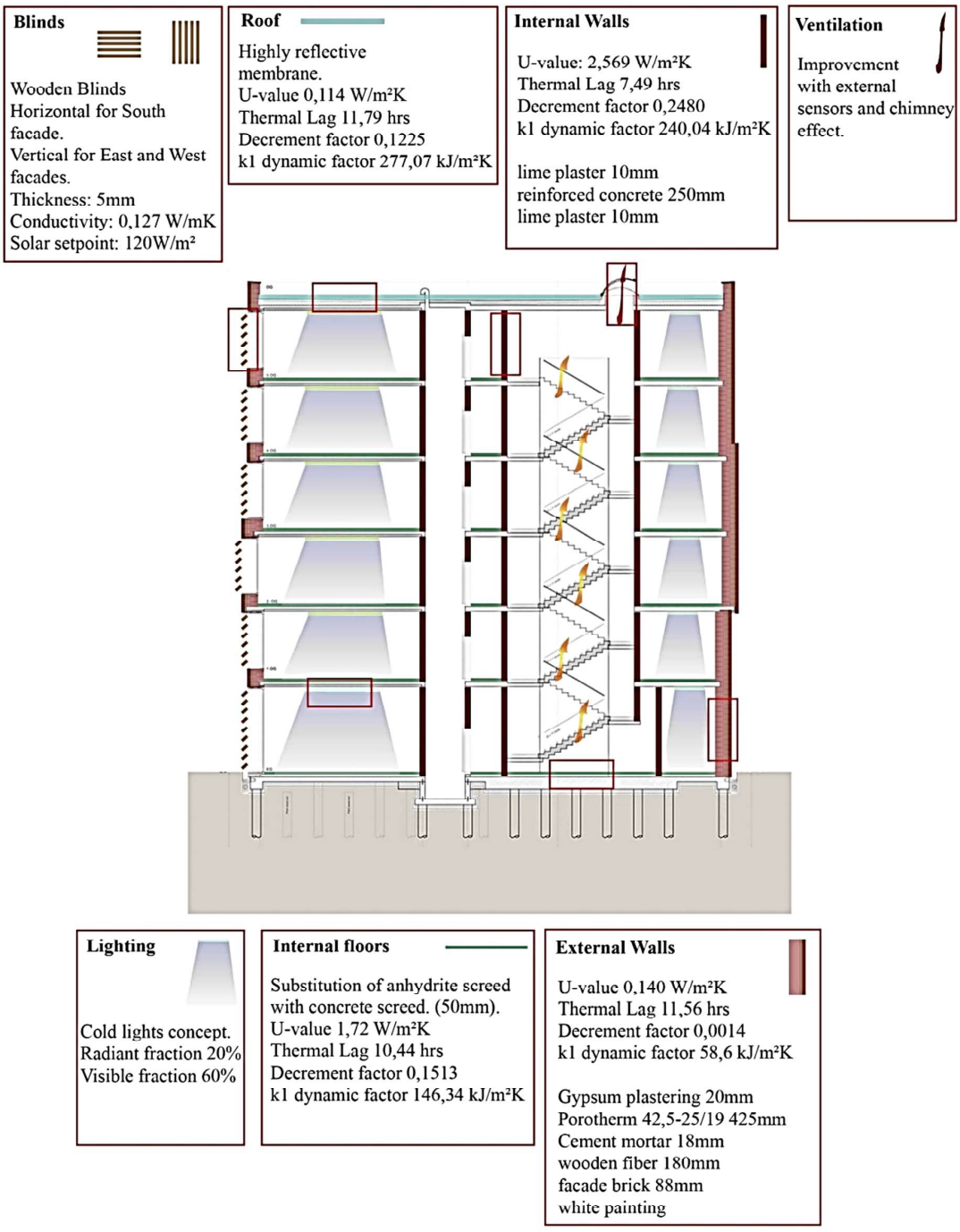
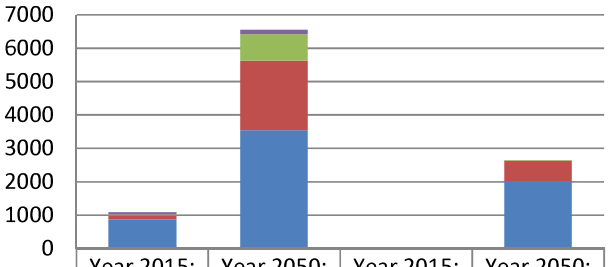


Figure 6.28
Final redesign strategy for climate change scenario.

STRENGHTS AND WEAKNESSES OF REDESIGN STRATEGIES				
Strategy	**Comfort**	**Life Cycle Assessment**	**Energy Consumption**	**Life Cycle Costing**
External wall with insulation	+	-	+	+
Internal reinforced concrete walls	+	-	+	+
Introduction of wooden blinds on the façade	+	-	-	-
Restructuring of inner floors	+	-	+	+
Roof with reflective membrane	+	-	+	+
Cool lighting	+	Not analysed	+	Not analysed
Newly proposed ventilation concept	+	Not analysed	+	-

Table 6.6
Trade-offs of the proposed final redesign measures between current and future scenario.

Such final re-shape of Building 2226 was remarkably promising from a comfort perspective both in 2015 and 2050, thanks to increased thermal mass and reduced solar gains. As a general rule, the impact of combined redesign strategies in 2015 is lower than in 2050 (**figure 6.29**).
In 2015 the most effective redesign strategy is the reinforced concrete inner wall, while wooden blinds was the best practice for 2050 (**figure 6.30**)



	Year 2015: Exisiting building	Year 2050: Exisiting building	Year 2015: redesigned building	Year 2050: Redesigned building
>30°C	0	8.65	0	0
>29°C & <=30°C	62.25	124.5	0	0
>28°C & <=29°C	46.45	799.3	0	17.4
>27°C & <=28°C	109.55	2079.3	0	614.75
>26°C & <=27°C	875.25	3547.2	3.3	2021.3

Figure 6.29
Comfort assessment for the final redesign: discomfort hours in 2015 and 2050

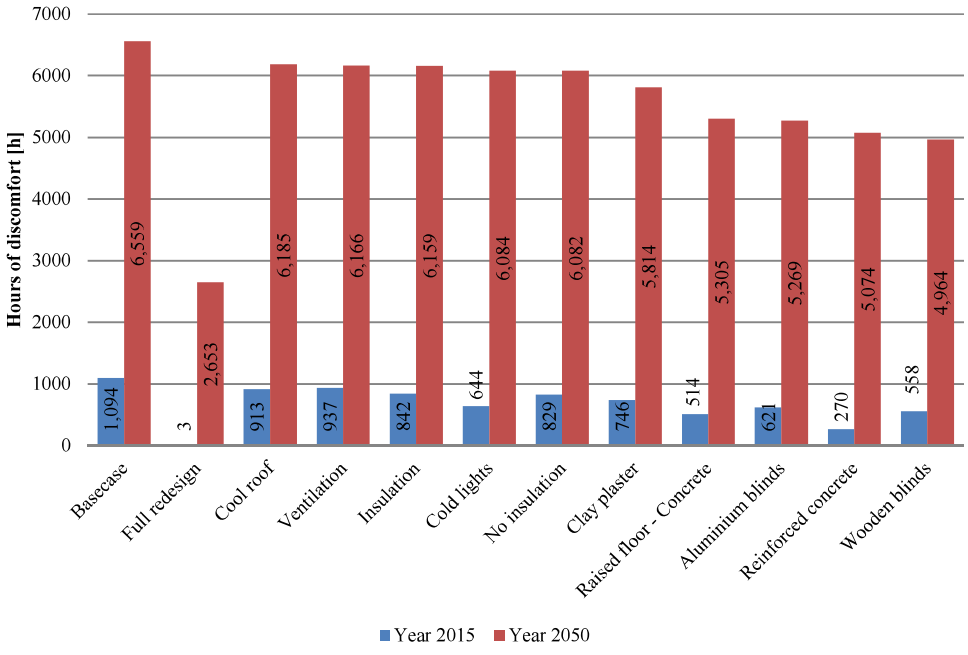


Figure 6.30
Overheating and related discomfort for each chosen redesign strategy: comparing 2015 and 2050 scenarios.

In terms of energy, the climate change scenario actually considered smaller energy demands in 2050. Out of all simulated configurations only the ones involving blinds, cold luminaires, change of structure of inner and outer walls had any, yet shallow impacts on energy use. An interesting finding was that the decrease of heat gains caused by blinds in winter and the consequent need to activate illumination was utterly compensated by the implementation of the other redesign measures (**figure 6.31**).

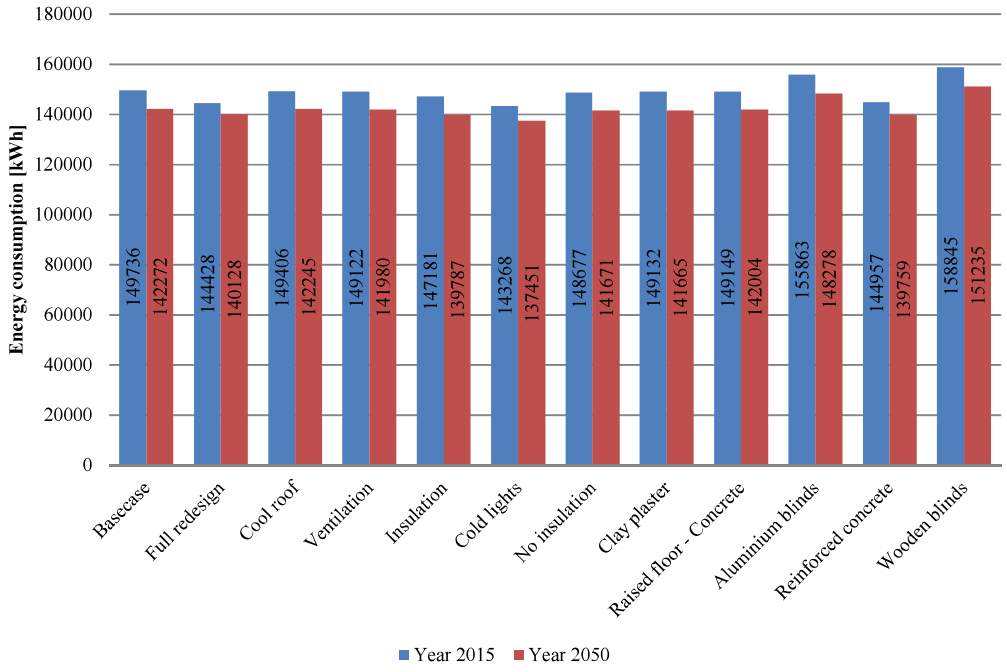


Figure 6.31
Energy consumptions for base and final redesigned case in 2015 and 2050.

6.8 – CONCLUSIONS

Building 2226 goes under the heading of energy efficient building.
Nevertheless, given that decisions made by designers in the present will have tremendous impacts on future economy, society, townscape as well as energy and ecological scenes, a 4-month-long assessment was made on the existing configuration to explore the potential threats and opportunities to cope with 2050 climate change.
The redesign was successful.
The user-centred vision beneath building 2226 conception was maintained: comfort and energy consumptions were selected as decisive aspects, while environmental impact and financial costs were screened to solve controversial choices.
A huge reduction of thermal discomfort was achieved and a slightly, yet present, benefit in terms of energy efficiency was noticed as well for the redesigned building in 2050 compared to the current state.
Conversely, LCA and LCC analyses revealed a higher financial and environmental impact: however, in both cases, the penalty was less than 10%.
Finally, some conclusions could be drawn.
Building 2226 can be improved to be resilient to climate change with low-tech redesign measures, which might lead to twice improved comfort conditions.
Most of the discomfort phenomena occurred for indoor temperatures exceeding the comfort boundary on a maximum of 1° C. Moreover, in naturally ventilated buildings adaptive comfort theory applies **[6.27]**, thereby users can accept higher indoor temperatures. Thus, the obtained result of discomfort hours after the climate change with applied redesign strategies should be reinterpreted as successful.

REFERENCES

[6.1] http://wisba.wienerberger.com/projects/
[6.2] (APCC), A. P. (2014). Austrian Assessment Report 2014 (AAR14). In A. P. (APCC).
[6.3] Climate Consultant 6.0 BETA
[6.4] climate-data.org
[6.5] A. Reilly, O. Kinnane,The impact of thermal mass on building energy consumption, Applied Energy 198 (2017) 108–121
[6.6] K. Gregory, B. Moghtaderi, H. Sugo, A. Page. Effect of thermal mass on the thermal performance of various australian residential constructions systems. Energy Build 2008;40(4):459–65.
[6.7] N Aste, A. Angelotti, M. Buzzetti. The influence of the external walls thermal inertia on the energy performance of well insulated buildings. Energy Build 2009;41(11):1181–7.
[6.8] H.Asan, Numerical computation of time lags and decrement factors for different building materials. Build Environ 2006;41(5):615–20.
[6.9] E. Kossecka, J. Kosny. Influence of insulation configuration on heating and cooling loads in a continuously used building. Energy Build 2002;34 (4):321–31.
[6.10] M.Lj Bojic´, D.L. Loveday . The influence on building thermal behavior of the insulation/masonry distribution in a three-layered construction. Energy Build 1997;26(2):153–7.
[6.11] Childs KW. Appraisal of the m factor and the role of building thermal mass in energy conservation. Technical report, Oak Ridge National Laboratory; 1980.
[6.12] M. Němeček, M. Kalousek, Influence of thermal storage mass on summer thermal stability in a passive wooden house in the Czech Republic,Energy and Buildings Volume 107, 15 November 2015, Pages 68–75
[6.13] H. Johra, P. Heiselberg, Influence of internal thermal mass on the indoor thermal dynamics and integration of phase change materials in furniture for building energy storage: A review, Renewable and Sustainable Energy Reviews Volume 69, March 2017, Pages 19–32
[6.14] 2008 ASHRAE Environmental Guidelines for Datacom Equipment
[6.15] AICCM Interim Temperature and Relative Humidity Guidelines March, 2014
[6.16] A.V. Arundel, E.M.Sterling, J.H. Biggin, T.D. Sterling. "Indirect health effects of relative humidity in indoor environments". Environ. Health Perspect. 65: 351–61. doi:10.1289/ehp.8665351. PMC 1474709. PMID 3709462.
[6.17] C. Eastman, P. Teicholz, R. Sacks, K. Liston. BIM Handbook: A Guide to Building Information Modeling. New Jersey, Canada: s.n., 2008.
[6.18] CEN/TC 442 - Building Information Modelling (BIM)

[6.19] Hosni, M. H., Jones, B. W., Xu, H. Experimental Results for Heat Gain and Radiant/Convective Split from Equipment in Buildings. [Online] 2011. http://www.kcashrae.org/wp-content/uploads/2011/09/Sept-05-Heat-Gain-Split.pdf.
[6.20] Solar, Wholesale. How much power do your appliances us. How to save energy. [Online] http://www.wholesalesolar.com/solar-information/how-to-save-energy/power-table.
[6.21] Saver&Score, Home Energy. Default Energy Consumption of MELs. Home Energy Saver&Score: Engineering Documentation.
[Online] http://hes-documentation.lbl.gov/calculation-methodology/calculation-of-energy-consumption/major-appliances/miscellaneous-equipment-energy-consumption/default-energy-consumption-of-mels.
[6.22] Architectural Record - 2226 Building.
[Online] http://archrecord.construction.com/projects/Building_Types_Study/Office_Buildings/2014/1407-2226-building-baumschlager-eberle.asp.
[6.23] Zumtobel. http://www.zumtobel.com/com-en/index.html. Zumtobel official web page. [Online] 2015.
[6.24] Lars Junghause, PhD. Sustainability and resilience of the 2226 building in Lustenau- What can we learn from the future. Michigan University: s.n.
[6.25] EN 15251:2007, Indoor environmental input parameters for design and assessment of energy performance of buildings addressing indoor air quality, thermal environment, lighting and acoustics, published: July 2008
[6.26] International Organization for Standardization, Geneva, Switzerland. ISO 13786:2007: Thermal performance of building components – dynamic thermal characteristics – calculation methods.
[6.27] R. J. de Dear, G. S. Brager, Thermal comfort in naturally ventilated buildings: revisions to ASHRAE Standard 55, Energy and Buildings 34 (2002) 549–561

7

Urban Heat Island Mitigation

Investigating and comparing the UHI mitigation potential of various technologies via on-site monitoring and urban-scale simulation: a case study in Australia

7.1 – ABSTRACT

This chapter collects the outcomes of one of the major project I took part to during the last year of my Doctorate path, spent as a member of the High Performance Architecture (HPA) cluster at the University of New South Wales (Sydney, Australia), under the lead of professor Mat Santamouris.

An urban heat island (UHI) study was conducted all over the Central Business District (CBD) of Darwin, the capital of the Northern Territory, requested and founded by the local Government, in the frame of a wider program to enhance urban liveability and outdoor comfort, in collaboration with the Bureau of Meteorology (BoM), the CSIRO and the Charles Darwin University. The aim was to counteract the local overheating via appropriate UHI mitigation technologies and solutions.

The target was achieved following a complex and structured roadmap, namely:

- statistical study of Darwin synoptic weather conditions both during the wet and the dry season to identify the dominant synoptic weather conditions and their percent weight over Darwin's typical meteorological year;
- interpretation of the weather data to define the most relevant inputs for the preliminary simulations (worst cases);
- identification of the hot spots and the anomalies in the air temperature distribution to conceive a proper monitoring plan (oriented to the validation of the simulation model);
- ground and aerial monitoring campaign to get on-site collected datasets of the main meteorological parameters and surface temperature;
- comparison between the measured data and those recorded in an "undisturbed" location (BoM airport station) to diagnose magnitude and characteristics of Darwin UHI;
- delineation of the most suitable mitigation strategies, based on UHI sources and local peculiarities;
- simulation of single mitigation measures and combined scenarios (for a total number of thirteen cases);
- detailed evaluation of pros and cons by comparing the distributions of the potential ambient temperature (normalized to standard pressure conditions to harmonize diverse altitudes and scenarios), potential temperature decrease, surface temperature and wind speed.
- gross estimation of the corresponding cost.

Since my personal involvement in the project mostly regarded the monitoring activity, the contents here addressed deal with the UHI diagnosis by means of on-site measurements. A less detailed description of the other operative steps is provided for the sake of comprehensiveness.

7.2 – INTRODUCTION

UHI is mainly provoked by the lack of vegetation, the density of heat sources and the widespread of low albedo materials (such as asphalt, metal roofs and brick pavements) throughout the cityscape.

Several, well established mitigation technologies are currently available, yet each single casuistry needs to be treated in a customized way.

Tropical climates represent a borderline case: averting inverse migration flows and enlivening the attractiveness of the cities in such areas are becoming pressing issues, given the exacerbated and self-empowering phenomena of local overheating and climate change (global warming mostly).

Moreover, the potential benefits of a proper intervention might have a resounding impact on energy and sustainability issues, by reducing the use of the HVAC systems, which does not only mean direct energy saving but even downsizing of the air conditioning plants and higher efficiencies. On top of that, comfort is enhanced even in free running buildings, CO_2 emission is contrasted, photochemical smog at street level is prevented, lighting needs are dampened...

For instance, the replacement of asphalt and concrete with cool materials (high solar reflectance - or albedo - and high thermal emittance) helps contrasting the heat storage within the urban fabric during hot, clear days; and, even though ageing processes affect cool materials' performance, their solar reflectance generally does not drop below 0.5 **[7.1]**.

Alternatively, canopy or street shading can be a valid passive tool when properly designed. They provide physical obstruction to sunlight thus preventing excessive temperatures of the surfaces underneath.

Trees and greenery, throught their daily dew and evaporation cycle (evapotranspiration), control the moisture content in the air and absorb heat, CO_2 and pollutants. Consequently, the overheating in the surrounding microclimate gets mitigated.

A different application of the same principle is that of green walls and green roofs: the plants produce both a cooling and an insultating effect with remarkable benefis in energy needs and peak power demand throughout the year.

Spraying water (sprinklers, fountains, …) is another effective countermeasure since it triggers evaporation. Even though the efficiency is largely affected by type and size of the intervention, they proved to strongly reduce local air temperature.

Combined solutions need to be carefully investigated since they are not synonymous of greater impact.

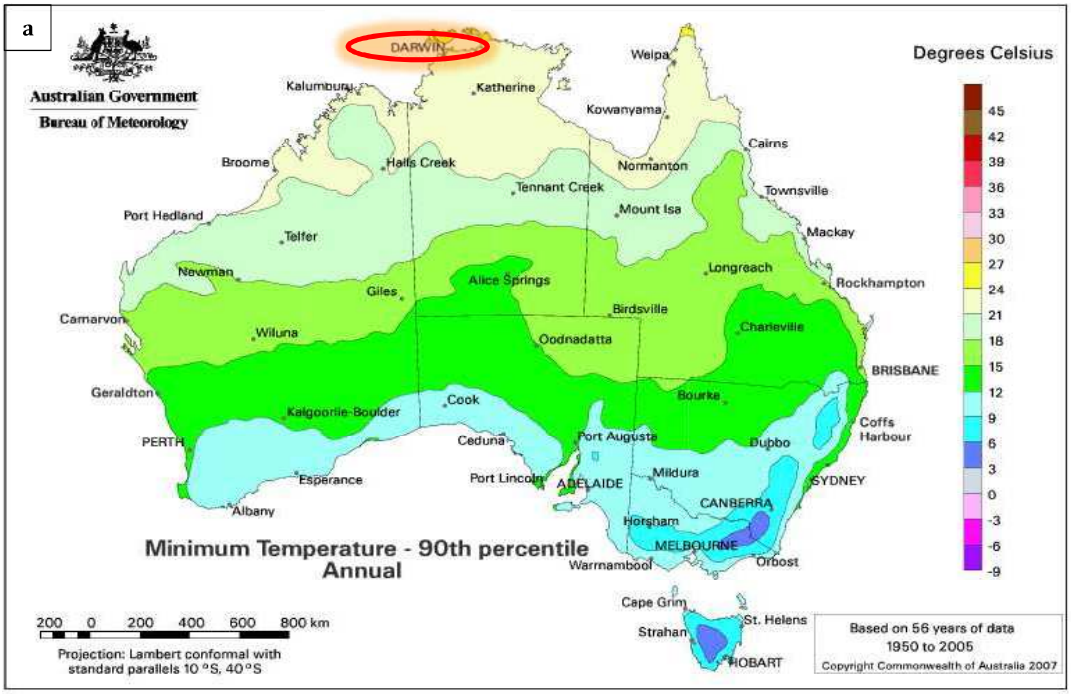
All these scientific findings are summed up by Santamouris et al. **[7.2]** and compared in terms of mitigation potential.

7.3 – DARWIN'S MICROCLIMATE

Darwin is the capital of the Tropical North of Australia. The Köppen Climate Classification subtype is "Aw" (Tropical Savanna Climate), which stands for equatorial, desert conditions.

There is no winter, yet monsoonal dry and wet seasons, with very little temperature variations, easily over 30°C thoughout the year. Moreover, cyclones are not unfamiliar.

F**igure 7.1** collects BoM's (Bureau of Meteorology) maps of annual minimum (**Figure 7.1a**), average (**Figure 7.1b**) and maximum (**Figure 7.1c**) temperature (90th percentile), calculated over a period of 56 years from 1950 to 2005. Darwin's location is highlighted with red circles.



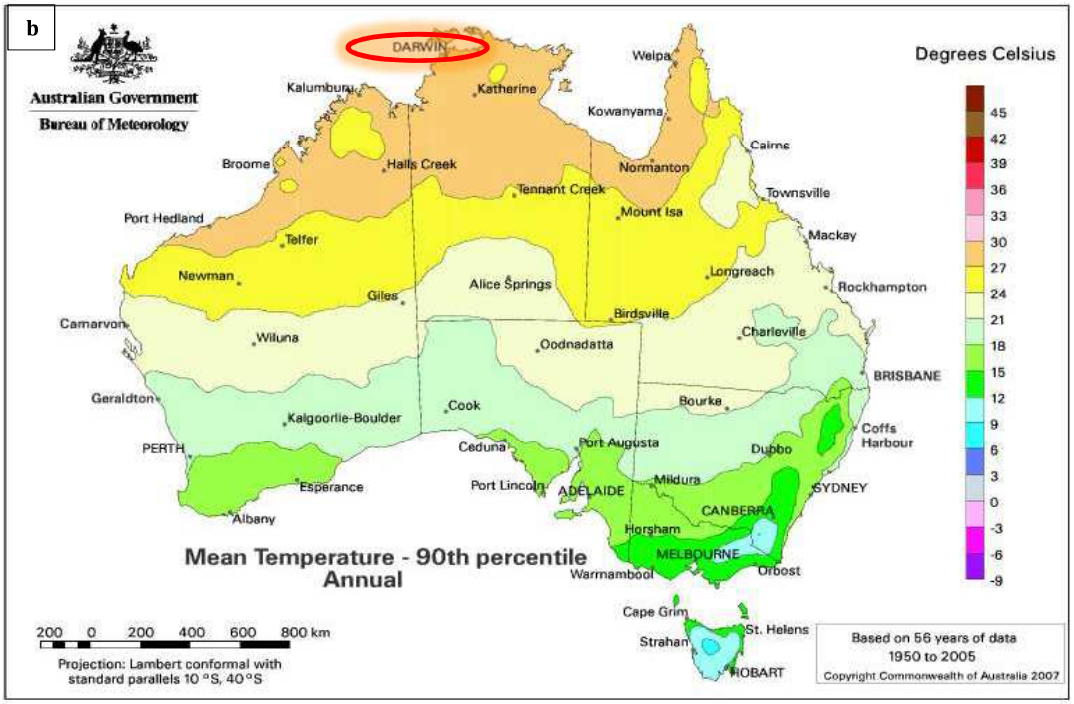


Figure 7.1

Annual temperature 90th percentile distribution over Australian territory – BOM maps of minimum (a), average (b) and maximum (c) values.

The first step in the investigation of Darwin CBD urban heat island was the identification of the most frequent synoptic weather conditions affecting the area.
Accordingly, a preliminary analysis based on clustering techniques was carried out on ambient temperature, relative humidity, wind speed & direction datasets retrieved from the BoM Darwin airport meteorological station and pertaining the period 2006-2016.
Twelve clusters were established in function of temperature, relative humidity and wind direction (four clusters each). Wind was found to be the pivotal parameter: by interpreting its four clusters the following conclusions could be drawn:

- NORTH-WESTERN WINDS: these strong winds (maximum over 15m/s) blow for about the 24% of the year advecting warm air from the desert. The highest temperatures (peak value of 37°C) are thereby recorded within these synoptic conditions. In view of such considerations, convective cooling was expected to be counterproductive since it is responsible for the penetration of warm air through the urban fabric, while evaporative solutions (although placed far from the coast to avoid excessive humidity) were likely helpful. Obviously, whereas wind is the driving force for the temperature rise, its physical obstruction or Venturi-driven divertion was outlined as the most promising mitigation strategy, although more complicated to be applied in a short-term scenario (placement of multi-story buildings, plantation of high trees in the North-West-due "entry door" to the CBD, …). A certain room for improvement was also identified in the use of widespread greenery to exploit local heat dissipation.
- SOUTHERN AND SOUTH-WESTERN WINDS: both temperature and humidity lie steadily on high levels when winds come from the South (22% of the time). As for western winds, the only potentially effective intervention was avoiding urban corridors aligned to these directions and placing heat sinks right at the entrance (which could require less redesign effort) to facilitate the advection of refreshing air.
- NORTHERN AND NORTH-EASTERN WINDS: they account for the 24% of the yearly conditions and represents the "best case". The city is mostly cooled by a certain, yet weak, sea breeze and maximum temperature do not overtake 36°C. Humidity remains high, touching saturation conditions sporadically. This is the only synoptic condition suitable for cooling convective solutions: thereby the highest facades, the narrowest corridors and the lowest pressure zones should be oriented accordingly.
- SOUTHERN AND SOUTH-EASTERN WINDS: these are the prevailing conditions (30%) and fortunately are linked to the lowest average temperature (even though maximum values still reach 37°C) and relative humidity (seldom

approaching 100%). The underlying reason is the cooling action exerted by the national parks bordering the southern parts of the city. Here, convective cooling reaches its highest potential, thus urban openings to natural ventilation were contemplated, particularly for the south-eastern zones of the CBD.

Quantitative details of each cluster are provided in **table 7.1** and were used to define the input data to the simulation software (ENVI-met V4.1.2).

DARWIN SYNOPTIC CONDITIONS (MEAN VALUES)			
Annual incidence [%]	**Average Ambient Temperature**	**Average Relative Humidity**	**Average Wind Speed**
WINDS FROM NORTH-WEST			
24	29.4°C	67%	4.7m/s
WINDS FROM SOUTH/SOUTH WEST			
22	27.7°C	77%	4.1m/s
WINDS FROM NORTH AND NORTH-EAST			
24	27°C	71%	3.4m/s
WINDS FROM SOUTH EAST AND SOUTH			
30	25.3°C	66%	4.1m/s

Table 7.1
Darwin climate specs categorized via clustering technique.

7.4 – CURRENT STATE SIMULATION

The weather data were used to build up the model of Darwin's urban environment and run the simulations. Since their interpretation was fundamental for the proceeding of all the project, some of the results and some information around the model and the boundary conditions are mentioned in this paragraph. No detailing is provided for the sake of intellectual honesty (I was not directly involved in this step of the project).

ENVI-met was used as software platform to perform the simulations: it is a three-dimensional numerical micro-climate model used to recreate the interactions among surfaces, plants and air in urban scale **[7.3].** Together with the post-processor tools included in its setup package (LEONARDO 2014, BioMet), it is used to investigate how cities microclimatic specifications affect human thermal comfort and to predict how it will be affected, in turn, by climate change **[7.4].**

Against this framework, two main sets of simulations were run according to the prevailing wind directions and the aftermaths in terms of local warming:

- North-West wind was investigated as worst case, since such cluster is the one showing the highest levels of average ambient temperature;

- South-East wind is the positive counterpart, since it corresponds to the lowest average ambient temperature.

In order to quantify the contribute of convective ad advective phenomena, two speeds were selected and tested:

- 5m/s to account for the average wind speed, recorded almost throughout the year;
- 1m/s to check on a low-dynamic condition which was expected to be detrimental in terms of apparent temperature and pollutants stagnation.

The simulations were run in summertime at the hottest hour of the day (2pm) and selecting the day with the highest average temperature.

The model was 780m x 1390m x 179.68 m: twice the height of the tallest building was applied to meet the recommendations for a proper use of the software. The spatial resolution was set to 6m horizontally and 0.5m vertically with a telescoping grid increase factor of 20% (to properly account for edge effects).

Urban fabric was modelled according to standard albedo values suitable for Darwin CBD, namely: 0.2 for roofs, walls and pavements, 0.05 for asphaltic materials, 0.15 for loamy soil.

The vegetation was represented by trees 15m tall, very dense foliage, distinct crown layer, and grassy areas, 20cm tall, with average density.

Once the simulations were completed, a series of chromatic-scale representations of the main environmental parameters was retrieved: ambient temperature and surface temperature - which were the key parameters to plan the subsequent monitoring campaign – are mapped in **Figure 7.2** and **Figure 7.3**, extracted from the official report **[7.5]**.

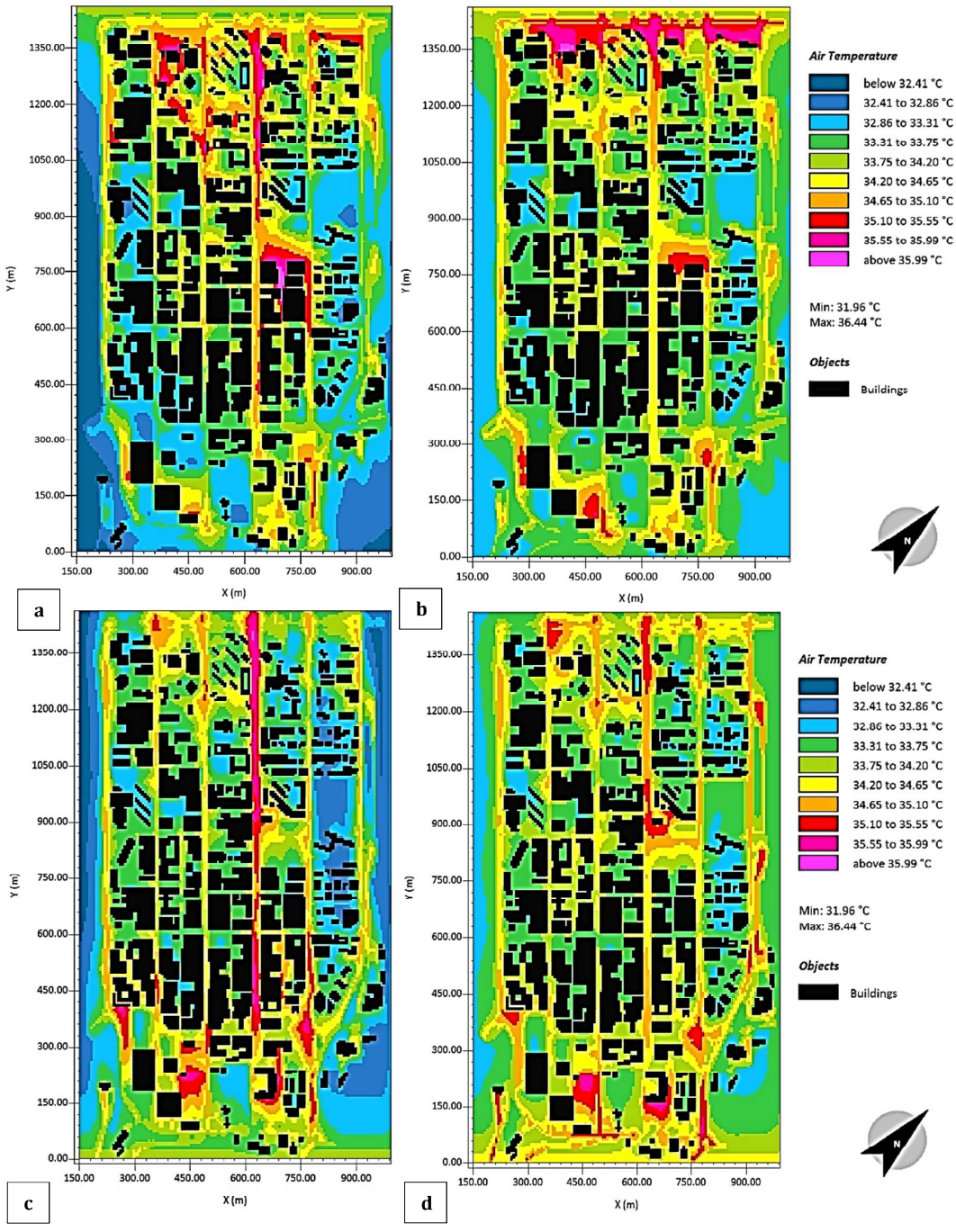


Figure 7.2
Ambient temperature distribution for Darwin reference model in summer, 2pm, with winds blowing from: (a)NW at 5m/s, (b) NW at 1m/s, (c) SE at 5m/s and (d) SE at 1m/s.

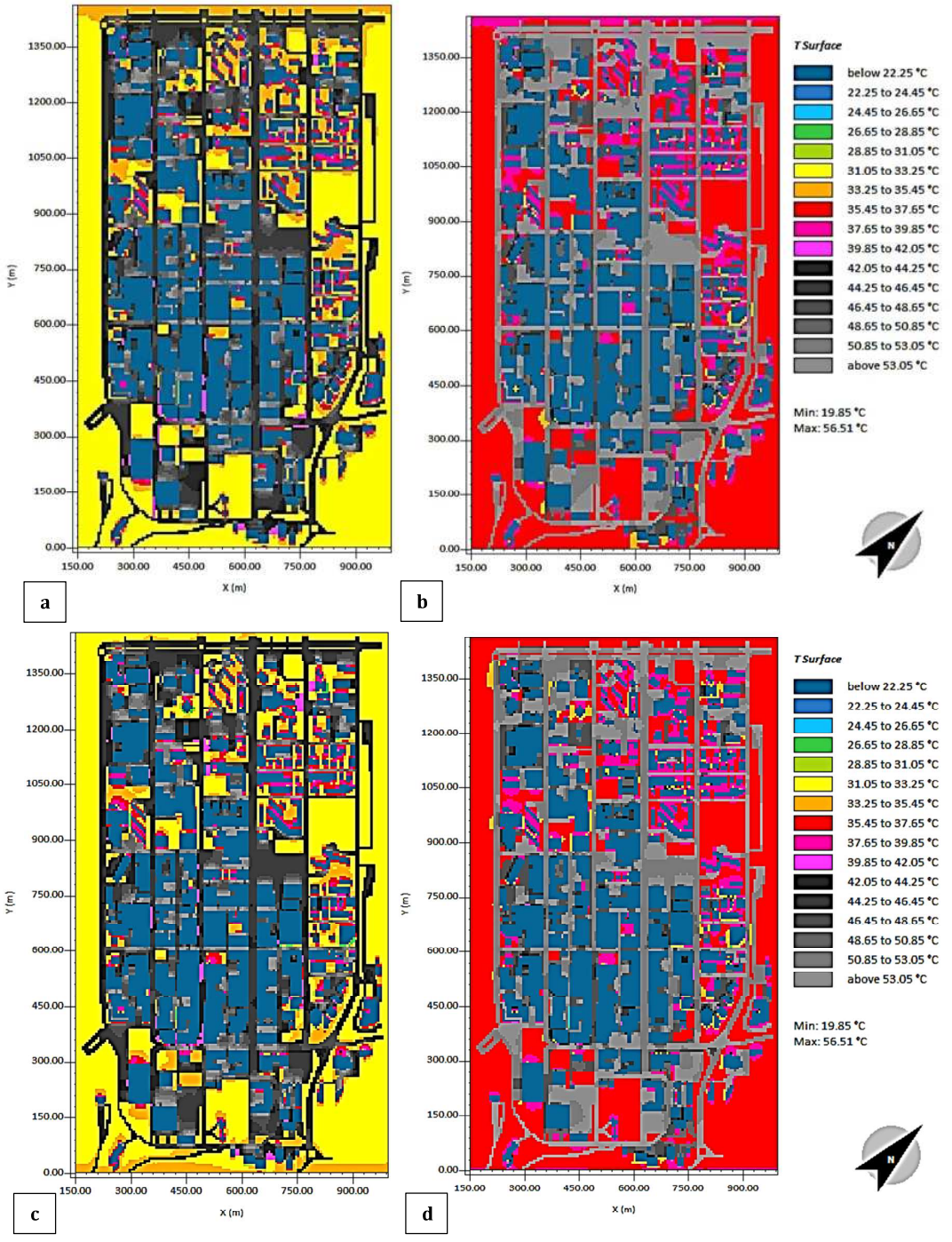


Figure 7.3
Surface temperature distribution for Darwin reference model in summer, 2pm, with winds blowing from: (a)NW at 5m/s, (b) NW at 1m/s, (c) SE at 5m/s and (d) SE at 1m/s.

At this stage, some conclusions were drawn both for air temperature and surface temperature. About the former:

- north-westerly winds, blowing at 5m/s were found to be responsible of the highest ambient temperature and the wider distribution of hot spots: thereby convection was deemed to exacerbate UHI since it encouraged massive hot air flows to pervade the urban fabric;
- ambient temperature at street level ranged between 31.9°C and 36.4°C;
- parking lots were found to be local heat concentrators;
- the main vertical streets acted as heat corridor, reinforcing winds momentum and thereby stimulating the penetration of the heat carried by the airflow;
- the horizontal streets, acting as entry doors for the north-westerly winds, are similarly affected by a considerable air temperature increase.

More detailed information about ambient temperatures in the different base cases are provided in **table 7.2.**

SUMMARY OF PREMILINARY SIMULATION RESULTS				
Darwin CBD Reference scenario	**Wind direction** NW		**Wind direction** SE	
Parameters	**Wind Speed**			
	5 m/s	**1m/s**	**5 m/s**	**1m/s**
Maximum Ambient Temperature	36.44°C	36.08°C	36.00°C	35.72°C
Minimum Ambient Temperature	31.96°C	32.84°C	32.04°C	32.97°C

Table 7.2

Statistics on temperatures for the reference scenario.

Similar findings (yet not equal, particularly about wind role) were achieved by perusing surface temperature maps (**Figure 7.3**):

- larger streets and parking lots showed the highest surface temperature because of longer periods of direct exposure (higher sky view factor) and the thermo-optical properties of the asphalt material: more in detail, asphaltic car parks and pavements reached surface temperatures of about 56.5°C when the wind blew from North West at a speed of 1m/s.
- A rule of thumb was found in the surface temperature distribution: it lowered when wind speed increased (unlike ambient temperature): accordingly, the maximum values were 55.60°C for 5m/s NW wind and 55.82°C for 5m/s SE wind; whilst 56.51°C and 56.26°C were the corresponding thresholds when the wind speed went down to 1m/s (NW and SE direction respectively)

The investigation of the reference scenario served the double purpose of getting an insight into the current situation in the city of Darwin (under two wind speeds and prevailing wind directions during summertime) and of planning the proper roadmap for the subsequent monitoring phase.
The results were then used as baseline to calculate the potential temperature decrease achieved by applying each mitigation technology (and some combos) and outline the best practice.

7.5 – MONITORING CAMPAIGN

The conjunction of increased absorption of solar radiation and heat storage, reduced heat losses, weakened air circulation, entrapped infrared radiation and higher anthropogenic heat gives birth to the heat island effect and to all the consequent drawbacks on energy consumption, outdoor comfort, health and economy.
No one-fits-all approach is feasible to counteract UHI **[7.6].** Each mitigation strategy, to be fully effective, has to be customized in order to address the right sources with impacting countermeasures.
Against this background, both aerial and terrestrial monitoring campaigns were carried out all over Darwin CBD area (**Figure 7.4**): a drone equipped with an infrared camera was used to measure the surface temperature, while a mobile mast equipped with several meteorological probes recorded ground-level climatic data.

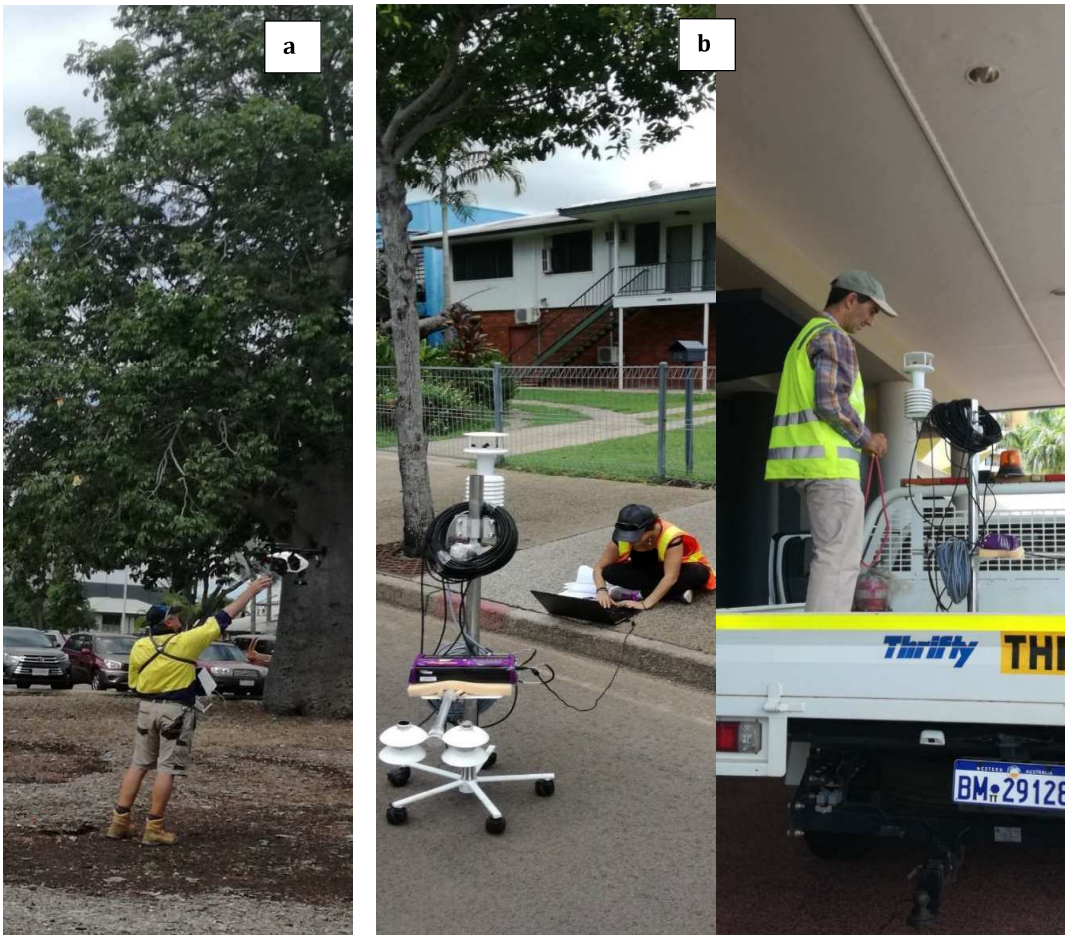


Figure 7.4
Darwin CBD monitoring campaign asset: (a) aerial survey by pilot Aaron Emmett (NT National Drones); (b) terrestrial survey by PhD candidates Giulia Ulpiani and Jonathan Fox.

By capturing aerial thermal shots and videos it was possible to characterize the materials composing the urban fabric and get the dimension of their weight on local weather conditions.
By detecting the local microclimatic parameters all along the hot spots of the city and the topographically strategic areas (according to the afore description of the prevailing synoptic conditions) it was possible to validate the results given by the preliminary model and gain more insight into the UHI inner workings.
The resulting database was used as scientific basis for planning and assessing ad-hoc conceived mitigation strategies.

7.5.1 – Monitoring plan

Based on the temperature maps simulated with ENVI-met, a structured plan to monitor all crucial points was conceived, considering both proper timing and priority targets (summarized in **table 7.3**).

UNSW, National Drones and local traffic management (Akron Group NT - Traffic Control Services) liaised to better coordinate the entire procedure in a time span of 3 days (from the 23rd to the 25th of March 2017).

It should be stressed here that approximately one month I spent in Australia was dedicated to pass all the examinations to get the relevant licence to fly remotely piloted aircrafts (RePL), released by the responsible Australian body (Civil Aviation Safety Authority – CASA) in order to be officially cleared to control UAVs (Unmanned Aerial Vehicles, drones) and be second in charge to the appointed pilot.

All the operations were conducted in full compliance of legal and good judgement-driven directives, thus respecting priorities and weather favourable conditions.

DARWIN CBD MONITORING CAMPAIGN	
TARGET PRIORITY SCALE	
1) MAIN VERTICAL STREETS	
TARGET	**SIDE NOTES**
Cavenagh St.	length 1.5 m - from Daly St. to Bennett St.
Woods St.	from Daly St. to Bennett St.
Michelle St.	mostly Daly st.side
Smith St.	mostly Daly st. side
Esplanade	mostly Daly st.side
2) PARKING LOTS	
TARGET	**SIDE NOTES**
P1	Cavenagh St. parking lot next to Australian Post Office
P2	all the area parking lots between Michelle St. and Cavenagh St., 260mX133m area in front of the petroleum stations
P3.1	130mx240m area between Woods and McMinn St.s, Daly St. as superior boundary
P3.2	parking lot along McMinn St. in front of McLachlan St.
P3.3	parking lot along McMinn St. in front of Manton St.
P4	parking lots in front of Supreme Court of the NT, Darwin City Library and NT Local Court
3) MAIN HORIZONTAL STREETS:	
TARGET	**SIDE NOTES**
Daly St.	length 800m
McLachlan St.	if deemed significant, in view of previous targets results
Lindsey St.	if deemed significant, in view of previous targets results
Knuckey St.	if deemed significant, in view of previous targets results
Bennett St.	if deemed significant, in view of previous targets results
DATA PRIORITY SCALE	
surface temperatures and meteo data along the streets	

surface temperatures of the pavements
surface temperatures and meteo data of parking lots (and asphaltic areas)
surface temperatures of the roofs (where compatible with the risk assessment and mitigation strategy)

Table 7.3
Darwin CBD monitoring campaign plan.

7.5.2 – Aerial survey

UAV technology has recently been widely adopted in the world of photography and filmography (by mounting a gimbal system to support digital and/or thermal cameras), because of its ability to capture aerial shots and videos thus sourcing information where traditional techniques tend to fail.

In the framework of Darwin project, the main goal behind conducting an aerial survey was to get immediate and wide overviews of surface temperature distributions, with the final aim of characterizing the different materials composing the cityscape to disclose their role in the CBD's UHI phenomenology.

The same methodology was recently applied by Gaitani et al. **[7.7, 7.8]** to map urban thermal properties.

7.5.2.1 Instruments and methods

The technical specifications of the employed equipment are summarized in **table 7.4** (drone specs) and **table 7.5** (thermal camera specs).

DRONE - DJI INSPIRE 1	



GENERAL SPECS	
Model	T600
Weight	6.27 lbs (2845 g, including propellers and battery, without gimbal and camera) 6.76 lbs (3090 g, including propellers, battery and Zenmuse XT)
GPS Hovering Accuracy	Vertical: ±1.64 feet (0.5 m) Horizontal: ±8.20 feet (2.5 m)
Max Angular Velocity	Pitch: 300°/s Yaw: 150°/s
Max Tilt Angle	35°
Max Ascent Speed	16.4 ft/s (5 m/s)
Max Descent Speed	13.1 ft/s (4 m/s)
Max Speed	49 mph or 79 kph (ATTI mode, no wind)
Max Wind Speed Resistance	10 m/s
Max Flight Time	Approx. 18 min
Motor Model	DJI 3510H
Propeller Model	DJI 1345T
Max Takeoff Weight	7.71 lbs(3500 g)
BATTERY TECHNICAL DETAILS	
Name	Intelligent Flight Battery
Model	TB47
Capacity	4500 mAh
Voltage	22.2 V
Battery Type	LiPo 6S
Energy	99.9 Wh
Net Weight	570 g

Table 7.4
DJI Inspire 1 technical details.

THERMAL CAMERA - ZENMUSE XT



GENERAL SPECS	
Dimensions	103 mm x 74 mm x 102 mm
Weight	270 g
Thermal Imager	Uncooled VOx Microbolometer
FPA/Digital Video Display Formats	640 × 512 336 × 256
Analog Video Display Formats	720 × 480 (NTSC); 720 × 576 (PAL)
Pixel Pitch	17 µm
Spectral Band	7.5 - 13.5 µm
Full Frame Rates	640 × 512 : 30 Hz (NTSC) 25 Hz (PAL) 336 × 256 : 30 Hz (NTSC) 25 Hz (PAL)
Exportable Frame Rates	7.5 Hz NTSC; 8.3 Hz PAL
Sensi ivity (NEdT)	<50 mK at f/1.0
Scene Range (High Gain)	640 × 512 : -13° to 275°F (-25° to 135°C) 336 × 256 : -13° to 212°F (-25° to 100°C)
Scene Range (Low Gain)	-40° to 1022°F (-40° to 550°C)
Spot Meter	Temperatures measured in central 4×4
File Storage	Mic o SD Card
Photo Format	JPEG, TIFF
Video Format	MP4
ENVIRONMENTAL SPECS	
Operating Temperature Range	14° to 104°F (-10° to 40°C)
Non-Operating Temperature Range	-22° to 158°F (-30° to 70°C)
Temperature Shock	5°C/min
Humidity	5% to 95%
GIMBAL TECHNICAL DETAILS	
Angular Vibration Range	±0.03
Mount	Detachable
Controllable Range	Tilt : +35° to -90°; Pan : ±320°; Roll : ±15°
Mechanical Range	Tilt : +45° to -135° Pan : ±320° Roll : ±45°

Max Controllable Speed	120°/s
IMAGE PROCESSING & DYSPLAY CONTROLS	
NTSC/PAL (field switchable)	yes
Image Optimization	yes
Digital Detail Enhancement	yes
Polarity Control (black hot/white hot)	yes
Color & Monochrome Palettes (LUTs)	yes
Digital Zoom	640 × 512 : 2x, 4x, 8x 336 × 256 : 2x, 4x

Table 7.5
Zenmuse XT thermal camera technical details.

When it comes to UAV management, all operations have to be planned in the safest possible way to preserve the drone structural integrity, avoid injuries to people and damages to properties.
All the potential issues have to be outlined in the risk assessment and means of mitigation have to be provided accordingly.
In the peculiar case of hovering over urban areas, several and redundant precautions must be taken in order to get CASA's approval.
As a first step, the task was appointed to an acknowledged pilot, boasting a standard area approval to operate within 3 nautical miles of Darwin International Airport (pilot Aaron Emmett, National Drones). A second pilot (the undersigned) was contemplated too.
Secondly, a strategy was set to meet CASA's regulations upon "populous areas" (min 30m distance from people not belonging to the briefed crew) and hazardous operation rules (CAST 101.055 **[7.9]**). Therefore, all monitoring operations were conducted:

- in parallel with traffic management and temporary closing of footpaths;
- with the collaboration of spotters whenever the line of sight was obstructed;
- around times od low vehicular and pedestrian hustle and bustle;
- straight over uninhabited bordering areas and mainly over parking lots (secured ex ante).

Since not the entire CBD could be patrolled (given CASA's prohibitions), oblique images were captured as well in order to help rebuild the "grey areas" in between take-off points.

The area overflown – on the 23rd of March 2017 (all the day long) and over the morning of the 24th of March 2017 - is displayed and codified in **Figure 7.5.**



Figure 7.5
Darwin aerial monitoring campaign – thermal shots strategic roadmap.

7.5.2.2 –Outputs

DJI FLIR Zenmuse XT returns radiometric greyscale shots and videos: both were taken during the monitoring campaign in object.

The raw thermal images were originally captured assuming the ideal behaviour of "black bodies": in order to get the energy fraction really irradiated by the urban materials (and so their real surface temperature), specific emissivity values for Australian cities landscape **[7.10]** were adopted.

A couple of examples among the hundreds of thermal shots collected and corrected are displayed in **Figure 7.6.**

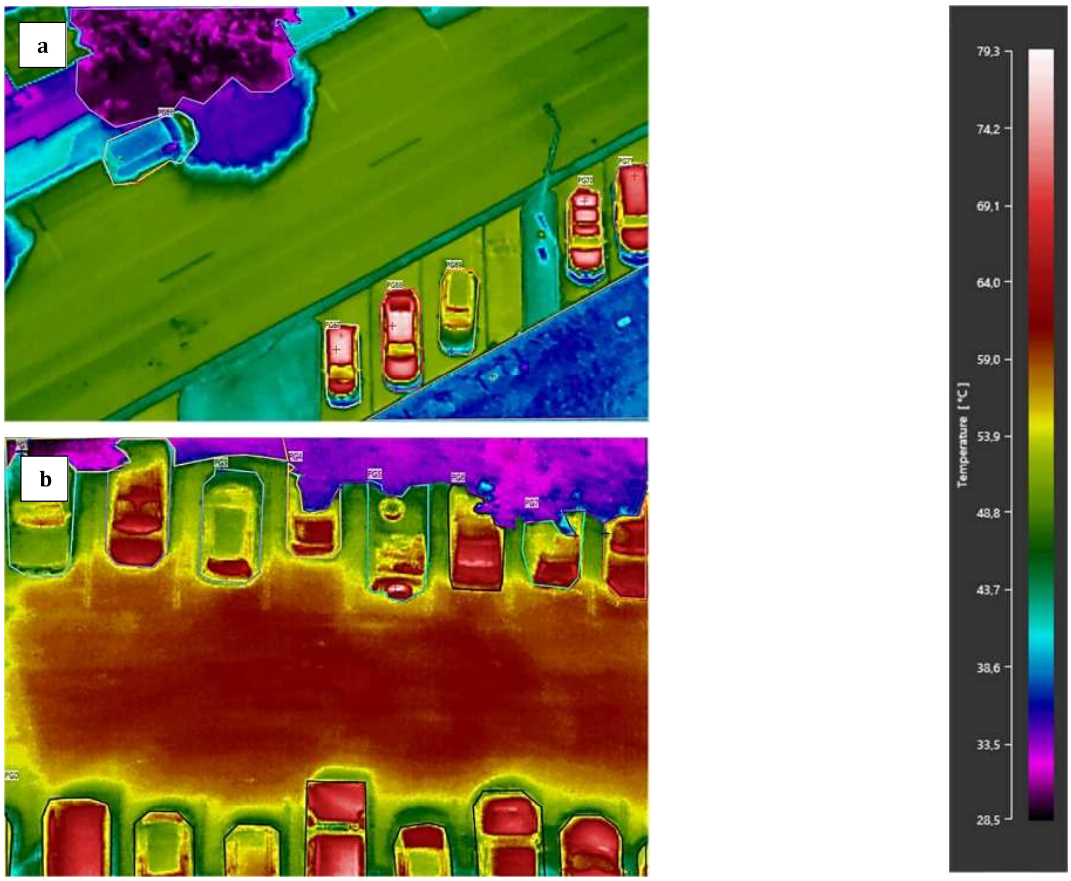


Figure 7.6
Darwin aerial monitoring campaign – thermal shots: (a) area 1.3, 23rd of March, 12pm; (b) area 2.3, 24th of March, 11:30am.

Along with the image capturing, aerial filming was performed as well, covering almost the same zones mapped via thermal shots and filling the gaps in between the shots (roadmap in **Figure 7.7**).



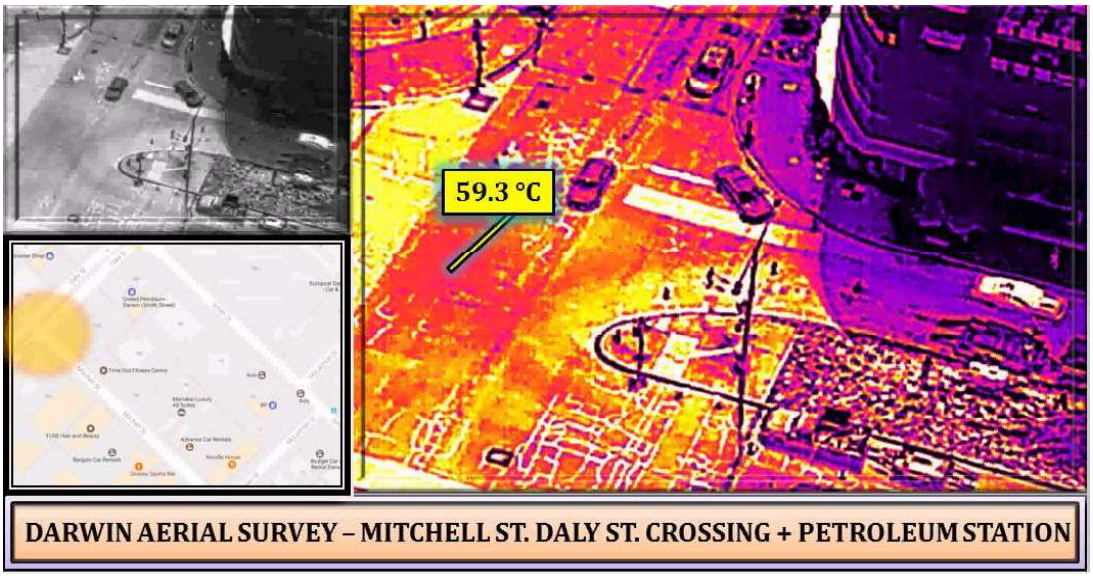
Figure 7.7
Darwin aerial monitoring campaign – thermal shots strategic roadmap.

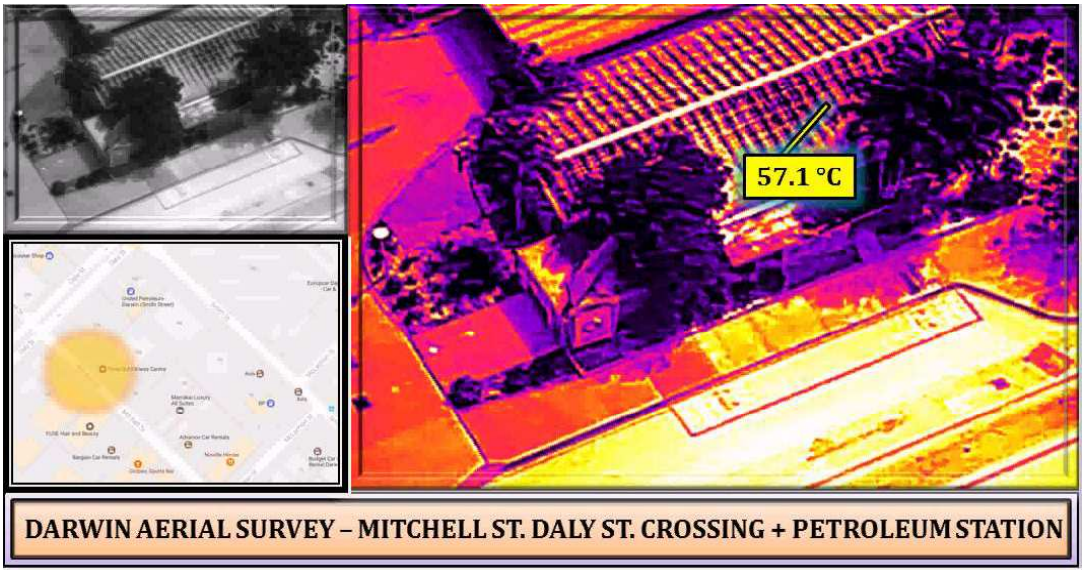
The raw videos were treated similarly to the thermal images, thus extending the corrective process to a series of frames rather than a single .jpeg file.
More in detail, the post-processing involved a series of operations:

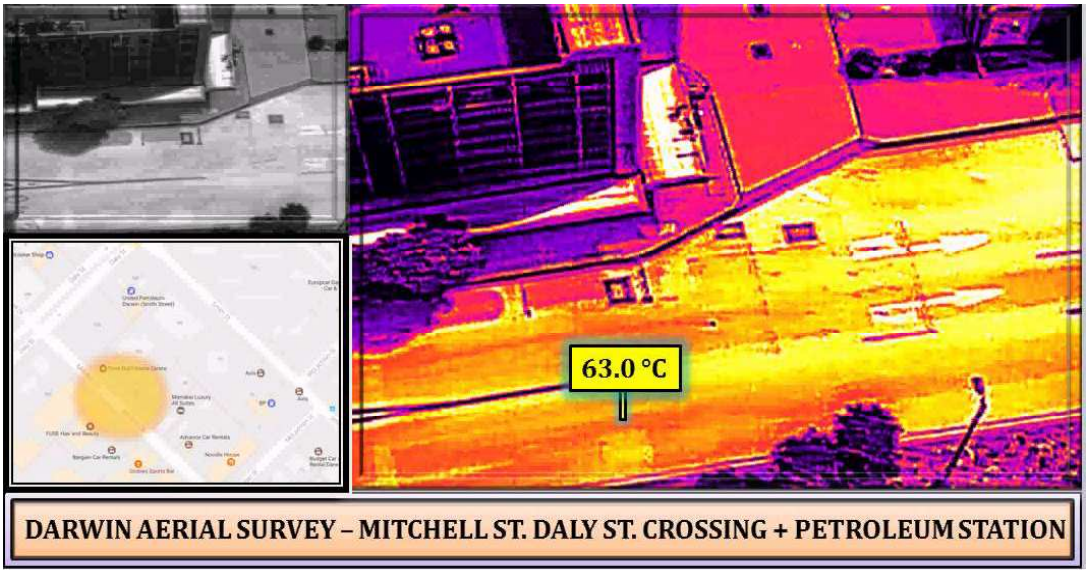
- defragmentation of each video into 100 frames;
- application of the corrected chromatic scale based on the radiosity information conveyed by each pixel and of the emissivity values;
- recomposition of the footages in both thermal and radiometric greyscale.

Thermo-chromatic videos were used to identify and quantify hot spots and catch immediately the differences among the materias composing the urban landscape; greyscale videos were added in synch to maintain the original radiometric acquisition.
Referential temperature values were overlapped to flash out during the visualization of the thermal videos whenever a major indication of the UHI phenomenon magnitude was detected.

Moreover, Darwin terrain maps were included alongside and supplemented by a moving viewer pane to keep track of the area spanned by the drone so as to make it easier to locate each point of interest and relate it to the CBD layout.
The information retrieved from both aerial images and videos converged into a powerful system to get an overarching diagnosis of the heat island effect, necessary to properly select the mitigation strategies which could best fit the peculiarities of such Australian, tropical cityscape.
Figure 7.8 shows some representative screenshots of the thermal videos in their ultimate format (area 1.2, referring to **Figure 7.7** codification).




57.1 °C
DARWIN AERIAL SURVEY – MITCHELL ST. DALY ST. CROSSING + PETROLEUM STATION


63.0 °C
DARWIN AERIAL SURVEY – MITCHELL ST. DALY ST. CROSSING + PETROLEUM STATION

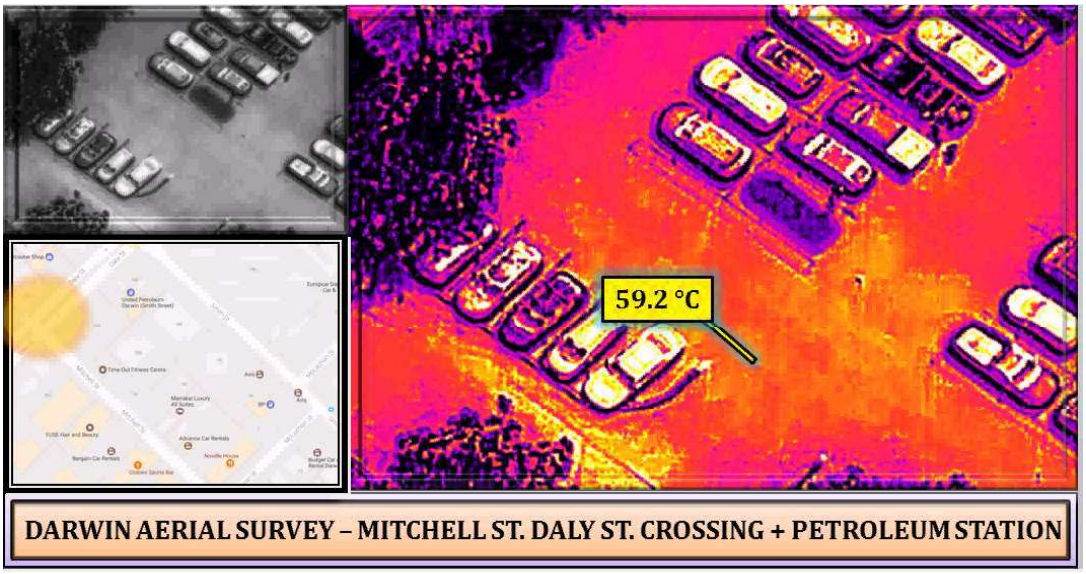


Figure 7.8
Mitchell Street – Daly Street crossing & petroleum station carpark (area 1.2) thermal video frames.

7.5.2.3 Conclusions

The thermodynamic phenomena occurring in highly urbanized areas can be virtually seen as an intertwined web of thermal fluxes: heat is absorbed, released, entrapped and generated because of diverse factors, either competing or mutual-empowering, either environmental or anthropogenic, thus depicting an extremely complex (chaotic indeed) energy scenario.
Against this backdrop, a suitable way to run a scientific investigation is to focus on the implications rather than on the root causes: for instance, surface temperature is a spying indicator of the contribution of urban fabric composition on the microclimatic conditions.
Such "visible" side of UHI is what was addressed via aerial patrolling and thermal measurements.
By perusing and comparing all post-processed data (privileging the least oblique views, as less biased), some pieces of information could be retrieved **[7.5]**:

- the minimum average surface temperature of the streets was 55.4°C recorded at the crossing between Esplanade and Bennett Street. The maximum was 63.2°C (Cavenagh Street – Daly street crossing).

- The minimum average surface temperature of the parking lots was 44.9°C recorded in front of Darwin Supreme Court. The maximum was 65.7°C (Darwin GPO Postshop carpark).
- The minimum average surface temperature of shadowed street portions was 34.7°C recorded in front of Darwin Supreme Court. The maximum was 54.6°C (Darwin GPO Postshop carpark).
- The minimum average surface temperature of the trees was 27.6°C recorded in front of Darwin Supreme Court. The maximum was 38.5°C (Darwin City Council).
- The minimum average surface temperature of the greenery was 32.3C recorded in McMinn Street (near the crossing with Knuckey Street). The maximum was 46.1°C (Darwin Supreme Court).
- The minimum average surface temperature of the roofs was 48.0°C recorded at the crossing between Esplanade and Peel Street. The maximum was 66.0°C (McMinn Street – Daly Street crossing).
- The minimum average surface temperature of the pavements was 49.2°C recorded at the crossing between Esplanade and Peel Street. The maximum was 56.4°C (Darwin City Council).
- The minimum difference between streets and pavements surface temperatures was 0.2°C recorded in the area of Darwin City Council. The maximum was 7.3°C (Cavenagh Street – Daly street crossing).
- The minimum difference between streets and shadowed portions surface temperatures was 9.3°C recorded in the area of the United Petroleum Darwin carpark. The maximum was 22.7°C (Bus Interchange – Parliament House).
- The minimum positive difference between streets and parking lots surface temperatures was 1.7°C recorded in McMinn Street (near the crossing with Knuckey Street). The maximum was 11.2°C (Bus Interchange – Parliament House).
- The minimum negative difference between streets and parking lots surface temperatures was -2.7°C recorded at the crossing between McMinn Street and Daly Street. The maximum was -8.2°C (United Petroleum carpark).
- The minimum difference between pavements and greenery surface temperatures was 7.0°C recorded in front of Darwin Supreme Court. The maximum was 21.2°C (McMinn Street. near Knuckey Street crossing).

All things considered, some rule of thumbs driving the dynamics of urban heat island in Darwin could be drawn:

- trees and greenery are major actors in the mitigation of locally risen temperatures: as a matter of fact, the higher the proximity to the widest scrubs

(Harbour, City Council, Supreme Court area) the lower the average surface temperatures;
- The shadowing effect given by vegetation refreshes the underlying surfaces of over 10°C thus reducing the irradiative contribution of such patches of urban landscape to the rise of local ambient temperature;
- Streets and pavements hit approximately the same peak and average values: just where greenery replaces asphalt and concrete pavements the difference can soar up to 22°C;
- A certain surface temperature gap is recorded between carparks and the closest streets: the former might get heated up to 8°C more than the latter. The sole exception is when green cover over the parking lots is widely extended;

Therefore, all these findings reinforced the evidence of the beneficial contribution given by vegetation. Nevertheless, it should be stressed that increasing vegetation is not a purely rewarding measure: particularly in tropical climates, the implications on ambient relative humidity need to be considered before any massive intervention. That is the reason why, in the subsequent step of simulating mitigation scenarios, the percent increase of greenery was kept below 30%.

7.5.3 – Terrestrial survey

The main interest behind running a terrestrial survey was to collect the meteorological data in a series of strategical points in order to compile a thorough map of Darwin CBD characteristics in terms of air temperature, relative humidity, wind speed and direction, solar radiation and heat flux.
This operation allowed to get the spatial and temporal trends all along the main streets and the identified crucial points; nevertheless absolute values were not a sufficient indication of urban local peculiarities over the rural bordering area.
Accordingly, the second step consisted in comparing the outcomes of the measurement campaign with the corresponding recordings from BoM's (Bureau of Meteorology) closest meteo station (located near Darwin's airport), used as referential "undisturbed" dataset.
The differences revealed the magnitude of the UHI.

7.5.3.1 – Instruments and methods

The mobile weather station, employed to collect all necessary information consisted of two main pieces of instrumentation:

- Hukseflux NR01 net radiometer: it is the composition of four probes, each one measuring a different term of the surface radiation balance. Two pyranometers detect the downward ($G_{sw,down}$) and upward ($G_{sw,up}$) Solar radiation received by a plane surface, while two pyrgeometers record the longwave radiation in the same directions ($G_{lw,down}$ and $G_{lw,up}$). The voltage output of each single detector is then converted into a watt-per-square-meter value and finally introduced in the net radiation equation (G_{net}), according to the following series of mathematical formulas, appealing to Stefan-Boltzmann law for grey bodies:

$$G_{sw,down} = \frac{U}{S} \; ; \; G_{sw,up} = \frac{U}{S} \tag{7.1}$$

$$G_{lw,down} = \frac{U}{S} + \sigma(T + 273.15)^4 \; ; \; G_{lw,up} = \frac{U}{S}\sigma(T + 273.15)^4 \tag{7.2}$$

$$G_{net} = (G_{sw,down} + G_{lw,down}) - (G_{sw,up} + G_{lw,up}) \tag{7.3}$$

Where "U" is the output signal in volts, "S" the sensitivity of the probe (enabling the conversion from voltage to W/m^2), "σ" is the Stefan-Boltzmann constant and "T" is the temperature of the probe (measured by an embodied RTD), necessary to compensate the error given by the internal heating used to preserve condensation.

Several other measurands could be calculated from the same raw recordings, namely albedo (α) and equivalent blackbody temperatures of the surface (T_{surf}) and the sky (T_{sky}).

$$\alpha = G_{sw,up}/G_{sw,down} \tag{7.4}$$

$$T_{surf} = \left(\frac{G_{lw,up}}{\sigma}\right)^{\frac{1}{4}} - 273.15 \tag{7.5}$$

$$T_{sky} = \left(\frac{G_{lw,down}}{\sigma}\right)^{\frac{1}{4}} - 273.15 \tag{7.6}$$

All this matemathics was directly implemented in the LabVIEW Virtual Instrument, ad hoc conceived to store and manage Darwin terrestrial monitoring database (block diagram snapshots are provided in **Figure 7.9**).

Hukseflux NR01 technical specs are summarized in **table 7.6.** Each measurement was taken at 50cm from street level as a trade-off between proximity to the target and distance from interefering items (mounting mast, vehicles, pedestrians, …).

- Gill Instrument MetPak Pro, a professional weather station including several on-board sensors to measure barometric pressure, air temperature, humidity, dew point, wind speed and wind direction. Technical data are presented in **table 7.7.**

  Measurements were taken at 110cm, which is the recommended height when people are supposed to stand in upright position as it represents the position of the centre of gravity **[7.11].**

All the analogic outputs of the net radiometer and the serial outputs (in SDI-12) coming from the weather station were connected to the multi-acquisition system by Lontek, datalogger dataTaker DT85.

.

HUKSEFLUX NR01 NET RADIOMETER



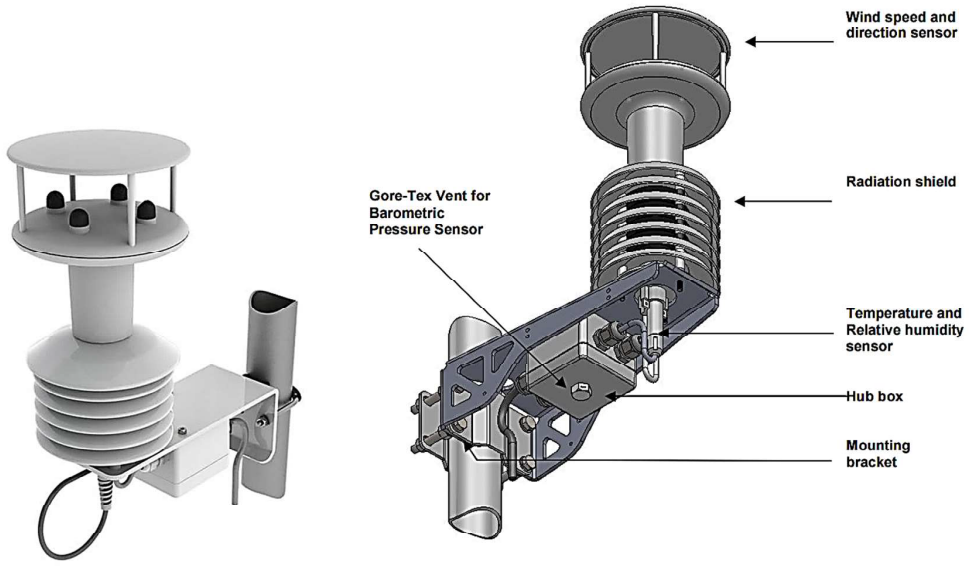
(1) upfacing pyrgeometer model IR01
(2) sun screens
(3,4) levelling assembly for x- and y-axis
(5) upfacing pyranometer model SR01
(6) downfacing pyranometer model IR01
(7) 4 x hex bolts for levelling adjustment
(8) downfacing pyrgeometer model IR02

GENERAL SPECS	
Product type	4-component net radiometer
Included sensors	2 x identical ISO 9060 second class pyranometer (see separate specification table for model SR01) 2 x identical pyrgeometer with 150 ° field of view angle (see separate specification table for model IR01)
Zero offset b (response to 5 K/h change in ambient temperature)	< ± 4 W/m2
Non-stability	< ± 1 % change per year
Non-linearity	< ± 1 % (100 to 1000 W/m2)
Directional response	< ± 25 W/m2
Spectral selectivity	< ± 5 % (0.35 to 1.5 x 10-6 m)
Temperature response	< ± 3 % (-10 to +40 °C)

Tilt response	< ± 2 % (0 to 90 ° at 1000 W/m2)
SPECIFICATIONS OF IR01 PYRGEOMETER	
Spectral range	4.5 to 40 x 10-6 m
Solar offset	< 15 W/m2 (at 1000 W/m2 global horizontal irradiance on the window)
Field of view angle	150 °
Response time (95 %)	18 s
Sensitivity (nominal)	15 x 10-6 V/(W/m2)
Sensitivity range	5 to 15 x 10-6 V/(W/m2)
Temperature dependence	< ± 3 % (-10 to +40 °C)
Required sensor power	zero (passive sensor)
Zero offset b (response to 5 K/h change in ambient temperature)	< ± 4 W/m2
Non-stability	< ± 1 % change per year
Non-linearity	< ± 2.5 % (100 to 300 W/m2, relative to 200 W/m2 sensor to source exchange)
Measurement range	-300 to +300 W/m2 (sensor to source exchange: U/S)
Tilt dependence	< ± 2 % (0 to 90° at 300 W/m2)

Table 7.6
Hukseflux NR01 technical details.

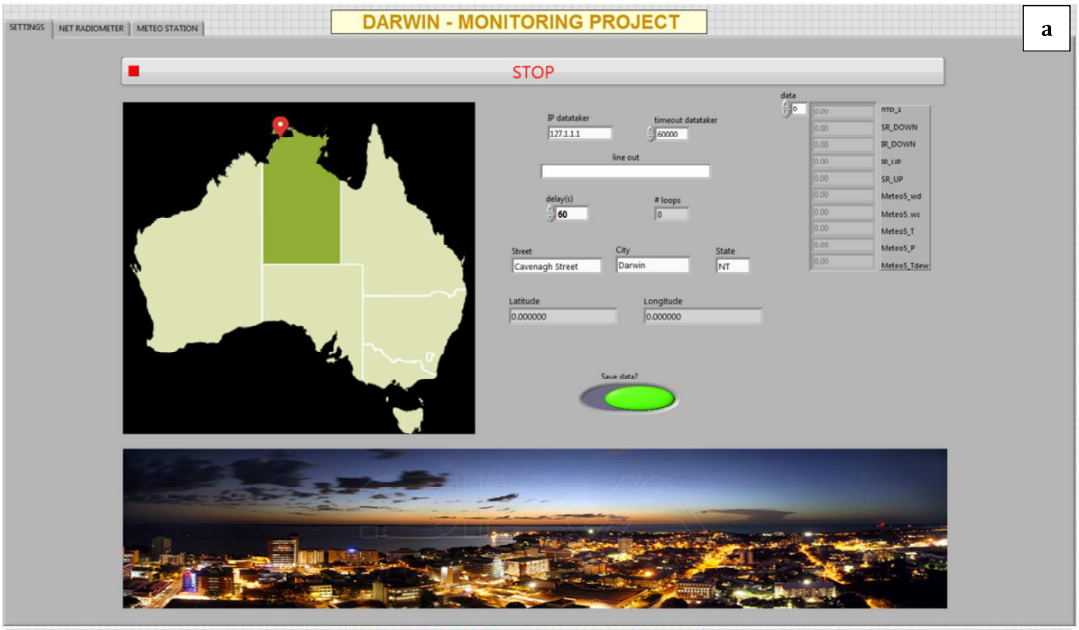
GILL INSTRUMENT METPAK PRO METEOROLOGICAL STATION

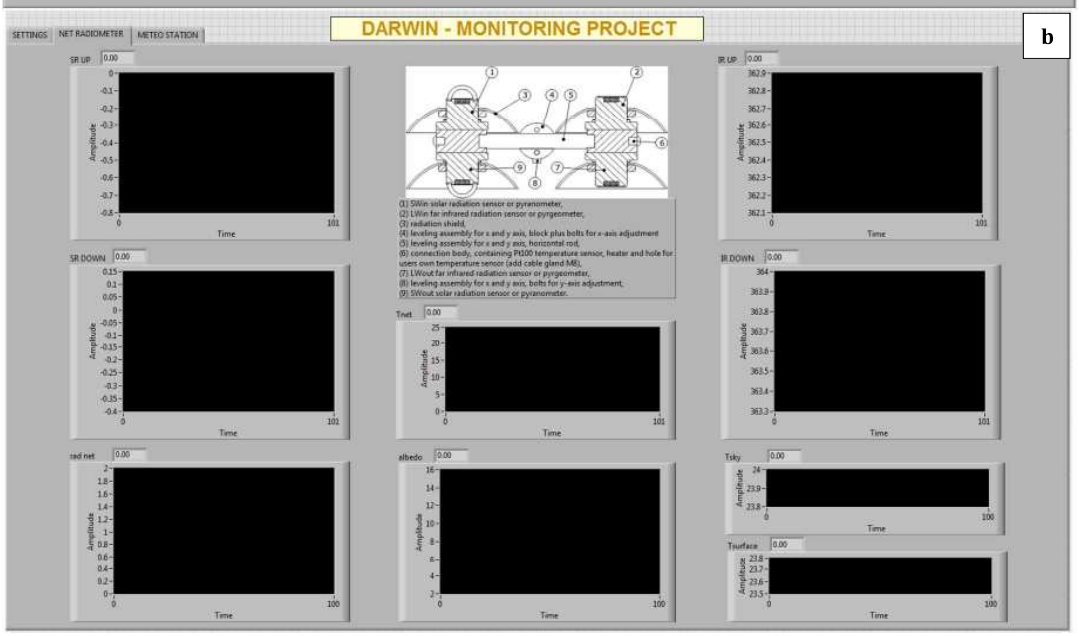


WIND MEASUREMENT

Parameters	Wind speed and direction
Wind Speed Range	0-60m/s
Wind Speed Accuracy	±2% @12m/s
Wind Speed Resolution	0.01m/s
Wind Direction Range	0 to 359º - No dead band
AIR TEMPERATURE	
Air Temperature	Pt100 1/3 Class B
Range	-50ºC to +100ºC
Accuracy	±0.1ºC
Resolution	0.1ºC (0.1ºF)
Units of measure	ºC or ºF
BAROMETRIC PRESSURE	
Range	600-1100hPa
Accuracy	±0.5hPa
Resolution	0.1hPa
Units of measure	hPa, mbar, mmHg, inHg
Compensated for temperature dependency	**-30ºC to +70ºC**
DEW POINT	
Resolution	0.1ºC (0.1ºF)
Units of measure	ºC or ºF
Accuracy	±0.15ºC (23ºC ambient temp @20ºC dew point)
OUTPUT	
Digital	**SDI-12** V1.3
Wind Direction Accuracy	±3º @12m/s
Wind Direction Resolution	1º

Table 7.7
Gill Instrument MetPak Pro technical details.


a
SETTINGS
NET RADIOMETER
METEO STATION
DARWIN - MONITORING PROJECT
STOP
IP datataker
127.1.1.1
timeout datataker
60000
line out
delay(s)
60
loops
0
Street
Cavenagh Street
City
Darwin
State
NT
Latitude
0.000000
Longitude
0.000000
Save data?
data
RTD_1
SR_DOWN
IR_DOWN
IR_UP
SR_UP
Meteo5_wd
Meteo5_ws
Meteo5_T
Meteo5_P
Meteo5_Tdew


b
SETTINGS
NET RADIOMETER
METEO STATION
DARWIN - MONITORING PROJECT
SR UP
SR DOWN
IR UP
IR DOWN
Tnet
rad net
albedo
Tsky
Tsurface
Amplitude
Time

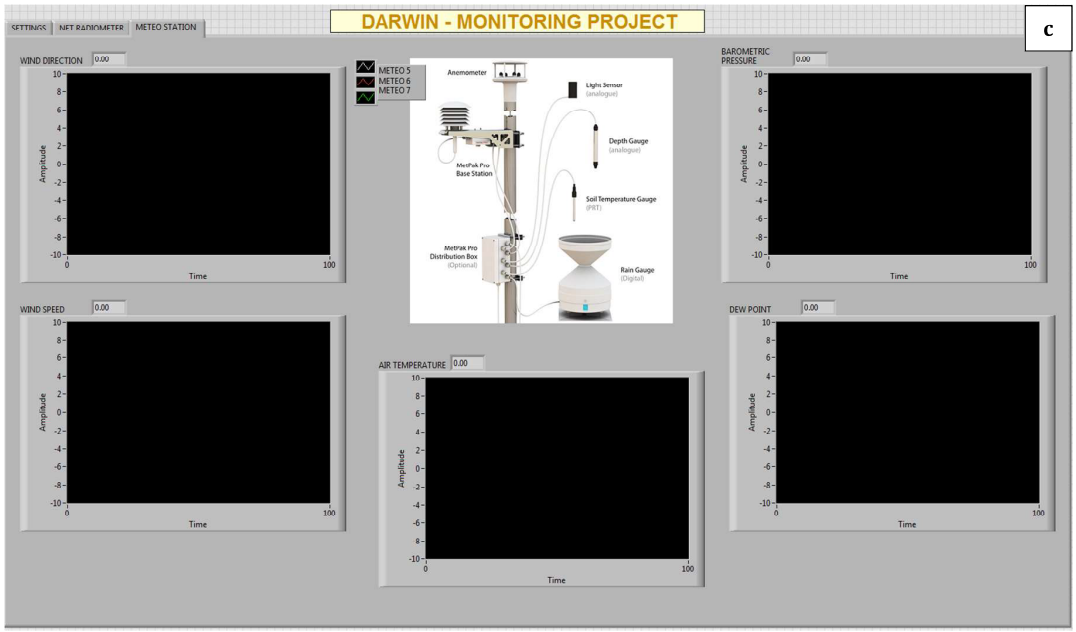


Figure 7.9
LabVIEW front panel: (a) setting screen - communication with the datataker, dt85 and geographic data retrieval; (b) graphical visualization of net radiometer output time trends; (c) graphical visualization of meteo station output time trends.

A preliminary investigation of the main causes leading to Urban Heat Island and of the most accredited methods to measure it, was run on the wide literature background available in literature and in the HPA group itself **[7.12-7.19]** in order to design the afore described sensor system.
On the other hand, a second preliminary investigation was carried out to match the monitoring plan (estimated in **sub-paragraph 7.5.1**) with the safety issues related to the operation of the drone and to the weather instabilities during the wet season in Darwin.
Figure 7.10 recaps the locations examined at the end of the monitoring campaign: the red drop-shaped cursors indicate on-road points of measurement, while the blue ones fall upon the coordinates where the sensors system was placed in parking lots. It is immediately noticeable that:

- the main vertical and horizontal streets were mapped through a matrix of points distributed at the crossroads;
- all main parking lots were included (less concerns in terms of CASA approval);
- some stand-alone points were explored in order to clarify (ENVI-met disclosed or in-loco experienced) anomalies;

- multiple points were investigated along Daly Street as it represents the "entry door" for western oriented winds and gusts, deemed to play a major role in the UHI phenomenon.



Figure 7.10
Darwin terrestrial monitoring campaign – points of measurement.

20 recordings were taken per point with an acquisition rate of 30 seconds covering a total time slot of 10 minutes per point. Refer to **table 7.8** (filled out with the data retrieved at the crossing between Cavenagh Street and Bennett Street), by way of example.

CAVENAGH ST. – BENNETT ST. CROSSING: METEOROLOGICAL DATASET			
DAY	START	LAT	-12.463854
25-mar	11:11:30	LONG	130.844378
	FINISH	DISTANCE FROM	

	11:22:30	WOODS STREET	170m
	TIMESTEP		
	30 s		

METEO STATION MEASUREMENTS AND PROCESSING

Wdir [°]	Ws [m/s]	Ta [°C]	P [hPa]	Tdew [°C]	RH [%]
208	0.46	29.7	1005.3	25,2	76,9
269	2.3	29.7	1005.3	25,2	76,9
184	0.5	29.7	1005.3	25,3	77,3
339	2.47	29.7	1005.3	25,1	76,4
352	0.33	29.8	1005.2	25,1	76,0
341	0.68	29.8	1005.2	25,1	76,0
97	0.3	29.9	1005.2	25,1	75,5
318	0.68	29.9	1005.2	25,2	76,0
307	0.33	30	1005.2	25,1	75,1
264	0.83	30	1005.2	25,2	75,5
18	0.84	30	1005.2	25,1	75,1
217	0.37	30.1	1005.2	25,3	75,6
250	0.74	30.2	1005.2	25,2	74,7
271	1.17	30.1	1005.2	25,3	75,6
244	0.79	30	1005.2	25,4	76,4
347	0.67	30	1005.2	25,3	76,0
8	1.68	30	1005.2	25,4	76,4
348	0.95	30.1	1005.2	25,4	76,0
2	1.3	30.1	1005.2	25,5	76,5
7	1.41	30.2	1005.2	25,6	76,5

NET RADIOMETER MEASUREMENTS AND PROCESSING

$G_{sw,down}$ [W/m²]	$G_{sw.up}$ [W/m²]	$G_{lw.down}$ [W/m²]	$G_{lw.up}$ [W/m²]
599,6288	60.6616	449.3339	528.2362
820,5590	82.5609	449.0764	528.8983
655,3705	66.6260	450.5702	531.2789
822,7535	82.7468	450.8167	532.3071
844,5934	84.0064	453.8360	534.1762
652,4236	65.2382	457 7321	536.1599
484,6077	46.9810	457.9436	533.6863
394,5162	39.2977	458.1366	532.5371
377,2989	37.9753	457.0203	530.9511
384,7717	38.7867	456.3188	530.1386
441,8178	44.4045	453.6571	529.5930
1122,6590	112.0454	459.7739	538.8346
1010,5725	98.2894	456.5740	541.7889
953,2220	93.7601	454.4453	542.5683
802,0932	78.2912	453.9261	543.1410

644,1379	61.6265	452.2718	541.3806
834,3616	81.3216	458.2134	545.3615
622,9993	59.0439	456.8550	543.9861
464,1217	43.9056	456.4524	541.6389
420,9435	39.7828	457.3908	539.9036
G_{net} [W/ m²]	**α**	**T_{surf} [°C]**	**T_{sky} [°C]**
460,0649	0.1012	37.5286	25.2141
658,1762	0.1006	37.6259	25.1713
508,0358	0.1017	37.9750	25.4191
658,5164	0.1006	38.1254	25.4599
680,2468	0.0995	38.3983	25.9587
508,7576	0.1000	38.6871	26.5985
361,8840	0. 969	38.3268	26.6332
280,8179	0.0996	38.1590	26.6647
265,3927	0.1007	37.9270	26.4819
272,1652	0.1008	37.8079	26.3669
321,4773	0.1005	37.7279	25.9292
931,5528	0.0998	39.0753	26.9322
827,0682	0.0973	39.5024	26.4088
771,3388	0.0984	39.6148	26.0590
634,5871	0.0976	39.6973	25.9735
493,4027	0.0957	39.4435	25.7006
665,8918	0.0975	40.0165	26.6773
476,8242	0.0948	39.8189	26.4548
335,0297	0.0946	39.4807	26.3888
298,6479	0.0945	39.2300	26.5426

Table 7.8

*Darwin terrestrial monitoring campaign – example of meteorological data collection: time and space details, terrestrial sensor network outputs and mathematical processing (as in **sub-paragraph 7.7.1**). Refer to the following legend: Wdir = Wind direction; Ws = Wind speed;Ta = Air temperature; P = Barometric pressure; Tdew = Dew-point; RH = Relative humidity*

7.5.3.2 – Outputs

The main outputs of the monitoring activity can be split into three macrocategories:

- inter-parameter comparative assessment in absolute terms, obtained by comparing a series of charts (**Figure 7.11**) that overlap the main weather parameters trends. In detail, air, surface and sky temperatures were displayed on the primary vertical axis; relative humidity (espressed in decimals) and

wind speed were plotted on the secondary vertical axis. That was a way to characterize the microclimate of the main urban areas of interest;

- inter-point comparative assessment in absolute terms, obtained by comparing the weather conditions between locations monitored in a limited window of time to depict the thermo-hygrometric profiles along potential urban corridors. Indeed, when it comes to meteorological monitoring campaigns during the wet season in a tropical climate, data analysis have to deal with a substantial lack of coherence and continuity in the readings: in many cases, the acquisition was interrupted by frequent rainfall events (from drizzles to squally storms).

  Nevertheless, some conclusions and observations could be drawn focusing on the difference in averaged air temperature (ΔTa) and relative humidity (ΔRH) within measurement points close both in space and time (a threshold of one hour was established). The graphical representation of this second assessment is given in **Figure 7.12.**

  On the other hand, the intermittent, but steady occurrence of short, sharp downpours of torrential rain and scattered thunder showers allowed to examine several other facets of the local microclimate:

- the mean rise of moisture content in the air after a storm: relative humidity was found to increase up to +16.5% on average;
- the average drop in ambient temperature after a storm (-4.52°C);
- the transient thermal behaviour of the asphaltic surfaces after a rainfall: surface temperature exhibited an increase of even more than 1°C in the 10-minute-time slot of measurement: the peak value for streets was 2.49°C, recorded at the crossing between Cavenagh Street and Bennett Street, while the correspondent value for parking lots was +1.7°C at the United Petroleum Darwin carpark.

  Those analyses furtherly disclosed the thermodynamics behind the UHI in Darwin (and in tropical cities by generalization) which is the role of the ongoing loop of evaporation processes: the average duration and magnitude of rainfall impel the formation of a quite thin film of water over hot asphaltic surfaces of street and pavements; as soon as the rain holds off, the liquid turns into moisture, almost saturizing the air layer within the canopy (which explains while both in the preliminary study of Darwin climate and in the terrestrial survey, the relative humidity mostly stood at 100%).

  Outdoor discomfort is thus emphasized.

- inter-point comparative assessment in relative terms: by calculating the differences between simoultaneous data retrieved in Darwin CBD and Darwin airport (BoM meteorological station). That was the actual analysis of UHI as

increased ambient temperature of urban landscape compared to rural settings. The reference datasets, coming from the "undisturbed" environment, were provided for the same days of the terrestrial monitoring campaign (24th-25th March 2017) with a time step of 1 minute for air temperature, wind speed and relative humidity.

Once both the sets were aligned in time, a suite of analyses was performed to identify magnitude and peculiarities of the UHI phenomenon. Both tabulated and graphical outputs were extracted and are here reported.

Figures 7.13 - 7.15 correspond to air temperature, wind speed and relative humidity differences plots respectively. The order of subtraction was set to CBD values minus reference values (sign convention) in order to directly get the UHI magnitude. Refer to **table 7.9** for the codification of the locations in the charts. Maximum, Minimum and average values are graphically displayed through the symbolization given in legend.

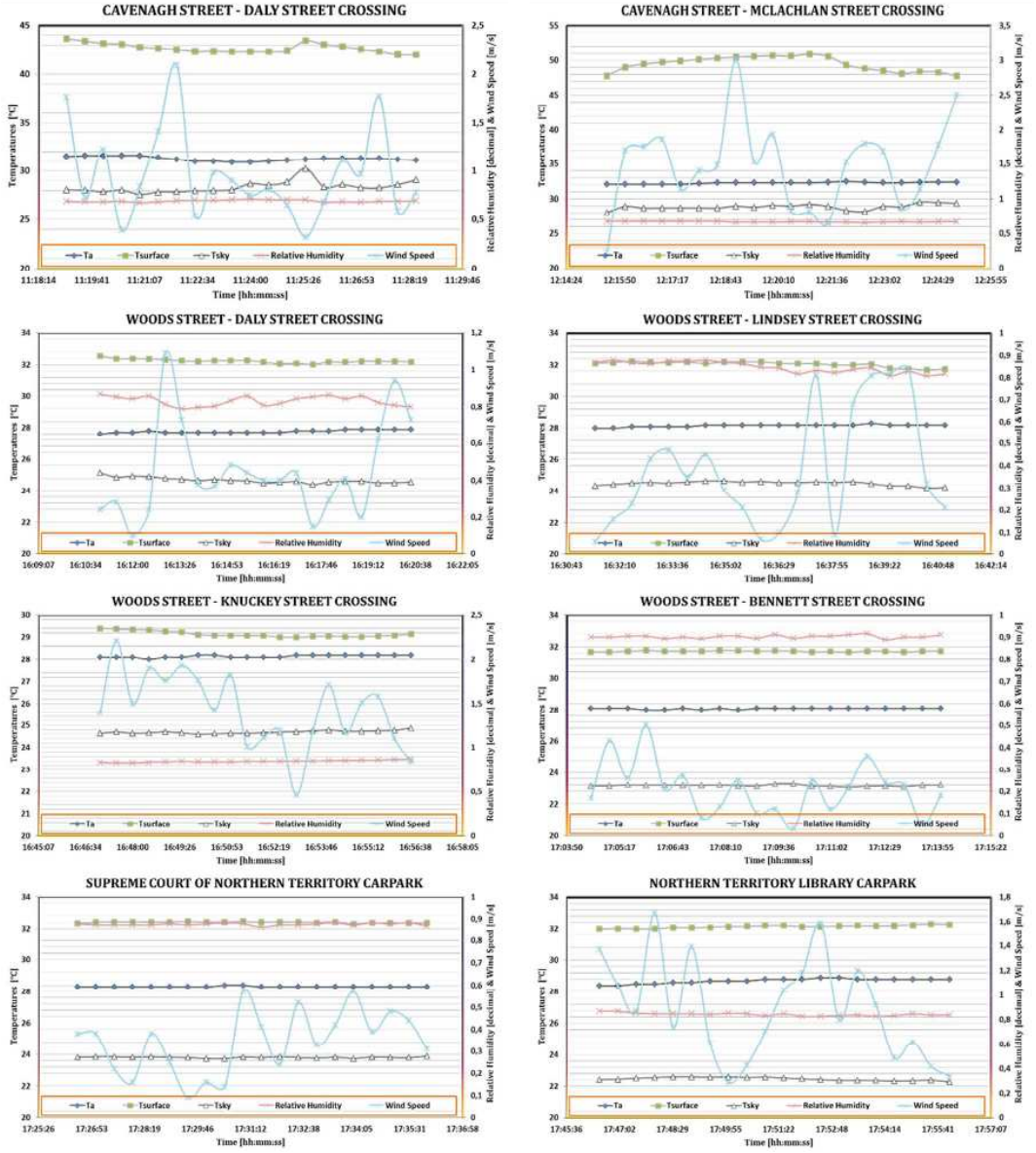
Below each figure is the table ranking all monitored points in order of decreasing average values (**tables 7.10-7.12**). The former and the latter three locations are highlighted (in red and blue respectively) both in the table rows and in the satellite map provided at the bottom.

The main findings arising from the analysis of these graphs are related to the identification of CDB landscape features leading to different magnitudes of heat island effect (urban pattern, population density, proximity to the sea, richness in vegetation, venturi corridors, …). Tabulated values (and their distribution over Darwin's satellite map), in particular, were used to discriminate regions of emphasized UHI and to strike correlations between temperature, wind speed and relative humidity differences.

The main results, drawn by merging the information given by each macro-category of analyses performed, are discussed in the following sub-paragraph.

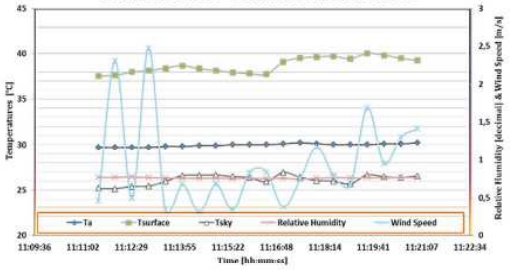
WEATHER TIME TRENDS

24th March 2017

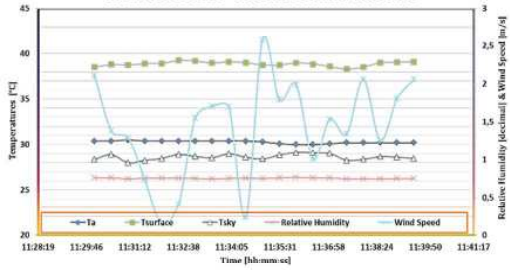


25th March 2017

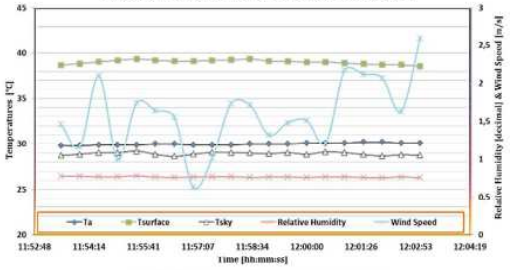
CAVENAGH STREET - BENNETT STREET CROSSING



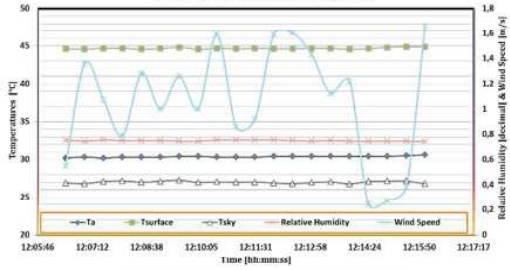
CAVENAGH STREET - KNUCKEY STREET CROSSING



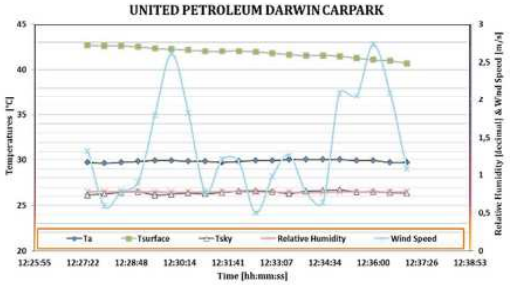
CAVENAGH STREET - LINDSEY STREET CROSSING



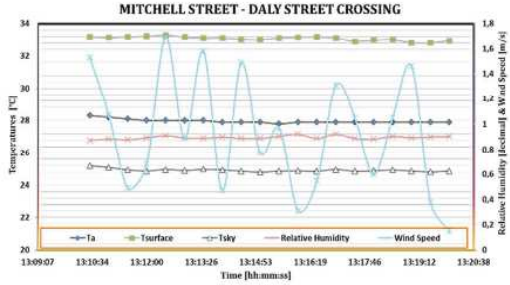
DARWIN GPO POSTSHOP CARPARK



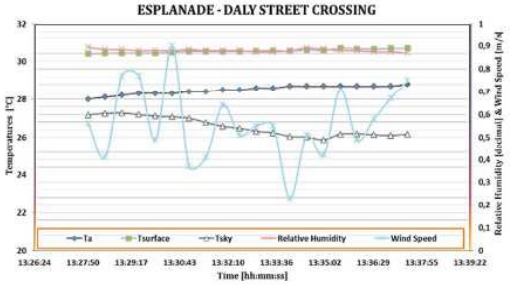
UNITED PETROLEUM DARWIN CARPARK



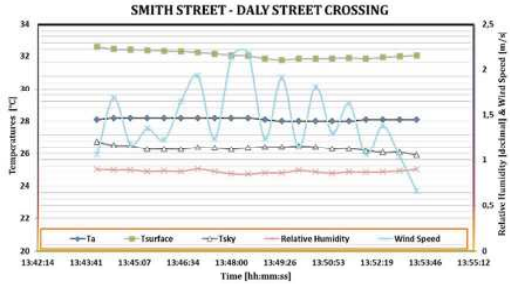
MITCHELL STREET - DALY STREET CROSSING



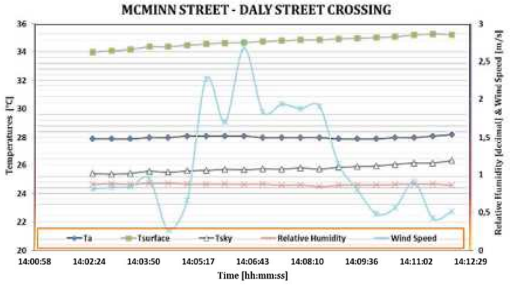
ESPLANADE - DALY STREET CROSSING



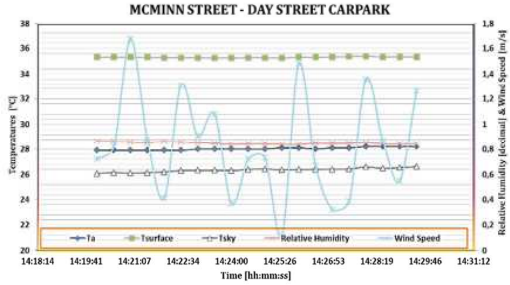
SMITH STREET - DALY STREET CROSSING



MCMINN STREET - DALY STREET CROSSING



MCMINN STREET - DAY STREET CARPARK



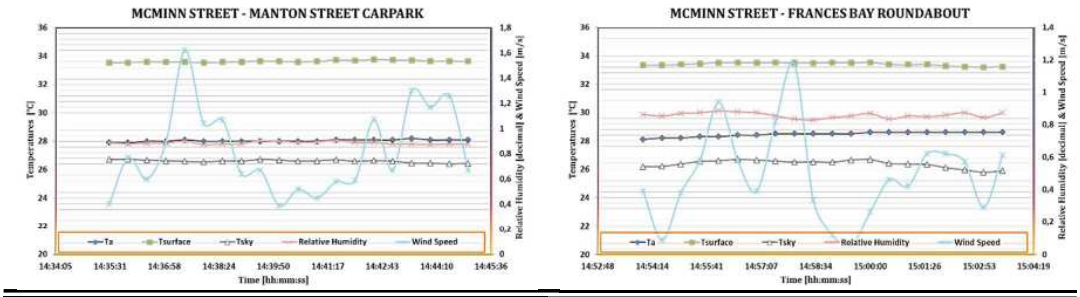
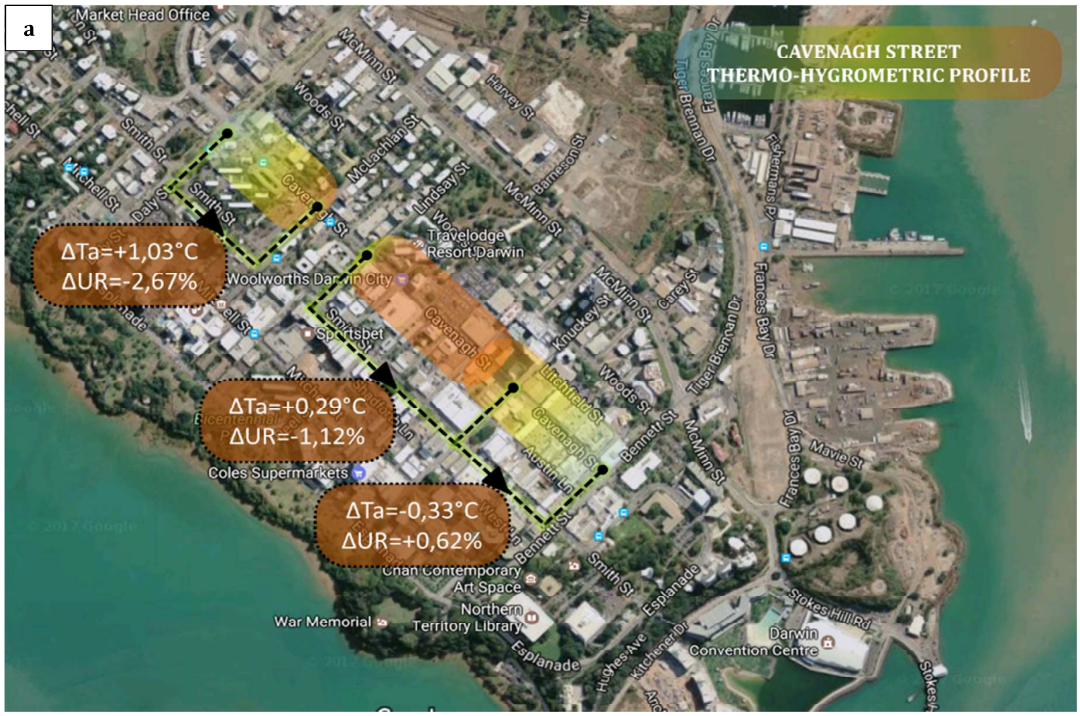


Figure 7.11
Darwin terrestrial monitoring campaign –meteo charts.



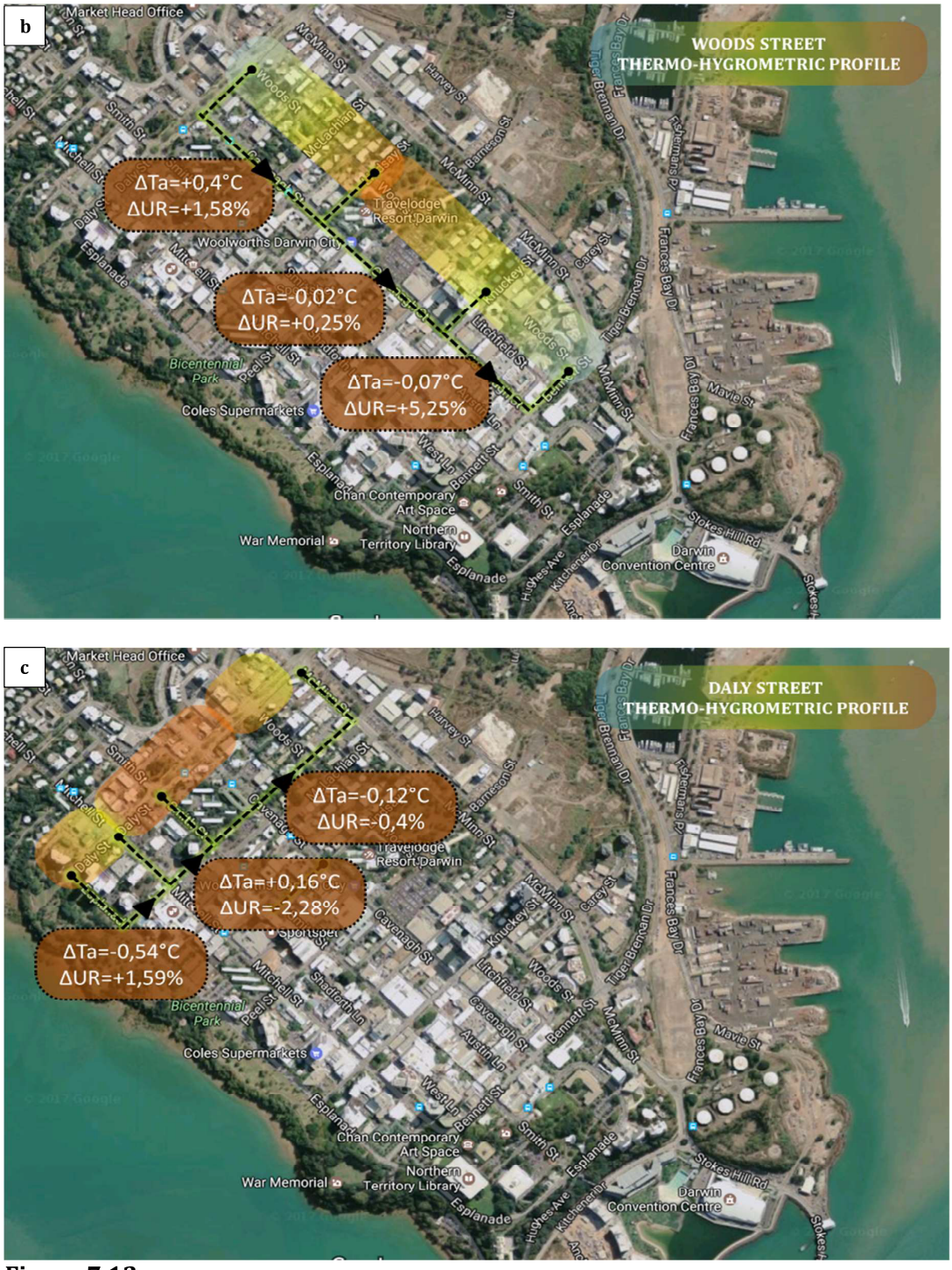


Figure 7.12

Darwin terrestrial monitoring campaign –thermohygrometric differences along Cavenagh Street (a), Woods Street (b) and Daly Street (c)

TERRESTRIAL SURVEY LEGEND	
X-AXIS INDICES	**MEASUREMENT POINT**
1	CAVENAGH STREET – DALY STREET CROSSING
2	CAVENAGH STREET – MCLACHLAN STREET CROSSING
3	WOODS STREET – DALY STREET CROSSING
4	WOODS STREET – LINDSEY STREET CROSSING
5	WOODS STREET – KNUCKEY STREET CROSSING
6	WOODS STREET – BENNETT STREET CROSSING
7	SUPREME COURT OF NORTHERN TERRITORY CARPARK
8	NORTHERN TERRITORY LIBRARY CARPARK
9	CAVENAGH STREET – BENNETT STREET CROSSING
10	CAVENAGH STREET – KNUCKEY STREET CROSSING
11	CAVENAGH STREET – LINDSEY STREET CROSSING
12	DARWIN GPO POSTSHOP CARPARK
13	UNITED PETROLEUM DARWIN CARPARK
14	MITCHELL STREET – DALY STREET CROSSING
15	ESPLANADE – DALY STREET CROSSING
16	SMITH STREET – DALY STREET CROSSING
17	MCMINN STREET – DALY STREET CROSSING
18	MCMINN STREET – DAY STREET CARPARK
19	MCMINN STREET – MANTON STREET CARPARK
20	MCMINN STREET – FRANCES BAY ROUNDABOUT

Table 7.9
Darwin terrestrial monitoring campaign – list and indexing of monitored points.

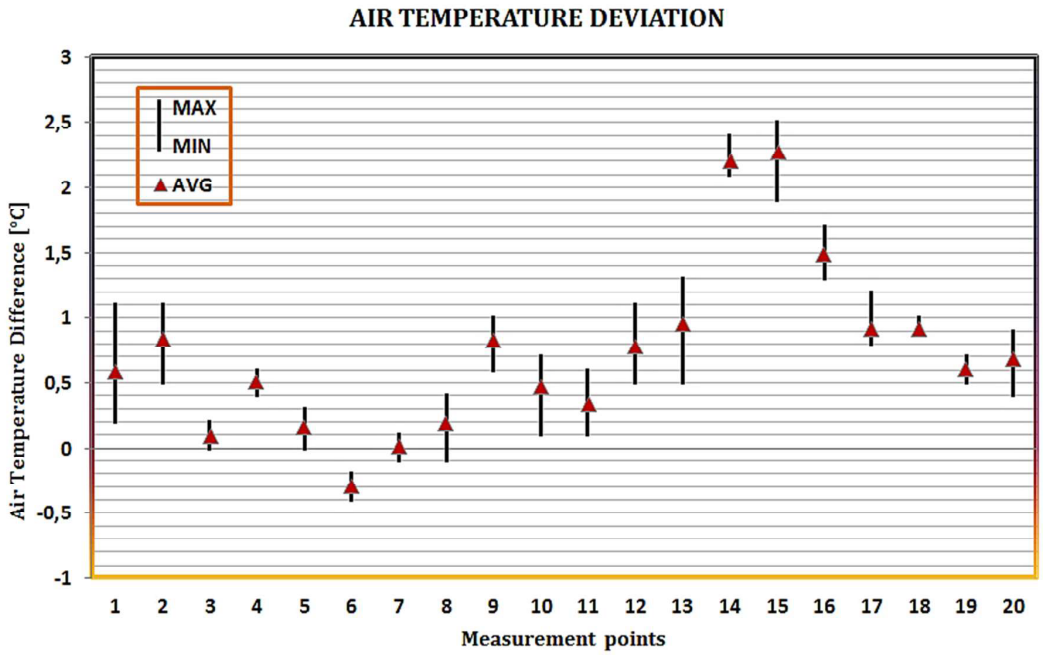


Figure 7.13
Darwin CBD air temperature differences distribution – maximum, minimum and average values displayed per each monitored location.

AIR TEMPERATURE DIFFERENCES IN ORDER OF DECREASING RANKING			
LOCATION INDEX	MAX_ΔT [°C]	MIN_ΔT [°C]	AVG_ΔT [°C]
15	2.5	1.9	2.27
14	2.4	2.1	2.21
16	1.7	1.3	1.49
13	1.3	0.5	0.95
18	1	0.9	0.92
17	1.2	0.8	0.92
2	1.1	0.5	0.84
9	1	0.6	0.83
12	1.1	0.5	0.78
20	0.9	0.4	0.69
19	0.7	0.5	0.61
1	1.1	0.2	0.59
4	0.6	0.4	0.5
10	0.7	0.1	0.47
11	0.6	0.1	0.33
8	0.4	-0.1	0.19
5	0.3	0	0.16
3	0.2	0	0.09
7	0.1	-0.1	0,01
6	-0.2	-0.4	-0.3



Table 7.10

List of the terrestrial survey monitoring points in order of decreasing average UHI magnitude – maximum and minimum values additionally showed.

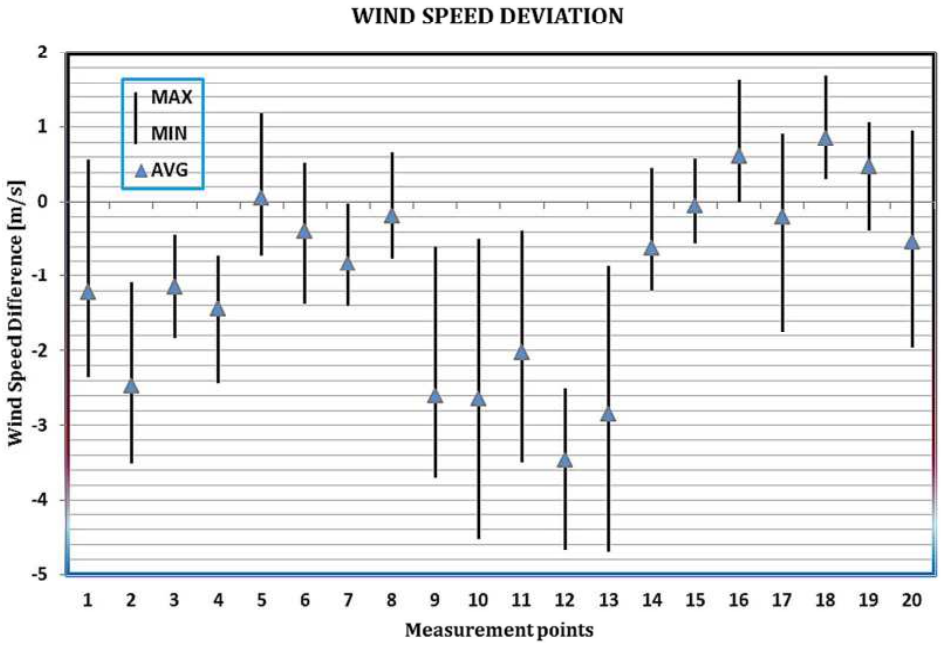


Figure 7.14
Darwin CBD wind speed differences distribution – maximum, minimum and average values displayed per each monitored location.

WIND SPEED DIFFERENCES IN ORDER OF DECREASING RANKING			
LOCATION INDEX	**MAX_Δws [m/s]**	**MIN_ Δws [m/s]**	**AVG_ Δws [m/s]**
3	1.67	0.32	0.85
8	1.62	0.01	0.61
7	1.04	-0.36	0.47
18	1.18	-0.69	0.06
11	0.55	-0.54	-0.05
9	0.64	-0.74	-0.18
5	0.90	-1.74	-0.20
17	0.50	-1.36	-0.38
6	0.94	-1.94	-0.53
10	0.43	-1.17	-0.62
2	-0.03	-1.38	-0.84
16	-0.45	-1.82	-1.14
15	0.55	-2.34	-1.21
13	-0.73	-2.41	-1.45
19	-0.40	-3.49	-2.02
14	-1.11	-3.49	-2.46
12	-0.62	-3.68	-2.60
20	-0.51	-4.50	-2.65
4	-0.87	-4.68	-2.85
1	-2.53	-4.66	-3.46



Table 7.11

List of the terrestrial survey monitoring points in order of decreasing average wind speed difference – maximum and minimum values additionally showed.

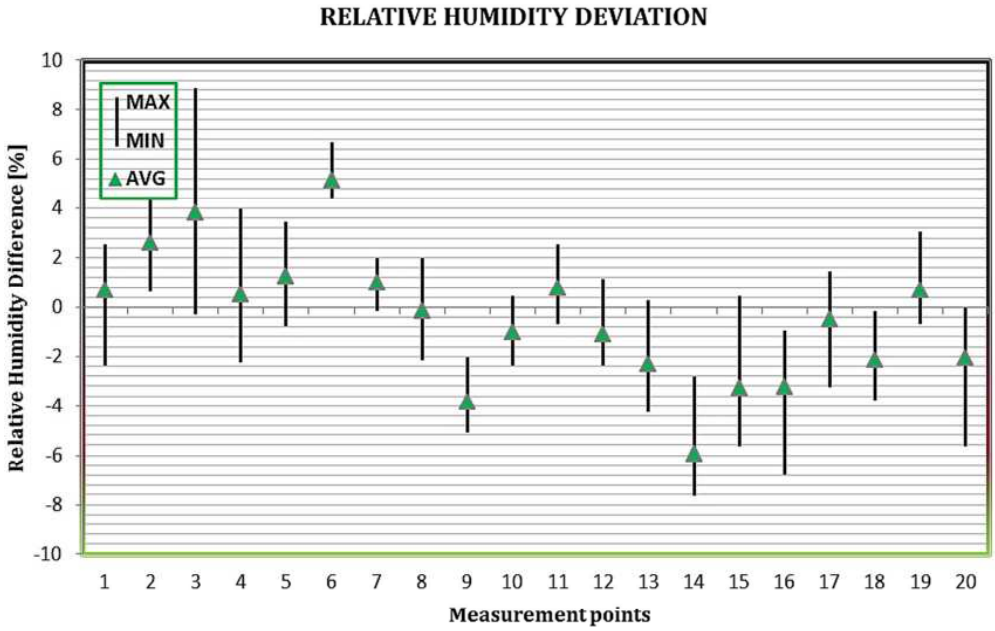


Figure 7.15
Darwin CBD relative humidity differences distribution – maximum, minimum and average values displayed per each monitored location.

RELATIVE HUMIDITY DIFFERENCES IN ORDER OF DECREASING RANKING

LOCATION INDEX	MAX_ΔRH [%]	MIN_ ΔRH [%]	AVG_ ΔRH [%]
9	6.6	4.5	5.12
7	8.8	-0.2	3.85
8	4.4	0.7	2.59
11	3.4	-0.7	1.26
5	1.9	-0.1	1
2	2.5	-0.6	0.8
4	3	-0.6	0.71
3	2.5	-2.3	0.68
18	3.9	-2.2	0.53
17	1.9	-2.1	-0.15
12	1.4	-3.2	-0.49
10	0.4	-2.3	-1
16	1.1	-2.3	-1.08
1	-0.1	-5.6	-2.06
20	-0.2	-3.7	-2.15
15	0.2	-4.2	-2.3
14	-1	-6.7	-3.22
19	0.4	-5.6	-3.29
6	-2.1	-5	-3.85
13	-2.9	-7.6	-5.94



Table 7.12

List of the terrestrial survey monitoring points in order of decreasing average relative humidity difference – maximum and minimum values additionally showed.

7.5.3.3 – Conclusions

The analysis on the results of the terrestrial survey demonstrated that significant temperature differences exist among the different zones of the CBD, up to 1°C, thus creating local microclimates within the urban layout. Such variability could be associated to topography and locally released anthropogenic heat mainly.

The area where the maximum UHI effect was observed is the north-west side of the CBD. That was an expected result since the hot western winds are the major natural trigger for temperature rise: accordingly, the external zones are those receiving the maximum advection.

On the other hand, the sea breeze effect was found to be negligible: the areas in close proximity to the Ocean (like those along Esplanade) did not show any evident air refreshing phenomena, actually some hot spots. That might be explained looking at

the wind speed values: here, the difference from the BoM station recordings reached the negative maximum because of the physical obstruction of the urban topography; consequently, convective flows are minimized and warm air is stuck within the canopy layer for a longer time.
Uhi magnitude hit its low in the area close to the Harbour. Many causes concur to this result: less building density, widespread greenery and massive evaporation phenomena (as witnessed by the positive difference in relative humidity too).
Given such diversification of reasons behind the formation of each local microclimate, it was likely that a combo rather than a one-fits-all mitigation solution had to be considered as the most promising.
Therefore, apart from a series of well-established corrective measures, some ad-hoc conceived blended alternatives were investigated too.

7.6 – MITIGATION SCENARIOS

In this paragraph, the selection and assessment of the mitigation scenarios is briefly addressed as part of the outputs HPA cluster was called upon to produce (yet not directly developed by the undersigned). Refer to the final report of the project **[7.5]** for pictures and tables and to find more detailed information.
Given the specific climatic characteristics and the overheating concerns emerging from the on-site data collection in Darwin CBD, fourteen mitigation scenarios (**table 7.13**) were proposed to reduce the ambient temperature and counteract the energy, comfort, health and economy-related drawbacks of UHI.
The macrocategories they belong to are:

- reflective technologies (cool roofs, cool pavements and increase of global albedo): the replacement of traditional materials with high-solar-reflectance ones is mirrored in lower surface temperatures, thus lower ambient temperature and lower radiant temperature affecting citizens' comfort in outdoor spaces;
- supplement of greenery (trees, grass, green roofs): their addition emphasizes the refreshment of ambient air occurring whenever an evaporative process (evapotranspiration) is activated;
- evaporative cooling systems (pools, fountains, sprinklers, …): in this case fountains were proposed since their integration with Darwin's cityscape and their mitigating potential outperformed the other solutions. The physical process is almost the same as for greenery (latent heat absorption during evaporation);

- shading devices and solar protections (shielding panels over street, technical tents, …): no specific solution was addressed. Their effect was simulated by increasing the albedo of streets, pavements and parking lots as much as necessary to align open-air and tree-shaded surface temperatures in the monitoring datasets.

A specific intervention on the State Square area was additionally designed in view of its high mitigation potential, to stand as exemplary model. In detail:

- all car parks in the square were covered by urban greenery;
- asphalt and concrete pavements in Smith Street and in the square, were replaced by cool pavements;
- Chan building was removed because of the massive encumbrance to air circulation (in accordance with the other interventions planned under the Heat Mitigation Program);
- spraying water fountains were installed along Smith street.

DARWIN URBAN HEAT ISLAND MITIGATION SCENARIOS

#	SCENARIO	DESCRIPTION
1	Reference Model	Albedo of walls and roofs=0.2; albedo of asphaltic streets and pavements=0.05, albedo of concrete pavements=0.2; albedo of loamy soil=0.15; Greenery<10% of the total pavements and open spaces.
2	Global albedo 0.4	Global albedo=0.4; Greenery<10% of the total pavements and open spaces.
3	Global albedo 0.6	Global albedo=0.6; Greenery<10% of the total pavements and open spaces.
4	Cool pavement	Albedo of streets and pavements=0.5; Greenery<10% of the total pavements and open spaces.
5	Shading	Albedo of streets=0.34; albedo of concrete pavements=0.44; Greenery<10% of the total pavements and open spaces.
6	Greenery 20%	Greenery=20% of the total pavements and open spaces.
7	Greenery 30%	Greenery=30% of the total pavements and open spaces.
8	Cool Roof	Albedo of roofs=0.85; Greenery<10% of the total pavements and open spaces.
9	Green Roof	Green roof for all buildings
10	Water fountain	Installation of water fountain on The Mall
11	State Square	Replacement of asphaltic carparks with greenery, removal of Chan building, application of water fountain in Smith Street
12	Combined scenario	Global albedo=0.6; greenery=30% and shading
13	Combined scenario with water fountain	Global albedo=0.6; greenery=30%; shading and water fountain across the Mall
14	Combined scenario – cold and dry season	Global albedo=0.6; greenery=30% and shading

Table 7.13
List of the proposed countermeasures for Darwin urban heat mitigation.

Two wind-driven synoptic conditions (NW and SE directions, 1 and 5m/s speeds) were simulated for the basic scenarios, while combined solutions were tested under cold (dry) season boundary settings too.
Each of the total 54 case studies was assessed by mapping the spatial distribution of: ambient temperature, surface temperature, wind speed and direction, reduction of ambient temperature (versus reference case).

7.7 – RESULTS AND DISCUSSION

The goodness of each mitigation measure proposed was essentially given in terms of reduction of the maximum ambient temperature, reduction of the minimum ambient temperature and maximum temperature decrease.
In order to simplify the presentation of the main ourcomes, the four simulated synoptic conditions are here codified in a XYZ format, where XY represent the direction of the wind (namely NW for North-Westerly winds and SE for South-Easterly winds) and Z is a number standing for the wind speed (namely 1 for 1m/s and 5 for 5m/s).
As a reminder, the ambient temperature in the reference scenario ranged from about 32°C to 36.5/36°C for NW5 and SE1 respectively and from about 33°C to 36°C for NW1 and SE1. The hottest surfaces were found to be the asphaltic ones composing the pavements, hitting a high of over 55°C, whichever wind was blowing.
Given such baseline, the following results were attained:

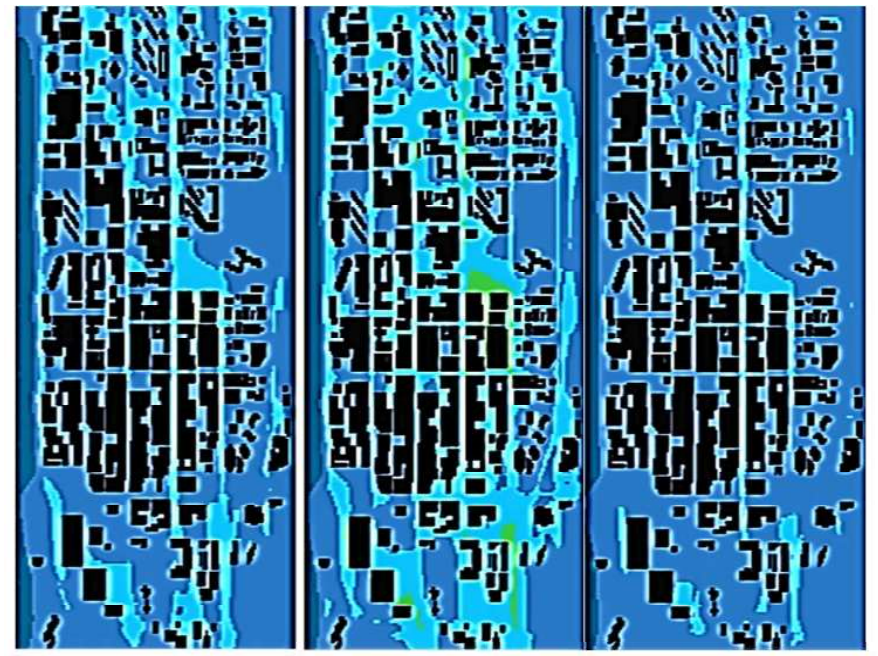
- the maximum reduction of maximum temperature for the NW5 boundary conditions was achieved in the combined scenarios (-2.72°C), even though an almost equal good result came out by increasing the global albedo up to 0.6 (-2.50°C) and in State Square (-2.42°C). Same placement for combined scenarios (-2.23°C) and increase of albedo to 0.6 (-2.14°C) when wind inverted direction. Third place for SE5 was reached by cool pavements instead of State Square (-1.82°C).
  When the wind speed decreased to 1m/s the best mitigation performances were achieved with the same scenarios, even if in a different order according to the direction of the wind: fountains (-2.56°C for NW1 and -1.23°C for SE1), global albedo up to 0.6 (-1.93°C for NW1 and -1.32 for SE1), combined scenarios (-1.87°C for NW1 and – 1.36°C for SE1).

The worst performance in terms of reduction of the maximum temperature was related to cool and green roofs (usually far less than 1°C), regadless of wind conditions.

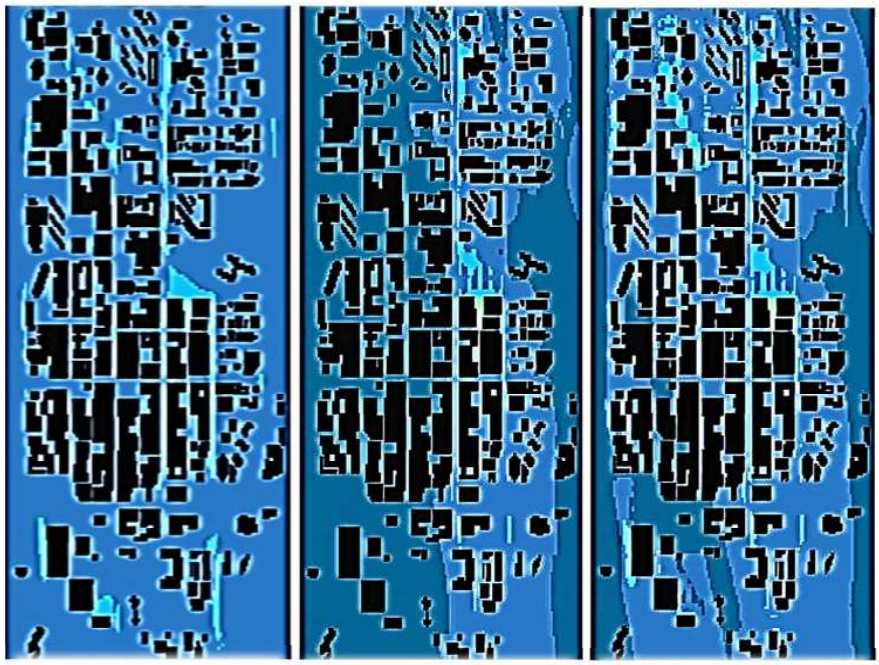
- the maximum reduction of minimum temperature for NW5 boundary conditions was achieved in the State Square scenario (-3.84°C), followed by conbined scenario with fountains (-3.09°C) and quite more distantly by fountains scenario (-1.86°C). Same ranking for SE5 (-4.80°C, -4.71°C and -3.42°C respectively). Same players yet inverting the first two positions with less windy conditions (-6.31°C, -5.77°C and -4.64 for NW1, -6.9°C, -5.94°C and – 5.77°C for SE1).

  All the other scenarios had a negligible impact in decreasing the minimum temperature (all below -0.3°C for NW5 and SE5, all below -1°C for NW1 and SE1);
- the reduction in maximum temperature improved when local scale was considered (boundaries close to where the mitigation strategy was implemented). In this context, State square scenario outperformed the others for all boundary conditions (-6.52°C for NW5, -8.02°C for SE5, -8.18°C for NW1 and -8.13°C for SE1), followed by the combined scenario with water (-5.15°C for NW5, -7.05°C for SE5, -7.15°C for NW1 and -7.80°C for SE1) and water fountain scenario (-3.92°C for NW5, -5.83°C for SE5, -5.46°C for NW1 and -6.67°C for SE1). As expected, the evaporation process contribution (the common line in all the three above mentioned scenarios) is much more emphasized near the source of phase change, while proximity plays a less evident role for the non-water scenarios. Cool roofs had a very poor local impact on maximum temperature, being the only scenario below -1°C for all wind conditions.

The following maps (produced in ENVI-met platform) provide a visual immediate comparison of the temperature drop distributions all over Darwin CBD (**Figure 7.16**) to better understand the spatial differences among the proposed scenarios and recap the afore presented conclusions.



GLOBAL ALBEDO 0.4 | GLOBAL ALBEDO 0.6 | COOL PAVEMENTS



SHADING | GREEN ROOF | WATER FOUNTAIN

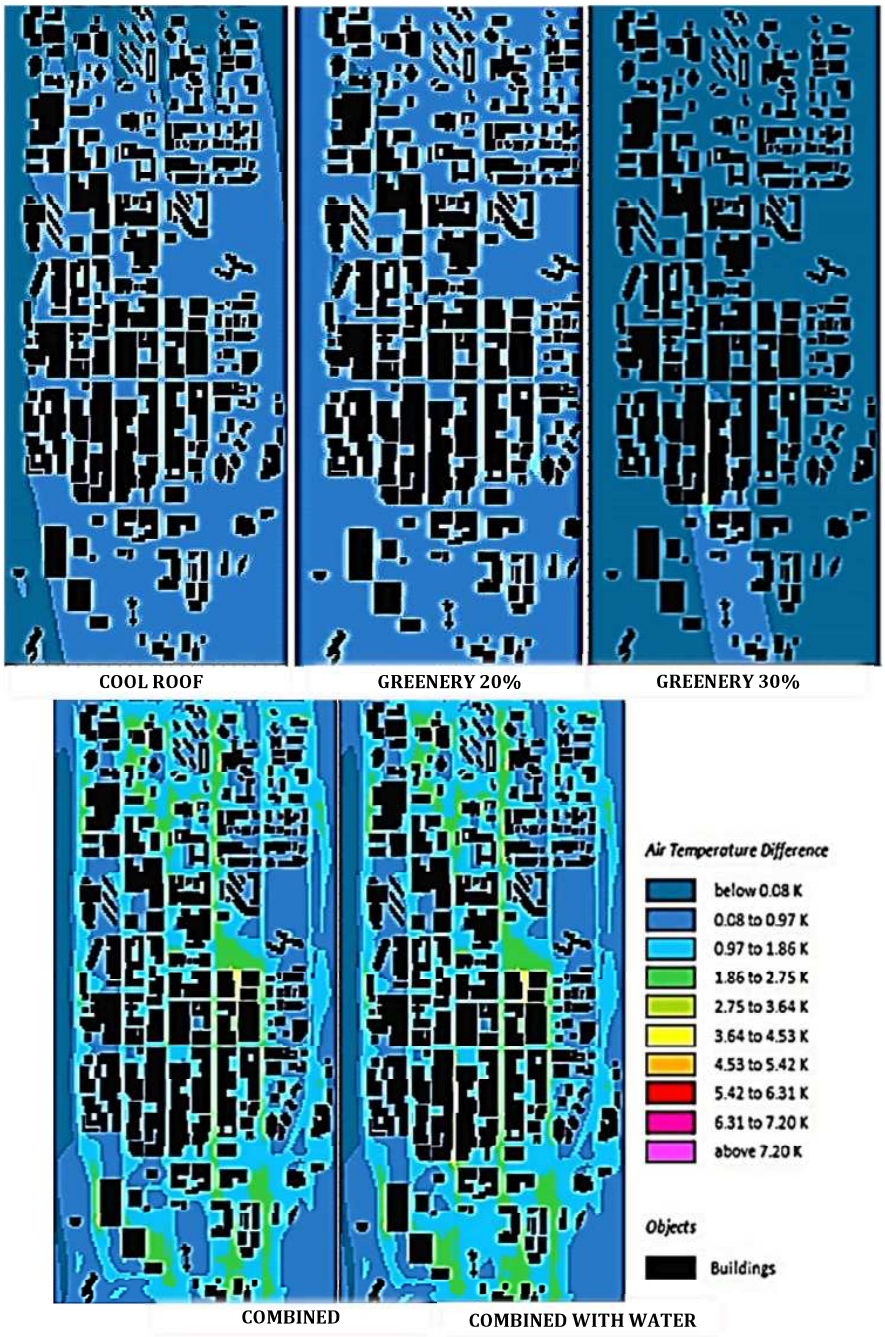


Figure 7.16
Distribution of the ambient temperature drop in Darwin CBD, according to the different simulated scenarios.

All the previous discussed simulations referred to the wet season: a separate investigation was conducted for the cold/dry period in a combined scenario, with the following settings: global albedo 0.6, greenery 30%, shadings over Woods St., Cavenagh St., Smith St., Mitchell St., Esplanade and McMinn St. plus over the car parks.
The outputs showed that:

- the maximum ambient temperature plummeted from more than 36°C in the reference scenario to about 30°C (for NW winds, between 30.3°C and 30.7 °C for SE winds);
- the minimum ambient temperature dropped from 32-33°C to about 27°C.

More detailed information is given in **table 7.14.**
Such figures confirmed the inherent assumption that the proposed mitigation techniques would improve outdoor comfort throughout the year.

DRY SEASON SIMULATION RESULTS							
Reduction of maximum ambient temperature [°C]				**Reduction of minimum ambient temperature [°C]**			
NW5	**NW1**	**SE5**	**SE1**	**NW5**	**NW1**	**SE5**	**SE1**
6.13	5.53	5.66	5.01	5.00	6.02	5.01	6.08

Table 7.14
Simulation results for the combined scenario developed for the dry season.

7.8 – CONCLUSIONS

Tropical cities are vulnerable to overheating phenomena and poor outdoor thermal comfort conditions due to the sinergies of synoptic weather conditions, global warming and urban heat island: Darwin, capital of the Northern Territory in Australia is not an exception, given its high-solar-absorbance materials and its layout which reduces wind speed and entraps warm air volumes within the urban canopy.
The research activity, run during the year of mobility spent at the UNSW in Sydney, aimed at investigating amplitude and characteristics of the UHI affecting the CBD area and return a full estimation of the mitigation potential.
The adopted methodology involved three macro-steps:

- preliminary statistical analyses over ten years of meteorological data (collected by the BoM station located near Darwin's airport): the main output was the identification of the dominant synoptic conditions via clustering technique. Wind speed and direction were found to be pivotal in the

microclimate variations throughout the year, thus among the four wind-related clusters the two extreme ones (North-Westerly winds and South-Easterly winds) were selected as boundary conditions for the following simulations;

- on-site monitoring campaign, by means of aerial thermal capturing and terrestrial meteorological mapping: the main output was the identification of magnitude and characteristics of the UHI by comparing simoultaneous datasets retrived in the CBD and in the airport area (used as undisturbed baseline).
- development of appropriate mitigation scenarios and quantification of the potential benefit: the main output was the ranking of a series of proposals of single and combined measures to counterbalance the local overheating in terms of ambient air temperature decrease.

The results of the latter two macro-steps are detailed below.

The use of the drone equipped with a thermal camera allowed to draw some relevant conclusions on surface temperature and the role of urban fabric materials on the formation of hot spots and local anomalies, in particular: streets exhibited very high surface temperatures, ranging between 55°C and 62°C; parking lots hitted even higher values (45°C - 67°C), close to those reached by roofs (49°C - 56°C) and pavements (48°C - 66°C); trees and greenery stayed much cooler, within the ranges 28°C - 38°C and 32°C - 46°C respectively; besides their shades locally decreased the surface temperatures of street-level materials by 10 to 23°C.

The use of a mobile meteorological sensor network allowed to record ambient temperature, relative humidity, wind speed and direction, solar radiation and heat flux all over the main areas of interest. The analysis of the results pointed out a series of local peculiarities to be taken into account in the design of the correct mitigation approach:

- the UHI reached a magnitude of 2.5°C along Daly Street on the Esplanade side, revealing the foundamental role of warm air advection (by westerly winds) and the almost negligible effect of sea breeze;
- ambient temperature distribution all over the CBD was found to be considerably heterogeneous: the north-west side of the city showed the highest ambient temperatures, while much lower values (-3/4°C) were recorded along Bennett Street and the Harbour district. Such findings reflected the different richness in vegetation and antropogenic density of the two poles, thus underpinning the efficacy of evapotranspiration.

Once sufficient information was retrieved by means of local monitoring, a systematic, broad-spectrum assessment of fourteen mitigation strategies was deployed through advanced simulation techniques involving 3D microclimate modelling.

The maximum temperature drop (over -2.7°C) witnessed between the reference and the mitigated scenarios corresponded to the combination of different technologies, simoultaneously applied. Such positive contribution was found to persist throughout the year (cold/dry season included). The minimum impact was achieved by the implementation of the sole cool roof. Evaporative technologies had a huge effect (exceeding -6°C ambient temperature decrease) on a very local scale, thus their installation was suggested just in specific locations where hot spots tended to concentrate.

Wind conditions affected the results of the considered scenarios: as a rule of thumb higher wind speeds were found to be beneficial in terms of UHI mitigation since convective cooling of the built surfaces and evapotranspiration potential were both emphasized. On the other hand, the potential of evaporation techniques was undermined since water droplets were faster and more efficiently removed.

Regarding the impact of wind direction, most of the mitigation technologies showed no bending between NW and SE boundary conditions: just evaporative solutions and greenery were strongly afftected (for the latter case the cooling potential dropped by 40-50%).

The afore described experimental and numerical study is framed in a wider program to enhance urban liveability and outdoor comfort in the Northern Territory: the obtained results will serve as guidelines for future real-scale implementation of the most promising mitigation solutions.

REFERENCES

[7.1] Paolini R., Zinzi M., Poli T., Carnielo E., Mainini A.G., Effect of ageing on solar spectral reflectance of roofing membranes: Natural exposure in Roma and Milano and the impact on the energy needs of commercial buildings, Energy and Buildings 84 (2014) 333–343

[7.2] Santamouris M., Ding L., Fiorito F., Oldfield P., Osmond P., Paolini R., Prasad D., Synnefa A., Passive and active cooling for the outdoor built environment – Analysis and assessment of the cooling potential of mitigation technologies using performance data from 220 large scale projects, Solar Energy, 2016, Article in press

[7.3] Bruse M., Fleer H., "Simulating surface-plant-air interactions inside urban environments with a three dimensional numerical model," Environmental Modelling and Software, vol. 13, no. 3-4, pp. 373–384, 1998

[7.4] Huttner S., Bruse M., Dostal P., Using ENVI-met to simulate the impact of global warming on the microclimate in central European cities, Berichte des Meteorologischen Instituts der Albert-Ludwigs-Universität Freiburg Nr. 18 (2008): Helmut Mayer and Andreas Matzarakis (eds.): 5th Japanese-German Meeting on Urban Climatology, October 2008, pp. 307-312

[7.5] Haddad S., Ulpiani G., Fox J., Paolini R., Synnefa A., Fiorito F., Garshasbi S., Heat Mitigation Program Darwin, NT, Final Report, 2017

[7.6] Santamouris M., Kolokotsa D., Urban Climate Mitigation Techniques, Routledge, 2016

[7.7] Gaitani N., Burud I., Thiis T., Santamouris M., High-resolution spectral mapping of urban thermal properties with Unmanned Aerial Vehicles, Building and Environment, Volume 121, 15 August 2017, Pages 215–224

[7.8] Gaitani N., Burud I., Thiis T., Santamouris M., Aerial Survey and In-situ Measurements of Materials and Vegetation in the Urban Fabric, Procedia Engineering, Volume 180, 2017, Pages 1335-1344

[7.9] Civil Aviation Safety Regulations 1998 (CASR) PART 101 Unmanned aircraft and rocket operations

[7.10] Lehmann S., Low Carbon Cities – transforming urban systems, 2015

[7.11] Mayer H., Hoppe P. 1987. Thermal comfort of man in different urban environments. Theoretical and Applied Climatology 38: 43–49

[7.12] U.S. Environmental Protection Agency. 2008. Reducing urban heat islands: Compendium of strategies.

[7.13] Santamouris M., Analyzing the heat island magnitude and characteristics in one hundred Asian and Australian cities and regions, Science of The Total Environment, Volumes 512–513, 15 April 2015, Pages 582-598

[7.14] Giannopoulou K., I. Livada., Santamouris M., Saliari M., Assimakopoulos M.,Caouris Y.G., On the characteristics of the summer urban heat island in Athens, Greece, Sustainable Cities and Society, Volume 1, Issue 1, February 2011, Pages 16-28
[7.15] Santamouris M., Cartalis C., Synnefa A., Local urban warming, possible impacts and a resilience plan to climate change for the historical center of Athens, Greece, Sustainable Cities and Society, Volume 19, December 2015, Pages 281-291.
[7.16] Synnefa A., Karlessi T., Gaitani N., Santamouris M., Papakatsikas C., Experimental testing of cool colored thin layer asphalt and estimation of its potential to improve the urban microclimate, Building and Environment, Volume 46, Issue 1, January 2011, Pages 38-44
[7.17] Voogt J.A., Oke. T.R. Thermal Remote Sensing of Urban Areas. Remote Sensing of Environment. 86. (Special issue on Urban Areas): 370-384, 2003.
[7.18] Akbari H., Levinson R.M., Rainer L., "Monitoring the Energy-Use Effects of Cool Roofs on California Commercial Buildings," Energy and Buildings, 37(10): 1007-1016, 2005.
[7.19] Akbari H., Rose L. S., Taha H.,. "Characterizing the Fabric of the Urban Environment: A Case Study of Sacramento, California," LBNL-44688, Lawrence Berkeley National Laboratory, Berkeley, California (December) 1999a.

8

Conclusions

Contribution, novelty and perspectives.

8.1 – FOREWORD

Several research activities have been carried out during the three years of the Doctorate path to investigate the potential in terms of energy efficiency, comfort and climate change resilience of different techniques and technologies applied both inside and outside the building stock.
The energy performance and the quality of life achievable inside a building depends on countless variables: from external microclimate to internal use and occupancy patterns, from walls composition to HVAC's characteristics, from solar shading devices to solar reflectance of the sunlit surfaces…
Indeed, the "optimization" problem is not an easy one to address, whether the target is energy or comfort, or both. What is certain is that a holistic, climate-specific design tends to be rewarding compared to building concepts that disregard both positive and negative effects of the outdoors.
The harmonization of architecture, construction and building service engineering could potentially led to very efficient energy ensembles, yet it should not be underestimated that "only a satisfied user will not intervene with the designed energy concept or the indoor climate control; dissatisfaction results in multiple system interventions which may cause waste of energy and sometimes even damage to building envelope components. Satisfaction with the indoor environment also increases working productivity or enables effective recreation of residents" **[8.1].**
As a consequence, each single research activity run in the framework of my PhD dealt with both reduction of energy consumption and enhancement of the ergonomics.
Moreover, the findings are not the result of a mere simulation-based activity. Conversely, the experimental component is dominant in each research study. The outcomes are thereby sustained by a robust and articulated monitoring phase, involving all the pivotal parameters at stake.

In the following paragraphs the main contribution, novelty and open issues are described.

8.2 – ADVANCES IN THE FIELD OF SMART CONTROL

Nowadays high performance architecture cannot ignore the contribute that intelligent networks, customized dashboards and advanced functionality might provide to the efficient use of the built environment.
It is a given that building systems and components fully cooperate when they act as receptive terminals of a hierarchically higher supervising system both by sourcing inputs and accepting command outputs to track the desired behaviour.
Arguably, the potential of automatic, sensor or data-driven control of the building systems is a rather promising path to be pursued in the perspective of net zero energy buildings, given the high degree of customization and easy integration with the HVACs and passive systems.
Moreover, it represents a fairly powerful strategy in dealing with challenging environments (extreme climates, massively dispersive architectural designs, considerably transient indoor conditions, …) which might require particular care to be respectful of both the needs of the occupants inside and the equilibriums of the outdoors.
The advantages mirror at operative and maintenance level too.
Several approaches and several configurations were conceived and tested in the framework of my research.
Below are the main considerations coming out of an overarching analysis of all the encompassed casuistry:

- heating systems, electrically powered, might be effectively driven by fuzzy controllers contemplating both indoor and outdoor temperatures in the decision making process, with no need for complex mathematical models nor time consuming tuning procedures;
- the benefit compared to conventional on/off and PID controllers is rather pronounced both in terms of energy consumption and ergonomics in the context of hyper-insulated buildings were fine regulation is necessary to avoid overshooting and hysteric operation of the terminals. The difference might narrow down with less energy efficient envelopes since they are much less sensitive to small heating/cooling calls;
- the same conclusions might not apply to "slower" terminal units, such as water-based ones. Inertial systems, indeed, might benefit from predictive controllers which could amortize the downtime required for the thermal balance to be established each time, through preventive adjustments.
- Vulnerability to poor indoor air quality in naturally ventilated school buildings can be addressed by means of smart automation of window opening and closing,

by properly contemplating both the role of temperature and of CO_2 content in the decision making process;

- it was demonstrated that IAQ can be preserved in an efficient, comfort-respective way by pondering the timing and the percentage of opening, thus avoiding local drafts and excessive environmental variability: consequently, the occupants could run their activities in the context of a self-adaptive building, with no need to undertake corrective actions to restore their thermal neutrality;
- the above results are meant to be achievable when the automatic system operates upper located, hopper windows: other design solutions (i.e. casement windows) might require a slightly different control algorithm, yet retaining the user-centred, flexible approach.
- Sunspaces might improve the energy performance of hyper-insulated buildings, given the proper selection of the window panes; additionally, when controlled mechanical ventilation adequately mixes the air volumes on the interface partition wall the benefit gets emphasized;
- the optimal percentage of glazed surface lies between 30% and 70%, depending on the dimensions of the indoor space. The roof should remain opaque to mitigate the drawback given by the lower thermal insulation of the transparent layers;
- low-e, double glazed panels should be preferred to single glazed solutions, notably when the VMC is implemented: the heat stored by the sunspace needs to persist longer to maximise the frequency of positive activation of the convective transfer;
- the potential drawback of a sunspace over summertime in the Mediterranean climate was not assessed. Anyway, by providing the solar collector with solar shadings and transversal openings (or other ventilation provisions), the disadvantages could be strongly mitigated.
- Indoor overheating, provoked by overabundant solar gains, can be mitigated by implementing a befitting control logic of the AC terminal units, but not solved at all unless accompanied by other retrofit strategies: neither a rule-based, heuristic, fuzzy logic over summertime, nor a model-predictive control over wintertime could avert the occurrence of discomfort phenomena inside the relevant case study, yet the severity was significantly dampened;
- in such casuistry, apart from the contribution of direct solar radiation, a second trigger for global and local discomfort was the heat re-irradiated by the hot sunlit surfaces (for instance, the glazed façade stayed frequently over 40°C on the internal side) which strongly contributed to the rise of the operative temperature;

- the need for pronounced interventions of the AC terminal units to counteract the positive thermal balance inside the indoor spaces, led to further sources of discomfort, namely temperature stratification, air turbulence, draughts and emphasized environmental asymmetries;
- despite the inherent deficiency, the tested controllers achieved non-negligible improvements by keeping the operative temperature closer to the setpoint. As a result, the PMV exceeded vote 2 in none of the ultimate configurations and category B conditions were established for a remarkable period of time (23% in summertime and between 85% and 50% in wintertime);
- from the energy perspective, the more rewarding logic was the predictive one since, by anticipating the perturbing action of weather changes it could better ponder its control action and make use of lower power emissions so as to adjust the indoor temperature more gently and loosely with all relevant benefits at both global and local scale;
- a certain room for improvement was pinpointed in the design of a cooperative fuzzy model predictive control (CFMPC) to combine the advantages of both the algorithms and extend the benefit to all seasons and all buildings and technical systems typologies, by achieving high control performance at less energy expenditure.

As a general remark, temperate climate (Mediterranean) constituted the boundaries for the above experiments. More extreme weather conditions were not investigated during the monitoring campaigns thus no field validated data are available to confirm the suitability of such configurations at other latitudes.

8.3 – ADVANCES TOWARDS CLIMATE CHANGE RESILIENCE

Understanding climate change is a truly daunting challenge. The ramifications are countless and usually self-empowering.
The building sector is one of most sensitive to such phenomenon, given that outdoor conditions dramatically impinge on the energy demand profile and undermine the efficacy of passive cooling approaches **[8.2, 8.3].** In this context, global warming and increased extremes in local weather patterns might jeopardize the optimal performance of buildings conceived to provide thermal comfort 'passively' under the aegis of bioclimatic design principles.
Nevertheless, there is plenty of scope to respond to changing climatic scenarios by boosting the widespread of adaptive buildings and mitigation technologies, which aim to increase the physical resilience of building structure and fabric to evolving weather and climatic events **[8.4, 8.5].**
This might include minimizing the operation costs, the GHG emissions, the vulnerability of people to extreme weather conditions, the energy poverty, the risk of disruption to energy supply, the heat island effect **[8.6, 8.7].**
For instance, bearing in mind that building roofs and pavements constitute over 60% of most urban surfaces **[8.8, 8.9]**, the room for improvement in terms of better management of radiation and air quality by shifting from dark, low-reflectance material to cool ones is fairly promising **[8.10, 8.11].**
Nowadays, cost-effective mitigation opportunities are abundant all over the world; the know-how is easily accessible and the payback period more than affordable, particularly if we consider monetizable some of the major social co-benefits (reduced mortality and morbidity, poverty alleviation, improved social welfare, employment, energy security, …).
However, the potential still needs to be unlocked and markets to be catalysed, by undertaking a suite of actions, one of which could be to fill the lack of awareness and information.
The research studies carried out during the last two years of my PhD aimed at disclosing some of these opportunities, by focusing on two of the major climate-change-related threats the building sector suffers of:

- premature obsolescence of construction and technical systems currently implemented;
- urban sprawl and escalation of the urban heat island effects.

The following sub-paragraphs summarize the pursued progresses and the main outcomes.

8.3.1 – Low-tech buildings and future scenarios

In the framework of WISBA 2015, Building 2226 designed by the architectural office Baumschlager and architect Eberle was selected to test if its low-tech concept could persist the climate change expected by 2050 since it represented the borderline case of ultra-low energy buildings.

As a matter of fact, the absence of heating, cooling or mechanical ventilation systems in favour of temperature and CO_2 controlled natural ventilation system, although rewarding in terms of current energy consumption, is rather vulnerable to premature obsolescence and failure in case of weather extremes.

A 4-month-long research activity was carried out on the existing configuration to explore the potential threats and opportunities and customize a potential suitable redesign, respectful of the original user-centred concept but resilient to wider outdoor conditions.

The trade-offs/conflicting benefits of the proposed redesign measures in comparison with the current state for the climate change scenario were balanced by giving priority to (in order): comfort, energy consumption, LCA, LCC.

Finally, the discomfort occurrence was strongly mitigated in the future scenario by:

- implementing a shading system and air circulation through the staircases: wooden blinds were beneficial in terms of comfort and LCA, but detrimental in terms of energy and LCC;
- replacing the inner walls with reinforced concrete walls (R.C. Core): the benefit in terms of comfort outweighed the environmental impacts and slightly impinged on the overarching energy consumption;
- increasing density and thermal capacity of the materials composing the external walls were: all options slightly enhanced discomfort (less than 0,1% impact) and improved all other aspects;
- increasing density and thermal capacity of the inner floors and roof: such intervention was rewarding from all perspectives since comfort was reinforced and the other issues remained almost unaffected.

All things considered, the re-shaped version of Building 2226 was remarkably promising from a comfort perspective both in 2015 and 2050 (-72% and -59% discomfort hours respectively – adaptive comfort theory thresholds), thanks to increased thermal mass and reduced solar gains.

8.3.2 – Urban Heat Island mitigation in tropical climates

It is well acknowledged that the urban heat island (UHI) effect has serious consequences on thermal comfort, energy consumption, health and economy and thus affects negatively the sustainability and liveability of cities.
In the framework of the "Heat Mitigation Program Darwin" two main outputs were developed so as to take a step forward towards the definition of a commendable diagnostic and prognostic routine, namely:

1. guidelines to the correct procedure to measure magnitude and characteristics of the UHI phenomenon through an interrelated chain of measurements, simulations and analyses;
2. methodology for the customization of the best single/combined countermeasures to ensure the overheating mitigation without penalizing the wintertime outdoor comfort conditions.

The city of Darwin, tropical capital of the Northern Territory (Australia), served as case study.
The first step of the study was the statistical analysis of the meteorological data collected by the local BoM (Bureau of Meteorology) station over ten years (2006-2016). The prevailing synoptic conditions were identified to guide the design of well-purposed mitigation solutions.
The second phase was the experimental campaign: aerial infrared monitoring via drone technologies and terrestrial monitoring of meteorological parameters were run all over the CBD: the on-site measurements were compared with the concomitant BoM recordings to assess the UHI magnitude: the CBD was found to be 2°C-3°C hotter than the surrounding rural area.
The third phase was the analysis of the hot spots location to pinpoint the potential causes: high surface temperatures of the urban fabric (frequently above 60°C), reduced wind speeds, lack of sea breeze and substantial release of anthropogenic heat were identified as driving forces for local overheating. Conversely, trees and greenery exerted a significant direct (evapotranspiration) and indirect (street shading) cooling effect. The hottest spots were found to be concentrated in the north-west area that represents the "entry door" for the warm western winds. However, remarkable temperature differences were observed between the various zones of the CBD.
The fourth step was the simulation: based on the experimental results, fourteen mitigation scenarios (involving single or combined technologies) were designed, simulated via 3D microclimate modelling (ENVI-met) and assessed in terms of ambient temperature, surface temperature, wind speed and direction for two synoptic conditions, NW and SE wind direction, and for low and high wind speeds, (1 and 5 m/sec).

The final combined scenario (use of reflective materials for roofs and pavements, application of shadings in specific zones of the city and a 30% increase of the urban greenery) was tested under the climatic conditions of the cold (dry) period too. In total 54 scenarios were evaluated. Additionally, the cost of the proposed mitigation scenarios was estimated using data received from various credible market sources.
All considered mitigation technologies, except of the green roofs, were found to be economically suitable for implementation in the Darwin CBD area. The achieved decrease of the maximum ambient temperature compared to the actual situation was close to 2.8°C (from 36.5°C down to 33.7°C), while the corresponding decrease of the minimum temperature was nearly 3.1°C. The maximum temperature drop was attained in the final combined scenario, while the minimum performance corresponded to the use of only cool roofs. Some of the considered mitigation scenarios (mainly evaporative systems and greenery) showed a rather significant local cooling (up to -6°C), although the global impact was negligible.
The maximum surface temperature drop was achieved when shading, greenery and cool pavement technologies, were implemented (local reduction exceeding 20-25°C).
The main conclusion is that very efficient mitigation technologies are currently available and promising results are expected from their implementation.

It should be stressed that the same procedure was furtherly applied to other major Australian cities (Sydney and Alice Springs, in the framework of akin projects run during the last year at the University of New South Wales).
Given the wide variety of climatic circumstances, the ultimate mitigation strategy was every time different and tailored to the specific casuistry.
Next step would be the physical implementation of some of the suggested interventions and subsequent monitoring campaign to check on the actual aftermaths.
These two further operative phases conclude the proposed methodology to tackle UHI pragmatically, yet in a scientifically sound and objective way.

REFERENCES

[8.1] Mitterer C, Künzel HM, Herkelb S, Holm A. Optimizing energy efficiency and occupant comfort with climate specific design of the building. Frontiers of Architectural Research (2012) 1, 229–235

[8.2] Artmann N, Gyalistras D, Manz H, Heiselberg P. Impact of climate warming on passive night cooling potential. Building Research and Information (2008) 36, 111 – 128.

[8.3] Chow DH, Levermore GJ. The effects of future climate change on heating and cooling demands in office buildings in the UK. Building Services Engineering Research and Technology (2010) 31, 307 – 323.

[8.4] Gerdes A, Kottmeier C, Wagner A. Climate and Construction. In: International Conference 24 and 25 October 2011, Karlsruhe, Germany / Competence Area "Earth and Environment" KIT Scientific Reports; 7618. KIT Scientific Publishing (2011). 367 pp

[8.5] Pyke CR, McMahon S, Larsen L, Rajkovich NB, Rohloff A. Development and analysis of Climate Sensitivity and Climate Adaptation opportunities indices for buildings. Building and Environment(2012) 55, 141 – 149.

[8.6] Roaf S, Crichton D, Nicol F. Adapting Buildings and Cities for Climate Change : A 21st Century Survival Guide. Architectural Press / Elsevier, Kidlington, (2009) 385 pp.

[8.7] Atkinson JGB, Jackson T, Mullings-Smith E. Market influence on the low carbon energy refurbishment of existing multi-residential buildings. Energy Policy (2009) 37, 2582 – 2593.

[8.8] Ihara T, Kikegawa Y, Asahi K, Genchi Y, Kondo H. Changes in year-round air temperature and annual energy consumption in office building areas by urban heat-island countermeasures and energy-saving measures. Applied Energy (2008) 85, 12 – 25.

[8.9] Taha H. Urban Surface Modification as a Potential Ozone Air-quality Improvement Strategy in California: A Mesoscale Modelling Study. Boundary-Layer Meteorology (2008) 127, 219 – 239.

[8.10] Akbari H, Damon Matthews H, Seto D. The long-term effect of increasing the albedo of urban areas. Environmental Research Letters(2012) 7, 024004.

[8.11] Akbari H, Menon S, Rosenfeld A. Global cooling: increasing world-wide urban albedos to offset CO2. Climatic Change (2009) 94, 275 – 286.

Acknowledgments

Through the voice of Indira Gandhi – Speech at the plenary session of United Nations Conference on Human Environment (Stockholm, 1972).

STOCKHOLM 14TH JUNE 1972

[…]

"My deep interest in this our `only earth' was not for itself but as a fit home for man. One cannot be truly human and civilized unless one looks upon not only all fellow-men but all creation with the eyes of a friend. […]"

"It is said that in country after country, progress should become synonymous with an assault on nature. We who are a part of nature and dependent on her for every need, speak constantly about "exploiting" nature. When the highest mountain in the world was climber in 1953, Jawaharlal Nehru objected to the phrase "conquest of Everest" which he thought was arrogant. It is surprising that this lack of consideration and the constant need to prove one's superiority should be projected onto our treatment of our fellowmen? […]".

We are gathered here under the aegis of the United Nations. We are supposed to belong to the same family sharing common traits and impelled by the same basic desires, yet we inhabit a divided world.

[…] We are bound by our own ideals. We owe allegiance to the principles of the rights of workers and the norms enshrined in the charters of international organizations. Above all we are answerable to the millions of politically awakened citizens in our countries. All these make progress costlier and more complicated.

On the one hand the rich look askance at our continuing poverty--on the other, they warn us against their own methods. We do not wish to impoverish the environment any further and yet we cannot for a moment forget the grim poverty of large numbers of people. Are not poverty and need the greatest polluters? […] The environment cannot be improved in conditions of poverty. Nor can poverty be eradicated without the use of science and technology.

Must there be conflict between technology and a truly better world or between enlightenment of the spirit and a higher standard of living? […]

For the last quarter of a century, we have been engaged in an enterprise unparalled in human history--the provision of basic needs to one-sixth of mankind within the span of one or two generations. When we launched on that effort our early planners had more than the usual gaps to fill.

There was not enough data and no helpful books. No guidance could be sought from the experience of other countries whose conditions--political, economic, social and technological--were altogether different.

Planning in the sense we were innovating, had never been used in the context of a mixed economy.

But we could not wait.

The need to improve the conditions of our people was pressing. Planning and action, the improvement of data leading to better planning and better action, all this was a continuous and overlapping process. Our industrialization tended to follow the paths which the more advanced countries had traversed earlier.

With the advance of the 60's and particularly during the last five years, we have encountered a bewildering collection of problems, some due to our shortcomings but many inherent in the process and in existing attitudes. The feeling is growing that we should re-order our priorities and move away from the single-dimensional model which has viewed growth from certain limited angles, which seems to have given a higher place to things rather than to persons and which has increased our wants rather than our enjoyment. We should have a more comprehensive approach to life, centred on man not as a statistic but an individual with many sides to his personality. The solution of these problems cannot be isolated phenomena of marginal importance but must be an integral part of the unfolding of the very process of development […].

Acknowledgements

The inherent conflict is not between conservation and development, but between environment and reckless exploitation of man and earth in the name of efficiency. Historians tell us that the modern age began with the will to freedom of the individual. And the individual came to believe that he had rights with no corresponding obligations. The man who got ahead was the one who commanded admiration. No questions were asked as to the methods employed or the price which others had to pay.
The industrial civilization has promoted the concept of the efficient man, he whose entire energies are concentrated on producing more in a given unit of time and from a given unit of manpower. Groups or individuals who are less competitive and according to this test, less efficient are regarded as lesser breeds--for example the older civilizations, the black and brown peoples, women and certain professions.
Obsolescence is built into production, and efficiency is based on the creation of goods which are not really needed and which cannot be disposed of when discarded. What price such efficiency now, and is not recklessness a more appropriate term for such a behaviour?

All the `isms' of the modern age--even those which in theory disown the private profit principle--assume that man's cardinal interest is acquisition. The profit motive, individual or collectives, seems to overshadow all else. This overriding concern with self and Today is the basic cause of the ecological crisis.

Pollution is not a technical problem. The fault lies not in science and technology as such but in the sense of values of the contemporary world which ignores the rights of others and is oblivious of the longer perspective [...].

The environmental problems of developing countries are not the side effects of excessive industrialization but reflect the inadequacy of development. The rich countries may look upon development as the cause of environmental destruction, but to us it is one of the primary means of improving the environment for living, or providing food, water, sanitation and shelter; of making the deserts green and the mountains habitable. The

research and perseverance of dedicated people have given us an insight which is likely to play an important part in the shaping of our future plans. We see that however much man hankers after material goods; they can never give him full satisfaction. Thus the higher standard of living must be achieved without alienating people from their heritage and without despoiling nature of its beauty, freshness and purity so essential to our lives […].

Life is one and the world is one, and all these questions are inter-linked. The population explosion; poverty; ignorance and disease, the pollution of our surroundings, the stockpiling of nuclear weapons and biological and chemical agents of destruction are all parts of a vicious circle. Each is important and urgent but dealing with them one by one would be wasted effort.
It serves little purpose to dwell on the past or to apportion blame, no one of us is blameless. If some are able to dominate over others, it is at least partially due to the weakness, the lack of unity and the temptation of gaining some advantage on the part of those who submit […]. If there is to be a change of heart, a change of direction and methods of functioning, it is not an organization or a country-no matter how well intentioned--which can achieve it. While each country must deal with that aspect of the problem which is most relevant to it, it is obvious that all countries must unite in an overall endeavour. There is no alternative to a cooperative approach on a global scale to the entire spectrum of our problems.

I have referred to some problems which seem to me to be the underlying causes of the present crises in our civilization. This is not in the expectation that this Conference can achieve miracles or solve all the world's difficulties, but in the hope that the opinions of each national will be kept in focus, that these problems will be viewed in perspective and each project devised as part of the whole.

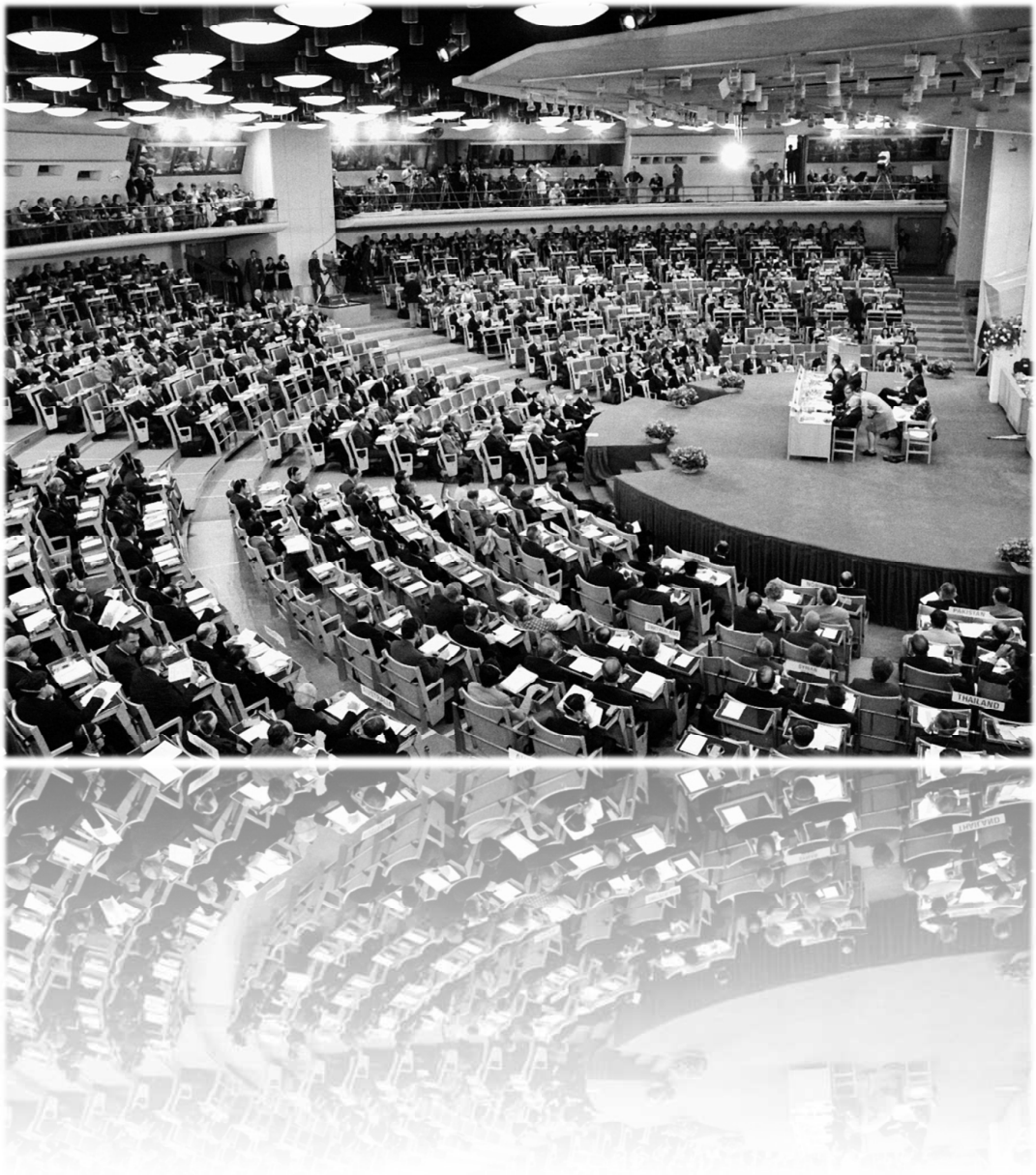
On a previous occasion I have spoken of the unfinished revolution in our countries I am now convinced that this can be taken to its culmination when it is accompanied by a revolution in social thinking. In 1968 at the 14th General Conference of UNESCO the

Indian delegation, along with others, proposed a new and major programme entitled "a design for living". This is essential to grasp the full implications of technical advance and its impact on different sections and groups. We do not want to put the clock back or resign ourselves to a simplistic natural state. We want new directions in the wiser use of the knowledge and tools with which science has equipped us. And this cannot be just one upsurge but a continuous search into cause and effect and an unending effort to match technology with higher levels of thinking. We must concern ourselves not only with the kind of world we want but also with what kind of man should inhabit it. Surely we do not desire a society divided into those who condition and those who are conditioned. We want thinking people capable of spontaneous self-directed activity, people who are interested and interesting, and who are imbued with compassion and concern for others.

It will not be easy for large societies to change their style of living. They cannot be coerced to do so, nor can governmental action suffice. People can be motivated and urged to participate in better alternatives.

It has been my experience that people who are at cross purposes with nature are cynical about mankind and ill-at-ease with themselves. Modern man must re-establish an unbroken link with nature and with life […]. I quote,

"What of thee I dig out, let that quickly grow over, Let me
not hit thy vitals, or thy heart".
So can man himself be vital and of good heart and
conscious of his responsibility



I thank everyone who made me think this way…

